OKLAHOMA GEOLOGICAL SURVEY
Charles J. Mankin, *Director*

CIRCULAR 93

ISSN 0078-4397

SOURCE ROCKS IN THE SOUTHERN MIDCONTINENT, 1990 SYMPOSIUM

KENNETH S. JOHNSON AND BRIAN J. CARDOTT
Editors

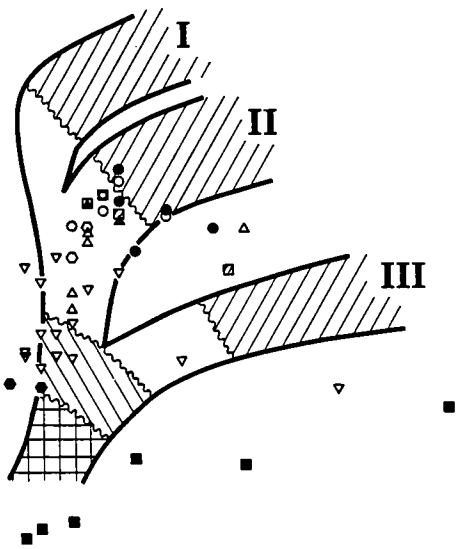

Proceedings of a symposium held February 6–7, 1990, in Norman, Oklahoma.

Co-sponsored by:
Oklahoma Geological Survey
and
Bartlesville Project Office,
U.S. Department of Energy

The University of Oklahoma
Norman
1992

OKLAHOMA GEOLOGICAL SURVEY

CHARLES J. MANKIN, *Director*
KENNETH S. JOHNSON, *Associate Director*

SURVEY STAFF

JAMES H. ANDERSON, *Cartographic Draftsperson II*
ROBERT H. ARNDT, *Economic Geologist*
BETTY D. BELLIS, *Word-Processing Operator II*
TOM L. BINGHAM, *Geologist II*
MITZI G. BLACKMON, *Clerk-Typist*
JOCK A. CAMPBELL, *Petroleum Geologist IV*
BRIAN J. CARDOTT, *Organic Petrologist*
JAMES R. CHAPLIN, *Geologist III*
JANISE COLEMAN, *Office Assistant II*
CHRISTIE L. COOPER, *Editor*
VELMA L. COTTRELL, *Chief Clerk*
ELDON R. COX, *Manager, Core and Sample Library*
TAMMIE K. CREEL, *Data-Entry Specialist*
CHARLES DYER III, *Drilling Technician*
WALTER C. ESRY, *Core and Sample Library Assistant*
ROBERT O. FAY, *Geologist IV*
SAMUEL A. FRIEDMAN, *Senior Coal Geologist*
T. WAYNE FURR, *Manager of Cartography*
L. JOY HAMPTON, *Petroleum Geologist III*
PATRONALIA HANLEY, *Chemist*
LEROY A. HEMISH, *Coal Geologist III*
SHIRLEY A. JACKSON, *Research Specialist I*
PRISCILLA A. JOHNSON, *Office Assistant III*
RUTH KING, *Research Specialist I*
JAMES E. LAWSON, JR., *Chief Geophysicist*
CHARLOTTE C. LLOYD, *Cartographic Draftsperson I*
KENNETH V. LUZA, *Engineering Geologist*
TODD MCCORMICK, *Electronic Technician*
RICHARD MURRAY, *Copy Center Operator*
LINDA NERO, *Receptionist-Clerk*
DAVID O. PENNINGTON, *Operations Assistant*
JO LYNN PIERCE, *Publications Assistant*
JUDY A. SCHMIDT, *Office Manager*
CONNIE G. SMITH, *Promotion and Information Specialist*
PAUL E. SMITH, *Supervisor, Offset Press Copy Center*
MICHELLE J. SUMMERS, *Coordinator Geological Computer Systems*
NEIL H. SUNESON, *Stratigrapher/Geologist IV*
DANNY L. SWINK, *Drilling Technician*
JANE L. WEBER, *Organic Chemist*
STEPHEN J. WEBER, *Chief Chemist*
GWEN C. WILLIAMSON, *Assistant to Director*

Title-Page Illustration

Van Krevelen-type diagram of elemental data showing kerogen type and thermal maturity of Upper Devonian source-rock samples of Oklahoma and Arkansas (adapted from Comer, fig. 2, this volume).

This publication, printed by the Transcript Press, Norman, Oklahoma, is issued by the Oklahoma Geological Survey as authorized by Title 70, Oklahoma Statutes, 1981, Sections 231–238. 1,200 copies have been prepared for distribution at a cost of $11,113 to the taxpayers of the State of Oklahoma. Copies have been deposited with the Publications Clearinghouse of the Oklahoma Department of Libraries.

CONTENTS

PREFACE

This is the third symposium in as many years dealing with topics of major concern to geologists and others involved in petroleum-resource development in Oklahoma and adjacent states. These symposia are intended to foster the exchange of information that will improve our ability to recover our Nation's oil and gas resources. Proceedings of the first symposium (on the Anadarko basin) were published as OGS Circular 90, and proceedings of the second symposium (Late Cambrian–Ordovician geology of the southern Midcontinent) were published as OGS Circular 92.

Hydrocarbon source rocks consist of organic-rich sediments that contain kerogen (disseminated insoluble organic matter) that can be converted to oil and/or gas through thermal maturation. Oklahoma and adjacent states are underlain by thousands to tens of thousands of feet of marine sedimentary rocks that contain known or potential hydrocarbon source rocks. Understanding the distribution, character, and thermal history of these source rocks can provide valuable insight into the occurrence, distribution, and character of oil and gas contained in petroleum reservoirs.

To facilitate the exchange of information on source rocks, petroleum occurrence, and petroleum recovery, the Oklahoma Geological Survey (OGS) and the Bartlesville Project Office of the U.S. Department of Energy (BPO–DOE) cosponsored this symposium dealing with source rocks and the generation and migration of hydrocarbons in the southern Midcontinent. The symposium was held on February 6–7, 1990, at the Oklahoma Center for Continuing Education, The University of Oklahoma, in Norman. This volume contains the proceedings of the symposium.

Research reported upon at the symposium focused on the organic geochemistry, diagenesis, and thermal history of the major source rocks in the region, with special emphasis on the Woodford–Chattanooga Shale, on various Pennsylvanian shales, and on carbonate units such as the Arbuckle and Viola Groups. Other research includes characterization of oil types, deep pressure compartments, diagenetic aureoles, and the hydrodynamics of fluid migration to reservoirs. We hope that the symposium and these proceedings will bring such research to the attention of the geoscience and energy-research community, and will help foster exchange of information and increased research interest by industry, university, and government workers.

Twenty-two papers were presented orally at the symposium, and they are presented here as full papers or abstracts. An additional 11 reports were given as posters, and they are presented here as short reports or abstracts. About 200 persons attended the symposium. Stratigraphic nomenclature and age determinations used by the various authors in this volume do not necessarily agree with those of the OGS.

Persons involved in the organization and planning of this symposium include Kenneth Johnson, Brian Cardott, and Charles Mankin of the OGS, and Tom Wesson and Michael Ray of BPO–DOE. Other OGS personnel who contributed include: Michelle Summers and Tammie Creel, Registration Co-Chairs; Jock Campbell, Poster Session Chair; Connie Smith, Publicity Chair; and Helen Brown and Gwen Williamson, Exhibits Coordinators. Appreciation is expressed to each of them and to the many authors who worked toward a highly successful symposium.

KENNETH S. JOHNSON
AND BRIAN J. CARDOTT
General Chairmen

PART I

PAPERS PRESENTED ORALLY AT THE SYMPOSIUM

The Role of Source Rock Studies in Petroleum Exploration

Colin Barker
University of Tulsa

ABSTRACT.—Mature source rocks are organic-rich rocks that have been heated hot enough and long enough to generate petroleum. They are an essential ingredient in forming commercial oil accumulations and their recognition is important in exploration. Most techniques for identifying source rocks stress maturation status. This can be established using either the complex, insoluble organic material called "kerogen" or the simple solvent-soluble "bitumen." For kerogen, physical characteristics such as color and reflectivity can be used and values for vitrinite reflectance are probably the single most widely used maturity parameter. Changes in kerogen chemical composition also indicate maturity and plots of atomic hydrogen/carbon (H/C) vs. atomic oxygen/carbon (O/C) ratios (called van Krevelen diagrams) are commonly used because they show organic matter type as well as maturity. Bitumen quantities change systematically with maturity, but chemical composition is usually more diagnostic. In particular, the very characteristic chemical fossils, now usually called biomarkers, are widely used. Biomarker structures are modified thermally and changing ratios have been calibrated in terms of source-rock maturity status. Pyrolysis techniques also give very useful thermal stability information. These methods are quick and convenient and are widely used for screening source-rock samples. In practice it is good policy to combine both kerogen-based and bitumen-based methods in evaluating source-rock generation status. Thermal models that consider the kinetics of petroleum generation and that mathematically combine temperature and time throughout the history of a source rock are becoming important in constraining the timing of the onset of generation and the cracking of oil to gas.

INTRODUCTION

The term "petroleum" is commonly used to include both crude oil and natural gas. For petroleum to accumulate in commercial quantities there must be both an effective source rock and a reservoir, and they must be linked by a migration pathway. In addition, the correct timing of the generation–migration–accumulation sequence is needed. The presence of an oil field shows that all the conditions were satisfied and implies that there must have been an effective source rock in the area. If it has been established that a source rock was present, what is to be gained by identifying the specific rock that generated the oil? Most geologists recognize that with better understanding comes improved success in exploration, and a simple example will illustrate how recognizing source rocks can help. Figure 1 shows a north–south section from the San Juan basin that crosses the Papers Wash field (full to the spill point), South Papers Wash field (partially filled), and a southern structure that is dry. What conclusions could have been drawn if the first well had penetrated the South Papers Wash structure and found it incompletely filled? If the area is thermally mature (Fig. 1A), all the traps probably would be partially filled. In contrast, if the source rock is only mature deeper downdip to the north, the traps would be filled in sequence by the migrating oil spilling updip from one to the next (Fig. 1B). A partially filled trap then shows that the updip traps are unlikely to contain petroleum, and in this case suggests that the southerly structure is not a prime exploration target.

For many years explorationists have assumed that "black shales" are source rocks. There is at least a grain of truth in this because red beds, for example, usually indicate oxidizing conditions and imply low organic matter contents. But color alone is a poor guide to source-rock quality, and it now seems that an evaluation of a shale, or other rock type, for source-rock character must provide answers to the following questions (Barker, 1979):

1) Does the rock have sufficient organic matter?
2) Is the organic matter capable of generating?
3) Has this organic matter generated petroleum?
4) Has the generated petroleum migrated out?
5) Is the rock oil-prone or gas-prone?

These questions will be discussed individually below.

At present, there are no generally applicable methods for establishing the percent of generated bitumen that migrated out of a source rock. It is assumed that the generation of petroleum drives the migration process and that a certain minimum quantity of bitumen is needed before expulsion can occur. This threshold value is set by the need

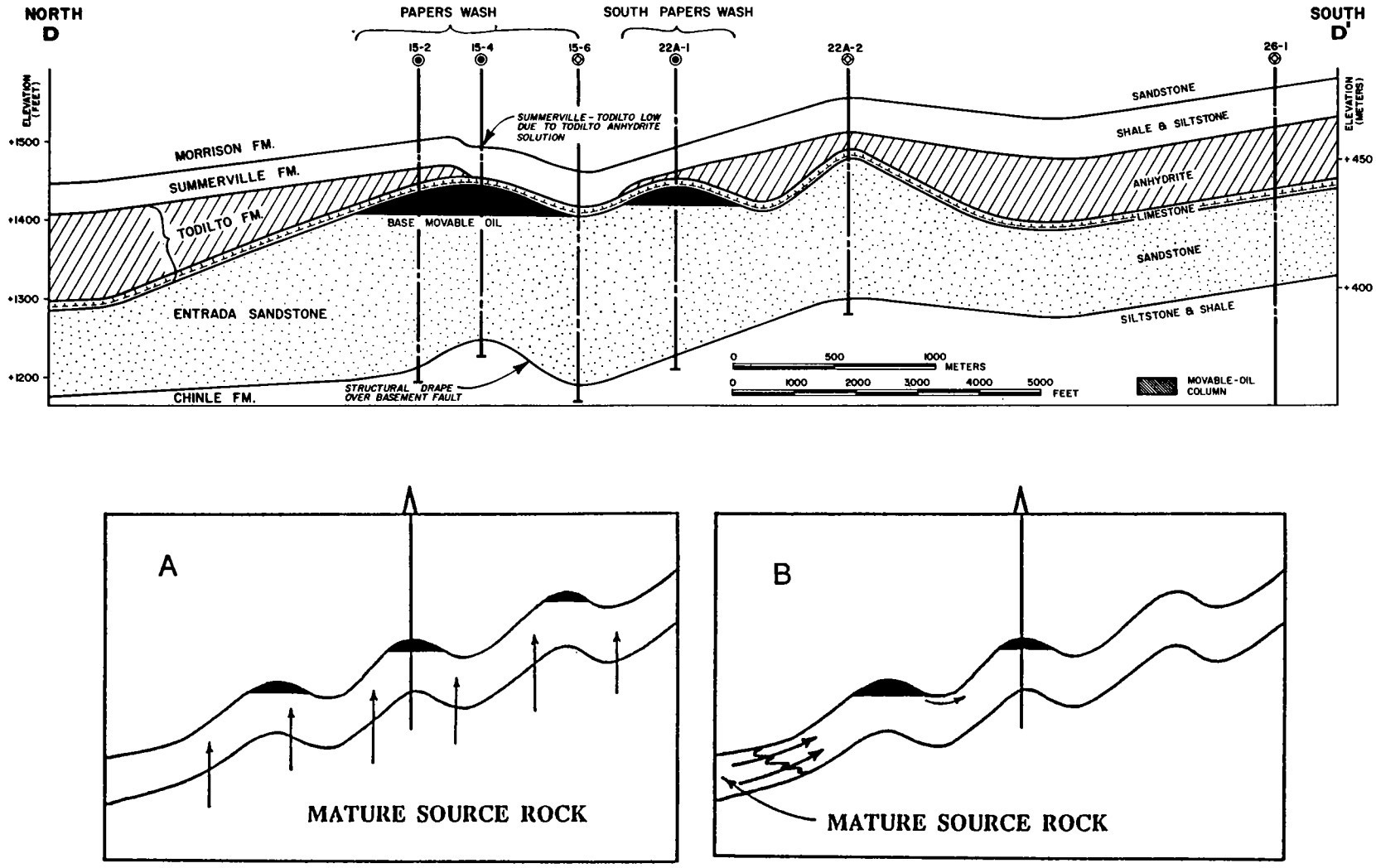

Figure 1. *Top:* North–south section across the Papers Wash field and nearby structures in the Entrada Sandstone, San Juan basin, New Mexico (Vincelette and Chittum, 1981). *Bottom:* Alternative oil migration directions depending on the location of mature source rocks.

to saturate adsorbers in the rock and to fill (at least partially) the pore system. Momper (1978) estimated that on average this requires 850 ppm of bitumen, so that a rock will not be an effective petroleum source rock until >850 ppm of bitumen have been generated.

QUANTITY OF ORGANIC MATTER

The requirement that source rocks generate commercially significant quantities of oil and gas implies that there is probably some lower limit for the organic carbon content in effective source rocks. A relation between high organic matter content in rocks and the occurrence of reservoired petroleum is well documented both globally and regionally. Statistics for giant fields worldwide show a remarkably good correlation with the available organic material as indicated by the average organic carbon content of sedimentary rocks. Ronov (1958) analyzed nearly 26,000 samples from both petroliferous and nonpetroliferous areas and found that the average organic content in the latter was <0.5%, whereas in petroliferous areas it was nearly three times as high. These studies (and others) have led to the widely accepted use of 0.5% total organic carbon (TOC) as a lower cut-off for effective source character. A lower limit for organic carbon also appears to be consistent with the idea that it is necessary to generate a certain amount of bitumen before migration can start. This is an important concept because it means that a lean rock with <0.5% TOC will never generate enough oil to initiate migration, and therefore it is not possible to offset low organic contents with large volumes of rock.

In the last couple of years improved understanding of the mechanism of migration has led to the idea that minimum organic contents for source rocks are somewhat higher, in the 1–2% range (Doligez, 1987; Lewan, 1987).

The organic content of rocks is commonly measured on individual samples from specific formations, composite samples, or samples taken at intervals down a well (e.g., every 10 or 50 ft). For many wells, no geochemical analyses are made. In an attempt to interpolate between sample control, or to extrapolate to surrounding areas, electric log response has been used to infer organic contents (Schmoker, 1979,1981; Meyer and Nederlof, 1984). This can be helpful locally for organic-rich rocks, especially in areas where the response can be calibrated in well-documented wells.

TYPE OF ORGANIC MATTER

The organic matter in potential source rocks must be a type that is capable of generating petroleum. Recycled material, which has already been buried and is now no longer capable of generating, should be excluded from the total when establishing the percentage of organic matter in the rock. Since clastic sediments are formed from weathered and transported preexisting rocks, it is possible for some remnants of older, once-buried organic matter to be remobilized and redeposited with younger sediments.

Most clastic rocks contain at least a few particles of recycled material and, in exceptional cases, >80% of the organic material may be recycled. The presence of recycled vitrinite can often be recognized by multiple populations in vitrinite-reflectance data. In general, the primary vitrinite fits a smooth trend with depth, but R_o values for the recycled vitrinite show considerable scatter to higher values. Because reworked organic matter has been buried once, it will be darker in color in transmitted light than the more recently deposited material. When visual examination of separated kerogen shows some light-colored material along with darker pieces, a recycled contribution is probably present.

GENERATION STATUS ("MATURITY")

Introduction

Petroleum generation depends on temperature modified by time (Tissot and Welte, 1984; Hunt, 1979), and its progress is shown by the changing composition of organic materials in the rock. Both physical and chemical characteristics of kerogen change, showing the combined effects of time and temperature and indicating present thermal maturity (Héroux and others, 1979). With increasing time-temperature exposure, kerogen color intensifies and darkens; vitrinite reflectance increases; palynomorph translucency decreases; thermal stability (as indicated by pyrolysis) increases; and the elemental composition of kerogen shows a progressive increase in percent carbon and decrease in H/C ratio. These changes in the kerogen lead to changes in both the amount and chemical composition of the bitumen. A wide range of techniques has been developed for evaluating the maturity of source rocks using these changes in kerogen and bitumen. The more important ones are discussed below.

Kerogen

Physical Characteristics

Color.—Kerogen color darkens and intensifies in transmitted light as increasing maturity drives the kerogen towards higher carbon contents and ultimately to black graphite. Color starts very pale yellow and progresses through darker yellow, orange-browns and darker browns to black. This sequence can be assigned a numerical ranking scale called a Thermal Alteration Index (TAI). Unfortunately

several schemes are being used, and while all of them start with 1.0 for the palest yellow, immature kerogen, the black-end member is assigned a value of 4, 7, or 10. Similar schemes can be used with spores to give a Spore Coloration Index (SCI) and with conodonts to give a Conodont Alteration Index (CAI).

Vitrinite Reflectance (R_o).—The single most important maturity indicator is the reflectivity of vitrinite, and most other maturity indicators have been calibrated to give corresponding R_o values. In spite of its importance, the interpretation of vitrinite-reflectance data is often not unambiguous. It is important for the operator to select only vitrinite particles for measurement. Vitrinite may be hard to identify and the situation is further complicated by the existence of more than one type of vitrinite. Generally, the material called Vitrinite 1 (Vitrinite A) is used, since Vitrinite 2 is more variable and shows lower reflectivities with more scatter (Buiskool Toxopeus, 1983).

Clearly, for R_o to be used as a maturity indicator, the sample must contain vitrinite. Because vitrinite is a wood-derived, type III kerogen that originates on the land surface, it is transported mainly by rivers and accumulates with clastic rocks. Carbonates, which commonly develop in clear waters (indicating lack of clastic input), frequently do not have vitrinite. Cambrian–Ordovician and older rocks will not have vitrinite, because higher land plants had not evolved at that time.

Reflectivity is usually measured for at least 30 pieces of vitrinite in a sample. A large number of measurements is needed because there are natural variations in vitrinite reflectance due to minor variations in chemical composition, and because particles are cut randomly during polishing and reflectivity varies somewhat with orientation. An ideal, single vitrinite population in a low-maturity sample will produce a histogram with a single, narrow, bell-shaped curve, but at high maturities (≥1.5% R_o) the peak broadens considerably, because vitrinite becomes increasingly anisotropic. Real samples commonly show multiple populations in the histogram, such as those shown in Figure 2. Peak A may be due to primary vitrinite with B and C being oxidized and/or recycled material. It is also possible that B is the primary population, C is oxidized, and A is due to caved material from shallower in the well. In the absence of any other information, it may be difficult or impossible to decide among alternative interpretations. For this reason, it can be very dangerous to depend on vitrinite-reflectance data obtained from a single sample of cuttings. The most reliable estimates of maturity come from vitrinite-reflectance profiles down a well.

In geologically simple settings, vitrinite reflectance starts at ~0.2% near surface and increases steadily with depth (Figs. 3,4). The rate increases with depth and plots of log R_o against depth are close to straight lines (Dow, 1977) (Fig. 4). Simple R_o profiles can be modified by several geologic processes including (1) faulting, (2) erosional unconformities, and (3) igneous intrusions.

Thrust faulting can move deeper, more mature samples with higher R_o values to shallow depths. In a well that crosses a thrust fault, the vitrinite-reflectance profile will show an abrupt break from high values to lower ones with increasing depth (Fig. 5).

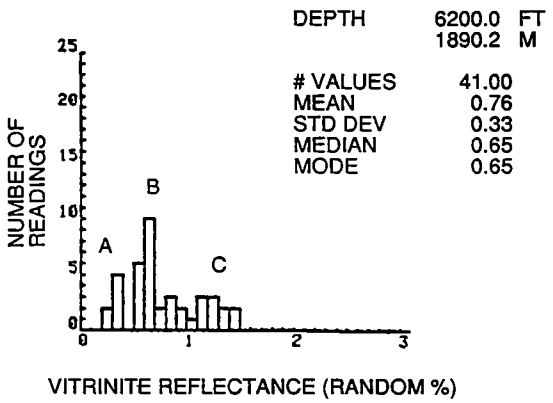

Figure 2. Vitrinite reflectance data for 41 particles showing several populations (from Dow and O'Conner, 1982). See text for discussion.

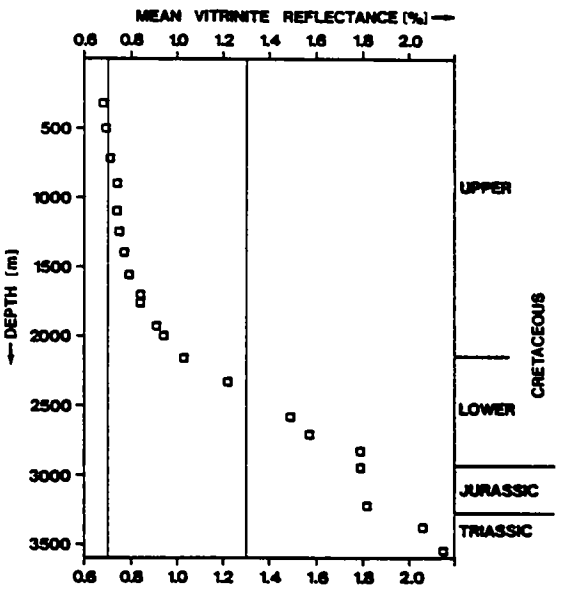

Figure 3. Profile of vitrinite reflectance with depth for a well in the Elmworth field, Deep basin of western Canada (Welte and others, 1984).

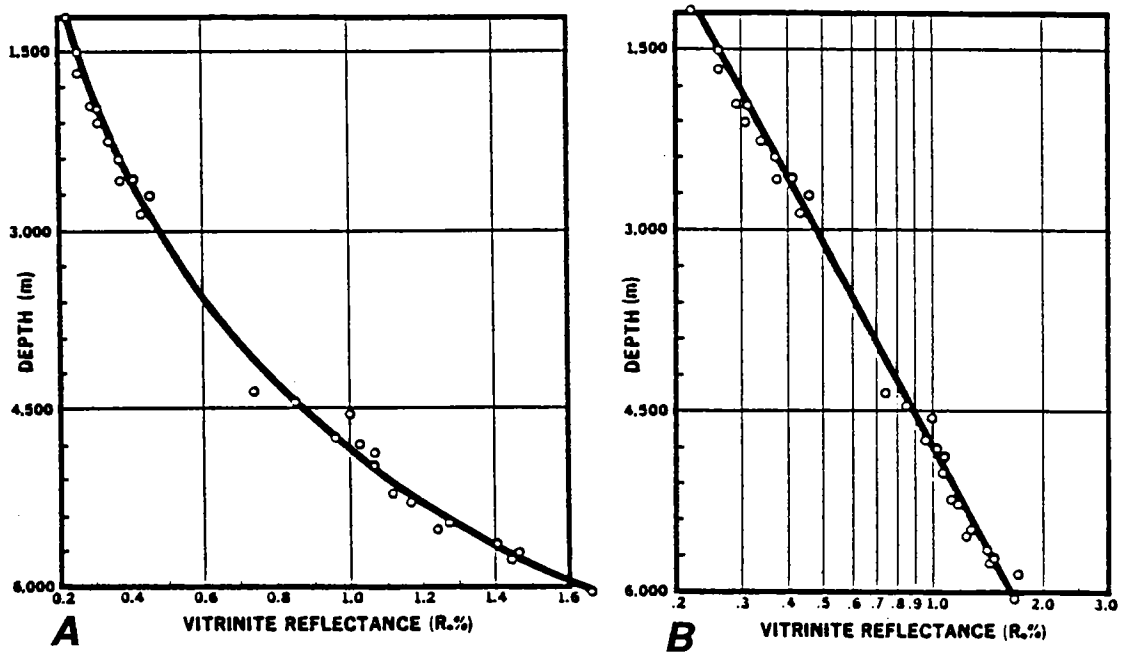

Figure 4. Kerogen maturation profile of a typical Gulf Coast well showing reflectance increase with depth. Both depth and average R_o values are plotted on linear scales in A. The same maturation profile is shown in B but with R_o values plotted on a logarithmic scale. This is the simplest case of a continuously subsiding basin (Dow, 1977).

Erosional unconformities show that part of the section has been removed and imply that material with the lowest range of R_o values has been lost. Subsequent sedimentation will deposit vitrinite with an R_o value of ~0.2% onto the erosional surface, so that the profile will show an abrupt increase at the unconformity (Fig. 5).

Igneous intrusions indicate locally high temperatures (though generally of short duration), and close to dikes and sills the R_o values will be increased due to the elevated thermal regime. Intrusions, however, have only a rather localized effect, and if a dike or sill is D units thick, thermal effects can be expected for 2D units on either side (Fig. 5).

In all three cases, an abrupt change in the trend of vitrinite-reflectance values with depth is formed. If the section is later buried more deeply, the vitrinite will continue to mature, with the lower R_o material maturing more rapidly since it is further from equilibrium. As a consequence, abrupt changes in R_o values tend to be smoothed out, leaving "kinks" in the profile (Katz and others, 1988).

Vitrinite is just one of the many types of organic matter that may be present in a rock. It has its own characteristic kinetic parameters (E—activation energy; A—frequency factor), and these may differ from those for other organic materials, so that on burial, rates of reaction (including petroleum generation) can be different. While R_o values have been calibrated to give a measure of thermal stress (essentially time-temperature influence), they may not always give a precise indication of maturation status for other types of organic matter. Kinetic parameters vary with both the nature of the organic matter and its past diagenetic history; differences do not vary systematically, but depend on the details of thermal history. Coals, for example, may give quite different values depending on whether the vitrinite is in a massive, bedded coal or in finely disseminated particles. This is because coal seams generally developed under conditions that remain reducing, while transport of smaller particles is more likely to involve a higher degree of degradation and oxidation. Thick coal seams can lead to other problems, because they are very friable and prone to caving, contaminating samples from deeper parts of the well.

Chemical Composition

Changes in the physical characteristics of kerogen are a reflection of changing chemical composition. The simplest indication of these changes is the variation of elemental composition with maturity. Carbon, hydrogen, and oxygen weight percentages are frequently measured (LaPlante, 1974;

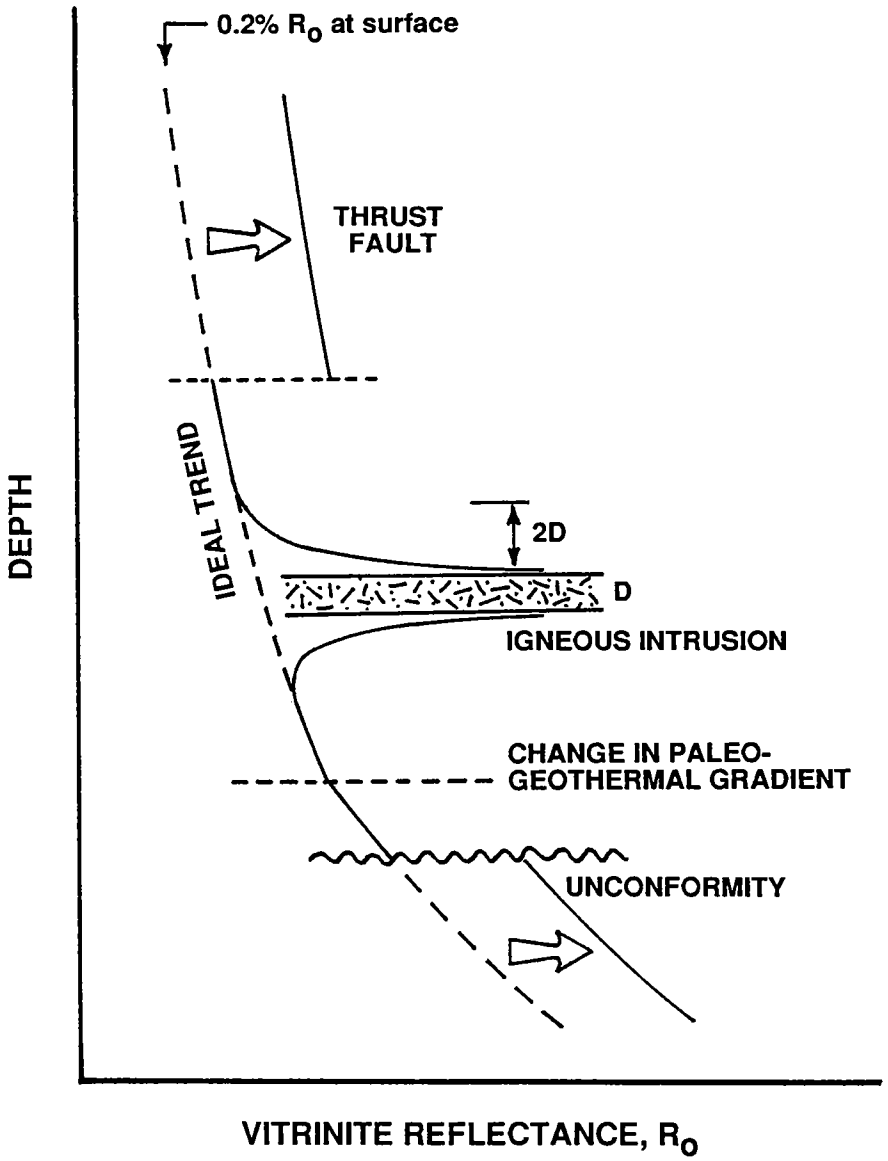

Figure 5. Schematic diagram showing some of the geologic processes that can disturb vitrinite-reflectance profiles.

Durand and Monin, 1980). This data can be presented in several different ways, but the most common is either as weight percent carbon (e.g., Swift and Williams, 1980), atomic hydrogen/carbon ratios (e.g., Ayers and others, 1982), or as a van Krevelen diagram where hydrogen/carbon ratios are plotted against oxygen/carbon ratios.

Van Krevelen diagrams present kerogen compositions in a way that not only shows maturity but may also indicate organic matter type (Tissot and others, 1974). The high hydrogen tracks for kerogen types I and II are oil prone while the type III, low hydrogen kerogen track is gas prone. Figure 6 shows kerogen elemental data plotted on a van Krevelen diagram.

Bitumen

Amount

Although kerogen accounts for the major part of the organic matter in rocks, it is the bitumen which eventually migrates and accumulates in the reservoir as petroleum. The most direct way of establishing the amount and composition of generated material is to analyze this solvent-extractable bitumen fraction. With increasing maturity, both

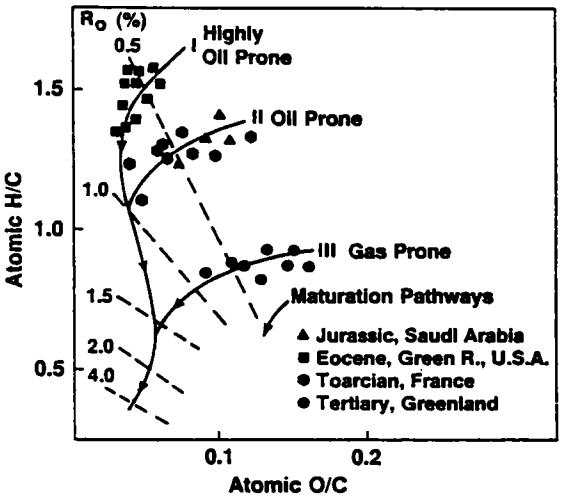

Figure 6. Plot of kerogen atomic H/C vs. O/C (van Krevelen diagram) showing various hydrocarbon-generative types. Plot is correlated to vitrinite reflectance (R_o) shown by dashed lines. Thermal maturity is indicated by distance along converging maturation pathways (solid lines), with the most mature samples in lower-left corner. Mixed samples showing compositions between each pathway are common (Peters, 1986).

the amount of bitumen and its chemical composition change. Either (or both) of these parameters can be used to help assess source-rock maturity. Since bitumen is generated mainly from kerogen, maturity is usually established from bitumen/kerogen ratios, but it is worth remembering that the absolute concentration of bitumen is what initially controls the onset of migration. Strictly, the term "bitumen" refers to all extractable organic material, but it is often restricted to just C_{15+} when being used with source-rock data. Figure 7 shows that bitumen/kerogen ratios are initially low, but with increasing depth they increase and pass through a maximum before decreasing to low values again.

Composition

The decrease in C_{15+} bitumen/kerogen ratio that occurs with depth (Fig. 7) is due to cracking of larger molecules to smaller ones that are part of the C_{15-} fraction. This is one of the clearest indications that bitumen composition is changing with depth, the trend being from oil-like materials toward gas. The overall changes in bitumen with increasing maturity are shown by the gas chromatograms for the total solvent extract. Figure 8 shows the changes associated with increasing depth for Kimmeridgian shale samples from the North Sea (Thomas and others, 1985).

The trend is for normal alkanes to increase relative to other components. Initially, these other materials are simply diluted, but with rising temperature, many biologically derived compounds break up, either to smaller fragments or to more complex residues that are not part of the soluble bitumen. The small hump in the gas chromatogram that is due to multi-ring biomarkers steadily diminishes with maturity and the main hump in the overall chromatogram also becomes less prominent. Alkane/isoprenoid ratios, such as n-C_{17}/pristane, are initially <1.0 but continue to rise with maturity until at very high maturity levels essentially there are no isoprenoid chains left (Fig. 8).

The normal alkanes change in composition as well as in relative amount with increasing maturity. In immature samples that include some terrestrial organic matter, the long chains often show an odd-even predominance and frequently normal n-C_{29} is the most abundant n-alkane. With increasing maturity n-alkane relative abundances tend toward a smooth distribution and increasingly toward shorter chain lengths. Odd-even preference can be expressed as a Carbon Preference Index (CPI) (Bray and Evans, 1961) with a value >1.0 indicating odd predominance. Although this is easy to measure and is commonly reported, it is only a rough indicator of maturity. It can only be used with rocks that initially contained significant terrestrial material, since a rock dominated by marine algae, for example, will have no odd-even preference and a CPI close to 1.0 from the time it is deposited.

Biomarkers

The bitumen in sediments and rocks contains a wide variety of compounds including the complex, but characteristic, molecules derived directly from organisms. These "chemical fossils" are now generally called "biological markers" or "biomarkers" (Mackenzie, 1984; Philp, 1985). They have variable, but limited, thermal stabilities and change in structure and composition as the sediment is buried. These changes can be used to indicate maturity level.

Organisms synthesize compounds with very specific three-dimensional structures, because these molecules must fit like a key in a lock if they are to work with the biochemical processes. Any time there are four different groups around a single carbon atom it is called "asymmetric," and two different configurations are possible—in essence, a left-handed and a right-handed form (Fig. 9). These structures are distinguished as R and S. For example, the C-20 carbon atom in the sterane ring structure is asymmetric (Fig. 10) and can assume either an S or an R form. Organisms, however, only make the 20R form so that initially 20S is

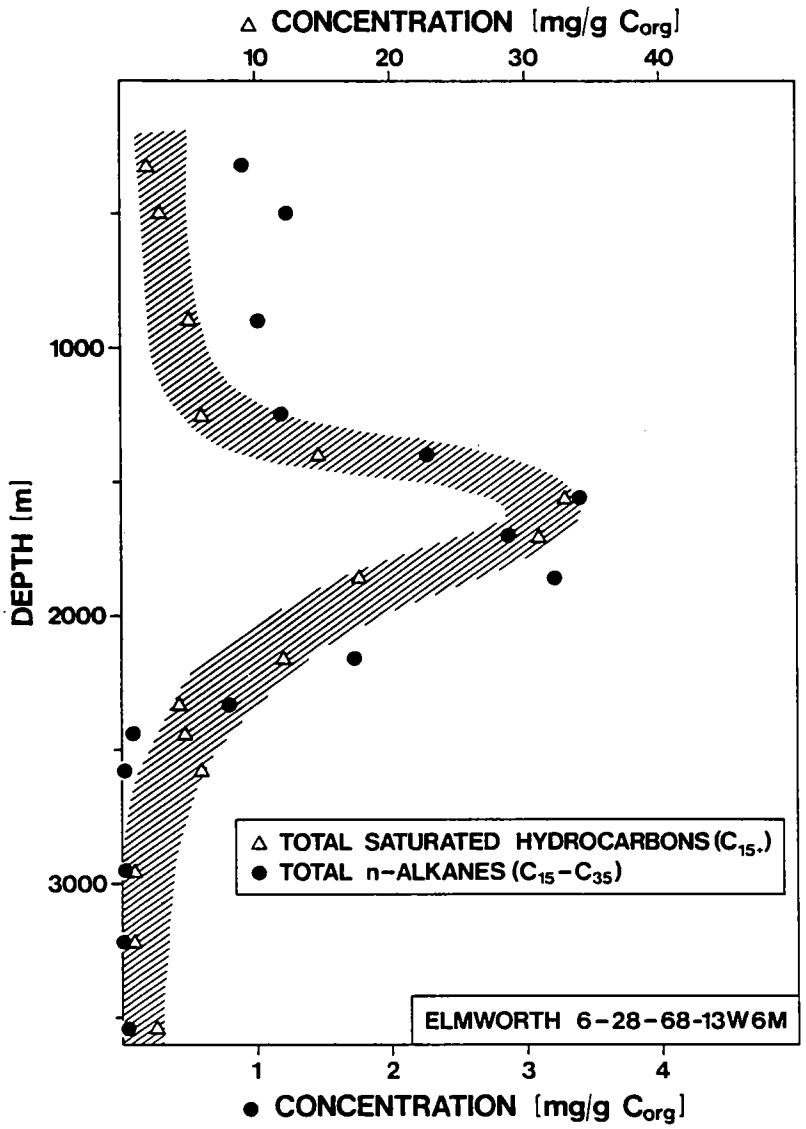

Figure 7. Total saturated hydrocarbons (C_{15+}) and total n-alkane (C_{15}–C_{35}) concentrations plotted against depth for selected rock samples from well 6–28–68–13W6M, Deep basin, western Canada (Welte and others, 1984).

0, but with increasing maturity the ratio (20S)/(20R + 20S steranes) rises from 0 to 0.50–0.55 (Fig. 11). An exactly analogous isomerization occurs at the 22-carbon in the hopanes (Table 1).

Some molecules show systematic changes in chemical composition in response to increasing thermal exposure, and several of these changes are widely used to establish source-rock maturity. Steranes are four-ring naphthenes, but compounds in which one of the rings (either A or C) is aromatic can occur. With increasing maturation, there is a trend toward triaromatic steranes, in which all three six-membered rings become aromatic (Mackenzie and others, 1981). Since there are no triaromatic steranes in living organisms or recent sediments, this provides a convenient maturity indicator (Table 1). Aromatic molecules themselves show compositional trends with maturity and a pair of ratios involving relative concentrations of methylphenanthrenes have been proposed as maturity indicators (Radke and others, 1982).

When a reaction involving the biomarkers has gone to completion (i.e., reached equilibrium) it is no longer controlled by time and temperature and cannot be used as an indicator of maturity. In gen-

eral, biomarkers are not useful for establishing maturation much above an equivalent vitrinite reflectance of ~1.0% (Fig. 11). They are very useful, however, because they cover the important phases of oil generation and expulsion.

Pyrolysis

A variety of pyrolysis techniques are being used for evaluating source-rock generation status, as well as providing information about organic matter type (Barker and Wang, 1988; Horsfield, 1984; Larter, 1984). These methods offer some important advantages over the more conventional kerogen and bitumen evaluation techniques, because they are rapid and use very small samples, typically 20–100 mg. In one widely used pyrolysis procedure, small rock samples are heated in an inert gas (helium) at a steadily increasing temperature while the total evolved hydrocarbons are monitored as a function of temperature. Hydrocarbon release curves are called "pyrograms" and generally show a first peak around 200°C which is produced by hydrocarbons already present in the rock due to generation in the subsurface (Peak 1), and a second peak at higher temperature which can be assigned to the thermal breakdown products of the kerogen (Peak 2) (Fig. 12). Peak 1 is the bitumen peak and Peak 2 provides an indication of

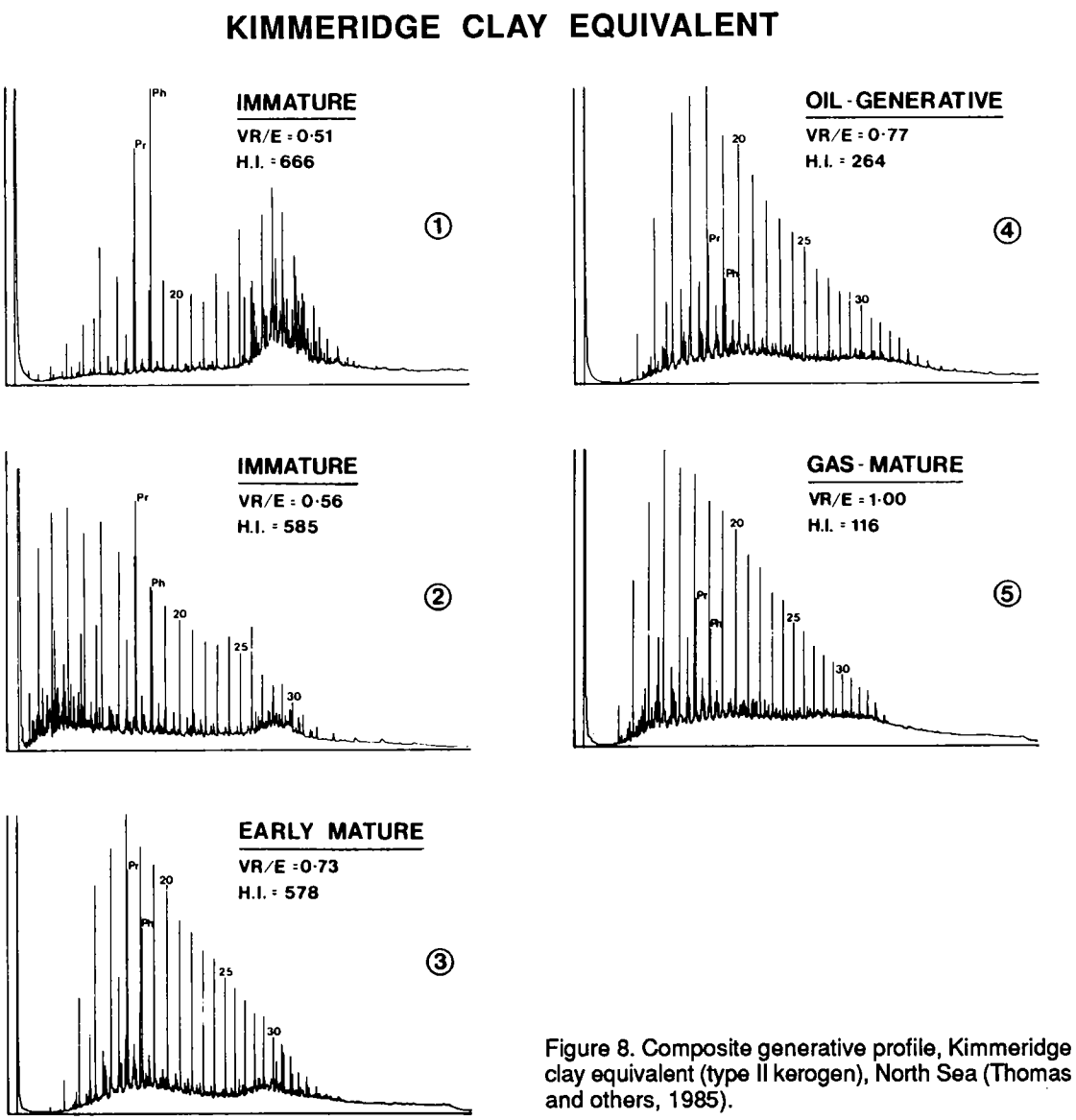

Figure 8. Composite generative profile, Kimmeridge clay equivalent (type II kerogen), North Sea (Thomas and others, 1985).

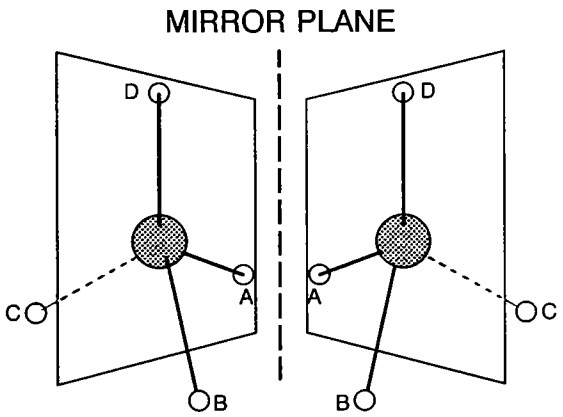

Figure 9. Asymmetric carbon atom bonded to four different groups. Two spatial configurations are possible and they are related as though the dotted line represents a mirror.

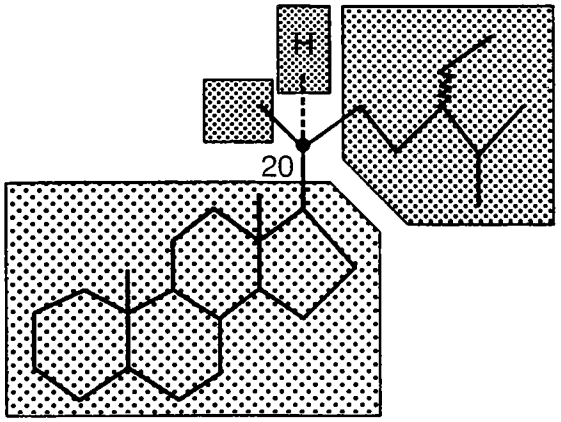

Figure 10. Generalized sterane molecule showing the asymmetric carbon atom (at C-20) with the four different groups (shaded) bonded to it that lead to an R and S configuration.

remaining generation potential (but is maturity related). As rocks are buried more deeply in the subsurface and subjected to higher temperatures, increasing amounts of hydrocarbons are generated and Peak 1 gets larger. This increase occurs at the expense of Peak 2, which not only decreases in size, but also moves to higher temperatures because the less thermally stable material is broken down first during natural maturation leaving a thermally more stable kerogen residue in the rock (Fig. 12) (Barker, 1974). Both the relative sizes of the peaks and the temperature of the maximum in the hydrocarbon release curve for Peak 2 can be used to indicate maturity (Fig. 13).

Relative peak sizes are usually given by the Generation Index (G.I.) defined by Barker (1974), although it is now generally called a Production Index (P.I.) or a Transformation Ratio (TR) (Espitalié and others, 1977).

$$\text{G.I., P.I., TR} = \frac{\text{amount generated}}{\text{total potential for generation}}$$

This ratio steadily increases with maturity (Fig. 13), and a value of 0.1 corresponds to the onset of generation and 0.4 marks the end of the oil window.

The temperature corresponding to the maximum value for Peak 2 is called "T_{max}". Values increase with maturity (Fig. 13).

Rock-Eval Pyrolysis

A commercial pyrolysis instrument called a Rock-Eval is being widely used for routine analysis of large numbers of rock samples. Like many other pyrolysis systems, the hydrocarbons released from heated samples are monitored as a function of increasing temperature, but in addition there is another type of detector (called a thermal conductivity detector) that can detect the carbon dioxide collected over a preselected temperature range. The two hydrocarbon peaks (Peak 1, Peak 2) and the carbon dioxide peak (Peak 3) are usually called S_1, S_2, and S_3, respectively (Table 2).

The temperature range chosen for carbon dioxide collection has been selected to include the main stage of carbon dioxide generation from kerogen, but to avoid thermally decomposing carbonates. The quantity of carbon dioxide then becomes a measure of the oxygen content of the kerogen and S_3/TOC has been called the "Oxygen Index." Similarly, Peak 2 is a measure of the hydrogen content of the kerogen so that S_2/TOC is a "Hydrogen Index." A plot of Oxygen Index against Hydrogen Index produces a pseudo-van Krevelen diagram (Espitalié and others, 1977). The position of a point on this diagram shows not only the maturity of the organic matter, but also organic matter type.

Final Comments

Not all of the techniques discussed for evaluating maturity are equally effective or applicable to all samples. In a comprehensive program it is advisable to have some preliminary analysis to screen samples and eliminate those with very low organic contents that have no potential as source rocks. Pyrolysis is often used in this way, because it needs small samples and is quick and cheap. Contents of total organic carbon can also be used to eliminate lean samples.

It is good practice to combine at least one kerogen-based method with at least one bitumen-based method (Table 3) in evaluating maturity.

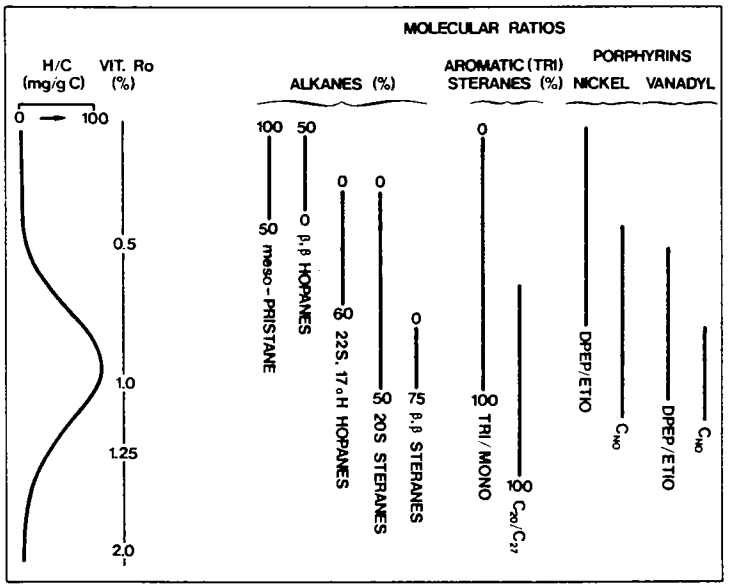

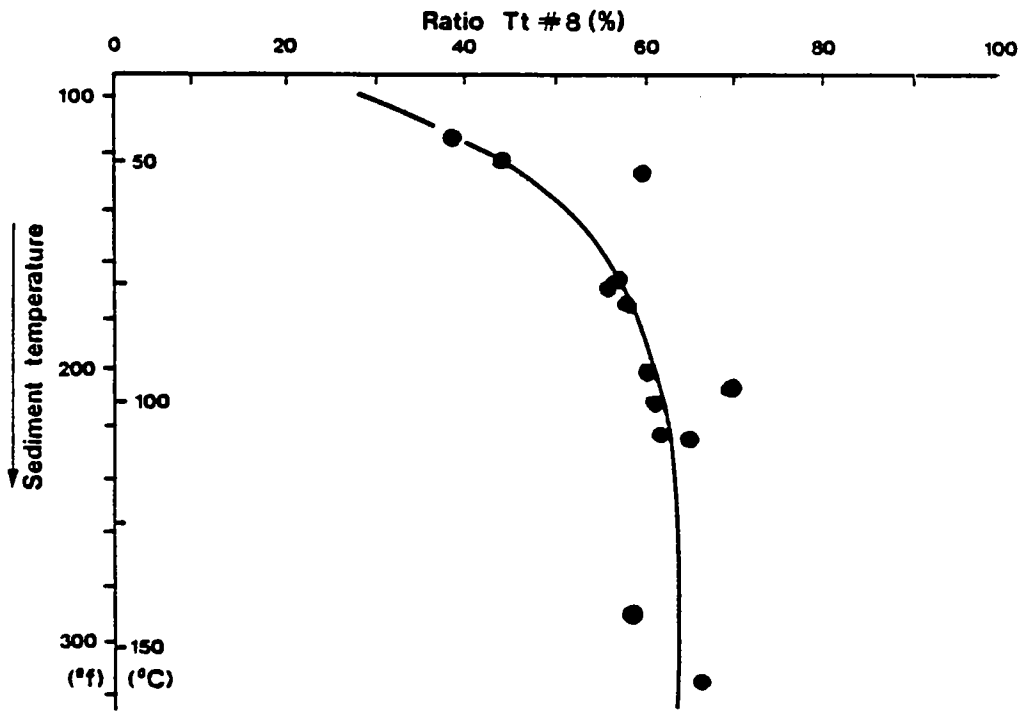

Figure 11. *Top:* Ranges of individual molecular measurements of thermal maturation, including those for steroids, plotted against the downhole hydrocarbon generation curves and vitrinite reflectance values. This was compiled from results for the Toarcian shales of the Paris basin and for the Pliensbachian shales of N.W. Germany (Mackenzie, 1984). *Bottom:* Variation in the 22R/(22R + 22S) ratio (Ratio Tt#8) of the C_{31} hopane, with source-rock maturity showing that an equilibrium of 60% is attained within the immature zone (modified from Cornford and others, 1983).

TABLE 1. — SOME REACTIONS OF BIOMARKERS USED IN DETERMINING THERMAL MATURITY (Mackenzie, 1984)

Reaction	Ratio (2)	Starting Value of (2)	End Value of (2)
Configurational isomerization	$\frac{RR + SS}{\text{total pristane}}$	0	0.5
	$\frac{22R}{(22R + 22S) - 17\alpha(H)\text{-hopanes}}$	0	0.6
	$\frac{24R}{(24R + 24S)\text{-steranes}}$	variable	0.5
	$\frac{20S}{(20R + 20S)\text{-steranes}}$	0	0.5–0.55
	$\frac{17\alpha(H),21\beta(H)\text{-hopanes}}{\text{total hopanes}}$	variable	0.9
	$\frac{5\alpha(H),14\beta(H),17\beta(H)\text{-steranes}}{\text{total steranes}}$	variable	0.8
Aromatization	$\frac{\text{triaromatic steroid hc.}}{\text{mono + triaromatic steroid hc.}}$	0	1.0
Apparent C–C bond cleavage	(e.g.) $\frac{C_{20}\text{ triaromatic steroid hc.}}{C_{20} + C_{28}\text{ triaromatic steroid hc.}}$	variable	1.0
	$\frac{\text{Aetio}}{\text{DPEP + Aetioporphyrins}}$	variable	1.0

NATURE AND AMOUNT OF PETROLEUM PRODUCTS

Introduction

In many areas, particularly those that are hostile or remote from consumers, the economics of transportation make oil much more desirable than gas. The ability to use source-rock character to predict the nature of the hydrocarbons generated is important in exploration. At intermediate depths, the type of organic matter exercises primary control over whether oil or gas is the main petroleum product, but any type of organic matter will generate gas if buried deeply enough. It follows that recognizing organic matter type is a prerequisite for predicting the nature of the petroleum products. A range of techniques is available for characterizing organic matter type, and clear distinctions can usually be made at intermediate maturity levels. Unfortunately, at high maturity all types of organic materials begin to appear similar—they all become black in transmitted light, tracks on a van Krevelen diagram converge, etc. While this may show that the rock is currently gas generating or overmature, it does not help in deciding whether it followed a gas-prone or oil-prone track as it was buried. There is no easy solution to this dilemma.

Microscopic Characterization

Microscopic examination of kerogen concentrates often provides considerable information about the types of organic materials present. However, it can be difficult to get estimates of weight percentages of the various components. Several classification schemes have been developed and a variety of terms introduced, some with overlapping meanings (Fig. 14). Frequently, much of the organic material seen under the microscope lacks any recognizable structure even at high magnifications. This "amorphous kerogen" is frequently algal-derived, and although recognizable remnants of algae are commonly observed it is very unwise to assume that this is the case in the absence of any supporting data. All types of organic matter can be physically degraded and retain no identifiable structure.

The term "herbaceous" has been used to cover

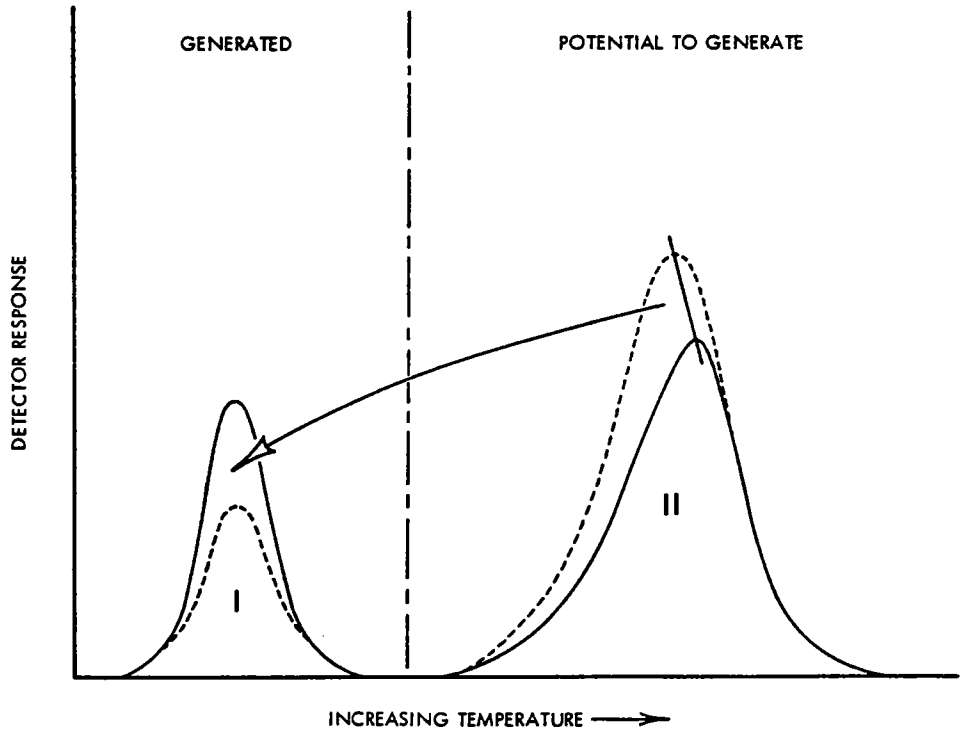

Figure 12. Schematic representation of the way in which the low-temperature pyrolysis peak (Peak 1) increases with depth at the expense of the high-temperature peak (Peak 2). Dashed line, response for shallow sample; solid line, response for deep sample.

a broad range of organic materials including spores, pollen grains, cuticles, leaf epidermis, cellular structures of plants, and other recognizable discrete cell material. Woody kerogen is derived from the structural support of higher land plants and often has a compact, angular morphology. Angular to subangular fragments of naturally charred plant material (fossil charcoal or "fusain") and recycled material are usually called "coaly."

Woody and herbaceous materials are terrestrially derived and are mainly associated with clastic rocks. Carbonates are usually dominated by amorphous and/or algal kerogens.

Organic matter type becomes increasingly difficult to characterize as the size of the particles diminishes (especially below 1 μ), and as the organic material becomes increasingly mature and darker.

Elemental Analysis

Carbon, hydrogen, and oxygen elemental data are conveniently displayed on van Krevelen diagrams (Fig. 6). These show not only the type of organic matter but also the stage of petroleum generation. As organic matter moves down the type I or type II tracks, it generates first oil, then gas. The gas is formed at decreasing rates until eventually the material is metamorphosed. Type III kerogen, in contrast, generates little, if any, oil before it forms gas. While the microscopic examination of kerogen provides information on single particles, chemical methods, such as the van Krevelen diagrams, present weighted averages of all the types of organic materials in the sample.

Pyrolysis Techniques

The information provided by pyrolysis can be interpreted in terms of organic matter type. Different types of organic matter have different thermal convertibilities (see below) and, since pyrolysis is causing the thermal breakdown of the kerogen, the quantity of hydrocarbon products will depend on organic matter type. Specifically, oil-prone kerogens generate roughly two and a half times as much hydrocarbon products as do gas-prone kerogens, so that the ratio of pyrolitic hydrocarbons to total organic carbon is a measure of organic matter type at a given maturity level.

The hydrocarbons in Peaks 1 and 2 can be analyzed by suitable trapping procedures coupled with gas chromatography (Dembicki and others, 1983). The composition of the hydrocarbons, particularly the character of the gas chromatograms

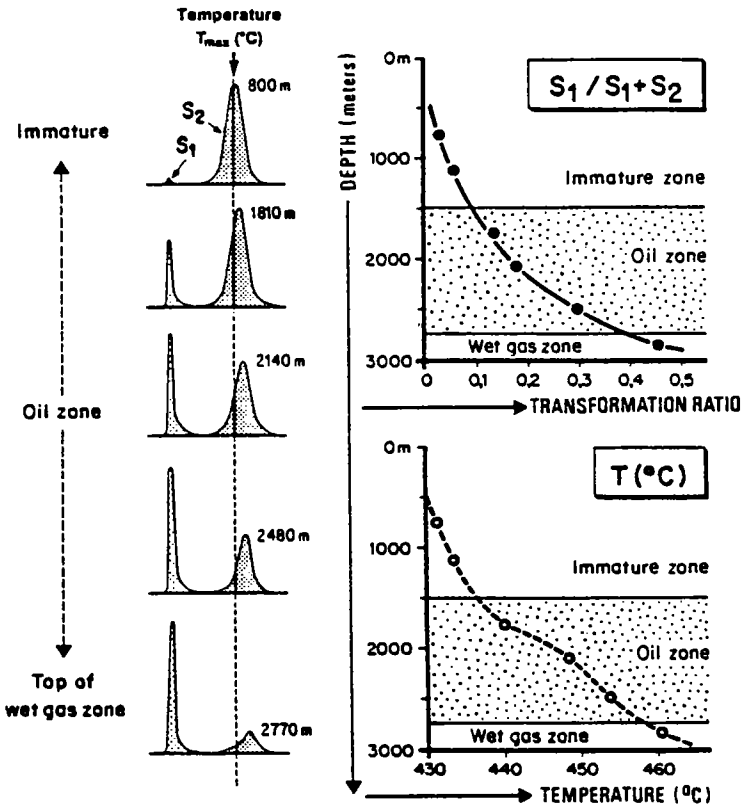

Figure 13. Characterization of source-rock maturity by pyrolysis methods. Transformation ratio and/or peak temperature T_{max} may be used as indicators of thermal evolution (from Espitalié and others, 1977).

and the relative abundances of short and long chains, can be useful indications of the oil- or gas-generating ability of the rock.

Convertibilities

The quantity of petroleum generated from a given weight of organic matter varies with organic matter type. Oil-prone kerogens generally produce two and a half times as much gas (if deeply buried) as gas-prone (type III) kerogens (Tissot and Welte, 1984). Type I oil-prone kerogen is somewhat more prolific than type II oil-prone kerogen.

Lean rocks (<0.5 wt% organic carbon) that contain oil-prone kerogen may never generate enough bitumen to migrate as oil. However, with increasing burial, this bitumen may crack to gas, and this gas may subsequently migrate. In this case, the organic matter type does not have the major role in controlling the nature of the hydrocarbon products.

CARBONATES AS SOURCE ROCKS

Oil and gas are generated from the organic matter in rocks. Some carbonates can have sufficient organic material of the right type to generate petroleum (Palacas, 1984a,b). Since clays appear to have no role as catalysts, and are not needed to provide water for migration, shales have no intrinsic advantages over carbonates as source rocks (Jones, 1984). As in clastic systems, anoxic conditions favor preservation of oil-prone organic matter, and generally it is the finer-grained, laminated carbonate muds laid down in anoxic environments that become source rocks. The organic matter in carbonates tends to be oil-prone, and gas-prone facies are rare. Indications of clastic input, such as long-chain alkanes, are rare, and carbonates do not source waxy crudes. Sulfur content is generally above average for carbonate-sourced crudes, presumably because the iron-poor system does not lead to the formation of pyrite.

COALS AS SOURCE ROCKS

Coals provide an extreme example of organic-rich rocks. The organic matter is terrestrial and is often dominated by wood, so that the kerogen is type III and gas-prone. The role of coals in generating the gas in the southern North Sea, San Juan basin of New Mexico, and other areas is well docu-

TABLE 2. — GEOCHEMICAL PARAMETERS USED TO ESTABLISH SOURCE ROCK MATURITY, GENERATING POTENTIAL, AND TYPE OF HYDROCARBON PRODUCT

Level of Maturation

Maturation	PI [S1/(S1 + S2)]	T_{max} (°C)	R_o (%)
Top oil window (birthline)	~0.1	~435-445*	~0.6
Bottom oil window (deadline)	~0.4	~470	~1.4

*Many maturation parameters (particularly T_{max}) depend on type of OM.

Source Rock Generative Potential

Quantity	TOC (wt. %)	S1*	S2*
Poor	0-5	0-0.5	0-2.5
Fair	0.5-1	0.5-1	2.5-5
Good	1-2	1-2	5-10
Very good	2+	2+	10+

*Nomenclature:
S1 = mg HC/g rock
S2 = mg HC/g rock

Type of Hydrocarbon Generated

Type	HI (mg HC/g C_{org})*	S2/S3*
Gas	0-150	0-3
Gas and oil	150-300	3-5
Oil	300+	5+

*Assumes a level of thermal maturation equivalent to R_o = 0.6%.

NOTE: Values are from Peters (1986), but there are variations among values quoted by other authors.

TABLE 3. — SUMMARY OF SOME OF THE MORE IMPORTANT TECHNIQUES AVAILABLE FOR ESTABLISHING SOURCE-ROCK MATURITY

SOURCE ROCK EVALUATION

KEROGEN	Chemical	%C, O/C vs H/C, IR
	Physical	TAI, R_o
BITUMEN	Amount	ppm
	Composition	CPI, % normals, biomarkers
PYROLYSIS	O.M. type	response/TOM, GC
	O.M. maturity	$S_1/(S_1+S_2)$, Tmax

mented (Lutz and others, 1975; Meissner, 1984).

The role of coals as possible source rocks for oil is still being debated (Thomas, 1982; Durand and Paratte, 1983; Thompson and others, 1985). Part of the uncertainty comes from the fact that coals have a very wide compositional range; furthermore, most of the detailed studies have been made for northern hemisphere Paleozoic coals. Recent studies have shown that some coals (mainly those of Tertiary age) appear to have the potential to generate oils, and these are the paraffinic, high pour point, low sulfur crudes. Coal source rocks have been proposed for the prolific fields of the Gippsland basin, Australia, and for some fields in the South China Sea and the Mahakam Delta, but the role of massive bedded coals relative to disseminated coaly material has not been fully resolved.

SOURCE-ROCK MODELING

The traditional methods for source-rock evaluation have two major limitations: (1) they require sample material so that wells must have been drilled, and (2) they provide information only about the present-day generation status. If a rock is currently thermally overmature, there is no information about when it entered the oil window and started generating. Recently theoretical models have been developed that permit a quantitative combination of time and temperature throughout the burial history of the rock, and this makes it possible to calculate generation status through time. The simplest method, usually associated with the name of Lopatin, assumes that reaction rate doubles for every 10°C rise in temperature and then considers time-temperature combinations for each 10°C increment through the rock's burial history (Waples, 1980). The cumulative time-temperature increments (TTI) are calibrated in terms of maturity data from well-understood basins. A more rigorous alternative uses the kinetic equations and pertinent kinetic parameters (activation energy [E], and frequency factor [A]) to calculate generation status through time. This approach was introduced by Tissot and Espitalié (1975).

The most important application of thermal models has been in establishing the timing of oil generation. This is especially important relative to the timing of trap formation, since the development of traps must precede oil generation and migration. An interesting example of the use of thermal models is provided by Jackson and others (1984) for the Amadeus basin of central Australia.

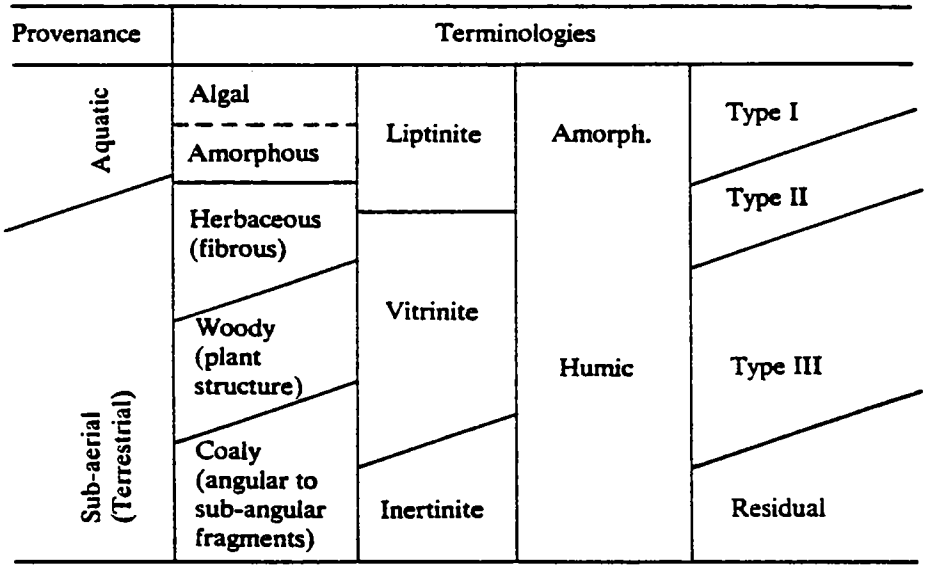

Figure 14. Approximate equivalents of various terms used in describing kerogen (after Cornford and others, 1983).

The major fields are Palm Valley, which is a gas field, and Mereenie, which is an oil field. At the location of Palm Valley thermal modeling shows that the Precambrian and Ordovician source rocks were either overmature or into gas generation before the trap formed, while at Mereenie the Ordovician was still generating oil after the time of trap formation.

EXPLORATION SIGNIFICANCE OF SOURCE-ROCK STUDIES

Establishing the probable distribution of mature source rocks in a new exploration area can have a major impact on wildcat success. This is well illustrated by exploration in the North Sea (Demaison, 1984). The central and northern areas are blanketed by the organic-rich Kimmeridge shale, but the mature areas are generally in the central parts of the grabens. Here drilling success has been 1 to 3 which is very much better than the 1 in 30 achieved outside the mature fairway. It should be noted, however, that in a rift setting such as the North Sea faulting breaks up long-distance continuity of carrier beds, and petroleum accumulations tend to be on local high blocks with little lateral migration. In contrast, in structurally simple areas, such as many intracratonic basins, there is long-distance continuity of carrier beds so that long-distance migration is possible and oil accumulations may be >100 mi from mature source rocks. Source rock studies and thermal modeling are often less useful in these settings.

REFERENCES

Ayers, M. G.; Bilal, M.; Jones, R. W.; Slentz, L. W.; Tartir, M.; and Wilson, A. O., 1982, Hydrocarbon habitat in main producing areas, Saudi Arabia: American Association of Petroleum Geologists Bulletin, v. 66, p. 1–9.

Barker, C., 1974, Pyrolysis techniques for source rock evaluation: American Association of Petroleum Geologists Bulletin, v. 58, p. 2349–2361.

_____1979, Organic geochemistry in petroleum exploration: American Association of Petroleum Geologists Continuing Education Course Note Series, no. 10, 159 p.

Barker, C.; and Wang, L., 1988, Applications of pyrolysis in petroleum geochemistry: a bibliography: Journal of Analytical and Applied Pyrolysis, v. 13, p. 9–61.

Bray, E. D.; and Evans, E. D., 1961, Distribution of n-paraffins as a clue to recognition of source beds: Geochimica et Cosmochimica Acta, v. 22, p. 2–15.

Buiskool Toxopeus, J. M. A., 1983, Selection criteria for the use of vitrinite reflectance as a maturity tool, *in* Brooke, J. (ed.), Petroleum geochemistry and exploration of Europe: Blackwell Scientific Publications, Oxford, p. 295–307.

Cornford, C.; Morrow, J. A.; Turrington, A.; Miles, J. A.; and Brooks, J., 1983, Some geological controls on oil composition in the U.K. North Sea, *in* Brooks, J. (ed.), Petroleum geochemistry and exploration of Europe: Blackwell Scientific Publications, Oxford, p. 175–194.

Demaison, G., 1984, The generative basin concept: American Association of Petroleum Geologists Memoir 35, p. 1–14.

Dembicki, H., Jr.; Horsfield, B.; and Ho, T. T. Y., 1983,

Source-rock evaluation by pyrolysis gas chromatography: American Association of Petroleum Geologists Bulletin, v. 67, p. 1094–1103.

Doligez, B. (ed.), 1987, Migration of hydrocarbons in sedimentary basins: Editions Technip, Paris, 681 p.

Dow, W. G., 1977, Kerogen studies and geological interpretations: Journal of Geochemical Exploration, v. 7, p. 79–99.

Dow, W. G.; and O'Connor, D. I., 1982, Kerogen maturity and type by reflected light microscopy applied to petroleum exploration, *in* Staplin, F. L.; and others (eds.), How to assess maturation and paleotemperatures: Society of Economic Paleontologists and Mineralogists Short Course No. 7, p. 133–157.

Durand, B.; and Monin, J. C., 1980, Elemental analysis of kerogen (C, H, O, N, S, Fe), *in* Durand, B. (ed.), Kerogen: Editions Technip, Paris, p. 113–142.

Durand, B.; and Paratte, M., 1983, Oil potential of coals, *in* Brooks, J. (ed.), Petroleum geochemistry and exploration of Europe: Blackwell Scientific Publications, Oxford, p. 285–292.

Espitalié, J.; Laporte, J. L.; Madec, M.; Marquis, F.; Leplat, P.; Paulet, J.; and Boutefeu, A., 1977, Méthode rapide de charactérisation des roches mères, de leur potentiel pétrolier et de leur degré d'évolution: Revue de L'Institut Francais du Pétrole, v. 32, p. 23–42.

Héroux, Y.; Chagnon, A.; and Bertrand, R., 1979, Compilation and correlation of major thermal maturation indicators: American Association of Petroleum Geologists Bulletin, v. 63, p. 2128–2144.

Horsfield, B., 1984, Pyrolysis studies and petroleum exploration, *in* Brooks, J.; and Welte, D. (eds.), Advances in petroleum geochemistry, vol. 1: Academic Press, New York, p. 247–298.

Hunt, J. M., 1979, Petroleum geochemistry and geology: W. H. Freeman, San Francisco, 617 p.

Jackson, K. S.; McKirdy, D. M.; and Deckelman, J. A., 1984, Hydrocarbon generation in the Amadeus basin, central Australia: Australian Petroleum Exploration Association Journal, v. 24, p. 42–65.

Jones, R. W., 1984, Comparison of carbonate and shale source rocks: American Association of Petroleum Geologists, Studies in Geology No. 18, p. 163–180.

Katz, B. J.; Pheifer, R. N.; and Schunk, D. J., 1988, Interpretation of discontinuous vitrinite reflectance profiles: American Association of Petroleum Geologists Bulletin, v. 72, p. 926–931.

LaPlante, R. E., 1974, Hydrocarbon generation in Gulf Coast Tertiary sediments: American Association of Petroleum Geologists Bulletin, v. 58, p. 1281–1289.

Larter, S. R., 1984, Application of analytical pyrolysis techniques to kerogen characterization and fossil fuel exploration exploitation, *in* Vorhees, K. J. (ed.), Analytical pyrolysis techniques and explorations: Butterworth, London, p. 212–275.

Lewan, M. D., 1987, Petrographic study of primary petroleum migration in the Woodford Shale and related rock units, *in* Doligez, B. (ed.), Migration of hydrocarbons in sedimentary basins: Editions Technip, Paris, p. 113–130.

Lutz, M.; Kaasschieter, J. P. H.; and van Wijhe, D. H., 1975, Geological factors controlling Rotliegend gas accumulations in the mid-European basin: Proceedings of the Ninth World Petroleum Congress, v. 2, p. 93–103.

Mackenzie, A. S., 1984, Applications of biological markers in petroleum geochemistry, *in* Brooks, J.; and Welte, D. (eds.), Advances in petroleum geochemistry, vol. 1: Academic Press, New York, p. 115–214.

Mackenzie, A. S.; Hoffmann, C. F.; and Maxwell, J. R., 1981, Molecular parameters of maturation in the Toarcian shales, Paris basin, France. III.—Changes in aromatic steroid hydrocarbons: Geochimica et Cosmochimica Acta, v. 45, p. 1345–1355.

Meissner, F. F., 1984, Cretaceous and lower Tertiary coals as sources for gas accumulations in the Rocky Mountain area, *in* Woodward, J.; Meissner, F. F.; and Clayton, J. L. (eds.), Hydrocarbon source rocks of the greater Rocky Mountain region: Rocky Mountain Association of Geologists, Denver, p. 401–431.

Meyer, B. L.; and Nederlof, M. H., 1984, Identification of source rocks on wireline logs by density/resistivity and sonic transit time/resistivity crossplots: American Association of Petroleum Geologists Bulletin, v. 68, p. 121–129.

Momper, J. A., 1978, Oil migration limitations suggested by geological and geochemical considerations, *in* Physical and chemical controls on petroleum migration: American Association of Petroleum Geologists Continuing Education Course Note Series, no. 8, p. B1–B60.

Palacas, J. G., 1984a, Carbonate rocks as sources of petroleum: geological and chemical characteristics and oil-source correlations: Proceedings of the 11th World Petroleum Congress, v. 2, p. 31–43.

_____(ed.), 1984b, Petroleum geochemistry and source rock potential of carbonate rocks: American Association of Petroleum Geologists Studies in Geology, no. 18, 208 p.

Peters, K. E., 1986, Guidelines for evaluating petroleum source rock using programmed pyrolysis: American Association of Petroleum Geologists Bulletin, v. 70, p. 318–329.

Philp, R. P., 1985, Fossil fuel biomarkers: applications and spectra: Methods in geochemistry and geophysics, No. 23: Elsevier, Amsterdam, 294 p.

Radke, M.; Welte, D. H.; and Willsch, H., 1982, Geochemical study on a well in the western Canada basin: relation of the aromatic distribution pattern to maturity of organic matter: Geochimica et Cosmochimica Acta, v. 46, p. 1–10.

Ronov, A. B., 1958, Organic carbon in sedimentary rocks (in relation to the presence of petroleum) [translated from Russian]: Geochemistry , v. 5, p. 510–536.

Schmoker, J. W., 1979, Determinations of organic content of Appalachian Devonian shales from formation-density logs: American Association of Petroleum Geologists Bulletin, v. 63, p. 1504–1537.

_____1981, Determination of organic-matter content of Appalachian Devonian shales from gamma-ray logs: American Association of Petroleum Geologists Bulletin, v. 65, p. 1285–1298.

Swift, J. H.; and Williams, J. A., 1980, Petroleum source rocks, Grand Banks area: Canadian Society of

Petrology Geological Memoir 6, p. 567–587.
Thomas, B. M., 1982, Land-plant source rocks for oil and their significance in Australian basins: Australian Petroleum Exploration Association Journal, v. 22, p. 164–178.
Thomas, B. M.; Moller-Pedersen, P.; Whitaker, M. F.; and Shaw, N. D., 1985, Organic facies and hydrocarbon distributions in the Norwegian North Sea, *in* Thomas, B. M.; and others (eds.), Petroleum geochemistry in exploration of the Norwegian Shelf: Graham and Trotman, London, p. 3–26.
Thompson, S.; Cooper, B. S.; Morley, R. J.; and Barnard, P. C., 1985, Oil-generating coals, *in* Thomas, B. M.; and others (eds.), Exploration of the Norwegian Shelf: Graham and Trotman, London, p. 59–73.
Tissot, B.; and Espitalié, J., 1975, L'évolution thermique de la matière organique des sédiments: application d'une simulation mathématique: Revue de L' Institut Francais du Pétrole, v. 30, p. 743–777.
Tissot, B. P.; and Welte, D. H., 1984, Petroleum formation and occurrence [second edition]: Springer-Verlag, New York, 699 p.
Tissot, B.; Durand, B.; Espitalié, J.; and Combaz, A., 1974, Influence of nature and diagenesis of organic matter in formation of petroleum: American Association of Petroleum Geologists Bulletin, v. 58, p. 499–506.
Vincelette, R. R.; and Chittum, W. E., 1981, Exploration for oil accumulations in Entrada Sandstone, San Juan basin, New Mexico: American Association of Petroleum Geologists Bulletin, v. 65, p. 2546–2570.
Waples, D. S., 1980, Time and temperature in petroleum formation: application of Lopatin's method to petroleum exploration: American Association of Petroleum Geologists Bulletin, v. 64, p. 916–926.
Welte, D. H.; Schaefer, R. G.; Stoessinger, W.; and Radke, M., 1984, Gas generation and migration in the Deep basin of western Canada: American Association of Petroleum Geologists Memoir 38, p. 35–47.

Geologic Framework and Hydrocarbon Source Rocks of Oklahoma

Kenneth S. Johnson and Brian J. Cardott
Oklahoma Geological Survey

ABSTRACT.—Sedimentary rocks in Oklahoma are mostly marine in origin, ranging from 20,000–40,000 ft thick in the major basins to 0–10,000 ft thick over some of the uplifts. Upper Cambrian through Mississippian strata are a thick sequence of marine carbonates, interbedded with several widespread but relatively thin shales and sandstones. The carbonates typically were deposited in warm, aerated, and shallow waters, whereas some of the shales (particularly the Upper Devonian–Lower Mississippian Woodford Shale) were deposited in anaerobic marine environments favorable for preservation of organic matter. Other Cambrian through Mississippian shales or shaley units with some prospect for being source rocks are Middle–Upper Ordovician Simpson Group shales, the Upper Ordovician Sylvan Shale, and some Upper Mississippian shales.

Pennsylvanian strata in Oklahoma are sequences of marine and nonmarine shale, sandstone, conglomerate, and limestone that thicken markedly into rapidly subsiding basins. Anaerobic and/or phosphate-rich environments existed in local and basin-sized areas during the Pennsylvanian Period, causing deposition of known and potential source rocks. In Permian and post-Permian times, environments in Oklahoma favored deposition of red beds, evaporites, and terrestrial sediments, none of which is considered favorable for development of source rocks.

Based primarily on geochemical data (e.g., total organic carbon [TOC], elemental, Rock-Eval pyrolysis), source rocks can be divided into those that generate oil (and gas) from types I and II kerogen, and those that generate only gas from type III kerogen.

Source rocks of Oklahoma identified in the literature are: Simpson Group shales (types I and II kerogen); Sylvan Shale (type II); Woodford Shale (types II and III); Springer Formation shales (Upper Mississippian–Lower Pennsylvanian, type III); Morrowan shales (Lower Pennsylvanian, type III); and Middle and Upper Pennsylvanian shales (types II and III). Source rocks of the Ouachita Mountains uplift identified in the literature are: Womble Shale (Middle–Upper Ordovician, type II); Bigfork Chert (Upper Ordovician, type II); Polk Creek Shale (Upper Ordovician); Missouri Mountain Shale (Lower Silurian); Arkansas Novaculite (Silurian–Lower Mississippian, types II and III); and Stanley Group shales (Mississippian, type III).

By far, the most important known petroleum source rocks in Oklahoma are the Woodford Shale and Middle and Upper Pennsylvanian marine shales. These have TOC values generally ranging from 1 to 25%. Other known or potential source rocks mentioned above have TOC values generally <1%, although in a few samples they are >3%. Known or potential source rocks in most regions of Oklahoma have thermal maturities sufficient to have generated oil and/or natural gas.

INTRODUCTION

Oklahoma is one of the leading petroleum-producing states in the nation. In 1989 it ranked fifth in crude-oil production, third in natural-gas production, and second in number of wells drilled. Major production and reserves are in the Anadarko, Arkoma, Ardmore, and Marietta basins, and in the northern shelf areas (Fig. 1); unknown, but presumably large, reserves also remain to be discovered in the Ouachita Mountain uplift. With petroleum exploration and production being of such great importance to the State, it is critical to understand the hydrocarbon source rocks from which these oil and gas resources have been derived.

This paper provides an overview of the geologic history and structure of Oklahoma, with special emphasis on known and potential hydrocarbon source rocks, and also discusses what is known about Oklahoma's source rocks up to the time of this symposium. The paper thus helps set the stage for the other reports that are given in this symposium volume.

GEOLOGIC FRAMEWORK

The geology of Oklahoma is complex, but it is remarkably well understood as a result of the extensive amount of drilling and seismic exploration in search of oil and gas. Great thicknesses of sedimentary rock are preserved in a series of major

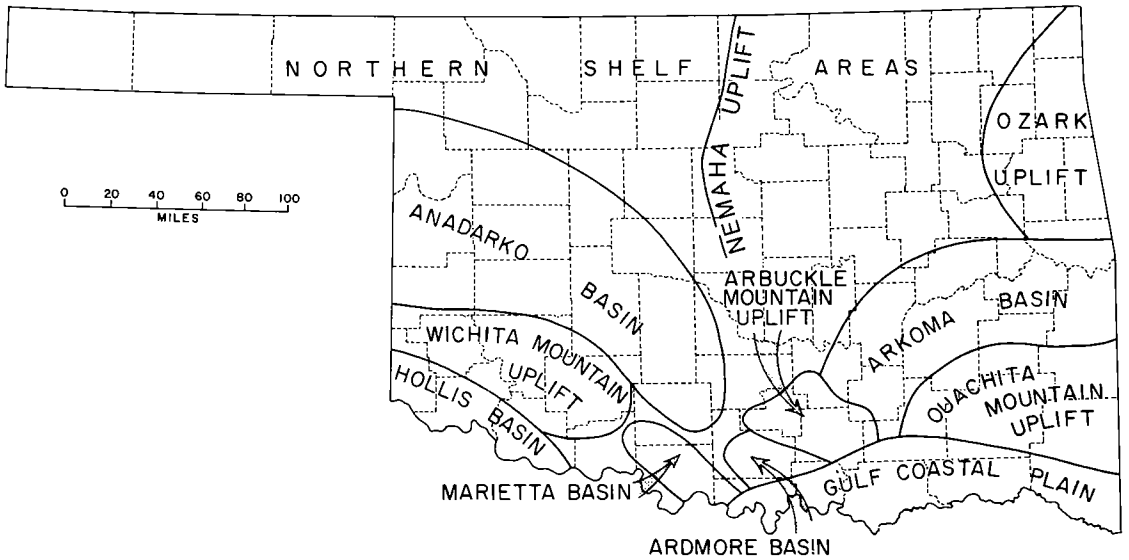

Figure 1. Map showing major geologic provinces of Oklahoma.

depositional and structural basins separated by orogenic uplifts that formed mainly during Pennsylvanian time (Fig. 1). The major sedimentary basins contain as much as 20,000–40,000 ft of sediments, most of which are Paleozoic and marine, resting upon a basement complex of igneous rocks and some low-rank metasedimentary rocks (Denison and others, 1984; Johnson and others, 1988). Basement rocks beneath most of Oklahoma are Precambrian granites and comagmatic rhyolites, but beneath the southern Oklahoma aulacogen they are Early and Middle Cambrian granites, rhyolites, gabbros, and basalts. Basement rocks beneath the Ouachita province have not been drilled and are unknown.

By early Paleozoic time, Oklahoma had three major tectonic/depositional provinces: the Oklahoma basin, the southern Oklahoma aulacogen, and the Ouachita trough (Fig. 2). The Oklahoma basin was a broad, shelf-like area that received a sequence of remarkably thick and extensive, shallow-marine carbonates interbedded with thinner marine shales and sandstones (Johnson and others, 1988). The southern Oklahoma aulacogen was the depocenter for the Oklahoma basin. It was a west–northwest-trending trough where sediments are generally similar to those elsewhere in the basin, but they are two to three times as thick. The aulacogen embraced the Anadarko, Ardmore, and Marietta protobasins, along with the Arbuckle anticline and the Wichita Mountain uplift. The Ouachita trough was the site of deep-water sedimentation along a rift at the southern margin of the North American craton. These sediments were thrust some 50 mi northward to their present position in the Ouachita Mountain uplift.

These three provinces persisted through the middle Paleozoic until Pennsylvanian time, when the Oklahoma basin and the aulacogen were divided into a series of well-defined marine basins by sharply uplifted crustal blocks. The Ouachita trough was destroyed by Pennsylvanian uplift and northward thrusting. Orogenic activity throughout the State was limited to folding, faulting, and uplift, and was not accompanied by igneous or high-grade metamorphic activity.

For purposes of this report, it is practical to discuss the sedimentary rocks and associated tectonic history of the State in four major time periods: early Paleozoic (Late Cambrian and Ordovician), middle Paleozoic (Silurian, Devonian, and Mississippian), late Paleozoic (Pennsylvanian and Permian), and post Paleozoic (Triassic through Holocene). Early and middle Paleozoic sediments tend to be quite persistent laterally, and thus the same formations are recognized in most geologic provinces outside of the Ouachitas (Fig. 3). In contrast, late Paleozoic (mainly Pennsylvanian) strata are markedly different from basin to basin, and even within the same basin. Post Paleozoic strata are laterally persistent, but their thickness and distribution are generally limited.

Early Paleozoic

Late Cambrian and Ordovician strata in the Oklahoma basin are characterized by 1,000–10,000 ft of shallow-marine carbonates (limestone and dolomite) interbedded with several quartzose sandstone and green shale units (Fig. 4). These strata commonly are referred to as the "Arbuckle facies," owing to their excellent exposure in the

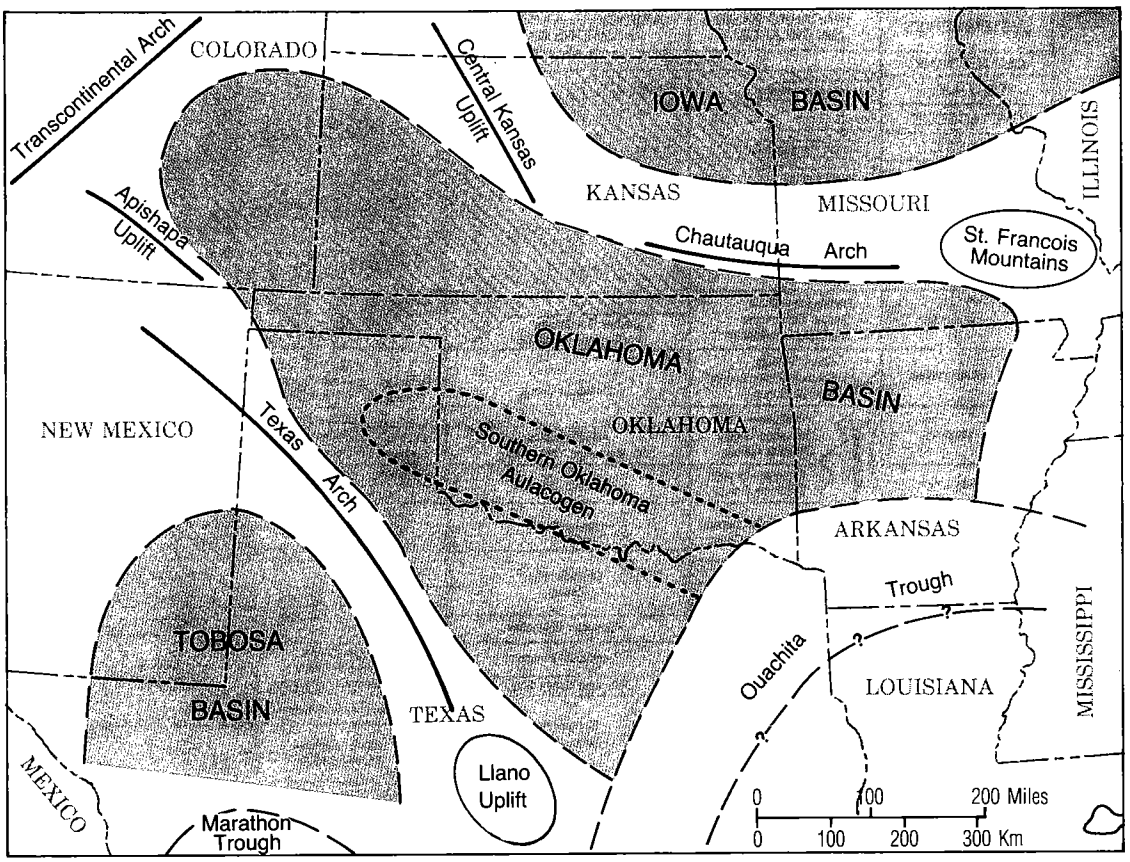

Figure 2. Map of southwestern United States, showing approximate boundary of the Oklahoma basin and other major features that existed in early and middle Paleozoic time (after Johnson and others, 1988).

Arbuckle Mountains, and they result from deposition in environments ranging mainly from the intertidal zone to water depths of several hundreds of feet. Equivalent Late Cambrian and Ordovician strata in the Ouachita trough, the so-called "Ouachita facies," consist of several thousand feet of mainly black shales, cherts, and sandstones deposited in several thousand feet of marine water. Recent reports on early Paleozoic strata include those by Ham (1959,1969), Schramm (1964,1966), McHugh (1964), Herndon (1965), Ham and Wilson (1967), Donovan (1986), Johnson and others (1988), Fay (1989), and Johnson (1991). We draw upon each of these earlier reports.

Late Cambrian seas transgressed to the north and west, covering a basement-rock surface of modest to locally rugged relief. The time-transgressive basal Reagan Sandstone was deposited throughout most of the Oklahoma basin. It is a feldspathic and glauconitic sandstone that grades upward into bioclastic limestones and sandy dolomites of the Honey Creek Limestone. Those two formations, both deposited in open, shallow-marine environments, constitute the Timbered Hills Group (Fig. 3).

The overlying Arbuckle Group is the thickest sequence of lower Paleozoic strata in Oklahoma. It is as much as 6,700 ft of limestone in the aulacogen, on the flank of the Arbuckle anticline (Fay, 1989), thinning to ~4,000 ft of dolomite in the eastern Arbuckle Mountains and about 1,000–4,000 ft of dolomite in most other shelf areas of the Oklahoma basin (Johnson and others, 1988). The transition from mainly limestone to mainly dolomite occurs near the boundary of the aulacogen (Fig. 4) and, in part, reflects differences in water depths and local restrictions in water circulation. Dolomite probably results from deposition and diagenesis of carbonates in shelf areas characterized by alternating shallow-marine and supratidal environments.

It is likely that hydrocarbon source rocks in the Arbuckle Group were deposited in the more rapidly subsiding aulacogen. Limestones here contain algal mats and algal boundstones (Donovan, 1986), bedded and disseminated anhydrite (La-

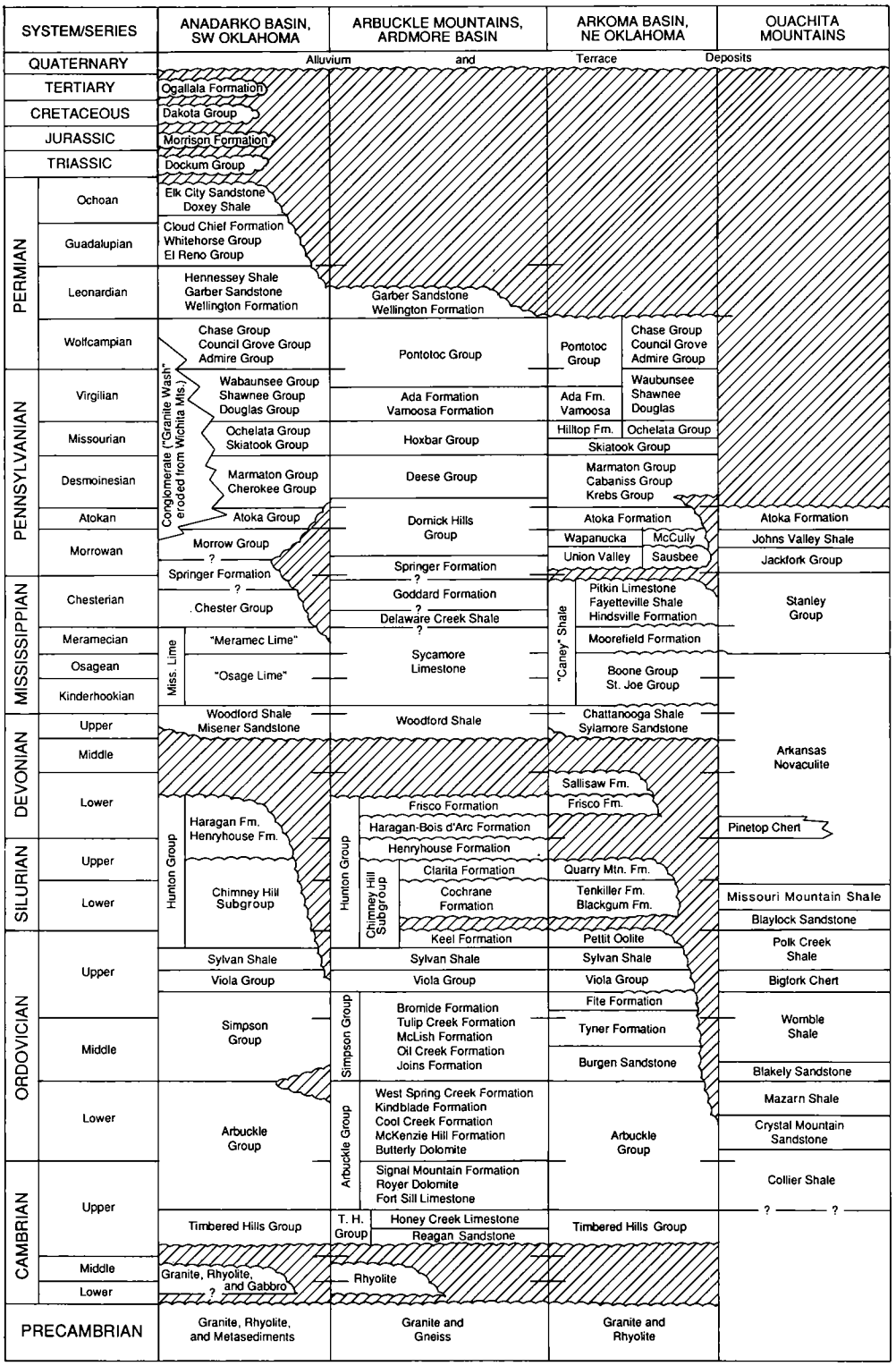

Figure 3. Generalized correlation of rock units in Oklahoma (modified from COSUNA charts by Hills and Kottlowski, 1983; Mankin, 1987). Height of boxes is not related to thickness of rock units.

tham, 1970; St. John and Eby, 1978; Ragland and Donovan, 1985; Donovan, 1986), and gray to dark-gray limestones and some shales (Fay, 1989). These lithologies, most prevalent in the Cool Creek Formation, indicate occasional lagoonal and sabkha-like environments that may have favored deposition and preservation of sufficient organic (algal) matter to locally make the Arbuckle Group a potential source rock for hydrocarbons. At the end of Ordovician time, the burial depth of the Arbuckle in the aulacogen was ~2,500 ft (top of Arbuckle) to 9,000 ft (base) (Fig. 4); at the end of Mississippian time it was ~6,000 ft (top) to 12,500 ft (base); and after Permian time it was as much as 26,000 ft (top) to >30,000 ft (base). Thus parts of the Arbuckle Group would have been buried to depths of 6,000–13,000 ft (the approximate range of the "oil window") from as early as Middle Ordovician time until as late as the Middle Pennsylvanian. Arbuckle Group source rocks may exist and may be buried (but not yet identified) in the deeper parts of the present Anadarko, Arkoma, Ardmore, and Marietta basins.

Simpson Group strata in the Oklahoma basin are cleanly washed quartzose sandstones interbedded with thick, shallow-water marine limestones and thin to moderately thick greenish-gray shales; in a gross sense, these lithologies are present in roughly equal amounts in the basin (Statler, 1965). The shales, which tend to be more abundant in the aulacogen, range mainly from shades of dark-green and gray-green to bright-green, bluish-green, and olive green. Small amounts of red shale are interbedded with green shale in east-central and northeast Oklahoma, and minor amounts of dark-gray and black shale are present in the subsurface of southeastern Oklahoma (Statler, 1965).

Simpson strata are identified as oil source rocks in the Anadarko basin (Hatch and others, 1986; Burruss and Hatch, 1989). These strata in the aulacogen were buried at depths of 6,000–13,000 ft from Late Mississippian through Middle Pennsylvanian times, whereas those outside the aulacogen were in that depth range from the Middle Pennsylvanian through the Holocene. Burruss and Hatch (1989) documented that Simpson Group shales are the source of oil and gas in the Forest City and Salina–Sedgwick basins in Kansas.

The Viola Group is a marine-limestone sequence widespread in the Oklahoma basin. It contains chert at several stratigraphic levels and commonly is highly fossiliferous. Terrigenous detritus, including some organic and graptolitic shale, is present in the lower Viola, particularly in the aulacogen; these components decrease upward and the strata grade into clean-washed skeletal limestones (Johnson and others, 1988). This vertical change indicates an upward decrease in water depth, and a corresponding increase in the energy level and aerobic activity of the depositional environment. The Viola is reported as a source rock for oil in the Pauls Valley area of the Anadarko basin (Jones and Philp, 1990).

The Sylvan Shale, a widespread green and greenish-gray shale in the Oklahoma basin, ranges from 300–400 ft thick in the aulacogen to 30–200 ft thick in most shelf areas. Locally abundant graptolites and chitinozoans, and well-developed laminations, suggest that the Sylvan was deposited in water deeper than other early Paleozoic formations (Ham, 1969). Limited data indicate that the source-rock potential for the Sylvan Shale is only poor to moderate (Burruss and Hatch, 1989).

In the Ouachita trough, early Paleozoic sediments consist mainly of black shales interbedded with sandstones, dark limestones, siliceous shales, and cherts (Fig. 4). These Ouachita-facies strata, deposited as deep-water equivalents of the Arbuckle facies, include the Collier, Crystal Mountain, Mazarn, Blakely, Womble, Bigfork, and Polk Creek Formations. Total thickness of the exposed early Paleozoic Ouachita facies is ~2,500 ft, but the base of the Collier has not been recognized. The Viersen and Cochran No. 25-1 Weyerhaeuser well, drilled in the core of the Broken Bow uplift, penetrated ~10,000 ft of complexly folded and faulted black phyllite, quartzite, and dolomitic marble without reaching basement (Goldstein, 1975). Curiale (1983) tested the Womble, Bigfork, and Polk Creek strata, and found them to be good oil-generative source rocks.

Middle Paleozoic

The Oklahoma basin persisted as the site for deposition of shallow-marine carbonates through Silurian and Early Devonian times. Subsequent Paleozoic strata in the aulacogen are mainly clastic units, and the first of these sediments (Late Devonian and Mississippian) are almost entirely dark shales. Ham (1969, p. 7–8) noted that this "sharply defined change from long-continued, shallow-marine environments to those of euxinic deeper waters marks one of the great divisions in the Paleozoic evolution of southern Oklahoma."

Middle Paleozoic strata range from about 3,000–6,000 ft thick in the aulacogen to about 1,000–3,000 ft thick in most other parts of the Oklahoma basin. The aulacogen, which subsided rapidly and accumulated a thick column of sediments during the Cambrian and Ordovician, subsided at a much slower rate during the Silurian and Devonian. Rapid subsidence was then renewed during the Mississippian, chiefly in the eastern part of the aulacogen. At the same time, as much as 10,000 ft of black shale, novaculite, and flysch sediments were dumped into the Ouachita

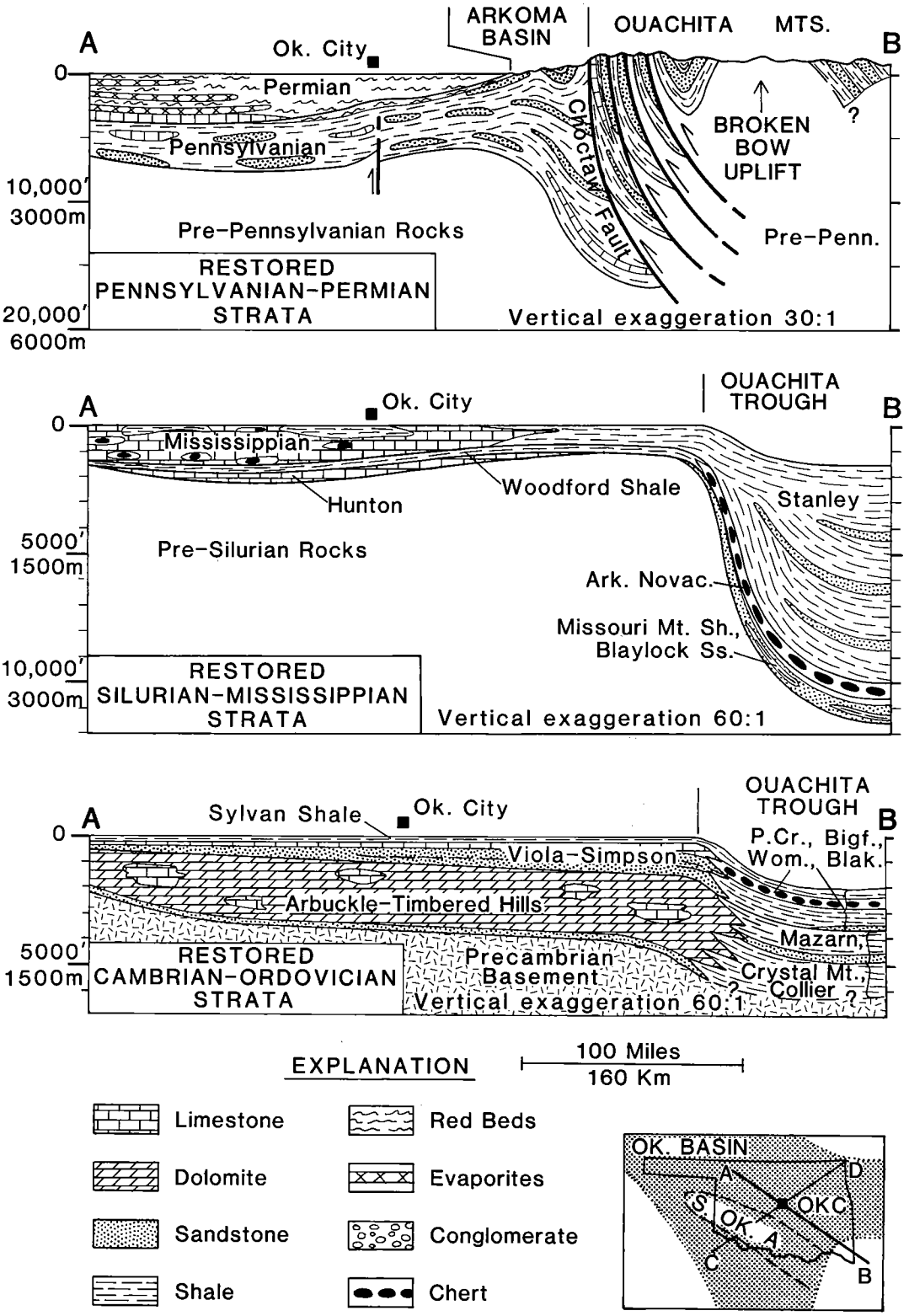

Figure 4. Schematic cross sections showing restored thickness of strata in Oklahoma at the end of early,

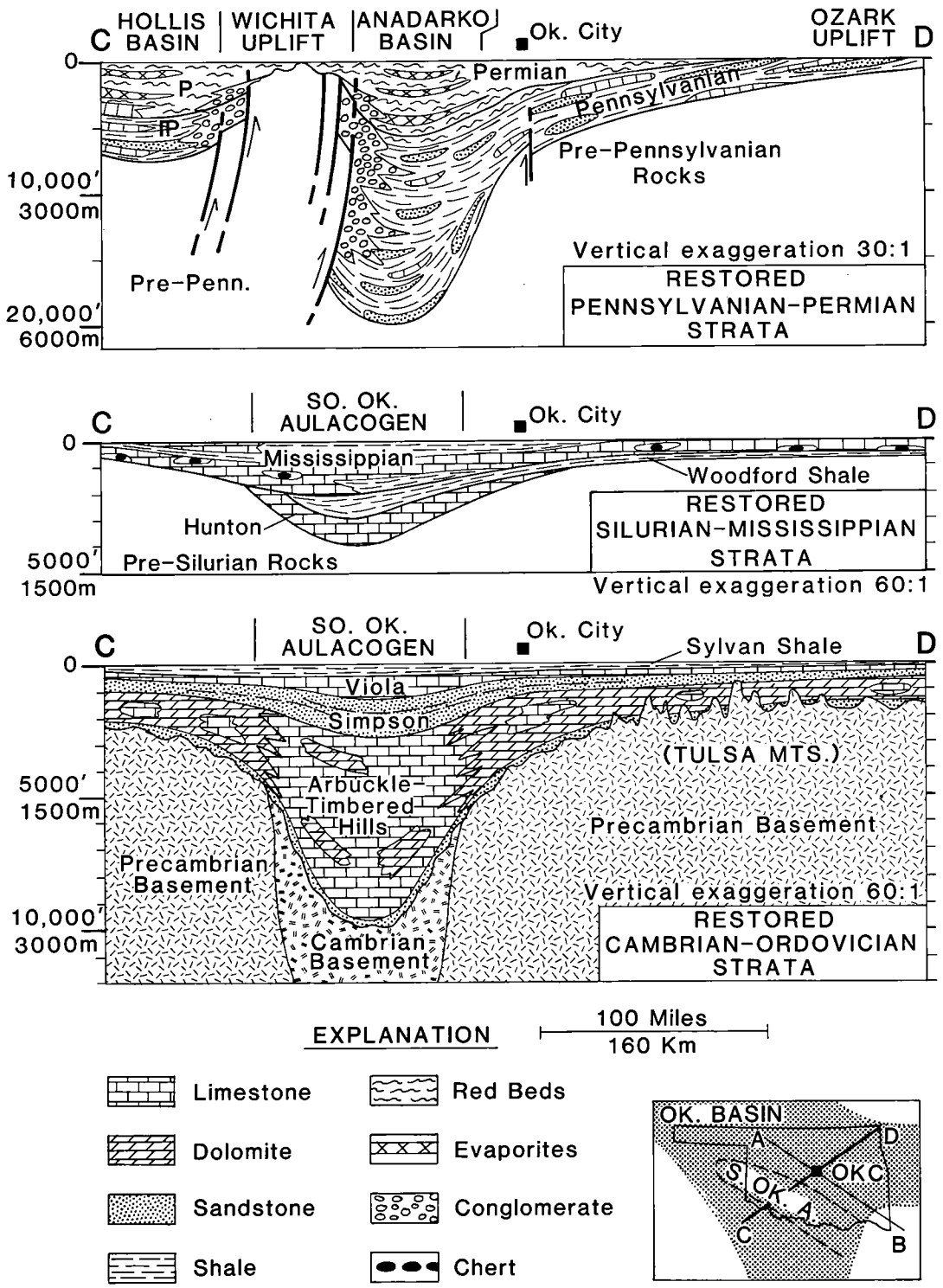

middle, and late Paleozoic times (based upon data in Johnson and others, 1988). Top cross sections (Pennsylvanian–Permian) have less vertical exaggeration than other cross sections.

trough, mainly during the Mississippian Period. Recent reports on middle Paleozoic strata include those by Ham (1959,1969), Ham and Wilson (1967), Amsden (1975,1980), Craig and others (1979), Johnson and others (1988), and Fay (1989).

The Hunton Group consists mainly of shallow-water, clean-washed skeletal limestones in the lower part (Chimneyhill Subgroup), argillaceous and silty carbonates in the middle (Henryhouse and Haragan–Bois d'Arc Formations), and clean-washed limestone at the top (Frisco Formation). Silt- and clay-sized detritus is largely restricted to the aulacogen area. Most of the Hunton carbonates are moderately to highly dolomitized in the northern shelf. The Hunton is not known to be a source rock for hydrocarbons.

Unconformably above the Hunton is the Woodford Shale, unquestionably the most prolific source rock for oil and gas in Oklahoma. The Woodford, which is equivalent to the Chattanooga Shale to the northeast, is dark-gray to black fissile shale that also contains chert and siliceous shale. Anaerobic conditions on the Woodford sea floor inhibited almost all benthic organisms, and favored the preservation of organic matter that settled to the bottom. The Woodford is present throughout most parts of the Oklahoma basin; it ranges from 200–900 ft thick in the aulacogen to 50–100 ft thick in most of the shelf areas (Amsden, 1975; Johnson and others, 1988).

Mississippian strata above the Woodford are shallow-marine limestones and shales in most parts of the Oklahoma basin, but thick, dark-gray fissile shales (Caney, Goddard, and Springer) predominate in the eastern part of the aulacogen. Cherty limestone was significant in the northern half of the State during Osagean and Meramecian time. The environment for most Mississippian strata was well-aerated, warm, shallow seas that supported an abundance of benthic life forms. Thicknesses generally range from 200 to 2,000 ft in the northern shelf areas, but the dark-shale sequence in the aulacogen typically is 2,000–5,000 ft thick. In spite of this great thickness of dark shales, there are no data to show their source-rock potential.

Sedimentation in the Ouachita trough during the middle Paleozoic produced a thick sequence of black shale, novaculite, and sandstones (Fig. 4). Silurian and Devonian strata are nearly 1,000 ft of shale and sandstone in the Blaylock and Missouri Mountain Formations, overlain by at least 600 ft of Arkansas Novaculite. The Ouachita trough then sank sharply to receive 7,000–14,000 ft of Stanley shale, which contains small to moderate amounts of sandstone, chert, and volcanic tuff. These strata reflect continued deposition in slope to deep-water (abyssal) environments. The Missouri Mountain, Arkansas Novaculite, and Stanley all have potential as hydrocarbon source rocks (Curiale, 1983), with the Stanley being especially good. Mississippian and Devonian rocks probably would generate natural gas, although the Missouri Mountain may also generate oil.

Late Paleozoic

Major changes took place in Oklahoma in Pennsylvanian time. Early and middle Paleozoic epeirogenic movements, accompanied by the deposition of relatively simple sequences of shelf carbonates (with some shales and sandstones) over vast regions of the Oklahoma basin, ended with a series of orogenic movements that subdivided the State into the tectonic provinces so easily recognized today (Figs. 1,4). First, an episode of Late Mississippian–Early Pennsylvanian epeirogenic uplift and erosion throughout most of the Oklahoma basin produced a widespread pre-Pennsylvanian unconformity, except where sedimentation apparently was continuous along the axis of the aulacogen (deep Anadarko and Ardmore basins). Then a series of orogenic pulses in the aulacogen and the Ouachita trough through Early, Middle, and Late Pennsylvanian time caused, or contributed to, the following: folding and thrusting of the Ouachita foldbelt; raising of the Wichita, Criner, Arbuckle, Nemaha, and Ozark uplifts; and pronounced downwarping of the Anadarko, Ardmore, Marietta, Arkoma, and Hollis basins (Ham and Wilson, 1967; Johnson and others, 1988). Other comprehensive reports on late Paleozoic strata include those of Tomlinson and McBee (1959), Cline (1960), McKee and others (1967,1975), Rascoe and Adler (1983), Sutherland (1988), and Elmore and others (1990).

Pennsylvanian strata in the State are sequences of marine and nonmarine shale, sandstone, conglomerate, and limestone that thicken markedly (to as much as 10,000–15,000 ft thick) into the rapidly subsiding basins (McKee and others, 1975). The thick wedges of terrigenous clastic sediments were shed from nearby uplifts; thinner carbonates were deposited in shallow-water shelf areas distal to the uplifts. Successively younger Pennsylvanian strata commonly overlap older units at the margins of the basins and across some of the uplifts. Thin coal beds are abundant in Desmoinesian strata, mainly in the Arkoma basin and on its northern shelf area (Cherokee platform). Among the clastic units deposited in the newly formed Pennsylvanian basins and their shelf areas are a number of organic-rich, dark-gray to black shales that are known or potential source rocks for hydrocarbons; these units are in the Morrowan, Desmoinesian, and Missourian Series (Burruss and Hatch, 1989).

In the Ouachita trough, deep-water flysch sedi-

mentation continued through Morrowan and Atokan time, although the depocenter shifted northward in Atokan time to the southern part of the Arkoma basin. The trough was then destroyed during the Ouachita orogeny (Desmoinesian), with northward thrusting and complex folding of Ouachita-facies rocks to form the present-day Ouachita Mountains (Fig. 4). Data presented by Guthrie and others (1986) indicate that locally the organic content of the Jackfork and Atoka make them favorable as potential source rocks.

Permian strata are limited to the western half of Oklahoma. Clastics were eroded from the Ouachitas (reduced to low mountains by this time) on the east, the ancestral Rocky Mountains on the west, and the Wichita uplift in southwestern Oklahoma. Sediments accumulated mainly in the Anadarko basin, and also in the Hollis basin and the Panhandle region. Early Permian (Wolfcampian) carbonates and shales, both gray and red beds, are overlain by a major evaporite and red-bed sequence of Leonardian, Guadalupian, and Ochoan age. Evaporites (salt and gypsum/anhydrite) thicken into the basins that continued to subside more than the adjacent uplifts and arches. Permian strata are as much as 7,000 ft thick in the Anadarko basin, 4,000 ft thick in the Hollis basin, and 1,000–3,000 ft thick in nearby shelf or platform areas.

The predominantly evaporite and red-bed sequence of the Permian does not have source-rock potential. Campbell and others (1988), however, point out that the lack of good source-rock data for Early Permian strata should not preclude them as source rocks, and also note that several of these shales are good source rocks in Kansas.

Post Paleozoic

Post Paleozoic rocks of Oklahoma include Triassic, Jurassic, Cretaceous, and Tertiary strata in the west; Cretaceous strata in the southeast; and Quaternary deposits at many places throughout the State (Johnson and others, 1988). By the time these strata were deposited, the structural geology of Oklahoma was much the same as it is today (Fig. 5). Triassic and Jurassic units are mostly thin, continental red-bed shales and sandstones deposited in mixed fluvial, lacustrine, and deltaic environments; they are largely eroded, and now are limited to 100–600 ft of strata in the Panhandle. Cretaceous units are shales, sandstones, and limestones deposited at the edge of the Gulf Coastal Plain (southeast Oklahoma) and as part of the Cretaceous seaway that covered the western interior of the country (western Oklahoma). Strata in southeast Oklahoma are up to 1,000–2,000 ft thick, whereas those in the west typically are 50–300 ft thick.

The Tertiary consists of interbedded fluvial and windblown sediments of the Ogallala Formation (Miocene–Pliocene age), deposited from low-gradient streams that flowed east and southeast from the Rocky Mountains. The Ogallala is typically 100–600 ft thick in Oklahoma, restricted to the Panhandle and the western counties of the Anadarko basin. Quaternary sediments are alluvial, eolian, and lacustrine deposits derived from rivers and streams flowing to the east and southeast across the State. Typically these deposits are 10–50 ft thick, although locally they are 100 ft thick along the major rivers.

There are no data to indicate that any of the post Paleozoic rocks in Oklahoma are potential hydrocarbon source rocks.

HYDROCARBON SOURCE ROCKS

Hydrocarbon source rocks are formed from organic-rich sediments containing kerogen (disseminated insoluble organic matter) that can be converted to oil or gas during thermal maturation (coalification). Potential hydrocarbon source rocks are characterized by quantity of organic matter, both kerogen (insoluble) and bitumen (soluble), type of kerogen, and level of thermal maturation (Tissot and Welte, 1984).

The minimum quantity of organic matter for a potential hydrocarbon source rock is generally accepted to be 0.5% TOC (total organic carbon) for shales, and 0.3% TOC for carbonates (Tissot and Welte, 1984). Some workers now place the lower limit closer to 1% TOC. Hatch and others (1989, p. 4) stated, "The minimum organic carbon content necessary to generate and expel oil from a shale source rock lies between 0.4% and 1.4%, with the minimum probably closer to the higher of these two values." Kerogen types, determined from van Krevelen-type diagrams of elemental data (carbon, hydrogen, and oxygen) and Rock-Eval pyrolysis data (Tissot and Welte, 1984), are divided into those that generate oil and gas (types I and II kerogen), and those that generate only gas (type III kerogen). The level of thermal maturation is determined by several parameters (Héroux and others, 1979), the most common of which is vitrinite reflectance.

The two most important characteristics for identifying potential hydrocarbon source rocks are the quantity of organic matter and type of kerogen. In this report, potential hydrocarbon source rocks of Oklahoma are identified from published geochemical data (TOC, van Krevelen-type diagrams of elemental data, and Rock-Eval pyrolysis data). Identified hydrocarbon source rocks in most regions of Oklahoma have thermal maturities sufficient to have generated oil and/or natural gas. Recent reports on the thermal maturation of

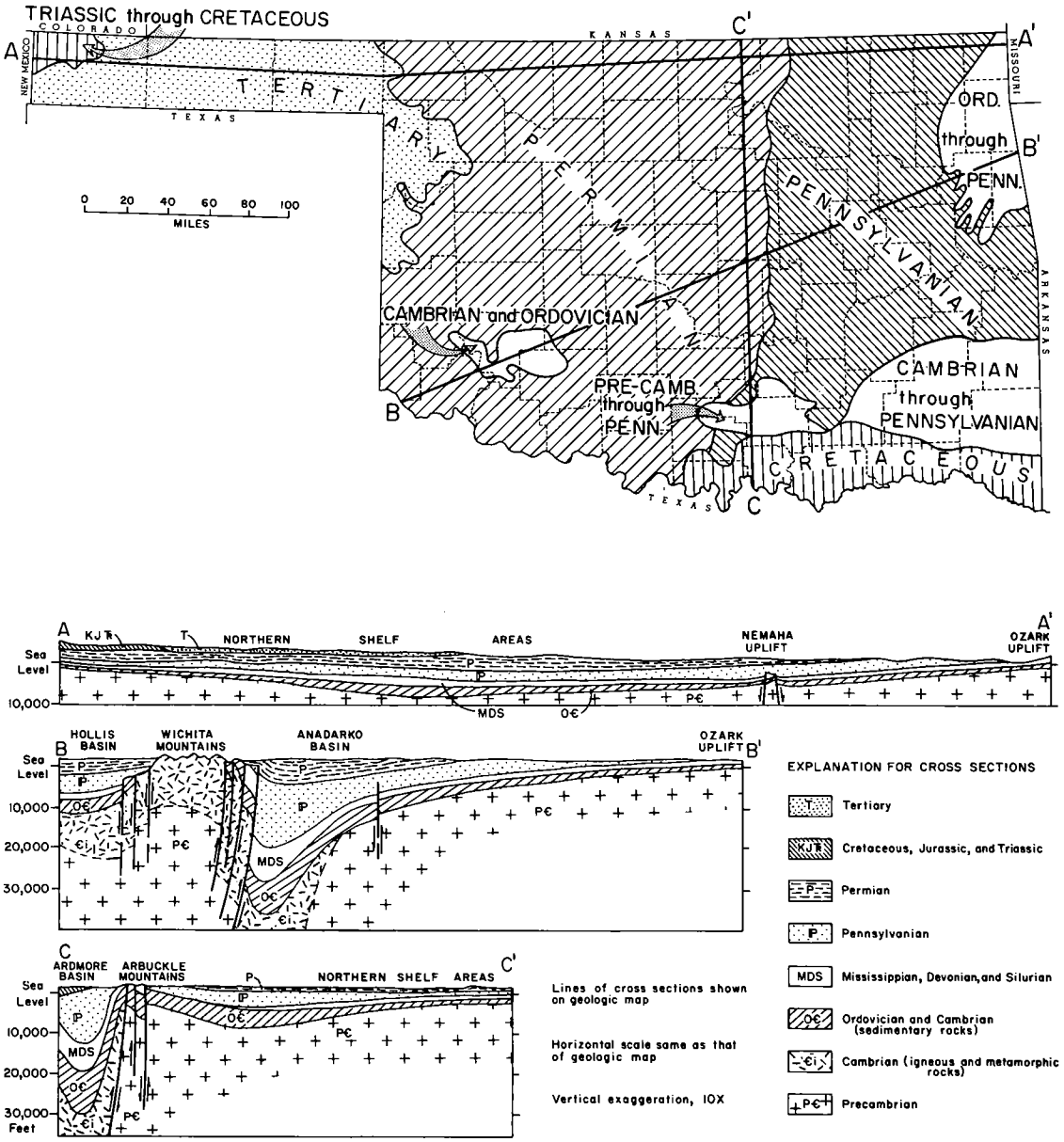

Figure 5. Generalized geologic map and cross sections of Oklahoma (after Johnson, 1971).

Oklahoma strata include those by Houseknecht and Matthews (1985), Cardott and others (1986), Walker (1986), Carr (1987), Cardott (1989), Pawlewicz (1989), and Cardott and others (1990).

Oklahoma Basin

Adler (1971), Webster (1980), Hatch and others (1986), and Wavrek (1989) indicated that Oklahoma basin hydrocarbon source rocks are of three time sequences: Ordovician (Simpson Group shales), Devonian–Mississippian (Woodford Shale), and Pennsylvanian (thick, dark shales). Figure 6 summarizes the geochemical data (kerogen type, TOC) available on potential hydrocarbon source rocks in the Oklahoma basin.

The source-rock potential of Arbuckle Group formations (Upper Cambrian to Lower Ordovician, Fig. 3) has long been debated, with many conflicting opinions. Bartram and others (1950) and Webb (1976) considered the hydrocarbons reservoired in Arbuckle Group formations to be

SYSTEM	PRODUCING INTERVAL	HYDROCARBON-SOURCE ROCK	KEROGEN TYPE	TOC %
PERMIAN	PERMIAN (UNDIFFERENTIATED)			
PENNSYLVANIAN	VIRGILIAN	UPPER AND MIDDLE PENNSYLVANIAN	II III	<1-25
	DESMOINESIAN			
	ATOKAN			
	MORROWAN	MORROWAN	III	0.5-3.4
MISSISSIPPIAN	SPRINGER FORMATION	SPRINGER FORMATION	III	
	PRE-CHESTER MISSISSIPPIAN (UNDIFFERENTIATED)	WOODFORD SHALE	II III	<1-14
DEVONIAN	HUNTON GROUP			
SILURIAN				
ORDOVICIAN	SIMPSON GROUP	SYLVAN SIMPSON GROUP	II I II	<1-9
UPPER CAMBRIAN	ARBUCKLE GROUP			

Figure 6. Paleozoic producing intervals, hydrocarbon source rocks, kerogen type, and total organic carbon content (TOC %) of Oklahoma basin (after Wenger and Baker, 1986; Rice and others, 1989; Burruss and Hatch, 1989).

sourced indigenous to the formation. Based on a geochemical study of oil composition, Zemmels and Walters (1987) concluded that Hoover field A-type oil in the Arbuckle Group (Garvin County, Oklahoma) was derived from an Arbuckle Group shale. Whitmire (1989) stated that most major Arbuckle gas produced from the Arkoma basin was externally sourced. Based on a geochemical study of oil composition, Wavrek (1989) concluded that the Arbuckle-reservoired oil in the Cottonwood Creek and Hewitt fields (Carter County, Oklahoma) was sourced by the Woodford Shale. Jones and Philp (1990) concluded that the Arbuckle Group was not a likely source of the oil that was geochemically analyzed from the Pauls Valley area of the Anadarko basin. Two published reports contain TOC data for Arbuckle Group carbonates and clastics. Trask and Patnode (1942) reported 0.10–1.30% TOC in 81 Arbuckle samples from 16 wells in the Midcontinent region. Cardwell (1977) indicated that 21 Arbuckle and Ellenburger carbonate samples had 0.03–0.24% TOC, with an average of 0.10%. Cardwell (1977) reported the most detailed geochemical study on oils, extracts, and samples from Arbuckle and Ellenburger rocks of the southern Midcontinent. Cardwell (1977,1985) concluded that Arbuckle and Ellenburger rocks did not source any of the oils investigated in his study. The low TOC content of Arbuckle carbonates and limited geochemical data on Arbuckle shales preclude proving that the Arbuckle Group is a hydrocarbon source rock.

Simpson Group shales from the Kansas shelf and Anadarko basin are reported to contain oil-

prone types I and II kerogen (Rice and others, 1989; Burruss and Hatch, 1989), based on Rock-Eval pyrolysis data. Hatch and others (1986) and Burruss and Hatch (1989) indicated that the Simpson Group and Sylvan Shale are generally organic lean (<1% TOC), although samples from the Kansas shelf of the Anadarko basin had TOC values between 1 and 9%. The source-rock potential of the Simpson Group is poor to moderate overall, with good potential on the Kansas shelf (Burruss and Hatch, 1989). Zemmels and others (1987) concluded that the Woodford Shale was the source of shallow Simpson Group oils in Murray County, Oklahoma.

Data are not available on the kerogen type and TOC content of the Viola Group. However, Jones and others (1987), Michael and others (1989), and Jones and Philp (1990) concluded that the Viola limestones are the source and reservoir of oil in the Pauls Valley area, Anadarko basin, based on biomarker analysis of oils and source-rock extracts. Zemmels and Walters (1987) stated that Viola oil from Love County, Oklahoma, was typical Ordovician oil.

Burruss and Hatch (1989) included geochemical data for the Sylvan Shale with geochemical data for the Simpson Group. The Sylvan Shale contains type II kerogen, with generally low TOC content (<1%). The source-rock potential for the Sylvan Shale is poor to moderate in the Anadarko basin (Burruss and Hatch, 1989).

The Woodford Shale is considered to be one of the most important hydrocarbon source rocks of the Anadarko basin and other regions of Oklahoma (Imbus and others, 1987; Cardott, 1989; Burruss and Hatch, 1989; Jones and Philp, 1990). The Woodford Shale contains predominantly type II kerogen (Lewan, 1983,1987; Crossey and others, 1986; Comer and Hinch, 1987; Burwood and others, 1988; Roberts and Mitterer, 1988; Surdam and others, 1989; Rice and others, 1989; Burruss and Hatch, 1989; Schmoker and Hester, 1989), with varying amounts of type III (terrestrial) kerogen (Hatch and others, 1986; Burruss and Hatch, 1989). Comer and Hinch (1987) and Burruss and Hatch (1989) illustrated van Krevelen-type diagrams of elemental and Rock-Eval pyrolysis data for the Woodford Shale and age-equivalent rocks of Oklahoma and Arkansas. TOC content of the Woodford Shale ranges from <1 to 14% (Sullivan, 1985; Comer and Hinch, 1987; Hester and Schmoker, 1987; Lewan, 1987; Burruss and Hatch, 1989). The source-rock potential for the Woodford Shale is moderate to good (Burruss and Hatch, 1989).

Upper Mississippian–Lower Pennsylvanian Springer Formation and Lower Pennsylvanian Morrowan shales contain gas-generating type III kerogen, with TOC content from 0.5 to 3.4% (Rice and others, 1989).

Middle and Upper Pennsylvanian (Atokan, Desmoinesian, Virgilian) marine shales are considered to be some of the most important hydrocarbon source rocks of Oklahoma (Burruss and Hatch, 1989). Baker (1962) and James and Baker (1972) indicated that the Excello Shale and other Cherokee Group shales (Desmoinesian) were the source of hydrocarbons in southeastern Kansas and northeastern Oklahoma. Hatch and others (1989) concluded that the Chattanooga Shale of Kansas (Woodford Shale equivalent) was the source of Cherokee Group oils. Atokan, Desmoinesian, and Virgilian offshore shales contain a mixture of type II and type III kerogen (Ece, 1989; Rice and others, 1989; Burruss and Hatch, 1989; Hatch and others, 1989). Nearshore shales contain degraded type III kerogen (Hatch and others, 1989). Ece (1989), Burruss and Hatch (1989), and Hatch and others (1989) illustrated van Krevelen-type diagrams of elemental and Rock-Eval pyrolysis data for Pennsylvanian shales of Kansas, Missouri, and Oklahoma. TOC content ranges from <1 to 25% (Baker, 1962; James and Baker, 1972; Wenger and Baker, 1986,1987; Ece, 1989; Burruss and Hatch, 1989; Hatch and others, 1989). The source-rock potential for the Middle and Upper Pennsylvanian marine black shales is good (Baker, 1962; Burruss and Hatch, 1989; Hatch and others, 1989).

Data are not available on the kerogen type and TOC content of Permian shales of Oklahoma. Murphy and others (1972) reported that two Lower Permian shales of northeastern Kansas, the Florena and Neva shales, contained appreciable amounts of extractable organic matter, indicative of good hydrocarbon source rocks. Rice and others (1989) concluded that Permian reservoir gas in the Panhandle-Hugoton field was sourced by Pennsylvanian and/or older source rocks. It is probable that Lower Permian shales, including some potential hydrocarbon source rocks, are mature in the Anadarko basin, Oklahoma and Texas, based on their depth of burial (Campbell and others, 1988).

Ouachita Trough

Hydrocarbon source rocks in the Ouachita trough can be divided into those that contain oil-prone, type II kerogen (Womble Shale through Arkansas Novaculite) and those that contain gas-prone, type III kerogen (Arkansas Novaculite through Atoka Formation) (Curiale, 1983; Curiale and others, 1984). Figure 7 summarizes the geochemical data (kerogen type, TOC) available on potential hydrocarbon source rocks in the Ouachita trough.

Curiale (1983) reported the most detailed geochemical study of oils, solid bitumens, and samples from Womble Shale through Stanley Group rocks of the Ouachita Mountains. Womble

Shale and Bigfork Chert contain oil-prone, type II kerogen (Fowler and Douglas, 1984), with TOC content <1 to 3.4% (Curiale, 1983). Polk Creek and Missouri Mountain Shale probably contain oil-prone, type II kerogen based on good oil source-rock potential, with TOC content of <1 to 1.6% (Curiale, 1983). Zemmels and others (1985) indicated that shale units in the Arkansas Novaculite contained oil-prone organic matter (type II? kerogen).

SYSTEM	OUACHITA MOUNTAINS	KEROGEN TYPE	TOC %
PENNSYLVANIAN	ATOKA FORMATION	III ?	<1
	JOHNS VALLEY SHALE		
	JACKFORK GROUP	III ?	1
MISSISSIPPIAN	STANLEY GROUP	III	<1-1.9
DEVONIAN	ARKANSAS NOVACULITE	II, III	<1-1.4
SILURIAN	MISSOURI MOUNTAIN SHALE	II ?	<1-1.4
	BLAYLOCK SANDSTONE		
ORDOVICIAN	POLK CREEK SHALE	II ?	<1-1.6
	BIGFORK CHERT	II	<1
	WOMBLE SHALE	II	<1-3.4
	BLAKELY SANDSTONE		
	MAZARN SHALE		
	CRYSTAL MOUNTAIN SANDSTONE		
	COLLIER SHALE		
CAMBRIAN			
PRECAMBRIAN			

Figure 7. Paleozoic strata, kerogen type, and total organic carbon content (TOC %) of Ouachita trough (after Curiale, 1983; Curiale and others, 1984; Fowler and Douglas, 1984; Zemmels and others, 1985; Guthrie and others, 1986).

Curiale and others (1984) considered the Arkansas Novaculite and Stanley to be gas-generative, based on the predominance of vitrinite (type III kerogen). TOC content of the Arkansas Novaculite is <1 to 1.4% (Curiale, 1983). TOC content of the Stanley Group is <1 to 1.9% (Curiale, 1983; Guthrie and others, 1986). Jackfork Group and Atoka Formation shales probably contain gas-prone organic matter (type III? kerogen), with TOC content ≤1% (Guthrie and others, 1986; Pyron and Gray, 1986).

Womble Shale, Bigfork Chert, Polk Creek Shale, Missouri Mountain Shale, and Arkansas Novaculite are considered to have good oil source-rock potential, while the Stanley Group shales are considered to have good gas source-rock potential (Curiale, 1983; Curiale and others, 1984; Zemmels and others, 1985). Lower Paleozoic oil-prone source rocks are thin, whereas Upper Paleozoic gas-prone source rocks are thick (Stone and Haley, 1984).

ACKNOWLEDGMENTS

We are grateful to J. A. Campbell and J. L. Weber, Oklahoma Geological Survey, for critical reviews of an earlier version of part of this paper.

REFERENCES

Adler, F. J., 1971, Anadarko basin and central Oklahoma area, *in* Future petroleum provinces of the United States—their geology and potential: American Association of Petroleum Geologists Memoir 15, v. 2, p. 1061–1070.

Amsden, T. W., 1975, Hunton Group (Late Ordovician, Silurian, and Early Devonian) in the Anadarko basin of Oklahoma: Oklahoma Geological Survey Bulletin 121, 214 p.

_____1980, Hunton Group (Late Ordovician, Silurian, and Early Devonian) in the Arkoma basin of Oklahoma: Oklahoma Geological Survey Bulletin 129, 136 p.

Baker, D. R., 1962, Organic geochemistry of the Cherokee Group in southeastern Kansas and northeastern Oklahoma: American Association of Petroleum Geologists Bulletin, v. 46, p. 1621–1642.

Bartram, J. G.; Imbt, W. C.; and Shea, E. F., 1950, Oil and gas in Arbuckle and Ellenburger Formations, Mid-Continent region: American Association of Petroleum Geologists Bulletin, v. 34, p. 682–700.

Burruss, R. C.; and Hatch, J. R., 1989, Geochemistry of oils and hydrocarbon source rocks, greater Anadarko basin: evidence for multiple sources of oils and long-distance oil migration, *in* Johnson, K. S. (ed.), Anadarko basin symposium, 1988: Oklahoma Geological Survey Circular 90, p. 53–64.

Burwood, R.; Drozd, R. J.; Halpern, H. I.; and Sedivy, R. A., 1988, Carbon isotopic variations of kerogen pyrolyzates: Organic Geochemistry, v. 12, p. 195–205.

Campbell, J. A.; Mankin, C. J.; Schwarzkopf, A. B.; and Raymer, J. H., 1988, Habitat of petroleum in Permian rocks of the Midcontinent region, *in* Morgan, W. A.; and Babcock, J. A. (eds.), Permian rocks of the Midcontinent: Society of Economic Paleontologists and Mineralogists Special Publication 1, p. 13–35.

Cardott, B. J., 1989, Thermal maturation of the Woodford Shale in the Anadarko basin, *in* Johnson, K. S. (ed.), Anadarko basin symposium, 1988: Oklahoma Geological Survey Circular 90, p. 32–46.

Cardott, B. J.; Hemish, L. A.; Johnson, C. R.; and Luza, K. V., 1986, The relationship between coal rank and present geothermal gradient in the Arkoma basin, Oklahoma: Oklahoma Geological Survey Special Publication 86-4, 65 p.

Cardott, B. J.; Metcalf, W. J., III; and Ahern, J. L., 1990, Thermal maturation by vitrinite reflectance of Woodford Shale near Washita Valley fault, Arbuckle Mountains, Oklahoma, *in* Nuccio, V. F.; and Barker, C. E. (eds.), Applications of thermal maturity studies to energy exploration: Society of Economic Paleontologists and Mineralogists, Rocky Mountain Section, p. 139–146.

Cardwell, A. L., 1977, Petroleum source-rock potential of Arbuckle and Ellenburger Groups, southern Mid-Continent, United States: Quarterly of the Colorado School of Mines, v. 72, no. 3, 134 p.

_____1985, Petroleum source rock potential of Arbuckle and Ellenburger Groups, Oklahoma and north Texas [abstract]: American Association of Petroleum Geologists Bulletin, v. 69, p. 142.

Carr, J. L., III, 1987, The thermal maturity of the Chattanooga Formation along a transect from the Ozark uplift to the Arkoma basin: Shale Shaker, v. 38, p. 32–40.

Cline, L. M., 1960, Stratigraphy of the Late Paleozoic rocks of the Ouachita Mountains, Oklahoma: Oklahoma Geological Survey Bulletin 85, 113 p.

Comer, J. B.; and Hinch, H. H., 1987, Recognizing and quantifying expulsion of oil from the Woodford Formation and age-equivalent rocks in Oklahoma and Arkansas: American Association of Petroleum Geologists Bulletin, v. 71, p. 844–858.

Craig, L. C.; and others, 1979, Paleotectonic investigations of the Mississippian System in the United States: U.S. Geological Survey Professional Paper 1010, part I, p. 1–369; part II, p. 371–559; part III, 15 plates.

Crossey, L. J.; Hagen, E. S.; Surdam, R. C.; and Papoint, T. W., 1986, Correlation of organic parameters derived from elemental analysis and programmed pyrolysis of kerogen, *in* Gautier, D. L. (ed.), Roles of organic matter in sediment diagenesis: Society of Economic Paleontologists and Mineralogists Special Publication 38, p. 35–45.

Curiale, J. A., 1983, Petroleum occurrences and source-rock potential of the Ouachita Mountains, southeastern Oklahoma: Oklahoma Geological Survey Bulletin 135, 65 p.

Curiale, J. A.; Harrison, W. E.; and Smith, Garmon, 1984, Hydrocarbon occurrences in the frontal and central Ouachita Mountains, Oklahoma, *in* Borger, J. G., II (ed.), Technical proceedings of the 1981 American Association of Petroleum Geologists

Mid-Continent Section meeting: Oklahoma City Geological Society, p. 90–115.
Denison, R. E.; Lidiak, E. G.; Bickford, M. E.; and Kisvarsanyi, E. B., 1984, Geology and geochronology of Precambrian rocks in the central interior region of the United States: U.S. Geological Survey Professional Paper 1241-C, 20 p.
Donovan, R. N. (ed.), 1986, The Slick Hills of southwestern Oklahoma—fragments of an aulacogen?: Oklahoma Geological Survey Guidebook 24, 112 p.
Ece, O. I., 1989, Organic maturation and paleoceanographic/paleogeographic implications of the Desmoinesian cyclothemic Excello black shale of the Midcontinent, USA: Shale Shaker, v. 39, p. 90–104.
Elmore, R. D.; Sutherland, P. K.; and White, P. B., 1990, Middle Pennsylvanian recurrent uplift of the Ouachita fold belt and basin subsidence in the Arkoma basin, Oklahoma: Geology, v. 18, p. 906–909.
Fay, R. O., 1989, Geology of the Arbuckle Mountains along Interstate 35, Carter and Murray Counties, Oklahoma: Oklahoma Geological Survey Guidebook 26, 50 p.
Fowler, M. G.; and Douglas, A. G., 1984, Distribution and structure of hydrocarbons in four organic-rich Ordovician rocks, *in* Schenck, P. A.; De Leeuw, J. W.; and Lijmbach, G. W. M. (eds.), Advances in organic geochemistry 1983: Organic Geochemistry, v. 6, p. 105–114.
Goldstein, A., Jr., 1975, Geologic interpretation of Viersen and Cochran's 25-1 Weyerhaeuser well, McCurtain County, Oklahoma: Oklahoma Geology Notes, v. 35, p. 167–181.
Guthrie, J. M.; Houseknecht, D. W.; and Johns, W. D., 1986, Relationships among vitrinite reflectance, illite crystallinity, and organic geochemistry in Carboniferous strata, Ouachita Mountains, Oklahoma and Arkansas: American Association of Petroleum Geologists Bulletin, v. 70, p. 26–33.
Ham, W. E., 1959, Correlation of pre-Stanley strata in the Arbuckle–Ouachita Mountain regions, *in* Cline, L. M. (ed.), The geology of the Ouachita Mountains, a symposium: Dallas Geological Society and Ardmore Geological Society, p. 71–86. [Reprinted in Oklahoma Geology Notes, v. 21, p. 204–224.]
_____1969, Regional geology of the Arbuckle Mountains, Oklahoma: Oklahoma Geological Survey Guidebook 17, 52 p.
Ham, W. E.; and Wilson, J. L., 1967, Paleozoic epeirogeny and orogeny in the central United States: American Journal of Science, v. 265, p. 332–407.
Hatch, J. R.; Rice, D. D.; Burruss, R. C.; Schmoker, J. W.; and Clayton, J. L., 1986, Thermal maturity modeling and geochemical characterization of hydrocarbon source rocks, oils, and natural gases of the Anadarko basin, *in* Carter, L. M. H. (ed.), USGS research on energy resources—1986, program and abstracts: U.S. Geological Survey Circular 974, p. 21–23.
Hatch, J. R.; King, J. D.; and Daws, T. A., 1989, Geochemistry of Cherokee Group oils of southeastern Kansas and northeastern Oklahoma: Kansas Geological Survey Subsurface Geology Series 11, 20 p.
Herndon, T. (ed.), 1965, Symposium on the Simpson: Tulsa Geological Society Digest, v. 33, 308 p.
Héroux, Y.; Chagnon, A.; and Bertrand, R., 1979, Compilation and correlation of major thermal maturation indicators: American Association of Petroleum Geologists Bulletin, v. 63, p. 2128–2144.
Hester, T. C.; and Schmoker, J. W., 1987, Determination of organic content from formation-density logs, Devonian–Mississippian Woodford Shale, Anadarko basin, Oklahoma: U.S. Geological Survey Open-File Report 87-20, 11 p.
Hills, J. M.; and Kottlowski, F. E. (coordinators), 1983, Correlation of stratigraphic units in North America—southwest/southwest Mid-Continent correlation chart: American Association of Petroleum Geologists.
Houseknecht, D. W.; and Matthews, S. M., 1985, Thermal maturity of Carboniferous strata, Ouachita Mountains: American Association of Petroleum Geologists Bulletin, v. 69, p. 335–345.
Imbus, S. W.; Engel, M. H.; and Zumberge, J. E., 1987, A geochemical correlation study of Oklahoma crude oils using a multivariate statistical method [abstract]: American Association of Petroleum Geologists Bulletin, v. 71, p. 570.
James, G. W.; and Baker, D. R., 1972, Organic geochemistry of the Pennsylvanian black shale (Excello) in the Midcontinent and the Illinois basin, *in* Kellogg, J. A. (ed.), Short papers on research in 1971: Kansas Geological Survey Bulletin 204, part 1, p. 3–10.
Johnson, K. S., 1971, Introduction, guidelines, and geologic history of Oklahoma, *book 1 of* Guidebook for geologic field trips in Oklahoma: Oklahoma Geological Survey Educational Publication 2, 15 p.
_____1991, Geologic overview and economic importance of Late Cambrian and Ordovician rocks in Oklahoma, *in* Johnson, K. S. (ed.), Late Cambrian–Ordovician geology of the southern Midcontinent, 1989 symposium: Oklahoma Geological Survey Circular 92, p. 3–14.
Johnson, K. S.; Amsden, T. W.; Denison, R. E.; Dutton, S. P.; Goldstein, A. G.; Rascoe, B., Jr.; Sutherland, P. K.; and Thompson, C. M., 1988, Southern Midcontinent region, *in* Sloss, L. L. (ed.), Sedimentary cover—North American craton, U.S.: Geological Society of America, The Geology of North America, v. D-2, p. 307–359. [Reprinted as Oklahoma Geological Survey Special Publication 89-2, 53 p.]
Jones, P. J.; and Philp, R. P., 1990, Oils and source rocks from Pauls Valley, Anadarko basin, Oklahoma, U.S.A.: Applied Geochemistry, v. 5, p. 429–448.
Jones, P. J.; Lewis, C. A.; Philp, R. P.; Lin, L. H.; and Michael, G. E., 1987, Geochemical study of oils, source rocks, and tar sands in Pauls Valley area, Anadarko basin, Oklahoma [abstract]: American Association of Petroleum Geologists Bulletin, v. 71, p. 574.
Latham, J. W., 1970, Healdton field, Carter County, Oklahoma: American Association of Petroleum Geologists Memoir 14, p. 255–276.
Lewan, M. D., 1983, Effects of thermal maturation on stable organic carbon isotopes as determined by hydrous pyrolysis of Woodford Shale: Geochimica et Cosmochimica Acta, v. 47, p. 1471–1479.
_____1987, Petrographic study of primary petroleum migration in the Woodford Shale and related rock

units, *in* Doligez, Brigitte (ed.), Migration of hydrocarbons in sedimentary basins: Collection Colloques et Séminaires, Editions Technip, Paris, p. 113–130.

Mankin, C. J. (coordinator), 1987, Correlation of stratigraphic units in North America—Texas–Oklahoma tectonic region correlation chart: American Association of Petroleum Geologists.

McHugh, J. W. (ed.), 1964, Symposium on the Arbuckle: Tulsa Geological Society Digest, v. 32, 186 p.

McKee, E. D.; and others, 1967, Paleotectonic maps of the Permian System: U.S. Geological Survey Miscellaneous Geologic Investigations Map I-450, scale 1:5,000,000.

McKee, E. D.; and others, 1975, Paleotectonic investigations of the Pennsylvanian System in the United States: U.S. Geological Survey Professional Paper 853, part I, 349 p.; part II, 192 p.; part III, 17 plates.

Michael, G. E.; Lin, L. H.; Philp, R. P.; Lewis, C. A.; and Jones, P. J., 1989, Biodegradation of tar-sand bitumens from the Ardmore/Anadarko basins, Oklahoma. II.—Correlation of oils, tar sands and source rocks: Organic Geochemistry, v. 14, p. 619–633.

Murphy, M. E.; Narayanan, S.; Gould, G.; Lawlor, S.; Noonan, J.; and Prentice, D., 1972, Organic geochemistry of some Upper Pennsylvanian and Lower Permian Kansas shales: hydrocarbons, *in* Kellogg, J. A. (ed.), Short papers on research in 1971: Kansas Geological Survey Bulletin 204, part 1, p. 19–25.

Pawlewicz, M. J., 1989, Thermal maturation of the eastern Anadarko basin, Oklahoma: U.S. Geological Survey Bulletin 1866-C, 12 p.

Pyron, A. J.; and Gray, John, 1986, Initial data indicate good chance for Ouachita production: World Oil, v. 203, no. 3, p. 62–65.

Ragland, D. A.; and Donovan, R. N., 1985, The Cool Creek Formation (Ordovician) at Turner Falls in the Arbuckle Mountains of southern Oklahoma: Oklahoma Geology Notes, v. 45, p. 132–148.

Rascoe, B., Jr.; and Adler, F. J., 1983, Permo–Carboniferous hydrocarbon accumulations, Mid-Continent, U.S.A.: American Association of Petroleum Geologists Bulletin, v. 67, p. 979–1001.

Rice, D. D.; Threlkeld, C. N.; and Vuletich, A. K., 1989, Characterization and origin of natural gases of the Anadarko basin, *in* Johnson, K. S. (ed.), Anadarko basin symposium, 1988: Oklahoma Geological Survey Circular 90, p. 47–52.

Roberts, C. T.; and Mitterer, R. M., 1988, Laminated black shale-chert cyclicity in Woodford Formation (Upper Devonian of southern Mid-Continent) [abstract]: American Association of Petroleum Geologists Bulletin, v. 72, p. 240–241.

St. John, J. W., Jr.; and Eby, D. E., 1978, Peritidal carbonates and evidence for vanished evaporites in the Lower Ordovician Cool Creek Formation, Arbuckle Mountains, Oklahoma: Gulf Coast Association of Geological Societies Transactions, v. 28, part 2, p. 589–599.

Schmoker, J. W.; and Hester, T. C., 1989, Formation resistivity as an indicator of the onset of oil generation in the Woodford Shale, Anadarko basin, Oklahoma, *in* Johnson, K. S. (ed.), Anadarko basin symposium, 1988: Oklahoma Geological Survey Circular 90, p. 262–266.

Schramm, M. W., Jr., 1964, Paleogeologic and quantitative lithofacies analysis, Simpson Group, Oklahoma: American Association of Petroleum Geologists Bulletin, v. 48, p. 1164–1195.

_____(ed.), 1966, Symposium on the Viola, Fernvale and Sylvan: Tulsa Geological Society Digest, v. 34, 151 p.

Statler, A. T., 1965, Stratigraphy of the Simpson Group in Oklahoma, *in* Herndon, T. (ed.), Symposium on the Simpson Group: Tulsa Geological Society Digest, v. 33, p. 162–211.

Stone, C. G.; and Haley, B. R., 1984, A guidebook to the geology of the central and southern Ouachita Mountains, Arkansas: Arkansas Geological Commission Guidebook 84-2, p. 5.

Sullivan, K. L., 1985, Organic facies variation of the Woodford Shale in western Oklahoma: Shale Shaker, v. 35, p. 76–89.

Surdam, R. C.; Crossey, L. J.; Hagen, E. S.; and Heasler, H. P., 1989, Organic-inorganic interactions and sandstone diagenesis: American Association of Petroleum Geologists Bulletin, v. 73, p. 1–23.

Sutherland, P. K., 1988, Late Mississippian and Pennsylvanian depositional history in the Arkoma basin area, Oklahoma and Texas: Geological Society of America Bulletin, v. 100, p. 1787–1802.

Tissot, B. P.; and Welte, D. H., 1984, Petroleum formation and occurrence [second edition]: Springer-Verlag, New York, 699 p.

Tomlinson, C. W.; and McBee, W., Jr., 1959, Pennsylvanian sediments and orogenies of Ardmore district, Oklahoma, *in* Petroleum geology of southern Oklahoma: American Association of Petroleum Geologists, v. 2, p. 3–52.

Trask, P. D.; and Patnode, H. W., 1942, Source beds of petroleum: American Association of Petroleum Geologists Report of Investigation, 566 p.

Walker, P. E. G., 1986, A regional study of the diagenetic and geochemical character of the Pennsylvanian Morrow Formation, Anadarko basin, Oklahoma: Oklahoma State University unpublished M.S. thesis, 156 p.

Wavrek, D. A., 1989, Characterization of oil types along Hewitt trend, Carter County, Oklahoma: implications for future exploration [abstract]: American Association of Petroleum Geologists Bulletin, v. 73, p. 424.

Webb, G. W., 1976, Oklahoma City oil—second crop from preserved subunconformity source rocks: American Association of Petroleum Geologists Bulletin, v. 60, p. 115–122.

Webster, R. E., 1980, Evolution of S. Oklahoma aulacogen: Oil and Gas Journal, v. 78, no. 7, p. 150–172.

Wenger, L. M.; and Baker, D. R., 1986, Variations in organic geochemistry of anoxic-oxic black shale-carbonate sequences in the Pennsylvanian of the Midcontinent, U.S.A., *in* Advances in organic geochemistry 1985: Organic Geochemistry, v. 10, p. 85–92.

_____1987, Variations in vitrinite reflectance with organic facies—examples from Pennsylvanian cyclothems of the Midcontinent, U.S.A.: Organic

Geochemistry, v. 11, p. 411–416.
Whitmire, M. G., 1989, Industry "hot spot"—the Arkoma basin: Oil and Gas Journal, v. 87, no. 29, p. 76–78.
Zemmels, I.; and Walters, C. C., 1987, Variation of oil composition in vicinity of Arbuckle Mountains, Oklahoma [abstract]: American Association of Petroleum Geologists Bulletin, v. 71, p. 998–999.
Zemmels, I.; Grizzle, P. L.; Walters, C. C.; and Haney, F. R., 1985, Devonian novaculites as source of oil in Marathon–Ouachita thrust system [abstract]: American Association of Petroleum Geologists Bulletin, v. 69, p. 318–319.
Zemmels, I.; Tappmeyer, D. M.; and Walters, C. C., 1987, Source of shallow Simpson Group oils in Murray County, Oklahoma [abstract]: American Association of Petroleum Geologists Bulletin, v. 71, p. 245.

Geology and Organic Geochemistry of the Woodford Shale in the Criner Hills and Western Arbuckle Mountains, Oklahoma

D. W. Kirkland, R. E. Denison, D. M. Summers, and J. R. Gormly
Mobil Research and Development Corp., Dallas

ABSTRACT.—Exposures in southern Oklahoma afford a convenient opportunity to examine one of North America's richest and most important marine source rocks for oil—the Upper Devonian Woodford Shale. In the study area the Woodford is a laminated black shale composed by volume of approximately one-fifth organic matter, one-quarter illite, and the remainder silica. The silica is derived largely from Radiolaria and sponge spicules. The organic matter is predominantly type II kerogen with a hydrogen index of 500–800 mg hydrocarbons/gram of organic carbon. The Woodford contains a variety of features visible in outcrop and in thin section including microflora (e.g., *Tasmanites* sp. and *Foerstia* sp.), terrestrial macroflora (*Calamites*(?) sp. and *Callixylon* sp.), microfauna (various species of Radiolaria), macrofauna (aptychi of ammonoids and *Mooreoceras* sp.), phosphate nodules, pyrite concretions, large (~5 ft diameter) calcite concretions, seasonal(?) laminations, bitumen-filled fractures, and tar-balls. These features provide clues to the shale's depositional setting and early diagenetic environment. In the area of our investigation the Woodford sediments probably accumulated at a slow rate (e.g., ~0.01 mm/yr) in water several hundred feet deep, in a broad, persistently thermally stratified, tropical or subtropical, intracratonic sea. The anoxic bottom water, and consequent lack of bottom-dwelling fauna, and the slow rate of sedimentation were principal factors contributing to the large amount of organic matter in the Woodford. Within the sediment column, phytoplanktonic remains and their degradation products were fermented; by-products of the fermentation were then oxidized via microbial agents, by sulfate anions, and by carbon dioxide. A fraction of the remains, however, were nonmetabolizable and were preserved within the fine-grained clastic and biogenic sediments. Preservation of this organic matter provided the Woodford with an immense capacity to generate oil at thermal maturity.

INTRODUCTION

The Woodford Shale, one of North America's richest and most important source rocks, is well exposed in southern Oklahoma. We examined excellent exposures of the Woodford Shale at the McAlester (also spelled McAlister) Cemetery Quarry in the Criner Hills, our primary focus, at the Henry House Falls Quarry and at a road cut along Interstate-35 on the south flank of the Arbuckle Mountains (Fig. 1).

The Upper Devonian–Lower Mississippian Woodford Shale and its lateral equivalents (e.g., the Antrim, Bakken, Chattanooga, New Albany, Ohio Shales, etc.) are important source rocks throughout the eastern and central United States. The Woodford has been estimated to be the source for ~70% of the oil discovered in central and southern Oklahoma (Comer and Hinch, 1987). Shales that originated in a depositional and early diagenetic environment similar to that of the Woodford are the source of an important fraction of the world's oil. Source rocks of this type occur only intermittently in the Phanerozoic rock record and are the result of a specific and uncommon set of geologic circumstances.

The Woodford and its stratigraphic equivalents were deposited in a Late Devonian–Early Mississippian intracratonic sea that stretched from New York to North Dakota and south to Mexico. Throughout much of this extent, these units accumulated within anoxic bottom water, an environmental setting that favors preservation of organic matter. The intracratonic sea was generally shallow, probably less than several hundred feet deep (Shaw, 1964; Irwin, 1965; Hallam, 1981). Yet waters without oxygen were able to persist near the sea floor for millions of years throughout much of this vast epeiric sea. Anoxia probably resulted because the persistent thermal stratification of the Woodford Sea prevented oxygen-bearing currents from moving downward into the bottom water, and because the relatively shallow depth of the sea prevented oxygen-bearing currents from the open ocean from moving laterally beneath the thermocline into the interior of the Woodford Sea.

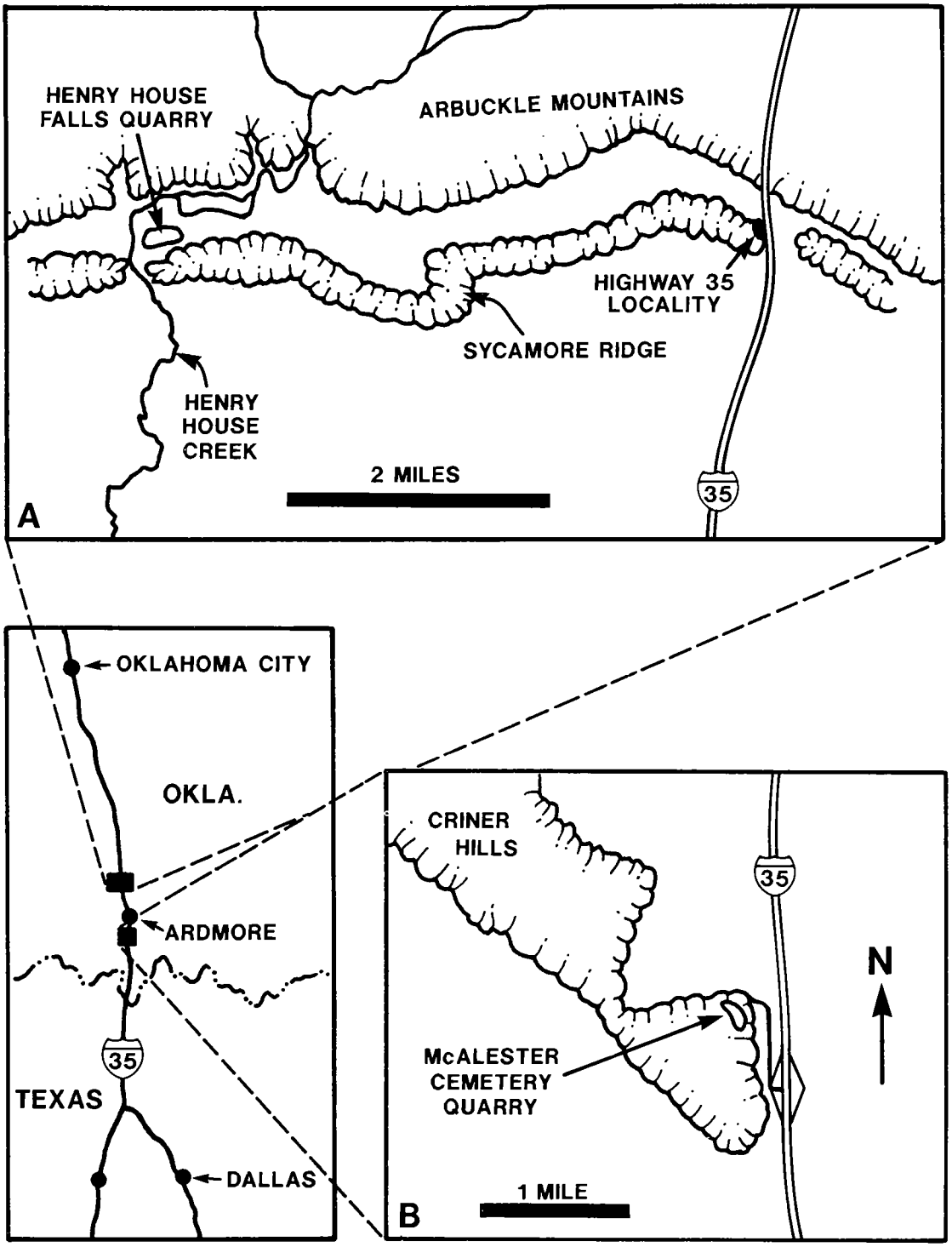

Figure 1. Location of (A) Henry House Falls Quarry and I-35 road cut, and (B) McAlester Cemetery Quarry.

REGIONAL STRATIGRAPHIC AND TECTONIC SETTING

Pre-Woodford erosion exposed rocks as old as Arbuckle (Late Cambrian–Early Ordovician) in northern Oklahoma and as old as latest Ordovician in southern Oklahoma (Fig. 2). The pre-Woodford unconformity was the first of significance in Oklahoma after that of the Late Cambrian. Although well exposed in southern Oklahoma, the unconformity rarely shows physical evidence of the time disparity. A thin conglomerate (as much as 4 in. thick) is sporadically developed; a distinct discordance in dips does not occur (Amsden, 1960). Only the progressive truncation of pre-Woodford rocks shows the magnitude of the unconformity. A basal sandstone, the Misener, is found in areas in which a source for sand was available. The Misener sand, derived largely from reworking of Middle Ordovician Simpson sands in north-central Oklahoma (Amsden and Klapper, 1972), is sporadically interbedded with the lowermost Woodford. The lack of both a well-defined basal conglomerate and a dip discordance suggests gentle regional warping rather than severe local deformation.

The sea that ultimately deposited the Woodford muds transgressed generally from the south–southeast out of the deep-water Ouachita depositional basin. The shelf-edge was 120–150 mi from the Woodford exposure at the McAlester Cemetery Quarry (Fig. 3). The surface on which the sea transgressed was exceptionally flat and substantially clear of debris. Although the original regional distribution of the Woodford and its equivalents is imprecisely known, the general pattern of their depositional facies is clear (Fig. 3A). The Arkansas Novaculite, a siliceous equivalent of the Woodford, was deposited in deep water to the southeast while black shale, green shale, and dolomite were deposited in shallower water to the northwest (Fig. 3B). The clastic component was probably derived from the northeast, from rocks uplifted during the Acadian orogeny (see King, 1977, p. 60–62).

The Woodford Sea probably completely covered Oklahoma. In much of Oklahoma the Woodford Shale is <200 ft thick, but in southern Oklahoma it is >700 ft thick (maximum drilled thickness; Amsden, 1975). Intraformational unconformities are unknown and probably absent. Erosion, chiefly in the Late Paleozoic, removed the Woodford from parts of Oklahoma. The restored depositional thickness in Oklahoma is shown in Figure 4. The Woodford Shale is the youngest unit in Oklahoma that retains an essentially identical character, with the exception of thickness, in the southern Oklahoma aulacogen as well as on the platform.

The contact with the overlying Sycamore has been interpreted as conformable (Ham, 1969). In

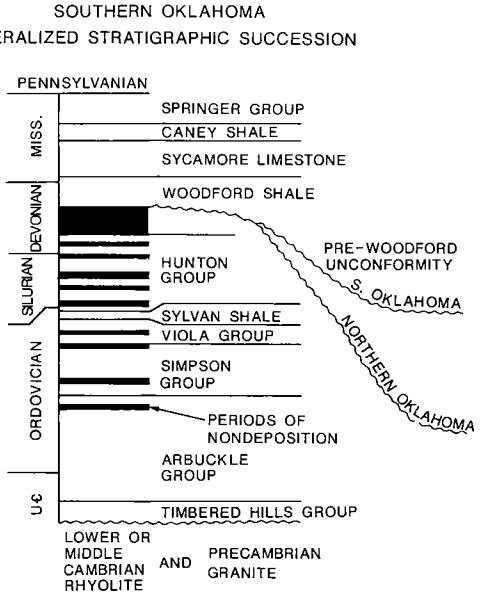

Figure 2. Generalized stratigraphic section for the pre-Pennsylvanian of southern Oklahoma showing periods of nondeposition (black) and extent of pre-Woodford unconformity. After Ham (1969), Ross and others (1982), and Amsden (1973).

southern Oklahoma the Mississippian strata consist of 5,000 ft of mostly deep-water sandstone, shale, and limestone, with the limestone being subordinate. Elsewhere in Oklahoma the Woodford is overlain by a relatively thin (300–400 ft), largely carbonate, shallow-water shelf-sequence.

AGE

The age of the Woodford is based principally on conodonts. The conodont fauna from southern Oklahoma indicates that most of the formation is Late Devonian (Hass and Huddle, 1965). The oldest conodonts in the formation are early Late Devonian and the youngest conodonts, in the uppermost part (1–8 ft) at some sections, are earliest Mississippian (Kinderhookian). Conodonts from cores and outcrops of the Misener show that the Misener is diachronous (Amsden and Klapper, 1972). Locally it is as old as latest Middle Devonian, but generally it is of Late Devonian age. The basal Sycamore, which immediately overlies the Woodford, contains a sparse conodont fauna of middle to late Kinderhookian age (Spesshardt, 1985). The Woodford was therefore deposited from latest Middle Devonian to Early Mississippian, an interval of ~15 million years (using the time scale of Harland and others, 1982).

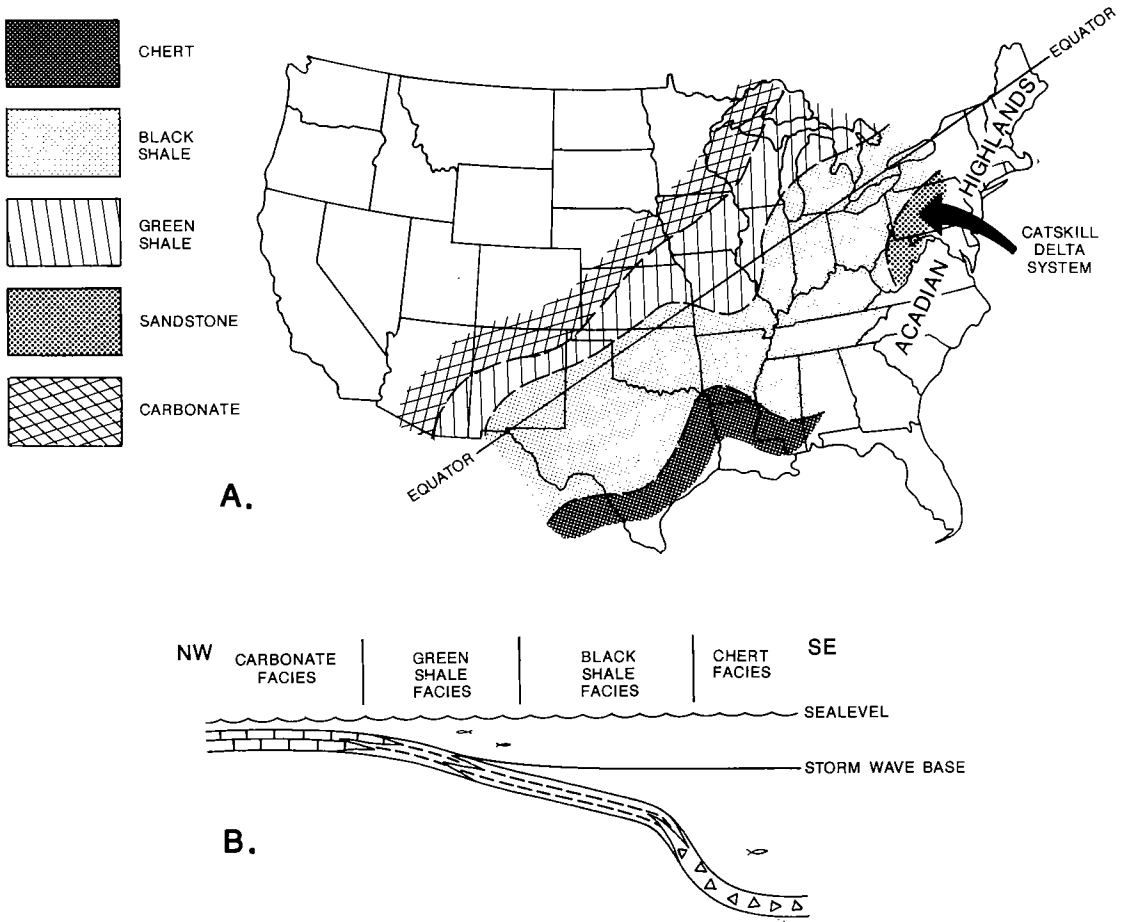

Figure 3. *A*—Paleogeography and facies distribution in the Late Devonian (modified from Cook and Bally, 1975). Location of the paleoequator is from Scotese and others (1979). Heckel and Witzke (1979) and Miller and Kent (1986) interpret the paleoequator to pass through Canada. *B*—Northwest–southeast cross section through the Woodford depositional basin showing the relationship of facies to relative water depth.

GEOLOGY

Introduction

The McAlester Cemetery Quarry, located on the northeast flank of the Criner Hills uplift (Fig. 1B), has an area of several acres (Fig. 5). Near-surface rock to a depth of probably <75 ft was removed during the quarrying operation. The Woodford strikes ~N. 40° W. and dips steeply (~34° NE).

A complete sequence of the Woodford, ~365 ft of section, is exposed in the quarry. The basal 240 ft is intercalated papery and blocky, black-to-brown shale. This stratification is well illustrated in the Henry House Falls Quarry (Fig. 6). The upper 125 ft in the Criner Hills consists of alternating hard (siliceous) and soft (shaly) beds with little apparent internal structure. The upper section was severely weathered, probably in Quaternary time, to a white-to-cream color. The upper 50 ft of the weathered section contain abundant phosphate nodules.

Fossils

The fossil assemblage in the Woodford Shale at the McAlester Cemetery Quarry includes many species of microflora (Figs. 7–10), one species of macroflora (Fig. 12), microfauna (Fig. 13), and several species of macrofauna (Figs. 14,15). Petrified wood, *Callixylon* sp., unobserved at the McAlester Cemetery Quarry, is conspicuous in the basal section at the Henry House Falls Quarry (Fig. 11). Spores and hystrichosphaerids (acritarchs) are abundant throughout the Woodford (Urban, 1960; Von Almen, 1970). Plankton include *Foerstia* sp. (probably of algal affinity), *Tasmanites* sp. (an alga), and Radiolaria. *Foerstia* is restricted to a nar-

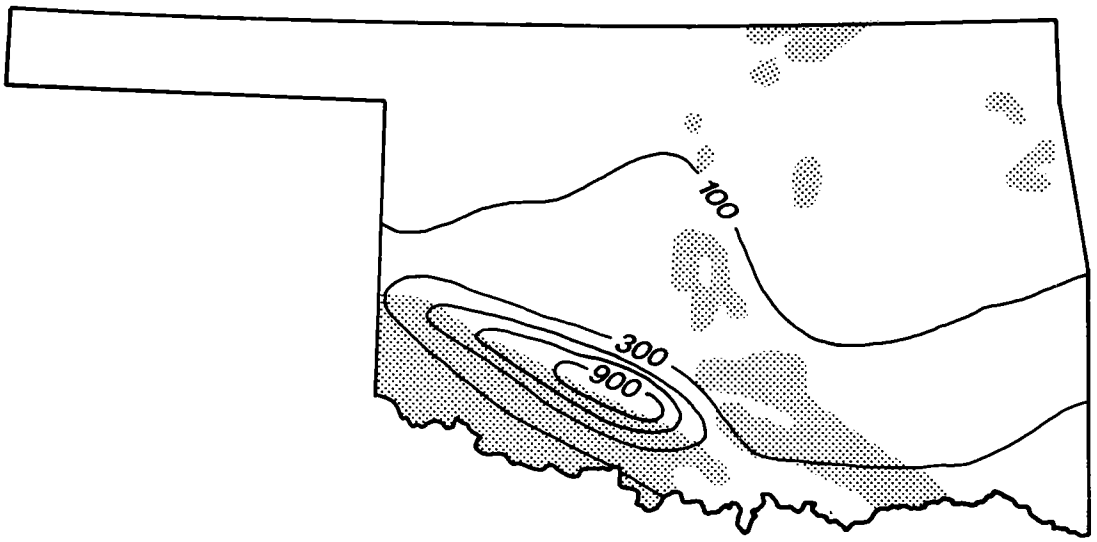

Figure 4. Restored depositional thickness of the Woodford Shale (100-, 300-, 500-, 700-, and 900-ft contours). Shading designates generalized areas from which the Woodford has been removed. (Reconstruction largely from data of Amsden [1975,1980]).

Figure 5. General view of the McAlester Cemetery Quarry (September 1986).

row zone near the middle of the section. (Previously unknown from the Woodford, *Foerstia* was discovered at the McAlester Cemetery Quarry by L. E. Roberts). Nekton—including crustaceans, ammonoids, and conodonts—lived in the near-surface water and fed on plankton. The remains of fossil crustaceans and ammonoids have been found only in the upper one-seventh of the formation (i.e., within the nodular zone). The track of a bottom-dwelling(?) organism (Fig. 16) and macroscopic remains of terrestrial plants—*Calamites*(?) sp. and *Callixylon* sp.—have been found only in the lower one-fourth of the formation. Sponge spicules (monaxons) are common in, at least, the

Figure 6. Rhythmic bedding in the Woodford Shale at the Henry House Falls Quarry. Silica-rich beds are intercalated with shaley beds. Scale in centimeters.

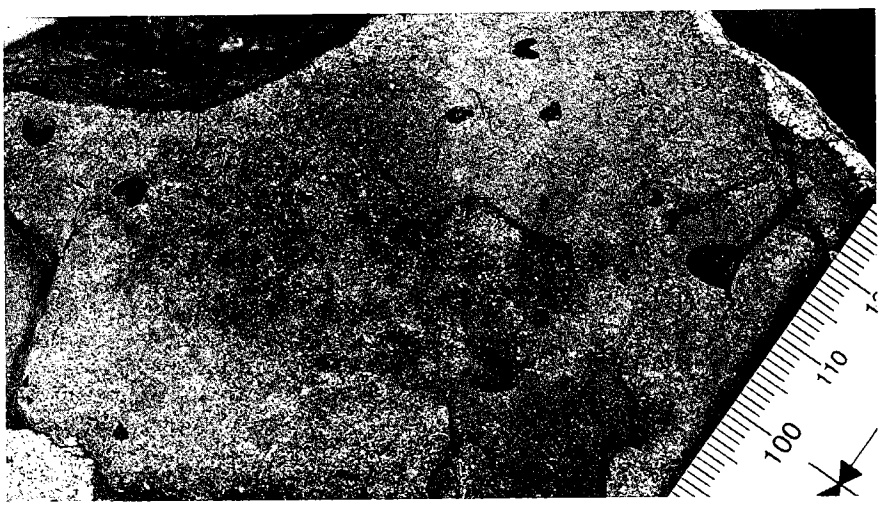

Figure 7. *Foerstia* sp., a fossil of problematic affinities, on bedding surface of Woodford Shale, McAlester Cemetery Quarry.

upper part of the Woodford. These spicules, because of their small size, could be transported long distances from areas of the Woodford Sea in which bottom waters were oxic.

The virtual absence of evidence of bottom-dwelling animals indicates that the sea floor and uppermost sediment-column were uninhabitable by metazoans during most of Woodford deposition. The bottom waters apparently contained insufficient oxygen to support respiration. During the earliest stage of Woodford deposition, as the Devonian sea transgressed, the sea floor at the McAlester Cemetery Quarry was intermittently above storm wave-base. The bottom waters then mixed with overlying waters, dissolved oxygen was transported to the sea floor, and green organic-

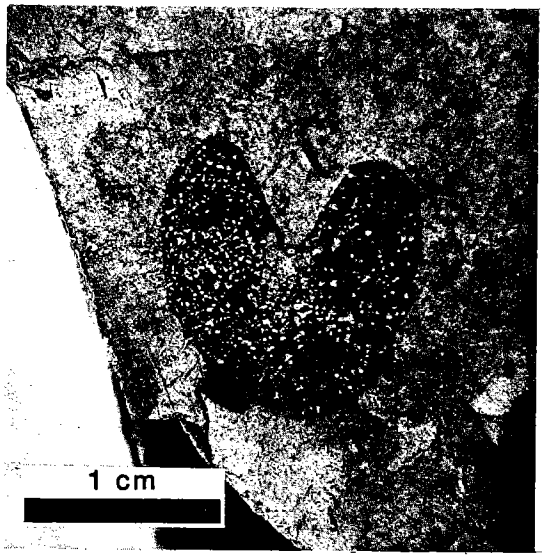

Figure 8. Close-up of *Foerstia* sp. at the McAlester Cemetery Quarry.

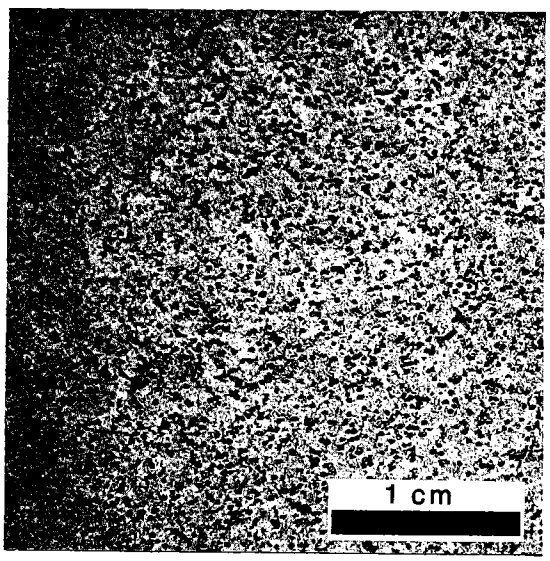

Figure 9. Densely distributed *Tasmanites* sp. on a bedding surface in the McAlester Cemetery Quarry. Scale in millimeters.

carbon-poor muds accumulated. These episodes of oxygenation were apparently too short to allow benthic animals to become established.

Petrography and Composition

We used petrographic examination together with X-ray diffraction and X-ray fluorescence analysis to understand the appearance and origin of the shale. Megascopically, most of the outcrop is a massive, silica-rich shale with conchoidal fracture (the blocky facies). This facies is interstratified with a highly fissile, paper-shale facies. In thin section these facies are similar. The rock appears to be composed of reddish-brown clay and organic matter and is distinctly laminated. Scattered within this laminated clay-organic matrix are siliceous spheres, flattened yellow bodies (*Tasmanites*), tiny lenses of silica, and opaque minerals (Fig. 17A,B). Roberts and Mitterer (1990) reported that the organic carbon content at the I-35 locality (Fig. 1A) ranges from 3 to 9% in the silica-rich beds and from 10 to 25% in the black shale beds. The total organic carbon content of samples we analyzed was usually in the range of 5–15 wt%. Given the average density of the mineral matrix, the organic material occupies 10–30% of the rock volume.

Laminae such as those shown in Figure 17A probably represent a lithified record of seasonal climatic change. The depositional environment into which the Woodford sediments rained was extremely quiet, currents were virtually absent, and animal and plant life were absent. Subtle changes in temperature, precipitation, humidity, or wind intensity may be reflected in the composition and thickness of the laminae. Couplets of organic matter and mineral matter similar to those in the Woodford have been shown elsewhere to represent varves—annual increments of sediment (e.g., Hallam, 1967).

The Woodford has a relatively low clay-content (Table 1). None of 10 samples analyzed has as much as 50% by weight clay (illite plus kaolinite). In fresh samples illite is as much as three times as abundant as kaolinite. In weathered samples the relative proportion of kaolinite increases (based on three analyses). Of the samples investigated, quartz constitutes 29–96 wt% of the mineral portion. In some beds, dolomite forms >50 wt% of the mineral matter. In thin section, dolomite is obvious and quartz is inconspicuous.

Clay and silt are the only detrital components. The silt is mostly quartz, with lesser amounts of muscovite, glauconite, and feldspar. Grains tend to be angular and <0.05 mm in length. No sample contains as much as 2% silt. The silt was probably transported by wind, whereas the clay was transported primarily in suspension. In the paper-shale sections (as compared to the blocky-shale sections) the amount of silt is large relative to the amount of clay. If the rate of accumulation of the windblown silt was relatively constant, the paper-shale facies probably would have had a slower depositional rate than the blocky shale facies. A thickness of 365 ft of Woodford accumulating in ~15 million years amounts to an average rock accumulation rate of ~0.01 mm per year—a slow rate indeed. This rate is in accord with estimates of the rate of accumulation based on petrography, as-

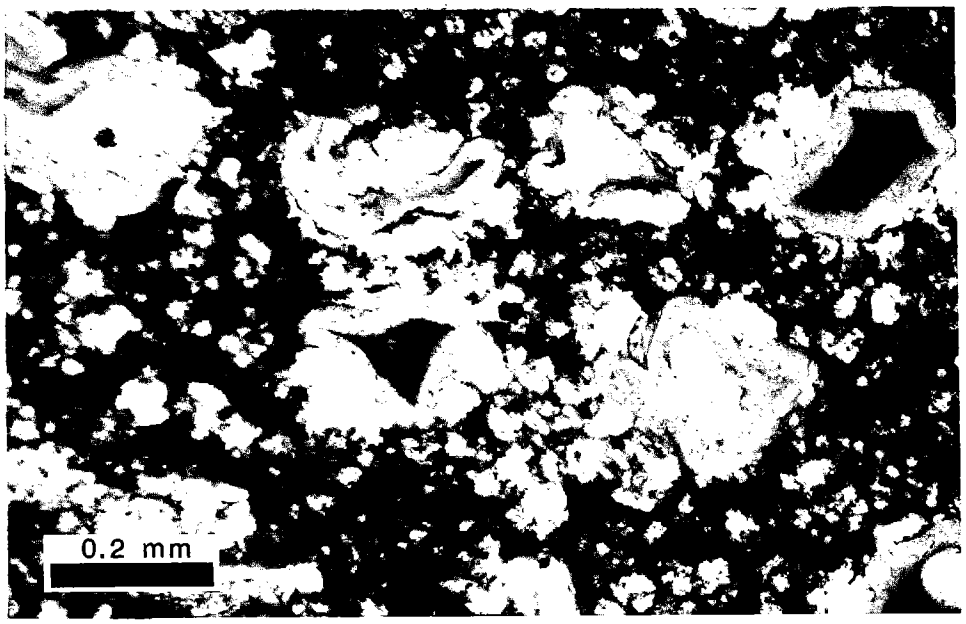

Figure 10. Photomicrograph of thin section of Woodford perpendicular to bedding showing unflattened individuals of *Tasmanites* sp. with body cavities filled with early diagenetic carbonate and collophane.

Figure 11. Fossil tree trunk of *Callixylon* sp. from basal Woodford Shale, Henry House Falls Quarry. Scale in centimeters.

suming continuous deposition and assuming that pairs of laminae represent varves.

Examination of the phosphatic nodules, which formed during early diagenesis, gives clues to the origin of quartz within the shale. Radiolarian tests with spines and delicate, lacy wall-structure are abundant (e.g., Fig. 13). They are about the same size as spheres and lenses of silica in the shale. However, in the host shale, even immediately adjacent to the nodules, definitive radiolarian remains cannot be identified. In the shale, the round, clear silica bodies, ~0.2 mm in diameter,

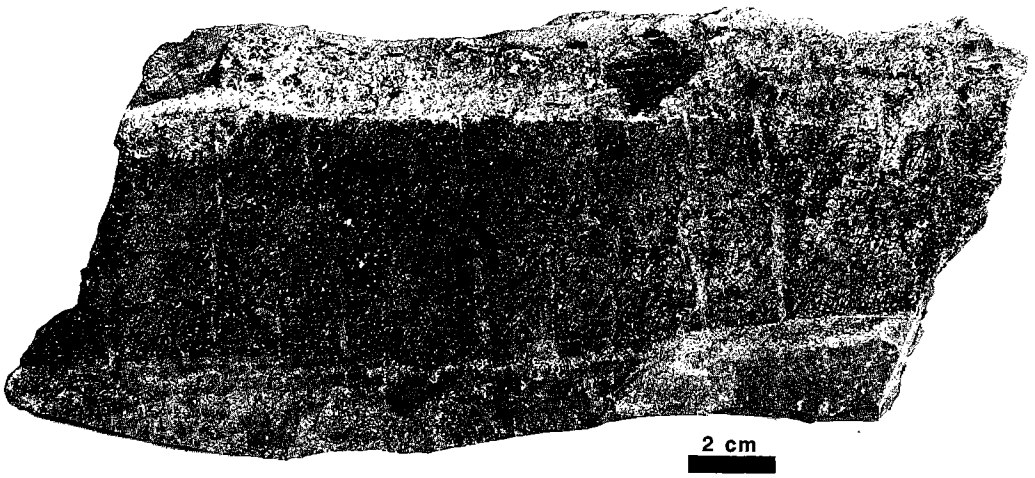

Figure 12. Carbonized stem of *Calamites*(?) sp. from the McAlester Cemetery Quarry. Carbonized wood from this specimen has a vitrinite reflectance of 0.34%.

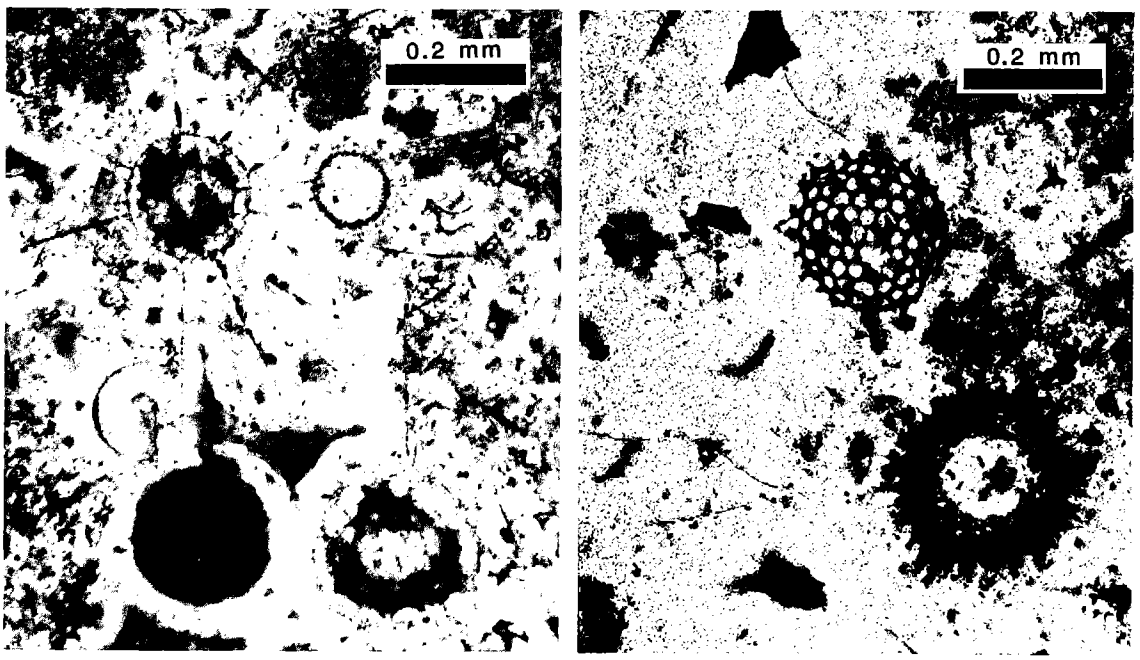

Figure 13. Photomicrographs of thin sections of phosphate nodules showing species of Radiolaria in various stages of preservation.

are composed of microcrystalline quartz or fibrous chalcedony. A reddish-brown (in transmitted light), nearly isotropic material fills some of these bodies. This material, principally collophane, is, in part, bitumen. The lens-shaped pods of silica, approximately 0.2–0.3 mm in length, tend to occur in zones that do not contain the round bodies. We interpret the round bodies to be uncrushed, filled radiolarian tests and the lenses to be crushed radiolarian tests.

The total quantity of petrographically identifiable quartz, represented by silt plus the lenses and spheres of silica, is less than the quantity of quartz indicated by X-ray diffraction. Apparently, some cryptocrystalline quartz occurs as cement derived probably from dissolution of biogenic opal.

Blocky strata of dolomitic (20–50+%) shale and replacement dolomite are interspersed within the Woodford section. The dolomite occurs as evenly distributed small (<0.03 mm), discrete rhombs

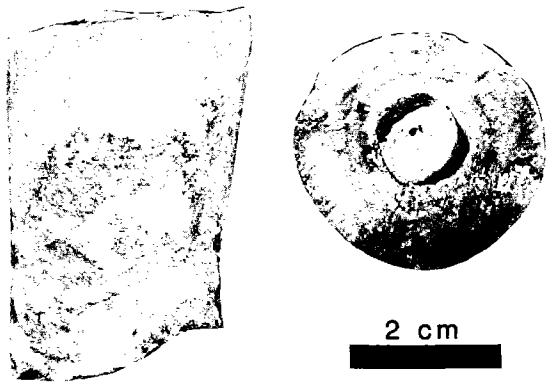

Figure 14. Cephalopod (*Mooreoceras* sp.) serving as nucleus of a phosphatic nodule (right), Upper Woodford (I-35 road cut, Fig. 1). The elongated phosphatic nodule (left) is in marked contrast to the more common near-spherical shape.

and spherules, and as lens-shaped pods (typically ~0.2 mm in length) of aggregate crystals. The pods may be crushed tests of an unknown plankton, possibly Radiolaria. This is based on their similarity in size, shape, and distribution to pods of silica believed on better petrographic grounds to be crushed Radiolaria. Most of the discrete rhombs and spherules of dolomite probably had an inorganic origin, but some may be replaced tests of a planktonic species.

At the I-35 road cut (Fig. 1A), dolomite has extensively replaced a siliceous mudstone bed near the top of the zone of phosphate nodules. A dolomite bed, ~0.5 ft thick, can be traced along strike for ~8 ft. The dolomite is dark brown, nearly the color of the fresh shale, and it incorporates phosphate nodules. The bedding contacts are nearly regular, but make small crosscutting excursions. The bed is formed of coarse, baroque dolomite crystals, 1–2 mm in diameter, with ragged, irregu-

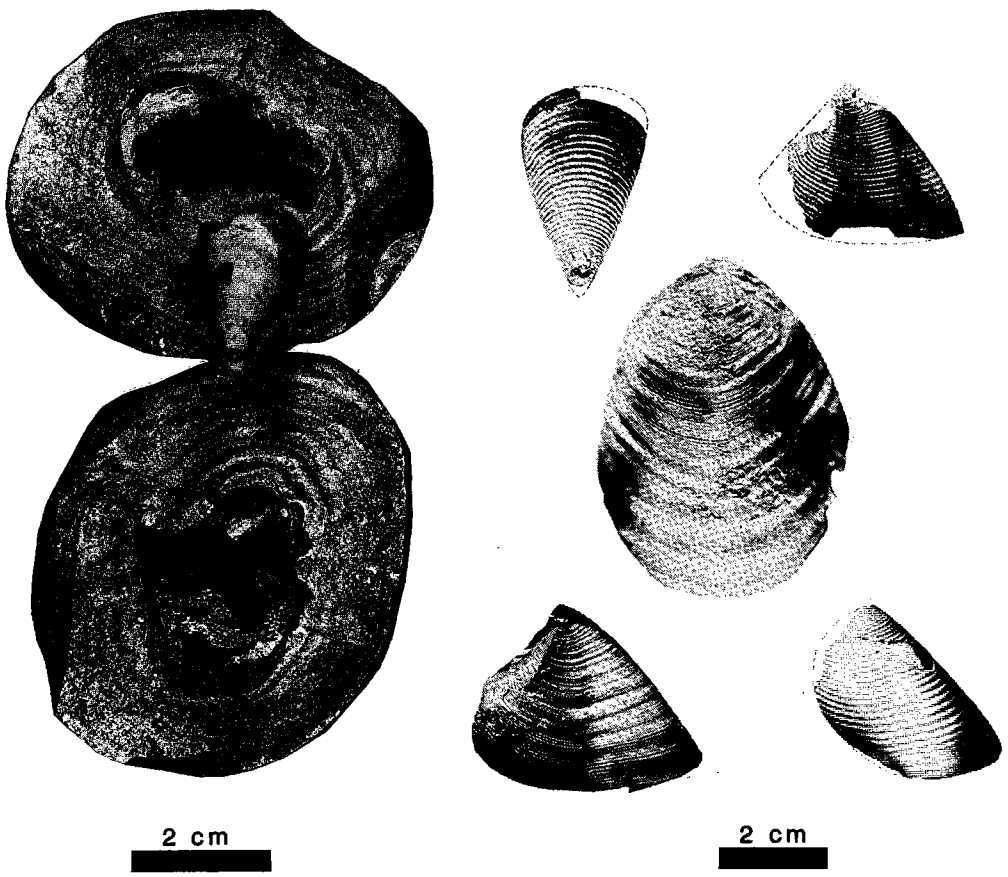

Figure 15. Broken phosphate nodule (left) showing enclosed aptychus of an ammonoid (the aptychus, which served as the nucleus, has been removed and is laying on the outer part of the nodule), McAlester Cemetery Quarry. Examples of aptychi (right) from nuclei of phosphate nodules in the Woodford Shale (from Cooper, 1932).

lar contacts and generally ovoid shapes. The dolomite contains <20% insoluble residue and ~2–5% organic carbon.

The most conspicuous petrographic feature of the dolomite is a complex of rod-like crystals, 0.3–0.7 mm in length and ~0.05 mm wide. The original crystals are mostly replaced by calcite, but in one sample, by quartz. The original composition of these rod-like features cannot be positively determined. Nonetheless, they are remarkably similar to lath-shaped crystals of gypsum. Only early replacement of the shale-silica matrix prevented the gypsum(?) pseudomorphs from being destroyed during compaction.

The soft, bleached upper Woodford, which also occurs at other localities (L. E. Roberts, personal communication, 1987), is well exposed at the McAlester Cemetery Quarry. The organic matter, which has a low content (Table 2) in the bleached (weathered) shale, was probably oxidized during Quaternary weathering. In thin section this rock is featureless and appears to be mostly poorly crystalline, clay-like material with sparse small quartz particles; to the contrary, X-ray analysis shows that the bleached shale actually contains more silica and less clay than the average fresh shale (Table 1).

Concretions

Three types of concretions have been found. We refer to these as phosphate nodules, pyrite concretions, and calcite concretions. Much of our focus is on description and origin of the phosphate nodules. They are more abundant than the other

Figure 16. Rare *Planolites*-like trace fossils on bedding surface of the Woodford Shale at the McAlester Cemetery Quarry (cf. with plate VIII of Barron and Ettensohn, 1981). The white mineral defining the trails(?) is calcium carbonate.

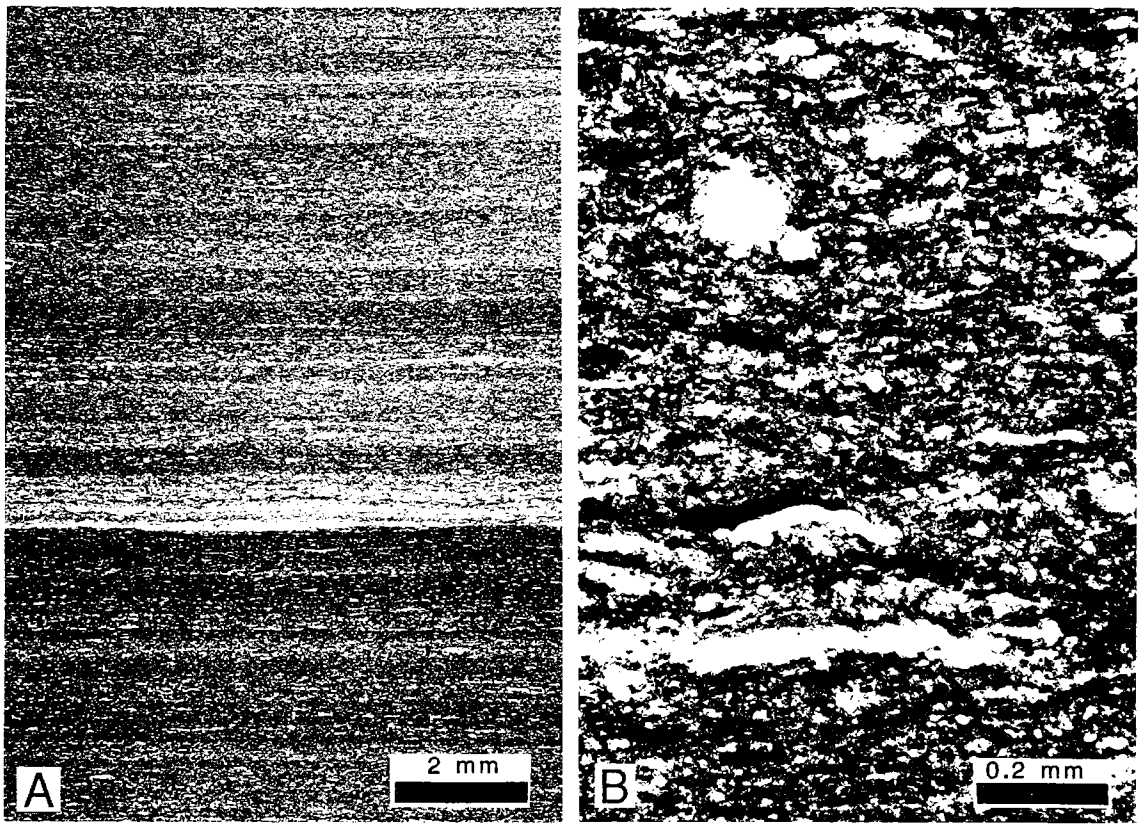

Figure 17. Photomicrographs of Woodford Shale. *A*—Fine laminae (from a silica-rich bed) probably represent seasonal layers; gross color changes may be related to type rather than the amount of organic matter. *B*—Siliceous spheres and flattened silica lenses, probably altered and crushed Radiolaria, are in a matrix of silica and clay, rich in organic matter and containing pale yellow, crushed palynomorphs.

types, and their occurrence is striking. Their presence is a clue that the matrix shale is probably a source rock (as defined by Tissot and Welte, 1984, p. 495). Each of the three types of concretions provides evidence of environmental conditions during deposition and early diagenesis of the Woodford Shale.

Phosphate Nodules

Phosphate nodules occur in abundance in the upper 50 ft of the Woodford at the McAlester Cemetery Quarry. Similar nodules occur at other localities including the upper 55 ft of the Henry House Falls Quarry and the upper 40 ft of the I-35 road cut. At the I-35 road cut, phosphate nodules are in greatest abundance in a zone 11.5–23.0 ft below the top of the Woodford (Spesshardt, 1985). The phosphate nodules are spherical to slightly flattened (Fig. 18) parallel to bedding. At the McAlester Cemetery Quarry they range in diameter as much as ~3.2 in. with a median diameter of ~1.4 in. (Fig. 19). The average ratio of maximum to minimum diameter (i.e., degree of flattening) is ~1.2. Thin sections of the nodules from the weathered zone show considerable (>10%) porosity. At the McAlester Cemetery Quarry, phosphate nodules comprise, overall, approximately 5–10% (by volume; visual estimate; e.g., Fig. 20) of the nodular section. Phosphate nodules appear to be less abundant at the Henry House Falls Quarry and at the I-35 road cut.

The nodules are composed chiefly of carbonate apatite—calcium phosphate with carbonate substituting for phosphate in varying amounts. The general formula is $Ca_5(PO_4,CO_3)_3$. The apatite was described as "brown microcrystalline collophane" by Spesshardt (1985). Quartz forms 7% of one nodule analyzed quantitatively and, judging from petrographic analysis, this value is probably representative. The quartz is probably derived from biogenic silica, detrital quartz being virtually absent.

Most nodules investigated by Spesshardt (1985) in the central Arbuckle Mountains showed little or no internal structure. On the other hand, most nodules at the Henry House Falls Quarry and al-

TABLE 1. — MINERAL COMPOSITION OF TYPICAL WOODFORD SAMPLES FROM X-RAY DATA (in wt%)

Locality[a]	Quartz	K-Feldspar	Dolomite	Apatite	Pyrite	Illite	Kaolin
MC	44.0	0.0	21.9	0.0	1.4	26.1	5.1
MC	69.2	1.1	0.0	0.0	1.2	26.1	2.4
MC	49.1	2.3	4.8	0.0	1.5	35.2	7.1
MC	29.4	0.6	56.3	0.0	0.9	11.2	1.3
MC[b]	71.5	0.0	2.1[e]	0.0	0.0	9.2	15.2
MC[b]	77.0	0.0	0.0	0.2	0.0	15.4	6.9
MC[b]	96.2	0.0	0.1	0.0	0.0	1.7	2.0
HHF	55.1	6.6[d]	3.0	0.0	1.0	27.1	7.3
HHF	59.7	2.5	0.1	0.0	0.4	33.9	3.3
HHF	87.0	0.0	0.0	1.2	0.4	8.1	3.3
HHF[c]	4.6	0.0	0.0	91.8	0.0	2.0	1.2

[a] MC, McAlester Cemetery Quarry; HHF, Henry House Falls Quarry
[b] Weathered shale
[c] Phosphate nodule
[d] Includes 2.8% plagioclase
[e] Calcite

most all nodules at the McAlester Cemetery Quarry exhibited marked concentric banding (Fig. 20). The banding in nodules from the McAlester Cemetery Quarry may have been enhanced by the extensive weathering. Based on the pattern of the banding (or its absence), we separated the nodules into 11 classes (Fig. 21). Nodules in the same stratigraphic horizon and within several feet of each other have similar banding (Fig. 20). The banding, based on microprobe analysis across two banded nodules, is not due to changes in mineralogy. The bands do, however, exhibit textural differences that probably resulted from subtle changes in the chemistry and microbiology of the environment of nodular growth.

Microfossils, especially Radiolaria and sponge spicules, are common throughout the phosphate nodules; Spesshardt (1985), in addition, observed conodonts. Preservation of these fossils, as seen in thin section, is usually good.

About 80% of the nodules that we slabbed (~200) show evidence of a nucleus. All the nodules probably have a nucleus, but because the central part was probably occasionally missed, some nodules do not show one. Many nodules have a thin, elongated (several millimeters) nucleus that is possibly a fragment of a carapace of a crustacean (e.g., *Colpocaris* sp.). The carapace may have been fragmented during predatory activity by ammonoids or fish. Other nodules contain a nucleus that is interpreted to be an operculum (a plate that closed over the aperture) of ammonoids (*Sidetes* sp.). Ammonoids, which inhabited the near-surface oxygenated water may have jettisoned these structures periodically during their growth, or the structures may have become detached from dead, floating ammonoids during decomposition of their soft tissue.

The nucleus of the phosphate nodules was originally investigated by Cooper (1932). Over a period of four years he collected macrofossils, which form the nucleus, from the phosphate nodules of the Arbuckle Mountains (e.g., Fig. 15, right). He estimated that ~1% of the nodules contain good fossil specimens, and he collected 50 specimens of a form that he assigned to the genus *Spathiocaris* and two specimens that he assigned to the genus *Colpocaris*. *Colpocaris*, a crustacean, belongs to the same class (Malacostraca) as shrimp. Cooper also considered *Spathiocaris* to be a crustacean. This genus is now a synonym of *Sidetes* (Rolfe, 1969, p. R329), which is an aptychi—a general term for structures interpreted to be opercula of ammonoid cephalopods.

The Upper Devonian–Lower Mississippian black-shale sequence in eastern Kentucky also

TABLE 2. — ORGANIC GEOCHEMICAL ANALYSES OF SAMPLES OF WOODFORD SHALE

Quarry[a] or Well Name	Sample Description[b]	Distance above base of Fm. (in feet)	Depth below surface (in feet)	Acid insoluble (%)	TOC (%)	S1 (mgHC/ g rock)	S2 (mgHC/ g rock)	S3 ($mgCO_2$ g rock)	Tmax (°C)	HI (mgHC/ g TOC)	EOM (ppm)	SAT (%)	AROM (%)	NSO (%)	Pr/ Ph	Pr/ $n\text{-}C_{17}$	Ph/ $n\text{-}C_{18}$
MC	green shale	45	0	10.2	0.3	0.0	0.0	0.3	nd[c]	nd	42	nd	nd	nd	2.10	0.28	0.27
MC		30	0	17.0	12.9	10.0	101.7	0.1	422	785	10545	6	47	48	1.56	1.22	0.95
MC		50	0	5.2	17.7	11.1	137.4	2.8	429	775	8778	10	39	52	1.42	1.42	1.12
MC		50	0.25	13.8	7.8	5.8	62.5	0.1	427	797	5266	9	44	48	1.49	1.23	0.98
MC		50	0.5	1.0	11.6	7.4	88.8	1.5	433	764	12708	9	45	46	1.38	1.52	1.24
MC		50	1.0	8.8	8.3	4.7	64.7	1.2	436	776	9368	9	45	46	1.34	1.56	1.10
MC		50	1.0	8.4	9.2	7.2	78.3	0.1	426	850	6626	9	37	54	1.57	1.34	0.99
MC		103	0	10.1	15.1	9.8	90.0	2.2	419	595	nd	nd	nd	nd	nd	nd	nd
MC		110	0	2.8	15.2	11.9	104.2	1.7	420	687	12292	17	46	37	1.45	1.35	1.30
MC		175	0	12.0	10.2	10.2	76.7	0.7	414	666	8530	11	42	48	1.44	0.47	0.45
MC		175	0	32.0	6.3	6.7	40.7	0.6	407	649	7790	12	39	49	1.40	1.67	1.70
MC		175	0.3	28.5	7.2	7.3	48.2	0.6	415	674	8623	14	39	48	1.41	1.88	1.99
MC		175	0.5	11.6	10.5	12.7	73.6	0.2	419	701	13427	10	41	49	1.51	0.56	0.51
MC		175	0.7	32.9	5.8	5.8	37.3	1.1	413	642	8147	11	41	48	1.47	1.87	1.90
MC		210	0	7.4	10.1	9.4	77.6	0.0	418	767	10311	11	45	45	1.41	2.18	1.84
MC	weathered (white)	250	0	9.8	0.2	0.0	0.0	0.2	nd	nd	nd	nd	nd	nd	nd	nd	nd
MC	weathered (white)	300	0	7.8	0.1	0.0	0.0	0.0	nd	nd	nd	nd	nd	nd	nd	nd	nd
MC	weathered (white)	350	0	6.1	0.1	0.0	0.0	0.0	nd	nd	nd	nd	nd	nd	nd	nd	nd
HHF	black massive shale[d]	220	0	3.0	13.7	1.2	77.8	1.5	435	569	2595	7	28	65	1.09	0.58	0.59
HHF	cherty shale[d]	220.5	0	1.6	3.2	0.3	16.1	0.3	429	510	883	10	23	67	1.05	0.92	0.95
HHF	dolomitic shale	225	0	63.7	4.3	0.5	27.9	0.6	430	645	1762	6	36	58	0.98	0.58	0.66
Calif. 1 Goodell[e]	green shale		9456-9459	12.0	0.8	1.0	3.9	0.4	435	497	2589	19	31	49	1.08	0.47	0.43
Calif. 1 Goodell			9460	nd	3.7	nd	18.6	0.5	449	501	2186	nd	nd	nd	1.64	0.28	0.25
Calif. 1 Goodell			9457	nd	4.4	nd	23.3	0.8	448	531	nd	nd	nd	nd	nd	nd	nd
Am. Quazar 1 Pate[f]			6431	11.1	4.7	0.7	28.4	0.5	443	607	2395	7	35	58	1.33	0.21	0.19
Texaco 1 Drummond[g]			3050-3052	6.7	12.8	7.2	68.0	1.0	419	529	1061	8	28	64	1.10	0.19	0.20

[a] MC, McAlester Cemetery; HHF, Henry House Falls
[b] Samples are black shale or black cherty shale unless otherwise noted
[c] nd = Not determined
[d] Adjacent beds
[e] 33-5S-2W
[f] 30-5S-6E
[g] 11-6S-6E

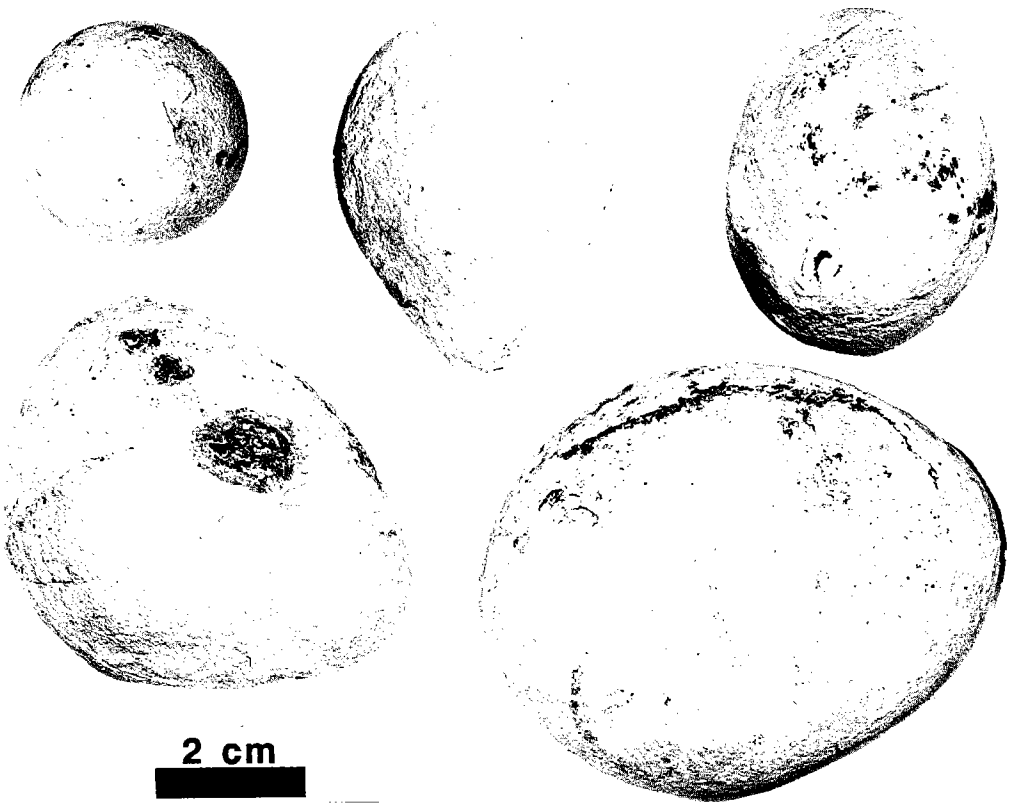

Figure 18. Phosphate nodules from upper 50 ft of the Woodford Shale at the McAlester Cemetery Quarry showing typical sizes and shapes.

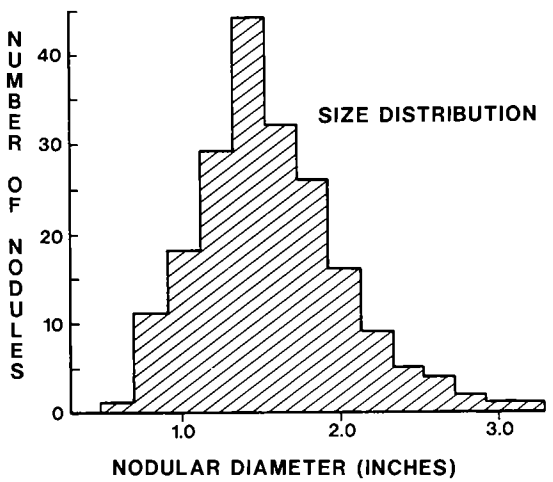

Figure 19. Distribution of diameters of phosphate nodules from McAlester Cemetery Quarry. The distribution may be skewed toward the right because small nodules were probably overlooked during sampling.

contains phosphate nodules in its upper part. These nodules contain various fossils that also served as nuclei. These include small bush-like or rush-like plants as well as stems from trees like *Callixylon*, in addition to remains of animals such as brachiopods, conodonts, crustaceans, and fish (Barron and Ettensohn, 1981, p. 29).

Several origins have been proposed for phosphate nodules within the Woodford Shale. Shead (1963) believed that the nodules formed like "snowballs," by accretion of particles from a bed of phosphate minerals on the sea floor. This hypothesis is unacceptable on a variety of grounds: evidence for bottom currents, for example, is absent. Spesshardt (1985) concluded that the nodules grew by displacement. He cited as evidence that the nodules appear to displace shale above and below. Spesshardt's hypothesis, although reasonable, is also unacceptable. The nodules contain abundant sponge spicules and radiolarian tests that were incorporated as the nodules grew. If the nodules had formed by displacive growth, the microfossils, originally part of the shale, would have been forced out as growth progressed.

Figure 20. Cross section of phosphate nodules in weathered shale at the McAlester Cemetery Quarry, showing typical proportion of nodules to matrix and showing similar banding of adjacent nodules at the same statigraphic level.

At the localities we investigated (Fig. 1), the origin of the nodules can be constrained by the configuration of laminations in the enclosing shale. The three possible configurations are shown diagrammatically in Figure 22. Based on these configurations, deductions can be made about how each of these hypothetical nodules originated.

Figure 22A represents a nodule that must have formed by replacement of consolidated host rock, inasmuch as the laminae are completely undeformed. None of the phosphate nodules we examined showed this configuration.

Figure 22B represents a nodule that had one of two possible origins. The first possibility is that the nodule formed on the sea floor and became buried; then, during compaction, laminae of the soft muds deformed around the hard nodule. The second possibility is that during its growth the nodule displaced the soft, laminated sediment resulting in deformation of the adjacent laminae. This deformation would have then been further enhanced by differential compaction. Displacement of sediment during nodular growth has commonly been proposed.

Figure 22C and Figure 23B show the type of configuration of laminae that we observed. Three origins are possible. The first possibility is that the nodule grew by replacement of the laminated muds, which would have resulted in an initial configuration like Figure 23A, and then, with burial, laminae were deformed by differential compaction resulting in a configuration like Figure 23B. The second possibility, also represented by Figure 23A,B, is that the laminae grew by cementation of the laminated muds, filling the space previously occupied by water. At the time of nodular growth, the sediment would have been about 70–80% water by volume, and the average lamina thickness in the newly deposited muds would have been about 2–3 times the average lamina thickness in the shale. Then, as in the first possibility, laminae were deformed differentially about the nodule during compaction. Only the laminae that project into the midsection of the nodule were undeformed. The third possibility is a combination of the first and second models.

The phosphate nodules of the Woodford Shale in the Criner Hills and southern Arbuckle Mountains formed in the uppermost part of the sediment-column by cementation and to a lesser extent by replacement of the uncompacted siliceous mud. With their formation, the nodules were hard, essentially uncompactible masses. Because the sediment in which they grew was so porous, cementation is likely to have been volumetrically more important than replacement. Also, the phosphate nodules contain abundant Radiolaria tests and abundant sponge spicules, only some of which are replaced by collophane. The microfossils within the nodules as well as the configuration of laminae adjacent to the nodules preclude an origin by displacement during growth.

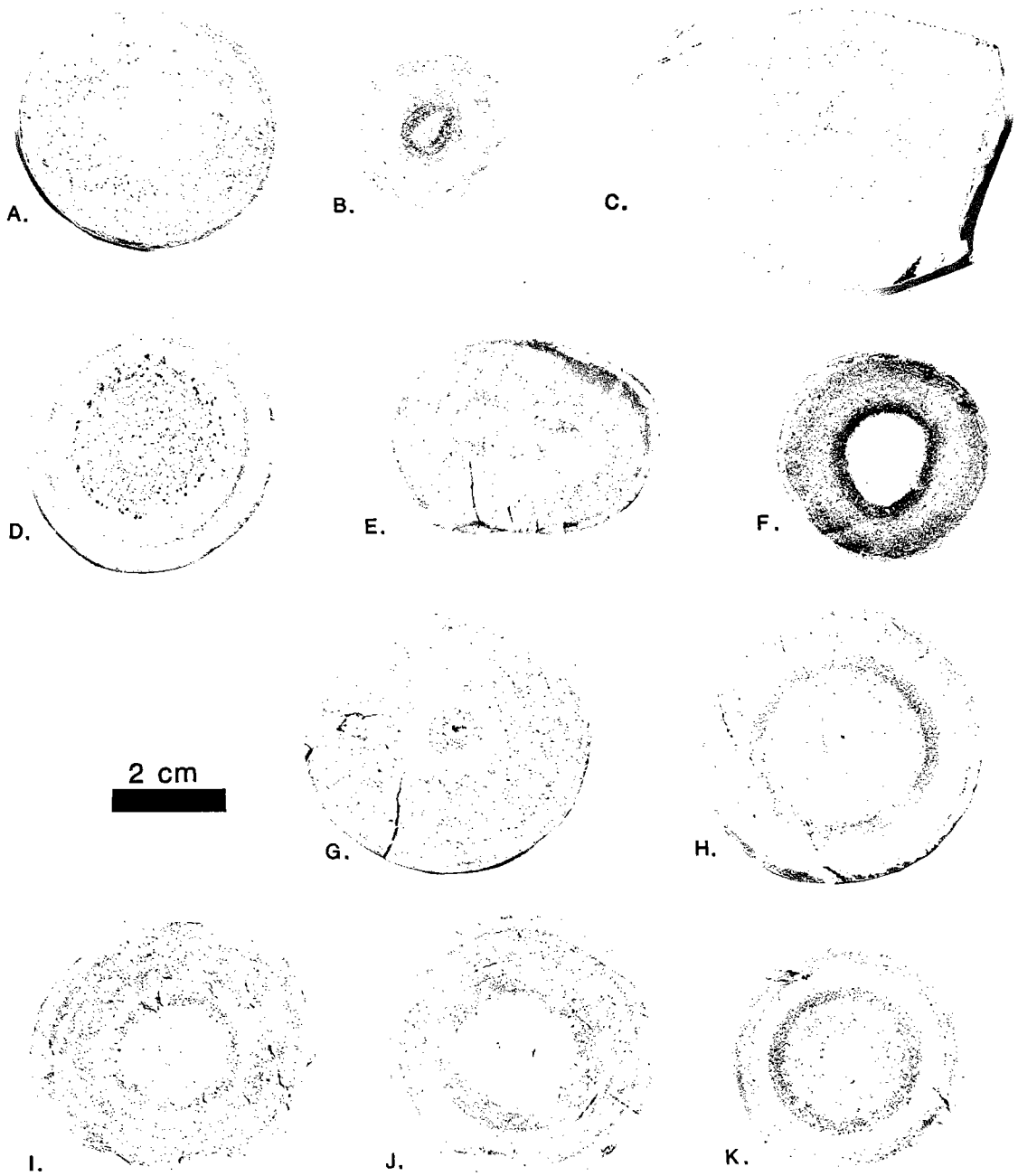

Figure 21. Slabbed phosphate nodules from upper 50 ft at the McAlester Cemetery Quarry, showing 11 varieties of internal structures. The approximate abundance of each type is: *A*—9%, *B*—11%, *C*—5%, *D*—7%, *E*—7%, *F*—25%, *G*—1%, *H*—5%, *I*—11%, *J*—14%, *K*—5%.

An interesting feature associated with some nodules is a zone of silica cementation near those laminae adjacent to the bedding-parallel midsection plane of the nodule. An example is illustrated in Figure 24. This zone was preserved as a zone of high porosity during compaction. The rigid nodule, in a sense, provided a scaffolding in a zone circumscribing the nodule. As a result, compaction in this zone was restricted, and more of the original porosity was preserved than in the same interval away from the nodule. Then, at an intermediate stage of compaction history, silica (probably derived from the dissolution of opaline radiolarian tests) was precipitated in the encircling void-

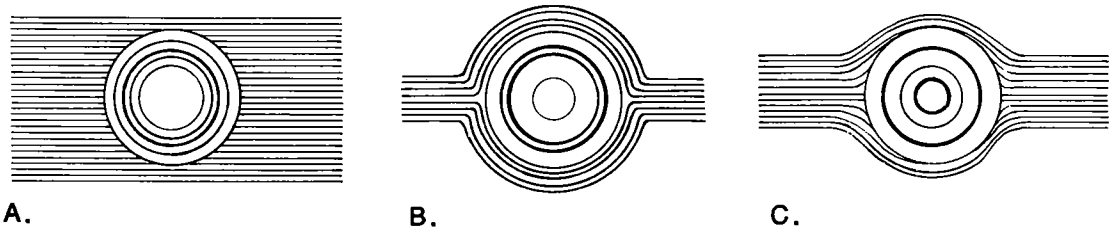

Figure 22. Theoretical configurations of shale laminate in the vicinity of phosphate nodules.

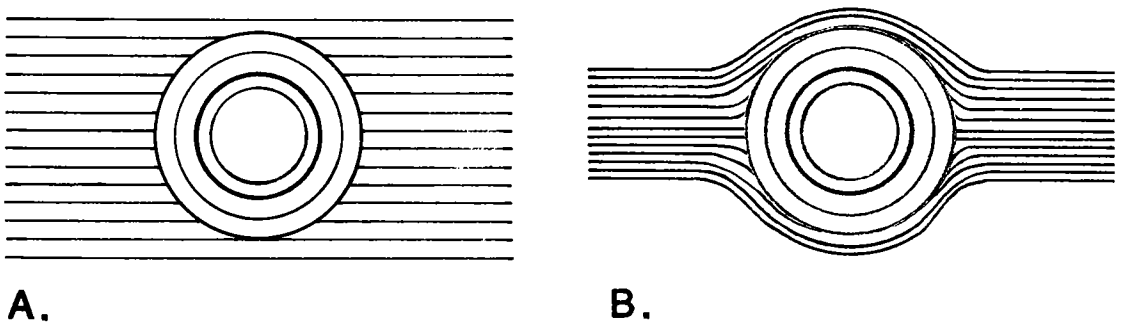

Figure 23. *A*—Diagrammatic representation of a nodule growing by replacement, cementation, or a combination of both, in soft laminated mud prior to compaction. *B*—The same nodule in shale; compaction has greatly reduced the thickness of the shale but not the diameter of the nodule; thus differential compaction has resulted in deformation of laminae about the nodule.

space. (Some carbonate concretions from the Late Devonian Ohio Shale have "... a ridge around the middle composed of material different from the main body" [Clifton, 1957]. This ridge may have originated in the same way as the zone of silica circumscribing some phosphate nodules from the Woodford.)

Our general account of the origin of the nodules follows: Phosphate anions transported by rivers into the Woodford Sea and phosphate transported from deeper waters into shallow waters, via diffusion and possibly via local upwelling, were utilized by phytoplankton as a nutrient. Ultimately, the bodies of the phytoplankton rained onto the sea floor chiefly within fecal pellets of zooplankton. Decomposition of the phytoplankton debris took place on the sea floor and in the shallow sediment by an assemblage of anaerobic bacteria. Decomposition culminated with oxidation of organic matter by sulfate-reducing bacteria, which use sulfate anions as an oxidizing agent and, at greater depth, by methane-producing bacteria, which use carbon dioxide as an oxidizing agent.

The processes of anaerobic oxidation, which probably resulted in degradation of more than one-half of the total organic matter, freed phosphate anions to interstitial water in the shallow sediment. These anions moved by diffusion and within the upward flux of water of compaction. Where the phosphate anions came into contact with calcareous substances suitable for nuclei—such as individuals of the genus *Sidetes*—nodules began to form. In pores surrounding the nucleus, the nodules grew chiefly by precipitation of carbonate apatite.

The reason phosphate nodules occur only in the uppermost part of the Woodford is unknown. Two possibilities are: (1) suitable calcareous nuclei may have been unavailable in the older Woodford; and (2) the concentration of phosphate entering the Woodford Sea may have increased markedly due to, for example, the unroofing of a phosphate-rich unit in the provenance.

Pyrite Concretions

Pyrite concretions are uncommon and occur sporadically throughout the Woodford. Most are almost spherical and as much as 2–4 in. in diameter (Fig. 25). Some are slightly flattened parallel to bedding. Pyrite crystals that form the concretions are of variable size; the outer surfaces of some concretions are smooth because the crystals are small and the outer surfaces of others are a mosaic of coarse crystals (Fig. 25, upper). The pyrite concretions have no obvious nucleus, but two features are typical of their interior (Fig. 25, lower): (1) vague relict bedding, parallel to the long axis; and (2) short (~1 cm) open cracks across the center

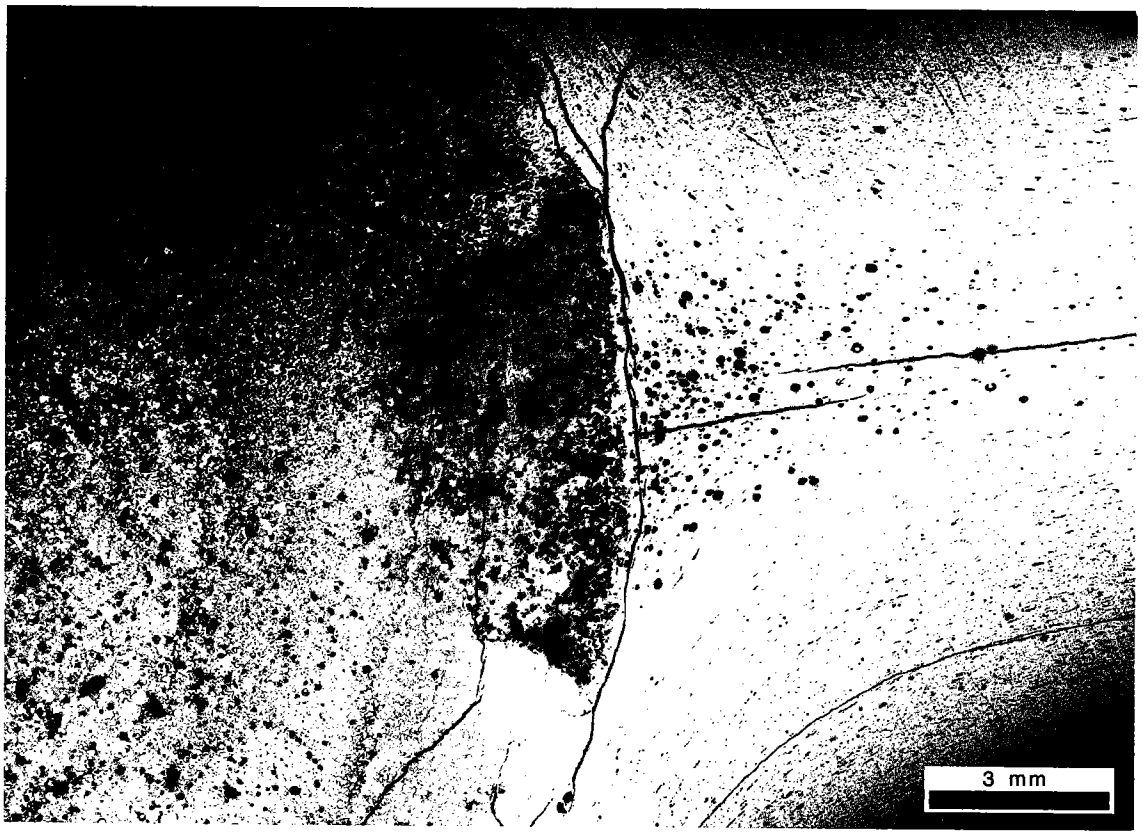

Figure 24. Photomicrograph of a phosphate nodule and adjacent shale showing the zone of silica cement that girdles some nodules.

perpendicular to the relict bedding. These may be tensile features that formed during burial and compaction (cf. Astin, 1986).

The pyrite concretions are a consequence of anaerobic oxidation of organic matter by sulfate-reducing bacteria. Sulfate-reducing bacteria, which function only in the complete absence of oxygen, use the reaction between sulfate (from seawater) and either hydrogen or organic compounds with simple structures (both derived from fermentation of labile organic matter) as a source of energy. By-products of this metabolic process are carbon dioxide (CO_2) and hydrogen sulfide (H_2S) (or their hydrolysis products). If ferrous iron is available, the H_2S reacts with it to form pyrite. Clay minerals are usually a ready source of iron. In the Woodford, pyrite concretions probably formed more commonly in zones that were relatively rich in iron (i.e., shaly zones rather than cherty zones). Sulfate reduction and pyrite formation would have taken place from the sediment surface to a depth at which the source of metabolizable organic matter was depleted or until diffusion of sulfate from seawater was so slow that the sulfate concentration was insufficient to support microbial degradation (probably a depth of feet to tens of feet).

Calcite Concretions

The calcite concretions are spectacular because of their size. The concretions at the McAlester Cemetery Quarry are approximately spherical and average ~5 ft in diameter. We found seven (Fig. 26). We know of no reports of concretions of this type from elsewhere in the Woodford, but large calcite concretions (as much as 13 ft in diameter) have been reported from equivalent Upper Devonian shale in the upper midwestern United States (e.g., Clifton, 1957; Gutschick, 1987). None of the concretions at the McAlester Cemetery Quarry were in place. When encountered during quarrying, they are pushed aside. Based on information from quarrymen, the concretions occur near the base of the zone of phosphate nodules.

The surfaces of some calcite concretions have a coating of calcite spar (Fig. 27). Also, phosphate nodules are sporadically embedded within and on the surface of the calcite concretions (Fig. 27). A 1-in.-diameter core into one of the large concre-

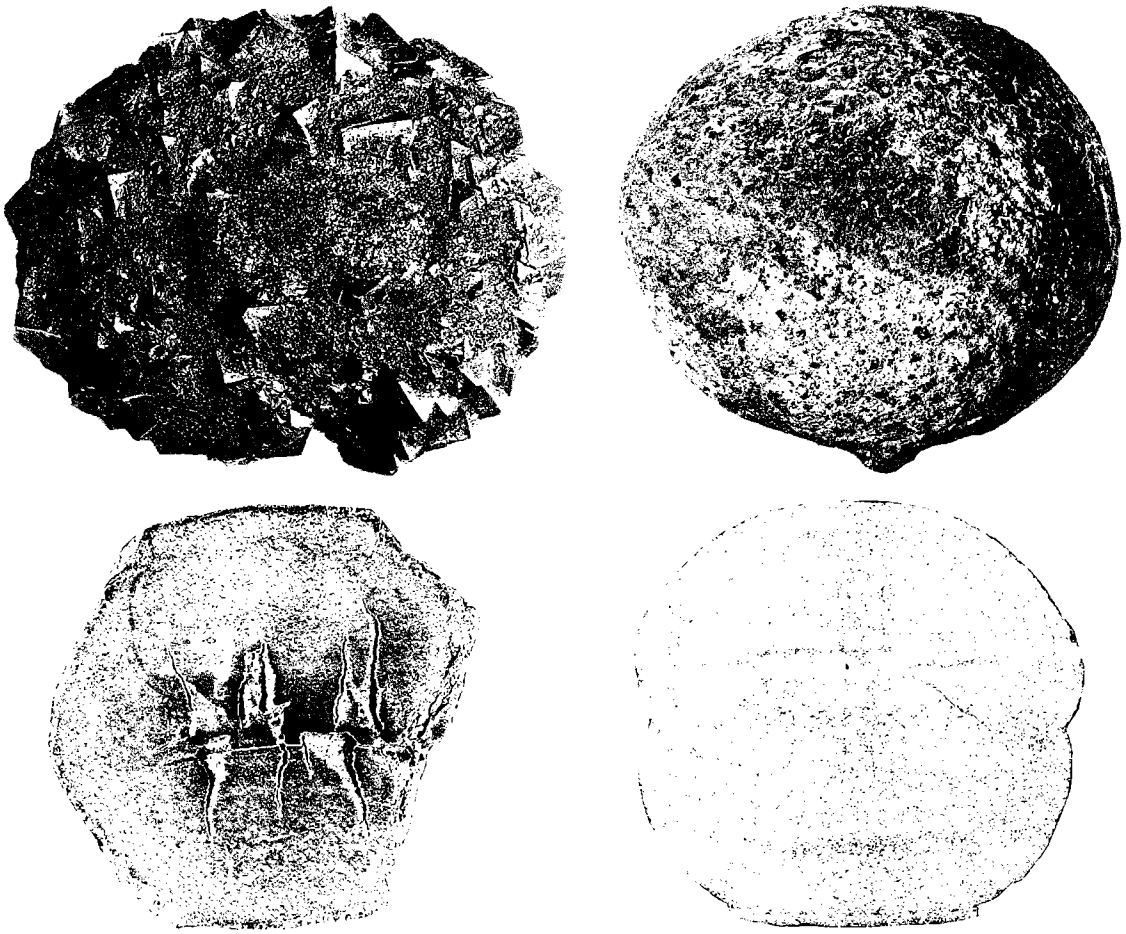

Figure 25. Four different pyrite concretions from the McAlester Cemetery Quarry. The upper two show different crystal sizes; the lower two are slabbed and show tensile features perpendicular to vague relict bedding.

tions: (1) encountered a single phosphate nodule ~2 in. from the surface of the calcite concretion; (2) revealed systematic (but disrupted) "bedding," distinct in the outer portion, but vague toward the center; and (3) did not encounter a nucleus. (A nucleus, however, could easily have been missed by our 1-in. core, since it may not have passed through the center of the concretion.)

The concretions are nonporous and are composed of coarsely crystalline calcite with minor quartz. Ghosts of replaced sponge spicules and Radiolaria are common, occurring in approximately the same abundance as in the phosphate nodules. Pyrite crystals were sparse. Like the phosphate nodules, the calcite concretions formed within shallow sediments by cementation and by replacement.

The strontium and oxygen isotope data, except from samples of the calcite spar rim, are consistent with an early diagenetic origin. The mean $^{87}Sr/^{86}Sr$ value for four samples from the interior of the concretion is 0.70813 (Table 3). This value is within the range of Late Devonian seawater ratios, showing that strontium ions were diffusing into the sediments from the overlying seawater. If the water from which the calcite precipitated is assumed to have had a $\delta^{18}O_{PDB}$ of +30.86‰ (a $\delta^{18}O_{SMOW}$ of 0‰), the mean $\delta^{18}O_{PDB}$ of –2.5‰ for four samples from the interior of one concretion (Table 3) suggests that the temperature at precipitation would have been ~25°C. The temperature of the bottom water probably would have approximated the coolest temperature attained by the surface water in its previous 1 to 50+ yrs. Although this calculated temperature is rather high, it is approximately what we would suspect for the bottom water of the tropical (or subtropical) epeiric sea in the vicinity of the McAlester Cemetery Quarry.

We are uncertain of how to interpret the carbon isotopic data. Judging from $\delta^{13}C$ values between –2.5 and –9.6‰ for samples from the interior of

Figure 26. Calcite concretions, McAlester Cemetery Quarry; seven were exposed in September 1986. The concretions were moved to this area during the quarrying operation.

Figure 27. Sparry calcite-rind on outer surface of a calcite concretion and phosphate nodule, McAlester Cemetery Quarry. Scale in centimeters.

the concretion (Table 3), the concretion might have formed below the zone of sulfate reduction in the zone of methanogenesis (where carbon dioxide was being reduced). Carbonate minerals that precipitated in the zone of methanogenesis would be expected to have carbon enriched in carbon-13 compared to the organic substrate (e.g., Gautier and Claypool, 1984). However, $\delta^{13}C$ values of two samples from the outer part of the concretion (0.5 in. and 2.25 in. from its surface; Table 3) do not fit

TABLE 3. — ISOTOPIC DATA FOR SAMPLES FROM A CARBONATE CONCRETION, MCALESTER CEMETERY QUARRY

Depth from surface (inches)	Percent residue (HCl - insoluble)	$^{87}Sr/^{86}Sr$[a]	$\delta^{13}C_{PDB}$‰	$\delta^{18}O_{PDB}$‰
0.0[b]	0.0	0.70925±3	+5.8	-13.3
0.5	4.2	0.70845±4	-23.8	-1.3
2.25	4.6	0.70867±4	-26.0	-0.3
16.0	5.2	0.70826±4	-2.5	-2.6
23.0	8.1	0.70807±5	-9.6	-2.5
28.0	6.3	0.70807±3	-7.3	-2.5
36.0	17.3	0.70811±4	-7.2	-2.3

[a] Data normalized to NBS 987; $^{87}Sr/^{86}Sr = 0.71014$
[b] Iceland spar on exterior of concretion

this interpretation. They have a mean $\delta^{13}C$ value of –24.9‰, which is typical of calcite precipitated in the zone of sulfate reduction. Such a burial and growth history is unlikely. Alternatively, isotopically light carbonate derived from early thermal maturation of organic matter may have become available in deeper levels of the zone of methanogenesis.

Another interpretation of the isotopically light calcite rim, and the one that we favor, is that much of the carbonate in the interior of the concretion was derived from seawater by diffusion to the growing concretion. This seawater carbonate was isotopically heavy compared to carbonate from sulfate reduction. With burial, permeability of the sediment decreased and less carbonate was able to diffuse to the concretion, and the carbonate making up the outer cortex, the isotopically light carbonate, was derived solely from sulfate reduction.

The final carbonate that precipitated—the surface spar—has a $\delta^{13}C$ of +5.8‰ and a $\delta^{18}O_{PDB}$ of –13.3‰—a marked departure from isotopic values from the interior (only 0.5 in. from the surface). This "rind" of calcite spar is apparently of late diagenetic origin.

ORGANIC GEOCHEMISTRY

The Woodford is so rich a source that it could account for all the known oil in Oklahoma. Nonetheless, geological reasoning and geochemical data suggest that some large oil fields in Oklahoma contain little or no Woodford-generated oil. If we use reasonable values obtained from Woodford samples from the McAlester Cemetery and Henry House Falls Quarries, some simple calculations can be made for oil generation and expulsion. Given an average total organic carbon (TOC) of 10%, a hydrogen index of 500 mgHC/g TOC, complete passage of the Woodford through the oil window, expulsion of 80% (Cooles and others, 1986), and a thickness of 100 ft, the Woodford would expel ~50 million barrels of oil per square mile or ~1.9 billion barrels per township. The American Petroleum Institute estimates that there are 39 billion barrels of oil-in-place in Oklahoma. The Woodford may account for much of this (Comer and Hinch, 1987).

In the Woodford Shale a direct relationship probably exists between the quantity of organic carbon and radioactivity. The Woodford, like many rich source beds, is uraniferous; the ura-

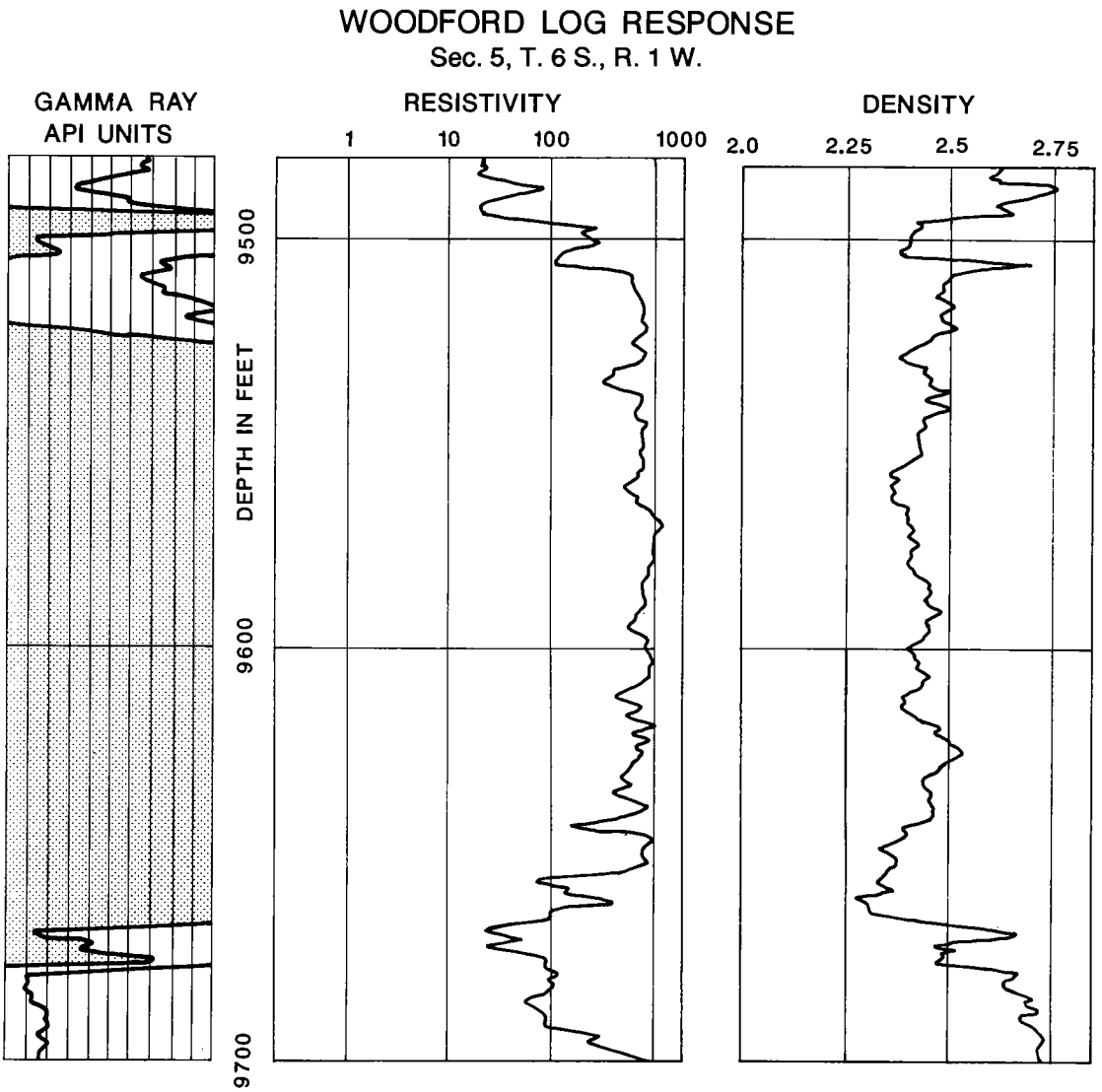

Figure 28. Log of Woodford section from the Criner Hills showing gamma ray, resistivity, and density response.

nium is closely associated with the organic matter. (A yellow crust, which one might expect to be a uranium mineral given the Woodford's radioactive components, is developed on weathered Woodford surfaces. This mineral, which contains no appreciable uranium, is jarosite [$KFe_3(SO_4)_2(OH)_6$], formed from the weathering of pyrite.) Gamma-ray logs show a marked response throughout Woodford sections (Fig. 28). The radioactivity in the lower part of the Woodford is reduced compared to the radioactivity of the middle part (Figs. 28,29); the radioactivity is also lower in the upper Woodford of the two well-sections investigated and at the Henry House Falls Quarry. A similar pattern occurs at the McAlester Cemetery Quarry (Fig. 29), but because of weathering it does not reflect original conditions. Rich source rocks are generally characterized on wireline logs by high resistivities (especially where thermally mature), high radioactivity, low densities, and long traveltimes (Meyer and Nederlof, 1984). The Woodford shows many of these log characteristics (e.g., Fig. 28).

Kerogen

The content of organic carbon in unweathered Woodford Shale at the McAlester Cemetery Quarry ranges from 4–18% (n = 14; Table 2). For comparison, conventional-core samples of Woodford from three wells: the California 1 Goodell (sec. 33, T. 5 S., R. 2 W.), the American Quazar 1 Pate (sec. 30, T.

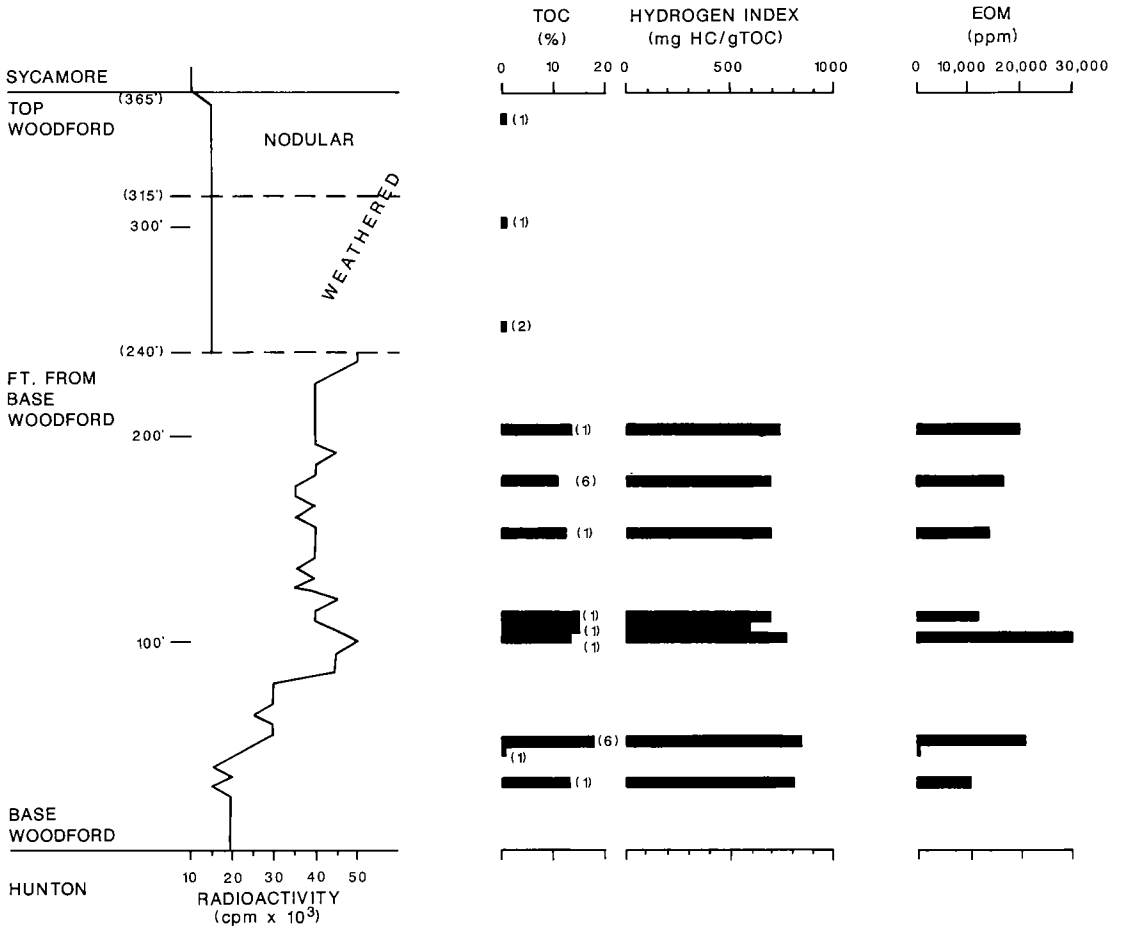

Figure 29. Log of radioactivity at the McAlester Cemetery Quarry; and intermittent values for total organic carbon (TOC), hydrogen index, and extractable organic matter (EOM). Numbers in parentheses represent the number of samples analyzed.

5 S., R. 6 E.), and the Texaco 1 Drummond (sec. 11, T. 6 S., R. 6 E.), have organic carbon contents ranging from 4 to 13% (Table 2). In the upper Woodford in the McAlester Cemetery Quarry the content of organic carbon ranges from 0.1 to 0.2% (Fig. 29; Table 2), a marked reduction due to weathering.

The organic carbon content in the unweathered Woodford is related to lithology. A sample of the green shale (representing ephemeral oxic bottom water) from 45 ft above the base of the formation at the McAlester Cemetery Quarry contains only 0.3% organic carbon (Table 2). At the Henry House Falls Quarry the organic carbon content of a sample of the black massive shale in the phosphatic nodule zone (~220 ft above the base) is 13.7%; that of a sample of the cherty layer immediately above (nominally the same level, at ~220.5 ft) is 3.2%. Five feet above these beds, in a dolomitic layer, the organic carbon content is 4.3% (Table 2). Most intervals analyzed have >3% organic carbon.

Except for the weathered shale and the green shale, the hydrocarbon potential of samples of Woodford that we measured is excellent. Hydrogen indices (HI) range from 500 to >800 mg hydrocarbons/gram of organic carbon (Table 2). Based on carbon-13 NMR, 57–69% of the organic matter in samples (n = 4) of Woodford Shale is of aliphatic character, which supports the Rock-Eval data. The Woodford is, indeed, a rich source rock for oil.

Two other shale sequences, the Sycamore and the Viola, were sampled at the I-35 road cut (Fig. 1A). The amount of organic carbon in the Sycamore (0.7–1.7%) and Viola (2.5–3.5%) shales is consistently lower than that in the Woodford Shale. The hydrocarbon potential of the Sycamore shale (HI = 100–200 mg HC/g TOC) and the Viola shale are also inferior to that of the Woodford Shale, although the potential of the "richest" thin bed at the base of the Viola (HI = 300–580 mg HC/g TOC) is nearly as good as that of the Woodford. In terms of volume, the hydrocarbon potentials of the Sycamore and Viola Formations are small compared to that of the Woodford Shale.

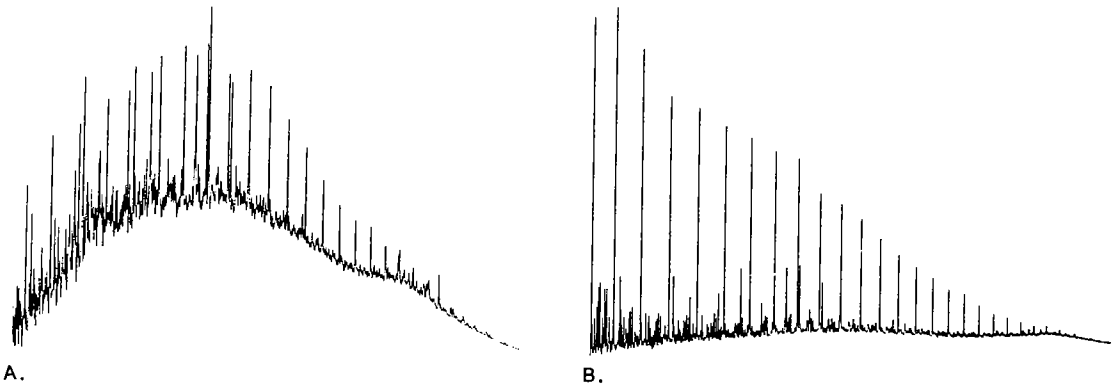

Figure 30. *A*—Gas chromatogram of the saturate fraction of extract from the Woodford Shale (sample from 30 ft above the base), McAlester Cemetery Quarry. *B*—Gas chromatogram of the saturated fraction of an oil sample expelled from the Woodford Shale; J. L. Martin 17 well, Milroy Field, Stephens County, Oklahoma.

Extractable Organic Material

Values of extractable organic matter (EOM) in virtually all samples of dark, unweathered Woodford Shale (Table 2) indicate that it is an excellent source rock for oil. EOM values for most samples range from 1,000 to 13,000 ppm, whereas a greenshale sample from the lowermost Woodford has an EOM of only 42 ppm (Table 2). Values for EOM/TOC are 0.02–0.15 for samples from the McAlester Cemetery Quarry. Assuming no migration in or out of the source rock, as much as 15% of the kerogen has been converted to bitumen. Woodford Shale at this quarry, however, has a low thermal maturity (e.g., the vitrinite reflectance of a sample of preserved wood, possibly suppressed, is 0.34%). Type II kerogen with a maturity this low would usually not generate a significant fraction of bitumen. The Woodford, however, contains kerogen with ~5% sulfur. Such medium-sulfur kerogen has many thermally labile bonds compared to kerogen with low levels of sulfur; thus a significant fraction of bitumen was probably generated at a low level of thermal exposure.

A representative gas chromatogram for the saturated hydrocarbon fraction of the extract from a sample of Woodford Shale from the McAlester Cemetery Quarry is shown in Figure 30A. Most chromatograms of extracts of Woodford Shale from this area show similar distributions of n-alkanes, dominated by low- to medium-molecular-weight compounds and a large elevated base line under the peaks. These distributions and a mean pristane/phytane value of about 1.0–1.5 suggest that the bitumen was derived from organic matter that accumulated in a reducing environment. The gas chromatogram (Fig. 30B) of the saturated hydrocarbon fraction of an oil from the J. L. Martin 17 well (Stephens County, ~30 mi northwest of the McAlester Cemetery Quarry) is similar to that of the Woodford extract (Fig. 30A), except that the saturated fraction of the oil has an elevated baseline under the peaks that is significantly reduced.

Based on an abundance of pristane and phytane relative to normal alkanes (Table 2), and on the elevated base line in the chromatograms, many Woodford extracts probably represent low-maturity samples. The amount of saturated hydrocarbons in extracts of samples of the Woodford Shale is 6–17%, and the amount of nitrogen-sulfur-oxygen (NSO) components is 40–70% (Table 2). These values are typical both of bitumen generated by immature source rocks and of mature bitumen that has undergone biodegradation. Since it is difficult to visualize biodegradation of bitumen in samples of tight, fresh shale from an active quarry, the extracts have probably been generated at low levels of thermal maturity. Biomarker data from extracts of various samples of Woodford Shale are similar, and they resemble biomarker data from samples of Woodford oil. Woodford oil, unfortunately, appears to have no obvious geochemical characteristics that can be used in its unambiguous identification.

Carbon-isotope ratios for samples of kerogen and bitumen of Woodford Shale at the McAlester Cemetery Quarry are listed in Table 4. Values for the samples are similar (approximately –30‰), indicating a uniform depositional environment and a uniform source of organic matter.

Tar Balls and Bitumen-Filled Fractures

"Tar balls" occur in a zone ≤10 ft in thickness ~140 ft from the base of the Woodford at the McAlester Cemetery Quarry. We were unable to locate "tar balls" at the Henry House Falls Quarry or the I-35 road cut. The structures that we call "tar balls" are spherical to oblate, up to ~1 cm in diam-

TABLE 4. — CARBON ISOTOPE RATIOS FOR EXTRACTS OF WOODFORD SHALE, MCALESTER CEMETERY QUARRY

Distance above base of Fm. (in feet)	Depth below surface (in inches)	$\delta^{13}C$‰ whole extract	$\delta^{13}C$‰ SAT	$\delta^{13}C$‰ AROM	$\delta^{13}C$‰ RESINS	$\delta^{13}C$‰ ASPHALTENES	$\delta^{13}C$‰ KEROGEN
30	0	-29.47	-30.28	-30.38	-29.09	nd[a]	-27.86
50	0	-30.01	-30.12	-30.19	-29.77	-29.89	-30.82
50	3	-30.01	-30.20	-30.28	-29.66	nd	-30.58
50	6	-30.21	-30.14	-30.13	-29.82	-29.91	-30.99
50	12	-29.89	-30.25	-30.17	-29.70	-29.83	-30.87
50	12	-29.93	-30.14	-30.25	-29.67	nd	-30.55
110	0	-29.98	-30.14	-30.29	-29.68	nd	-29.37
175	0	-30.00	-30.16	-30.38	-29.62	nd	-29.53
175	0	-29.94	-30.13	-30.38	-29.67	nd	-29.43
175	4	-30.01	-30.15	-30.36	-29.77	nd	-29.83
175	5	-30.10	-30.12	-30.31	-29.82	nd	-29.62
175	8	-29.94	-30.14	-30.36	-29.60	nd	-29.84
210	0	-29.91	-30.29	-30.28	-29.54	nd	-29.15

[a] not determined

eter, and are composed of a solid, shiny, organic material (Fig. 31A). Shale laminae are deflected around the tar balls, showing that the tar was emplaced before substantial compaction. Their smooth, rounded, commonly flattened form suggests that they were deposited as a semisolid material.

The tar balls probably represent remains of oil from a submarine oil seep. During Woodford deposition, oil from an older source (possibly Simpson) seeped onto the sea floor, rose to the surface of the sea, and floated. Ultimately, the oil oxidized into dense tar in small bodies of approximately spherical shape, sank, and became incorporated into the sediment. We do not understand why the tar balls are found only at the McAlester Cemetery Quarry. Perhaps they are present at other localities, but have not yet been observed. If they are not present elsewhere, the paleo-submarine seep was probably close to the Criner Hills locality.

The Woodford Shale is tectonically fractured at the McAlester Cemetery Quarry. Most of the fractures, which are abundant, are open, but some are filled with quartz cement, and some are filled with bitumen (Fig. 31B). Bitumen-filled fractures occur at both the McAlester Cemetery Quarry and the Henry House Falls Quarry.

The tar balls are virtually insoluble; only 3% could be dissolved (Table 5). The tar balls are, therefore, classified as pyrobitumen. Gas chromatography, gas chromatography/mass spectrometry, and carbon isotopic analyses show that the small amounts of extractable organic matter in the tar balls are probably absorbed bitumen from the surrounding Woodford Shale. Insoluble organic material is difficult to characterize. However, based on a carbon isotope ratio 1–2‰ more positive than that of Woodford kerogen (Table 4), the pyrobitumen in the tar balls does not appear to be related to Woodford kerogen. Elemental composition of a tar ball is as follows: C, 62.7%; H, 5.1%; O, 4.1%; N, 0.5%; S, 4.5%; Fe, 1.4%; and ash, 25.5%. When plotted on a diagram of H/C versus (N+S)/O (Hunt, 1978), the tar ball shows a value near the field for asphaltenes and pyrobitumen.

ORIGIN

The Woodford Shale is an extremely rich marine source rock. Such source rocks, uncommon in Phanerozoic sequences, are the product of an unusual set of depositional and diagenetic factors. Much of the organic matter that rained onto the Woodford, chiefly within fecal pellets of zooplankton, was preserved within the sediments. Three factors in particular promoted preservation.

First, the fine grain size of the clay and the radiolarian tests inhibited degradation of organic matter. Because of tortuosity of the diffusion path, the fine-grained sediments decreased the ability of sulfate anions, the principal oxidizing agent, to diffuse into the sediment. Also, organic matter adsorbed onto clay minerals was protected from microbial degradation (Gordon and Millero, 1985).

Second, the anoxic bottom water inhibited degradation of the organic matter. Under anoxic conditions, deposit-feeding metazoans cannot exist.

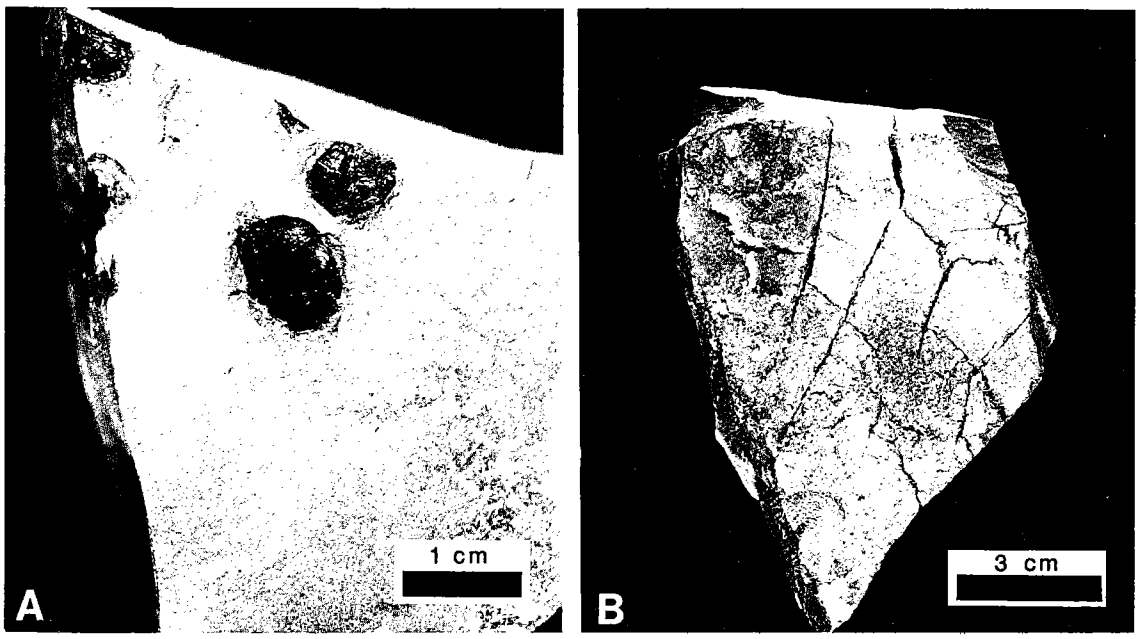

Figure 31. *A*—Tar balls on slab of Woodford Shale, McAlester Cemetery Quarry. *B*—Solid-bitumen-filled fractures exposed on bedding surface of Woodford Shale at the McAlester Cemetery Quarry.

Where present in oxic waters, as Demaison and Moore (1980) have shown, metazoans usually cause virtual elimination of hydrogen-rich organic matter—the type needed for formation of source rocks. Deposit feeders consume some organic debris for their metabolic needs. But, in addition, and probably of greater importance, their feeding activities result in circulation of the organic debris in the uppermost zone of sediments. This results in exposure of the organic debris to molecular oxygen for a longer duration (Demaison and Moore, 1980) and, hence, to greater degradation by microbial agents.

The third preservational factor of major importance is that under anoxic conditions a fraction of the algal organic matter cannot be metabolized by bacteria (see Emerson and Hedges, 1988). Organic matter that persisted in the Woodford sediments, a significant proportion of the total amount deposited, was essentially refractory to bacteria. These organic molecules were large, and they contained linkages that were intrinsically stable and of a variety of types (Emerson and Hedges, 1988). These large organic molecules served as a "trelliswork" to which smaller hydrogen-rich molecules became bound by condensation reactions (e.g., Ishiwatari and Machihara, 1982). Once bound, these hydrogen-rich structures were virtually refractory to anaerobic oxidation.

These preservational factors combined with a slow rate of sedimentation were largely responsible for the relatively large content of hydrogen-rich organic matter. Dilution of organic matter by mineral matter was never excessive. The Woodford Sea in the area of our investigation received only a minor annual input of detrital sediment. Much of the annual "rain" of inorganic sediment had a biogenic origin.

Crucial to the preservation of organic matter in the Woodford sediments and, therefore, to the formation of the rich, Woodford source rock was an anoxic bottom water. How could the bottom waters of the shallow Woodford Sea (and the seas of its laterally equivalent units) have remained anoxic over thousands upon thousands of square miles for millions of years?

Three principal models exist for development of anoxic bottom waters in the Woodford Sea. The most widely known involves versions of the upwelling model (e.g., Barron and Ettensohn, 1981, who used a modified model of Heckel, 1977; and Parrish, 1982). If organic productivity in the near-surface waters were great enough, a rain of organic debris into the bottom water would react with available oxygen faster than oxygen could be replenished. Anoxia would result. In modern oceans, upwelling of deep, nutrient-laden water into the euphotic zone results in extremely large phytoplankton productivity, which, in turn, results in a large rain of plankton debris into deeper waters. Oxidation of this debris may lead to anoxic bottom waters.

North America was thought by Parrish (1982) to be situated on the equator in the Late Devonian so

TABLE 5. — ORGANIC GEOCHEMICAL DATA FOR SELECTED SAMPLES FROM OUTCROPS OF WOODFORD SHALE

Sample Description	Quarry	Acid Soluble (%)	TOC (%)	S1 (mgHC/ g rock)	S2 (mgHC/ g rock)	S3 ($mgCO_2$/ g rock)	Tmax °C	HI (mgHC/ gTOC)	EOM (ppm)	R_o (%)	SAT (%)	AROM (%)	NSO (%)	Pr/ Ph	Pr/ $n\text{-}C_{17}$	Ph/ $n\text{-}C_{18}$
Specimen of *Calamites*(?)	MC	0.0	76.2	19.5	257.3	10.0	387	337	41256	0.34	nd	nd	nd	1.27	1.53	1.33
Tar ball	MC	11.8	49.3	15.3	215.5	4.6	434	437	2800	0.39	16	32	52	1.59	0.86	0.68
Bitumen in fracture	MC	7.5	34.1	10.0	134.9	3.5	425	395	8851	0.77	nd	nd	nd	1.38	1.67	1.27
Bitumen in fracture	HHF	7.7	26.7	9.6	227.9	6.0	431	852	39274	0.20	8	36	55	1.05	0.28	0.31
Bitumen in fracture[a]	MC	19.3	37.1	11.3	195.2	6.7	432	526	10000	nd	4	40	56	1.55	0.70	0.56
Bitumen in fracture[a]	MC	0.9	18.7	10.0	145.4	2.6	431	778	9187	nd	7	52	41	1.44	1.12	0.83
Bitumen in fracture[a]	MC	3.6	17.3	9.0	125.4	2.5	430	723	11050	nd	4	48	48	1.55	1.02	0.77
Phosphate nodule	HHF	88.5	7.4	1.4	24.3	1.3	426	325	nd	nd	nd	nd	nd	nd	nd	nd
Calcite concretion[b]	MC	92.4	1.1	0.4	5.2	0.5	431	482	nd	nd	nd	nd	nd	nd	nd	nd
Calcite concretion[c]	MC	88.1	0.2	0.0	0.1	0.2	435	58	nd	nd	nd	nd	nd	nd	nd	nd
Calcite concretion[d]	MC	89.7	1.0	0.4	4.6	0.5	426	445	nd	nd	nd	nd	nd	nd	nd	nd

[a] Three different samples from approximately 50 ft above base of formation
[b] 2.2 inches from surface of concretion
[c] 23.0 inches from surface of concretion
[d] 36.0 inches from surface of concretion

that the locus of equatorial divergence (equatorial upwelling) was thought to have been over Mexico, New Mexico, northern Texas, Oklahoma, Illinois, and Michigan (as is shown on Fig. 3A). Parrish thought that a band of high phytoplankton-productivity was parallel to either side of the Late Devonian equator, and was directly responsible for the Woodford source rocks. However, Miller and Kent (1986) have shown that previously interpreted Devonian magnetizations actually represent secondary, Late Paleozoic remagnetizations. Their reinterpreted pole positions suggest that the Late Devonian paleoequator actually transected Canada. The Late Devonian Woodford Sea, therefore, might have been subequatorial rather than equatorial. Based on these new data, Witzke (1987) states that an equatorial upwelling scenario for Late Devonian black-shale deposition in cratonic areas of the United States seems untenable.

An oceanic upwelling model, according to Cook (1984), can only be applied to epeiric seas with difficulty. An interpretation that the Woodford and its lateral equivalent units are upwelling deposits probably precludes shallow water such as proposed by Conant and Swanson (1961) for the Chattanooga Shale. The Late Devonian–Early Mississippian sea that transgressed over the North American craton was a classic epeiric sea. Hallam (1981, p. 91) argues that water depths over extensive regions of epeiric seas were appreciably <600 ft. (Similar arguments have been made by Shaw, 1964; Irwin, 1965; and others.) If the water in the Woodford Sea were indeed shallow, major ocean current systems transferring large volumes of water could not have existed (Hallam, 1981, p. 91). Hallam states, "Effectively the only water energy within extensive regions of epicontinental sea would be that of waves generated by local winds."

Phosphate-rich strata, such as those within the upper Woodford, are commonly cited as evidence of upwelling. In theory, upwelling does not appear to be necessary. Also, some phosphorites are clearly not reliable indicators of upwelling (O'Brien and Veeh, 1983).

Woodford black shale and its equivalent black shales (Antrim, Bakken, Chattanooga, New Albany, Ohio Shales, etc.) extend (or extended) over a large part of the interior of the United States. Areas of black shale occur outside Parrish's proposed area of upwelling and have characteristics similar to black shale within the proposed area of upwelling. The upwelling model, although widely advocated for epicontinental seas, appears to have deficiencies when applied to the Woodford Sea.

Another model that might be called upon to account for the anoxic bottom water of the Woodford Sea is that the water was derived from the oxygen-minimum zone of the Late Devonian ocean (e.g., Comer and Hinch, 1981; Jones, 1983). In modern oceans, the oxygen-minimum zone has an oxygen concentration that is reduced, but is usually not anoxic; its top commonly occurs at a depth of 1,500–6,500 ft and it is 650–1,600 ft thick (Schopf, 1980, p. 104). During major highstands such as that of the Late Devonian, the oxygen-minimum zone probably became anoxic. If the top of the oxygen-minimum zone in the Devonian ocean were at a similar depth-range as in modern oceans, the anoxic waters may have been at too great a depth to have transgressed far onto the continents. Also, currents to transport such water into the interior were probably absent. Tyson (1987), on other grounds, argues that epeiric black shales do not represent an expansion of an oxygen-minimum zone into an epeiric sea.

The model we propose, similar to one proposed by Hallam (1981), is that anoxic bottom waters developed when a persistent horizontal barrier within the water mass, a thermocline, prevented transfer of dissolved oxygen from the zone of water near the surface of the sea to the zone of water near the sea floor. Oxygen is incorporated into surface water by solution of atmospheric oxygen and as a by-product of photosynthesis. This dissolved oxygen was prevented from being carried to the bottom water by persistent density stratification of the water mass: the surface, oxygen-bearing water of low specific gravity being unable to sink through the bottom water of higher specific gravity.

The density stratification of the Late Devonian sea probably resulted from vertical temperature differences—warm water of low specific gravity persistently floated on cooler water of higher specific gravity. This situation is typical of present tropical and subtropical oceans of the world. At higher (but nonpolar) latitudes, temperature stratification is seasonal. The Woodford Sea was close to the equator (Fig. 3; Miller and Kent, 1986). Thus persistent thermal stratification of the equatorial or subequatorial Devonian epeiric sea probably existed over a vast area.

The temperature of the water mass below the thermocline (the zone of rapid vertical change in temperature separating the water masses) represented approximately the minimum temperature achieved by surface water during cool climatic events of the Late Devonian. During these events, the surface water, because its specific gravity exceeded that of the underlying water, sank, temporarily introducing oxygen into water just above the sea floor. These cool events were rare, probably occurring cyclically with periods of centuries. The oxygen introduced into the bottom water rarely persisted long enough for a benthic fauna to become established. The trail of an organism on a bedding plane in the McAlester Cemetery Quarry (Fig. 16) is probably that of an organism able to inhabit the sea floor after one of these events.

Oxygen could not be transported to Woodford

sediments from the open ocean by horizontal currents moving beneath the thermocline. Such currents would have been ineffective as a mechanism for transporting oxygen far into the cratonic sea. The shallowness of the Woodford Sea, with its extremely low, oceanward gradient resulted in restricted circulation and damping of tide- and wind-generated currents (see Irwin, 1965; Hallam, 1981). If the Woodford Sea were much shallower or much deeper, however, oxygen in solution might have contacted the sediments, a benthic fauna might have developed, and aerobic sediment-dwelling bacteria might have degraded much of the hydrogen-rich organic matter.

Chiefly because of the anoxic bottom water and the slow rate of sedimentation, rich source beds formed in the Woodford Sea and its laterally associated intracratonic seas over vast areas and for millions of years. Other important source beds may have originated in shallow, tropical to subtropical, epicontinental seas with anoxic bottom waters, with extremely slow sedimentation, and with low phytoplankton productivity.

CONCLUSIONS

1. The Woodford Shale was deposited largely in the Late Devonian as a transgressive unit upon a substantial erosional unconformity.

2. Siliceous- and clay-rich sediments were deposited in equatorial or subequatorial latitudes in a broad intracratonic sea that was deeper to the southeast and shallower to the northwest.

3. The sediments were deposited below storm wave base in an anoxic environment.

4. The depth of the Woodford Sea was probably <500 ft; anoxia was probably maintained by persistent thermal stratification.

5. The shale is typically laminated and composed of silica with lesser but substantial amounts of illite/kaolinite and organic matter. Both the laminations, which are probably seasonal, and the beds are caused by variations in the relative amount of the major constituents.

6. Organic matter usually constitutes between 10 and 30% of the rock volume. The organic matter is predominantly type II kerogen with hydrogen indices generally in the range of 500–800 mg hydrocarbons/gram organic carbon.

7. The accumulation rate was ~0.01 mm per year. This very slow rate was a factor contributing to the large relative amount of organic matter in the formation.

8. Fossil organisms found in the shale represent free swimming or floating forms that sank into the anoxic waters.

9. Known major contributors to the organic matter in the Woodford were *Tasmanites*, Radiolaria, spores, and hystrichosphaerids (acritarchs).

10. Ammonites, judging from the abundance of their aptychi, were common in the Woodford Sea, at least during the time represented by the upper 50 ft of Woodford Shale.

11. Phosphate nodules, and pyrite and calcite concretions in the Woodford are early diagenetic, and each type is directly or indirectly related to microbially aided anaerobic oxidation of organic matter.

12. The Woodford has wire-line log characteristics—high radioactivity, low density, high resistivity, and slow interval velocity—associated with rich source rocks.

ACKNOWLEDGMENTS

Field and laboratory investigations of both the Henry House Falls and the McAlester Cemetery Quarries were a group effort by geologists and geochemists of the Dallas Research Laboratory of Mobil Research and Development Corp., and we gratefully acknowledge the help of our many colleagues. In particular, we thank L. E. Roberts, who led us to many interesting features in the quarries; J. B. Comer of the Indiana Geological Survey, who generously shared his extensive knowledge of the Woodford; G. E. Claypool, who constructively reviewed the manuscript; T. H. McCulloh, who encouraged us to undertake the investigation; and F. B. Roof, who helped prepare the figures. In addition, we thank Wood Marris of Ardmore, Oklahoma, who kindly gave us permission to investigate the McAlester Cemetery Quarry; and B. J. Cardott of the Oklahoma Geological Survey, who provided us with core samples of the Woodford Shale. We also thank Mobil Research and Development Corp. for permission to publish this paper.

REFERENCES

Amsden, T. W., 1960, Stratigraphy, *pt. 6 of* Stratigraphy and paleontology of the Hunton Group in the Arbuckle Mountain region: Oklahoma Geological Survey Bulletin 84, 311 p.

_____1973, Stop 3: Late Ordovician, Silurian, and Early Devonian strata, *in* Ham, W. E. (ed.), Regional geology of the Arbuckle Mountains, Oklahoma: Geological Society of America Guidebook for Field Trip 5, p. 39–43.

_____1975, Hunton Group (Late Ordovician, Silurian, and Early Devonian) in the Anadarko basin of Oklahoma: Oklahoma Geological Survey Bulletin 121, 214 p.

_____1980, Hunton Group (Late Ordovician, Silurian, and Early Devonian) in the Arkoma basin of Oklahoma: Oklahoma Geological Survey Bulletin 129, 136 p.

Amsden, T. W.; and Klapper, G., 1972, Misener sandstone (Middle–Upper Devonian), north-central Oklahoma: American Association of Petroleum Geologists Bulletin, v. 56, p. 2323–2334.

Astin, T. R., 1986, Septarian crack formation in carbonate concretions from shales and mudstones: Clay Minerals, v. 21, p. 617–631.

Barron, L. S.; and Ettensohn, F. R., 1981, Paleoecology of the Devonian–Mississippian black-shale sequence in eastern Kentucky with an atlas of some common fossils: U.S. Department of Energy, Morgantown Energy Technology Center, DOE/ET/12040-151, 75 p.

Clifton, H. E., 1957, The carbonate concretions of the Ohio Shale: Ohio Journal of Science, v. 57, p. 114–124.

Comer, J.B.; and Hinch, H. H., 1981, Petrologic factors controlling internal migration and expulsion of petroleum from source rocks: Woodford–Chattanooga of Oklahoma and Arkansas [abstract]: American Association of Petroleum Geologists Bulletin, v. 65, p. 912.

_____1987, Recognizing and quantifying expulsion of oil from the Woodford Formation and age-equivalent rocks in Oklahoma and Arkansas: American Association of Petroleum Geologists Bulletin, v. 71, p. 844–858.

Conant, L. C.; and Swanson, V. E., 1961, Chattanooga Shale and related rocks of central Tennessee and nearby areas: U.S. Geological Survey Professional Paper 357, 91 p.

Cook, P. J., 1984, Spatial and temporal controls on the formation of phosphate deposits—a review, *in* Nriagu, J. O.; and Moore, P. B. (eds.), Phosphate minerals: Springer-Verlag, New York, p. 242–274.

Cook, T. D.; and Bally, A. W. (eds.), 1975, Stratigraphic atlas of North and Central America: Princeton University Press, 272 p.

Cooles, G. P.; Mackenzie, A. S.; and Quigley, T. M., 1986, Calculation of petroleum masses generated and expelled from source rocks, *in* Advances in organic geochemistry 1985: Organic Geochemistry, v. 10, p. 235–245.

Cooper, C. L., 1932, A crustacean fauna from the Woodford Formation of Oklahoma: Journal of Paleontology, v. 6, p. 346–352.

Demaison, G. J.; and Moore, G. T., 1980, Anoxic environments and oil source bed genesis: American Association of Petroleum Geologists Bulletin, v. 64, p. 1179–1209.

Emerson, S.; and Hedges, J. I., 1988, Processes controlling the organic carbon content of open ocean sediments: Paleoceanography, v. 3, p. 621–634.

Gautier, D. L.; and Claypool, G. E., 1984, Interpretation of methanic diagenesis in ancient sediments by analogy with processes in modern diagenetic environments, *in* McDonald, D. A.; and Surdam, R. C. (eds.), Clastic diagenesis: American Association of Petroleum Geologists Memoir 37, p. 111–123.

Gordon, A. S.; and Millero, F. J., 1985, Adsorption mediated decrease in the biodegradation rate of organic compounds: Microbial Ecology, v. 11, p. 289–298.

Gutschick, R. C., 1987, Devonian shelf-basin, Michigan basin, Alpena, Michigan: Geological Society of America, North-Central Section, Centennial Field Guide, p. 297–302.

Hallam, A., 1967, The depth significance of shales with bituminous laminae: Marine Geology, v. 5, p. 481–493.

_____1981, Facies interpretation in the stratigraphic record: W. H. Freeman, San Francisco, 291 p.

Ham, W. E., 1969, Regional geology of the Arbuckle Mountains, Oklahoma: Oklahoma Geological Survey Guidebook 17, 52 p.

Harland, W. B.; Cox, A. V.; Llewellyn, P. G.; Pickton, C. A. G.; Smith, A. G.; and Walters, R., 1982, A geological time scale: Cambridge University Press, London, 128 p.

Hass, W. H.; and Huddle, J. W., 1965, Late Devonian and Early Mississippian age of the Woodford Shale in Oklahoma, as determined from conodonts, *in* Geological Survey research 1965: U.S. Geological Survey Professional Paper 525-D, p. 125–D132.

Heckel, P. H., 1977, Origin of phosphatic black shale facies in Pennsylvanian cyclothems of Mid-Continent North America: American Association of Petroleum Geologists Bulletin, v. 61, p. 1045–1068.

Heckel, P. H.; and Witzke, B. J., 1979, Devonian world paleogeography determined from distribution of carbonates and related lithic paleoclimatic indicators, *in* House, M. R.; Scrutton, C. T.; and Bassett, M. G. (eds.), The Devonian System: Special Papers in Palaeontology No. 23, p. 99–123.

Hunt, J. M., 1978, Characterization of bitumens and coals: American Association of Petroleum Geologists Bulletin, v. 62, p. 301–303.

Irwin, M. L., 1965, General theory of epeiric clear water sedimentation: American Association of Petroleum Geologists Bulletin, v. 49, p. 445–459.

Ishiwatari, Ryoshi; and Machihara, Tsutomu, 1982, Algal lipids as a possible contributor to the polymethylene chains in kerogen: Geochimica et Cosmochimica Acta, v. 46, p. 1459–1464.

Jones, R. W., 1983, Organic matter characteristics near the shelf-slope boundary, *in* Stanley, D. J.; and Moore, G. T. (eds.), The shelf break: critical interface on continental margins: Society of Economic Paleontologists and Mineralogists Special Publication 33, p. 391–405.

King, P. B., 1977, The evolution of North America: Princeton University Press, 197 p.

Meyer, B. L.; and Nederlof, M. H., 1984, Identification of source rocks on wireline logs by density/resistivity and sonic transit time/resistivity crossplots: American Association of Petroleum Geologists Bulletin, v. 68, p. 121–129.

Miller, J. D.; and Kent, D. V., 1986, Synfolding and prefolding magnetizations in the Upper Devonian Catskill Formation of eastern Pennsylvanian: implications for the tectonic history of Acadia: Journal of Geophysical Research, v. 91, p. 12791–12803.

O'Brien, G. W.; and Veeh, H. H., 1983, Are phosphorites reliable indicators of upwelling?, *in* Suess, Erwin; and Thiede, Jörn (eds.), Coastal upwelling: its sediment record. Part A.—Response of the sedimentary regime to present coastal upwelling Plenum Press, New York, p. 399–419.

Parrish, J. T., 1982, Upwelling and petroleum source beds, with reference to Paleozoic: American Association of Petroleum Geologists Bulletin, v. 66, p. 750–774.

Roberts, C. T.; and Mitterer, R. M., 1990, Laminated black shale-chert cyclicity in the Woodford Formation [abstract]: Oklahoma Geological Survey workshop on source rocks, generation, and migration of hydrocarbons and other fluids in the southern Midcontinent, p. 29.

Rolfe, W. D. I., 1969, Phyllocarida, *in* Moore, R. C. (ed.), Treatise on invertebrate paleontology. Part R.—Arthropoda: Geological Society of America and University of Kansas Press, p. R296–R331.

Ross, R. J.; and others, 1982, The Ordovician System in the United States: International Union of Geological Sciences, Publication No. 12, 73 p.

Schopf, T. J. M., 1980, Paleoceanography: Harvard University Press, Cambridge, 341 p.

Scotese, C. R.; Bambach, R. K.; Barton, Colleen; Van Der Voo, Rob; and Ziegler, A. M., 1979, Paleozoic base maps: Journal of Geology, v. 87, p. 217–277.

Shaw, A. B., 1964, Time in stratigraphy: McGraw-Hill, New York, 365 pp.

Shead, A. C., 1963, Some phosphate nodules and the beds from which they were derived: Proceedings of the Oklahoma Academy of Science, p. 74–76.

Spesshardt, S. A., 1985, Late Devonian–Early Mississippian phosphorite-bearing shales, Arbuckle Mountain region, south-central Oklahoma: Texas Tech University unpublished M.S. thesis, 109 p.

Tyson, R. V., 1987, The genesis and palynofacies characteristics of marine petroleum source rocks, *in* Brooks, J.; and Fleet, A. J. (eds.), Marine petroleum source rocks: Geological Society Special Publication 26, Blackwell Scientific Publications, London, p. 251–261.

Tissot, B. P.; and Welte, D. W., 1984, Petroleum formation and occurrence [second edition]: Springer-Verlag, New York, 699 p.

Urban, J. B., 1960, Microfossils of the Woodford Shale (Devonian) of Oklahoma: University of Oklahoma unpublished M.S. thesis, 77 p.

Von Almen, W. F., 1970, Palynomorphs of the Woodford Shale of south-central Oklahoma with observations on their significance in zonation and paleoecology: Michigan State University unpublished Ph.D. dissertation, 180 p.

Witzke, B. J., 1987, Models for circulation patterns in epicontinental seas applied to Paleozoic facies of North American craton: Paleoceanography, v. 2, p. 229–248.

Organic Geochemistry and Paleogeography of Upper Devonian Formations in Oklahoma and Northwestern Arkansas

John B. Comer
Indiana Geological Survey

ABSTRACT.—The study of Upper Devonian formations in Oklahoma and Arkansas was undertaken to document the regional petroleum generation and expulsion history of these well-known hydrocarbon source beds. Paleogeographic implications derive from mapping organic geochemical data, such as organic-matter type, richness, and thermal maturity, in conjunction with stratigraphic and lithologic data. Data from 251 core and 191 outcrop samples covering an area of roughly 10^5 mi^2 provided the basis for the following observations.

Upper Devonian formations in most parts of Oklahoma and northwestern Arkansas are excellent petroleum source rocks with prolific hydrocarbon-generating capability. Exceptions occur in basal siliciclastic units and in the core area of the Ouachita tectonic belt where less organic-rich rocks (light-colored shale, chert, siltstone) are common.

In central and southern Oklahoma, Upper Devonian black shales are rich oil source rocks (6.8 ± 4.2% TOC) at an early stage of hydrocarbon generation. Seventy to 85% of the commercial oil reserves in the region (~15×10^9 bbl) correlates with bitumen from these source beds. The largest reserves of Devonian oil are along the basin margin, following the trend of oil source rocks that are least thermally mature. Although some of the oil migrated from more mature sections buried deeper in adjacent basins, much of the oil was expelled from local source beds at an early oil-generation stage.

In the Ozark uplift, Upper Devonian black shale contains less organic matter (3.5 ± 1.7% TOC) because of dilution by siliciclastic sediment. Type-II and type-III kerogens that are present document the contribution of marine and terrestrial organic matter. Although the kerogen reached the early to main stage of oil generation, catagenesis is now arrested because of the shallow depth of the source rock and the normal thermal gradient. Trapping conditions are not favorable here because both the source rocks and formations with reservoir potential crop out and are mostly unconfined.

Upper Devonian rocks in the Ouachita core area and locally in the deepest parts of the Arkoma and Anadarko basins have been metamorphosed and no longer have significant hydrocarbon-generating potential. Elsewhere in the Anadarko basin, age-equivalent source rocks are actively generating gas.

Upper Devonian strata in the Ouachita frontal zone are rich oil-prone source rocks (6.8 ± 5.4% TOC) at an early stage of oil generation. Significant hydrocarbon accumulations are possible at depth along the northwestern and western margin of the Ouachita tectonic belt.

Regional variations in organic richness and type reflect the Late Devonian paleogeography. The allochthonous Ouachita core area represents a deep trough in which open ocean circulation prevailed and that received abundant biogenic silica in a zone of oceanic upwelling and minor clastic sediment from distal source areas. The Anadarko basin was a linear trough that received terrigenous silt and terrestrial organic matter from a northwestern source area (Transcontinental Arch). Terrigenous sediment was transported southeastward along the basin axis, while the flanks were bypassed and distal regions received pelagic marine sediment in the form of biogenic silica and type-II organic matter. Increased proportions of terrestrial organic matter found along the Nemaha and Ozark uplifts indicate that they were positive topographic features during Late Devonian time.

INTRODUCTION

This report is a regional synthesis of organic geochemical data for Upper Devonian source rocks in Oklahoma and northwestern Arkansas (Fig. 1). The report includes an evaluation of organic richness, thermal maturity, and oil- versus gas-generating potential, and presents a series of contour maps documenting the geochemical characteristics in the study area. Also, a model of Late Devonian paleogeography is presented, based on regional and stratigraphic variations in

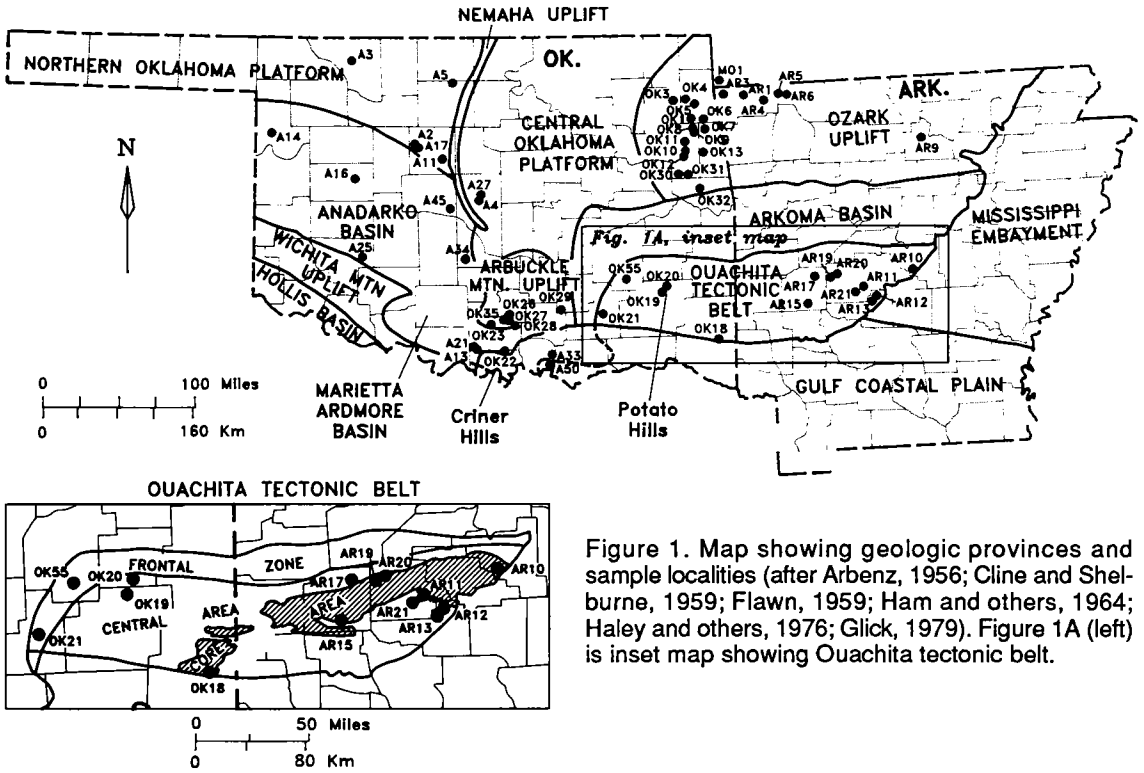

Figure 1. Map showing geologic provinces and sample localities (after Arbenz, 1956; Cline and Shelburne, 1959; Flawn, 1959; Ham and others, 1964; Haley and others, 1976; Glick, 1979). Figure 1A (left) is inset map showing Ouachita tectonic belt.

the organic geochemistry and petrology of the source beds.

The present report is largely an outgrowth of research sponsored by Amoco Production Co. to investigate petrologic factors that control expulsion of oil from source rocks (Comer and Hinch, 1987). Geochemical and petrologic data bearing on source-rock quality and related aspects of geologic history are summarized in this report.

DATA AND METHODS

Table 1 is a list of the core and outcrop localities sampled for this study, and Table 2 summarizes the geochemical data. In Figure 1 and Tables 1 and 2, sample localities and field numbers for cores begin with "A," whereas outcrop samples begin with either "OK" for localities in Oklahoma, "AR" for localities in Arkansas, or "MO" for localities in Missouri. The data in Table 2 are the means and standard deviations (1σ) for the geochemical data obtained at each of the 16 core and 43 outcrop localities shown in Figure 1. Maturity data are not expected to vary significantly at a given locality, because there are no significant unconformities in the Upper Devonian section. Although vertical variations in organic richness and type are observed, continuous sedimentation under consistent environmental conditions apparently prevailed throughout the epoch (Freeman and Schumacher, 1969; Amsden and Klapper, 1972; Amsden, 1975,1980). Consequently, samples from a given section can be viewed as having had similar depositional and diagenetic (burial) history. The degree of vertical variability within a section is indicated by the standard deviations listed in Table 2.

Data comprising the means in Table 2 include 300 total organic carbon (TOC) analyses, 257 Rock-Eval analyses, 181 solvent extract analyses (packed column and gas chromatography), 164 elemental analyses (C, H, O, N) of isolated, solvent extracted kerogen, and 115 vitrinite reflectance analyses. In addition, 181 slides of separated kerogen were visually analyzed, 185 thin sections were prepared and examined, and 50 samples were analyzed by scanning electron microscopy (SEM). A total of 251 core samples and 191 outcrop samples are represented covering an area of ~10^5 mi^2.

GEOLOGY AND ORGANIC GEOCHEMISTRY

The rock units studied include Woodford Shale, Chattanooga Shale, and the middle division of the Arkansas Novaculite. These strata are mostly Late Devonian in age but range from late Middle Devonian (Givetian) to Early Mississippian (Kinderhookian) (Hass and Huddle, 1965; Amsden and others, 1967; Amsden and Klapper, 1972; Amsden

TABLE 1. — CORE AND OUTCROP LOCALITIES

OKLAHOMA CORES

Map symbol	Depth (ft)	Company	Well	County	Location
A2	8,310–8,330	Calvert	#1 Bertie	Kingfisher	Sec. 35, T19N, R9W
A3	6,190–6,207	Calvert Midamerica	#2 Bloyd	Woods	Sec. 21, T27N, R15W
A4	6,477–6,486	Jones & Pellow	#1 Boyd	Oklahoma	Sec. 28, T12N, R2W
A5	6,103–6,113	Pan American	#1 Lowenhaupt	Grant	Sec. 34, T25N, R5W
A11	7,545–7,549	Cleary	#1-21 Gilbert	Kingfisher	Sec. 21, T17N, R6W
A13	9,456–9,460	California Oil	#1 Goodell	Carter	Sec. 33, T5S, R2W
A14	14,323–14,342	Lone Star	#1 Hanan	Ellis	Sec. 6, T19N, R24W
A16	14,251–14,267	Glover Hefner Kennedy	#1 Hoffman	Custer	Sec. 1, T14N, R16W
A17	8,521–8,534	Pan American	#1 York	Kingfisher	Sec. 13, T18N, R9W
A21	8,979–9,021	California Oil	#1 Mullen et al.	Carter	Sec. 29, T5S, R2W
A25	757–761	Columbia Fuel	#1 Rainy Mtn.	Kiowa	Sec. 23, T6N, R15W
A27	6,246–6,283	Gulf	#1 Schroeder	Oklahoma	Sec. 3, T12N, R2W
A33	3,052–3,074	Texaco	#1-K Drummond	Marshall	Sec. 11, T6S, R6E
A34	8,962–8,969	Gulf	#1 Dyer	McClain	Sec. 20, T6N, R3W
A45	8,515–8,524	Apexco	#2 Curtis	Canadian	Sec. 27, T11N, R5W
A50	5,290–5,320	Gulf-Conoco	#1-26 Pershica	Marshall	Sec. 26, T7S, R5E

(continued on next page)

1975,1980). The characteristic and dominant lithology is black shale, but chert, dolomite, sandstone, siltstone, and light-colored shale locally are common (Harlton, 1956; Amsden and others, 1967; Amsden, 1975,1980).

In the southern Midcontinent, Devonian black shale is known to be a petroleum source rock based on numerous oil-to-rock correlation studies (Brenneman and Smith, 1958; Hunt, 1961; Welte and others, 1975; Lewan and others, 1979; Winters and others, 1983; Iztan, 1985; Reber, 1988,1989; Burruss and Hatch, 1989; Philp and others, 1989; Rice and others, 1989). Recent estimates are that 70–85% of the oil produced in central and southern Oklahoma (on the order of 15×10^9 bbl) originated in the Upper Devonian Woodford Shale (Comer and Hinch, 1987; Philp, 1987).

Upper Devonian rocks typically contain very high concentrations of organic matter (Curiale, 1983; Sullivan, 1985; Comer and Hinch, 1987). The mean TOC content for the region is 5.4 wt% based on data from 300 samples representing the 59 localities shown in Figure 1 (Table 3). Individual samples range from <0.1 wt% TOC (i.e., below the detection limit) in some chert beds from the Ouachita core area to 26 wt% TOC in a highly compacted black shale from the Arbuckle Mountain uplift (locality OK35). The TOC data are not normally distributed but are strongly skewed toward the high TOC value.

Upper Devonian strata throughout the region contain predominantly oil-prone type-II kerogen representing a range of thermal maturities from marginally immature to metamorphic (Fig. 2). The lowest maturities are found in the Arbuckle Mountain uplift and on uplifted blocks in the Marietta–Ardmore basin (e.g., Criner Hills; OK22) (Fig. 2). The highest maturities are found in the Ouachita core area (Fig. 2). Most of the Upper Devonian source beds sampled for this project are in the oil or gas windows (Fig. 2). Present burial depths of the cored intervals (Table 1) are close to maximum burial depths estimated for the region (Cardott and Lambert, 1985; Schmoker, 1986; Cardott, 1989), indicating that Devonian source beds are actively generating hydrocarbons at most places in the subsurface. In contrast, sections that crop out are too shallow and cool to be actively generating petroleum by natural thermal-catalytic processes.

REGIONAL DISTRIBUTION OF SOURCE BEDS

Base Map

Figure 3 is the base map used for contouring the source rock data. Upper Devonian black shale is missing from the Wichita Mountain uplift and Hollis basin in southwestern Oklahoma, along parts of the Nemaha uplift in central Oklahoma, on parts of the Arbuckle Mountain uplift in south-central Oklahoma, and from much of the Ozark uplift in northern Arkansas (Fig. 3). Distribution of Upper Devonian strata beneath the Cretaceous overlap in Arkansas and southeastern Oklahoma was not mapped for this study.

TABLE 1. — *Continued*

OUTCROPS

Map symbol	County	Location
		Arkansas
AR1	Benton	Sec. 12, T20N, R31W (Hwy 71 at Belle Vista)
AR3	Benton	Sec. 1, T20N, R33W (Gravette)
AR4	Benton	Sec. 12, T19N, R29W (Hwy 12 5.5 mi. east of Rogers)
AR5	Carroll	Sec. 10, T20N, R27W (Beaver Dam)
AR6	Carroll	Sec. 15, T20N, R26W (Eureka Springs)
AR9	Stone	Sec. 21, T15N, R11W (Hwy 87 at Gayler Cemetary)
AR10	Pulaski	Sec. 28, T1N, R13W (I-430, mile post 2)
AR11	Garland	Sec. 21, T2S, R18W (Marvern Minerals Co. tripole mine)
AR12	Hot Springs	Sec. 14, T3S, R17W (Chamberlain Creek barite mine)
AR13	Hot Springs	Sec. 36, T3S, R18W (Remmel Dam)
AR15	Montgomery	Sec. 18–19, T4S, R24W (Caddo Gap)
AR17	Montgomery	Sec. 14, T1S, R24W
AR19	Garland	Sec. 3, T1S, R22W
AR20	Garland	Sec. 5, T2S, R21W (Hwy 298 at Smoking Hole)
AR21	Garland	Sec. 33, T2S, R19W (Hot Springs)
		Missouri
MO1	McDonald	Sec. 15, T21N, R33W
		Oklahoma
OK1	Delaware	Sec. 21, T20N, R24E (Hwy 33 3.5 mi. east of Kansas)
OK3	Mayes	Sec. 15, T22N, R21E (Spavinaw Dam)
OK4	Delaware	Sec. 14, T22N, R22E (north of Lake Eucha Dam)
OK5	Delaware	Sec. 26, T22N, R23E (Hwy 10 at Lake Eucha)
OK6	Delaware	Sec. 25, T20N, R24E (Hwy 33 at Flint Creek)
OK7	Adair	Sec. 7, T19N, R24E (Winset Hollow)
OK8	Cherokee	Sec. 23, T19N, R23E (Hwy 10)
OK9	Cherokee	Sec. 26, T19N, R23E (Hwy 10)
OK10	Cherokee	Sec. 12, T17N, R22E (Hwy 10)
OK11	Cherokee	Sec. 13, T18N, R22E (Hwy 10)
OK12	Cherokee	Sec. 26, T17N, R22E (Hwy 51)
OK13	Adair	Sec. 7, T17N, R24E (Hwy 62)
OK18	McCurtain	Sec. 31, T5S, R25E (Hwy 259)
OK19	Pushmataha	Sec. 1, T2N, R19E (Potato Hills)
OK20	Latimer	Sec. 31, T3N, R20E (Potato Hills)
OK21	Atoka	Sec. 14, T2S, R11E (Hwy 7 at Black Knob Ridge)
OK22	Carter	Sec. 36, T5S, R1E (Criner Hills)
OK23	Carter	Sec. 30–31, T2S, R1E (Henry House Creek)
OK26	Murray	Sec. 1, T2S, R2E (Hwy 110 2 mi. north of Dougherty)
OK27	Murray	Sec. 1, T2S, R2E (Hwy 110 0.25 mi. north of Dougherty)
OK28	Carter	Sec. 4, T3S, R3E (east of Gene Autry)
OK29	Coal	Sec. 22, T1S, R8E (north of Wapanuka)
OK30	Cherokee	Sec. 1, T14N, R21E
OK31	Cherokee	Sec. 32, T14N, R22E
OK32	Sequoyah	Sec. 10, T13N, R23E
OK35	Carter	Sec. 25, T2S, R1E (I-35, mile post 44)
OK55	Pittsburg	Sec. 4, T2N, R15E (Indian Nations Turnpike)

TABLE 2. — DATA BASE FOR REGIONAL MAPS

		Rock-Eval		Solvent extract		Kerogen					
Map symbol	TOC wt%	HI S_2/TOC (mg/g)	PI S_1/S_1+S_2	C_{15+} saturated hydrocarbons Total bitumen (mg/g)	Bitumen TOC (mg/g)	C wt%	H wt%	Atomic H/C	Atomic O/C	Vitrinite reflectance R_o(%)	Morphology
A2	8.2±2.3	310±70	0.04±.01	0.38±.02	40±10	85±1	6.3±.2	0.88±.01	0.05±.01	0.81±.0	Mixed
A3	5.4±1.1	580±60	0.08±.01	0.53±.15	30±10	83±1	7.3±.3	1.04±.04	0.06±.01	0.50±.04	Amorphous
A4	8.8±2.2	610±70	0.08±.02	0.33±.08	50±20	82±1	7.5±.1	1.11±.02	0.08±.01	0.38±.01	Amorphous
A5	2.9±0.6	—	—	0.74±.02	70±0	86±0	6.0±.1	0.83±.01	0.05±.01	0.72	Amorphous
A11	7.9	540	0.03	0.30	30	83	7.4	1.07	0.06	0..56	Amorphous
A13	6.6±1.8	480±110	0.06±.01	0.22	60	78	7.2	1.12	0.11	0.50±.04	Amorphous
A14	1.0±0.6	10±10	0.37±.10	0.50±.13	20±10	90	4.3	0.58	0.03	2.33	Structured
A16	5.8±2.5	20±10	0.19±.13	0.10±.03	<10±<10	91±1	4.4±.0	0.59±.00	0.01±.01	1.91±.03	Structured
A17	7.1±3.5	310±40	0.07±.02	0.31	30	74	6.5	1.06	0.16	0.72	Amorphous
A21	5.5±3.9	460±60	0.05±.02	0.26±.05	60±20	84±1	7.6±.0	1.09±.04	0.05±.01	0.51±.01	Amorphous
A25	8.1±1.7	400±40	0.03±.01	—	—	—	—	—	—	0.61±.03	Amorphous
A27	9.3±3.7	500±160	0.03±.02	0.37±.07	40±10	83±3	7.9±.2	1.16±.03	0.06±.03	0.40±.01	Amorphous
A33	7.7±3.7	740±60	0.06±.02	0.34±.07	40±10	82±1	7.7±.1	1.14±.01	0.07±.01	0.46±.05	Amorphous
A34	3.9±2.5	430±250	0.08±.02	0.43±.06	70±10	83±0	7.6±.1	1.09±.01	0.06±.00	0.41±.01	Amorphous
A45	6.7±1.7	510±60	0.07±.03	0.38±.05	50±10	85±0	7.0±.2	0.99±.02	0.05±.01	0.60±.01	Amorphous
A50	0.9	230	0.03	0.14	260	—	—	—	—	0.67	Mixed
AR1	2.1	250	0.33	0.52	250	87	6.6	0.91	0.03	1.11	Mixed
AR3	2.5±1.1	300±30	0.24±.04	0.42	150	89	5.5	0.75	0.03	1.10	Mixed
AR4	2.3±0.6	260±50	0.11±.02	0.44	110	86	5.6	0.78	0.05	0.85	Mixed
AR5	4.7±2.1	450±230	0.10±.08	0.35±.03	110±40	86±1	7.1±.0	0.99±.01	0.04±.01	0.56±.02	Amorphous
AR6	2.1	300	0.05	0.52	100	83	6.5	0.94	0.08	0.57	Structured
AR9	3.5±2.1	200±100	0.40±.03	0.40±.08	30±10	84±2	6.3±.9	0.89±.11	0.06±.03	0.83±.05	Amor/mix/struc
AR10	0.1±0.0	60±10	0.28±.13	—	80	69	3.0	0.51	0.29	—	—
AR11	1.6±1.9	40±70	0.37±.22	—	<10	93	1.0	0.13	0.03	3.66±.21	Amorphous
AR12	1.0±1.7	60±80	0.27±.14	—	10±10	90	1.1	0.15	0.05	4.59	Mixed
AR13	0.1±0.0	30±10	0.17±.02	0.01	310	86	2.5	0.35	—	—	—
AR15	1.4±1.2	20±40	0.21±.14	—	20±30	78±3	2.2±1	0.33±.01	0.16±.03	2.88±.16	Amorphous
AR17	0.1±0.1	30±30	0.21±.06	—	—	—	—	—	—	—	Mixed
AR19	0.6±0.1	10±0	0.13±.08	—	—	—	—	—	—	—	—
AR20	1.8±2.3	80±110	0.20±.21	—	—	—	—	—	—	—	—
AR21	1.3±0.2	<10±<10	0.42±.21	—	—	—	—	—	—	3.62	Amorphous
MO1	2.7±0.1	160±50	0.33±.17	0.58±.01	170±00	88±1	5.4±.1	0.75±.01	0.04±.00	0.84±.05	Amorphous
OK1	3.2	150	0.36	—	—	—	—	—	—	1.57	Mixed
OK3	3.3±2.2	190±160	0.12±.00	—	—	—	—	—	—	0.94±.26	Mixed/struc
OK4	3.2±0.1	240±60	0.12±.06	—	—	—	—	—	—	1.01±.04	Mixed
OK5	4.4±0.8	320±110	0.12±.02	—	—	—	—	—	—	1.00	Amorphous
OK6	3.2±0.6	90±40	0.16±.04	0.55	60	81	4.4	0.66	0.12	1.20±.08	Mixed
OK7	2.6	40	0.09	—	—	—	—	—	—	—	Mixed
OK8	3.7±0.5	210±20	0.19±.08	—	—	—	—	—	—	1.20±.07	Mixed
OK9	2.8±0.1	170±10	0.12±.02	—	—	—	—	—	—	1.28±.08	Mixed
OK10	4.9±0.2	200±10	0.26±.02	0.54±.01	60±20	89±4	7.0±2.5	0.96±.37	0.02±.01	1.18±.09	Amorphous
OK11	5.4±1.0	130±110	0.21±.03	0.48±.02	50±40	89±1	5.1±.6	0.69±.07	0.02±.01	1.05±.09	Amorphous
OK12	3.0±2.3	160±20	0.23±.04	0.65±.16	70±20	87±2	5.0±.3	0.68±.02	0.04±.03	1.20±.13	Amorphous
OK13	4.4±1.5	130±10	0.26±.04	0.54±.06	60±10	87±3	4.8±.7	0.67±.08	0.05±.04	1.11±.10	Amorphous
OK18	2.2	<10	0.83	0.06	20	95	0.8	0.10	0.02	—	—
OK19	1.0	190	0.07	0.16	40	76	6.0	0.95	0.15	0.65	Amorphous
OK20	7.0±12.0	—	—	0.29	100±90	81	7.7	1.13	0.08	0.69	Amorphous
OK21	3.2±4.1	490±150	0.05±.01	0.21±.03	20±10	81±2	8.0±.6	1.19±.09	0.07±.02	0.52±.01	Amorphous
OK22	10.3±5.4	540±210	0.14±.03	0.32±.09	130±50	80±2	8.2±.4	1.23±.05	0.08±.03	0.53±.02	Amorphous
OK23	7.8±11.8	340±170	0.05±.02	0.23±.07	40±30	80±1	7.8±.2	1.17±.02	0.08±.01	0.65±.03	Amorphous
OK26	8.5	430	0.09	0.19	30	76	6.9	1.10	0.14	—	—
OK27	4.5	500	0.07	0.12	10	78	7.5	1.14	0.11	—	—
OK28	6.7	540	0.05	0.25	10	81	8.5	1.27	0.08	0.56	Amorphous
OK29	3.6±0.1	370±90	0.05±.01	0.26±.05	30±10	82	6.9	1.01	0.09	0.63±.04	Amorphous
OK30	3.8	30	0.06	—	10	72	3.4	0.57	0.22	—	Mixed
OK31	4.2	70	0.14	0.61	20	88	4.5	0.62	0.03	1.09	Amorphous
OK32	6.3	70	0.18	0.39	10	89	5.0	0.68	0.02	1.40	Amorphous
OK35	8.4±5.2	—	—	0.48±.10	30±20	81±2	8.0±.2	1.19±.03	0.07±.02	0.52	Amorphous
OK55	7.8±5.3	—	—	0.51±.13	30±20	82±1	7.9±.3	1.16±.04	0.06±.01	0.63	Amorphous

NOTE: Values are means and 1σ standard deviations for data from localities shown in Figure 1 and Table 1. Where no standard deviation is shown, only one valid measurement was available.

TABLE 3. — MEAN AND STANDARD DEVIATION OF TOTAL ORGANIC CARBON BY GEOLOGIC PROVINCE

Geologic province	TOC mean and 1σ standard deviation (wt%)	Number of samples
Northern Oklahoma Platform and west side of Nemaha uplift	5.4 ± 2.6	26
Central Oklahoma Platform and east side of Nemaha uplift	8.8 ± 3.7	26
Ozark uplift	3.5 ± 1.7	65
Arbuckle Mountain uplift	6.9 ± 5.8	26
Anadarko basin	4.4 ± 3.0	52
Marietta–Ardmore basin and Criner Hills	7.1 ± 4.3	32
Ouachita frontal zone	6.8 ± 5.4	36
Ouachita core area	1.1 ± 1.3	37
Regional grand mean	5.4 ± 6.9	300

Isopach Map

Figure 4 is an isopach map of Upper Devonian rocks in the region. This map is a modification of more detailed maps published by Amsden (1975, 1980), Huffman (1960), Adler and others (1971), and Frezon and Glick (1959). The thicknesses shown on Figure 4 include not only black shale (i.e., source beds) but also nonsource facies (e.g., chert, siltstone, sandstone, dolomite, and organic-poor shale), such as the Misener and Sylamore Sandstones. Inclusion of the Misener and Sylamore follows the work of Amsden (1975,1980) and allows direct comparison with his isopach data for Upper Devonian sections in Oklahoma. Amsden (1980) noted that much of the southward thickening of the Woodford in Oklahoma is due to thickening of the basal siliciclastic unit (Misener) in the deepest parts of the Anadarko, Marietta–Ardmore, and Arkoma basins. Exposures of the Woodford Shale in the Criner Hills (OK22) include ~50 ft of basal siltstone and organic-poor shale underlying very rich (10.3% TOC; Table 2, OK22) oil source shale (Kirkland and others, this volume). Also, Harlton (1956) described 75 ft of basal green (presumably organic-poor) shale in the Harrisburg trough, a structurally complex area at the junction between the Anadarko and the Marietta–Ardmore basin provinces. These data show that significant thicknesses of the Woodford Shale in the deep cratonic basins of southern Oklahoma are not black shale (source rock) but organic-poor siliciclastics.

REGIONAL SOURCE BED QUALITY

Total Organic Carbon (TOC)

Figure 5 shows the geographic distribution of organic carbon based on the data in Table 2, and Table 3 lists mean total organic carbon (TOC) values for each geologic province. Except for some localities in the central and core areas of the Ouachita tectonic belt, all of the Upper Devonian sections represented in this study contain beds with petroleum source potential (>0.5 wt% TOC). The highest concentrations of organic carbon are found near the Nemaha uplift in central Oklahoma, in the Arbuckle Mountain uplift and Criner Hills of southern Oklahoma, and on upthrown blocks along the Anadarko basin–Wichita Mountain uplift boundary in southwestern Oklahoma (Fig. 5). The Anadarko and Marietta–Ardmore basins, which together comprise the deep basinal manifestation of the southern Oklahoma aulacogen (Shatski, 1946; Ham and others, 1964; Walper, 1977), show a general trend of low TOC in the northwest and high TOC in the southeast. Intermediate TOC values are found in axial parts of the Anadarko basin, on the northern and central Oklahoma platforms, and around the Ozark uplift. Limited data suggest that TOC increases toward the Arkoma basin in east-central Oklahoma and west-central Arkansas. The lowest TOC values are found in the core area of the Ouachita tectonic belt. In contrast, the western part of the Ouachita frontal zone has intermediate to high TOC.

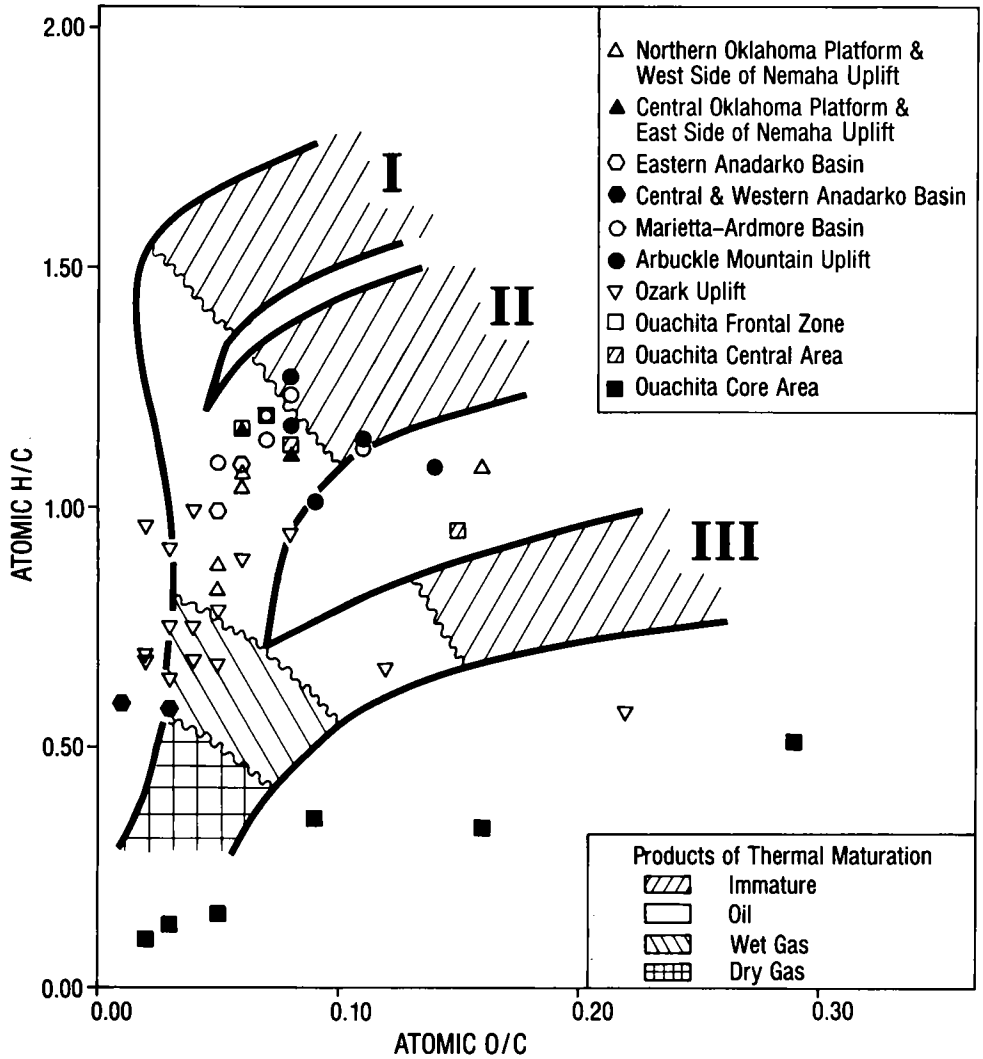

Figure 2. Van Krevelen plot for Upper Devonian source beds in Oklahoma and Arkansas (from Comer and Hinch, 1987). Frontal zone, central area, and core area refer to subdivisions of the Ouachita tectonic belt defined by Cline and Shelburne (1959). Thermal evolution trends are from Tissot (1984).

Hydrogen Index (HI)

The hydrogen index (HI) (Fig. 6; Table 2) is the ratio of generated hydrocarbons to TOC (S_2/TOC in mg/g) from Rock-Eval pyrolysis and is an indication of the convertibility of the organic matter in a rock to petroleum (Peters, 1986). If the rock is thermally immature, the magnitude of HI indicates whether the kerogen is a gas or an oil generating type. Hydrogen indices >300 indicate the rock has oil generating capability, whereas values <150 indicate gas generating capability (Peters, 1986). As rocks become more thermally mature, hydrogen indices approach 0.

Figure 6 shows that, on a regional scale, hydrogen indices vary due to thermal maturity. Kerogen in the Ouachita core area and in the deep parts of the Anadarko basin is at an advanced level of metagenesis (Cardott and Lambert, 1985; Houseknecht and Matthews, 1985; Schmoker, 1986; Comer and Hinch, 1987; Cardott, 1989) and has correspondingly low HIs (Fig. 6). Along the Nemaha uplift, northern Oklahoma platform, Marietta–Ardmore basin, Arbuckle Mountain uplift, and western part of the Ouachita frontal zone, HIs are >300, indicating relatively immature source rocks having significant unrealized oil-generating capability. Intermediate HIs around the Ozark uplift reflect both an intermediate level of thermal maturity in that area and a greater proportion of mixed and structured types of kerogen (Table 2), indicating potential for generating rela-

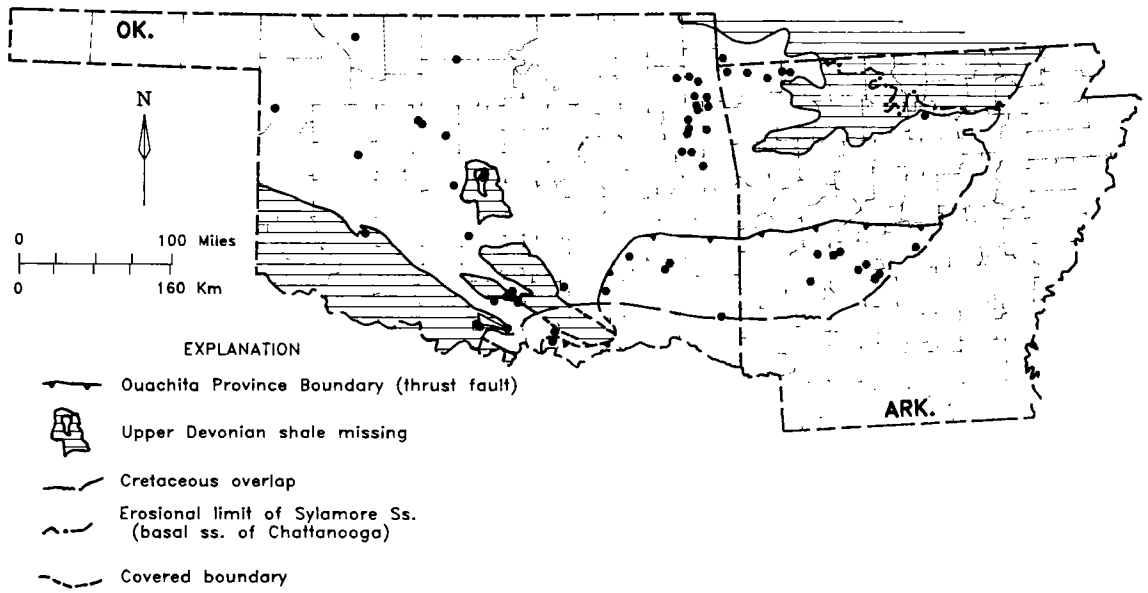

Figure 3. Base map showing limit of Upper Devonian strata, the Ouachita overthrust, and Cretaceous overlap. Patterned areas in the southwest (Wichita Mountain uplift), northeast (Ozark uplift), and center (Nemaha uplift) of the map show where Devonian black shale is missing. The dashed line running northeast–southwest through Arkansas and east–west through southern Oklahoma marks the limit of Cretaceous overlap and the boundary between Cretaceous rocks of the Gulf Coastal Plain and Mississippi Embayment and Paleozoic rocks of the Ozark, Ouachita, and Arbuckle provinces. The dashed line across northern Arkansas indicates the limit of Upper Devonian basal sandstone (Sylamore Sandstone Member of the Chattanooga Shale) by pinchout and erosion along the Ozark uplift. The heavy line with the sharp teeth marks the overthrust boundary of the Ouachita tectonic belt. Dashed lines extending south of the Cretaceous overlap represent Paleozoic province boundaries beneath the unconformity.

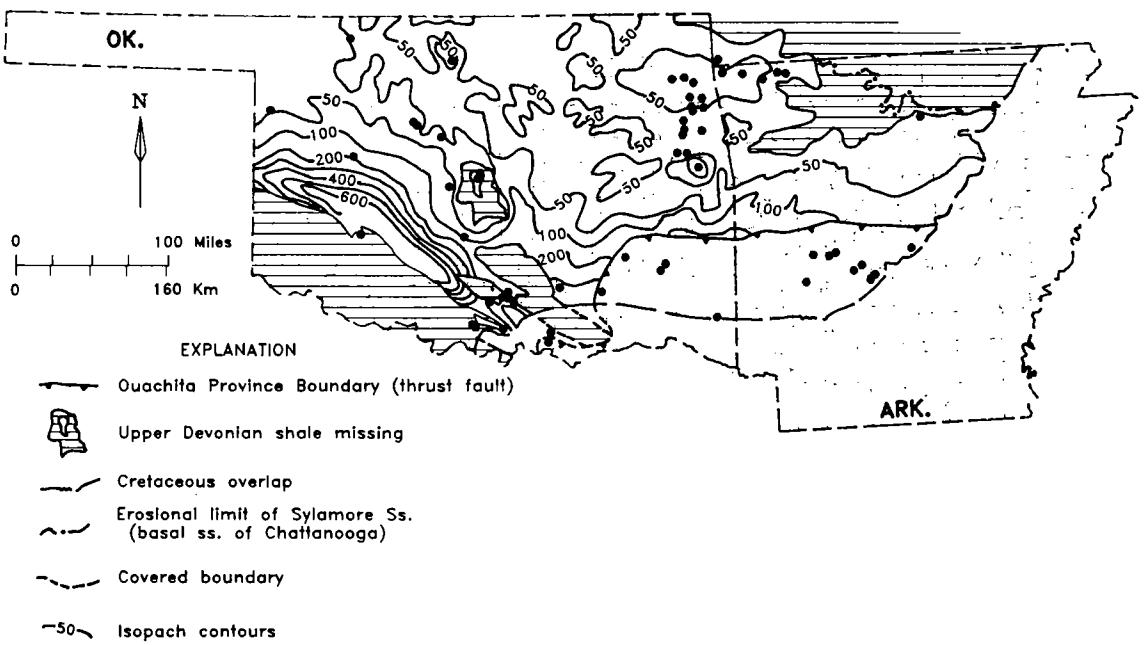

Figure 4. Isopach map of Upper Devonian strata (thickness in feet).

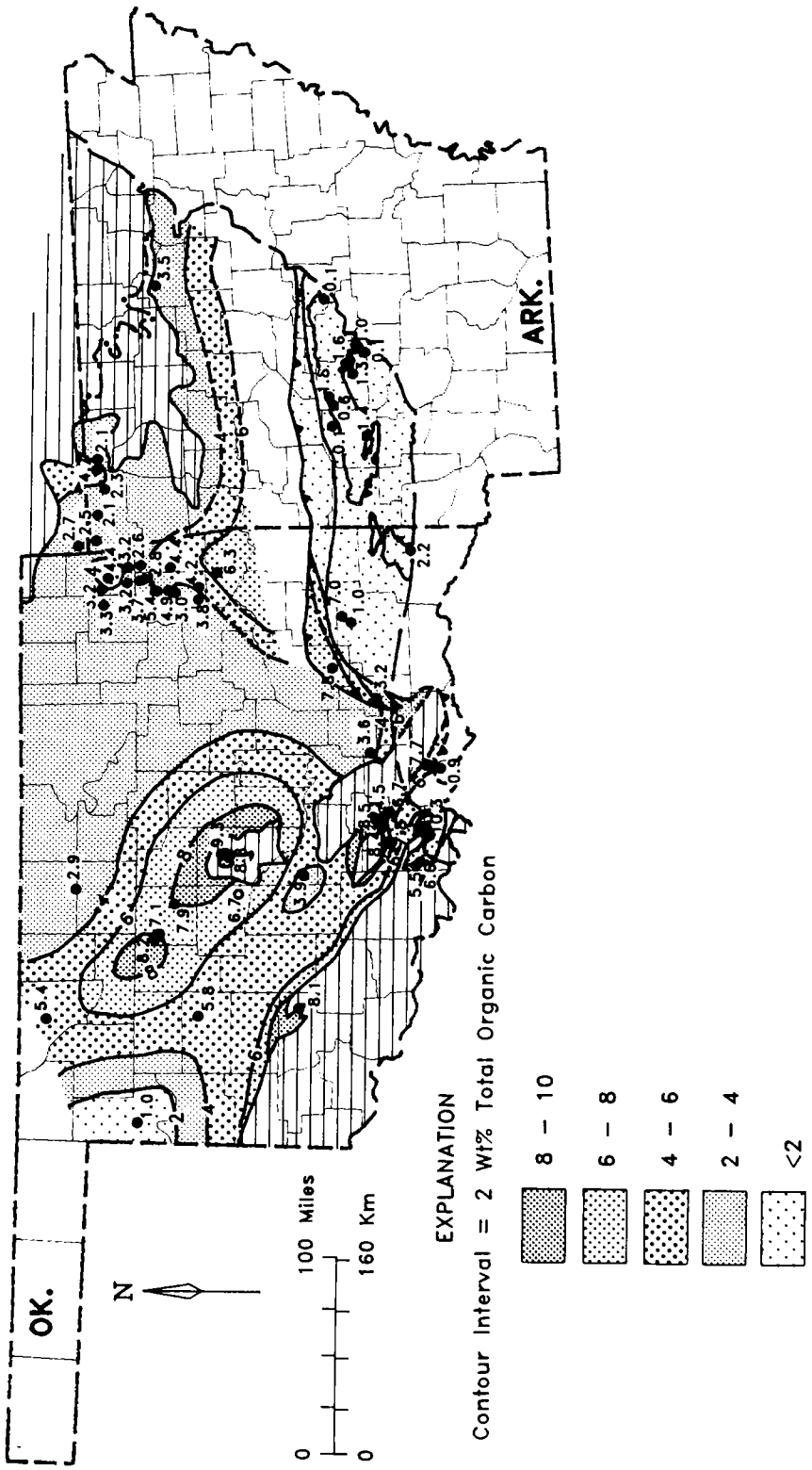

Figure 5. Map showing total organic carbon distribution.

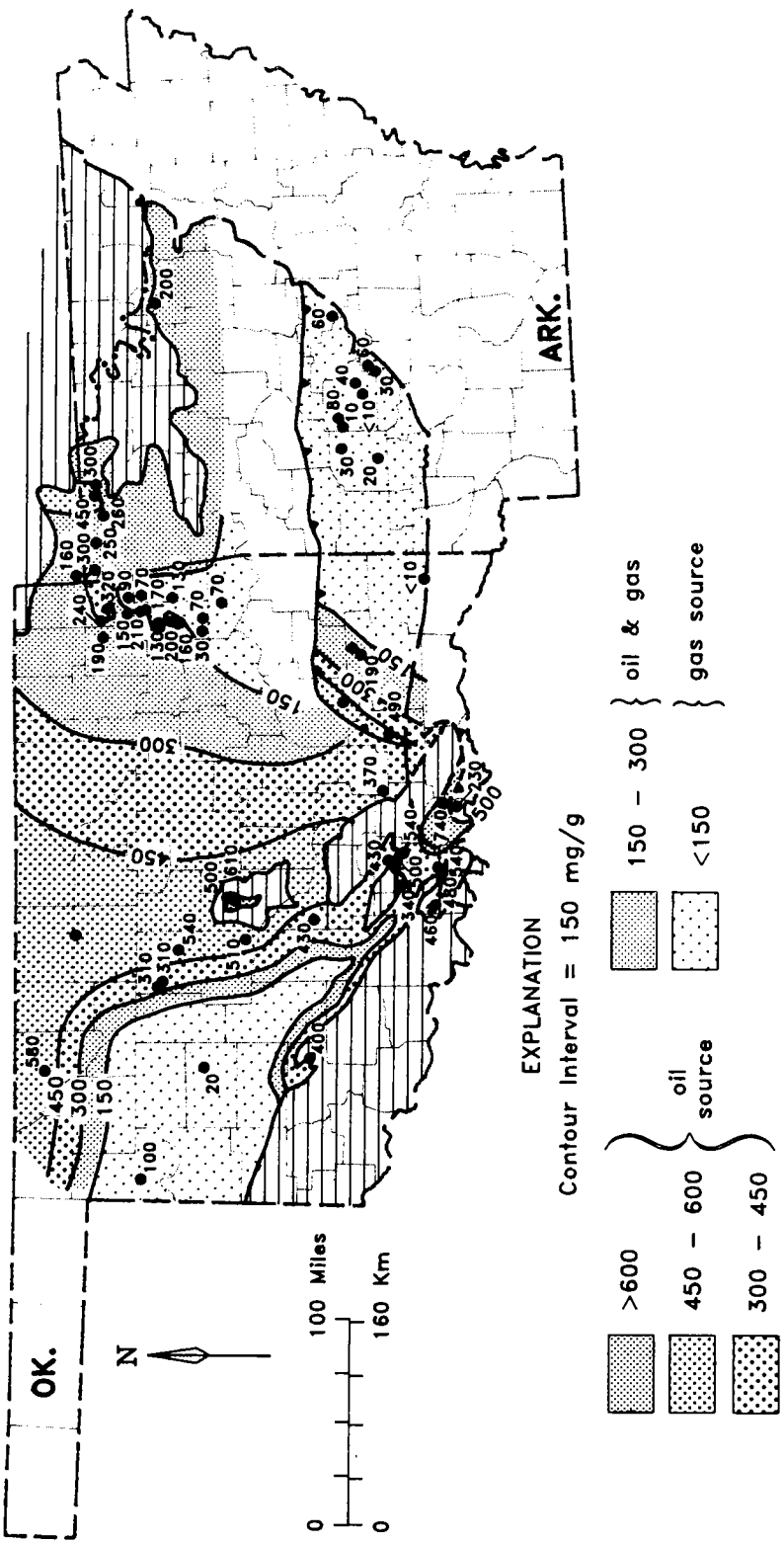

Figure 6. Map of hydrogen indices.

tively less oil and more gas. Although the data are limited, there appears to be a decrease in the HI from the Ozark uplift southward into the Arkoma basin. This trend is probably related to the very high thermal maturities in the deep part of the basin (Carr, 1987; Houseknecht and others, this volume). The decrease in HI from the Ouachita frontal zone into the core area (Fig. 6) is poorly constrained but appears to closely follow trends in thermal maturity recorded in Carboniferous strata (Houseknecht and Matthews, 1985).

Production Index (PI)

The production index is the ratio of volatile hydrocarbons to volatile plus generated hydrocarbon $[S_1/(S_1 + S_2)]$ from Rock-Eval pyrolysis. Values <0.1 indicate thermal immaturity, whereas values between 0.1 and 0.4 bracket the oil window (Peters, 1986). High indices (approaching 1.0) occur when the amount of generated hydrocarbons (S_2) approaches 0 (i.e., when the kerogen is "cooked out"). Also, high indices occur when migrated oil (excess S_1) is present.

High production indices (>0.4), reflecting very high thermal maturity, occur in the Ouachita core area and the Anadarko basin (Fig. 7). The patchy pattern around the Ozark uplift records local thermal anomalies, perhaps related to the migration of hydrothermal fluids and emplacement of Mississippi Valley-type lead–zinc deposits during the Late Paleozoic (Coveney, this volume; Filipek, this volume; Bagley and others, this volume; Gregg and others, this volume).

Low production indices (<0.10), indicating low thermal maturity, parallel the Nemaha uplift and include areas of the northern and central Oklahoma platforms. Low ratios and maturities also occur in the Marietta–Ardmore basin, Arbuckle Mountain uplift, Ouachita frontal zone, Potato Hills (OK19), and locally in the Ozark uplift. The Criner Hills anomaly (0.14; Table 2, OK22) is partly due to migrated oil because many of the samples contain prominent oil-lined fractures.

Bitumen/TOC

The ratio of bitumen (total material extractable in organic solvents) to TOC is another measure of thermal maturity. (Methylene chloride was the solvent used for most samples, but benzene was used for some. Extractions were performed using soxhlet apparatus.) Immature source rocks typically have ratios <50 mg/g. The ratios progressively increase during catagenesis (oil generation), then decrease during metagenesis as high molecular weight hydrocarbons are thermally cracked to gas (Hunt, 1979; Tissot and Welte, 1984). Anomalously high ratios (>300 mg/g) reflect contamination by migrated oil or petroleum-based drilling additives. Weathering can reduce both bitumen and kerogen concentrations and can variably alter the ratio by processes such as water washing, bacterial degradation, and oxidation (Leythaeuser, 1973; Clayton and Swetland, 1978; Hunt, 1979; Lafargue and Barker, 1988).

Ratios for Upper Devonian outcrops are widely scattered between <10 and 250 mg/g, whereas most core ratios fall in a narrow range between <10 and 70 mg/g (Table 2). Low ratios (<20 mg/g) occur in the Anadarko basin, Ouachita core area, and northern shelf of the Arkoma basin (Fig. 8), and indicate high thermal maturity. High ratios (>70 mg/g), which occur at localities in the Ozark uplift, Criner Hills (OK22), and Potato Hills (OK20) (Fig. 8), do not correlate very well with other thermal maturity indicators and apparently result from the combined effects of local differences in maturity, organic matter type, contamination by migrated oil, and weathering.

Throughout the rest of the map area the bitumen/TOC ratios fall between 20 and 70 mg/g (Fig. 8), and the pattern of thermal maturity evident on Figures 6 and 7 is not apparent. No direct relationship between bitumen/TOC ratios and thermal maturity is observed in cored intervals in the regions between the Nemaha uplift and Anadarko basin and between the Ozark province and Arkoma basin. As proposed by Comer and Hinch (1987), relatively early and efficient oil expulsion apparently suppress increases in the bitumen/TOC ratio because leakage of oil from confined, oil-saturated source rocks is required in order to maintain pressure stability during thermal generation. In Upper Devonian source beds, bitumen/TOC ratios are apparently controlled by oil storage capacity (e.g., porosity) rather than thermal maturity.

Carbon in Kerogen

Weight percent carbon in isolated solvent-extracted kerogen increases with increasing thermal maturity (Dow, 1977; Hunt, 1979). The highest carbon values (>90%) are found in the Anadarko basin and the Ouachita core area (Fig. 9). Carbon values >90% are indicated by the very high thermal maturities (as much as 5% R_o) recorded in kerogen from the deep Arkoma basin (Carr, 1987; Houseknecht and Hathon, 1987; Houseknecht and others, this volume).

A trend of intermediate carbon percentages (81–85%) follows the Nemaha uplift and includes parts of the northern and central Oklahoma platforms. Also, intermediate values are found in the frontal zone of the Ouachita tectonic belt and along the Ozark uplift near the erosional edge of the Chattanooga Shale. Somewhat higher values (85–90%) occur on the flanks of the Anadarko basin and throughout most of the central Oklahoma

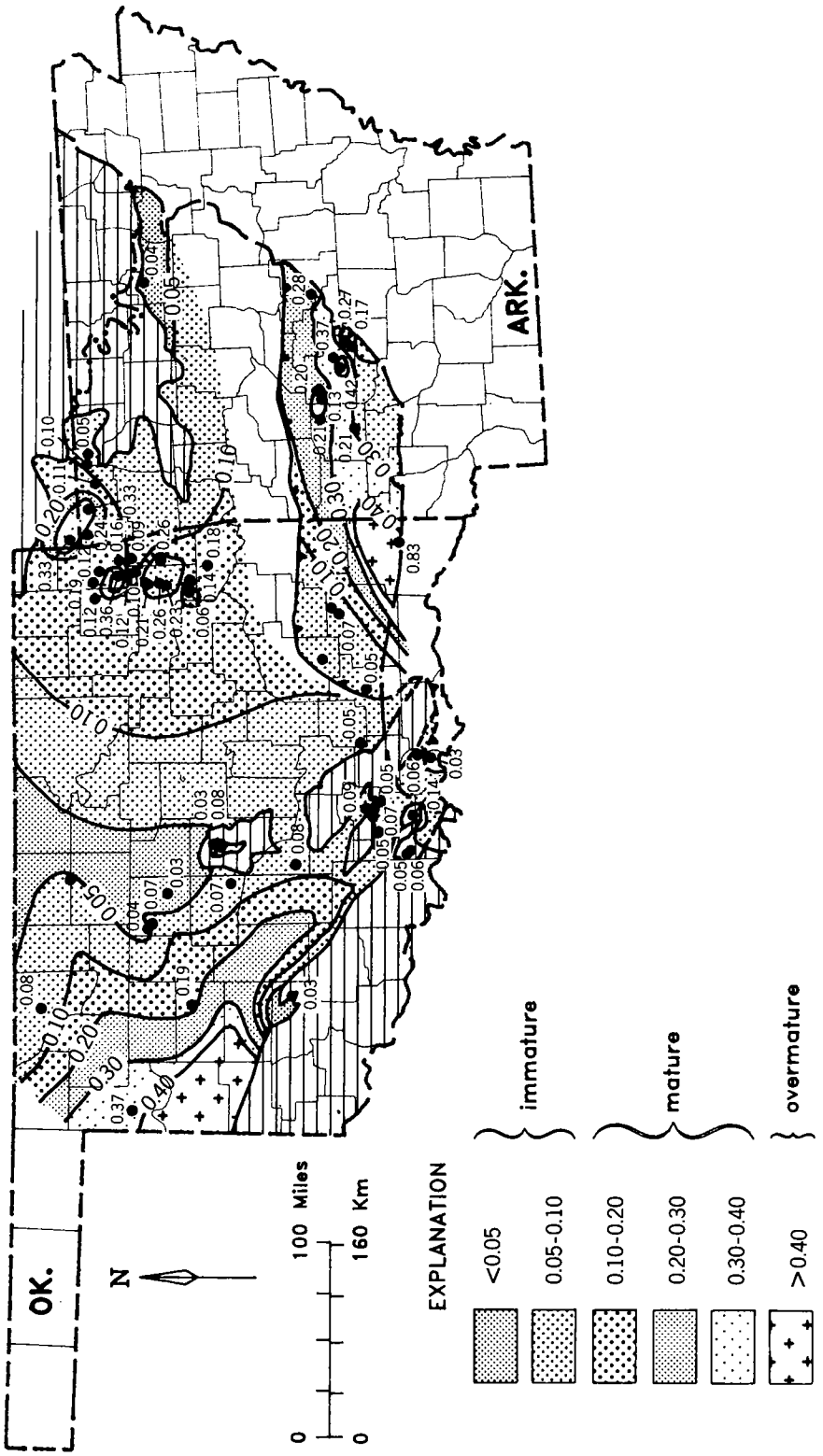

Figure 7. Map of production indices.

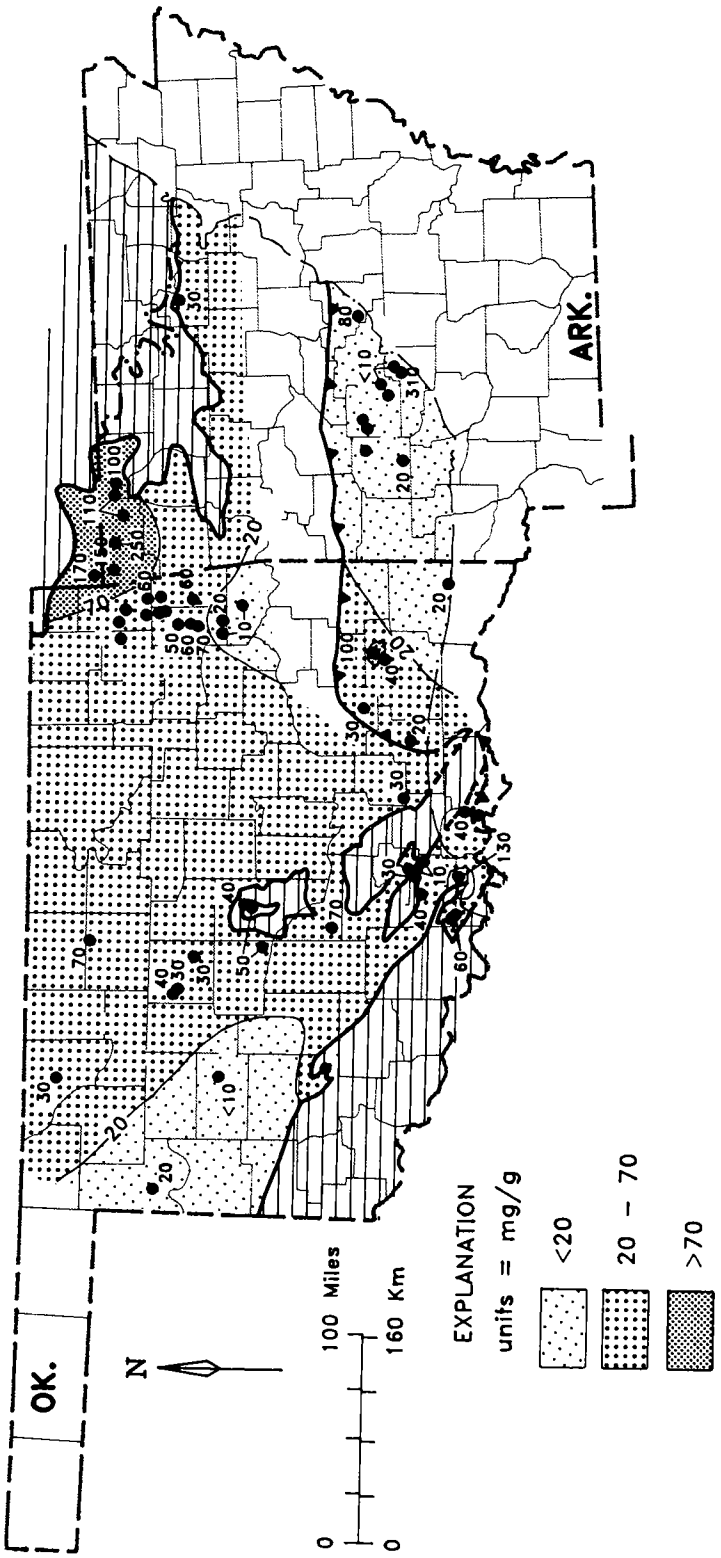

Figure 8. Map of bitumen/TOC ratios.

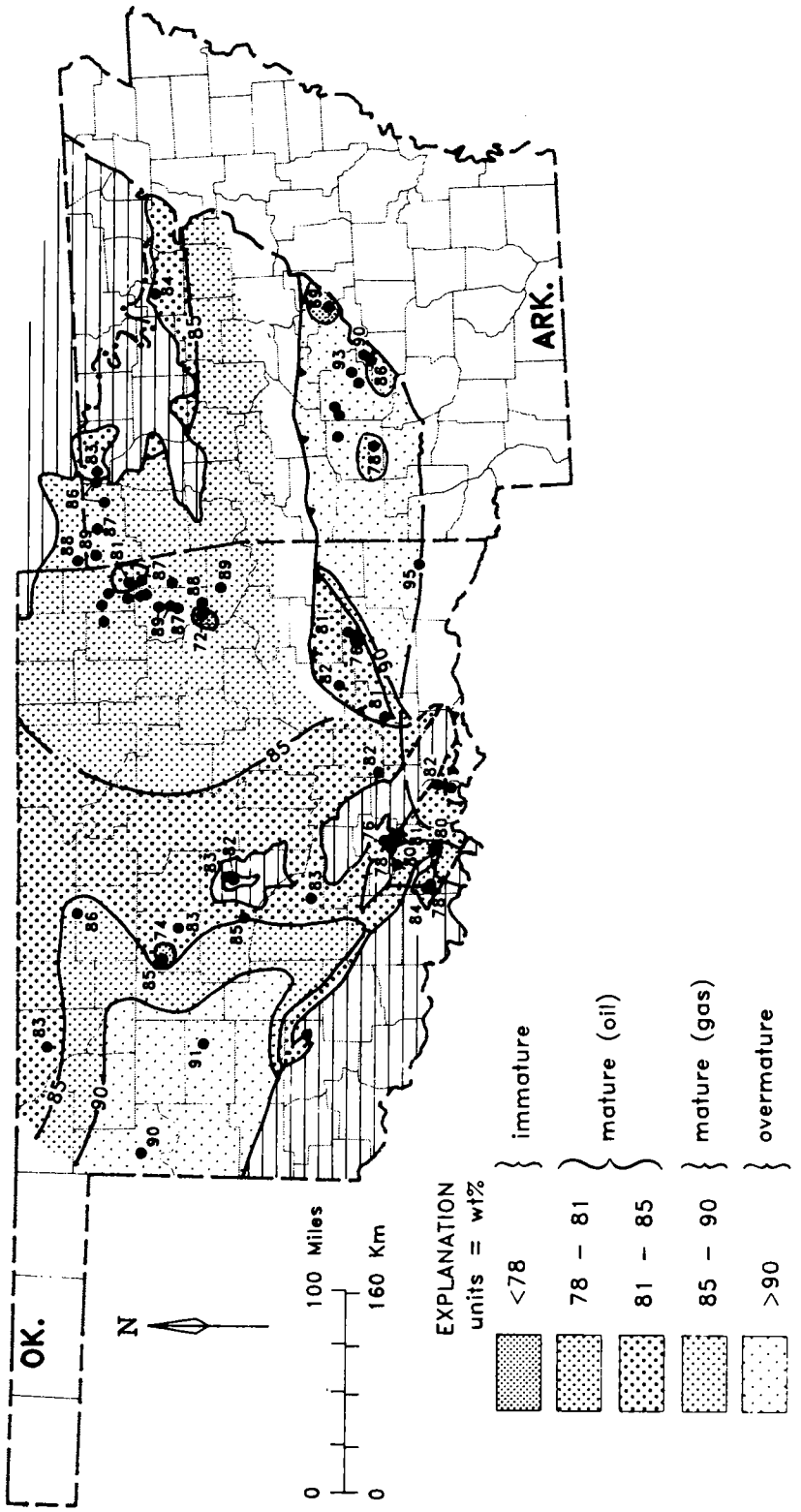

Figure 9. Map of carbon in kerogen.

platform and the Ozark uplift. The lowest carbon percentages (<81%) are in the Arbuckle Mountain uplift, the Criner Hills (OK22), and the Marietta–Ardmore basin.

The few carbon values <78% are anomalous and reflect either oxidation of kerogen due to outcrop weathering (OK19, OK30, AR10, AR13, AR15) or poor analytical data (core sample A17).

Hydrogen in Kerogen

The abundance of hydrogen in solvent-extracted kerogen depends on both the original type of organic matter and the thermal maturity. Oil-prone kerogen has >6% hydrogen and gas-prone kerogen, <6% (LaPlante, 1974; Hunt, 1979). Overmature kerogen contains <3% hydrogen (Hunt, 1979).

The large areas of low hydrogen abundance (<6%) in the Anadarko basin and the Ouachita core area (Fig. 10) result from the high thermal maturity arising from deep burial and metamorphism. The area of low hydrogen (<6%) around the Ozark uplift is due to a combination of localized moderate to high thermal maturity, a greater abundance of mixed and structured (terrestrial, low-hydrogen) types of organic matter, and oxidation of kerogen due to outcrop weathering.

Most of central Oklahoma, including parts of the northern and central Oklahoma platforms, the Nemaha uplift, the Arbuckle Mountain uplift, the Criner Hills (OK22), the Marietta–Ardmore basin, and the western part of the Ouachita frontal zone, contains oil-prone, high-hydrogen (>7%) kerogen at relatively low thermal maturity. The area of moderate to high hydrogen abundance (3.4–7.1%; Fig. 10) found in the Ozark uplift near the erosional edge of the Chattanooga Shale was never buried very deeply and includes source beds that locally contain mixed and structured kerogen (Table 2).

Atomic Hydrogen/Carbon Ratio

The atomic ratio of hydrogen to carbon (H/C ratio) in kerogen varies as a function of both thermal maturity and kerogen type (Fig. 2). With increasing temperature the H/C ratio will decrease as hydrocarbons are generated. Oil-prone kerogens will start out with much higher H/C ratios (>1.0) than gas-prone kerogens.

The patterns shown in Figure 11 mostly reflect increasing thermal maturity (decreasing H/C ratios) from structural highs into the deep basins and into the Ouachita core area. Central and southern Oklahoma, including the Nemaha uplift, parts of the northern and central Oklahoma platforms, the Arbuckle Mountain uplift, the Criner Hills (OK22), the Marietta–Ardmore basin, the western part of the Ouachita frontal zone, and the Potato Hills (OK19 and OK20), contain oil-prone kerogen (H/C >1.00; Fig. 11) at relatively low thermal maturity. In the Ozark uplift, intermediate H/C ratios (0.60–1.00) are due to both local thermal maturity anomalies and to increased abundances of mixed and structured types of organic matter (i.e., low-hydrogen kerogen). In general, kerogens in the Ozark province still have significant oil and gas generating potential, but thermal generation mostly is inactive because the source rock is too shallow and cool.

Atomic Oxygen/Carbon Ratio

The atomic ratio of oxygen to carbon (O/C ratio) in kerogen decreases as thermal maturity increases (Fig. 2) due primarily to the loss of CO_2 and H_2O (McIver, 1967; LaPlante, 1974). Oxygen can be reintroduced into kerogen by outcrop weathering, causing the O/C ratio to increase (Tissot and Welte, 1984).

Low ratios (<0.03) occur in the Anadarko basin and Ouachita core area (Fig. 12) and indicate high thermal maturity. Intermediate (0.03–0.06) to high (>0.06) values predominate throughout central and northeastern Oklahoma, the western parts of the Ouachita frontal and central zones, and the Ozark uplift (Fig. 12). Several localities have very high O/C ratios (>0.10) (Table 2) due to oxidation of kerogen at the outcrop. The well A17 anomaly (0.16) is due to poor quality data.

Vitrinite Reflectance

The reflectance of vitrinite steadily increases as thermal maturity of the kerogen increases (Dow, 1977; Hunt, 1979; Tissot and Welte, 1984). Current practice reflects the popularity of vitrinite reflectance as a reliable indicator of organic maturity. However, reflectance can be increased by oxidation at the outcrop and recent work suggests that reflectance may be suppressed in lipid-rich oil shales (Hutton and Cook, 1980; Price and Barker, 1985). Furthermore, the use of vitrinite reflectance for kerogens that have very low abundances of vitrinite macerals, such as most of the Upper Devonian marine source beds in this study, leads to difficulties in measurement and interpretation that should not be ignored.

Nevertheless, the vitrinite reflectance data reported here (Fig. 13; Table 2) are in general agreement with the other thermal maturity indicators and with the regional geology. Areas of high vitrinite reflectance (R_o >2.0%), indicating organic metagenesis, include the deep parts of the Anadarko basin (A14) and the Ouachita core area. In these areas, Upper Devonian source beds are in the late stage of gas generation (2.0–3.5% R_o)or have ceased significant hydrocarbon generation (>3.5% R_o; Hunt, 1979). A narrow band of intermediate vitrinite reflectance values (R_o = 0.8–2.0%), representing generation of gas (R_o = 1.2–2.0%) and

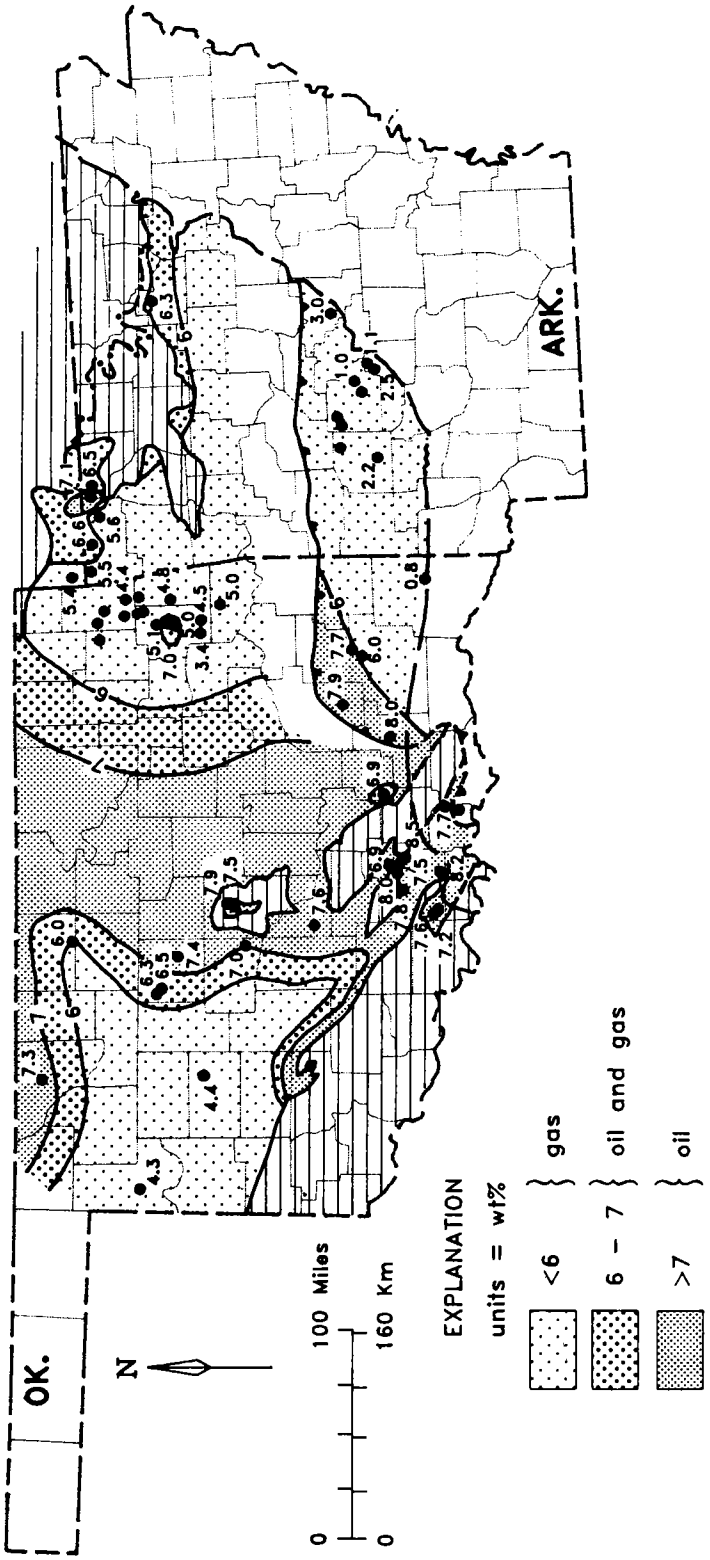

Figure 10. Map of hydrogen in kerogen.

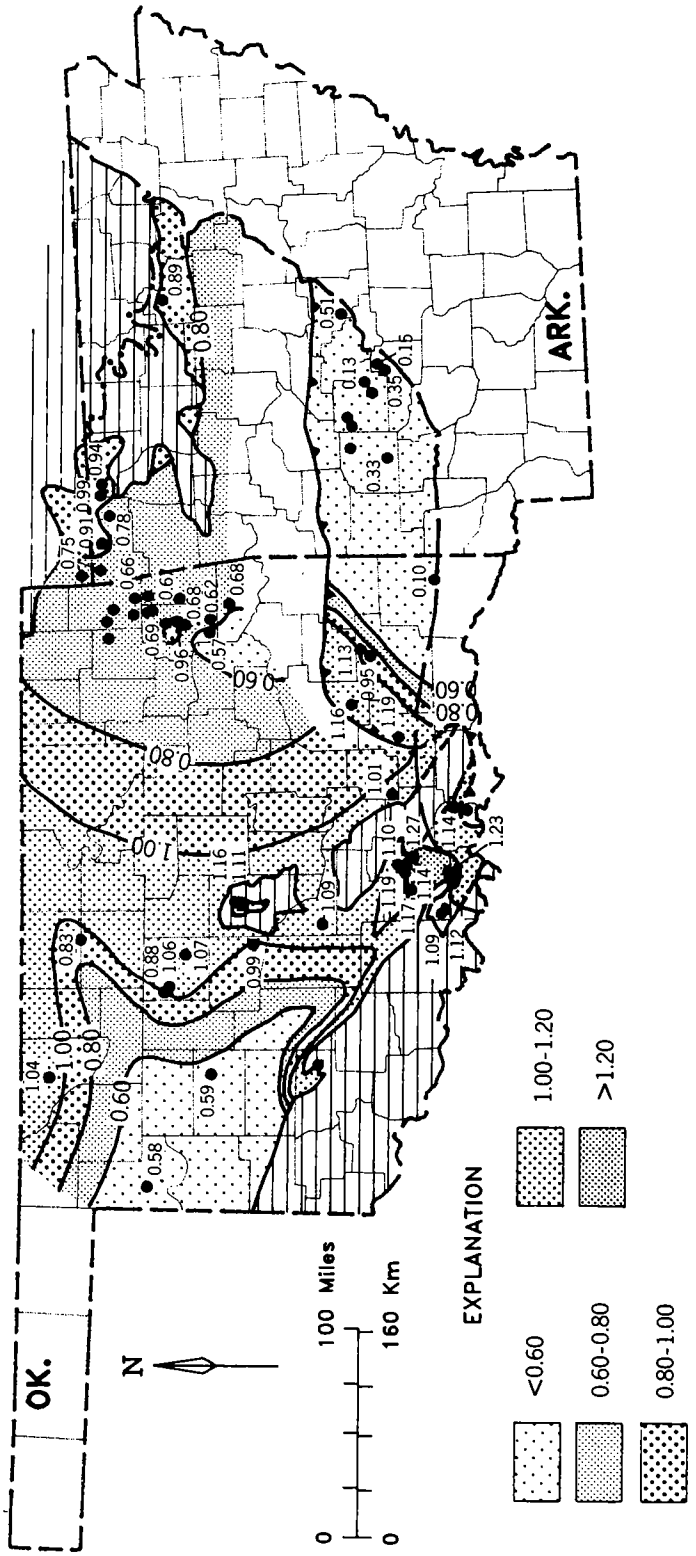

Figure 11. Map of atomic H/C ratios.

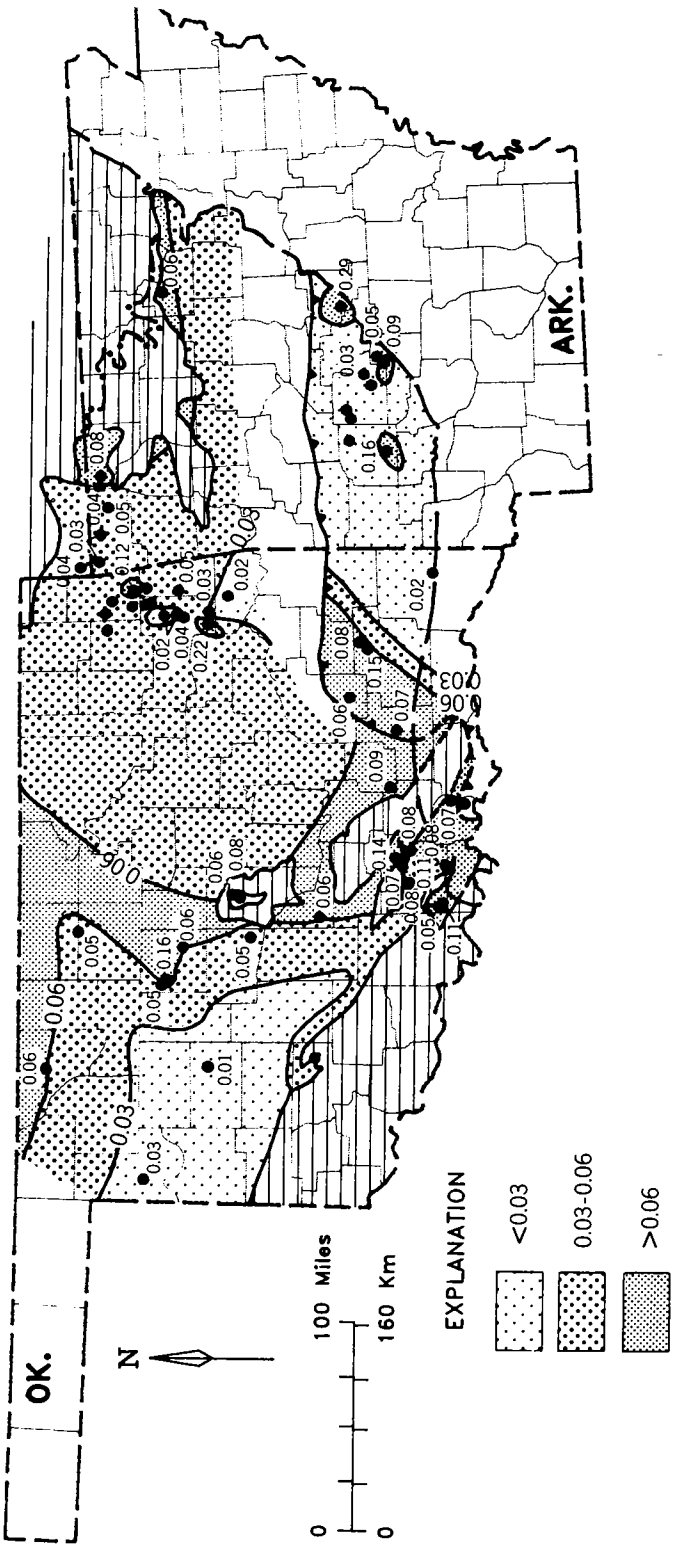

Figure 12. Map of atomic O/C ratios.

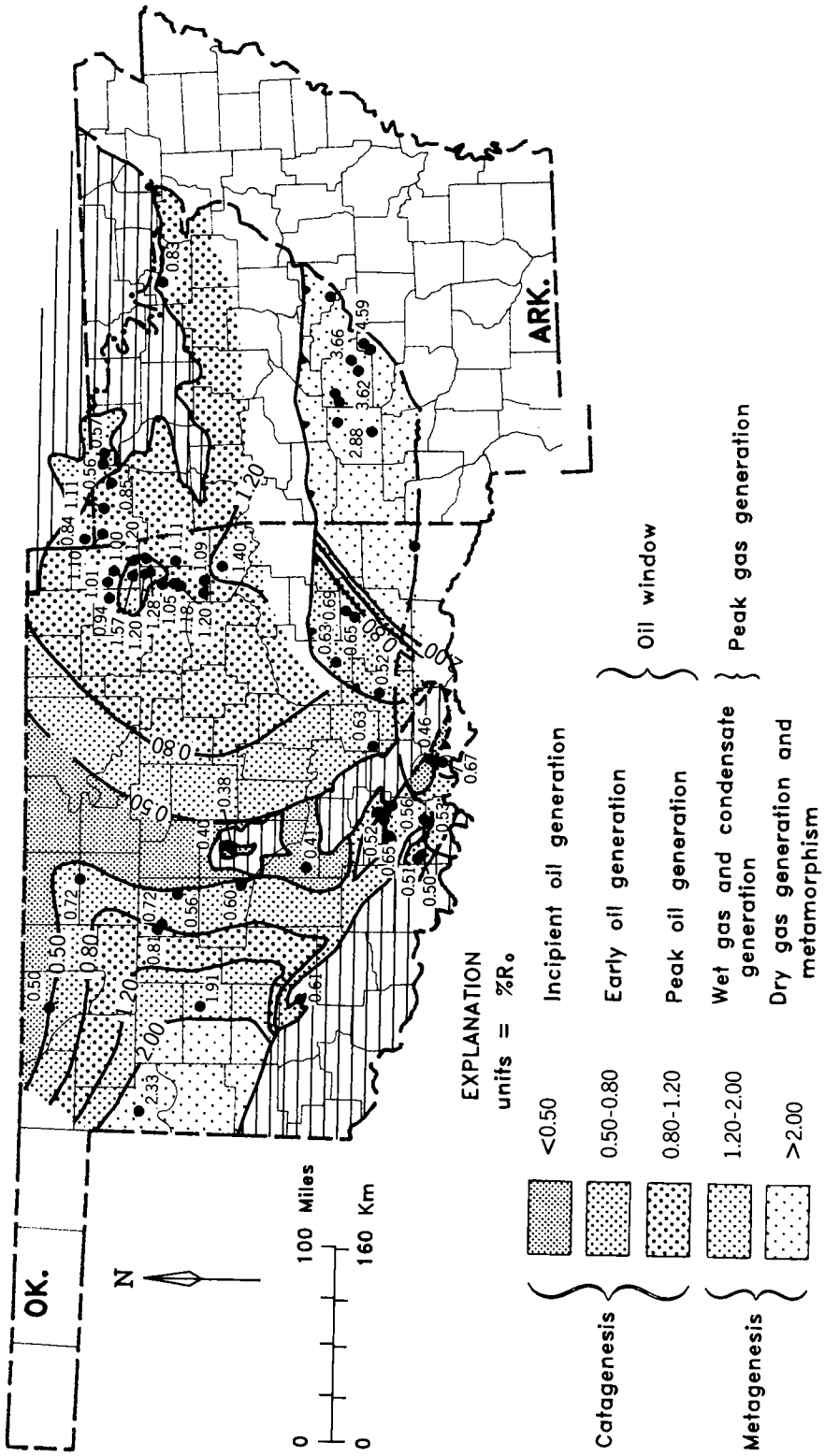

Figure 13. Map of vitrinite reflectance.

oil (R_o = 0.8–1.2%), occurs along the flanks of the Anadarko basin. A broad area of intermediate vitrinite reflectance values (R_o = 0.8–2.0%) with local anomalies occurs in the Ozark province (Fig. 13). Extremely high values (as much as 5% R_o) have been mapped in the Arkoma basin by Houseknecht and others (this volume).

Areas of low vitrinite reflectance (R_o <0.5–0.8%), indicating early catagenesis, dominate central Oklahoma along the Nemaha uplift, adjacent parts of the northern and central Oklahoma platforms, the Arbuckle Mountain uplift, the Criner Hills (OK22), and the Marietta–Ardmore basin. Also, source rocks found locally in the northern part of the Ozark uplift and in the western part of the frontal and central zones of the Ouachita tectonic belt are in the early stage of oil generation. The increase in maturity from the Ouachita frontal zone into the core area is schematically shown by narrow reflectance contours in the central area (Fig. 13), but these changes most likely occur across thrust fault boundaries. The low reflectance values (0.65%, 0.69%; Fig. 13) in the Potato Hills (OK19 and OK20) are similar to those in surrounding Carboniferous rocks which are part of a different, overlying thrust sheet (Houseknecht and Matthews, 1985).

PALEOGEOGRAPHY

The regional distribution of TOC (Fig. 5) and organic matter type is best explained as a response to the Late Devonian paleogeography. The relatively low TOC values that occur in the Ozark uplift (3.5 ± 1.7%; Table 3) and adjacent parts of the central Oklahoma platform are due to dilution by siliciclastic sediment. Black shales in the region have the highest concentrations of clay minerals (mostly illite), and commonly texturally mature quartz sandstone is present at the base of the section. Detrital quartz has been documented as coming from Middle Ordovician sandstones exposed nearby (Freeman and Schumacher, 1969; Amsden and Klapper, 1972; Pittenger, 1981,1988). Locally, some black shale beds contain marine (amorphous) and terrestrial (structured) kerogen and beds with mixed types are common throughout the province (Table 2). The increased proportions of detrital quartz, clay, and terrestrial kerogen reflect the presence of land nearby and indicate that parts of the Ozark uplift were subaerially exposed during the Late Devonian.

Beds of mixed amorphous and structured kerogens are found locally along the Nemaha uplift indicating that it also was topographically high during the Late Devonian. Local increases in structured material suggest the presence of a low-relief archipelago with scattered islands that supported terrestrial plants.

Low TOC values occur in the middle division of the Arkansas Novaculite in the Ouachita core area (1.1 ± 1.3%; Table 3). Many sections are notably deficient in black shale, whereas organic-poor cherts, siltstones, and shales are abundant. These rocks are allochthonous, having been displaced from the south (Miser, 1929; Viele, 1973), and represent deposits of a deep marginal trough that experienced open ocean circulation (Park and Croneis, 1969; Cline, 1970; Morris, 1974). The predominance of radiolarian and spiculitic chert indicates deposition in a zone of oceanic upwelling (Lowe, 1975).

The western part of the frontal zone of the Ouachita tectonic belt contains organic-rich source rocks composed of interbedded black shales and both organic-rich and organic-poor cherts (6.8 ± 5.4% TOC; Table 3). Frontal zone sections are unmetamorphosed and lithologically similar to Arbuckle Mountain sections (6.9 ± 5.8% TOC; Table 3). They most likely represent a transitional slope environment between shallow northern platforms and the deep Ouachita trough.

The organic content of the Woodford Shale in Oklahoma is dominated by a northwest–southeast trend of high TOC (6–>9%) located in the center of the state (Fig. 5). To the southwest, a parallel trend of high TOC (6–>10%) follows the northern edge of the Wichita Mountain uplift and dominates the Marietta–Ardmore basin, the Arbuckle Mountain uplift, and the Criner Hills (OK22). These two high TOC trends are separated by a zone of lower TOC that reaches a minimum (1.0%) in the northwestern part of the Anadarko basin (A14). Comer (1986) and Burruss and Hatch (1989) noted that the Woodford Shale changes facies, becoming more silty and less organic-rich to the northwest and more cherty to the southeast in the Anadarko basin. Also, the type of organic matter changes from almost purely marine to more terrestrial from southeast to northwest. Sections in the basin are thicker and contain thicker siliciclastic units than sections along the margins. Changes in thickness, lithology, and organic matter type show that the Anadarko basin was a topographic trough during the Late Devonian, receiving terrigenous sediment from a major source area to the northwest. The two high TOC trends along the basin flanks represent areas of clastic sediment bypassing and suggest that clastics were deposited by bottom flows sensitive to intrabasinal relief. Comer (1989, 1991) documented the presence of fine-grained bottom flow deposits (graded siltstones and fine-grained Bouma sequences) in the Upper Devonian rocks of West Texas and southeastern New Mexico and showed that the Transcontinental arch was the dominant clastic sediment source area. The same source region would have fed the Anadarko basin in the Late Devonian.

CONCLUSIONS

Throughout most of Oklahoma and northwestern Arkansas, Upper Devonian formations are organic-rich (5.4 ± 6.9% TOC; Table 3) and have prolific petroleum generating capability, much of which has not yet been realized. In the Ozark uplift, the Chattanooga Shale has less TOC (3.5 ± 1.7%; Table 3) than the regional mean and higher proportions of mixed and structured kerogen (oil and gas, and gas generating types, respectively). These differences are due to increased terrestrial sediment influx from land exposed along the Ozark uplift during the Late Devonian. Source rocks here would generate significant amounts of both oil and gas if sufficiently deeply buried.

In the Ouachita core area, highly variable but generally small proportions of the Upper Devonian section are organic-rich source beds (1.1 ± 1.3% TOC; Table 3). Organic-rich chert and shale are commonly replaced in the section by organic-poor biogenic chert, shale, and siltstone. The lack of carbonates suggests that core area rocks were mostly deposited in deep water. The predominance of radiolarian and spiculitic chert and the low amounts of organic matter indicate that there was good vertical circulation and oceanic upwelling. Although the organic-rich lithologies once had significant oil and gas generating capability, the present advanced level of metagenesis precludes current or future hydrocarbon generation by core area rocks.

Low maturity rocks (early oil-generation stage) are found in the central area (OK19 and OK20) and frontal zone (OK21 and OK55) of the Ouachita tectonic belt. Frontal zone rocks have high TOC (6.8 ± 5.4% TOC; Table 3) and consist of interbedded dark, organic-rich chert and black shale similar to equivalent rocks in the Arbuckle Mountain uplift. Organic richness and thermal maturity show that oil and gas accumulations are possible at depth in the frontal zone, particularly along the northwestern and western boundary of the Ouachita province in Oklahoma.

In the Anadarko basin, organic content decreases toward the northwest (Fig. 5) and the organic matter type changes from dominantly amorphous (oil-prone) on the basin flanks and in the southeast, to dominantly structured (gas-prone) in the basin axis and to the northwest. These changes coincide with a change in the type of hydrocarbon accumulations, with oil mostly along the flanks and gas in the deep basin and to the northwest. Although the change can be attributed to changes in thermal maturity (Figs. 2,6,7,9–13), the type of organic matter must have had some control over the proportions of oil and gas generated in the basin.

The richest oil source beds are in the northern and southern flanks of the Anadarko basin, the Nemaha uplift, the Marietta–Ardmore basin, the Arbuckle Mountain uplift, the Criner Hills (OK22), and the Ouachita frontal zone (Table 3; Figs. 1,5,6, 10,11). The largest commercial accumulations of Woodford oil are found in central Oklahoma along the trend of the least thermally mature oil source rocks (R_o <0.8%). This association has led to conflicting interpretations. The conventional view is that Woodford oil was generated deeper in the Anadarko basin and migrated into reservoirs along the Nemaha uplift and the northern Oklahoma platform (Burruss and Hatch, 1989). Undoubtedly, some Woodford oil originated in this manner from oil-prone kerogen in the basin. However, the increase in gas-prone kerogen toward the depocenter suggests that long-distance migration may not account for all of the Woodford oil along the basin flanks and in shelf regions farther to the north. Locally, biomarker analysis (Reber, 1988) showed that indigenous oil produced from the Woodford correlates with bitumen in the enclosing low maturity source beds (R_o = 0.4–0.8%). Typically, these beds contain petrographic features interpreted as evidence of oil expulsion, such as oil-lined fractures and oil-impregnated nodules (Comer and Hinch, 1987; Reber, 1988). If early expulsion is characteristic of very rich, low-maturity oil source beds like the Woodford, as suggested by Comer and Hinch (1987), then much local sourcing is likely throughout the southern Midcontinent.

ACKNOWLEDGMENTS

Amoco Production Co., Tulsa, Oklahoma, provided financial support for the research and granted permission to publish. H. H. Hinch (Amoco) helped collect core and outcrop samples and engaged in numerous seminal discussions during the project. O. A. Wise and C. G. Stone (Arkansas Geological Commission) guided our sampling of outcrops in Arkansas and H. A. Pittenger (University of Tulsa) provided some of the samples from northeastern Oklahoma. Most of the analytical work was done at the Amoco Research Center with the assistance of Amoco staff. Jim McDonald performed elemental analysis of solvent-extracted kerogen, Carl Bennett assisted with kerogen isolation, Robert Littlejohn performed visual-kerogen and vitrinite-reflectance analyses, Bruce Torkelson and John Kearns ran soxhlet extractions and column chromatography, Jerry McClendon performed TOC analyses, and Kirk Rovang and Cheryl Birciw helped compile the data. Numerous discussions with Amoco colleagues Roger Ames, John Grayson, Robert Harwood, Michael Lewan, James Momper, Larry Ross, Paul Basan, and Robert Thompson led to improvements in the data and interpretations. The manuscript was reviewed at the Indiana Geologi-

cal Survey by A. Fleming, N. R. Hasenmueller, N. R. Shaffer, and C. W. Zuppann and at Indiana University by J. M. Hayes. At the Indiana Geological Survey, Marilyn DeWees typed the manuscript and Kimberly Sowder and Rea Kersey, under the supervision of Richard Hill, drafted the figures. Publication is authorized by the State Geologist, Indiana Geological Survey. The author is deeply indebted to each of the above for contributing time, knowledge, and resources to the project.

REFERENCES

Adler, F. J.; Caplan, W. M.; Carlson, M. P.; Geobel, E. D.; Henslee, H. T.; Hicks, I. C.; Larson, T. G.; McCracken, M. H.; Parker, M. C.; Rascoe, B.; Schramm, M. W.; and Wells, J. S., 1971, Future petroleum provinces of the Midcontinent, Region 7: American Association of Petroleum Geologists Memoir 15, p. 985–1042.

Amsden, T. W., 1975, Hunton Group (Late Ordovician, Silurian, and Early Devonian) in the Anadarko basin of Oklahoma: Oklahoma Geological Survey Bulletin 121, 214 p.

_____1980, Hunton Group (Late Ordovician, Silurian, and Early Devonian) in the Arkoma basin of Oklahoma: Oklahoma Geological Survey Bulletin 129, 136 p.

Amsden, T. W.; and Klapper, G., 1972, Misener Sandstone (Middle–Upper Devonian), north-central Oklahoma: American Association of Petroleum Geologists Bulletin, v. 56, p. 2323–2334.

Amsden, T. W.; Caplan, W. M.; Hilpman, P. L.; McGlasson, E. H.; Rowland, T. L.; and Wise, O. A., 1967, Devonian of the southern Midcontinent area, United States, *in* Oswald, D. H. (ed.), International symposium on the Devonian System: Alberta Society of Petroleum Geologists, Calgary, v. 1, p. 913–932.

Arbenz, J. K., 1956, Tectonic map of Oklahoma: Oklahoma Geological Survey Map GM-3, scale 1:750,000.

Brenneman, M. C.; and Smith, P. V., Jr., 1958, The chemical relationships between crude oils and their source rocks, *in* Weeks, L. G. (ed.), Habitat of oil: American Association of Petroleum Geologists, p. 818–849.

Burruss, R. C.; and Hatch, J. R., 1989, Geochemistry of oils and hydrocarbon source rocks, greater Anadarko basin: evidence for multiple sources of oils and long-distance oil migration, *in* Johnson, K. S. (ed.), Anadarko basin symposium, 1988: Oklahoma Geological Survey Circular 90, p. 53–64.

Cardott, B. J., 1989, Thermal maturation of the Woodford Shale in the Anadarko basin, *in* Johnson, K. S. (ed.), Anadarko basin symposium, 1988: Oklahoma Geological Survey Circular 90, p. 32–46.

Cardott, B. J.; and Lambert, M. W., 1985, Thermal maturation by vitrinite reflectance of Woodford Shale, Anadarko basin, Oklahoma: American Association of Petroleum Geologists Bulletin, v. 69, p. 1982–1998.

Carr, J. L., 1987, The thermal maturity of the Chattanooga Formation along a transect from the Ozark uplift to the Arkoma basin: Shale Shaker, v. 38, p. 32–40.

Clayton, J. L.; and Swetland, P. J., 1978, Subaerial weathering of sedimentary organic matter: Geochimica et Cosmochimica Acta, v. 42, p. 305–312.

Cline, L. M., 1970, Sedimentary features of Late Paleozoic flysch, Ouachita Mountains, Oklahoma, *in* Lajoie, J. (ed.), Flysch sedimentology in North America: Geological Association of Canada Special Paper No. 7, p. 85–101.

Cline, L. M.; and Shelburne, O. B., 1959, Late Mississippian–Early Pennsylvanian stratigraphy of the Ouachita Mountains, Oklahoma, *in* Cline, L. M.; Hilseweck, W. J.; and Feray, D. E. (eds.), The geology of the Ouachita Mountains–a symposium: Dallas Geological Society and Ardmore Geological Society, p. 175–208.

Comer, J. B., 1986, Organic geochemistry, diagenesis and depositional environments of Late Devonian–Early Mississippian formations in Oklahoma and western Arkansas [abstract]: *in* Bennison, A. P. (ed.), Upper Pennsylvanian source beds of northeastern Oklahoma and adjacent Kansas: Tulsa Geological Society Guidebook, p. 46–47.

_____1989, Depositional model for Upper Devonian black shale (Woodford Formation) in Permian basin, West Texas and southeastern New Mexico [abstract]: American Association of Petroleum Geologists Bulletin, v. 73, p. 346.

_____1991, Stratigraphic analysis of the Upper Devonian Woodford Formation, Permian basin, West Texas and southeastern New Mexico: Texas Bureau of Economic Geology Report of Investigations 201, 63 p.

Comer, J. B.; and Hinch, H. H., 1987, Recognizing and quantifying expulsion of oil from the Woodford Formation and age-equivalent rocks in Oklahoma and Arkansas: American Association of Petroleum Geologists Bulletin, v. 71, p. 844–858.

Curiale, J. A., 1983, Petroleum occurrences and source-rock potential of the Ouachita Mountains, southeastern Oklahoma: Oklahoma Geological Survey Bulletin 135, 65 p.

Dow, W. G., 1977, Kerogen studies and geological interpretations: Journal of Geochemical Exploration, v. 7, p. 79–99.

Flawn, P. T., 1959, The Ouachita structural belt, *in* Cline, L. M.; Hilesweck, W. J.; and Feray, D. E. (eds.), The geology of the Ouachita Mountains—a symposium: Dallas Geological Society and Ardmore Geological Society, p. 20–29.

Freeman, T.; and Schumacher, D., 1969, Qualitative pre-Sylamore (Devonian–Mississippian) physiography delineated by onlapping conodont zones, northern Arkansas: Geological Society of America Bulletin, v. 80, p. 2327–2334.

Frezon, S. E.; and Glick, E. E., 1959, Pre-Atoka rocks of northern Arkansas: U.S. Geological Survey Professional Paper 314-H, p. 171–189.

Glick, E. E., 1979, Arkansas, *in* Craig, L. C. (coordinator), Paleotectonic investigations of the Mississippian System in the United States. Part I.—Introduction and regional analyses of the Mississippian System: U.S. Geological Survey Professional Paper

1010-H, p. 125–145.
Haley, B. R.; Glick, E. E.; Bush, W. V.; Clardy, B. F.; Stone, C. G.; Woodward, M. B.; and Zachry, D. L., 1976, Geologic map of Arkansas: Arkansas Geological Commission and U. S. Geological Survey.
Ham, W. E.; Denison, R. E.; and Merritt, C. A., 1964, Basement rocks and structural evolution of southern Oklahoma: Oklahoma Geological Survey Bulletin 95, 302 p.
Harlton, B. H., 1956, The Harrisburg trough, Stephens and Carter Counties, Oklahoma, *in* Hicks, I. C.; Westheimer, J.; Thomlinson, C. W.; Putman, D. M.; and Elk, E. L. (eds.), Petroleum geology of southern Oklahoma, a symposium: American Association of Petroleum Geologists, p. 135–143.
Hass, W. H.; and Huddle, J. W., 1965, Late Devonian and Early Mississippian age of the Woodford Shale in Oklahoma, as determined from conodonts: U.S. Geological Survey Professional Paper 525-D, p. D125–D132.
Houseknecht, D. W.; and Hathon, L. A., 1987, Relationships among thermal maturity, sandstone diagenesis, and reservoir quality in Pennsylvanian strata of the Arkoma basin [abstract]: American Association of Petroleum Geologists Bulletin, v. 71, p. 568–569.
Houseknecht, D. W.; and Matthews, S. M., 1985, Thermal maturity of Carboniferous strata, Ouachita Mountains: American Association of Petroleum Geologists Bulletin, v. 69, p. 335–345.
Huffman, G. G., 1960, Regional relations of pre-Desmoinesian rocks, central Midcontinent region: Kansas Geological Society Guidebook, p. 48–71.
Hunt, J. M., 1961, Distribution of hydrocarbons in sedimentary rocks: Geochimica et Cosmochimica Acta, v. 22, p. 37–49.
_____1979, Petroleum geochemistry and geology: Freeman, San Francisco, 617 p.
Hutton, A. C.; and Cook, A. C., 1980, Influence of alginite on the reflectance of vitrinite from Joadja, NSW, and some other coals and oil shales containing alginite: Fuel, v. 59, p. 711–714.
Iztan, Y. H., 1985, Geochemical correlation between crude oils from Misener reservoirs and potential source rocks in central and north-central Oklahoma: University of Tulsa unpublished M.S. thesis, 191 p.
Lafargue, E.; and Barker, C., 1988, Effect of water washing on crude oil composition: American Association of Petroleum Geologists Bulletin, v. 72, p. 263–276.
LaPlante, R. E., 1974, Hydrocarbon generation in Gulf Coast Tertiary sediments: American Association of Petroleum Geologists Bulletin, v. 58, p. 1281–1289.
Lewan, M. D.; Winters, J. C.; and McDonald, J. H., 1979, Generation of oil-like pyrolyzates from organic-rich shales: Science, v. 203, no. 4383, p. 897–899.
Leythaeuser, D., 1973, Effects of weathering on organic matter in shales: Geochimica et Cosmochimica Acta, v. 37, p. 113–120.
Lowe, D. R., 1975, Regional controls on silica sedimentation in the Ouachita system: Geological Society of America Bulletin, v. 86, p. 1123–1127.
McIver, R. D., 1967, Composition of kerogen—clue to its role in the origin of petroleum: Proceedings of the Seventh World Petroleum Congress, v. 2, p. 25–36.
Miser, H. D., 1929, Structure of the Ouachita Mountains of Oklahoma and Arkansas: Oklahoma Geological Survey Bulletin 50, 30 p.
Morris, R. C., 1974, Sedimentary and tectonic history of the Ouachita Mountains, *in* Dickinson, W. R. (ed.), Tectonics and sedimentation: Society of Economic Paleontologists and Mineralogists Special Publication 22, p. 120–142.
Park, D. E.; and Croneis, C., 1969, Origin of Caballos and Arkansas Novaculite formations: American Association of Petroleum Geologists Bulletin, v. 53, p. 94–111.
Peters, K. E., 1986, Guidelines for evaluating petroleum source rock using programmed pyrolysis: American Association of Petroleum Geologists Bulletin, v. 70, p. 318–329.
Philp, R. P., 1987, A study of the source material, mechanisms of generation, and migration of oils in the Anadarko basin, Oklahoma [abstract]: Summary of Physical Research in the Geosciences, U.S. Department of Energy, Office of Energy Research, Division of Engineering and Geosciences, DOE/ER-0349, p. 92.
Philp, R. P.; Jones, P. J.; Lin, L. H.; Michael, G. E.; and Lewis, C. A., 1989, An organic geochemical study of oils, source rocks, and tar sands in the Ardmore and Anadarko basins, *in* Johnson, K. S. (ed.), Anadarko basin symposium, 1988: Oklahoma Geological Survey Circular 90, p. 65–76.
Pittenger, H. A., 1981, Provenance, depositional environment and diagenesis of the Sylamore Sandstone in northeastern Oklahoma and northern Arkansas: University of Tulsa unpublished M.S. thesis, 109 p.
_____1988, Provenance and depositional environment of the Sylamore Sandstone in northeastern Oklahoma and northern Arkansas: Shale Shaker, v. 38, p. 50–61.
Price, L. C.; and Barker, C. E., 1985, Suppression of vitrinite reflectance in amorphous rich kerogen—a major unrecognized problem: Journal of Petroleum Geology, v. 8, p. 59–84.
Reber, J. J., 1988, Correlation and biomarker characterization of Woodford-type oil and source rock, Aylesworth Field, Marshall County, Oklahoma: University of Tulsa unpublished M.S. thesis, 96 p.
_____1989, Biomarker characterization of Woodford-type oil and correlation to source rock, Aylesworth Field, Marshall County, Oklahoma, *in* Johnson, K. S. (ed.), Anadarko basin symposium, 1988: Oklahoma Geological Survey Circular 90, p. 271.
Rice, D. D.; Threlkeld, C. N.; and Vuletich, A. K., 1989, Characterization and origin of natural gases of the Anadarko basin, *in* Johnson, K. S. (ed.), Anadarko basin symposium, 1988: Oklahoma Geological Survey Circular 90, p. 47–52.
Schmoker, J. W., 1986, Oil generation in the Anadarko basin, Oklahoma and Texas: modeling using Lopatin's method: Oklahoma Geological Survey Special Publication 86-3, 40 p.
Shatski, N. S., 1946, The Great Donets basin and the Wichita System—comparative tectonics of ancient

platforms: Akademiia Nauk SSSR, Izvestiia Seriia Geologicheskaia, no. 6, p. 57–90.

Sullivan, K. L., 1985, Organic facies variation of the Woodford Shale in western Oklahoma: Shale Shaker, v. 35, p. 76–89.

Tissot, B. P., 1984, Recent advances in petroleum geochemistry applied to hydrocarbon exploration: American Association of Petroleum Geologists Bulletin, v. 68, p. 545–563.

Tissot, B. P.; and Welte, D. H., 1984, Petroleum formation and occurrence [second edition]: Springer-Verlag, New York, 699 p.

Viele, G. W., 1973, Structure and tectonic history of the Ouachita Mountains, Arkansas, *in* DeJohn, K. E.; and Scholten, R. T. (eds.), Tectonics and sedimentation: Wiley-Interscience, New York, p. 361–377.

Walper, J. L., 1977, Paleozoic tectonics of the southern margin of North America: Gulf Coast Association of Geological Societies Transactions, v. 27, p. 230–241.

Welte, D. H.; Hagemann, H. W.; Hollerbach, A.; Leythaeuser, D.; and Stahl, W., 1975, Correlation between petroleum and source rock: Proceedings of the Ninth World Petroleum Congress, v. 2, p. 179–191.

Winters, J. C.; Williams, J. A.; and Lewan, M. D., 1983, A laboratory study of petroleum generation by hydrouspyrolysis, *in* Bjorøy, M.; Albrecht, P.; Cornford, C.; deGroot, K.; Eglinton, G.; Galimov, E.; Leythaeuser, D.; Pelet, R.; Rullkötter, J.; and Speers, G. (eds.), Advances in organic geochemistry 1981: John Wiley, Chichester, United Kingdom, p. 524–533.

Internal Stratigraphy of the Chattanooga Shale in Kansas and Oklahoma

Michael W. Lambert
Kansas Geological Survey
and University of Kansas

ABSTRACT.—The Late Devonian–Early Mississippian-age Chattanooga Shale contains organic-rich shale that is of considerable economic importance as a petroleum source rock in the Midcontinent. The results presented here represent a preliminary step in assessing the nature, extent, and causal mechanisms of microfabric units within the Chattanooga Shale of Kansas and Oklahoma. The Chattanooga-equivalent Woodford Shale in the Anadarko basin of western Oklahoma has previously been subdivided on the basis of palynology and organic geochemistry (Urban, 1960; Sullivan, 1985). Hester and others (1990) used gamma-ray, density, and resistivity logs to trace distinctive, regionally persistent divisions within the Woodford Shale, which may indicate variations in organic content. This study uses gamma-ray logs to examine internal stratigraphy of the Chattanooga Shale in Kansas and extend the work of Hester and others (1990) northward.

The Chattanooga Shale in Kansas usually can be divided into an uppermost shale interval and a more radioactive underlying shale. The uppermost shale varies in gamma-ray response from 120 to 160 API units in southern Kansas, and from 80 to 110 API units in the northern part of the state. Similarly, the underlying shale registers from 180 to 320 API units in the south and from 110 to 140 API units in the north. Where available, well cuttings indicate that the uppermost shale is lighter in color than the underlying shale. An additional unit, a basal shale, is locally present in southern Kansas, where it has a gamma-ray response less than that of the uppermost shale. This tripartite division appears to correlate with the informally named upper, middle, and lower shale members identified by Hester and others (1990) in the Woodford Shale of western Oklahoma. A lenticular limestone bed as much as 40 ft thick is locally developed at the base of the upper member along the southwest margin of the Iowa basin and the adjacent part of the Central Kansas arch.

Presence of the lower shale member only in southern Kansas is consistent with a transgression from the south that progressively flooded more of the craton. Variations in middle and upper member thicknesses are indicative of a migration of the major Chattanooga Shale depocenter from northeastern to central Kansas as deposition progressed, and of initial development of the Sedgwick basin of south-central Kansas along the northern margin of the Oklahoma basin.

Internal stratigraphic units of the Chattanooga Shale can be correlated regionally across Kansas, providing detailed refinement of depositional patterns during latest Devonian and earliest Mississippian time. In addition, gamma-ray signature is being used to provide a framework for ongoing analysis of Chattanooga Shale microfabric. Recognition of microfabric units can be used to evaluate controls on shale microfabric and on petroleum generative capacity of the Chattanooga Shale.

INTRODUCTION

The Chattanooga Shale of Kansas and the age-equivalent Woodford Shale of western Oklahoma have thermal histories that range from immature to post-mature with regard to the generation of petroleum (Lambert, 1982; Cardott and Lambert, 1985; J. Senftle, personal communication, 1990). Thermal maturity of the shale increases with progressively greater burial from the relatively shallow northern shelf areas to the deep Anadarko basin of southwestern Oklahoma. Geochemical comparisons of Oklahoma crude oils suggest that organic matter in the Woodford is the source of much of the petroleum produced in Oklahoma (Hunt, 1961; Lewan and others, 1979; Comer and Hinch, 1987).

The present study is a preliminary step in establishing an internal stratigraphy that will serve as a framework for characterizing the distribution of microfabric units within the Chattanooga (Woodford) Shale of Kansas and Oklahoma. Microfabric refers to the distribution and arrangement of mineral flakes between 1 and 4 microns in size (Foster and De, 1971; Bennet and Hulbert, 1986). In shales microfabric is developed in elon-

gate phyllosilicate grains that may be either poorly or well oriented with respect to bedding. The degree of orientation helps determine shale porosity and permeability (Magara, 1978; Hunt, 1979), which in turn influences hydrocarbon flow out of a petroleum source rock.

Degree of orientation of microfabric in shale has been positively correlated with increasing organic content (Meade, 1964; Gipson, 1965; Odom, 1967; Polley, 1982), although why the two are related remains unknown. Quantity and type of organic matter are also important in determining how much petroleum a particular source rock will produce (Demaison and Moore, 1980; Tissot and Welte, 1984). The concept of organic facies (Jones and Demaison, 1980; Jones, 1982,1987), which are stratigraphic subdivisions based on differences in organic content, is therefore useful in evaluating geometries of microfabric units, controls on shale microfabric and the generative capacity of fine-grained source rocks.

Urban (1960) divided the Woodford Shale in one locality on the margin of the Ardmore basin in south-central Oklahoma into zones on the basis of paleoecological inferences drawn from palynology. He found three zones: a lower and upper zone that appeared to have been deposited within relative proximity to shore and a middle zone that was deposited in an open-marine setting. Sullivan (1985) used geochemical analysis of organic matter in Woodford Shale cores and cuttings from the Anadarko basin of western Oklahoma to detect organic facies variation. She found a bipartite division of the Woodford that may correspond to the upper and middle zones of Urban (1960).

Hester and others (1990) were the first to systematically follow internal divisions of the Woodford Shale across western Oklahoma. Using gamma-ray, resistivity, and density logs they divided the Woodford into three informal members and used regional variation in member thickness to make inferences about depositional and structural events during Woodford deposition. Based on calculations from density logs, they determined that their lower and upper members had respective total organic carbon (TOC) contents of 3.2 and 2.7 wt%, and that the middle member had a TOC of 5.5 wt%. Therefore, the internal divisions they recognized seem to be indicative of organic facies.

Since the late 1950s, gamma-ray logs commonly have been run in Kansas wells, and the Chattanooga Shale has a characteristically high gamma-ray response. This high radioactivity is due to the fixing of uranyl ions by organic matter, and therefore the gamma-ray response of a shale is related to the amount of organic matter it contains (Schmoker, 1981; Doveton, 1986). In this study gamma-ray logs from 74 wells in eastern Kansas have been used to prepare three north–south and three east–west stratigraphic cross sections through the Chattanooga Shale in order to extend the work of Hester and others (1990) northward.

DEPOSITIONAL SETTING OF THE CHATTANOOGA (WOODFORD) SHALE

Conodonts have been used to date the Woodford Shale of western and south-central Oklahoma as Late Devonian–Early Mississippian in age (Hass and Huddle, 1965; Amsden, 1975; Over and Barrick, 1990). The Woodford is stratigraphically equivalent to other dark, organic-rich shales that are widely distributed across the eastern and central United States (e.g., Chattanooga Shale of Kansas and eastern Oklahoma, New Albany Shale of the Illinois and Appalachian basins, Bakken Shale of the Williston basin, and others).

Figure 1 is a Late Devonian (Frasnian and Famennian) lithofacies map for North America, after Heckel and Witzke (1979). It is based on the distribution of climate-sensitive lithologies such as carbonates, evaporites, bauxites, and coals, and is unique in that it places North America in the Southern Hemisphere during this time. Witzke and Heckel (1988) believed that alternate interpretations based on paleomagnetic data placed the lithologies in unlikely latitudinal settings. They also suggested that diagenetic overprinting and other problems may have introduced error into the paleomagnetically based reconstructions.

The high organic content of the Chattanooga and equivalent shales is believed to be due to deposition during the inundation of the shelf and cratonic basins in North America by anoxic marine water (Jones, 1983). Some of these deposits may represent the distal basinal facies of the Catskill Delta complex that developed concurrently in what is now the northeastern United States (Ettensohn, 1985).

Figure 2 shows the major structural features of Kansas during Chattanooga Shale deposition and the location of the six cross sections used in the present study. The Iowa basin was present in northeastern Kansas, while the southern and western parts of the state were occupied by the northern part of the Oklahoma basin (Johnson, 1989). Separating these two basins were the Ancestral Central Kansas uplift and the Chautauqua arch, which were submerged extensions of the Transcontinental arch and the Ozark dome, respectively, and which were linked by the Central Kansas arch (Merriam, 1963).

The Chattanooga Shale belongs to the Kaskaskia cratonic sequence of Sloss (1963). The deposition of the Chattanooga Shale followed regional exposure and erosion that resulted in the incision of major stream channels, such as the McPherson

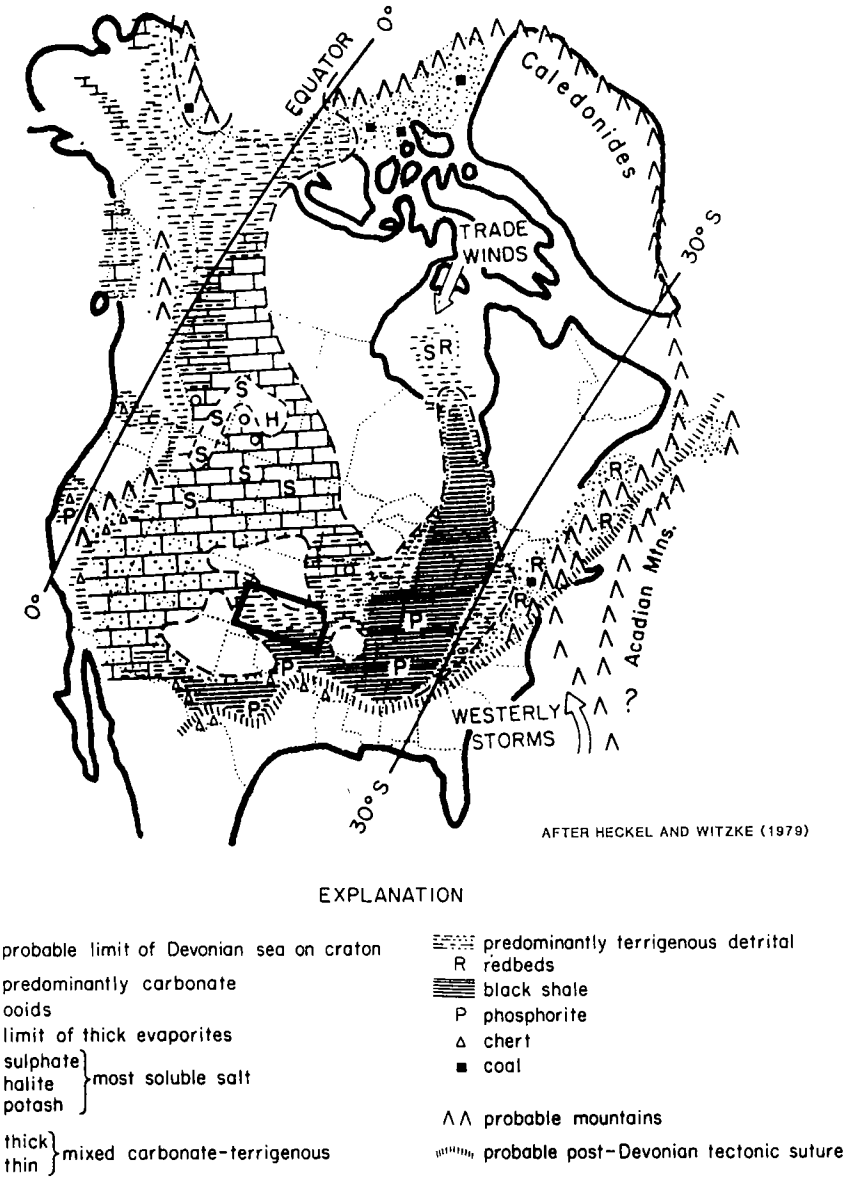

Figure 1. Late Devonian (Frasnian and Famennian) lithofacies map. The state of Kansas is shown in outline.

Valley of central Kansas (first described by Lee, 1956), in pre-Chattanooga strata. The Late Devonian marine transgression advanced from the south, flooding the craton and resulting in deposition of the Chattanooga Shale (Bunker and others, 1988).

DEPOSITIONAL PATTERNS IN TOTAL CHATTANOOGA SHALE ISOPACH

The isopach map (Fig. 3) of the Chattanooga Shale in Kansas and Oklahoma (after Lambert, this paper, and Hester and others, 1990) shows total thickness of the entire formation. This map does not distinguish shale members within the Chattanooga, and the thickness includes the basal Misener sandstone, which is only sporadically present and is at most a few feet thick in Kansas and Oklahoma. However, a few general trends can be seen from the total thickness distribution.

The Chattanooga Shale is <50 ft thick over the Chautauqua arch in southeastern Kansas (area 1 on the isopach map). It can be >200 ft thick in the Iowa basin of northeastern Kansas, and >250 ft thick in the McPherson Valley area of central Kansas (areas 2 and 3 on the isopach map, respec-

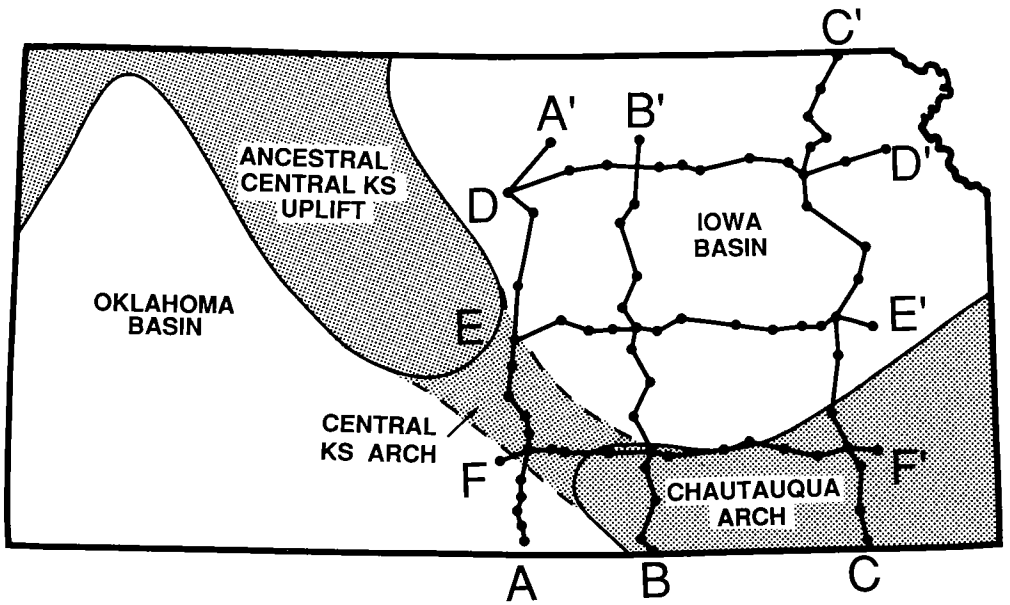

Figure 2. Location of cross sections used in this study superimposed on a map of structural features in Kansas during Chattanooga Shale deposition. Names and locations of wells used in these cross sections are listed in the appendix at the end of this paper.

tively). The Chattanooga is absent from part of area 2 due to post-depositional erosion associated with the Nemaha anticline.

Consideration of variations in the thickness of shale members within the Chattanooga Shale will permit a more detailed analysis of events during deposition. For example, the major Chattanooga depocenter migrated from northeastern to central Kansas as Chattanooga deposition progressed and the eastern part of the Chautauqua arch in Kansas subsided relatively late in the deposition of the Chattanooga Shale.

TYPE LOGS IN OKLAHOMA AND KANSAS

Figure 4 shows the Oklahoma type log selected by Hester and others (1990) for the Woodford Shale (from the Texas #1-B Jellison well in Major County, western Oklahoma, sec. 1, T. 20 N., R. 16 W.) and the Kansas type log that I selected for the Chattanooga Shale (from the Phoenix #1 Orme well in Kingman County, south-central Kansas, sec. 4, T. 28 S., R. 6 W.). Both logs show the upper, middle, and lower members of the Chattanooga (Woodford), with the middle member in each case having a much more radioactive response (and therefore a higher organic content) than either the upper or lower members.

Hester and others (1990) commonly found all three members of the Woodford Shale in western Oklahoma, but in Kansas often only the upper and middle members are present. The Chattanooga (Woodford) is conformable with overlying Kinderhookian shales and carbonates but unconformably overlies Lower Paleozoic formations of various ages in Kansas and Oklahoma.

In extreme northeastern Kansas a red shale or ferruginous oolite (the "Boice shale") is sometimes reported to disconformably overlie the Chattanooga Shale (Lee, 1956; Goebel, 1968). Some well-cutting descriptions from this part of the study area do include such a lithology, which may be the result of reworking and oxidation of the top of the Chattanooga. Carlson (1963) and Thompson (1986) suggested that the Boice is equivalent to the Lower Kinderhookian Hannibal Shale of northeastern Missouri.

CHATTANOOGA SHALE CROSS SECTIONS IN KANSAS

A total of 74 different well logs were used in constructing the six stratigraphic cross sections upon which this study is based. The datum for these cross sections is the base of the Mississippian carbonates (where they are present) or the tops of the pre-Chattanooga formations where both the Mississippian carbonates and the Chattanooga Shale have been removed by erosion. In those areas where the Mississippian carbonates are absent but the Chattanooga Shale is still present, the base of a carbonate unit within the upper member of the Chattanooga Shale was used as the

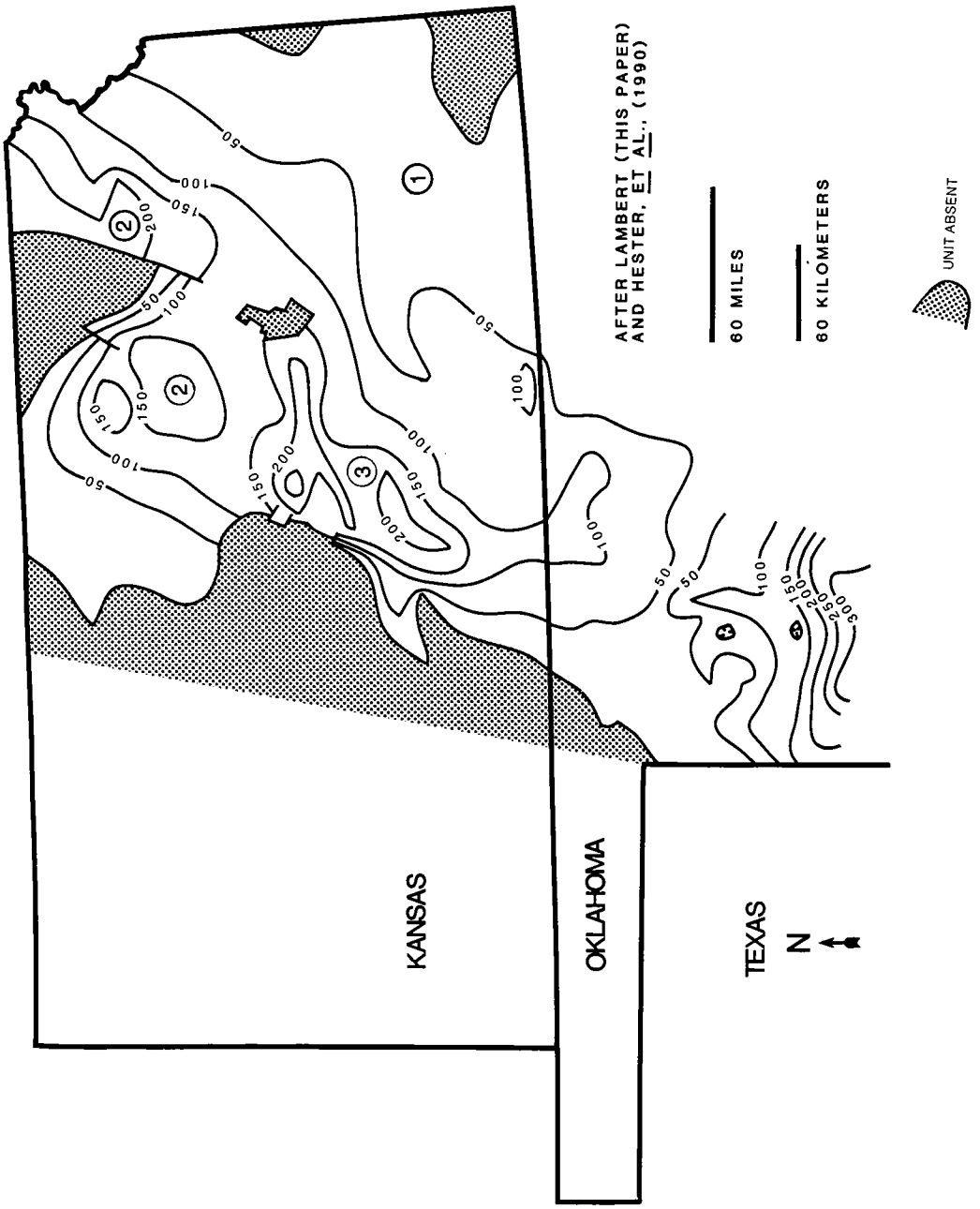

Figure 3. Isopach map for the Chattanooga Shale in Kansas and Oklahoma. Relatively thin Chattanooga over the Chautauqua arch is shown as area 1; major depocenters in northeastern and central Kansas are shown as areas 2 and 3, respectively.

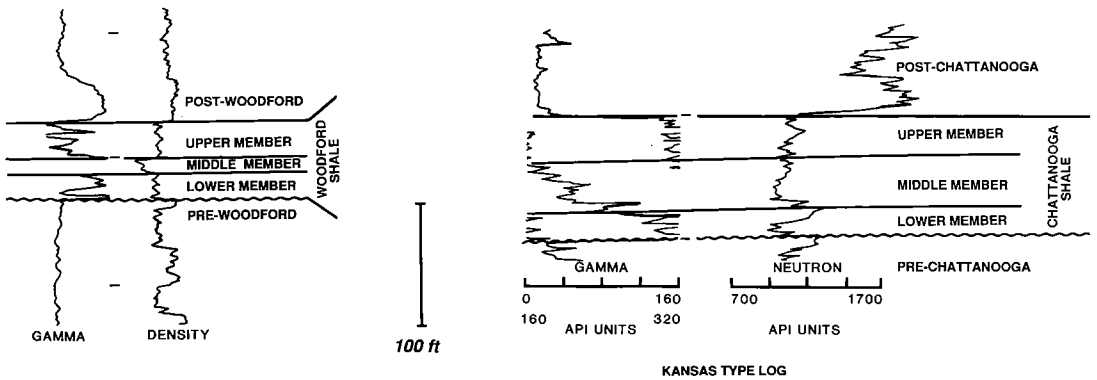

Figure 4. Oklahoma type log for the Woodford Shale and Kansas type log for the Woodford-equivalent Chattanooga Shale. Oklahoma type log of Hester and others (1990).

datum. The Misener sandstone occurs below the base of Chattanooga Shale members in parts of several cross sections, but is never more than a few feet thick and does not constitute a major internal division of the Chattanooga Shale Formation.

Section A–A′

This westernmost north–south cross section is 166 mi long and comprises 15 well logs, beginning in the eastern Oklahoma basin and continuing across the Central Kansas arch before terminating in the western Iowa basin (Fig. 2). The upper and middle members are the only shale members of the Chattanooga Shale present in this section. Their thicknesses (50 ft and 25 ft, respectively) remain more or less constant across the Oklahoma basin; however, as illustrated in Figure 5A, in the McPherson Valley area of the northeastern Central Kansas arch the upper member becomes 150 ft thick and near its base contains a lenticular limestone bed that is as much as 40 ft thick. It was in this area that Lee (1956), working with well cuttings and geophysical logs, described a limestone within the Chattanooga Shale. The fact that the upper member thins and pinches out to the north in the Iowa basin while having thickened in the McPherson Valley suggests that it was not until late in the deposition of the Chattanooga Shale that the McPherson Valley area became a major depocenter.

In the southern part of section A–A′, the upper member has a gamma-ray response of 140–150 API units, decreasing to 80 or 90 API units in the northern part of the section. Similarly, the middle member registers 240–320 API units in the south, but only 110–120 API units in the north. This trend is found in all my Chattanooga Shale cross sections, and in general the upper member has a response of 120–160 API units in southern Kansas and 80–110 API units in the north. The middle member registers anywhere from 180 to 320 API units in the south and from 110 to 140 API units in the northern part of the state.

Because gamma-ray response is indicative of the organic content of a shale, this systematic decrease in radioactivity to the north documents a progressive decrease in organic content of the Chattanooga Shale. This may have been because the more northerly locations were high enough on the shelf to be above the pycnocline that separated well-oxygenated surface water from deeper, anoxic water. Preservation potential of organic matter deposited in the north would have been low due to bioturbation of the unconsolidated sediment. Alternatively, the major source of organic matter deposited with the Chattanooga Shale may have been located south of Kansas. Comer (1989) proposed that organic productivity during Chattanooga Shale deposition was high in what is now the south-central United States due to the coastal upwelling of nutrient-rich water along the North American continental margin.

Wells 1, 3, and 5 of section A–A′ have corresponding well-cutting descriptions that show the upper member to be light-green to gray shale and the more radioactive middle member to be black shale. Because dark shales commonly contain more organic matter than shales that are light in color (McBride, 1974; Schmoker, 1980; Hosterman and Whitlow, 1983), the color difference is an additional indication that the middle member has a higher organic content than the upper member.

Sections B–B′ and C–C′

Section B–B′ is 194 mi long, incorporating 14 well logs, and section C–C′ is 208 mi long, including 16 well logs. Both sections extend from the Chautauqua arch into the Iowa basin (Fig. 2), and in both only the upper and middle shale members are present.

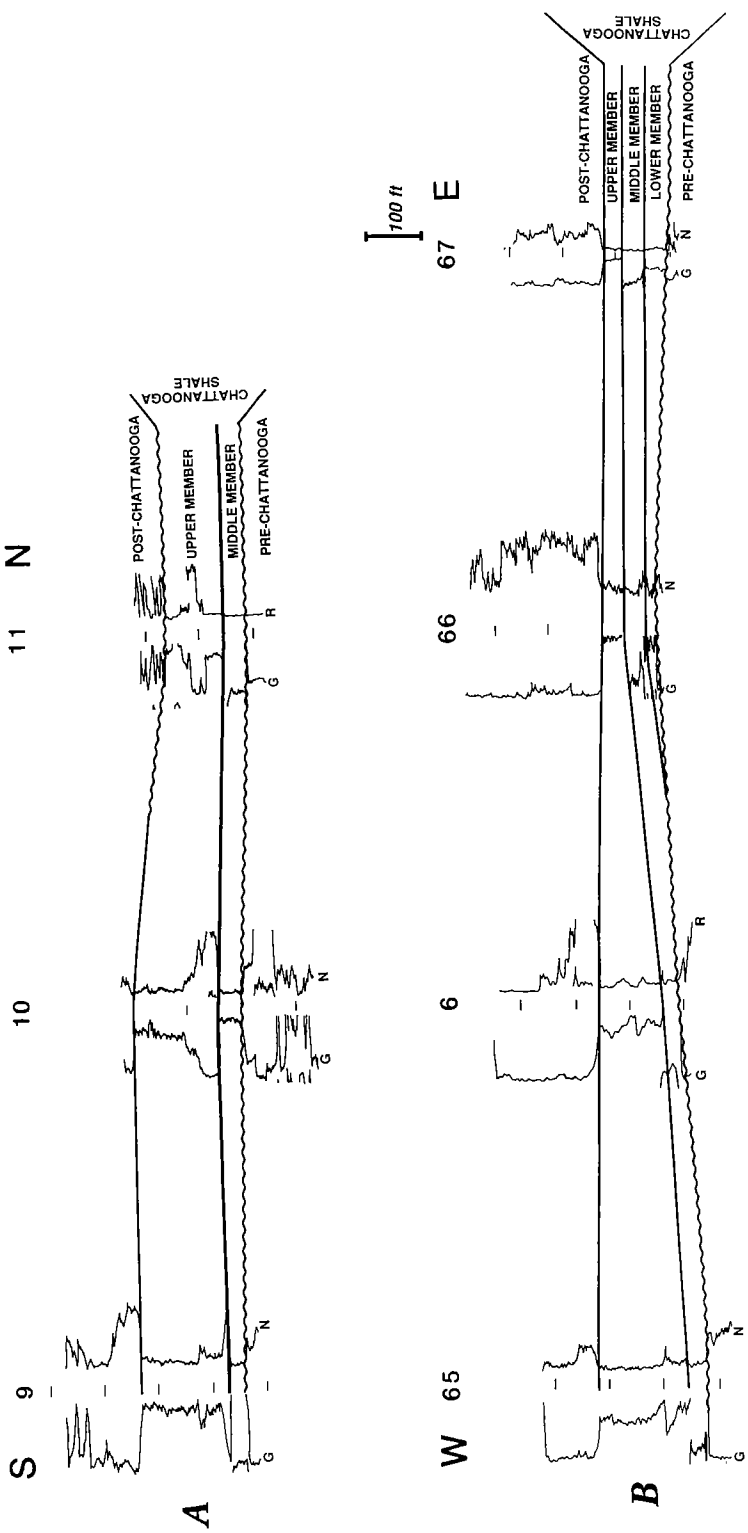

Figure 5. *A*—North–south stratigraphic cross section for Chattanooga Shale over the northeastern Central Kansas arch (the McPherson Valley area of Lee, 1956). *B*—East–west stratigraphic cross section for the Chattanooga Shale in the eastern Oklahoma basin and southern Central Kansas arch.

Judging from the variation in thickness of the upper and middle members in the southern part of section B–B′, the relative elevation of the western part of the Chautauqua arch with respect to sea level must have fluctuated a great deal. The upper member varies from <10 to >50 ft in thickness, and the middle member can be anywhere from 12 to 75 ft thick. The upper member onlaps the middle member over the Chautauqua arch in part of the southern half of section C–C′. At one point (log 31 in Appendix) the upper member rests on the unconformity at the base of the Chattanooga Shale. This suggests that the eastern part of the Chautauqua arch in Kansas remained emergent until late in the deposition of the Chattanooga Shale. The upper shale member in both cross sections thins and pinches out to the north in the Iowa basin, while the middle member becomes as much as 200 ft thick, indicating that the Iowa basin was a major depocenter early during deposition of the Chattanooga Shale in Kansas.

As in cross section A–A′, the radioactivity of both the upper and middle members decreases to the north in sections B–B′ and C–C′. However, the upper member consistently has a lower gamma-ray response than the middle member in any given well.

Section D–D′

This east–west cross section is 164 mi long and includes 11 well logs (Fig. 2). It lies completely within the northern part of the Iowa basin in Kansas and passes through one of the major Chattanooga Shale depocenters. The Chattanooga Shale in Kansas approaches its greatest thickness in the central part of section D–D′ (225 ft), although only the middle shale member is present.

Section E–E′

This section, which is 174 mi long and includes 13 well logs, begins in the McPherson Valley area of the Central Kansas arch and continues across the southern part of the Iowa basin in Kansas (Fig. 2). Both the upper and middle shale members of the Chattanooga are present.

In the westernmost well log of section E–E′ (northeastern part of the Central Kansas arch) the upper member of the Chattanooga Shale is twice as thick as the middle member (100 ft vs. 50 ft), and the upper member contains a limestone 25 ft thick. This limestone is only 12 ft thick in the next well log from the southwestern part of the Iowa basin, and it is not present in the rest of the cross section. Upper and middle member thicknesses in the southwestern Iowa basin average 60 and 132 ft, respectively. In the southeastern Iowa basin upper and middle member thicknesses average 54 and 16 ft, respectively. The upper member is thicker than the middle member over the northeastern Central Kansas arch and in the southeastern Iowa basin, and thinner than the middle member in the southwestern Iowa basin. This suggests that subsidence was greater in the southwestern Iowa basin early during Chattanooga Shale deposition and greater over the northeastern Central Kansas arch and in the southeastern Iowa basin late during Chattanooga deposition.

Section F–F′

This section is 200 mi long and contains 13 well logs (Fig. 2). It begins in the Oklahoma basin in the west, continues across the southern part of the Central Kansas arch, then follows the northern margin of the Chautauqua arch.

This cross section includes all three members of the Chattanooga Shale (see Fig. 5B). The fact that all three shale members are present only in the southernmost east–west cross section suggests that the transgression responsible for the deposition of the Chattanooga advanced onto the craton from the south. The lower member is present only over the southeastern Central Kansas arch (wells 66 and 67 in Fig. 5B), suggesting that this was the first part of the study area to subside below sea level during Chattanooga Shale deposition.

The middle member is much more radioactive than either the upper or lower members, and the upper member is somewhat more radioactive than the lower. This is similar to the situation reported by Hester and others (1990) in western Oklahoma, except that there the upper member is usually slightly less radioactive than the lower member.

Hester and others (1990) noted that the upper member in western Oklahoma thickens to the northeast toward Kansas. They cite this as evidence of the initial development of the Sedgwick basin of south-central Kansas in Early Mississippian time (Kelly and Merriam, 1964). The thickening of the upper member in the western end of section F–F′ is a further indication of this.

SUMMARY

Geophysical logs can be used to subdivide the Chattanooga Shale of Kansas into three informal shale members that correlate with internal stratigraphic units of the age-equivalent Woodford Shale of western Oklahoma. These members appear to represent organic facies of the Chattanooga that may influence its petroleum generative capacity.

The lower member of the Chattanooga Shale is present only in southern Kansas, supporting the idea of a transgression onto the craton from the south. The middle member is thickest in northeastern Kansas while the upper member is thickest in central Kansas, suggesting that the Chatta-

nooga Shale depocenter migrated from northeastern to central Kansas as deposition progressed. In the McPherson Valley area of central Kansas a lenticular limestone is developed in the lower part of the upper member, the same location in which Lee (1956) reported a limestone within the Chattanooga Shale. The upper member in southern Kansas thickens into the area now occupied by the Sedgwick basin and may indicate its early development.

ACKNOWLEDGMENTS

This paper represents part of my dissertation research in geology at the University of Kansas. I would like to thank the Kansas Geological Survey for financial support during my studies. I would also like to thank C. G. Maples, W. L. Watney, K. D. Newell, J. A. French, and L. F. Dellwig for their critical reviews of this manuscript.

REFERENCES

Amsden, T., 1975, Hunton Group (Late Ordovician, Silurian, and Early Devonian) in the Anadarko basin of Oklahoma: Oklahoma Geological Survey Bulletin 121, 214 p.

Bennet, R.; and Hulbert, M., 1986, Clay microstructure: IHRDC Press, Houston, 161 p.

Bunker, B.; Witzke, B.; Watney, W.; and Ludvigson, G., 1988, Phanerozoic history of the central Midcontinent, United States, *in* Sloss, L. (ed.), Sedimentary cover—North American craton; U.S.: Geological Society of America, The Geology of North America, v. D-2, p. 243–260.

Cardott, B.; and Lambert, M., 1985, Thermal maturation by vitrinite reflectance of Woodford Shale, Anadarko basin, Oklahoma: American Association of Petroleum Geologists Bulletin, v. 69, p. 1982–1998.

Carlson, M., 1963, Lithostratigraphy and correlation of the Mississippian System in Nebraska: Nebraska Geological Survey Bulletin 21, 46 p.

Comer, J., 1989, Depositional model for Upper Devonian black shale (Woodford Formation) in Permian basin, west Texas and southeastern New Mexico [abstract]: American Association of Petroleum Geologists Bulletin, v. 73, p. 346.

Comer, J.; and Hinch, H., 1987, Recognizing and quantifying expulsion of oil from the Woodford Formation and age-equivalent rocks in Oklahoma and Arkansas: American Association of Petroleum Geologists Bulletin, v. 71, p. 844–858.

Demaison, G.; and Moore, G., 1980, Anoxic environments and oil source bed genesis: American Association of Petroleum Geologists Bulletin, v. 64, p. 1179–1209.

Doveton, J., 1986, Log analysis of subsurface geology: John Wiley and Sons, New York, 273 p.

Ettensohn, F., 1985, Controls on development of Catskill Delta complex basin-facies, *in* Woodrow, D.; and Sevon, W. (eds.), The Catskill Delta: Geological Society of America Special Paper 201, p. 65–77.

Foster, R.; and De, P., 1971, Optical and electron microscopic investigation of shear induced structures in lightly consolidated (soft) and heavily consolidated (hard) kaolinite: Clays and Clay Minerals, v. 19, p. 31–47.

Gipson, M., 1965, Application of the electron microscope to the study of particle orientation and fissility in shale: Journal of Sedimentary Petrology, v. 35, p. 408–414.

Goebel, E., 1968, Undifferentiated Silurian and Devonian, *in* Zeller, D. (ed.), The stratigraphic succession in Kansas: Kansas Geological Survey Bulletin 189, p. 15–17.

Hass, W.; and Huddle, J., 1965, Late Devonian and Early Mississippian age of the Woodford Shale in Oklahoma as determined by conodonts, *in* Geological Survey research: U.S. Geological Survey Professional Paper 525-D, p. 125–132.

Heckel, P.; and Witzke, B., 1979, Devonian world paleogeography determined from distribution of carbonates and related lithic paleoclimatic indicators, *in* House, M.; Scrutton, C.; and Bassett, M. (eds.), The Devonian System: Special Papers in Paleontology No. 23, p. 99–123.

Hester, T.; Schmoker, J.; and Sahl, H., 1990, Log-derived regional source-rock characteristics of the Woodford Shale, Anadarko basin, Oklahoma: U.S. Geological Survey Bulletin 1866-D, 38 p.

Hosterman, J.; and Whitlow, S., 1983, Clay mineralogy of Devonian shales in the Appalachian basin: U.S. Geological Survey Professional Paper 1298, 31 p.

Hunt, J., 1961, Distribution of hydrocarbons in sedimentary rocks: Geochimica et Cosmochimica Acta, v. 22, p. 37–49.

_____1979, Petroleum geochemistry and geology: W. H. Freeman and Co., San Francisco, 617 p.

Johnson, K. S., 1989, Geologic evolution of the Anadarko basin, *in* Johnson, K. S. (ed.), Anadarko basin symposium, 1988: Oklahoma Geological Survey Circular 90, p. 3–12.

Jones, R., 1982, Organic facies distribution: contributor to both wins and losses [abstract]: American Association of Petroleum Geologists Bulletin, v. 66, p. 586.

_____1983, Organic matter characteristics near the shelf-slope boundary, *in* Stanley, D.; and Moore, G. (eds.), The shelfbreak: critical interface on continental margins: Society of Economic Paleontologists and Mineralogists Special Publication 33, p. 391–405.

_____1987, Organic facies, *in* Brooks, J.; and Welte, D. (eds.), Advances in petroleum geochemistry, vol. 2: Academic Press, New York, p. 1–90.

Jones, R.; and Demaison, G., 1980, Organic facies-stratigraphic concept and exploration tool [abstract]: American Association of Petroleum Geologists Bulletin, v. 64, p. 729.

Kelly, T.; and Merriam, D., 1964, Structural development of the Sedgwick basin, south-central Kansas: Transactions of the Kansas Academy of Science, v. 67, p. 111–125.

Lambert, M., 1982, Vitrinite reflectance of Woodford Shale in Anadarko basin, Oklahoma [abstract]: American Association of Petroleum Geologists Bulletin, v. 66, p. 591–592.

Lee, W., 1956, Stratigraphy and structural development of the Salina basin area: Kansas Geological Survey Bulletin 121, 167 p.

Lewan, M.; Winters, J.; and McDonald, J., 1979, Generation of oil-like pyrolyzates from organic-rich shales: Science, v. 203, p. 897–899.

Magara, K., 1978, Compaction and fluid migration: Elsevier, New York, 319 p.

McBride, E., 1974, Significance of color in red, green, purple, olive, brown, and gray beds of Difunta Group, northeastern Mexico: Journal of Sedimentary Petrology, v. 44, p. 760–773.

Meade, R., 1964, Removal of water and rearrangement of particles during the compaction of clayey sediment—review: U.S. Geological Survey Professional Paper 497-B, 23 p.

Merriam, D., 1963, The geologic history of Kansas: Kansas Geological Survey Bulletin 162, 317 p.

Odom, I., 1967, Clay fabric and its relation to structural properties in Mid-Continent Pennsylvanian sediments: Journal of Sedimentary Petrology, v. 37, p. 610–623.

Over, D. J.; and Barrick, J. E., 1990, The Devonian/Carboniferous boundary in the Woodford Shale, Lawrence uplift, south-central Oklahoma, *in* Ritter, S. M. (ed.), Early to Middle Paleozoic conodont biostratigraphy of the Arbuckle Mountains, southern Oklahoma: Oklahoma Geological Survey Guidebook 27, p. 63–73.

Polley, M., 1982, Petrology of the Ohio Shale: effect of clay fabric, mineralogy, and carbon content on fissility: Bowling Green State University unpublished M.S. thesis, 97 p.

Schmoker, J., 1980, Organic content of Devonian shale in western Appalachian basin: American Association of Petroleum Geologists Bulletin, v. 64, p. 2156–2165.

_____1981, Determination of organic-matter content of Appalachian Devonian shales from gamma-ray logs: American Association of Petroleum Geologists Bulletin, v. 65, p. 1285–1298.

Sloss, L., 1963, Sequences in the cratonic interior of North America: Geological Society of America Bulletin, v. 74, p. 93–114.

Sullivan, K., 1985, Organic facies variation of the Woodford Shale in western Oklahoma: Shale Shaker, v. 35, p. 76–89.

Thompson, T., 1986, Mississippian System, *pt. 4 of* Paleozoic success in Missouri: Missouri Geological Survey Report of Investigation 70, 182 p.

Tissot, B.; and Welte, D., 1984, Petroleum formation and occurrence: Springer-Verlag, New York, 699 p.

Urban, J. B., 1960, Microfossils of the Woodford Shale (Devonian) of Oklahoma: University of Oklahoma unpublished M.S. thesis, 77 p.

Witzke, B.; and Heckel, P., 1988, Paleoclimatic indicators and inferred Devonian paleolatitudes of Euramerica, *in* McMillan, N.; Embry, A.; and Glass, D. (eds.), Devonian of the world: Canadian Society of Petroleum Geologists, v. 1, p. 49–63.

APPENDIX: Wells Used in Cross Sections

	Well	Location	Operator	Well name
Section A–A′	1	10–34S–8W	Mull	1 Dusenbury
	2	16–33S–8W	Mack	1 McKenny
	3	18–32S–8W	Mull	1 Morse
	4	16–31S–8W	Rabinowitz	1 Sanders
	5	9–30S–8W	Petroleum	1 Evans
	6	1–28S–8W	Beardmore	1 Coleman
	7	1–27S–8W	Alpha	1 Stucky
	8	23–25S–8W	Ribbs	2 Krehbiel
	9	15–24S–9W	Smitherman	1 Dion
	10	12–22S–9W	Sterling	1 Proffitt
	11	19–20S–8W	Sutton	2 Sessler
	12	29–16S–8W	American	1 Harmon
	13	33–11S–7W	Rupp-Ferguson	1 Metz
	14	14–10S–9W	National	1 Peckham
	15	34–6S–6W	KAI	1 Thierolf
Section B–B′	16	9–35S–2E	Co-operative	1 Callender
	17	15–34S–1E	Raymond	1 Wolf
	18	26–31S–2E	Brant & Clark	1 Evers
	19	13–29S–1E	Brandt	1 Phillips
	20	9–28S–2E	Ash	4 Mollett
	21	29–25S–1E	Uxford	29-164 Mouser
	22	16–23S–2E	Hummon	1-A Dey
	23	7–21S–1E	Time	2 East
	24	22–19S–1E	Wildcat	2 Groening
	25	10–18S–1W	Osage	2 Dozier
	26	3–16S–1E	Rains & Wmson.	1 Jones
	27	16–12S–1W	Terra	1 Buhler
	28	9–11S–1E	Barnett	1 Nagley
	29	26–6S–1E	Gulf	1 Turner
Section C–C′	30	25–34S–16E	Benson	1 Britton
	31	27–32S–16E	Kennedy	D-1 Kennedy
	32	22–29S–16E	Crest	1 Crestwiles
	33	2–28S–15E	V. & N.	2 Midwest Minerals
	34	26–25S–14E	Mecca	4 Mecca-Sheedy
	35	29–21S–15E	MAI	1 Ward
	36	6–19S–15E	Brunson-Spines	1 Jones
	37	23–16S–16E	Winwell	1 Woodward
	38	8–14S–17E	Five Nations	1 Keller
	39	20–11S–13E	Kaiser-Francis	1A Adams
	40	12–9S–12E	Anschutz	1 Marshall
	41	15–7S–13E	Phillips	1A Leach
	42	35–6S–14E	Dance	1 Fernkopt
	43	9–5S–13E	Cities	1A Feldkamp
	44	17–3S–14E	Pendleton	1 Edelman-Baumgartner
	45	3–1S–15E	Slawson	2 National Bank of Commerce

APPENDIX: *Continued*

	Well	Location	Operator	Well name
Section D–D′	14	14–10S–9W	National	1 Peckham
	46	36–8S–5W	Thompson & Waterman	1 Yenni
	47	21–8S–2W	Rupp-Ferguson	1 Larson
	48	19–8S–3E	Wakefield	1 Chestnut
	49	22–8S–4E	Pendleton	1 Mall-Steinbach
	50	36–8S–5E	Waugh	1 Renz
	51	6–8S–9E	Gulf	1 Ewing
	52	13–8S–11E	Pendleton	1 Bouziden
	40	12–9S–12E	Anschutz	1 Marshall
	53	24–8S–15E	Palmer	1 Robb
	54	26–7S–18E	Lear	1-26 Ellerman
Section E–E′	11	19–20S–8W	Sutton	2 Sessler
	55	5–19S–5W	Durbin	1 Durland
	56	31–19S–3W	Natural	1 Quantius
	57	26–19S–2W	Derby	3 Unruh
	24	22–19S–1E	Wildcat	2 Groening
	58	36–19S–2E	Anadarko	1-A Bartel
	59	3–19S–4E	Rock Island	1 Boettcher
	60	20–19S–8E	Brandt	1 Rettinger
	61	2–20S–10E	Little George	1 Miller
	62	26–19S–12E	Magnum	1 Carpenter
	63	30–19S–14E	Gear	1 Smith
	36	6–19S–15E	Brunson-Spines	1 Jones
	64	34–19S–17E	Benson	1 James
Section F–F′	65	36–28S–10W	Anschutz	1 Adelhardt
	6	1–28S–8W	Beardmore	1 Coleman
	66	4–28S–6W	Phoenix	1 Orme
	67	9–28S–5W	Saphire	1 Padgett
	68	9–28S–2W	Pickrell	1 Miles
	20	9–28S–2E	Ash	4 Mollett
	69	22–28S–3E	Petro-American	3 McCall
	70	9–28S–7E	Gary	2A Bing
	71	25–27S–8E	Beaumont	31A Lewis
	72	8–28S–11E	Morrow	1 Knight
	73	26–28S–13E	McGinnis	1 Blinn
	33	2–28S–15E	V. & N.	2 Midwest Minerals
	74	13–28S–17E	Burroughs	C-33 Kepley

Effects of Weathering and Maturity on the Geochemical Characteristics of the Woodford Shale

R. Paul Philp, Junhong Chen, Alfredo Galvez-Sinibaldi, Huaida Wang, and Jonathan D. Allen
University of Oklahoma

ABSTRACT.—The Woodford Shale is an organic-rich black shale deposited in an euxinic open-sea environment and is thought to be one of the principal sources of hydrocarbons in the Anadarko basin. The effects of weathering and maturity on geochemical characteristics of the Woodford Shale have been investigated and will be reported in this paper. Five surface rock samples and 11 rock samples from different depths have been collected, extracted, and subjected to analysis by GC, GC–MS, Py/GC–MS, isotopic compositions and petrographic characterization.

It has been observed that the surface samples have changed in their hydrocarbon composition and stable isotopic composition as a result of weathering. According to the similarities in various chromatograms, distributions of steranes and terpanes, and isotopic data, the surface samples can be divided into two groups. Compared with Group II, the Group I samples contain lower contents of n-alkanes, lower tricyclic terpanes (or low values of tricyclic terpanes/hopanes), but higher contents of C_{21}–C_{22} steranes and αββ steranes.

The effects of maturity on the geochemical characteristics of Woodford Shale also have been investigated from pyrolysis and the distribution of alkanes, aromatics, steranes, and terpanes. The thermal maturity parameters of steranes and terpanes are used to assess the maturation. The hydrocarbon generation potential is significantly greater below 8,500 ft based on the S_1/S_1+S_2 data from Py/GC analysis. The MPI values are also observed to increase with increasing depth and maturity.

In conclusion, it is observed that significant alteration has occurred to the Woodford Shale as a result of weathering. Hence, as previously noted, a great deal of care needs to be exercised when collecting and selecting rock samples, particularly outcrop samples, for source rock characterization.

INTRODUCTION

During evolution of a sedimentary basin, sedimentary rocks containing significant quantities of organic matter are expected to produce liquid hydrocarbons, which will be expelled out of the source rocks and subsequently migrate to a reservoir or a trap. Thermal maturation of the organic matter in the source rocks is the principal step in the formation of oil accumulations. Thermal maturation will have a major effect on the composition of the organic matter in source rocks and crude oils. Other processes that will affect the composition of organic matter will be bacterial attack, water washing, and oxidation by free oxygen. A comprehensive knowledge of the effects of these various processes on the organic matter in source rocks will help us acquire better knowledge of the evolution of the source rocks and the fate of organic matter.

The Anadarko basin, located in western Oklahoma, is one of the greatest oil and gas provinces in the United States (Johnson, 1989). The geologic evolution of the Anadarko basin has been extensively studied by many researchers and recently described by Johnson (1989). Recently, some geochemical studies have been carried out in the basin, including a study by Philp and others (1989) on the evolution of oils, source rocks, and tar sands in this basin. Another geochemical study by Burruss and Hatch (1989) presented evidence for multiple sources of oils and long-distance oil migration.

The Woodford Shale is an organic-rich black shale deposited in an euxinic open-sea environment and is thought to be one of the principal sources of hydrocarbons in the Anadarko basin. In the present study the effects of weathering and maturity on geochemical characteristics of organic matter in the Woodford Shale have been investigated and will be reported in this paper.

EXPERIMENTAL

Sample Preparation

Five surface rock samples and 11 subsurface rock samples of Woodford Shale were collected from the Arbuckle Mountains and Anadarko basin in Oklahoma, respectively (Fig. 1). Total organic

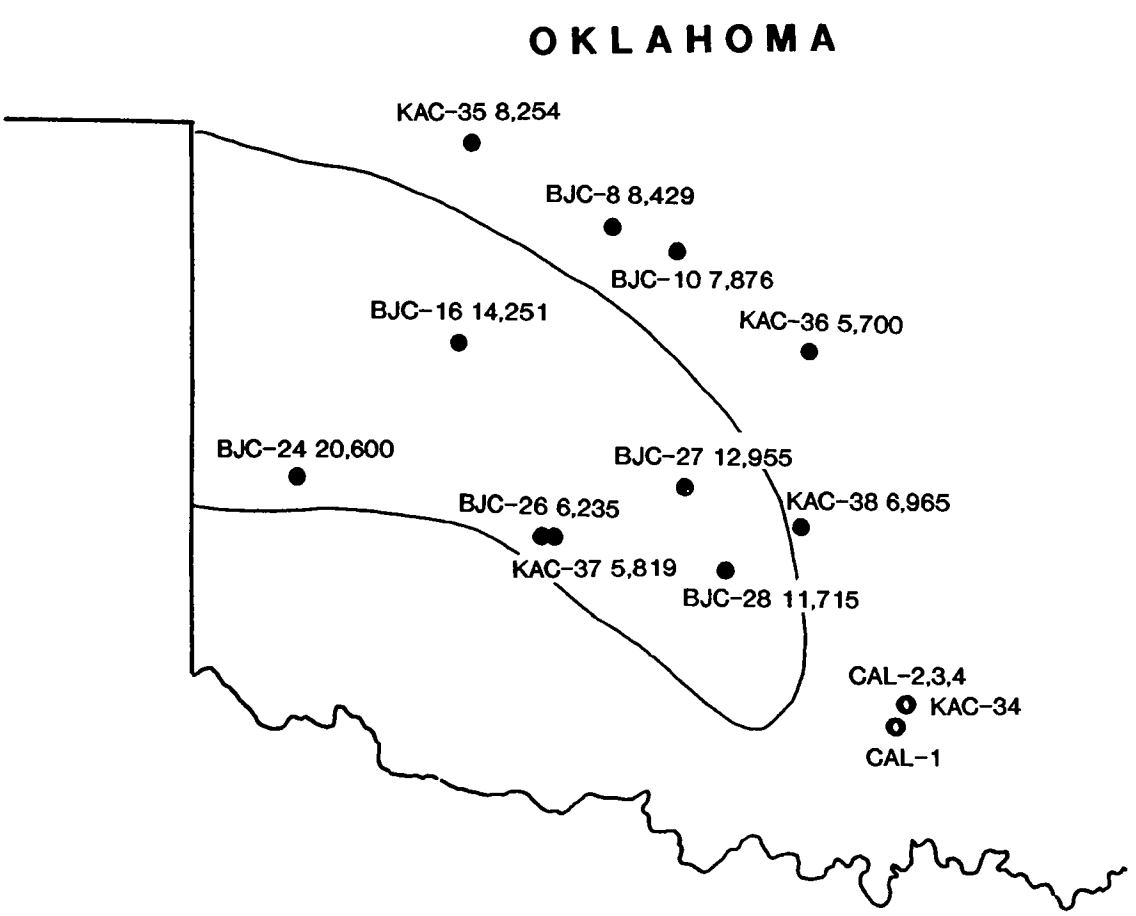

Figure 1. Map displaying the positions of samples which were used in our study. Dots are subsurface samples; the number following each sample's name is its depth in feet. Open circles are surface samples.

carbon (TOC) values for these samples were obtained by Core Lab and the rock samples were cleaned, crushed, and extracted with methylene dichloride. The rock extracts and crude oils were treated to remove asphaltenes by precipitation with n-pentane, and the n-pentane soluble fractions were further fractionated by thin layer chromatography (TLC) into aliphatic hydrocarbons, aromatic hydrocarbons, and NSO components prior to analysis by gas chromatography (GC), gas chromatography–mass spectrometry (GC–MS), and determination of the stable isotopic composition of the various fractions.

Analytical Procedures

Gas Chromatography (GC)

The saturate and aromatic fractions were analyzed by GC, using a Hewlett-Packard 5890A GC equipped with a 30 × 0.25 mm i.d. DB-5 column. The GC temperature conditions for the saturate fractions were as follows: injector temperature was 300°C; column temperature was initially 40°C and programmed to increase at 10°C/min for the first 10 minutes and then 3°C/min to 300°C where it was held for 20 minutes. The GC temperature conditions for the aromatic fractions were: injector temperature was 300°C; column temperature was initially 40°C for 1.5 min and programmed to increase at 4°C/min to 300°C where it was held for 30 minutes. Helium was employed as carrier gas. Peak heights were determined from the chromatograms and used for quantitative analysis.

Gas Chromatography–Mass Spectrometry (GC–MS)

GC–MS analyses were performed to determine distributions of steranes and terpanes using a Finnigan TSQ-70 interfaced to a Varian 3340 GC and equipped with a 30 × 0.25 mm i.d. DB-5 col-

umn. The GC conditions were as follows: injector temperature was 300°C; column temperature was isothermal at 40°C and programmed to increase at 10°C/min to 140°C and then at 3°C/min to 300°C where it was held isothermally for 20 minutes. Helium was employed as carrier gas. The ion source temperature was 200°C; electron energy and emission current were –70 eV and 200 uA, respectively.

Pyrolysis/GC–MS

A Pyran System was employed for the pyrolysis analysis. The pyrolysis conditions were as follows: isothermal at 300°C for 1 min, programmed to increase to 610°C at 30°C/min; held isothermally at 610°C for 5 min, then cooled down to ambient temperature. Helium was used as carrier gas (60 ml/min in level I; 30 ml/min in level II). Sample weights used were from 10 to 50 mg depending upon their TOC content and had been crushed to 200-mesh size.

^{13}C Isotopic Composition

The extracts and various fractions from the core samples were statically combusted according to the methods of Sofer (1980). Following combustion, the tubes were opened on a vacuum line (2×10^{-3} torr) and water was removed by trapping at –70°C (Neslab Cryocool CC-60 cooling unit). The CO_2 was collected in a gas sampling ampoule at –196°C (liquid N_2) and then transferred directly to the inlet system of a Finnigan MAT Delta E isotope ratio mass spectrometer equipped with a 90° sector magnetic deflector. The stable carbon isotopic composition is expressed as:

$$\delta^{13}C\ (‰) = [R_{sample}/R_{standard} - 1] \times 10^3$$

where R is the abundance ratio of the heavy to light isotope of carbon ($^{13}C/^{12}C$). The values are expressed relative to PDB carbonate (0‰) and are corrected for ^{17}O contribution.

RESULTS AND DISCUSSIONS

Thermal Maturation

The occurrence of hydrocarbons in organic-rich source rocks has been one of the major targets of petroleum geochemistry. Thermal maturation is a major factor affecting the formation and occurrence of hydrocarbons. With increasing temperature, hydrocarbon content will increase in source rocks with breakdown of the kerogen. During their formation from kerogen, the composition of hydrocarbons, including biomarkers, will undergo some changes. Studying these changes with increasing depth provides us with information on the fate of hydrocarbons during thermal maturation and an evaluation of the source rocks.

Bulk Composition

Rock-Eval type pyrolysis is a fast, convenient method to evaluate the source rocks. The S_1 peak represents the free hydrocarbons already produced from kerogen breakdown and ready for migration and accumulation. The S_2 peak represents the hydrocarbons formed from kerogen during pyrolysis under high analytical temperature (Fig. 2). The ratio of S_1/S_1+S_2 (calculated from peak area) has been used as a geochemical parameter for evaluation of source rock quality (Tissot and Welte, 1984; and references therein). An increase in the area of S_1 and the S_1/S_1+S_2 ratio with increasing depth (Fig. 2) indicates that the hydrocarbon content of the Woodford Shale was enhanced with the increasing thermal maturity. From Figure 2, it can also be noted that the ratio begins to increase at a greater rate at 8,500 ft where the vitrinite reflectance is ~0.6% which is at the threshold of the oil generation window.

It can also be noted that the ratio of S_1/S_1+S_2 of some samples is lower than other samples just below or above them although the overall trend is an increase in this ratio with depth. One possible reason for the shift in the S_1/S_1+S_2 ratio could be the facies changes causing some differences in composition of organic matter, which in turn causes the change in this ratio. There could be other reasons for variations in the values for the deeper samples at 11,715 ft (BJC-28) and 14,251 ft (BJC-16). The depth range from 11,000 to 11,900 ft was thought to correspond to the main phase of oil expulsion in Woodford Shale in the Anadarko basin (Cardott, 1989). These two samples are in, or already through, the oil expulsion phase. The low values for the S_1/S_1+S_2 ratio may be caused by a depletion in the liquid hydrocarbons which have undergone primary migration.

n-Alkanes

The hydrocarbons formed as a result of increasing maturity are dominated by n-alkanes. The composition of these hydrocarbons changes with depth. A major change to the n-alkane distributions observed in the Woodford Shale is that the relative content of light hydrocarbons increased compared with that of higher molecular weight n-alkanes with increasing depth (Fig. 3). This change in the n-alkane distribution was caused by the breakdown of long-chain alkanes into short-chain alkanes at higher temperatures.

Terpanes and Steranes

Terpanes and steranes are important cyclic biomarkers in crude oils and oil source rocks, al-

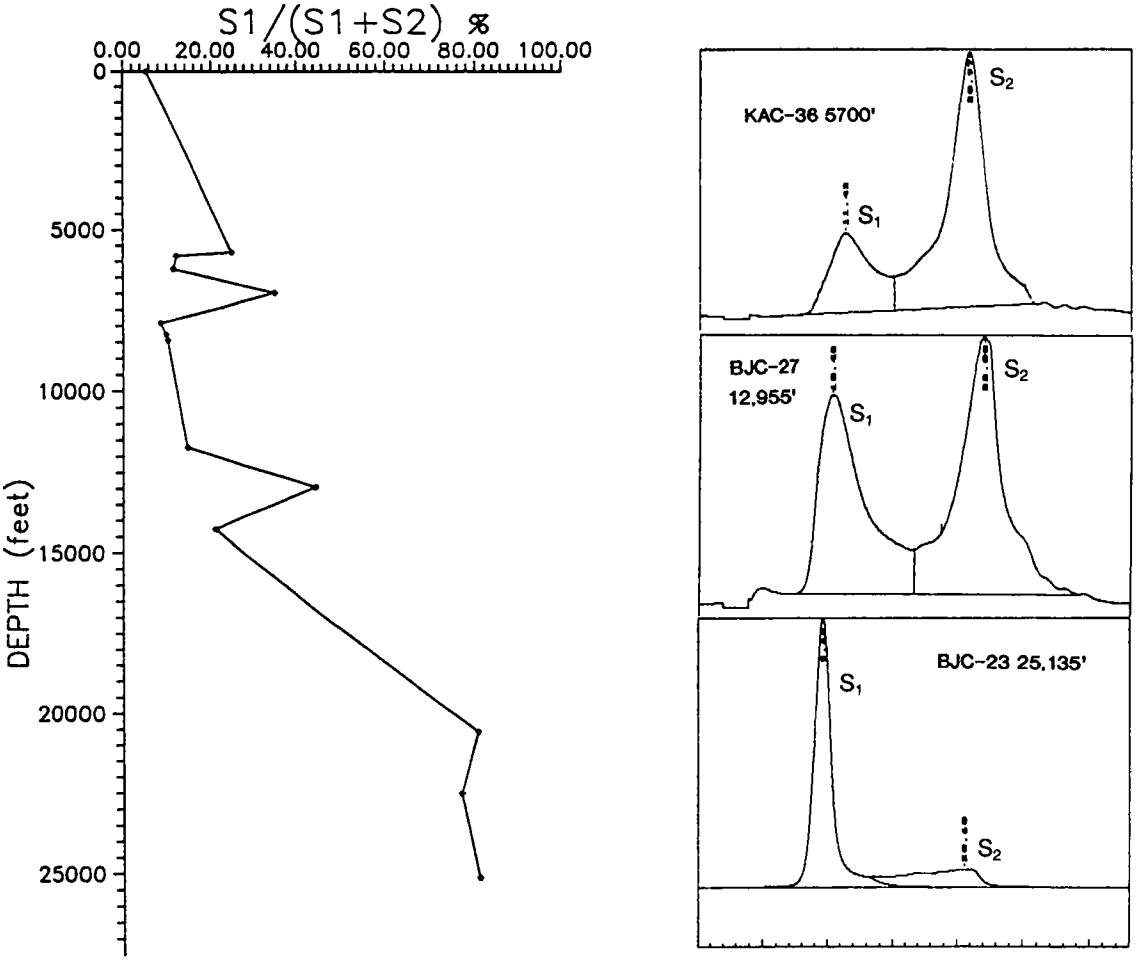

Figure 2. Diagram showing that the ratio of S_1/S_1+S_2 from Py/GC increases with increasing burial depth. The general increasing trend is caused by thermal maturation. The low ratios of samples at 11,715 ft (BJC-28) and 14,251 ft (BJC-16) might be caused by oil expulsion.

though their concentrations are generally lower than the n-alkanes. The distributions of these biomarkers are also subject to change with increasing maturity. A major change with increasing maturity was that the relative concentrations of extended tricyclic terpanes (C_{19}–C_{30}) increased compared to pentacyclic terpanes (mainly C_{27}–C_{35} hopanes) (Fig. 4A), and low molecular weight steranes (C_{21}–C_{22}) increased compared to regular steranes (C_{27}–C_{29}) (Fig. 4B). The probable reason for the changes in the sterane distributions is that the regular C_{27}–C_{29} steranes were broken down through cracking of side chain into low molecular weight steranes without changes in the cyclic nucleus. The situation for terpanes is presumably more complicated because the pentacyclic terpanes (here mainly hopanes) are not readily converted into extended tricyclic terpanes through cracking of D and E rings. Actually, extended tricyclic terpanes are thought to be structurally and biogenetically unrelated to the hopanes by virture of the point of attachment of the side chain (Seifert and Moldowan, 1986). One possible explanation for the distribution of the terpanes is that the tricyclic terpanes are more thermally stable than the hopane series. The relatively high concentrations of high molecular weight hopanes up to C_{35} were observed to occur in shallow (or immature) source rocks (e.g., KAC-37, Fig. 4A). In contrast, relative concentrations of the C_{33}–C_{35} hopanes in the deep samples (e.g., BJC-27, Fig. 4A), were extremely low as a result of the transformation of high molecular weight hopanes into low molecular weight hopanes through side-chain cracking. Meanwhile, the deeper source-rock extracts (e.g., BJC-27, 12,955 ft) have relatively weak responses for the steranes and terpanes in GC–MS analysis (Fig. 4) as a result of dilution by n-alkanes formed from

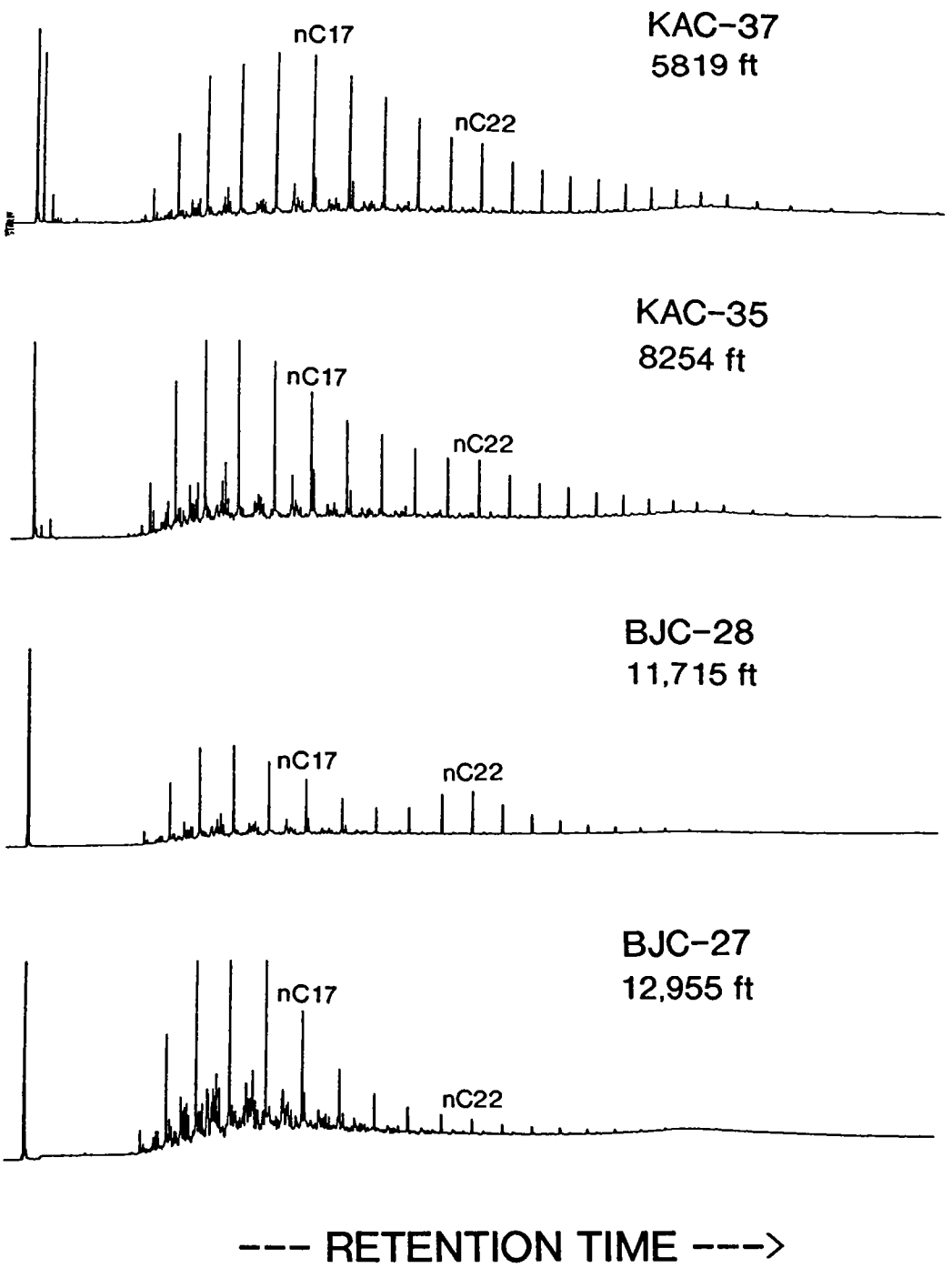

Figure 3. Representative GC chromatograms of saturate fractions of subsurface samples. The n-alkanes are dominated by light hydrocarbons.

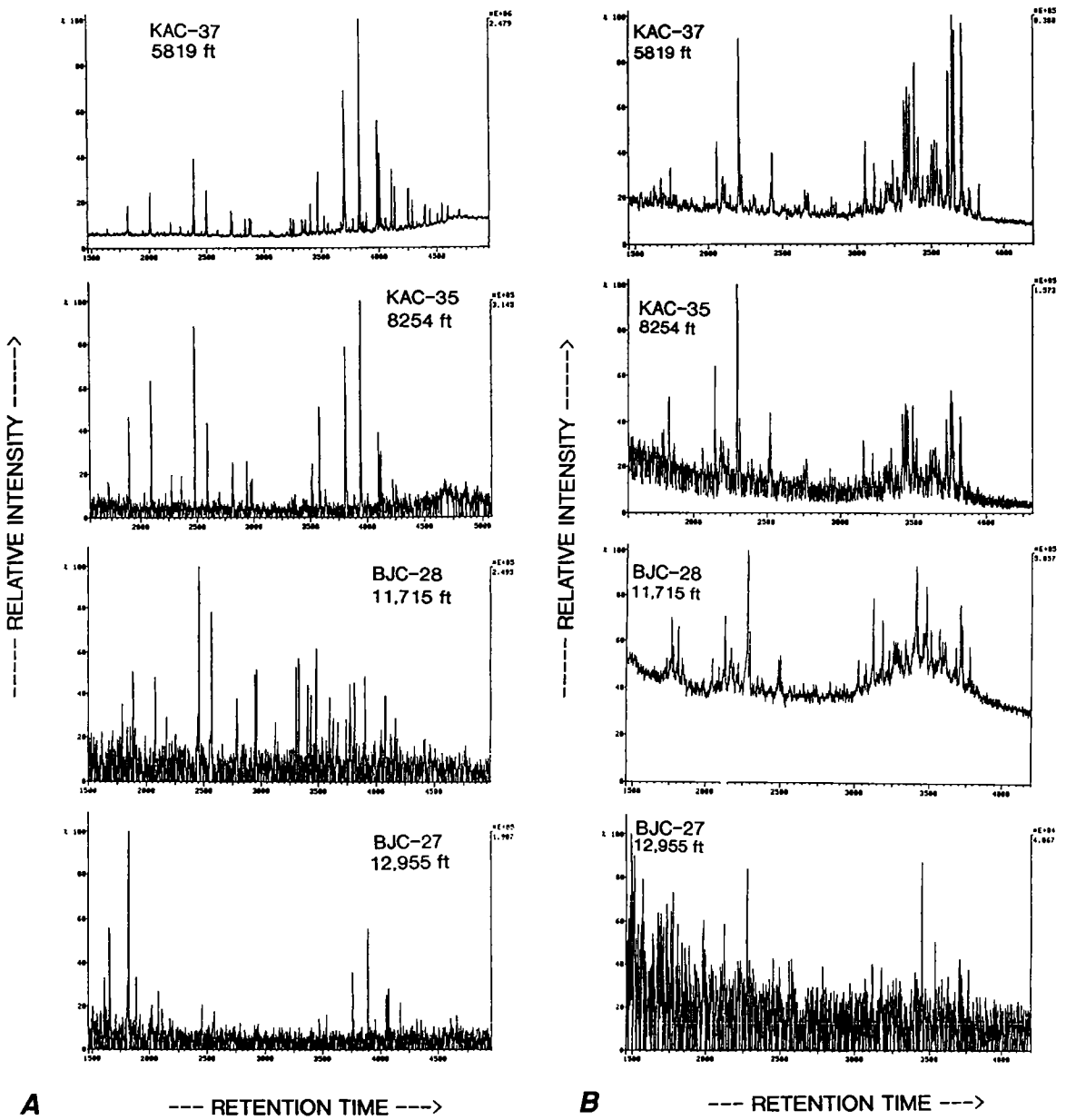

Figure 4. Mass chromatograms from GC–MS analysis of four selected samples (same samples as in Fig. 3) display the distributions of (*A*) terpanes (m/z 191) and (*B*) steranes (m/z 217).

kerogen during thermal maturation and aromatization of these saturated biomarkers.

The isomerization of steranes and hopanes is an important consequence of thermal maturation and the ratios of the 20S/20S+20R of ααα–C_{29} steranes, ββ/αα+ββ C_{29} steranes and 22S/22S+22R C_{32}-hopanes are widely used thermal maturity parameters. The two sterane ratios in Woodford Shale were observed to increase with depth from 5,700 to ~10,000 ft and then decrease with increasing depth. The hopane ratio was relatively constant with increasing depth (Fig. 5). The decrease in sterane ratios below ~10,000 ft, after the oil threshold, may be explained by the addition of immature molecules, such as the 20R and ααα-isomers from kerogen (Rüllkotter and Marzie, 1989) or preferential degradation of the these sterane isomers.

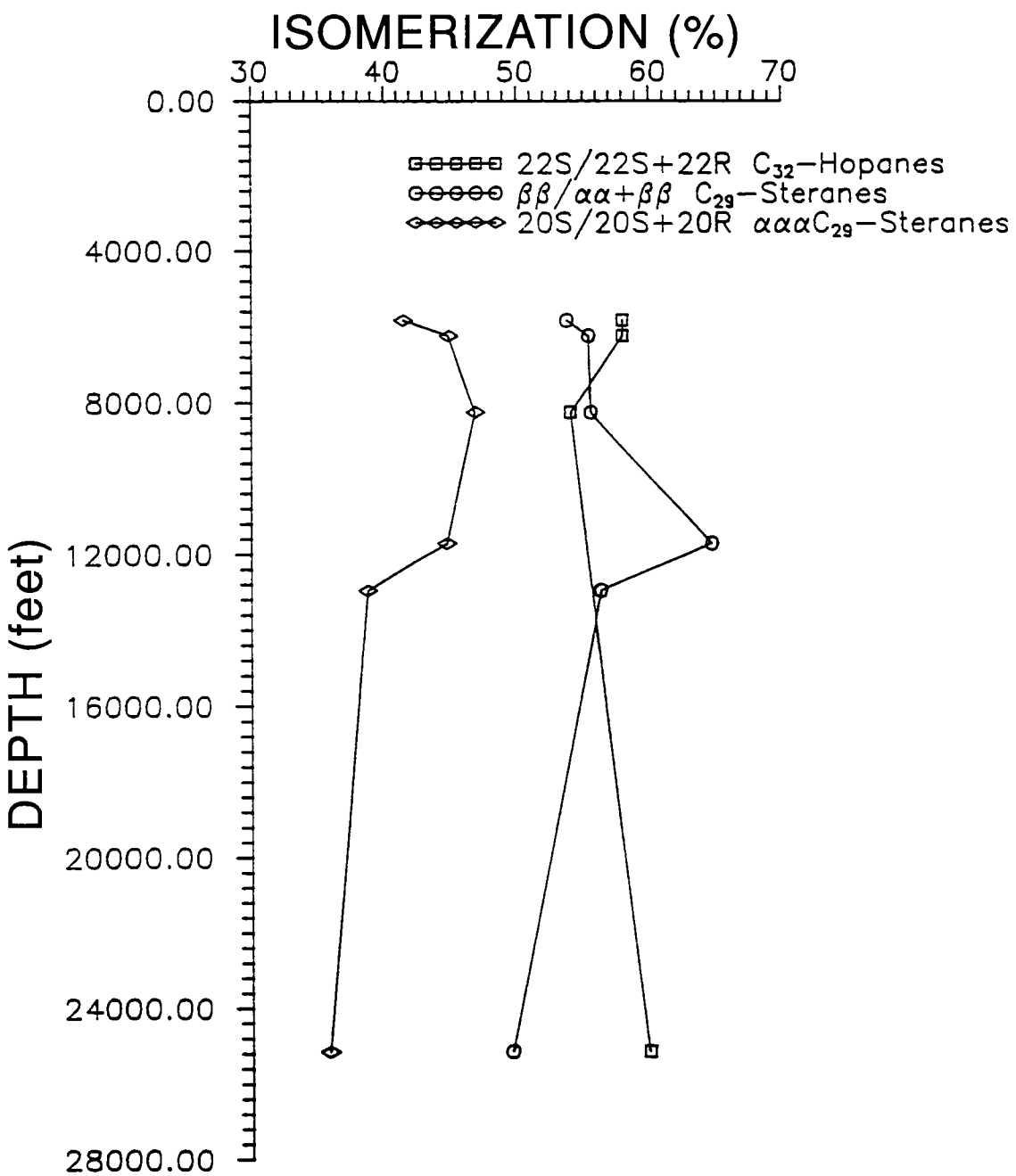

Figure 5. Diagram showing the distribution of isomerization of steranes and hopanes with depth.

Aromatics

From chromatograms of the aromatic fractions (Fig. 6), it was noted that phenanthrenes were important components of organic fractions of the Woodford Shale. Recently, the phenanthrene ratios have also been used as thermal maturity parameters (Radke and Welte, 1983). Similar distributions of phenanthrene ratios with increasing maturity have been observed in Woodford Shale. The methylphenanthrene index (MPI) (Fig. 7) and methylphenanthrene ratios (MPR-2 and MPR-3) increase with increasing maturity, at a higher rate after oil threshold. Meanwhile, MPR-1 (Fig. 7) and MPR-9 increase initially and then decrease after the oil threshold has been reached.

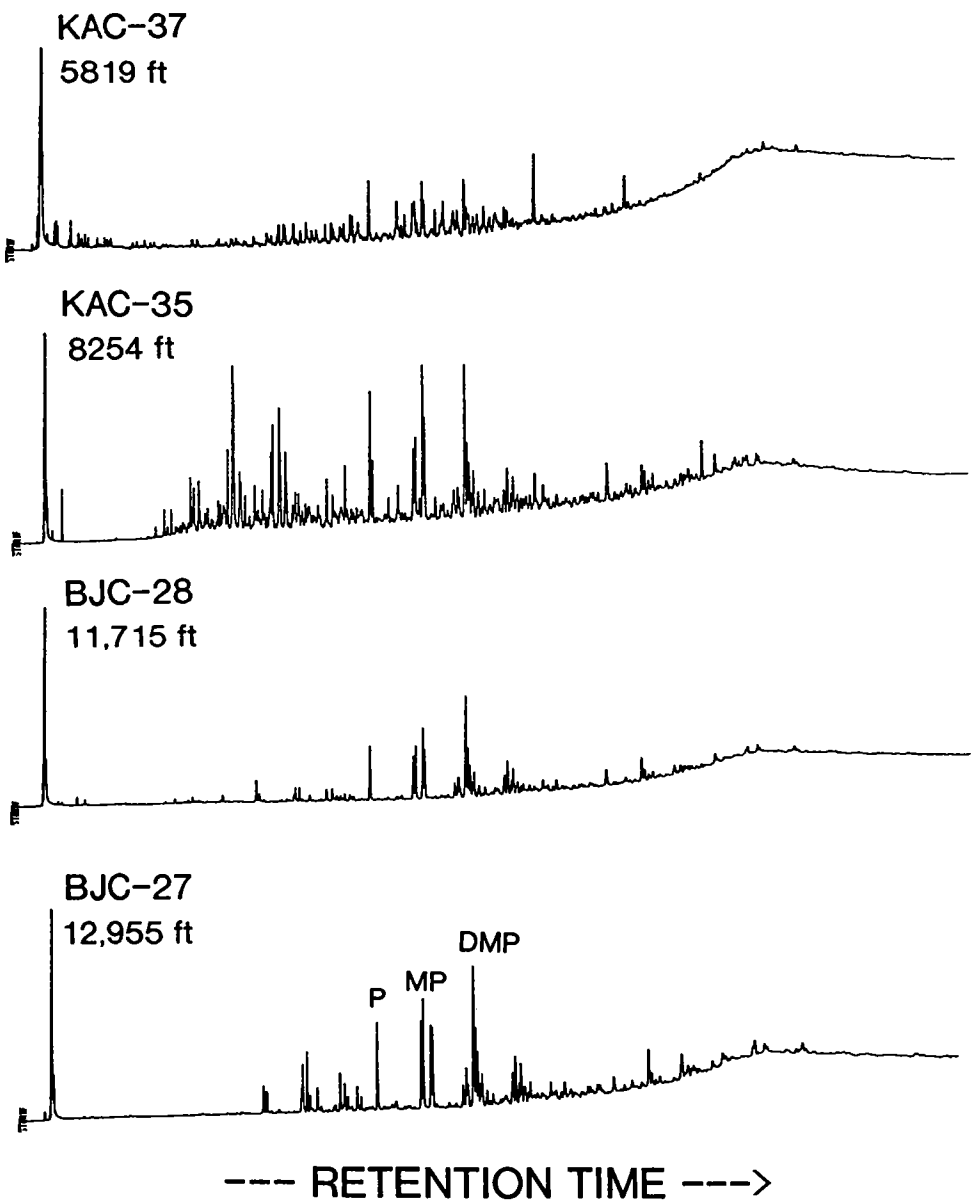

Figure 6. Representative GC chromatograms of aromatic fractions of subsurface samples. P—phenanthrene; MP—methylphenanthrene; DMP—dimethylphenanthrene.

Weathering Effects

The characteristics of organic matter in source rocks will be affected under weathering conditions. Five surface samples of Woodford Shale were collected from the Arbuckle Mountains outcrop area to study the effects of weathering on the organic matter of the Woodford Shale.

According to the distribution of the organic matter, the five samples could be divided into two groups: Group I—KAC-34 and CAL-2; Group II—CAL-1,3,4. These two groups of surface samples differ from each other in the distributions of n-alkanes, aromatics, terpanes, and steranes. The results of GC, GC–MS, and Py/GC analysis of KAC-34 and CAL-4 (representing Group I and Group II, re-

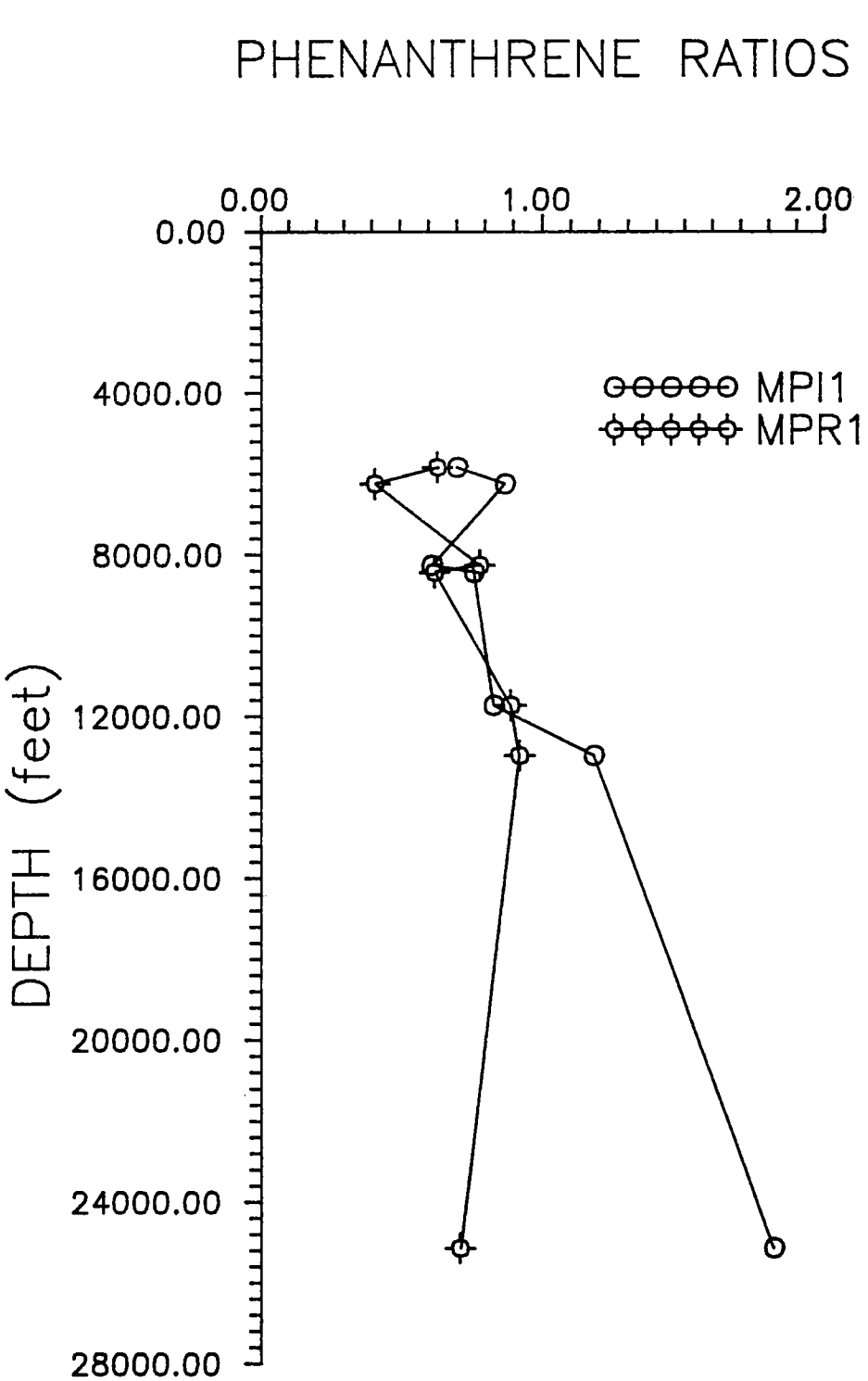

Figure 7. Changes of two representative phenanthrene ratios of subsurface samples with increasing depth.

spectively) are presented in Figures 8–13 to display how these two groups of samples differ from each other.

n-Alkanes

The saturate hydrocarbon chromatograms (Fig. 8) indicate that the n-alkanes in KAC-34 and CAL-4, representing Groups I and II, respectively, were removed to different extents compared to the subsurface samples. The n-alkanes have been almost totally removed from the Group I samples (e.g., KAC-34). The Group II samples (e.g., CAL-4) have a relatively higher content of residual n-alkanes compared with the Group I samples. The relative concentration of isoprenoid alkanes in Group II is also much higher than in the normal subsurface samples (Fig. 3). Previous studies have indicated that n-alkanes are readily removed by bacterial activity. The low n-alkane content in the Group I samples suggests that these surface samples have experienced more extensive weathering, probably biodegradation, than the surface samples belonging to Group II.

Terpanes and Steranes

KAC-34 and CAL-4 have low vitrinite reflectance values of 0.37% and 0.34%, respectively, indicating that these surface samples are of relatively low thermal maturity. Parameters based on extent of isomerization of various steranes and hopanes are widely used as maturity parameters of the organic matter in crude oils and source rocks. One advantage of using these parameters is that they are readily determined even when vitrinite is absent (as in oil) or difficult to measure (e.g., in carbonates). The disadvantage is that the distributions of steranes and hopanes are sometimes easily affected by factors other than maturation, such as bacterial activity and water washing. Surface or outcrop samples are believed to be more easily affected by these geochemical and biological processes as a result of weathering. Changes resulting from weathering conditions have been observed in the surface samples of the Woodford Shale used in this study. Although it has a low vitrinite reflectance value of 0.37%, KAC-34 has distributions of steranes similar to those of more mature samples,

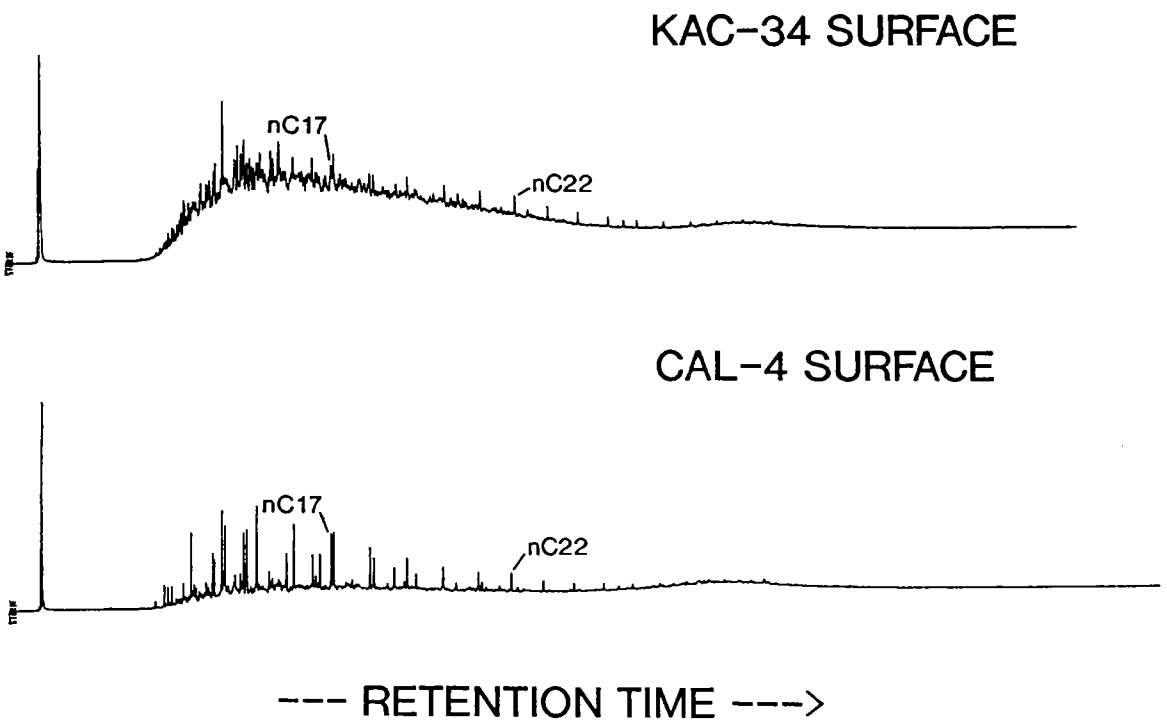

Figure 8. GC chromatograms of saturate fractions of two selected surface samples KAC-34 and CAL-4, representing Group I and Group II surface samples respectively. The n-alkanes in KAC-34 were more severely removed.

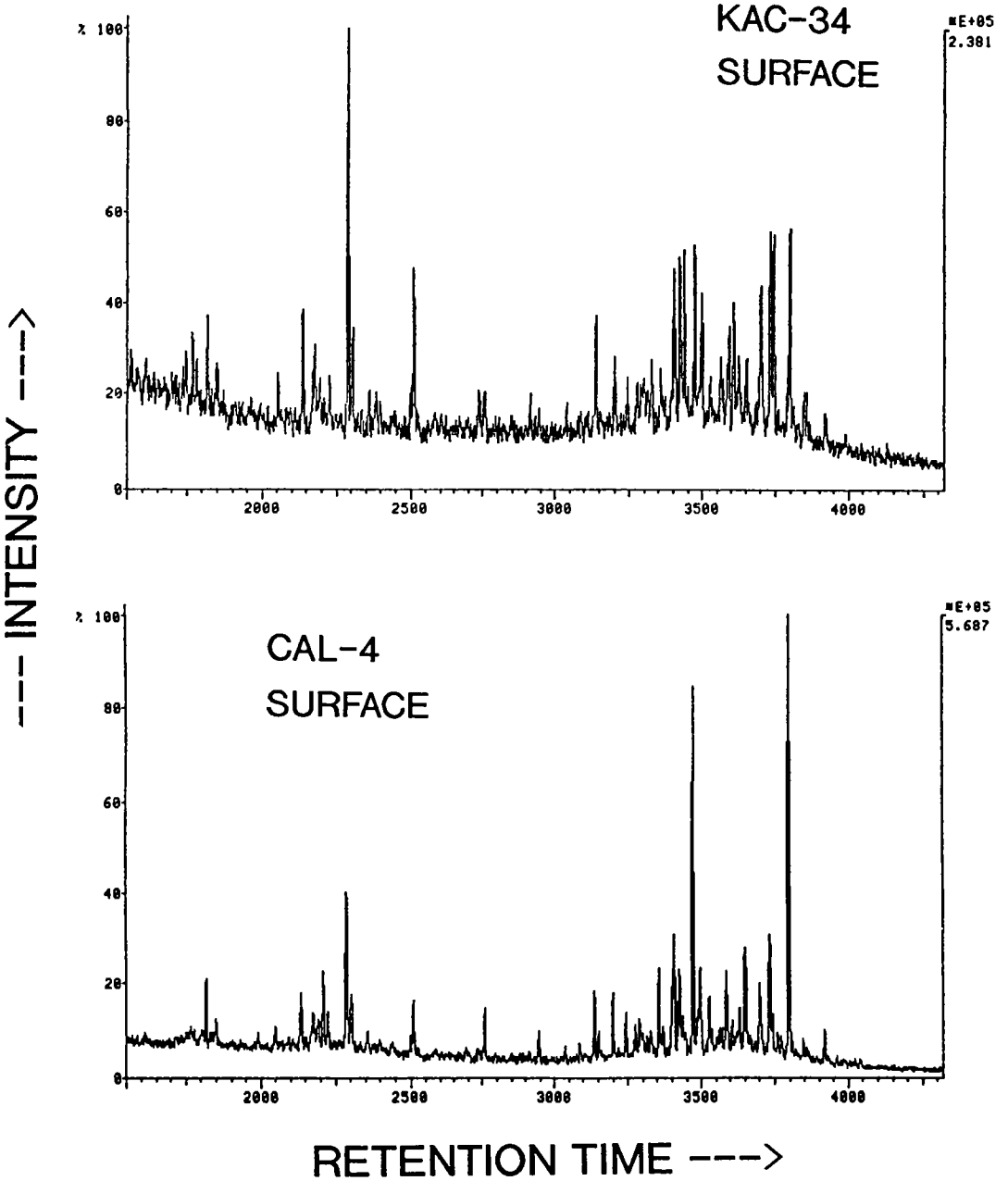

Figure 9. Mass chromatograms at m/z 217 displaying the distributions of steranes of KAC-34 (Group I) and CAL-4 (Group II).

high contents of pregnanes and ββ-steranes. Previous studies have indicated that the relative order of sterane removal by biodegradation is 20R-5α,14α17α steranes >20S- 5α14α,17α steranes and 5α,14β,17β steranes >5α,14α,17α steranes. The relatively high content of the αββ and 20S–ααα steranes in the Group I samples suggests that biodegradation has made these immature samples appear to be more "mature" on the basis of sterane parameters.

The terpane distributions in these two groups of surface samples look very different. In the m/z 191 mass chromatogram of the Group II samples (e.g., CAL-4, Fig. 10), there are many "abnormal" peaks observed, especially in the tricyclic and tetracyclic terpane range and the relative terpane concentration is quite low compared to KAC-34. The Group I samples (e.g., KAC-34, Fig. 10) have a

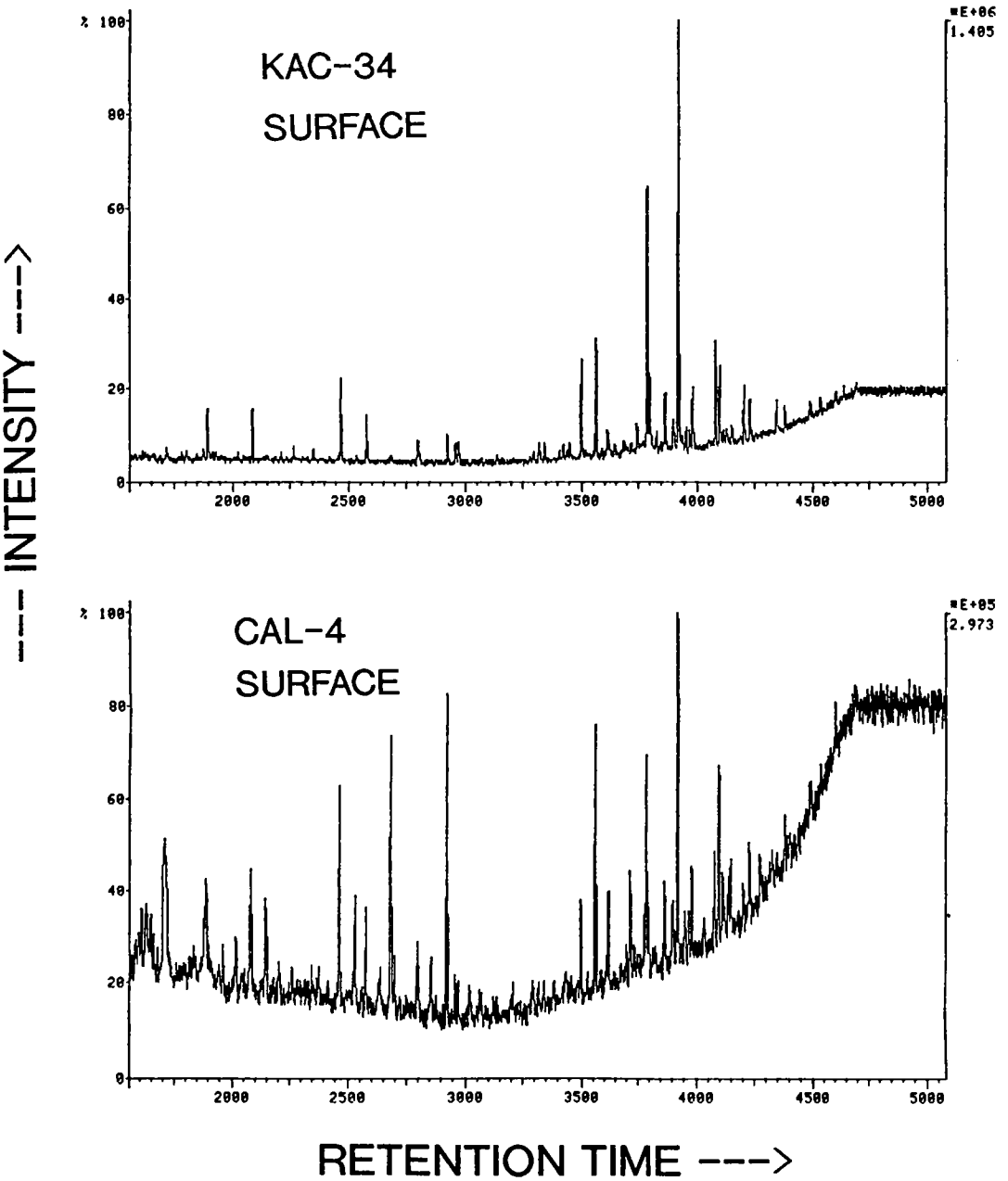

Figure 10. Mass chromatograms at m/z 191 displaying the distributions of terpanes of KAC-34 (Group I) and CAL-4 (Group II).

terpane distribution similar to that of the immature subsurface samples (e.g., KAC-37, 5,819 ft; Fig. 4A), but certain phenomena resulting from biodegradation or weathering can be observed. The preferential removal of 22R hopanes and the decreasing susceptibility to biodegradation of hopanes in the order $C_{35}>C_{34}>C_{33}>C_{32}>C_{31}>C_{30}>C_{29}$ has been previously documented by Goodwin and others (1983). The relative content of C_{31}–C_{35} hopanes to C_{29}–C_{30} hopanes is depleted in the surface samples although the 22S/22R ratio does not appear to be affected in the surface samples (especially in KAC-34).

Aromatics

The GC traces of the aromatic fractions from the surface samples showed some differences in

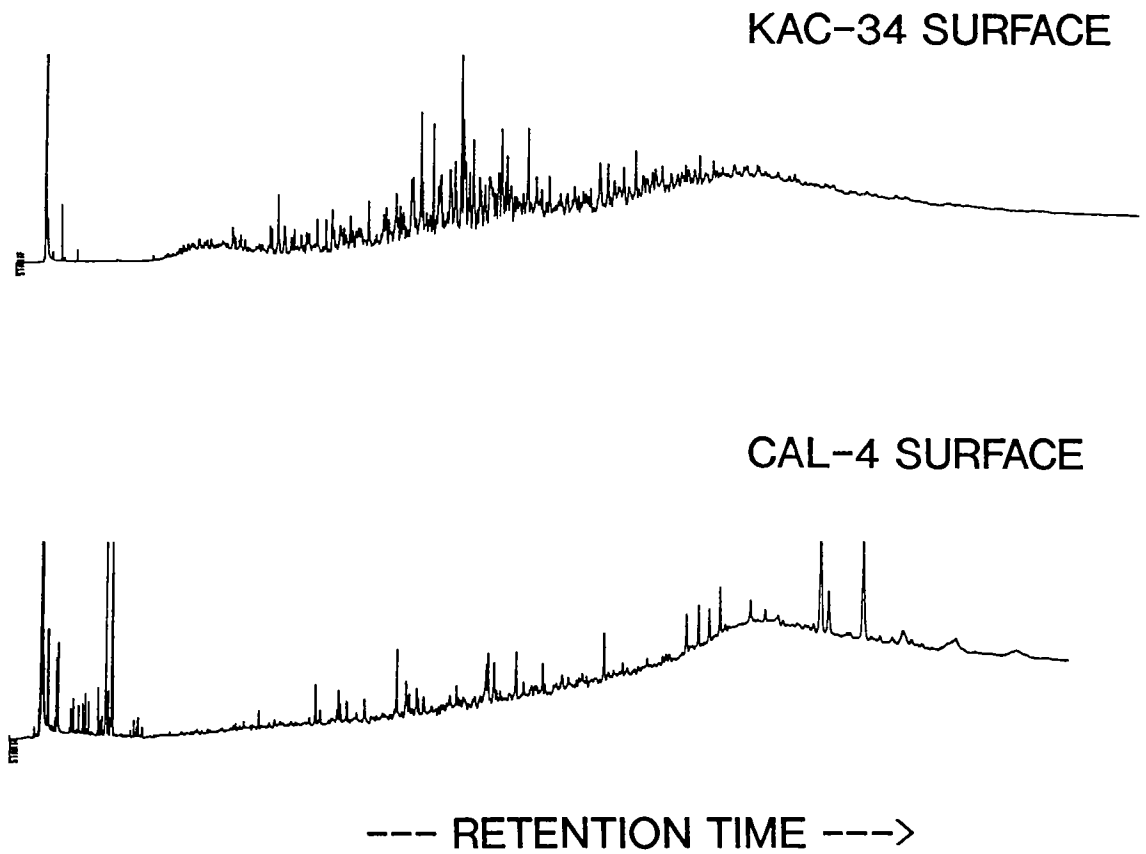

Figure 11. GC chromatograms of aromatic fractions of KAC-34 (Group I) and CAL-4 (Group II) surface samples.

their aromatic composition. Compared to Group I samples, the Group II samples have a higher content of high molecular weight components (Fig. 11) and compared to subsurface samples, the concentration of phenanthrenes in the surface samples is relatively low.

Isotope Composition

The stable carbon isotopic data for the saturates and aromatics of the Woodford Shale samples are plotted in Figure 12. Almost all of the subsurface samples (non-weathered) plot in the "marine" or "non-waxy" area of the Sofer-type plot (Sofer, 1984). In the beginning of the paper it was mentioned that the Woodford Shale was deposited in an euxinic open-sea environment. The Group I surface samples plot in the same general area as the subsurface samples. Therefore, it seems that little change has occurred to the stable isotopic composition of this group of samples. However, the Group II surface samples show an enhancement in the δC^{13} values of the aromatic fractions (Fig. 12) possibly as a result of weathering.

Bulk Composition

The surface samples were also subjected to the Rock-Eval type pyrolysis. The resulting chromatograms (Fig. 13) show low S_1 peaks. It could be caused by low maturity and/or weathering which resulted in the removal of free hydrocarbons (the S_1 peak) by washing and biodegradation.

CONCLUSIONS

1. The effects of increasing maturity on the geochemical characteristics of the Woodford Shale have been investigated by pyrolysis and isotopic data and the distribution of alkanes, aromatics, steranes, and terpanes. The hydrocarbon generation potential increases greatly below a depth of 8,500 ft based on the S_1/S_1+S_2 data from Rock-Eval type analysis. The MPI values are also observed to increase with increasing depth and maturity.

2. It has also been observed that the surface samples have changed in their hydrocarbon composition and stable isotopic composition as a result of weathering. According to the similarities in various chromatograms, distributions of steranes

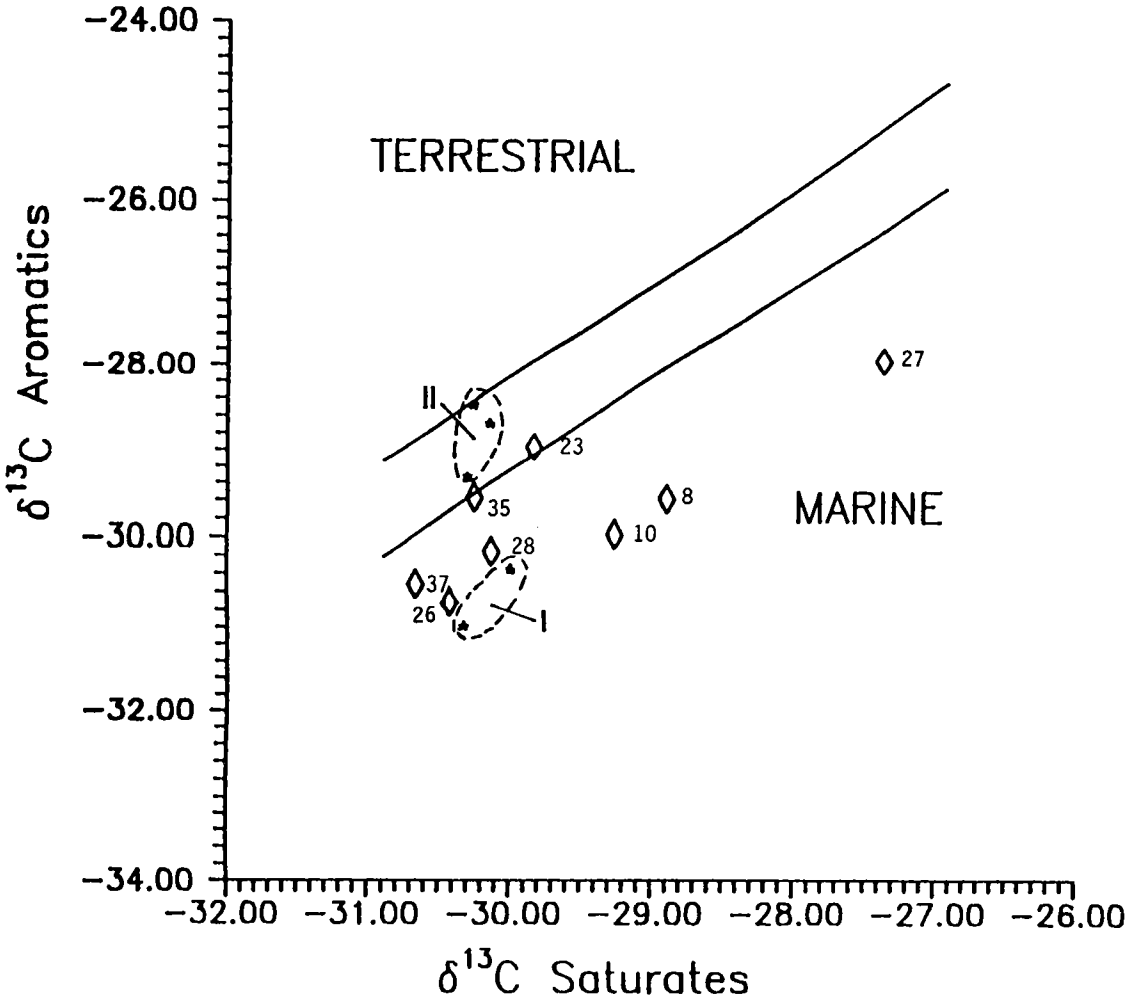

Figure 12. Plot of $\delta^{13}C$ saturates vs. $\delta^{13}C$ aromatics of subsurface samples (◊) and surface samples (*).

and terpanes and isotopic data, the surface samples can be divided into two groups. Compared with Group II, the Group I samples contain lower contents of n-alkanes, lower tricyclic terpanes (or low values of tricyclic terpanes/hopanes), but higher contents of C_{21}–C_{22} steranes and αββ steranes.

3. In conclusion, it can be observed that significant alteration can occur to the Woodford Shale as a result of weathering. Hence, as previously noted, a great deal of care needs to be exercised when collecting and selecting surface rock samples for source rock characterization.

REFERENCES

Burrus, R. C.; and Hatch, J. R., 1989, Geochemistry of oils and hydrocarbon source rocks, greater Anadarko basin: evidence for multiple sources of oils and long-distance oil migration, *in* Johnson, K. S. (ed.), Anadarko basin symposium, 1988: Oklahoma Geological Survey Circular 90, p. 53–64.

Cardott, B. J., 1989, Thermal maturation of the Woodford Shale in the Anadarko basin, *in* Johnson, K. S. (ed.), Anadarko basin symposium, 1988: Oklahoma Geological Survey Circular 90, p. 32–46.

Goodwin, N. S.; Park, P. J. D.; and Rawlinton, A. P., 1983, Crude oil biodegradation under simulated and natural conditions, *in* Bjorøy, M.; and others (eds.), Advances in organic geochemistry 1981: John Wiley, London, p. 650–658.

Johnson, K. S., 1989, Geologic evolution of the Anadarko basin, *in* Johnson, K. S. (ed.), Anadarko basin symposium, 1988: Oklahoma Geological Survey Circular 90, p. 3–12.

Philp, R. P.; Jones, P. J.; Lin, L. H.; Michael, G. E.; and Lewis, C. A., 1989, An organic geochemical study of oils, source rocks, and tar sands in the Ardmore and Anadarko basins, *in* Johnson, K. S. (ed.), Anadarko

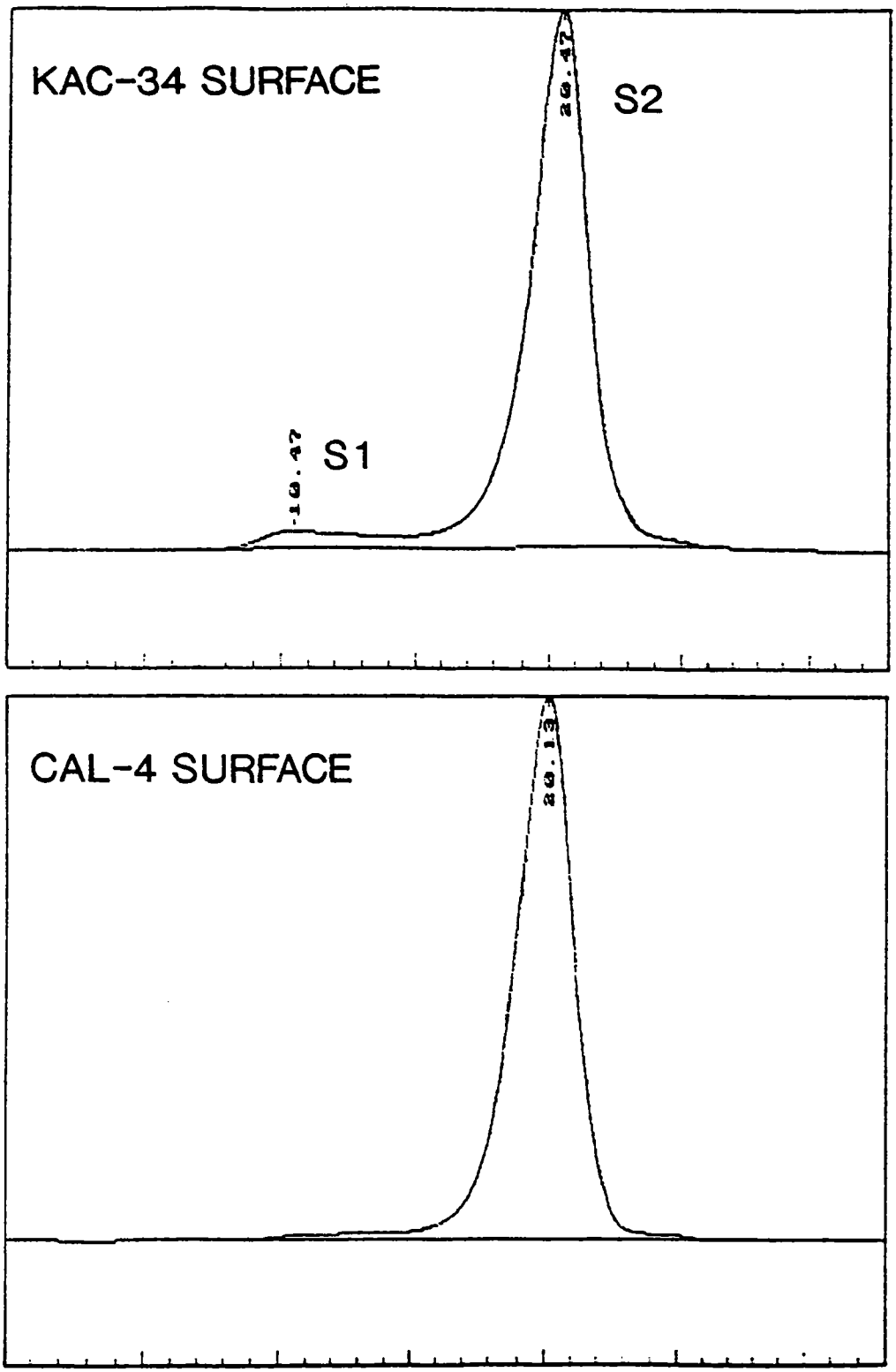

Figure 13. Py/GC chromatograms of KAC-34 (Group I) and CAL-4 (Group II). Low S_1 peak was caused by low maturity and/or weathering.

basin symposium, 1988: Oklahoma Geological Survey Circular 90, p. 65–76.

Radke, M.; and Welte, D. H., 1983, The methylphenanthrene index maturity parameter based on aromatic hydrocarbons, *in* Bjorøy, M.; and others (eds.), Advances in organic geochemistry 1981: John Wiley, London, p. 504–512.

Rüllkotter, J.; and Marzi, R., 1989, New aspects of the application of sterane isomerization and steroid aromatisation to petroleum exploration and the reconstruction of geothermal histories of sedimentary basins: Proceedings of the American Chemical Society 197th annual meeting, Dallas.

Seifert, W. K.; and Moldwan, J. M., 1986, Use of biological markers in petroleum exploration, *in* Johns, R. B. (ed.), Biological markers in the sedimentary record: Elsevier, Amsterdam, p. 261–290.

Sofer, Z., 1980, Preparation of carbon dioxide for stable carbon isotope analysis of petroleum fractions: Analytical Chemistry, v. 52, 1389–1391.

Sofer, Z., 1984, Stable carbon isotope compositions of crude oils: application to source depositional environments and petroleum alteration: American Association of Petroleum Geologists Bulletin, v. 68, p. 31–49.

Tissot, B. P.; and Welte, D. H., 1984, Petroleum formation and occurrence [second edition]: Springer-Verlag, Berlin, p. 520–523.

Thermal Maturity of Paleozoic Strata in the Arkoma Basin

David W. Houseknecht and Lori A. Hathon
University of Missouri, Columbia

Thomas A. McGilvery
HOCOL S.A., Cartegena, Colombia

ABSTRACT.—The Arkoma basin is a prolific natural gas province, despite thermal maturity levels in much of the stratigraphic column that are considered "supermature." Thermal maturity at the surface and in the shallow subsurface can best be characterized with a vitrinite reflectance map of the Hartshorne coal bed. That map reveals a pattern of increasing thermal maturity eastward, from vitrinite reflectance values of ~0.6% at the western end of the basin in Coal County, Oklahoma, grading to values >2.0% at the eastern erosional edge of the coal bed in Pope County, Arkansas. This pattern has discouraged exploration activity in the eastern end of the basin and in the adjacent Mississippi Embayment, because many explorationists expected thermal maturity to continue increasing eastward from Pope County.

Depth vs. reflectance data from six wells located along a strike-oriented traverse across the basin tend to confirm the thermal maturity pattern indicated by the Hartshorne reflectance map. However, when the reflectance data are considered relative to stratigraphic position, thermal maturity appears to increase eastward to a maximum in Logan and Yell Counties, Arkansas, and from there decrease eastward toward White County, Arkansas. This suggests that middle and lower Paleozoic strata in the eastern end of the Arkoma basin and in the Mississippi Embayment may be characterized by thermal maturities similar to those in Latimer County, Oklahoma, where prolific gas reserves have been discovered.

Preliminary interpretation of the thermal history of the basin suggests that the high levels of thermal maturity and the eastward increase in thermal maturity observed in the Arkoma basin are the result of anomalous heat flow along Atokan syndepositional faults combined with hydrothermal fluid flow away from the Ouachita orogenic belt. Contrasting orientations of facies patterns in shelf strata (basal Atokan and older) vs. foreland basin strata (Atokan and Desmoinesian) likely resulted in divergent hydrothermal fluid flow paths, which could translate into different thermal maturity patterns in shelf and foreland basin facies.

INTRODUCTION

The Arkoma basin is currently one of the most active areas of natural gas exploration in North America, despite the fact that much of the basin is characterized by levels of thermal maturity that are considered "supermature" by much of the current literature in organic geochemistry. This level of exploration activity has been fueled by the prolific nature of gas reserves that were discovered more than two decades ago (e.g., Red Oak field; Houseknecht and McGilvery, 1990) and by significant new discoveries that have been made in recent years (e.g., deep Wilburton field; Hook, 1989). Exploration successes in the main productive fairway of the basin have stimulated interest in the easternmost portion of the basin and in the adjacent Mississippi Embayment, neither of which has been thoroughly tested by exploration drilling. However, many explorationists find reason for hesitation in the high levels of thermal maturity that have been projected into the eastern part of the basin.

The objectives of this paper are to review relationships between thermal maturity and hydrocarbon occurrences, to discuss thermal maturity at the surface and in the shallow subsurface of the Arkoma basin, to present new subsurface data that suggest the presence of lower-than-expected thermal maturities in the eastern part of the basin, and to review current thinking regarding the origin of thermal maturity patterns in the Arkoma basin.

THERMAL MATURITY AND HYDROCARBON OCCURRENCE

David White (1915) was the first geologist to observe a relationship between coal rank (thermal maturity) and the occurrence of hydrocarbons in associated strata. He observed that low, intermediate, and high coal rank coincided with oil, gas,

and no hydrocarbon production, respectively, in the Appalachian basin. The relationships observed by White, along with additional examples, were summarized by Landes (1967) (Fig. 1). During the 1970s and '80s, much research concentrated on documenting thermal generation and thermal destruction of hydrocarbons. This led to the concept of *hydrocarbon windows*, specific ranges of thermal maturity within which oil, wet gas, and dry gas occur. Dow's (1977) correlation of thermal maturity and hydrocarbon windows is also illustrated in Figure 1.

The research summarized above demonstrated that oil and wet gas have thermal maturity *deadlines*, levels of organic metamorphism above which those phases do not commonly occur. Even though the oil and wet gas deadlines vary somewhat in absolute value depending upon the specific origin and composition of the hydrocarbons, they nevertheless represent a powerful exploration tool for predicting whether unexplored areas might contain oil or wet gas. The literature in organic geochemistry is almost unanimous in agreeing that oil and wet gas deadlines are fundamentally controlled by the thermal stability of the various organic geochemical compounds of which the hydrocarbons are composed and are mostly independent of reservoir diagenesis.

No such agreement exists with regard to the dry gas (methane) deadline. In fact, there is some question as to whether a thermal maturity deadline even exists for methane. Much early work suggested that the methane deadline may actually be a function of reservoir diagenesis rather than thermal stability of methane (e.g., Branner, 1937; Landes, 1967). Applying this line of thinking to the Arkoma basin, Houseknecht (1984) documented a thermal-maturity-controlled deterioration of reservoir quality in the Hartshorne Sandstone. Others implied that methane was chemically destroyed by very high temperatures (e.g., Dow, 1977), regardless of the diagenetic fate of reservoir rocks. However, Hunt (1975) demonstrated that methane is thermally stable up to temperatures approaching 600°C if the gas is not in communication with a source of sulfur.

Recent research in the Arkoma basin has demonstrated the preservation of reservoir quality and significant methane reserves at levels of thermal maturity higher than those cited as methane deadlines by Landes (1967) and Dow (1977). In Red Oak field (Latimer County, Oklahoma), good reservoir quality and >300 bcf of gas reserves are present in the Spiro sandstone (basal Atokan) characterized by vitrinite reflectance as high as 3.66% (Houseknecht and McGilvery, 1990). The good reservoir quality is only preserved in the charged gas column, whereas little porosity is preserved below a fossil hydrocarbon-water contact (Houseknecht and McGilvery, 1990). Thus, the presence of reser-

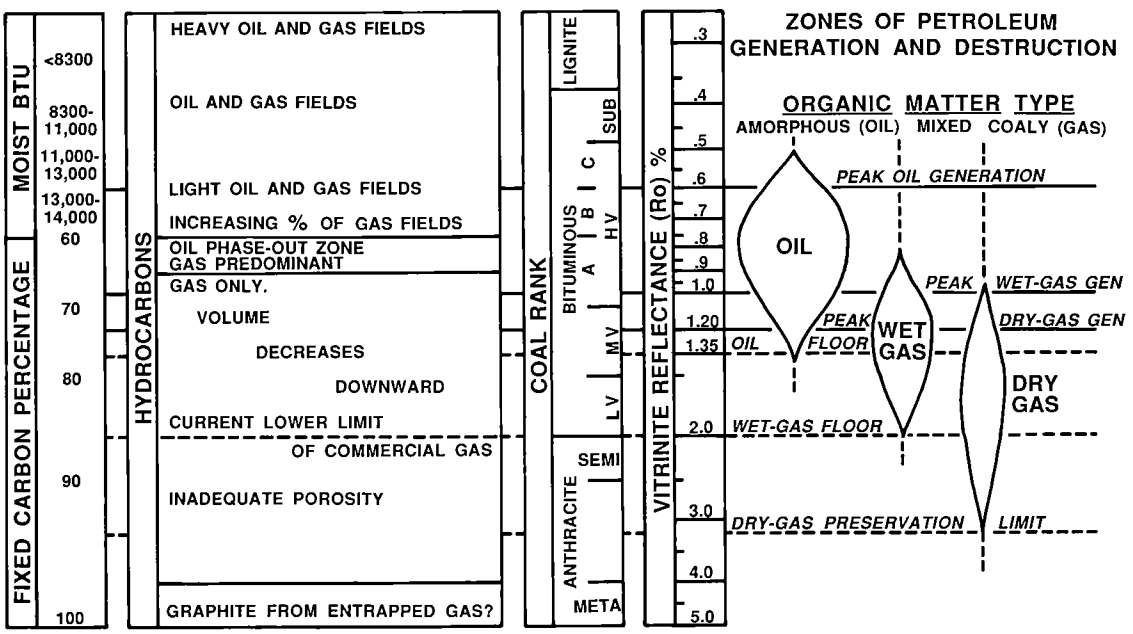

Figure 1. Relationship between thermal maturity and occurrence of hydrocarbons. Left two columns summarize knowledge as of 1967 (modified from Landes, 1967). Right part of figure summarizes more recent concepts regarding zones of hydrocarbon generation and destruction (*hydrocarbon windows*), expressed in terms of coal rank and vitrinite reflectance (modified from Dow, 1977).

voired hydrocarbons protected the reservoir from high temperature diagenesis that destroyed porosity in water-wet portions of the same rock. These observations suggest that good reservoir quality can be preserved to very high levels of thermal maturity if water (necessary for inorganic diagenetic reactions) has been displaced by accumulating hydrocarbons.

In light of these results, we now view Houseknecht's (1984) documentation of deterioration of Hartshorne Sandstone reservoir quality with increasing thermal maturity as a study of samples that were water-wet during high temperature diagenesis. All samples used in that research were collected from cores cut in synclines by coal companies or the U.S. Corps of Engineers, and from outcrops located on steep flanks of anticlines that have been breached by erosion. Thus, no samples were collected from locations favorable for hydrocarbon accumulation.

The recent discovery of significant methane reserves in the Arbuckle Group in Wilburton field (Latimer County, Oklahoma) demonstrates the preservation of good reservoir quality in carbonate rocks at elevated thermal maturity. Hendrick (1990) has estimated the thermal maturity of Arbuckle reservoir rocks to be equivalent to a vitrinite reflectance between 3.5 and 3.8%.

The work cited above provides clear evidence that good reservoir quality and prolific gas reserves are preserved in the Arkoma basin at levels of thermal maturity that are above the methane deadline (~3.2% R_o) according to conventional thinking and the current literature. However, this does not mean that thermal maturity can be ignored in future exploration efforts. As demonstrated in the Spiro sandstone in Red Oak field, at least some gas accumulations in the Arkoma basin have bottom seals that represent fossil hydrocarbon-water contacts. At certain locations in the Arkoma basin and Ouachita frontal thrust belt, such gas accumulations may have been structurally rotated during late phases of deformation. In these cases, seals that formed at hydrocarbon-water contacts may now form updip seals for gas trapped in positions that are not structurally high at present.

THERMAL MATURITY AT THE SURFACE AND IN THE SHALLOW SUBSURFACE

It has long been known that the Arkoma basin is characterized by relatively high thermal maturity, and that thermal maturity increases systematically from west to east. The first thermal maturity map of the basin was published by David White (1915) in his classic paper on relationships between rank (thermal maturity) of coals and the occurrence of petroleum in associated strata. During the subsequent 75 years, several workers have collected additional data and refined our understanding of thermal maturity at the surface and in the shallow subsurface, both in the Arkoma basin and in the Ouachita Mountains (White, 1915; Croneis, 1927; Hendricks, 1935; Branner, 1937; Wilson, 1961,1971; Burgess, 1974; Curiale, 1983; Houseknecht, 1984; Houseknecht and Matthews, 1985; Hathon and Houseknecht, 1987; Underwood and others, 1988).

There is no doubt that the most accurate thermal maturity patterns in the Arkoma basin can be mapped within Desmoinesian strata that contain widespread coal beds. Hundreds of analyses of Desmoinesian coals have been published during the past century, mostly by federal and state agencies, and additional data have been generated by industry and university laboratories. Data are from samples collected from outcrops, strip mines, underground mines, and coal exploration boreholes (cores). In our thermal maturity work, we have concentrated on the Hartshorne coal bed because it occurs over a very large part of the basin, it is an excellent coking coal and therefore has been the focus of numerous government and industry analytical studies, and it immediately overlies the Atoka Formation which has been the objective of much natural gas exploration within the basin. The Hartshorne Formation actually contains two or more coal beds in some parts of the basin (Houseknecht and Iannacchione, 1982), but they are stratigraphically close together and display nearly identical thermal maturity properties. Therefore, this paper treats the Hartshorne as a single coal bed horizon.

Figure 2 is our thermal maturity map of the Hartshorne coal bed. This map has been constructed using >300 control points, which include published and unpublished coal analyses (vitrinite reflectance, fixed carbon %, and Btu values) compiled from numerous sources. Fixed carbon and Btu data were converted to equivalent vitrinite reflectance percentages using published correlation charts (Hood and others, 1975; Héroux and others, 1979) and the validity of these correlations was confirmed by in-house vitrinite reflectance analyses of coal samples collected at numerous locations throughout the basin.

The map (Fig. 2) reveals a systematic eastward increase in thermal maturity. In the western end of the basin (Coal County, Oklahoma), vitrinite reflectance of the Hartshorne coal is ~0.65%. Thermal maturity of the coal rises steadily eastward through Coal, Pittsburg, and western Latimer Counties, and reaches a vitrinite reflectance of 1.0% in northeastern Latimer and western Haskell Counties. Thermal maturity continues to increase eastward, with the 1.5% vitrinite reflectance contour looping in a concave-eastward pattern within Le Flore County, Oklahoma. The southern part of

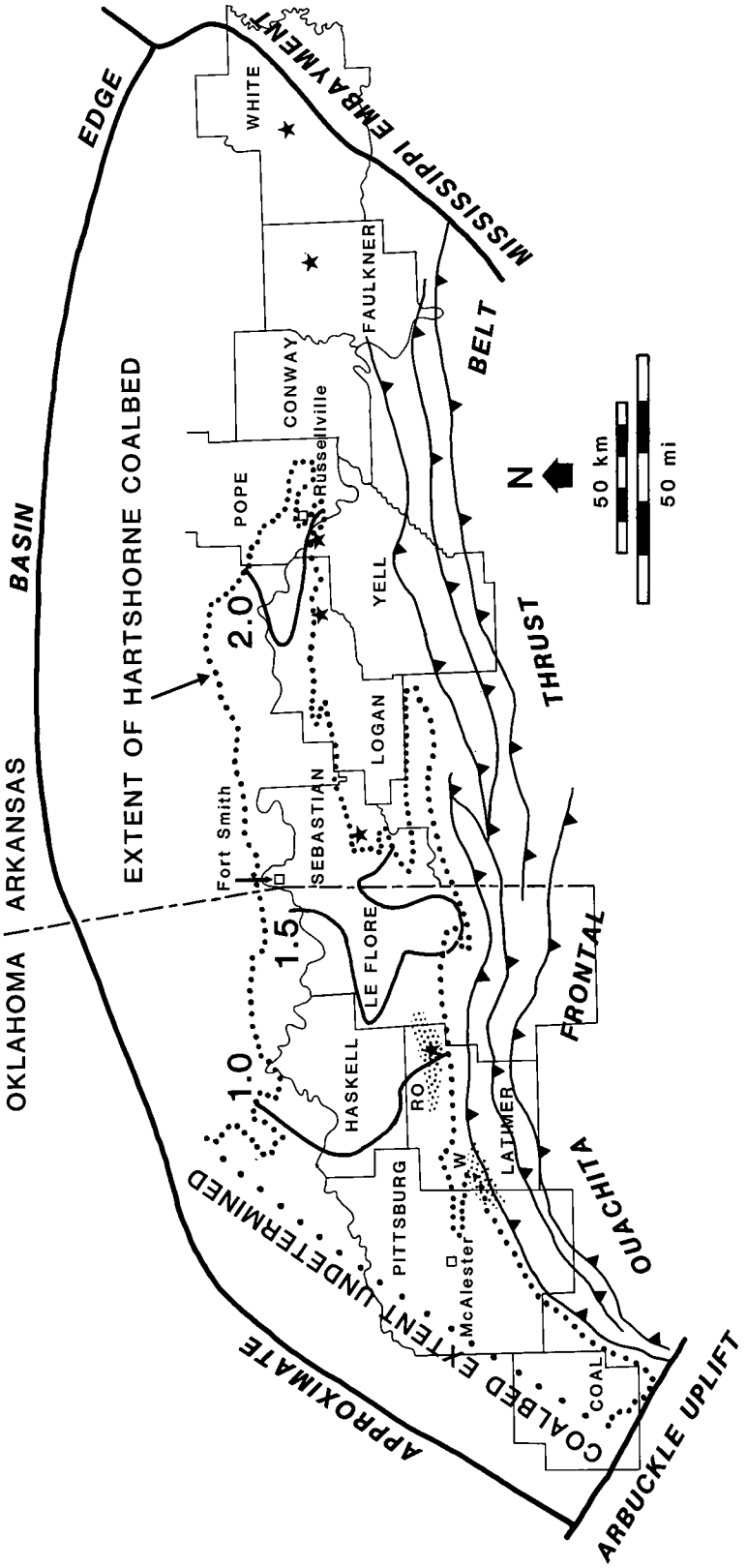

Figure 2. Thermal maturity map of the Hartshorne coal bed based on >300 control points. Contours are in units of vitrinite reflectance percentage. Stars indicate locations of wells discussed in text and summarized in Table 1. W = Wilburton gas field; RO = Red Oak gas field.

the 1.5% vitrinite reflectance contour continues into Sebastian County, Arkansas, where vitrinite reflectance of the Hartshorne coal is <1.5% in the south (adjacent to the Ouachita Mountains) and is >1.5% in the north. Data are insufficient to define the location of the northern part of the 1.5% vitrinite reflectance contour, but it presumably trends northeastward from Le Flore County, Oklahoma, and enters Arkansas in the vicinity of Fort Smith, in northwestern Sebastian County. Thermal maturity increases eastward through Sebastian and Logan Counties, Arkansas, and the 2.0% vitrinite reflectance contour is located near the border of Logan and Pope Counties, where it exhibits a concave-eastward shape, similar to that of the 1.5% contour.

The erosional limit of the Hartshorne coal bed occurs in Pope County, just east of the 2.0% contour line, and no coal beds are present to the east. We have analyzed dispersed organic matter concentrated from several shale samples collected from outcrops of the Atoka Formation (Atokan) and the Bloyd Formation (Morrowan) located east of the limit of the Hartshorne coal, in Pope, Conway, Faulkner, and White Counties, Arkansas (Fig. 2). In all cases, mean vitrinite reflectance values are between 2.0 and 2.5%, and there appears to be no systematic trend of either increasing or decreasing thermal maturity eastward toward the Mississippi Embayment.

The thermal maturity pattern described above has been known, at least in gross form, since White's (1915) map was published. The eastward increase in thermal maturity, combined with the high levels of thermal maturity at the eastern end of the "coal fields," have discouraged exploration activity in the eastern end of the basin and in the adjacent Mississippi Embayment.

THERMAL MATURITY PROFILES IN SIX WELLS ACROSS THE BASIN

Depth vs. Thermal Maturity Relationships

Thermal maturity data from six wells in a west–east traverse across the Arkoma basin are presented in this section. Well locations are shown on Figure 2 and well information, strata exposed at the surface at each location, and the oldest strata analyzed from each well are summarized in Table 1. These data were collected by a petroleum industry laboratory from dispersed organic matter concentrated from shale cuttings, and thermal maturity was estimated by measuring the reflectance of selected organic matter. Throughout most of the stratigraphic section analyzed, the selected organic matter is vitrinite, whereas the reflectance of *vitrinite-like* organic matter was apparently measured in pre-Devonian strata, and perhaps in certain younger strata. True vitrinite derived from terrestrial land plants is generally thought to be absent in pre-Devonian or pre-Silurian strata (woody land plants did not evolve until the Silurian and were not widely abundant until the Devonian). However, vitrinite-like organic matter is common in older strata (e.g., Buchardt and Lewan, 1990), and the reflectance of this type of organic matter can be measured using vitrinite reflectance techniques. In general, the reflectance of vitrinite-like organic matter increases with increasing temperature like the reflectance of vitrinite, but absolute reflectance values may differ somewhat between vitrinite and vitrinite-like organic matter, particularly over certain ranges of thermal maturity (Buchardt and Lewan, 1990). Nevertheless, reflectance of vitrinite-like organic matter is a reliable measure of relative thermal maturity in the absence of true vitrinite.

Depth vs. reflectance for the wells located in Latimer, Sebastian, Logan, and Yell Counties are plotted in Figure 3A. The general relationships displayed by these plots are not unexpected. That is, all four wells display a general increase in reflectance with depth and they project to reflectance values at the surface that are in good agreement with the Hartshorne thermal maturity map (Fig. 2). The details of these relationships, however, display complications that are difficult to explain. Each of the four wells plotted in Figure 3A displays at least one dogleg in depth vs. reflectance relationships. These doglegs are easier to see in Figure 3B, where "eyeball best fit" lines have been superimposed on the depth vs. reflectance data. Normally, such doglegs can be explained by the presence of faults or unconformities, or by changes in kerogen composition (e.g., Dow, 1977). However, none of the doglegs in these four wells corresponds to faults or unconformities that are of large enough magnitude to explain the changes in slope of the depth vs. reflectance profiles. Changes in kerogen composition cannot be evaluated with existing data. At present, we do not have adequate explanations for these doglegs although we continue to collect additional geologic information that may allow us to explain them in the future.

Regardless of the cause of the doglegs, it is apparent that surface and near-surface thermal maturity relationships are inadequate to predict deeper subsurface thermal maturity values with accuracy. For example, it is clear that the deeper strata in the Logan County well are characterized by a lower thermal maturity than the deeper strata in the Sebastian County well (Fig. 3B), whereas the opposite would be expected if only the Hartshorne thermal maturity map were used to anticipate thermal maturity at depth.

Figure 3C shows depth vs. reflectance trends for the four wells discussed above, plus depth vs. reflectance data for the two wells located in Faulkner and White Counties. This plot reinforces

TABLE 1. — WELL INFORMATION, STRATA AT SURFACE, AND OLDEST STRATA ANALYZED FOR THE SIX WELLS DISCUSSED IN TEXT

Location		Operator	Well name	Strata at surface	Oldest strata analyzed
County, State	Sec–T–R				
Latimer, OK	13–6N–21E	Midwest	#1 Gallagher	McAlester	Wapanucka
Sebastian, AR	25–6N–31W	Arkla	#1-25 Bell	middle Atoka	Arbuckle
Logan, AR	19–7N–23W	Tenneco	#1-19 Federal	upper Atoka/ Hartshorne*	Arbuckle
Yell, AR	22–7N–21W	Arkla	#1 McRay	upper Atoka	Arbuckle
Faulkner, AR	22–7N–12W	Lone Star	#1 Moore Estate	upper Atoka/ middle Atoka*	Arbuckle
White, AR	31–8N–7W	Arkla	#1 Baker	upper Bloyd	Arbuckle

*Two stratigraphic units separated by slash means that the surface location is near the contact between the two formations listed.

the notion that the eastern end of the basin is characterized by very high thermal maturity, even though the data suggest that the eastward increase in thermal maturity does not continue into Faulkner and White Counties. In fact, data from the Faulkner County well match those from the Yell County well in the upper 6,500 ft of penetration and are actually lower in the lower 4,000 ft of penetration. Data from the White County well indicate lower thermal maturity, more like that of the Logan County well (Fig. 3C).

Stratigraphy vs. Thermal Maturity Relationships

The depth vs. thermal maturity plots presented in Figure 3 provide useful indications of vertical thermal maturity gradients in various parts of the basin, but do not accurately illustrate lateral thermal maturity gradients at individual stratigraphic horizons. Figure 4 presents the same data adjusted to a single stratigraphic horizon, the basal Atokan Spiro sandstone. Presenting thermal maturity profiles in this way is essentially equivalent to hanging wire-line logs on a single stratigraphic horizon to produce a stratigraphic cross section.

Figure 4 shows stratigraphic position relative to the top of the basal Atoka (Spiro) vs. thermal maturity for the same wells with data plotted in Figure 3. On the vertical axis, zero corresponds to the top of the Spiro, positive numbers indicate footage above the top of the Spiro, and negative numbers indicate footage below the top of the Spiro. The data displayed in Figure 4 form approximately linear trends that appear to have different slopes from those shown in Figure 3 because the vertical scale is different. The total vertical scale is 25,000 ft in Figure 4, whereas it is 15,000 ft in Figure 3.

Stratigraphic position relative to the top of the basal Atoka vs. reflectance for the wells in Latimer, Sebastian, Logan, and Yell Counties are plotted in Figure 4A, and the "eyeball best fit" lines are superimposed on the data in Figure 4B. These figures illustrate the same basic information as Figures 3A and 3B, except data appear to be grouped more closely so that it is more difficult to discern differences in reflectance among the four wells. Data from the Latimer and Sebastian County wells are coincident in the upper portion of the plot (more than 3,000 ft above the Spiro; Fig. 4A,B), and this is much different from the impression made by Figure 3A,B, where the two wells appear to differ markedly in thermal maturity. Data from those two wells appear to diverge below 3,000 ft above the Spiro, with the Sebastian County well displaying higher reflectance values at individual stratigraphic horizons than the Latimer County well.

Data from the Logan and Yell County wells are coincident over most of the stratigraphic section penetrated by the two wells, and both clearly display higher reflectance values at individual stratigraphic horizons than the Latimer and Sebastian County wells (Fig. 4A,B). Again, these impressions are significantly different from those made by Figure 3A,B, where substantial differences in reflectance appear to be present from top to bottom of

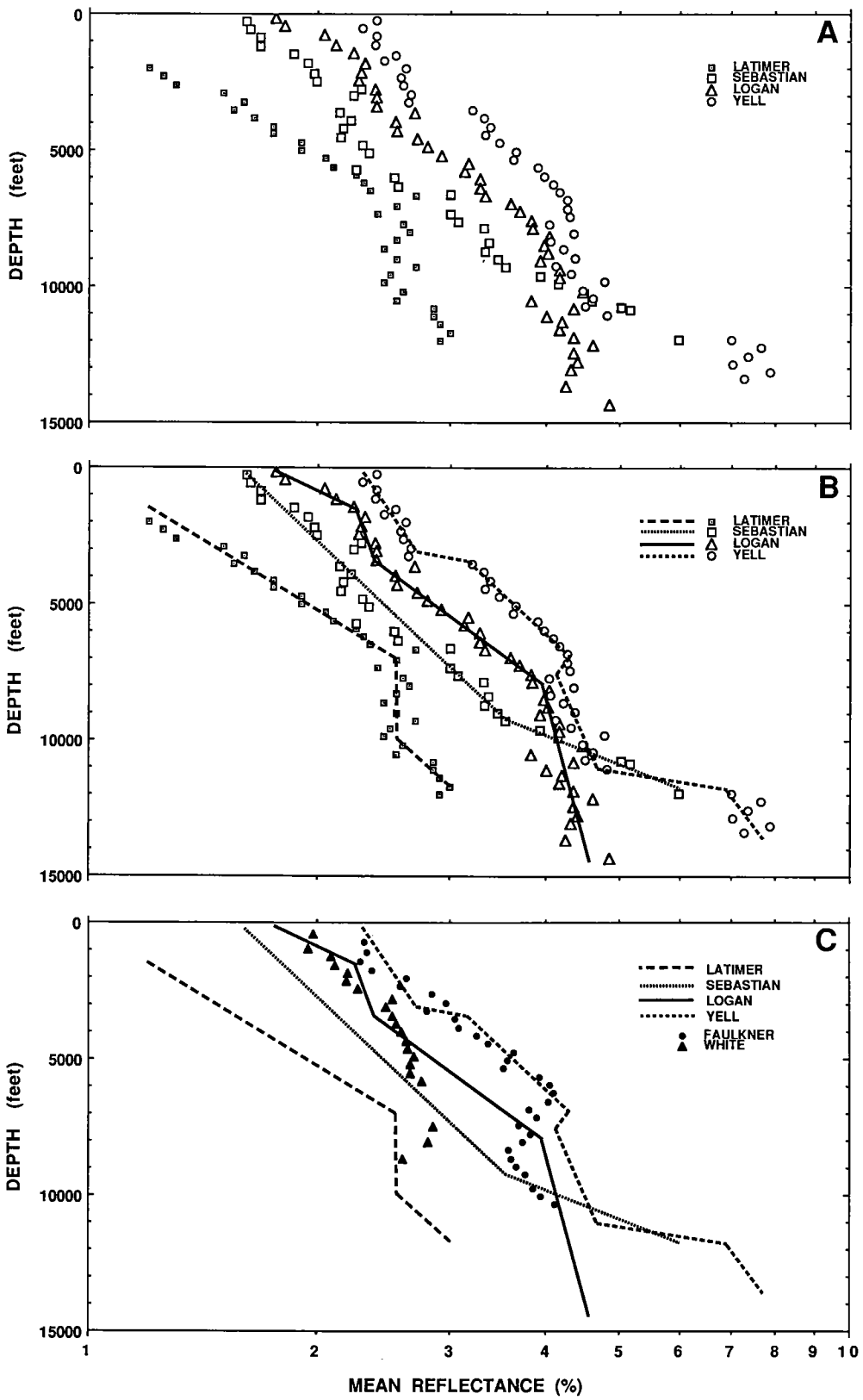
A
LATIMER
SEBASTIAN
LOGAN
YELL
DEPTH (feet)
0
5000
10000
15000
B
LATIMER
SEBASTIAN
LOGAN
YELL
C
LATIMER
SEBASTIAN
LOGAN
YELL
FAULKNER
WHITE
1
2
3
4
5
6
7
8
9
10
MEAN REFLECTANCE (%)

the two wells. There does appear to be significant divergence of reflectance data in the lowest stratigraphic horizons analyzed in the Logan and Yell County wells, as illustrated in Figure 4A,B.

The biggest surprise is provided by Figure 4C, where stratigraphic position relative to the basal Atoka vs. reflectance trends for the four wells discussed above is plotted with data from the Faulkner and White County wells. This figure clearly demonstrates that the reflectance of basal Atokan and older strata is significantly *lower* in the Faulkner and White county wells than in the Logan and Yell County wells. In fact, thermal maturity data from the Faulkner County well most nearly matches the trend of the Latimer County well, and thermal maturity data from the White County well is lower than any other data plotted in Figure 4! These stratigraphically "hung" data suggest that a thermal maturity maximum occurs in the vicinity of Logan and Yell Counties, and that thermal maturity *decreases eastward* from those counties toward the Mississippi Embayment. In fact, the reflectance values of the upper Arbuckle in the Faulkner County well are approximately equal to those of the productive Arbuckle in Wilburton field, and the reflectance values of the upper Arbuckle in the White County well are significantly lower than those of the productive Arbuckle in Wilburton field! These conclusions are based on comparing the data of Figure 4C with estimates of Hendrick (1990) for reflectance of productive Arbuckle in Wilburton field.

Use of the basal Atoka Spiro sandstone as a stratigraphic datum for thermal maturity data is informative, but does not provide a complete solution to deciphering thermal maturity patterns at various stratigraphic horizons. Figure 4C shows the position of the Woodford–Chattanooga Shale and the top of the Arbuckle Group in five of the wells from which samples were analyzed. The stratigraphic positions (relative to the Spiro) of these important strata vary by thousands of feet between Sebastian and White Counties, Arkansas. For this reason, even stratigraphically "hung" thermal maturity plots like those of Figure 4C fall short of accurately conveying the lateral gradients that exist at individual stratigraphic horizons such as the Woodford–Chattanooga and Arbuckle. These observations demonstrate the need for additional data throughout the stratigraphic section so that thermal maturity maps, like the Hartshorne map of Figure 2, can be constructed for other important stratigraphic horizons.

Figure 3 (facing page). *A*—Depth vs. reflectance for wells in Latimer County, Oklahoma, and Sebastian, Logan, and Yell Counties, Arkansas. Well locations shown in Figure 2. *B*—Same depth vs. reflectance profiles shown in A, but with superimposed "eyeball best fit" lines. *C*—"Eyeball best fit" lines from B with depth vs. reflectance data for wells in Faulkner and White Counties, Arkansas. Well locations shown in Figure 2.

THERMAL HISTORY

Perhaps the most enigmatic aspect of thermal maturity in the Arkoma basin is interpretation of thermal history. This is a topic of current research and a comprehensive interpretation is not possible at this time. The following discussion summarizes our current thoughts on the thermal history of the basin.

Two aspects of Arkoma basin thermal maturity are difficult to explain: the high absolute levels of thermal maturity and the lateral gradients in thermal maturity within individual formations. Neither can be adequately explained by stratigraphic burial, structural burial, or igneous intrusions. We believe that the high absolute values of thermal maturity are, at least in part, the result of anomalous heat flow along Atokan syndepositional normal faults. During the Atokan, basement beneath the Arkoma basin was broken by a series of normal faults (mostly S-dipping) that apparently formed as the result of the tectonic load exerted by the incipient phases of Ouachita orogeny (Houseknecht, 1986). These faults were active during deposition of the Atoka Formation, as indicated by growth of the Atokan section across them, and displacement had mostly ceased by the Desmoinesian. We believe that such faults would have enhanced heat flow into the basin, in the same way that heat flow is enhanced by growth faults of the modern Gulf Coast basin (e.g., Bodner and Sharp, 1988).

In recent years, appealing explanations for lateral thermal maturity gradients within individual formations have been provided by work published on the hydrology of foreland basins and resultant "hydrothermal" fluid migration within foreland basin strata. Three general mechanisms have been proposed to provide the head for such fluid migration: overpressuring of thick foreland basin strata because of rapid sediment accumulation (e.g., Cathles and Smith, 1983) and/or gas generation (e.g., Spencer, 1987); loading of thick foreland basin strata by advancing thrust sheets (e.g., Oliver, 1986); and gravity drive provided by recharge in orogenic mountain belts adjacent to foreland basins (e.g., Garven and Freeze, 1984; Bethke and Marshak, 1990). Regardless of specific mechanism, fluid flow out of the deepest portion of the foreland basin and adjacent orogenic belt effectively transports heat to shallower portions of foreland basins and to platform strata of the adjacent craton. Naturally, specific flow paths are controlled by the geometry of fluid conduits (permeable strata, faults, etc.), but the overall flow pattern

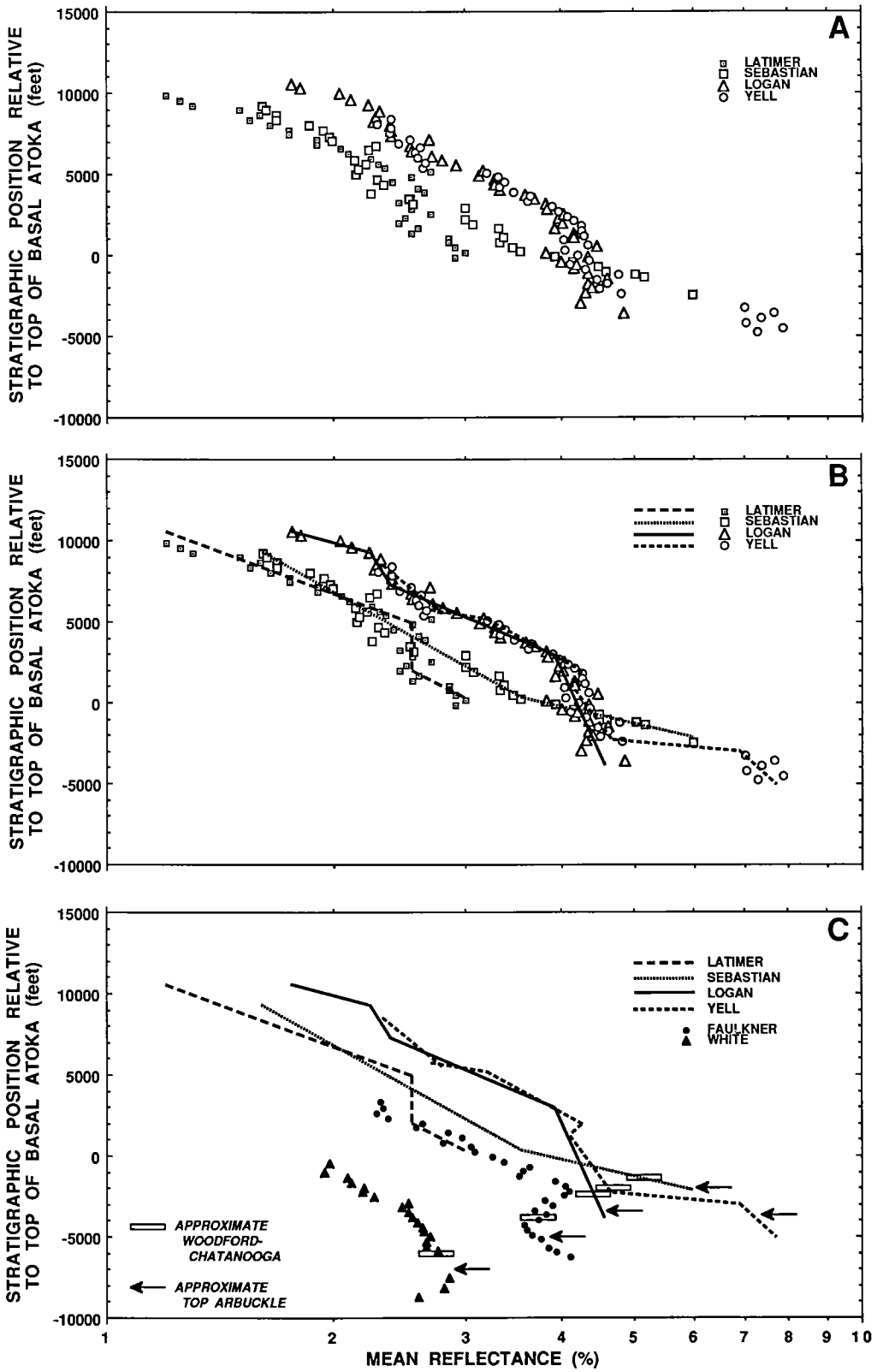
A
B
C
STRATIGRAPHIC POSITION RELATIVE TO TOP OF BASAL ATOKA (feet)
15000
10000
5000
0
-5000
-10000
LATIMER
SEBASTIAN
LOGAN
YELL
FAULKNER
WHITE
APPROXIMATE WOODFORD-CHATANOOGA
APPROXIMATE TOP ARBUCKLE
1
2
3
4
5
6
7
8
9
10
MEAN REFLECTANCE (%)

results in transport of heat away from the orogenic belt.

Combining these concepts of fluid flow and heat transport through foreland basins with tectonic, stratigraphic, and facies information specific to the Arkoma basin (Houseknecht, 1986; Houseknecht and others, 1989) results in a working hypothesis for Arkoma basin thermal maturation. Fluid flow out of the deepest part of the Arkoma basin would likely follow divergent flow paths in shelf vs. foreland basin facies. Within Cambrian through basal Atokan strata, deposited on a tectonically stable shelf prior to formation of the foreland basin and juxtaposed against Atokan shales across Arkoma basin normal faults, fluid flow would most likely be directed cratonward (up depositional dip). Within Atokan and Desmoinesian foreland basin strata, deposited by westward progradation of clastic depositional systems within the elongate foreland basin (Houseknecht, 1986), fluid flow would most likely be directed eastward for two reasons. First, the presence of E-striking normal faults that display thousands of feet of displacement would probably have focused fluid migration along flow paths parallel to their strike. Second, facies-controlled permeability conduits would tend to concentrate flow up depositional dip into sandier facies in the eastern part of the basin.

This interpretation has several important implications. High thermal maturity values located away from the orogenic belt and significant lateral thermal maturity gradients within individual formations (Fig. 2) are consistent with heat transport by migrating fluids away from the orogenic belt. However, the contrast in orientation of facies tracts and nature of porosity-permeability systems in basal Atokan and older shelf strata vs. Atokan and younger foreland basin strata (Houseknecht, 1986,1987) probably resulted in divergent fluid flow during heat transport. Therefore, thermal maturity patterns may differ among strata of various ages within the Arkoma basin; it is anticipated that "shelf" strata may display different thermal maturity patterns than "foreland basin" strata, but additional work is necessary to evaluate this hypothesis. This hypothesis may explain the reversal of thermal maturity that appears to be present in shelf strata in the eastern part of the basin (Fig. 4C).

Figure 4 (facing page). *A*—Stratigraphic position relative to top of basal Atoka (Spiro Sandstone) vs. reflectance for wells in Latimer County, Oklahoma, and Sebastian, Logan, and Yell Counties, Arkansas. Compare to Figure 3A. Well locations shown in Figure 2. *B*—Same plots shown in A, but with superimposed "eyeball best fit" lines. Compare to Figure 3B. *C*—"Eyeball best fit" lines from B with stratigraphic position relative to top of basal Atoka (Spiro sandstone) vs. reflectance for wells in Faulkner and White Counties, Arkansas. Compare to Figure 3C. Well locations shown in Figure 2.

CONCLUSIONS

The Hartshorne coal bed displays a regional pattern of eastward increasing thermal maturity within the Arkoma basin. Along a strike-oriented traverse from Coal County, Oklahoma, to Pope County, Arkansas, vitrinite reflectance values grade from <1% to >2%. These high thermal maturity values in the east, combined with the pattern of increasing thermal maturity eastward, have discouraged gas exploration in the eastern end of the basin and in the adjacent Mississippi Embayment.

Depth vs. reflectance data from six wells located along a strike-oriented traverse from Latimer County, Oklahoma, to White County, Arkansas, tend to reinforce the negative prognosis for exploration in the eastern end of the basin and in the adjacent Mississippi Embayment. However, when those same data are considered relative to stratigraphic position, thermal maturity appears to increase eastward to a maximum in the vicinity of Logan and Yell Counties, Arkansas. From there, thermal maturity appears to decrease eastward toward White County, Arkansas. This pattern suggests that middle and lower Paleozoic strata in the eastern end of the Arkoma basin and in the Mississippi Embayment may be characterized by thermal maturities similar to those of Latimer County, Oklahoma.

Interpretation of the thermal history of the Arkoma basin is difficult and currently in a preliminary stage. Enhanced heat flow along basement rooted normal faults combined with hydrothermal fluid migration away from the Ouachita orogenic belt provides the only adequate explanation for the high levels of thermal maturity and the lateral thermal maturity patterns that have been observed in the basin. It is likely that such fluid migration would have followed diverse flow paths in shelf vs. foreland basin strata; this could potentially result in different patterns of thermal maturity in shelf and foreland basin facies.

REFERENCES

Bethke, C. M.; and Marshak, S., 1990, Brine migrations across North America—the plate tectonics of groundwater: Annual Review of Earth and Planetary Sciences, v. 18, p. 287–315.

Bodner, D. P.; and Sharp, J. M., Jr., 1988, Temperature variations in south Texas subsurface: American Association of Petroleum Geologists Bulletin, v. 72, p. 21–32.

Branner, G. C., 1937, Sandstone porosities in Paleozoic region in Arkansas: American Association of Petroleum Geologists Bulletin, v. 21, p. 67–79.

Buchardt, B.; and Lewan, M. D., 1990, Reflectance of vitrinite-like macerals as a thermal maturity index for Cambrian–Ordovician Alum Shale of southern Scandinavia: American Association of Petroleum Geologists Bulletin, v. 74, p. 394–406.

Burgess, J. D., 1974, Microscopic examination of kerogen (dispersed organic matter) in petroleum exploration, *in* Dutcher, R. R.; Hacquebard, P. A.; Schopt, J. M.; and Simon, J. A. (eds.), Carbonaceous materials as indicators of metamorphism: Geological Society of America Special Paper 153, p. 19–30.

Cathles, L. M.; and Smith, A. T., 1983, Thermal constraints on the formation of Mississippi Valley-type lead–zinc deposits and their implications for episodic basin dewatering and deposit genesis: Economic Geology, v. 78, p. 983–1002.

Croneis, C., 1927, Oil and gas possibilities in the Arkansas Ozarks: American Association of Petroleum Geologists Bulletin, v. 11, p. 279–297.

Curiale, J. A., 1983, Petroleum occurrences and source-rock potential of the Ouachita Mountains, southeastern Oklahoma: Oklahoma Geological Survey Bulletin 135, 65 p.

Dow, W. G., 1977, Kerogen studies and geological interpretations: Journal of Geochemical Exploration, v. 7, p. 79–99.

Garven, G.; and Freeze, R. A., 1984, Theoretical analysis of the role of groundwater flow in the genesis of stratabound ore deposits. I.—Mathematical and numerical model. II.—Quantitative results: American Journal of Science, v. 284, p. 1085–1174.

Hathon, L. A.; and Houseknecht, D. W., 1987, Hydrocarbons in an overmature basin. I.—Thermal maturity of Atoka and Hartshorne Formations, Arkoma basin [abstract]: American Association of Petroleum Geologists Bulletin, v. 71, p. 993–994.

Hendrick, S. J., 1990, Vitrinite reflectance and deep Arbuckle maturation at Wilburton field, Latimer County, Oklahoma [abstract]: Oklahoma Geological Survey workshop on source rocks, generation, and migration of hydrocarbons and other fluids in the southern Midcontinent, p. 12.

Hendricks, T. A., 1935, Carbon ratios in part of Arkansas–Oklahoma coal field: American Association of Petroleum Geologists Bulletin, v. 19, p. 937–947.

Héroux, Y.; Chagnon, A.; and Bertrand, R., 1979, Compilation and correlation of major thermal maturation indicators: American Association of Petroleum Geologists Bulletin, v. 63, p. 2128–2144.

Hood, A.; Gutjahr, C. C. M.; and Heacock, R. L., 1975, Organic metamorphism and the generation of petroleum: American Association of Petroleum Geologists Bulletin, v. 59, p. 986–996.

Hook, R. C., 1989, Recent developments at Wilburton field, Latimer County, Oklahoma [abstract]: American Association of Petroleum Geologists Bulletin, v. 73, p. 1047.

Houseknecht, D. W., 1984, Influence of grain size and temperature on intergranular pressure solution, quartz cementation, and porosity in a quartzose sandstone: Journal of Sedimentary Petrology, v. 54, p. 348–361.

_____1986, Evolution from passive margin to foreland basin: the Atoka Formation of the Arkoma basin, south-central U.S.A., *in* Allen, P.A.; and Homewood, P. (eds.), Foreland basins: International Association of Sedimentologists, Special Publication No. 8, p. 327–345.

_____1987, The Atoka Formation of the Arkoma basin: tectonics, sedimentology, thermal maturity, sandstone petrology: Tulsa Geological Society Short Course Notes, 72 p.

Houseknecht, D. W.; and Iannacchione, A. T., 1982, Anticipating facies-related coal mining problems in the Hartshorne Formation, Arkoma basin: American Association of Petroleum Geologists Bulletin, v. 66, p. 923–930.

Houseknecht, D. W.; and Matthews, S. M., 1985, Thermal maturity of Carboniferous strata, Ouachita Mountains: American Association of Petroleum Geologists Bulletin, v. 69, p. 335–345.

Houseknecht, D. W.; and McGilvery, T. A., 1990, Red Oak field, *in* Beaumont, E. A.; and Foster, N. H. (eds.), Structural traps. II.—Traps associated with tectonic faulting: American Association of Petroleum Geologists, Treatise of petroleum geology, Atlas of oil and gas fields, p. 201–225.

Houseknecht, D. W.; Woods, M. O.; and Kastens, P. H., 1989, Transition from passive margin to foreland basin sedimentation: the Atoka Formation of the Arkoma basin, Arkansas and Oklahoma, *in* Vineyard, J. D.; and Wedge, W. K. (eds.), Geological Society of America 1989 Field Trip Guidebook: Missouri Department of Natural Resources Special Publication 5, p. 121–137.

Hunt, J. M., 1975, Is there a geochemical depth limit for hydrocarbons?: Petroleum Engineer, March 1975, p. 112–127.

Landes, K. K., 1967, Eometamorphism, and oil and gas in time and space: American Association of Petroleum Geologists Bulletin, v. 51, p. 828–841.

Oliver, J., 1986, Fluids expelled tectonically from orogenic belts: their role in hydrocarbon migration and other geologic phenomena: Geology, v. 14, p. 99–102.

Spencer, C. W., 1987, Hydrocarbon generation as a mechanism for overpressuring in Rocky Mountain region: American Association of Petroleum Geologists Bulletin, v. 71, p. 368–388.

Underwood, M. B.; Fulton, D. A.; and McDonald, K. W., 1988, Thrust control on thermal maturity of the frontal Ouachita Mountains, central Arkansas, U.S.A.: Journal of Petroleum Geology, v. 11, p. 325–340.

White, D., 1915, Some relations in origin between coal and petroleum: Journal of the Washington Academy of Sciences, v. 5, p. 189–212.

Wilson, L. R., 1961, Palynological fossil response to low-grade metamorphism in the Arkoma basin: Tulsa Geological Society Digest, v. 29, p. 131–140.

_____1971, Palynological techniques in deep-basin stratigraphy: Shale Shaker, v. 21, p. 124–139.

Evidence for Expulsion of Hydrothermal Fluids and Hydrocarbons in the Midcontinent during the Pennsylvanian

Raymond M. Coveney, Jr.
University of Missouri, Kansas City

ABSTRACT.—Zn- and organic-rich, marine black Pennsylvanian shales are widespread in the Midwest, type region for Late Paleozoic(?) Mississippi Valley-type (MVT) Pb–Zn ores. Interactions between the MVT mineralizing fluids and surface waters (meteoric or marine) are implied by the presence of oxidized species such as the goethite daughter crystals found in primary fluid inclusions hosted by calcite from MVT ores. Hence timing and depths of mineralization may have been conducive to derivation of metals for black shales from MVT ore fluids. Primary oil inclusions in MVT ore deposits show that metals and hydrocarbons were transported by the same hydrothermal fluids. Pennsylvanian country rocks, distal to ores, contain traces of ZnS with 80–120°C saline fluid inclusions. Some minor occurrences of MVT minerals found in Pennsylvanian beds along the Kansas/Missouri border occur as vertical tubes that may have been expulsion vents for hydrothermal fluids (undersea smokers). Thus, MVT hydrothermal systems may have leaked to the sea floor during Pennsylvanian time, providing metals for black shales.

INTRODUCTION

In previous articles, Coveney and Glascock (1989) and Coveney (1989) suggested that black shales may have gained metals from escaping hydrothermal fluids. This article presents further evidence for this possibility and for the additional likelihood that hydrocarbons were transported by the same hydrothermal fluids that mineralized the shales. Coveney and Goebel (1983), Coveney and others (1987a), and Goebel and others (1988) reported the widespread occurrence of fluid inclusions with high salinities and moderately high homogenization temperatures (80–120+°C) in minor and trace occurrences of sphalerite in the Midwest (Fig. 1). Pennsylvanian black shales (Fig. 2A) enriched in Zn, V, U, Mo, and other elements occur in the same region and may have been sinks rather than sources of Zn and Pb during Mississippi Valley-type (MVT) ore deposition, which others have inferred took place during the Late Paleozoic (Table 1). Pennsylvanian limestones, intercalated with the shales, contain tubes mineralized with calcite, dolomite, kaolinite or dickite, and sphalerite or barite (Fig. 3). The tubes commonly contain petroleum (Fig. 2B) and may have been submarine expulsion vents for hydrothermal fluids. Evidence in MVT ores suggests meteoric waters or oxidizing sea water were present during ore genesis, which would be consistent with the interpretation that black shales were enriched by metals derived from escaping MVT brines.

SHALES

For many years, thin (<1.0 m) midwestern Pennsylvanian black shales have been known to be enriched in uranium and other metals (Swanson, 1961; Zangerl and Richardson, 1963; Vine and Tourtelot, 1970; Coveney and Martin, 1983). For example, the U-rich Mecca Quarry Shale (Fig. 1) can be traced through Indiana, Iowa, Missouri, Kansas, and Oklahoma. Metals such as Mo, Se, and V are also present in enriched quantities and have been emphasized in other publications (e.g., Coveney and Glascock, 1989). Zinc, a characteristic MVT metal, is consistently enriched in the shales which contain whole-rock concentrations varying from 0.1 to 0.3 wt% in contrast with a tenor of 0.01 wt% Zn for average shale. Values exceeding 100 ppm are common for U, Se, and Pb (Table 2). Fourteen other extensive Pennsylvanian black shales are probably just as enriched in Zn as the Mecca Quarry Shale (Coveney, 1989).

Metals in black shales are often assumed to have been derived from sea water, but mass balance calculations based on chemical analyses and durations of sedimentation suggest that sea water alone could not have supplied the metals found in Pennsylvanian black shales (Coveney and Glascock, 1989). Possible solutions to the metal supply problem include epigenetic addition of metals. At least some MVT mineralization, which evidently was caused by large scale migration of chloride brines, may have postdated lithification of the

Pennsylvanian beds (Hatch and others, 1976; Coveney and others, 1987b). However, textural evidence suggests early deposition of sphalerite (e.g., Zangerl and Richardson, 1963). Coveney and Shaffer (1988) concluded that sulfur contained by Pennsylvanian black shales was fixed during or shortly after sedimentation. Therefore, Coveney and Glascock (1989) argue for an influx of metals during sedimentation as a result of submarine exhalative processes.

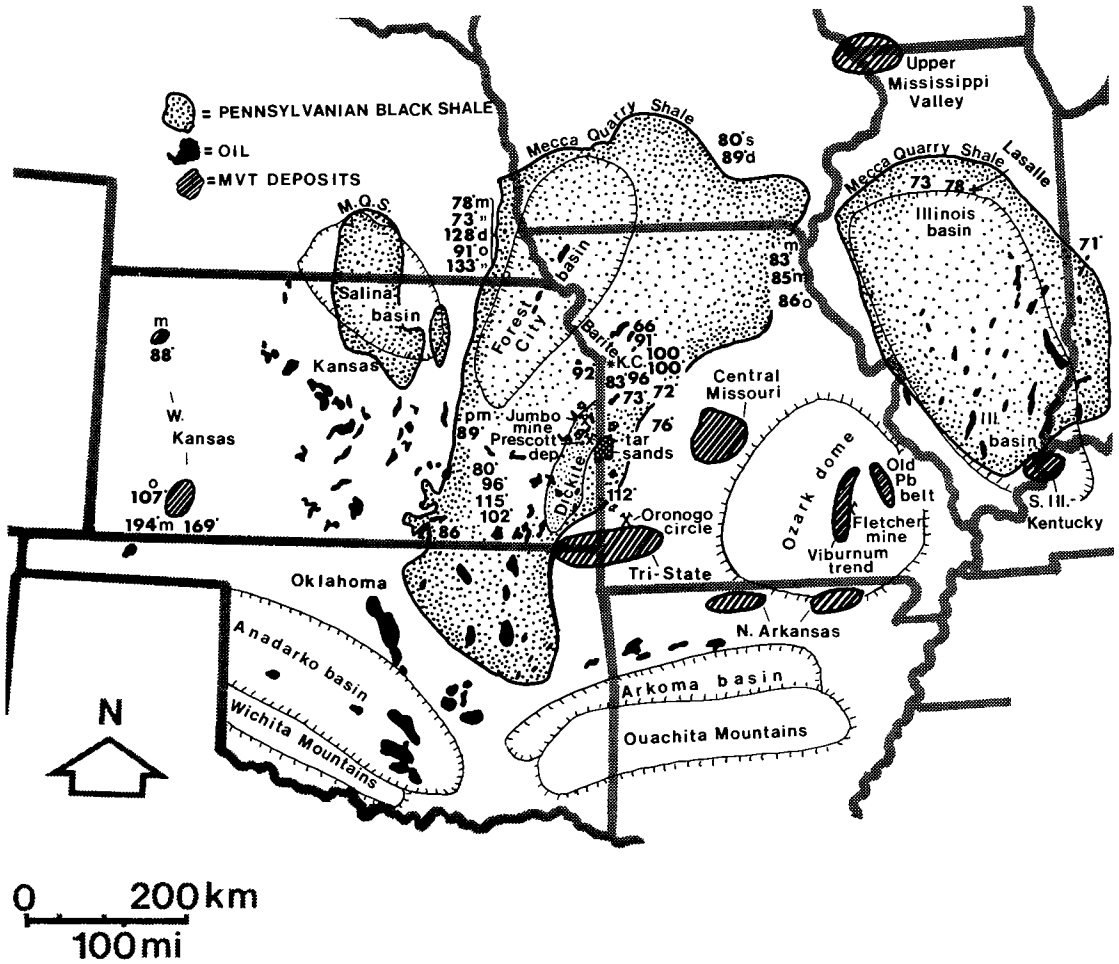

Figure 1. Distributions of MVT ores, hydrocarbon deposits, and Pennsylvanian black shales and tectonic features of the Midcontinent modified from Dozy (1970), Anderson and Macqueen (1982), and Coveney (1989). Black Pennsylvanian shales are represented by the present areal extent of Mecca Quarry Shale Member (modified from Wanless and Wright, 1978). Homogenization temperatures for fluid inclusions in minor occurrences of sphalerite (mainly in limestones) are indicated by bold-faced numbers (data from Coveney and Goebel [1983], Coveney and others [1987a], and Goebel and others [1988]). About half of the temperatures are from Pennsylvanian strata. Temperatures from other strata are labeled: c—Cambrian, o—Ordovician, s—Silurian, d—Devonian, m—Mississippian, and pm—Permian beds. Average temperatures from midwestern ore districts range from 95°C (central Missouri) to 140°C (southern Illinois) (Coveney and others, 1987a). Numerous other minor occurrences have been reported by others (e.g., Heyl, 1968). Hydrothermal dickite occurrences after Schroeder and Hayes (1968) are denoted by the encircled small dot pattern. Locations of major oil pools are from Goebel and others (1961) (Kansas), Johnson and others (1972) (Oklahoma), and Dozy (1970) (Illinois, Missouri, and Arkansas); tar sands (asphaltic rock) in Kansas and Missouri from Jewett (1940) and Searight (1957).

MVT ORES

MVT ores are characterized by enriched values for Zn and Pb. Seven major mining districts (Fig. 1) occur in the Midwest where MVT ores were first described. One of these, the Viburnum trend, remains the chief domestic source for Pb and Zn. Two unmined subsurface zones of MVT mineralization, of uncertain extent, occur in western Kansas (Fig. 1). The ores typically occur in carbonate host rocks and commonly contain such ore minerals as barite, chalcopyrite, marcasite, and pyrite in

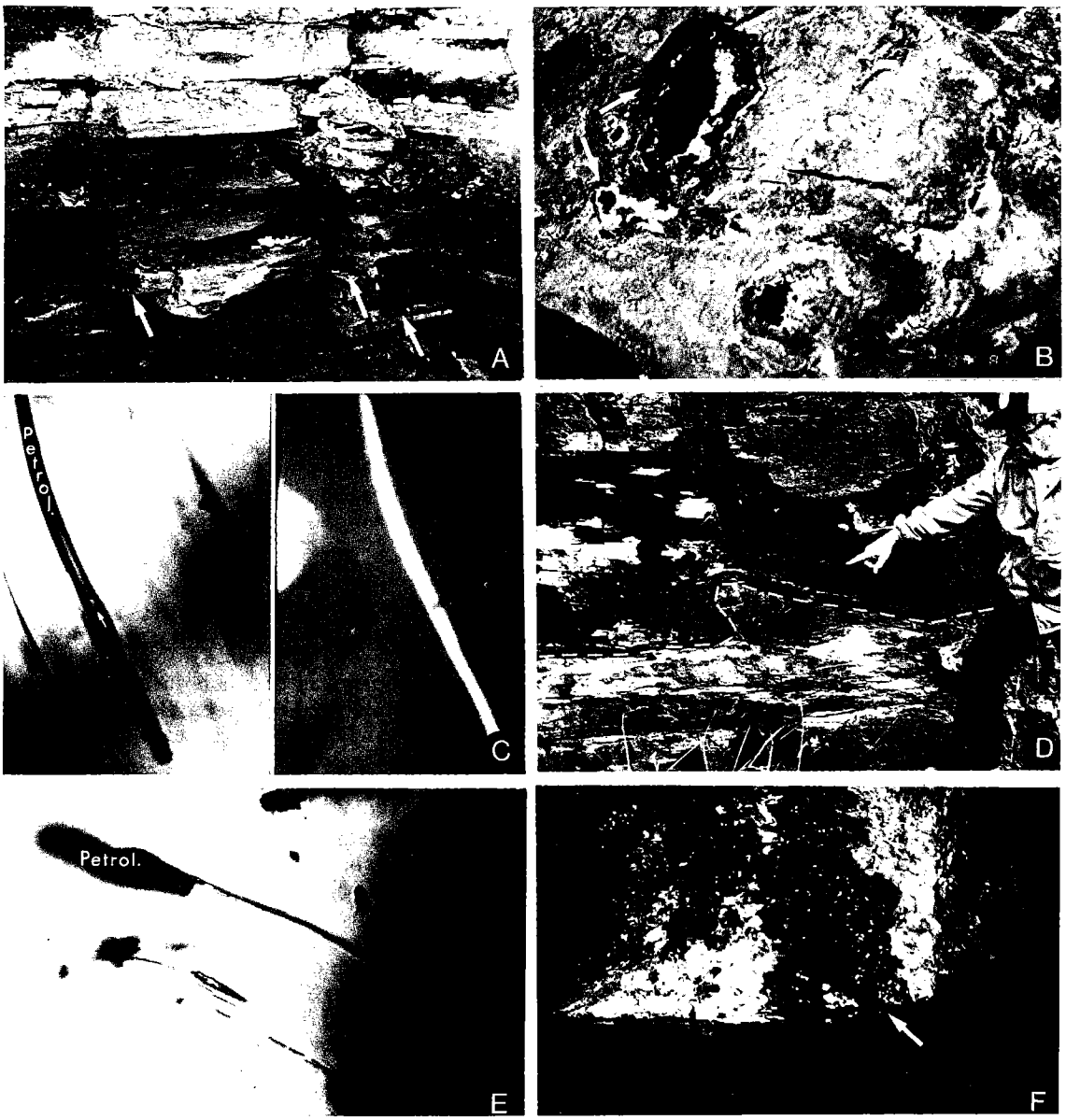

Figure 2. *A*—Stark Shale Member, Kansas City, Missouri (note oil on joint surfaces [arrows]). *B*—Oil seepage around mineralized tubes, Bethany Falls Limestone, McAdams Quarry, Prescott, Kansas (photo from Ragan, 1987). *C*—Primary petroleum fluid inclusions in sphalerite (~100 μm long) from Jumbo Pb mine (left in plane light, right under epifluorescent illumination). *D*—Pennsylvanian asphaltic rock ("tar sand"), Nevada, Missouri. Dashed line indicates contact between asphaltic rock (dark) and underlying barren zone. *E*—Primary petroleum fluid inclusion in sphalerite from the Oronogo Circle Zn–Pb mine, Missouri on north edge of Tri-State district. *F*—Oil dripping along pillar in Van Pool Zn–Pb mine, Picher field, Oklahoma.

TABLE 1. — COMPARATIVE AGES FOR DEPOSITION OF MVT ORE DEPOSITS AND PENNSYLVANIAN BLACK SHALES

Midcontinental USA MVT Ores		
>250 Ma	Post-ore illite	Rothbard (1983)
262 Ma	K–Ar Ba–adularia	Shelton and others (1986)
Penn.–Perm.	Paleomagnetics	Wu and Beales (1981)
Penn.–Perm.	Paleomagnetics	Wisniowiecki and others (1983)
283 Ma	Ouachita adularia	Bass and Ferrara (1969)
~235–290 Ma	Paleomagnetics	Pan and others (1989)
359 Ma	Rb–Sr glauconite	Stein and Kish (1985)
Metal-Rich Black Shales		
~290–303 Ma	Heebner Shale	
~291–302 Ma	Hushpuckney and Stark shales	
~296–309 Ma	Mecca Quarry Shale*	

*Ages of shales interpolated from Ross and Ross (1987), Palmer (1983), and Hess and Lippolt (1986).

addition to ubiquitous galena and sphalerite. Calcite, dolomite, and quartz (commonly jasperoid) are the predominant gangue minerals. Alteration assemblages include dolomite, quartz, and (in some cases) kaolinite or dickite. MVT deposits are characteristically associated with flat-lying, unmetamorphosed sedimentary country rocks, usually far removed from igneous rocks young enough to have provided the heat to drive the hydrothermal systems which deposited the MVT ores at temperatures between ~80 and 120°C from solutions having equivalent NaCl salinities >20 wt%.

A long and controversial history of interpretations concerning the origins of MVT ores has recently lead to a general consensus favoring deposition from migrating basinal brines, without the intervention of igneous processes. Recent articles by Sharp (1978), Cathles and Smith (1983), Garven (1985), Bethke (1986), and Oliver (1986) stressed the importance of the Ouachita–Arkoma region and the margins of other fold belts and basins in the formation of such ores. While favoring an important role for fluids from northern Arkansas, Leach and Rowan (1986) and Bauer and others (1989) also point out the possible influence of cratonic basins in the Midwest. The possibility of interaction between hydrothermal fluids and waters at the edges of basins has been raised by several workers including Dozy (1970). Near-surface deposition may be inferred on the basis of (1) the presence of sulfates such as barite (Barnes, 1983); (2) the dilute nature of fluid inclusions contained by barite (Leach, 1980); (3) the presence of marcasite (stable only at low pH values, likely to have been attained by oxidation of sulfide) (Murowchick and Barnes, 1986); (4) the presence of sphalerite color bands that may reflect astronomical cycles and/or climate changes (Barnes, 1989) and the likely presence of seasonal cycles in barite (Leach, 1980); and (5) the presence of oxidized Fe in fluid inclusions (Blasch and Coveney, 1988). Goethite daughter crystals in primary brine inclusions hosted by calcites from the Jumbo mine of eastern Kansas and the Fletcher mine of the Viburnum trend of southeast Missouri (Fig. 4), give evidence for oxidizing conditions, which would be consistent with a shallow setting of ore emplacement.

Leach and Rowan (1986), Sangster (1986), and Coveney (1989) summarized data concerning the age(s) of MVT mineralization in the Midwest. Although the available data summarized in Table 1 are not conclusive, ores in several midwestern MVT mining districts were probably emplaced during the Kiaman (Late Pennsylvanian–Early Permian) paleomagnetic stage (Wu and Beales, 1981; Wisniowiecki and others, 1983; Pan and others, 1989).

FLUID INCLUSIONS IN SPHALERITE FROM COUNTRY ROCKS

Many occurrences of sphalerite and barite resembling miniature MVT assemblages are found in the Midwest. Minor occurrences of sphalerite or barite associated with gangue minerals are widespread in Midcontinent country rocks (Goebel, 1968; Heyl, 1968). Not all of these occurrences are necessarily related to MVT mineralization events but many may be.

Numerous sphalerite–carbonate–kaolinite veinlets (Coveney, 1989) occur in the Winterset Limestone of Kansas City at a scale similar to the cleat fillings from coals studied by Cobb (1981). Sphalerite veins in the Winterset are so thin (<0.5 cm) that they must record rock temperatures.

Mineralized tubes occur in Missouri and Kansas. For example in Linn County, Kansas, the Bethany Falls Limestone Member of the Swope Formation contains vertical tubes that probably originated as root casts (Watney and others, 1989), which now contain abundant Fe-dolomite, calcite, and kaolinite (or dickite) with and without sphalerite (Fig. 3A). Many such occurrences ooze heavy oil (Fig. 2B). Similar structures are present in the Stoner Limestone Member of the Stanton

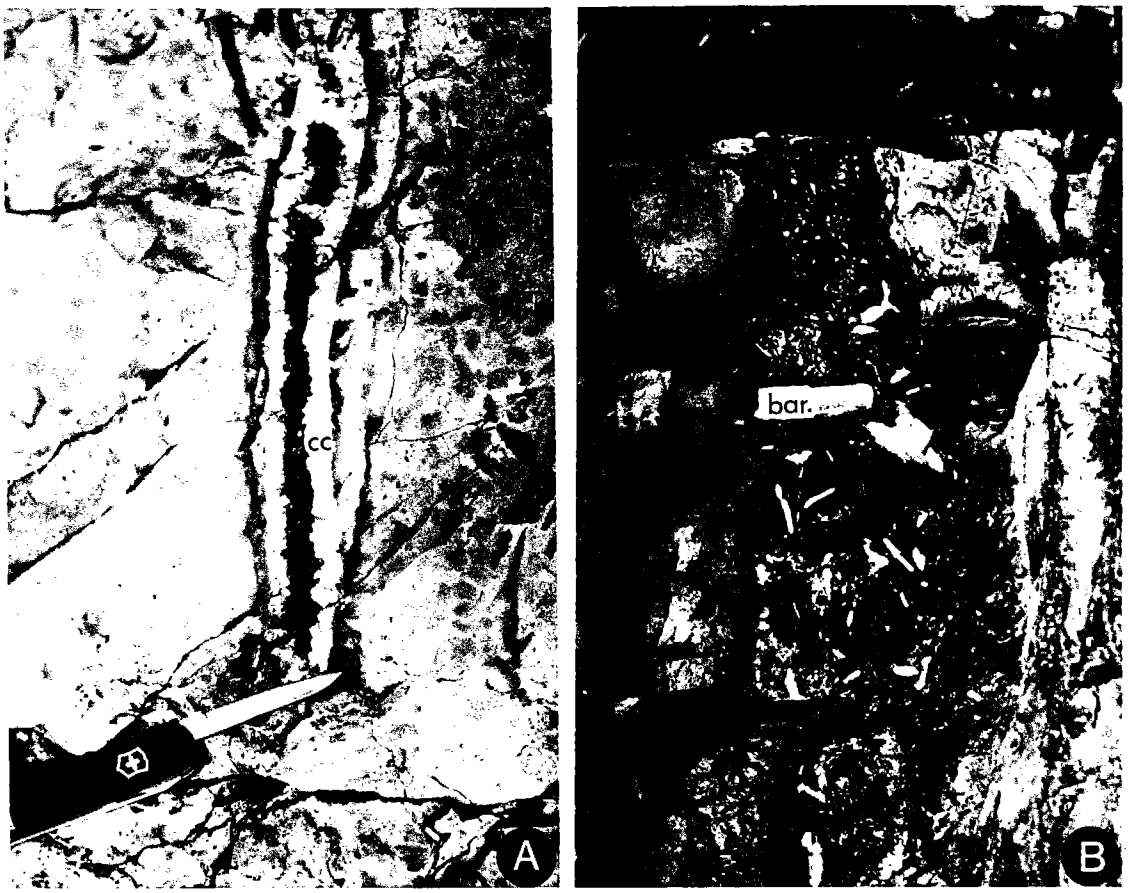

Figure 3. Mineralized tubes (possible vents). *A*—Hollow root cast or clam burrow lined with calcite crystals (cc), Bethany Falls Limestone, Mound City, Kansas; adjacent tubes contain oil. *B*—Barite (bar.) with ferroan dolomite and kaolinite in mineralized clam burrow from Stoner Limestone, Platte City, Missouri. Tubes in other locations are commonly filled with dolomite, calcite, barite, kaolinite or dickite, and contain minor amounts of sulfide minerals such as sphalerite, pyrite, marcasite, and chalcopyrite.

Limestone, near Platte City in Missouri (Gentile, 1979). These tubes, ~1 m long, probably formed as razor-clam burrows and are now lined with ferroan dolomite and pyrite. Many tubes contain pink barite crystals ranging to 40–60 mm long, which are so well formed as to suggest growth in soft sediment (Fig. 3B). The mineralized tubes certainly record the passage of large amounts of hydrothermal fluids and hydrocarbons and may be the remains of expulsion vents to the sea floor.

It has become increasingly clear that briny hydrothermal fluids were once ubiquitous in Paleozoic country rocks of the Midwest. Following the pioneering work of Leach (1973,1979) on the Missouri Ozark region, subsequent studies of fluid inclusions in ZnS, which broadened the area of coverage, include Cobb (1981) and Coveney and Goebel (1983). Salinities of inclusions hosted by country rock sphalerite are typically >20 wt% (Cobb, 1981; Coveney and others, 1987a). Goebel and others (1988) summarized their data on homogenization temperatures, which typically range from 80 to 120°C (see Fig. 1). Wojcik and others (1989,1990) found comparable homogenization temperatures for diagenetic carbonate minerals in southeast Kansas. It should be noted that there is a complete overlap between mineralization temperatures inferred from fluid inclusion data from both country rocks and the major ore districts, and that these temperatures correspond to the upper part of the oil window as defined by many authors (Hunt, 1989). Widespread trace occurrences of hydrothermal sphalerite suggest that country rock temperatures were elevated over broad areas during mineralization (Leach, 1979; Coveney and Goebel, 1983; Leach and Rowan, 1986; Bauer and others, 1989). Leach (1979) noted that temperatures recorded by fluid inclusions in ore deposits

TABLE 2. — METAL CONCENTRATIONS IN MECCA QUARRY SHALE AND EQUIVALENTS (PENNSYLVANIAN)

County:	Nowata	Bourbon	Randolph	LaSalle	Parke	Average
State:	Okla.	Kansas	Missouri	Illinois	Indiana	Crust
Sample no.:	A8 & A9	A6	BM2.3–2.4	Bed B	Bed B (U)	Value
Vanadium	290	400	912	3,200	2,850	135
Copper	65	85	105	160	144	55
Zinc	310	1,860	5,220	8,290	3,350	70
Selenium	73	78	84	272	230	0.05
Molybdenum	20	40	160	521	1,430	2
Lead	95	85	55	45	25	13
Thorium	11	10	7	5	7	7
Uranium	23	39	71	105	165	2
Gold (ppb)	2	2	3	2	2	4

Note: Data shown are for typical samples of organic-rich beds from the Mecca Quarry Shale Member and equivalent strata (data by neutron activation analysis from the University of Missouri–Columbia reactor, M.D. Glascock analyst). Copper and lead by atomic absorption were conducted at commercial laboratories. All values but gold in ppm (g/t). Some data from Coveney and Glascock (1989).

could not have been reached by normal geothermal gradients. An enhanced geothermal gradient may have been present in the Midcontinent during the Late Paleozoic from several possible causes including passage of the Midwest over a hot spot (Coveney and Goebel, 1983), global heat flow rates exceeding those of modern times, and, as previously mentioned, migration of hot brines into the Midwest (e.g., from the Ouachita region).

HYDROCARBONS

Dozy (1970) documented the striking relationships between occurrence of MVT ores and petroleum deposits in the Midwest (Fig. 1). In general, commercial oil fields show an antipathetic spatial relationship with respect to MVT mining districts (Fig. 1). On the other hand, hydrocarbons are known from many MVT mining districts (Fig. 2F). The presence of oil during mineralization can be documented in some cases. Most notable is the southern Illinois district where primary fluid inclusions of hydrocarbons have long been recognized in fluorite, the main ore mineral. References to hydrocarbon inclusions from other districts are rare, but Blasch and Coveney (1988) recently reported abundant primary petroleum inclusions from the Jumbo mine, Kansas (Fig. 2C), and Oronogo Circle, Missouri, on the fringe of the Tri-State mining district (Fig. 2E), as did Ragan (1987) for the Prescott, Kansas, Zn deposit. In most cases petroleum inclusions register homogenization temperatures 10–15°C lower than coeval brine inclusions because hydrocarbons are more compressible than aqueous fluids. For example, homogenization temperatures for sphalerite-hosted primary brine inclusions from the Jumbo mine average ~107°C, whereas adjacent primary petroleum inclusions register temperatures between 85 and 95°C (Blasch and Coveney, 1988). It should be noted that temperatures for emplacement of MVT ores and for sphalerite in the adjacent country rocks are well within the oil window as estimated by various workers (e.g., Hunt, 1989). Given the presence of organic-rich Pennsylvanian shales in the area (Fig. 1), local oil generation is likely, although in some areas the bulk of the oil probably originated from older beds (e.g., see Hatch and others, 1989). Outcrops of Pennsylvanian asphaltic rocks containing heavy (volatile-poor) oil are widespread in Kansas and Missouri near the Jumbo and Prescott mines (Figs. 1,2D).

RELATIONSHIPS AMONG BLACK SHALES, HYDROCARBONS, AND MVT DEPOSITS

Available results suggest that most MVT ores, certain hydrocarbon deposits, and Pennsylvanian black shales may have formed from the same hydrothermal system (or systems). Figure 5 illus-

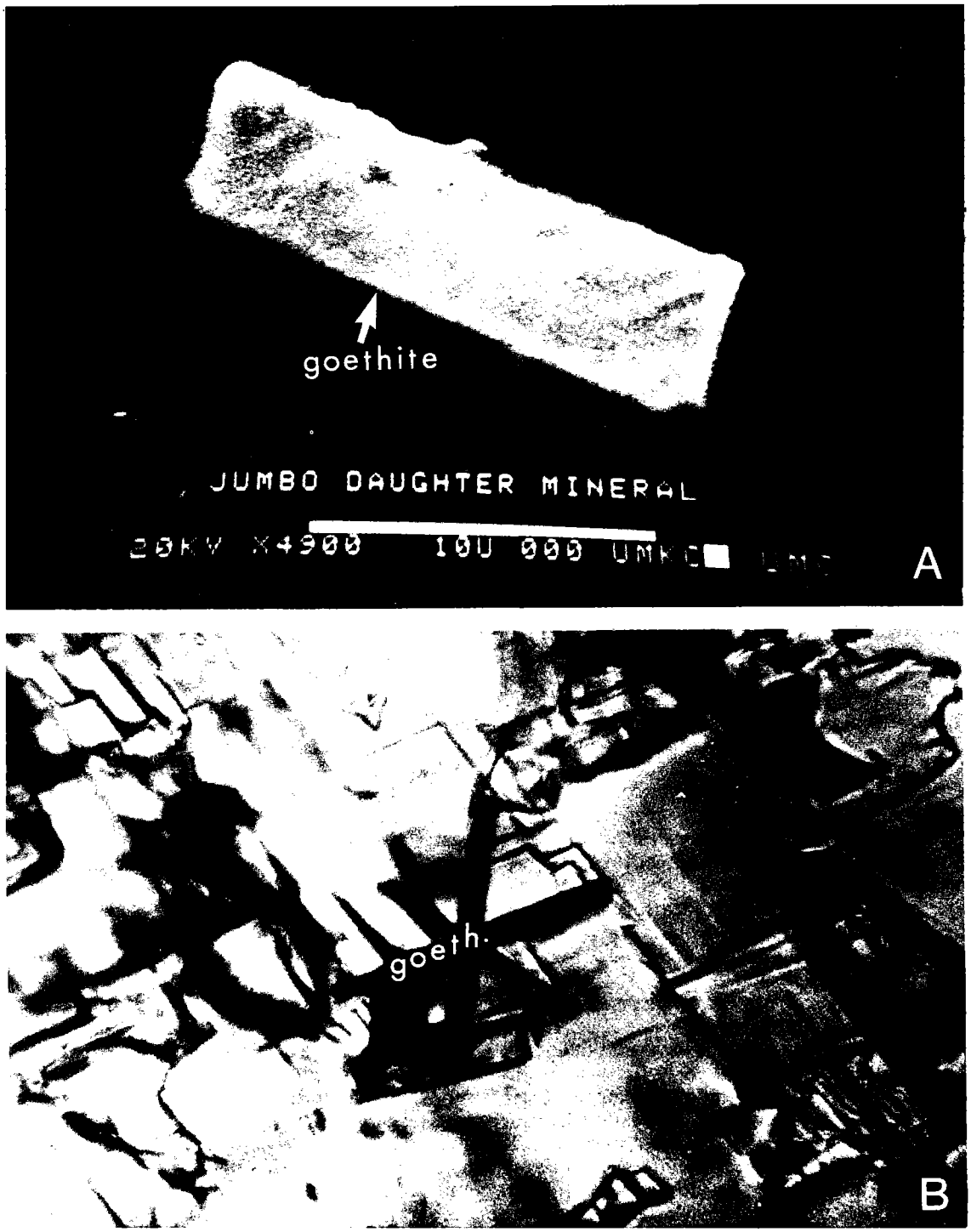

Figure 4. Iron oxide daughter minerals in primary fluid inclusions in calcite. *A*—Jumbo mine, Linn County, eastern Kansas. *B*—Fletcher mine, Viburnum trend, southeast Missouri (see Blasch and Coveney [1988] for details).

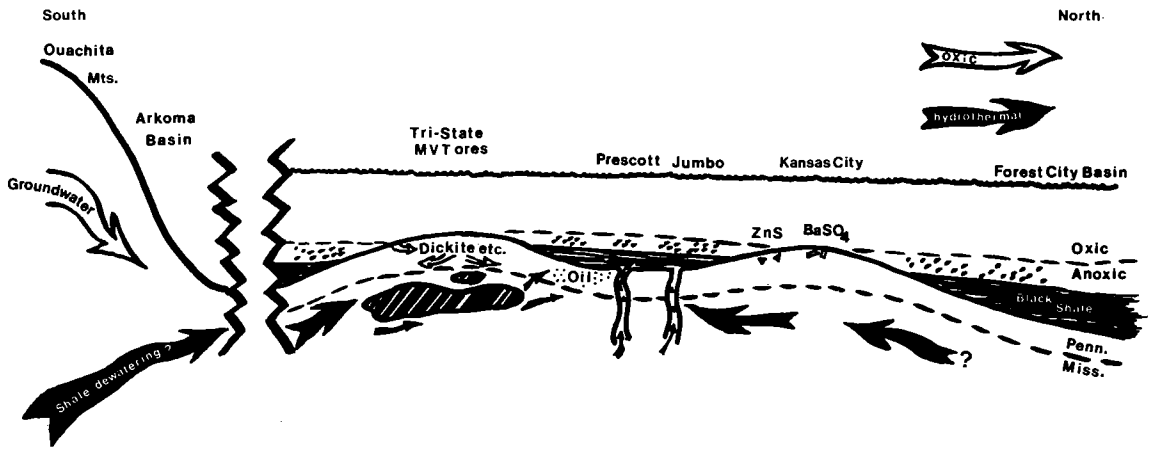

Figure 5. Schematic model. MVT ores, dickite occurrences, minor sphalerite and barite occurrences, and petroleum fields of western Missouri and eastern Kansas may all have formed from the same hydrodynamic system. (Refer to text for discussion of model).

trates a very general model showing how this may have occurred. Beginning in Middle or Late Pennsylvanian time, hydrothermal fluids were expelled from midwestern depositional basins to shelf areas. These fluids caused the deposition of MVT ores and carried hydrocarbons, now found in oil and gas fields. Major hydrocarbon deposits that remain are generally located peripheral to MVT districts, but some may have originally overlain mining districts only to be eroded away. As the MVT hydrothermal fluids passed through intervening country rocks, they left traces in the form of sphalerite containing high-temperature fluid inclusions (Coveney and others, 1987a) and other minerals (Wojcik and others, 1989,1990). Goebel and Ragan (1989) stressed the role of regional unconformities in fluid migration. In Kansas, former passageways for ore fluids and hydrocarbons include phylloid algal reefs now containing abundant hydrothermal dickite or kaolinite MVT gangue minerals, and traces of sphalerite and barite (Schroeder and Hayes, 1968; Keller, 1988). Tourtelot and others (1986) have proposed that filled-sink clay and iron deposits in the Missouri Ozarks may have been formed by paleohydrologic processes. Ultimately the fluids responsible for such features had to go somewhere, and here it is suggested that they escaped into the overlying water column or laterally along paleoaquifers. During the Pennsylvanian, where the overlying bottom waters were anoxic (i.e., during deposition of black shale), sulfides such as sphalerite were preserved. As in the Selwyn basin of Canada (Lydon and others, 1985; Goodfellow, 1987), in cases where sea water was oxygenated, Zn was largely flushed out of the system and barite was precipitated (e.g., when the Stoner and Bethany Falls Limestone Members were deposited). Such processes may have been active during the Middle or Late Pennsylvanian when black shales were deposited periodically throughout the Midwest.

Among the virtues of this very general model is a possible explanation for the origins of the exceptionally high metal concentrations in shales. Such concentrations are probably too high to have been derived solely from sea water (Coveney and Glascock, 1989). It also explains the ultimate fate of MVT ore fluids. The proposed model fits well with evidence of near-surface interactions between ore fluids and oxidized surface waters as has been suggested by the work of others (e.g., Murowchick and Barnes, 1986). It can also be reconciled with all essential aspects of the quantitative models focusing on the Arkoma–Anadarko region (e.g., Sharp, 1978). Nevertheless, along with Leach and Rowan (1986), I wish to stress the likelihood of a role for cratonic basins such as the Illinois basin and the Forest City basin in contributing metals, brines, and hydrocarbons to at least some MVT deposits and trace occurrences of sphalerite.

There are some possible problems with the model as it now stands. In particular the model rests on certain assumptions about timing of mineralization which may not survive as better radiometric dates for the length of the Pennsylvanian and the age of midwestern MVT mineralization become available. Also the sources of heat and the highly saline fluids contained by sphalerite-hosted inclusions remain unknown. Wojcik and others (1989,1990) found that multiple stages of alteration may have preceded the development of the most briny inclusions in their field area in southeast Kansas and have suggested that these brines may have been formed by dissolution of Permian

salt. They also suggested other possible origins including dissolution of as-yet-undiscovered pre-Permian evaporite deposits in the Arkoma–Ouachita region. If Permian salt proves to be critical for development of MVT brines, there would clearly be a time problem for some of the interpretations reported here.

Finally, it is possible that venting and expulsion of hydrothermal fluids into basins during deposition of metal-rich shales and Pennsylvanian brine migration were merely a harbinger for the main pulse(s) of MVT ore fluid and hydrocarbon migration that resulted in the formation of commercial deposits at a later time.

CONCLUSIONS

Fluid inclusions hosted by sphalerite in country rock in the Midwest imply that at one or more times in the past, moderately hot (80–120+°C) chloride brines were virtually ubiquitous in Paleozoic strata of the Midwest. The Paleozoic section of the Midwest also contains widespread black shales of Pennsylvanian age containing tremendous enrichments of Zn, a major component of MVT ores. The Midwest is the type region for Zn-rich Mississippi Valley-type ore deposits which likely formed during the Late Paleozoic. Hydrocarbon deposits are widespread in the Midwest although the distribution of commercial quantities of oil and gas differs from that of major MVT ores.

All three phenomena (fluid inclusions hosted by Paleozoic strata, the metal-rich Pennsylvanian shales, and the main MVT ores) may be genetically related. The same warm brines that escaped from sedimentary basins during the Late Paleozoic to deposit MVT ores may have provided metals for the black mud precursors of shales. Thus the metalliferous shales and the minor and trace occurrences of MVT mineralization may be by-products of the main MVT mineralization event (or events) of the Midwest. Hence it is conceivable that metal enrichments in black shales were deposited syngenetically from escaping MVT ore fluids because of the presence of abundant organic matter and H_2S in bottom waters or in the underlying sediments. Evidence favoring this interpretation includes the presence of Zn tenors in black shales that are too large to explain by derivation from sea water, radiometric dates of mineralization that fit with Late Paleozoic deposition, widespread evidence of passage of MVT hydrothermal fluids through country rocks, and the presence of what may be expulsion vents in Pennsylvanian carbonates. Whether the heating of country rocks resulted mainly from invasive hot brines, deeper burial than previously believed, passage of the Midcontinent over a hot spot, or some other cause is unknown but an interesting area for speculation.

ACKNOWLEDGMENTS

This paper has benefited from readings by Edwin D. Goebel, James B. Murowchick, Virginia M. Ragan, and Anthony W. Walton. Discussions with S. R. Blasch, R. J. Gentile, D. L. Leach, K. L. Shelton, and D. F. Sangster have been extremely helpful although few, if any, of these colleagues are likely to agree with all of the opinions expressed in this article. This research has been done with support from the National Science Foundation. It is also connected with IGCP Programme Project #254 ("Metalliferous Black Shales and Related Ore Deposits") funded by UNESCO. I thank Michael D. Glascock for neutron activation analyses of shale samples.

REFERENCES

Anderson, G. M.; and Macqueen, R. W., 1982, Ore deposit models. 6.—Mississippi Valley-type lead–zinc deposits: Geoscience Canada, v. 9, p. 108–117.

Barnes, H. L., 1983, Ore-depositing reactions in Mississippi Valley-type deposits, *in* Kisvarsanyi, G.; Grant, S. K.; Pratt, W. P.; and Koenig, J. W. (eds.), Proceedings of the international conference on Mississippi Valley-type lead–zinc deposits: University of Missouri–Rolla Press, p. 77–85.

_____1989, Constraints on the genesis of Mississippi Valley-type deposits from sphalerite banding [abstract]: Geological Society of America Abstracts with Programs, v. 21, p. A8.

Bass, M. N.; and Ferrara, G., 1969, Age of adularia and metamorphism, Ouachita Mountains, Arkansas: American Journal of Science, v. 257, p. 491–498.

Bauer, R. M.; Shelton, K. L.; and Gregg, J. M., 1989, Fluid inclusion studies of regionally extensive epigenetic dolomites, Bonneterre dolomite, S.E. Missouri: evidence of multiple fluids during Pb–Zn ore mineralization [abstract]: Geological Society of America Abstracts with Programs, v. 21, p. A3.

Bethke, C. M., 1986, Hydrologic constraints on the genesis of the Upper Mississippi Valley district from Illinois basin brines: Economic Geology, v. 81, p. 233–249.

Blasch, S. R.; and Coveney, R. M., Jr., 1988, Goethite-bearing brine inclusions, petroleum inclusions, and the geochemical conditions of ore deposition at the Jumbo mine, Kansas: Geochimica et Cosmochimica Acta, v. 52, p. 1007–1017.

Cathles, L. M.; and Smith, A. T., 1983, Thermal constraints on the formation of Mississippi Valley-type lead–zinc deposits and their implications for episodic dewatering and deposit genesis: Economic Geology, v. 78, p. 983–1002.

Cobb, J. C., 1981, Geology and geochemistry of sphalerite in coal: University of Illinois unpublished Ph.D. dissertation, 204 p.

Coveney, R. M., Jr., 1989, Relationships among metal-rich Pennsylvanian marine black shales, minor occurrences of sphalerite in country rocks and Mississippi Valley-type ore deposits of the midwestern United States, *in* Hagni, R. D.; and Coveney, R. M.,

Jr. (eds.), Mississippi Valley-type mineralization of the Viburnum Trend, Missouri: Society of Economic Geologists Guidebook 5, p. 166–181.

Coveney, R. M., Jr.; and Glascock, M. D., 1989, A review of the origins of metal-rich Pennsylvanian black shales, central U.S.A., with an inferred role for basinal brines: Applied Geochemistry, v. 4, p. 347–367.

Coveney, R. M., Jr.; and Goebel, E. D., 1983, New fluid inclusion homogenization temperatures for sphalerite from minor occurrences in the Mid-continent area, *in* Kisvarsanyi, G.; Grant, S. K.; Pratt, W. P.; and Koenig, J. W. (eds.), Proceedings of the international conference on Mississippi Valley-type lead–zinc deposits: University of Missouri–Rolla Press, p. 234–242.

Coveney, R. M., Jr.; and Martin, S. P., 1983, Molybdenum and other heavy metals of the Mecca Quarry and Logan Quarry shales: Economic Geology, v. 78, p. 132–149.

Coveney, R. M., Jr.; and Shaffer, N. R., 1988, Sulfur-isotope variations in Pennsylvanian shales of the midwestern United States: Geology, v. 16, p. 18–21.

Coveney, R. M., Jr.; Leventhal, J. S.; Glascock, M. D.; and Hatch, J. R., 1987a, Origins of metals and organic matter in the Mecca Quarry Shale Member and stratigraphically equivalent beds across the Midwest: Economic Geology, v. 82, p. 915–933.

Coveney, R. M., Jr.; Goebel, E. D.; and Ragan, V. M., 1987b, Pressures and temperatures from aqueous fluid inclusions in sphalerite from Midcontinent country rocks: Economic Geology, v. 82, p. 740–751.

Dozy, J. J., 1970, Genesis of lead–zinc ores of the Mississippi Valley, U.S.A.: Transactions Institute of Mining and Metallurgy, London, v. 79, p. B163–B170.

Garven, G., 1985, The role of regional fluid flow in the genesis of the Pine Point deposit, western Canada sedimentary basin: Economic Geology, v. 80, p. 307–324.

Gentile, R. J., 1979, Bivalve burrows as sites of barite crystal growth in an upper Carboniferous limestone, western Missouri [abstract]: Ninth International Congress on Carboniferous Stratigraphy and Geology, Abstracts, p. 69–70.

Goebel, E. D., 1968, Mississippian rocks of western Kansas: American Association of Petroleum Geologists Bulletin, v. 52, p. 1732–1778.

Goebel, E. D.; and Ragan, V. M., 1989, Fluid inclusions and sulfur isotopes from MVT deposition and the role of intra-cratonic unconformities [abstract]: Geological Society of America Abstracts with Programs, v. 21, p. A359.

Goebel, E. D.; Hilpman, P. L.; Beene, D. L.; and Noever, R. J., 1961, Oil and gas developments in Kansas during 1960: Kansas Geological Survey Bulletin 155, 229 p.

Goebel, E. D.; Coveney, R. M., Jr.; and Ragan, V. M., 1988, Fluid inclusion evidence from country rocks bearing on the extent of ore-forming systems in the Midcontinent U.S., *in* Kisvarsanyi, G.; and Grant, S. K. (eds.), Proceedings of the North American conference on tectonic control of ore deposits and the vertical and horizontal extent of ore systems: University of Missouri–Rolla Press, p. 447–454.

Goodfellow, W. D., 1987, Anoxic stratified oceans as a source of sulphur in sediment-hosted stratiform Zn–Pb deposits (Selwyn basin, Yukon, Canada): Chemical Geology, v. 65, p. 359–382.

Hatch, J. R.; Gluskoter, H. J.; and Lindahl, P. C., 1976, Sphalerite in coals from the Illinois basin: Economic Geology, v. 71, p. 613–624.

Hatch, J. R.; King, J. D.; and Daws, T. A., 1989, Geochemistry of Cherokee Group oils of southeastern Kansas and northeastern Oklahoma: Kansas Geological Survey, Subsurface Series 11, 20 p.

Hess, J. C.; and Lippolt, H. J., 1986, $^{40}Ar/^{39}Ar$ ages of tonstein and tuff sanidines: new calibration points for the improvement of the Upper Carboniferous time scale: Chemical Geology, v. 59, p. 143–154.

Heyl, A. V., 1968, Minor epigenetic, diagenetic, and syngenetic sulfide, fluorite, and barite occurrences in the central United States: Economic Geology, v. 63, p. 585–594.

Hunt, J. M., 1989, Review of "Geochemistry," American Association of Petroleum Geologists, Petroleum Geology Reprint Series No. 8, compiled by E. A. Beaumont and N. H. Foster: Geochimica et Cosmochimica Acta, v. 53, p. 3343.

Jewett, J. M., 1940, Asphalt rock in eastern Kansas: Kansas Geological Survey Bulletin 29, 23 p.

Johnson, K. S.; Branson, C. C.; Curtis, N. M., Jr.; Ham, W. E.; Harrison, W. E.; Marcher, M. V.; and Roberts, J. F., 1972, Geology and earth resources of Oklahoma—an atlas of maps and cross sections: Oklahoma Geological Survey Educational Publication 1, 8 p.

Keller, W. D., 1988, Authigenic kaolinite and dickite associated with metallic sulfides-probable indicators of a regional thermal event: Clays and Clays Minerals, v. 36, p. 153–158.

Leach, D. L., 1973, A study of the barite–lead–zinc deposits of central Missouri and related mineral deposits in the Ozark region: University of Missouri–Columbia unpublished Ph.D. dissertation, 186 p.

_____1979, Temperature and salinity of the fluids responsible for minor occurrences of sphalerite in the Ozark region of Missouri: Economic Geology, v. 74, p. 931–937.

_____1980, Nature of mineralizing fluids in the barite deposits of central and southeast Missouri: Economic Geology, v. 75, p.1168–1180.

Leach, D. L.; and Rowan, E. L., 1986, Genetic link between Ouachita foldbelt tectonism and the Mississippi Valley-type lead–zinc deposits of the Ozarks: Geology, v. 14, p. 931–935.

Lydon, J. W.; Goodfellow, W. D.; and Jonasson, I. R., 1985, A general genetic model for stratiform baritic deposits of the Selwyn basin, Yukon Territory and District of Mackenzie: Geological Survey of Canada Paper 85-1A, p. 651–660.

Murowchick, J. B.; and Barnes, H. L., 1986, Marcasite precipitation from hydrothermal solutions: Geochimica et Cosmochimica Acta, v. 50, p. 2615–2629.

Oliver, J., 1986, Fluids expelled from orogenic belts: their role in hydrocarbon migration and other geologic phenomena: Geology, v. 14, p. 99–102.

Palmer, A. R., 1983, The Decade of North American

Geology 1983 geologic time scale: Geology, v. 11, p. 503–504.

Pan, H.; Symons, D. T. A.; and Sangster, D. F., 1989, Paleomagnetism of mineralized and host Paleozoic carbonates from the northern Arkansas and Tri-State Pb–Zn districts [abstract]: Geological Society of America Abstracts with Programs, v. 21, p. A4–A5.

Ragan, V. M., 1987, Geothermometry and organic matter-mineral link for the mineralization at the Prescott zinc deposit and adjacent country rocks of Linn County, Kansas: University of Missouri–Kansas City unpublished M.S. thesis, 96 p.

Ross, C. A.; and Ross, J. R. P., 1987, Late Paleozoic sea levels and depositional sequences, *in* Ross, C. A.; and Haman, D. (eds.), Timing and depositional history of eustatic sequences: constraints on seismic stratigraphy: Cushman Foundation for Foraminiferal Research Special Publication, v. 24, p. 137–149.

Rothbard, D. R., 1983, Diagenetic history of the Lamotte sandstone, *in* Kisvarsanyi, G.; Grant, S. K.; Pratt, W. P.; and Koenig, J. W. (eds.), Proceedings of the international conference on Mississippi Valley-type lead–zinc deposits: University of Missouri–Rolla Press, p. 385–395.

Sangster, D. F., 1986, Age of mineralization in Mississippi Valley-type (MVT) deposits: a critical requirement for genetic modeling, *in* Andrews, C. J.; Crowe, R. W. A.; Finlay, S.; Pennell, W. M.; and Pyne, J. F. (eds.), Geology and genesis of mineral deposits in Ireland: Irish Association for Economic Geology, Dublin, p. 625–634.

Schroeder R. J.; and Hayes, J. B., 1968, Dickite and kaolinite in Pennsylvanian limestones of southeast Kansas: Clays and Clay Minerals, v. 16, p. 41–49.

Searight, W. V., 1957, Asphaltic rocks in western Missouri: Missouri Division of Geological Survey and Water Resources Information Circular 13, 26 p.

Sharp, J. M., Jr., 1978, Energy and momentum transport model of the Ouachita basin and its possible impact on formation of economic mineral deposits: Economic Geology, v. 73, p. 1057–1068.

Shelton, K. L.; Reader, J. M.; Ross, L. M.; Viele, G. W.; and Seidemann, D. E., 1986, Ba-rich adularia from the Ouachita Mountains, Arkansas: implications for a postcollisional hydrothermal system: American Mineralogist, v. 71, p. 916–923.

Stein, H. J.; and Kish, S. A., 1985, The timing of ore formation southeast Missouri: Rb–Sr glauconite dating at the Magmont mine Viburnum trend: Economic Geology, v. 80, p. 739–753.

Swanson, V. E., 1961, Geology and geochemistry of uranium in marine black shales—a review: U.S. Geological Survey Professional Paper 356-C, 112 p.

Tourtelot, H. A.; Goldhaber, M. B.; Fitzpatrick, J. J.; and Satterfield, I. R., 1986, Filled-sink deposits of refractory clays, iron-rich clays, hematite, and marcasite–pyrite in Missouri—possible results of unified paleohydrologic processes [abstract]: Geological Society of America Abstracts with Programs, v. 18, p. 775.

Vine, J. D.; and Tourtelot, E. B., 1970, Geochemistry of black shale deposits—a summary report: Economic Geology, v. 65, p. 253–273.

Wanless, H. R.; and Wright, C. R., 1978, Paleoenvironmental maps of Pennsylvanian rocks, Illinois basin, and northern Midcontinent region: Geological Society of America Map Series MC-23.

Watney, W. L.; French, J. A.; and Franseen, E. K., 1989, Sequence stratigraphy interpretations and modeling of cyclothems: Guidebook for 41st Annual Field Trip, Kansas Geological Survey, Lawrence, 211 p.

Wisniowiecki, M. J.; Van der Voo, R.; McCabe, C.; and Kelly, W. C., 1983, A Pennsylvanian pole from the mineralized Late Cambrian Bonneterre Formation, southeast Missouri: Journal of Geophysical Research, v. 88, p. 6540–6548.

Wojcik, K. M.; Goldstein, R. H.; and Walton, A. W., 1989, Fluid migration and thermal history recorded in diagenetic phases of Pennsylvanian sandstones and limestones, SE Kansas [abstract]: Geological Society of America Abstracts with Programs, v. 21, p. A4.

Wojcik, K. M.; McKibben, M. E.; Goldstein, R. H.; and Walton, A. W., 1990, Diagenesis and fluid migration, Middle and Upper Pennsylvanian rocks, southeastern Kansas [abstract]: Oklahoma Geological Survey/U.S. Department of Energy workshop on source rocks, generation, and migration of hydrocarbons and other fluids in the southern Midcontinent, p. 9.

Wu, Y.; and Beales, F. W., 1981, A reconnaissance study by paleomagnetic methods of the age of mineralization along the Viburnum trend, southeast Missouri: Economic Geology, v. 76, p. 1879–1894.

Zangerl, R.; and Richardson, E. S., 1963, The paleoecologic history of two Pennsylvanian black shales: Chicago Natural History Museum, Fieldiana Geology Memoirs, v. 4, 352 p.

Diagenesis, Thermal History, and Fluid Migration, Middle and Upper Pennsylvanian Rocks, Southeastern Kansas

K. M. Wojcik, M. E. McKibben*,
R. H. Goldstein, and A. W. Walton
University of Kansas

ABSTRACT.—Pennsylvanian sandstones, mudrocks, and limestones of southeastern Kansas form a regional confining unit that overlies mostly carbonate pre-Pennsylvanian strata containing regional permeable horizons. The diagenetic succession in both Pennsylvanian sandstones and limestones includes three stages. (1) Early, pre-compactional stage is characterized by pyrite and siderite in sandstones, and formation of moldic pores and zoned calcite cements in limestones. (2) Intermediate, syn-compactional stage is characterized by quartz and feldspar overgrowths in sandstones, and by iron-rich calcite and megaquartz in limestones. (3) Late stage of diagenesis represents the effects of a regional event and is characterized by a widespread dissolution event followed by precipitation of Ca–ankerite in sandstones, Ca–Fe–dolomite in limestones, and kaolinite in both lithologies. Ca–ankerite is more ferroan and somewhat more calcian than Ca–Fe–dolomite. Major element composition of late carbonate cements was controlled by local rock-water interaction.

Isotopic data indicate that Ca–ankerite and Ca–Fe–dolomite did not form in equlibrium with the same fluid and carbon sources. Ca–Fe–dolomite has $\delta^{18}O$ of –5.9‰ and $\delta^{13}C$ averaging +5.6‰. Ca–ankerite has $\delta^{18}O$ of –7.3‰ and $\delta^{13}C$ of –5.2‰. In limestones, matrix $\delta^{13}C$ values are distinctly lighter than dolomite $\delta^{13}C$ values from the same sample. The light carbon values for ankerite suggest its origin via reactions involving organic matter. Positive carbon values for dolomite and their shift relative to matrix values, suggest that a source of heavy carbon other than the rock reservoir may have influenced the dolomite $\delta^{13}C$.

Fluid inclusion data indicate that iron-rich calcite of the intermediate stage of diagenesis precipitated at temperatures below 50°C from a brine of 14.5 wt% NaCl equivalent. The data from late-stage carbonate cements show that high temperatures (100–150°C) affected the study area during, and perhaps after, precipitation of Ca–ankerite and Ca–Fe–dolomite. These temperatures are distinctly higher than maximum burial temperatures calculated for the studied section. Most fluids present during the late stage were highly saline, about 19–25 wt% NaCl equivalent.

Models of diagenesis must account for our three chief results: high salinity of diagenetic fluids, which imply their association with evaporites; compositional differences of late carbonate cements, suggesting local lithologic control; and temperatures above calculated burial temperatures, which suggest a source of heat other than simple burial. Lateral flow of hydrothermal fluids from the Ouachita–Arkoma region can account for the heat. Small amounts of heated water could have entered the Pennsylvanian section vertically through fractures and faults, driving diagenesis but permitting local lithologic control. Salt may have come from descending Permian evaporitic brines or dissolution of Permian evaporites by meteoric water. Simpler flow patterns would be possible if meteoric or connate water dissolved evaporites that could be postulated to exist in the Lower Paleozoic aulacogen or continental margin sequences of the Ouachita–Arkoma region.

INTRODUCTION

Indications of high paleotemperatures in the Ouachita foreland shelf (north of the Arkoma basin) of southeastern Kansas and adjacent areas of Missouri and Oklahoma (Leach, 1979; Coveney and Goebel, 1983) are at odds with the lack of support for either substantially greater burial in the past, or higher heat flow from the basement in this tectonically quiescent area. To resolve this paradox one can postulate lateral flow of heated water from the Ouachita tectonic belt or the Arkoma basin up onto the craton. Such a hydrogeologic event may have accompanied and been driven by deformation and uplift of the Ouachita–Arkoma system (Sharp, 1978; Oliver, 1986; Bethke and others, 1988).

This postulated flow of water has drawn much

*Present address: Exxon USA, Houston, Texas.

attention for its possible role in forming Mississippi Valley-type (MVT) lead–zinc deposits in the Ozarks (Leach and others, 1984; Leach and Rowan, 1986; Gregg, 1985; Gregg and Hagni, 1987; Shelton and others, 1986; Farr, 1989). However, heating and mineral reactions that accompanied it might have affected other rocks as well, possibly in areas well outside the mineralized districts. We have investigated interbedded Desmoinesian and Missourian (Pennsylvanian) sandstones and limestones in southeastern Kansas and a small area of western Missouri (Fig. 1). Our objectives were to describe the diagenetic history, to constrain the patterns of flow of fluids, and to compare these fluids to those involved in MVT mineralization in the Ozark region to the east. Preliminary results of this ongoing study include:

1) Results of diagenetic events in Middle and Upper Pennsylvanian sandstones are petrographically and chemically similar over an area >20,000 km^2.

2) Results of diagenetic events in Middle and Upper Pennsylvanian limestones are similar over the same area.

3) These internal similarities and the existence of identical or analogous diagenetic events in both sandstones and limestones suggest that the controls of this diagenesis were regional rather than local in extent.

4) Marked differences between chemical and isotopic compositions of analogous minerals in limestones and those in sandstones imply that diagenesis involved some lithology-dependent rock-water interaction.

5) Clear indications of temperatures in the 100–150°C range are found in diagenetic minerals in Middle and Upper Pennsylvanian sandstones and limestones of southeastern Kansas. These temperatures are significantly higher than those calculated using reasonable estimates of maximum burial depth, surface temperature, and thermal gradient.

6) The fluids that precipitated certain minerals in the sequence were very saline, >20 wt% NaCl equivalent.

7) Certain of these temperatures and salinities are similar to those reported for MVT deposits in the Ozark region of Missouri and surrounding states, suggesting that diagenesis of Pennsylvanian rocks in Kansas and formation of MVT ores may have been genetically linked over a broad region.

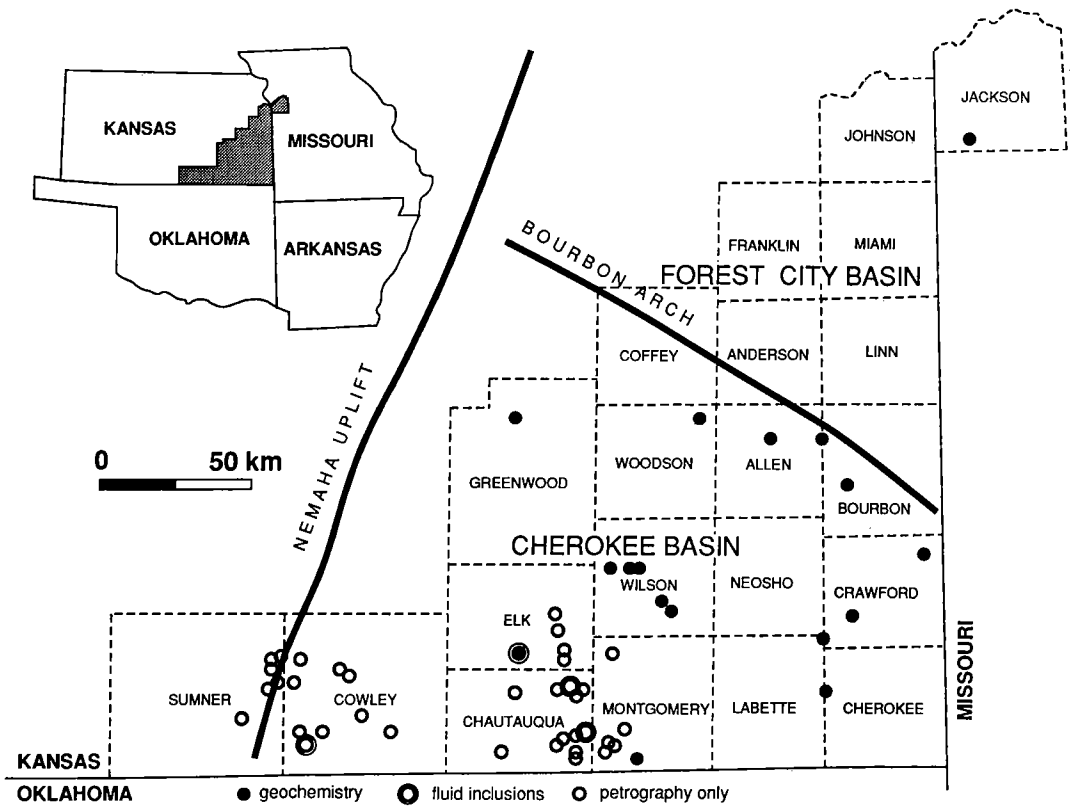

Figure 1. Map of southeastern Kansas showing location of samples studied.

GEOLOGIC SETTING

Pennsylvanian rocks of the Ouachita foreland shelf consist of limestones and sandstones interbedded with more abundant mudrocks (Fig. 2). Limestones are interpreted as cyclic deposits of transgressing and regressing seas, with black shales commonly marking the maximum transgression (Heckel, 1977). Mudstone-sandstone sequences are deposits of rivers, deltas, nearshore environments, and shallow-marine shelves (Murphy, 1978; Harris, 1984; Brenner, 1989). Coals interbedded in sandstone-mudstone sequences represent deposits of the earliest phases of transgressions. Dark-gray or black shales that immediately overlie coals may be similar to black shales associated with limestones; presumably they represent maximum transgression for each cycle.

The Nemaha uplift separates the shelf region of eastern Kansas from that of central and western Kansas. The anticlinal nature of that uplift was defined before deposition of Desmoinesian strata. The Cherokee basin occupies the southern part of the shelf of eastern Kansas (Fig. 1). The Bourbon arch separates the Cherokee basin from the Forest City basin, which extends into Missouri, Iowa, and Nebraska. These basins are best defined by the Cherokee Group, which ranges up to 150 m thick in southeastern Labette County on the Oklahoma border and up to 250 m thick in Brown County on the Nebraska border, but thins to ~100 m over the Bourbon arch and incompletely onlaps the crest of the Nemaha uplift. Since deposition, the area has undergone gentle tilting to the west–northwest and faulting that was concentrated along the east side of the Nemaha uplift.

The Pennsylvanian unconformably overlies Mississippian rocks over most of eastern Kansas, but older Paleozoic and Precambrian rocks subcrop along the Nemaha uplift. The pre-Pennsylvanian rocks are mostly carbonates, with transgressive sandstones (Lamotte, Simpson–St.Peter) and some shaly intervals (Maquoketa, Chattanooga). Both Cambrian–Ordovician (Arbuckle Group) and Mississippian carbonate rocks contain regional permeable horizons in eastern Kansas. In contrast, Pennsylvanian rocks are a regional confining unit (Jorgensen, 1989). They contain only discontinuous lenses of permeable sandstone or limestone embedded within extensive layers of shale.

METHODS AND RESULTS

Our study included reconnaissance over a broad area of the Cherokee and Forest City basins and a more concentrated study of samples from Cowley, Elk, and Chautauqua Counties of Kansas (Fig. 1). Most of the intensely studied samples came from oil-well cores; some were collected at outcrops.

Paragenesis

Paragenesis was determined by petrographic examination of stained thin sections (Dickson, 1965) of Desmoinesian and Missourian rocks and

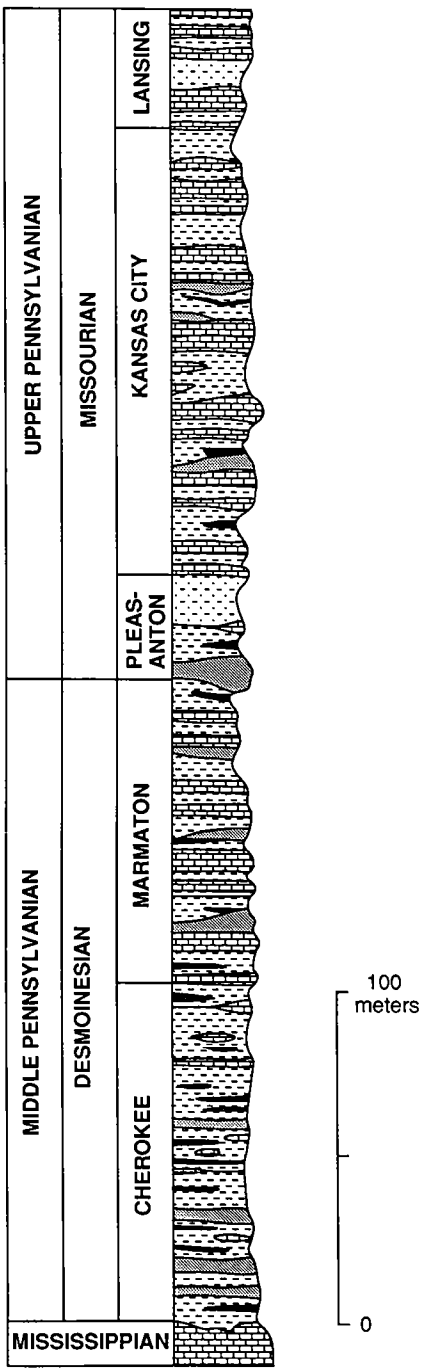

Figure 2. Generalized stratigraphic and lithologic section of eastern Kansas (from Ebanks and others, 1979). Our studied samples provide coverage of the entire sequence.

corroborated by examination of back-scattered electron images on a scanning electron microscope. For the purpose of this discussion, the paragenetic sequence has been divided into three stages of diagenesis (Fig. 3). The early stage predates most compaction. In sandstones it is characterized by formation of pyrite (Fig. 4A), siderite (Fig. 4B), and minor ferroan calcite, gypsum, and dolomite. In limestones it is characterized by formation of molds, nonferroan calcite, zoned nonferroan and ferroan calcite (Fig. 5A,D), pyrite, and minor gypsum, chalcedony, dolomite, and megaquartz. There is no sharp break between the early and intermediate stages. The intermediate stage of diagenesis took place during compaction. In sandstones it is characterized by quartz and feldspar overgrowths (Fig. 4B). In limestones it is characterized by fractures filled with very iron-rich calcite (Fig. 5B), megaquartz, and minor sphalerite of unclear paragenetic position. The final (late) stage follows a regional episode of dissolution (Fig. 4A,B; Fig. 5C,D). In sandstones it is dominated by ubiquitous baroque (saddle) Ca–ankerite (Fig. 4A, B), kaolinite (Fig. 4B), and minor barite. In limestones it is dominated by irregularly distributed baroque (saddle) Ca–Fe–dolomite (Fig. 5C), kaolinite (Fig. 5D), and minor calcite. The sandstone paragenetic sequence is in accord with other investigations of diagenesis of the Cherokee Group (e.g., Woody, 1983a,b).

In each stage, some diagenetic events affected both sandstones and limestones. Pyrite is a widespread early-stage mineral in both rock types. In the intermediate stage quartz precipitated in sandstones and limestones. The boundary between the intermediate and late stages is marked by a widespread dissolution event in both lithologies. Dissolution affected carbonate minerals (Fig. 5C,D) and detrital feldspars (Fig.4B). During the late stage, growth-zoned Ca–ankerite precipitated in sandstone and growth-zoned Ca–Fe–dolomite precipitated in limestone, whereas kaolinite formed in both lithologies. The ankerite and dolomite are petrographically similar and precipitated in paragenetically analogous positions. Several diagenetic minerals (pyrite, ferroan calcite, quartz, and kaolinite) are common to both sandstones and limestones and the Ca–ankerite and Ca–Fe–dolomite probably represent the same event. The minerals in common and the dissolution event developed in the same paragenetic order in both rock types (Fig. 3).

The apparent similarity of diagenesis between sandstones and limestones should be expected in

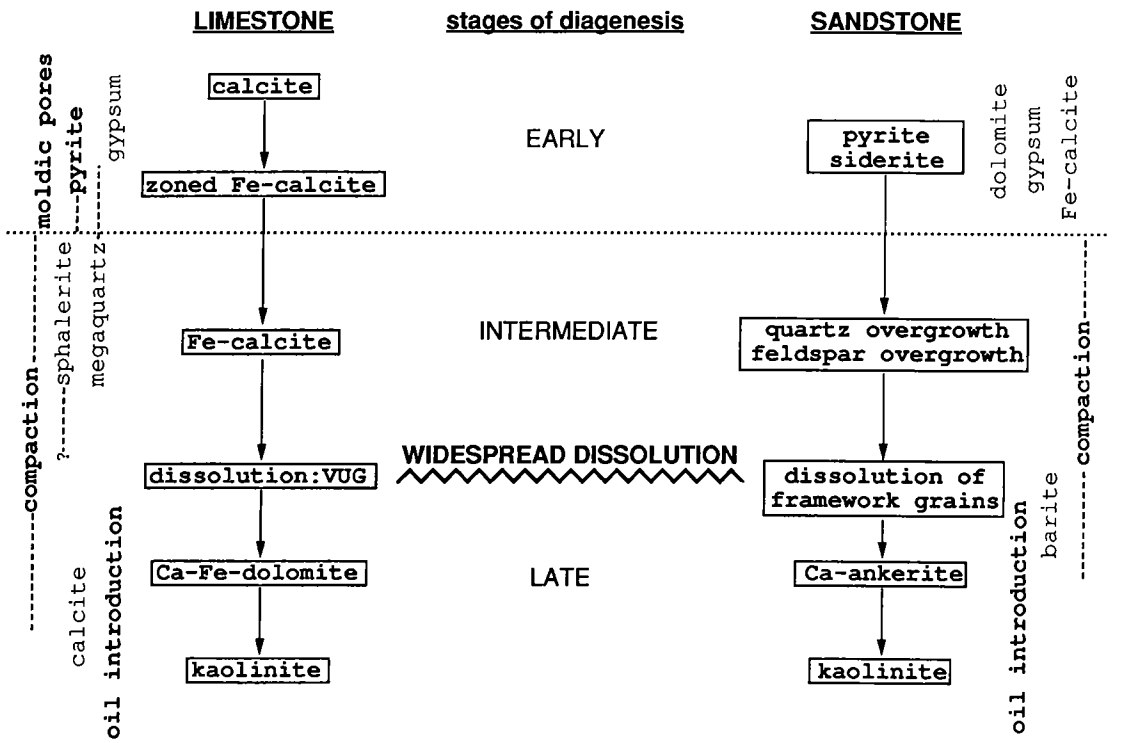

Figure 3. Summary of paragenesis observed in Pennsylvanian limestones and sandstones in southeastern Kansas. Diagenetic phases and events in boxes mark the general progression from early to late diagenesis. These phases and events may actually overlap in time to some degree.

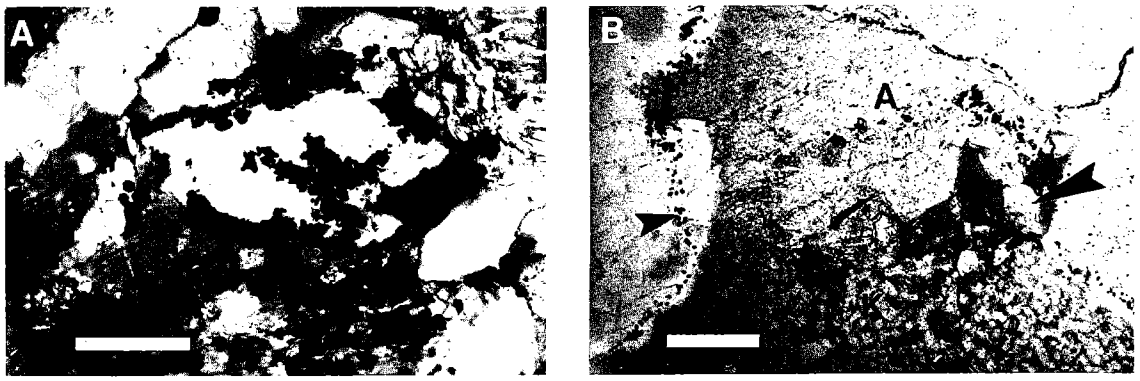

Figure 4. Thin-section photomicrographs showing paragenetic relations in sandstones: *A*—Early pyrite that outlines former margin of a framework grain which has been dissolved. The primary and secondary pores are now occluded by Ca–ankerite. Scale bar is 0.1 mm. *B*—Early siderite (small arrow) outlining detrital quartz and predating quartz overgrowth. In the center of photomicrograph, secondary pore has formed from dissolution of feldspar. Remnant of feldspar is still present (large arrow). Former margin of feldspar grain is outlined by finely crystalline siderite. Primary and secondary pores are occluded by Ca–ankerite (A) and kaolinite (K). Scale bar is 0.2 mm.

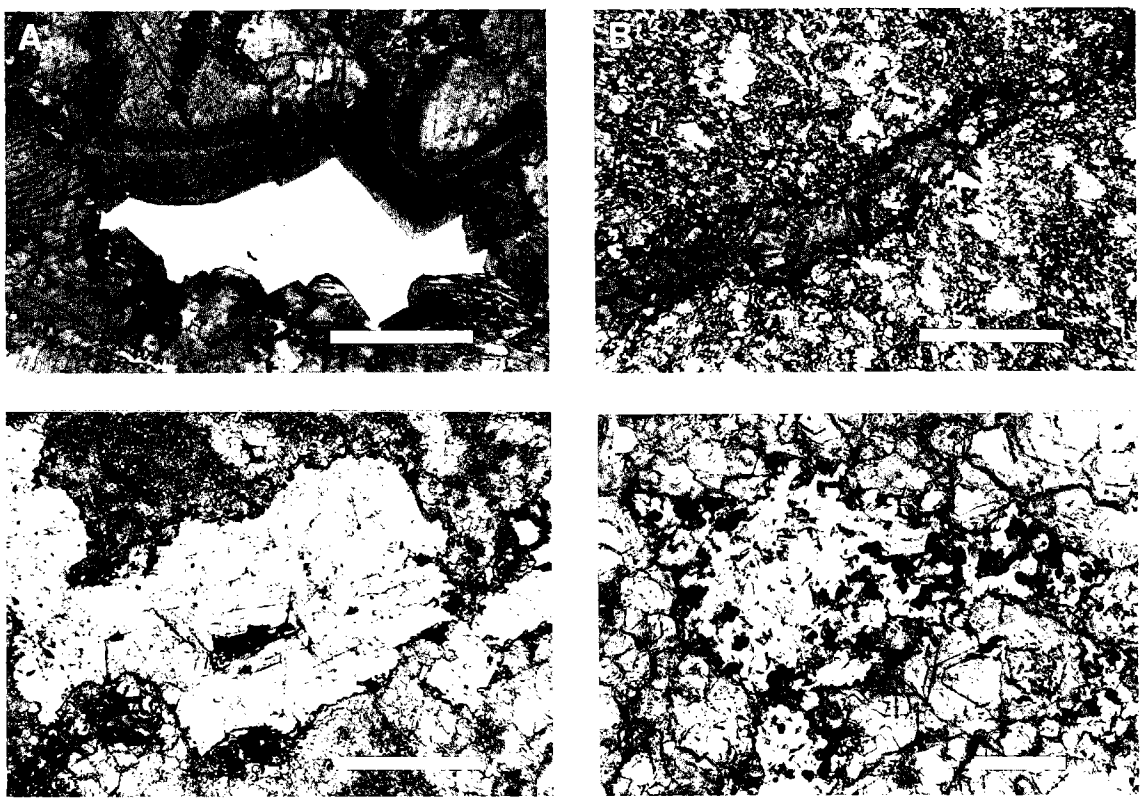

Figure 5. Thin-section photomicrograph of diagenetic minerals in limestones. All samples are stained with potassium ferricyanide and Alizarin red-S (Dickson, 1965). *A*—Early calcite shows zoning reflecting variations in iron content. Scale bar is 0.5 mm. *B*—Fracture occluded by very Fe-rich calcite. Scale bar is 0.5 mm. *C*—Vuggy pore filled by late Ca–Fe–dolomite. Scale bar is 0.5 mm. *D*—Vuggy pore truncates early zoned calcite and is occluded by late kaolinite. Scale bar is 0.2 mm.

an intimately interbedded sequence. The early diagenesis may be the consequence of repeated development of similar conditions, perhaps related to the environments of deposition or resulting from alternating subaerial exposure and drowning of the shelf, which could have affected many of these cyclothemic units (cf. Heckel, 1983). For the intermediate stage, diagenesis occurs during deeper burial with less evidence for near-surface controls. Finally, it is reasonable that the late stage of diagenesis of both sandstones and limestones represents the effects of the same regional events that postdate deposition of the entire Pennsylvanian sequence studied.

Chemical Composition

Analysis of major elements was conducted on polished thin sections using the ARL electron microprobe at the University of Missouri–Columbia. The beam current was 0.05 microamps, the spot size was 8 μm, and the accelerating potential was 15 kV. Normally, each spot was analyzed five times and each analysis was terminated when a preset integrated beam current was reached. Standards were University of Missouri #32 (calcite, for Ca), #31 (dolomite, for Mg) and #25 (siderite, for Fe and Mn) or #33 (ankerite, for Fe). Approximate detection limits (by weight) were CaO = 0.08%, MgO = 0.04%, MnO = 0.06%, and FeO = 0.14%. Data were corrected to the third approximation (Bence and Albee, 1968). Carbonate was determined by stoichiometry. Acceptable analyses ranged from 95 to 105% by weight CaO + MgO + MnO + FeO + CO_2.

Investigations of the chemical composition of the carbonate cements concentrated on late diagenetic Ca–ankerite and Ca–Fe–dolomite. Before the geochemical analyses of these minerals were done, they had been thought to be identical because of their petrographic and paragenetic similarity (cf. Fig. 3). Results are summarized in Figure 6 and in Table 1. Ca–ankerite of sandstones has a remarkably narrow compositional range. More than 90% of the analyses plot in a small area in Figure 6. The composition of the Ca–Fe–dolomite of the limestones is more variable, but this phase is generally less ferroan than the Ca–ankerites.

Analytical results on late baroque Ca–Fe–dolomite and Ca–ankerite are complicated by zoning, which becomes apparent when these materials are examined with back-scattered electron imaging (Fig. 7). The microprobe analyses fortuitously included a range of the different compositional zones. Major element composition of the Ca–Fe–dolomite in limestones is distinct from that of Ca–ankerite in sandstones despite the zoning.

Chemical differences between the baroque carbonate phases of the two lithologies is surprising considering their similar paragenetic occurrence, regional nature, and close stratigraphic association. If the two minerals precipitated as the result of a regional event, as suggested from petrography, then local rock-water interaction must have been important in controlling their composition.

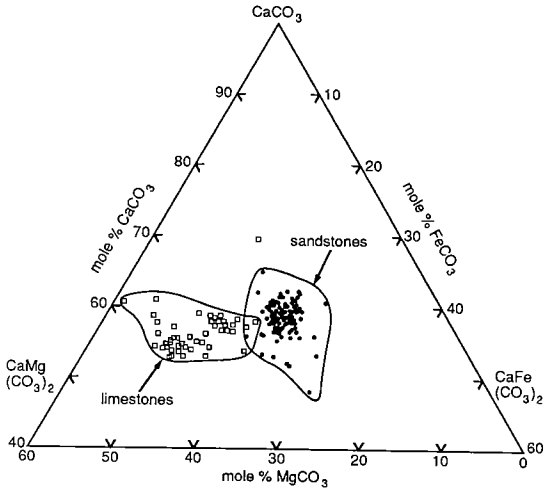

Figure 6. Major element composition of late baroque Ca–ankerite in sandstones and Ca–Fe–dolomite in limestones.

We also analyzed other carbonate cements in studied rocks. The most iron-rich phase is loosely referred to as siderite, but actually is sideroplesite because nearly all samples have >5 mole% $MgCO_3$. Sideroplesite is an early cement in sandstones (Fig. 4B). Fe–calcites have variable composition, but do not differ systematically from sandstones to limestones (Table 1).

Isotopic Composition

Small samples of limestone matrix, ferroan calcite, and Ca–Fe–dolomite were drilled out of limestones for analysis of carbon and oxygen isotopic composition. These were digested at 25°C in 100% phosphoric acid until reaction ceased. Sandstone samples containing only the carbonate phase of interest were crushed and reacted in 100% phosphoric acid at 25°C until activity ceased, and then analyzed. Splits of some samples were also reacted at 50°C.

Isotopically, the two late-stage minerals (Ca–Fe–dolomite and Ca–ankerite) are distinct (Fig. 8; Table 2). Ca–Fe–dolomite has moderately negative $\delta^{18}O$ of –5.9‰ and moderately positive $\delta^{13}C$ averaging +5.6‰. Ca–ankerite has somewhat lighter oxygen (–7.3‰), but much lighter carbon, averaging –5.2‰. In limestones, matrix $\delta^{13}C$ values are distinctly lighter than dolomite $\delta^{13}C$ from the same sample.

The isotopic results, especially the carbon isotope signatures, imply that Ca–Fe–dolomite and

TABLE 1. — AVERAGE NORMALIZED COMPOSITION OF DIAGENETIC CARBONATE PHASES FROM SANDSTONES AND LIMESTONES IN SOUTHEASTERN KANSAS[a]

Phase	n	Composition			
		$CaCO_3$	$FeCO_3$	$MgCO_3$	$MnCO_3$
Sandstone					
Sideroplesite[b]	6	6.4	77.5	14.7	1.4
range		4.4–10.0	72.9–86.3	3.9–17.6	0.3–3.8
Fe–calcite[b]	3	97.4	1.5	0.6	0.5
range		96.6–98.1	1.1–2.0	0.38–0.9	0.4–0.5
Ca–ankerite[b]	27	58.2	20.5	19.6	1.6
range		55.4–64.2	15.7–24.5	16.0–25.5	0.8–2.9
Ca–ankerite[c]	27	57.6	20.7	21.7	n.d.
range		55.3–59.9	18.5–22.3	21.4–22.8	
Ca–ankerite[d]	48	58.7	22.2	19.0	n.d.
range		48.0–63.3	19.4–30.0	15.1–22.5	
Limestone					
Fe–calcite[b]	5	98.0	0.9	0.9	0.2
range		96.8–98.9	0.3–1.8	0.6–1.0	0.1–0.5
Late, baroque Ca–Fe–dolomite[b]	13	55.0	12.1	32.5	0.5
range		52.9–58.1	7.5–18.3	23.3–37.5	0.1–1.2
Late, baroque Ca–Fe–dolomite[e]	16	54.9	12.6	32.3	0.2
range		52.8–57.9	9.8–16.0	27.5–36.0	0.1–0.5

[a]Mole % metal carbonates, averaged from microprobe analyses.

[b]Analyses reported in Bouquet (1984) and McKibben (1986), normalized to 100% $CaCO_3 + FeCO_3 + MgCO_3 + MnCO_3$.

[c]Samples from Covert Lease, Greenwood County, Kansas. Not analyzed for $MnCO_3$, analyses normalized to 100% $CaCO_3 + MgCO_3 + FeCO_3$. (A. W. Walton, unpublished data.)

[d]Brazos #O-5 Pierpoint and Colt #101A Lauber; n.d. = $MgCO_3$ not determined. Normalized to 100% $CaCO_3 + MgCO_3 + FeCO_3$. (A. W. Walton, unpublished data.)

[e]Samples from Brazos #0-11 Pierpoint and Union Gas #16 Leffingwell, normalized to 100% $CaCO_3 + FeCO_3 + MgCO_3 + MnCO_3$. (A. W. Walton, unpublished data.)

Ca–ankerite did not form in equilibrium with the same fluid. This is surprising considering their petrographic and paragenetic similarities and the fact that the host rocks are interbedded over a large area in this regional occurrence. On the other hand, it is in accord with the pronounced chemical differences between these phases.

At this time, it is difficult to attach much significance to the $\delta^{18}O$ compositions without a more thorough knowledge of fractionation factors for Ca–ankerite. The negative $\delta^{13}C$ values for ankerite suggest the importance of reactions involving organic matter which provided isotopically light carbon. The positive values for dolomite and the positive shift relative to matrix values, suggest that a source of heavy carbon other than the rock reservoir may have influenced the dolomite $\delta^{13}C$. The $\delta^{13}C$ contrast between dolomite and ankerite clearly indicates that different processes controlled the isotopic compositions of these cements.

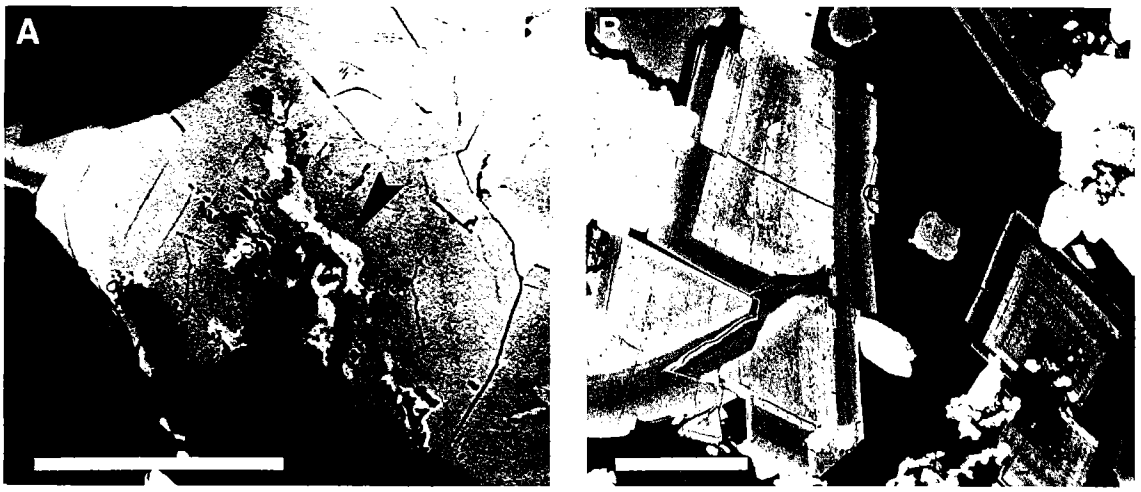

Figure 7. Back-scattered electron images of late diagenetic cements. *A*—Ca–ankerite in sandstones showing growth-zoning and possible dissolution and recementation or replacement by the late, bright cement (e.g., arrow). Scale bar is 0.1 mm. *B*—Ca–Fe–dolomite in limestones showing intricate zoning and possible dissolution surface within the dark crystal core. Scale bar is 0.1 mm.

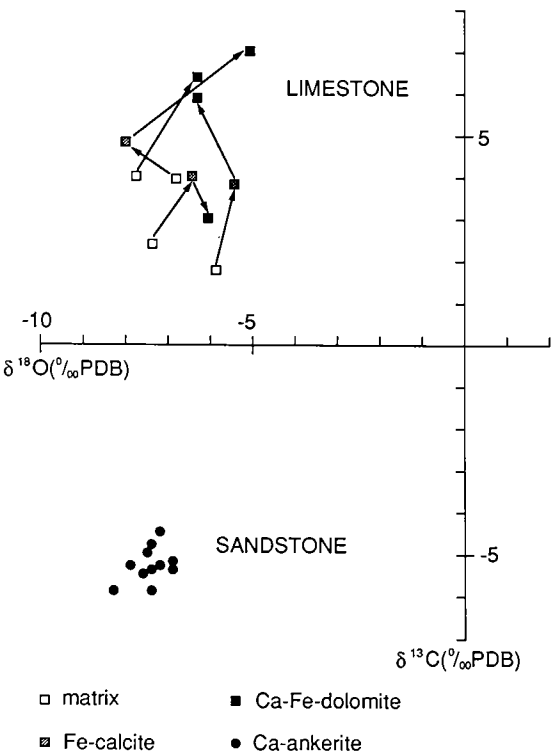

Figure 8. Isotopic composition of late Ca–ankerite in sandstones and Ca–Fe–dolomite, matrix, and Fe–calcite from limestones. Arrows show paragenetic order of components from same sample.

Fluid Inclusions

Fluid inclusions in ferroan calcite, Ca–Fe–dolomite and Ca–ankerite have been examined in several samples from Cowley, Elk, and Chautauqua Counties, Kansas (Fig. 1). Doubly polished plates, prepared from rock samples that had never been heated in the laboratory, were cold mounted on glass slides. Fluid inclusions were studied petrographically and then were heated and cooled using a gas-flow heating and freezing stage adapted from a USGS design by Fluid Inc. and mounted on a Leitz Ortholux II microscope. Homogenization temperature (Th) was measured before freezing runs. Fluid inclusions were not overheated in the lab before Th was measured. Originally one-phase, all-liquid fluid inclusions were intentionally overheated before freezing runs so that they would generate a vapor bubble. During freezing runs the first melting event (Te) and any intermediate melting events (Ti) were recorded if observable. The final melting temperature of ice (Tm ice) was recorded with a vapor bubble present to avoid metastable superheating of the ice (Roedder, 1967).

It is now well known that fluid inclusions in calcite may reequilibrate during natural overheating (Goldstein, 1986; Prezbindowski and Larese, 1987). Our samples were studied with the process of reequilibration in mind so reequilibrated populations of fluid inclusions are not treated in simple statistical terms (cf. Goldstein, 1988). In our study, fluid inclusions that showed petrographic distri-

TABLE 2. — ISOTOPIC DATA FOR Ca–Fe–DOLOMITES AND Ca–ANKERITES, SOUTHEASTERN KANSAS*

Phase	Sample	$\delta^{13}C$	$\delta^{18}O$
Ca–Ankerite			
		Sandstone	
		KB area, Bronson-Xenia Field Upper Bluejacket Interval	
	3H-736.5	–4.85±.27	–7.50±.20
	5J-738	–5.83±.14	–8.33±.09
		Strauss Field Skinner Sandstone	
	H21-201	–5.22±.09	–7.19±.05
	H1-201.3	–5.33±.06	–7.49±.11
	H8-208.6	–4.43±1.22	–7.21±.16
	H23-219.5	–4.66±.05	–7.31±.05
	F3-197	–5.87±.12	–7.40±.14
		Belvedere Field, Jackson County, MO Upper Bluejacket Interval	
	BBK	–5.3	–7.4
		Covert Lease, Greenwood County, KS Bluejacket Interval	
		Reacted at 25°C	
	C-92 094.3	–5.3	–6.9
	C-77 292.4	–5.1	–6.6
	replicate	–5.4	–7.1
	C-28 930.5	–5.1	–6.9
		Reacted at 50°C	
	C-92 094.3	–6.0	–7.2
	C-77 292.4	–6.3	–6.8
	replicate	–6.4	–7.1
	C-28 930.5	–6.9	–6.8
		Septarian Concretions	
		"V"-shale-Verdigris interval	
	S1	–2.73±.05	–7.08±.06
	S2	–4.77±.11	–6.93±.06
	U	–7.26±.09	–8.61±.10
		Lower Warner Interval (Harris, 1984)	
	H	–4.77±.11	–6.93±.06
Ca–Fe–dolomite			
		Limestone	
		Hertha Limestone	
	1189-1365	+5.93±.10	–6.24±.06
	1189-1369	+3.00±.24	–6.00±.12
		Raytown Member, Iola Limestone	
	1217-457	+7.00±.07	–4.99±.09
		Dennis Limestone	
	1221-343.5	+6.33±.16	–6.26±.07

TABLE 2. — *Continued*

Phase	Sample		$\delta^{13}C$	$\delta^{18}O$
Calcite				
		Limestone		
		Hertha Limestone		
	1189-1369	matrix	+2.3	–7.3
		sparite	+4.3	–7.9
		replicate	+3.7	–4.6
	1189-1365	matrix	+1.9	–5.9
		sparite	+3.9	–5.3
		Raytown Member, Iola Limestone		
	1217-457	matrix	+4.0	–6.8
		replicate	+3.9	–6.8
		sparite	+4.8	–8.0
		Dennis Limestone		
	1221-343.5	matrix	+4.0	–7.9

*Analyses courtesy of Lynton S. Land and Kitty Lou Milliken, University of Texas at Austin. Sample locations Table 1 and methods in McKibben, 1986.

butions associated with crystal growth were identified as primary. Because of reequilibration, primary fluid inclusions do not necessarily contain the fluid present during crystal growth.

Inclusions are common in certain zones of Ca–Fe–dolomites in limestones (Fig. 9A), but are found in usable quantities in only a few samples of Ca–ankerite (Fig. 9B). Useful inclusions are also found in some Fe–calcites in limestones, where they provide insight into conditions relatively early in diagenesis. The Te data for inclusions cluster around –50°C and suggest the brines are dominantly Na–Ca–Cl solutions (Crawford, 1981).

Fe–calcite in the Hertha Limestone contains primary aqueous fluid inclusions. These are mixtures of one-phase, all-liquid fluid inclusions and two-phase inclusions. All-liquid fluid inclusions suggest that ferroan calcite precipitated below 40–50°C and the two-phase inclusions with somewhat variable vapor-to-liquid ratios represent all-liquid inclusions reequilibrated during later heating. In such a system, the one-phase inclusions would be likely to retain the original fluid of calcite precipitation (Goldstein, 1990). The Tm ice measurements from the originally one-phase inclusions average –10.5°C and indicate cement precipitation from a brine of 14.5 wt% NaCl equivalent (Potter and others, 1978). Although these cements formed at low temperatures, they did not form from seawater or meteoric water but instead formed from a concentrated brine that had entered the rocks early in their history. Although the calcite was subjected to significantly increased temperature as diagenesis progressed, some of the lowest temperature inclusions (one-phase, all-liquid) were not reequilibrated. By analogy, this suggests that in later diagenetic minerals, inclusions with the lowest Th values in later diagenetic phases might also be unchanged by reequilibration.

The Ca–Fe–dolomite from the Hertha Limestone contains two-phase primary fluid inclusions that are confined to growth zones (Fig. 9A). These two-phase inclusions have relatively consistent vapor-to-liquid ratios and indicate that Ca–Fe–dolomite precipitated at a temperature above 40–50°C. The Th values range from ~97 to 158°C (Fig. 10). As yet no petrographic relationship has been noted to suggest an orderly progression of temperatures; attempts to identify a progression continue. The lowest Th measurements that suggest any petrographic consistency (such as position within one growth zone or within a small area of the crystal) are between ~100 and 115°C, indicating that at least some of the dolomite probably precipitated near this temperature. The Th mode at 130–135°C indicates that the rock was heated to at least this temperature. Some fields of view yield consistent populations of fluid inclusions at ~150°C and indicate the rocks were heated to at least 150°C. The Tm ice data (Fig. 11) cover a very narrow range (mean Tm ice = –18.5°C) and indicate the dolomite precipitated from a fluid of 21.5 wt% NaCl equivalent (Potter and others, 1978; see Fig. 12).

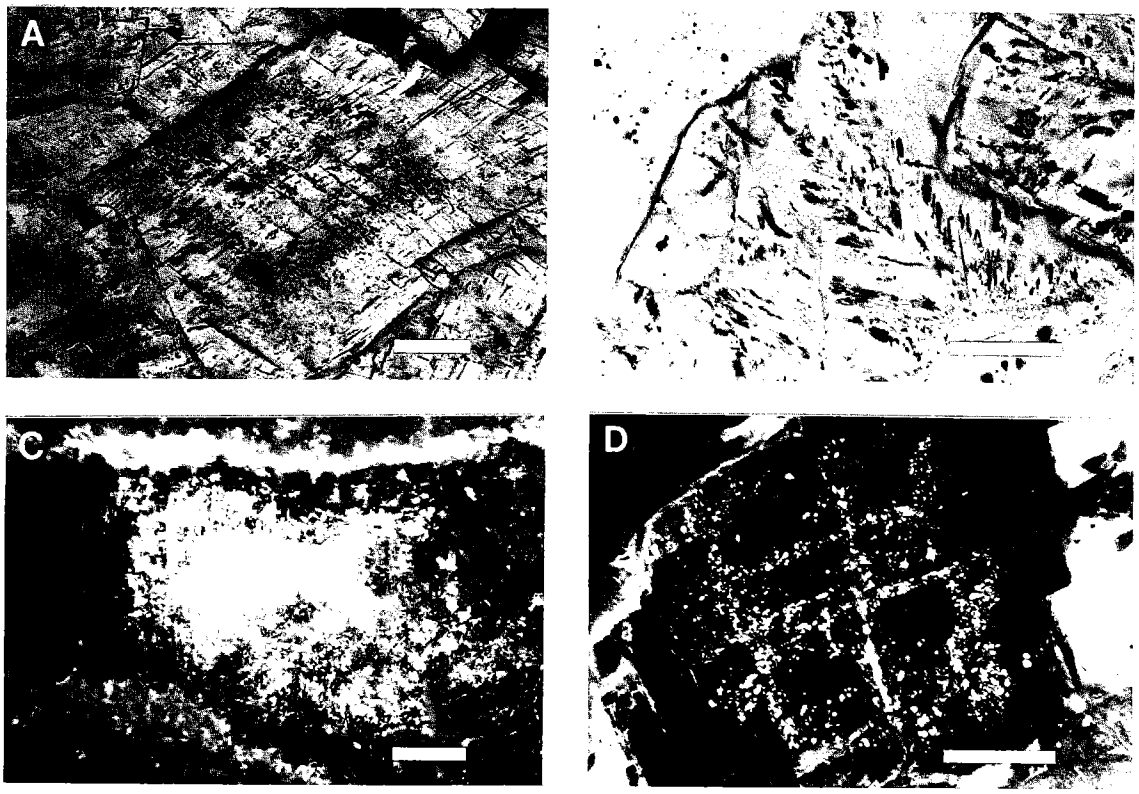

Figure 9. Thin-section photomicrographs showing fluid inclusions in late diagenetic cements. *A*—Primary aqueous fluid inclusions arranged in distinct growth zones in crystals of Ca–Fe–dolomite from the Hertha Limestone. Scale bar is 0.1 mm. *B*—Primary aqueous fluid inclusions concentrated inside a crystal of Ca–ankerite from a sandstone in the upper part of the Lansing Group (back-scattered electron image [cf. Fig. 7] suggests possible association with replacement or minor dissolution event). Scale bar is 0.1 mm. *C*—Primary oil-filled fluid inclusions outline a growth zone in Ca–Fe–dolomite from the Fort Scott Limestone. Ultraviolet epifluorescent illumination. Scale bar is 0.2 mm. *D*—Secondary oil-filled fluid inclusions in Ca–Fe–dolomite. Ultraviolet epifluorescent illumination. Scale bar is 0.1 mm

Samples of Ca–ankerite from sandstones of the Cherokee Group (probably the Bluejacket Sandstone) and from the Lansing Group also contain primary, two-phase fluid inclusions. The inclusions are abundant in internal zones of the crystal (Fig. 9B). However, the presence of several generations of cement revealed by back-scattered electron imaging (Fig. 7A) suggests that some of the inclusions may have been trapped during recrystallization or following internal dissolution and Ca–ankerite reprecipitation. In spite of this complexity, the presence of only two-phase, primary inclusions indicates precipitation of ankerite above 40–50°C.

The Th data on the inclusions in ankerite have a wide range from 78 to 162°C (Fig. 10), and no orderly petrographic progression has yet been related to compositional zoning of the cement. The lowest temperature inclusions that show some petrographic consistency suggest that at least some of the ankerite precipitated at temperatures near 100°C. The modes from various samples indicate that the rocks experienced temperatures from around 100 to 130°C and the uppermost Th data that show consistent temperatures in the same field of view indicate that the sandstones experienced temperatures in the range of about 135–140°C. The salinity data, Tm ice (Fig. 11), are highly variable, ranging from –8.1 to –23.0°C, with strong modes between –16 to –19.5°C. These data suggest only that the rocks experienced fluids ranging from 11.8 to 24.7 wt% NaCl equivalent (Potter and others, 1978; see Fig. 12).

Oil-filled fluid inclusions fluoresce brightly under UV illumination, and were found in both Ca–ankerite and Ca–Fe–dolomite from several localities. Most of these inclusions are secondary (Fig. 9D) and postdate precipitation of late baroque cements. This observation indicates the presence of oil after formation of microcracks in the late Ca–

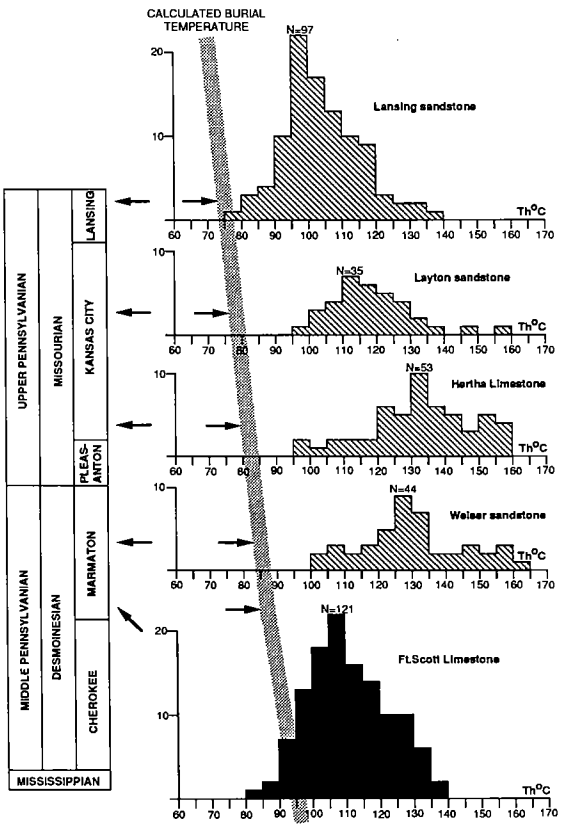

Figure 10. Frequency histograms of homogenization temperatures from aqueous (cross-hatched) and oil-filled (black) primary, two-phase fluid inclusions from late cements. Stratigraphic location of samples is shown by arrows. Broad line indicates temperatures calculated for maximum burial. Mean annual surface temperature of 25°C is assumed. Geothermal gradients are rough "high-end" estimates from present day values (Blackwell and Steele, 1989): 30°C/km for post-Wolfcampian Permian rocks, 42°C/km for Wolfcampian, Virgilian, Missourian and Upper Desmoinesian strata, and 55°C/km for the Cherokee Group. Maximum burial depth for the top of the Lansing Group is interpreted to have been 1,440 m. Note that fluid inclusions record temperatures that are consistently higher than those predicted during maximum burial.

Fe–dolomite and Ca–ankerite. However, in one sample of Ca–Fe–dolomite (Fort Scott Limestone, Elk County) oil-filled fluid inclusions are primary in origin (Fig. 9C), indicating that oil was locally present during precipitation of dolomite. The primary oil-filled fluid inclusions contain two phases in relatively consistent ratios. The Th values range from 82 to 138°C and have a single mode between 105 and 110°C (Fig. 10). Although these temperatures are lower than those obtained from aqueous fluid inclusions, they may reflect entrapment at similar temperatures because of the different PVT properties of oil and aqueous fluids.

DISCUSSION

Petrographic descriptions of paragenesis and major element composition of Ca–ankerite within all sandstones and Ca–Fe–dolomite cement in limestones are virtually identical over a very large area. The similarities extend at least from Cowley County, Kansas, to the Kansas City, Missouri, area

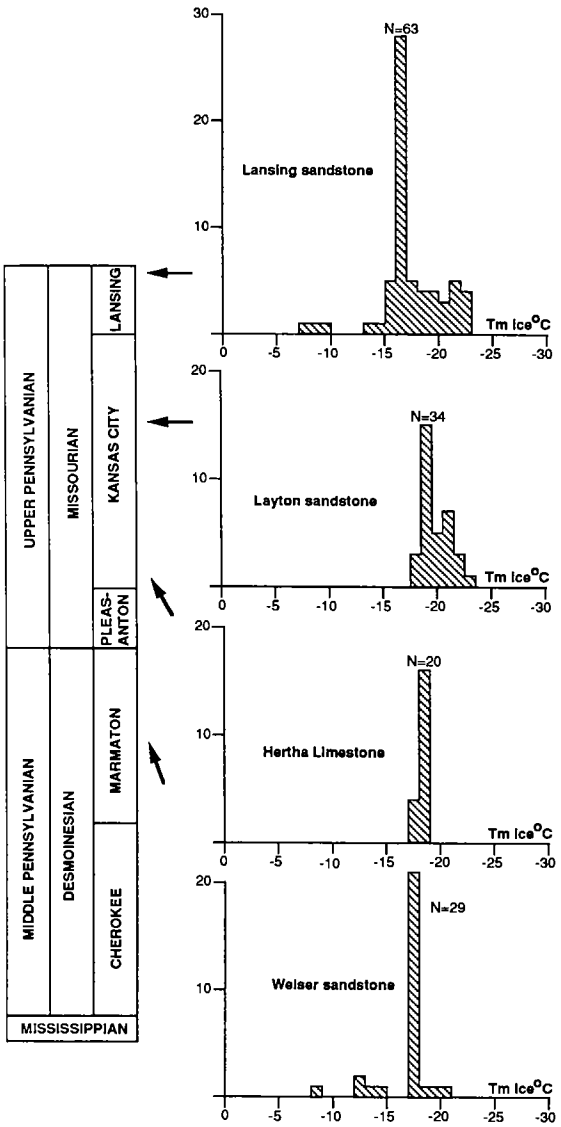

Figure 11. Frequency histograms of final melting temperature (Tm) of ice from two-phase aqueous fluid inclusions in late diagenetic cements. Stratigraphic location of samples is marked by arrows. Note similar range and salinity mode in all samples.

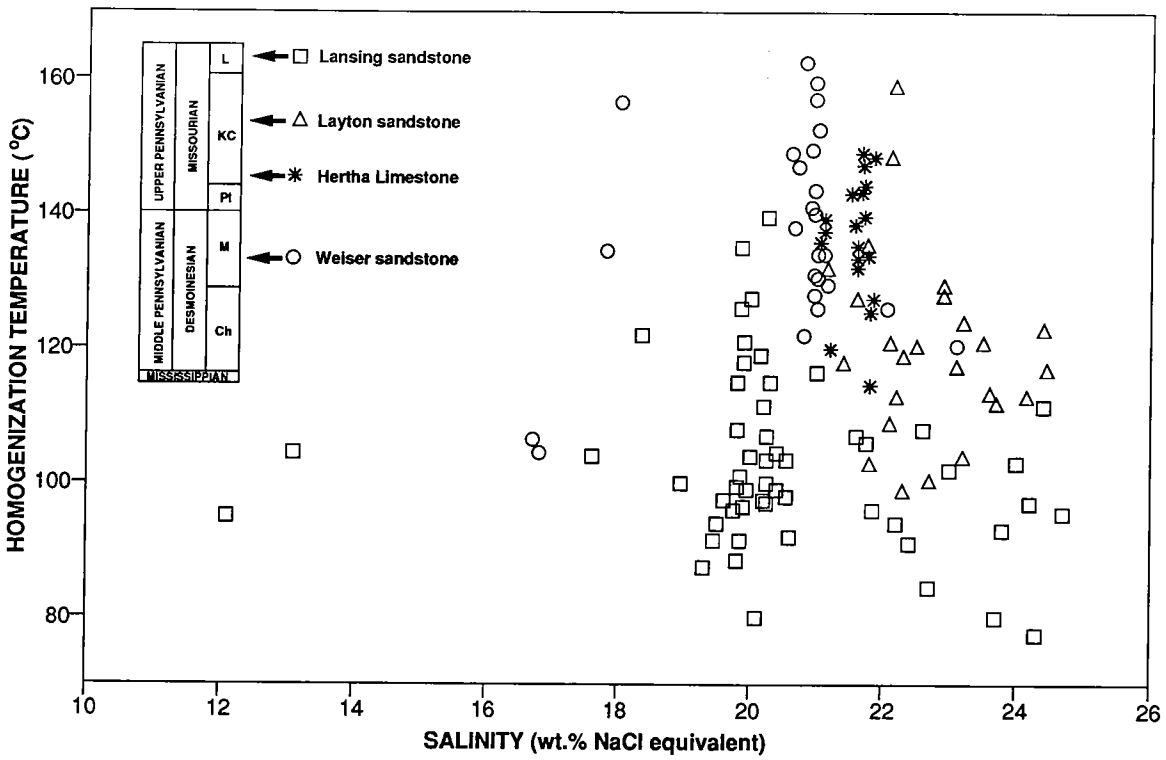

Figure 12. Plot of fluid-inclusion homogenization temperature vs. salinity from two-phase aqueous fluid inclusions in late cements.

and from Greenwood County to Labette County, Kansas, an area of at least 20,000 km^2 and vertically from the Cherokee Group to the Lansing Group, a stratigraphic interval of 400 m.

The fluid inclusion data from late-stage cements show that high temperatures (100–150°C) affected this region during, and perhaps after, precipitation of Ca–ankerite and Ca–Fe–dolomite. Most fluids present during the late stage were very saline, about 19–25 wt% NaCl equivalent (Fig. 12). Data from other studies agree with our data on paleotemperatures and salinity. For example, the Th and Tm ice measured on fluid inclusions in disseminated sphalerite occurrences in southeastern Kansas (Coveney and Goebel, 1983; Coveney and Ragan, 1987; Coveney, this volume) coincide with the higher salinity range and lower part of the temperature range of our results. Those workers used samples from Mississippian rocks as well as Middle and Upper Pennsylvanian beds. Gangue dolomite from MVT deposits in the Ozarks yield Th and Tm ice data that overlap with ours (Bauer and others, 1989), suggesting that similar fluids were important several hundreds of kilometers to the east. These results, together with ours, indicate that the fluid-temperature event and system of brine migration were regional in extent.

Hatch and others (1989) concluded that Desmoinesian shales and coals in eastern Kansas are thermally mature based on pyrolysis, gas chromatography, and gas-chromatography mass spectrometry of samples from the outcrop area and the subsurface. Vitrinite reflectance in rocks from Elk and Chautauqua Counties imply that carbonaceous black shales and coals of the Desmoinesian and Missourian are thermally mature and might be sources of oil or gas (Barker and others, this volume). The levels of maturity of organic matter in southeastern Kansas are also consistent with fluid inclusion data.

Two obvious questions result from these observations: (1) What was the origin of the heat and salt? and (2) What were the characteristics of the fluid flow regime?

Origin of High Temperatures and High Salinities

High temperatures imply either a great depth of burial or a high geothermal gradient. Barker and others (this volume) suggested that as much as ~1,100 m of Permian sediment was eroded from southeastern Kansas during the Late Permian and Mesozoic, based upon their projections of data in

Merriam (1963). In addition, 340–760 m of Pennsylvanian strata overlie or have been eroded from above the points where we took fluid inclusion samples. The thickness of later Mesozoic and Cenozoic sediment was negligible.

We calculated maximum burial paleotemperatures from estimates of maximum burial depth, the highest estimates of averaged geothermal gradients determined from modern thermal gradient data for eastern Kansas (Blackwell and Steele, 1989) and an assumed Permian surface temperature of 25°C. The maximum temperature calculated is 75°C for the top of the studied interval and 95°C for the bottom (Fig. 10). Normal burial heating does not account for the high temperatures measured from fluid inclusions (see Fig. 10). Therefore, one must propose alternative models to explain the combination of high temperatures and highly saline fluids. Sharp (1978), Cathles and Smith (1983), Garven and Freeze (1984), and Bethke (1986) proposed models whereby rapid updip migration of hot fluids from deeper parts of adjacent sedimentary basins cause heating of shallowly buried strata. With some modification, similar models could explain heating of the Pennsylvanian strata of southeastern Kansas and elevated salinities of diagenetic fluids.

The high salinity of the diagenetic brine implies that marine or fresh water originally present in these sediments has been displaced. Furthermore, a compactional system with generally upward movement of connate waters would not produce strongly saline brines. Such high salinity strongly suggests evaporites as a source of salt.

A brine reflux model might account for saline diagenetic fluids. Anderson (1989) postulated that the brine that effected diagenesis in Upper Pennsylvanian rocks of northwestern Kansas refluxed downward during deposition of Permian evaporites. This model could explain precipitation of the very iron-rich calcite of our intermediate stage, which contains low-temperature, high salinity fluid inclusions. However, it is not known that Permian evaporites ever extended into southeastern Kansas or eastern Oklahoma. And, to explain the high temperatures of the late-stage diagenesis, heating of the Pennsylvanian rocks and the previously introduced brines they contained would have to be invoked.

Saline fluids may also have originated through dissolution of Permian salt by fluids that were migrating through the strata containing salt. Permian salts have been proposed as a source of salinity in very saline fluids now present in the Arbuckle and Mississippian aquifers over most of Kansas and Oklahoma (Chaudhuri and others, 1987). However, such a process would not account for the heat during diagenesis, as downward-flowing waters should be cool, lowering the regional geothermal gradient. It would also involve a complex flow path, unless the Permian evaporites formerly extended far to the east of their current extent.

The alternative is to postulate unknown evaporites buried deep in the Arkoma basin or in the early Paleozoic continental margin and aulacogen succession of southern and eastern Oklahoma. If such evaporites existed, fluids driven from deep in the Arkoma basin could bring heat and high salinity onto the foreland shelf of Kansas. Hot brines could be injected into the Pennsylvanian strata along faults and fracture systems that tap the underlying aquifers. This model for late diagenesis and thermal history provides an explanation for both high temperatures and high salinities.

Models of Fluid Flow

Our results offer some constraints on the flow of brines in southeastern Kansas and surrounding areas. They show that connate fluids were displaced by saline brines in the rocks of the study area, and that rocks were likely heated by migration of hot fluids rather than through normal burial processes. This mode of heating requires rapid flow of large quantities of hot water through permeable rocks (Bethke and others, 1988). The rate of fluid flow through the Pennsylvanian rocks, however, must have been such that the observed local lithologic control of cement composition was possible.

Today, the Pennsylvanian strata comprise a regional confining unit and most water moves through the underlying Arbuckle and Mississippian aquifers (Jorgensen, 1989). Similarly, these aquifers could have provided effective fluid conduits and the shale-rich Pennsylvanian strata could have confined flow during the Late Paleozoic. However, during Late Paleozoic tectonic activity, brine could have entered the Pennsylvanian strata through hydrologic connections with the underlying aquifers. Possible connections could have been faults and fractures opened during minor tectonic jostling. The Pennsylvanian strata could have been heated by both conduction and by fluids transmitted into the Pennsylvanian rocks from the underlying aquifers.

CONCLUSIONS

Diagenesis in Middle and Upper Pennsylvanian sandstones and limestones of southeastern Kansas included three stages, each with several minerals common to both rock types. In both lithologies the paragenetic sequence is punctuated by a widespread dissolution event. Diagenesis progressed to a regional, late, high-temperature stage (>100°C) in which concentrated brines precipitated Ca–Fe–dolomite in limestones and Ca–ankerite in sandstones.

Many diagenetic reactions are driven by high temperatures; such temperatures can be achieved

simply by burying rocks to considerable depth. In such situations, water flow may be compactional or thermobaric (Galloway, 1984). In southeastern Kansas, temperatures during diagenesis were higher than those that could be inferred from maximum burial and appropriate geothermal gradients. Furthermore, diagenetic fluids were not connate waters modified by reaction with siliciclastics or membrane filtration. Instead, they were hot, concentrated brines that had replaced connate waters. Late diagenesis in Middle and Upper Pennsylvanian rocks of southeastern Kansas was not the result of simple burial, but the result of an active process that introduced heat and salty water to cause extensive diagenesis at depths of <2 km.

Lateral flow of water out of the Arkoma–Ouachita system can account for the observed high temperatures (Bethke and others, 1988). It was likely that hot fluids entered the Pennsylvanian section through faults and other passageways connected to the underlying aquifers. The origin of the salinity of the late diagenetic brines remains problematic, because it suggests either a complex flow associated with Permian evaporites or the presence of unknown evaporites somewhere to the south.

Key results of our investigation to date are constraints on the diagenetic processes in southeastern Kansas that may relate to other areas in similar geologic settings. The diagenetic reactions appear to have been influenced by local lithologic conditions. The high salinities observed offer constraints on fluid-flow history. The fluid-flow patterns permitted large transfer of heat into the relatively impermeable Pennsylvanian strata of the Arkoma foreland shelf.

ACKNOWLEDGMENTS

Research was partially supported by the Kansas Geological Survey, the University of Kansas General Research Fund (3815-X0-0038) and the National Science Foundation (EAR-8721229). Lou Ross of the University of Missouri assisted with electron microprobe analyses. Isotopic analyses were run by Lynton Land and Kitty Lou Milliken of the University of Texas at Austin. Charles Barker, Paul Enos, Randy Farr, and Raymond Coveney offered many helpful suggestions.

REFERENCES

Anderson, J. E., 1989, Diagenesis of the Lansing and Kansas City Groups (Upper Pennsylvanian), northwestern Kansas and southwestern Nebraska: University of Kansas unpublished M.S. thesis, 259 p.

Bauer, R. M.; Shelton, K. L.; and Gregg, J. M., 1989, Fluid inclusion studies of regionally extensive epigenetic dolomites, Bonneterre Dolomite, S.E. Missouri: evidence of multiple fluids during Pb–Zn ore mineralization [abstract]: Geological Society of America Abstracts with Programs, v. 21, p. A3.

Bence, A. E.; and Albee, A. L., 1968, Empirical correction factors for the electron microanalysis of silicates and oxides: Journal of Geology, v. 76, p. 382–403.

Bethke, C. M., 1986, Hydrologic constraints on the genesis of Upper Mississippi Valley mineral district from Illinois basin brines: Economic Geology, v. 81, p. 233–249.

Bethke, C. M.; Harrison, W. J.; Upson, C.; and Altaner, S. P., 1988, Supercomputer analysis of sedimentary basins: Science, v. 239, p. 261–267.

Blackwell, D. D.; and Steele, J. L., 1989, Heat flow and geothermal potential of Kansas: Kansas Geological Survey Bulletin 226, p. 267–291.

Bouquet, D .J., 1984, Depositional environment, diagenesis, reservoir quality, and enhanced oil-recovery potential of a reservoir in the Skinner Sandstone (Desmoinesian), Crawford, Labette, and Neosho Counties, Kansas: University of Kansas unpublished M.S. thesis, 121 p.

Brenner, R. L., 1989, Stratigraphy, petrology, and paleogeography of the upper portion of the Cherokee Group (Middle Pennsylvanian), eastern Kansas and northeastern Oklahoma: Kansas Geological Survey Geology Series, v. 3, 70 p.

Cathles, L. M.; and Smith, A. T., 1983, Thermal constrains on the formation of Mississippi Valley-type lead–zinc deposits and their implications for episodic basin dewatering and deposit genesis: Economic Geology, v. 78, p. 983–1002.

Chaudhuri, S.; Broedel, V.; and Clauer, N., 1987, Strontium isotopic evolution of oilfield waters from carbonate reservoir rocks in Bindley field, central Kansas, U.S.A.: Geochimica et Cosmochimica Acta, v. 51, p. 45–53.

Coveney, R. M., Jr.; and Goebel, E. D., 1983, New fluid-inclusion homogenization temperatures for sphalerite from minor occurrences in the Mid-continent area, *in* Kisvarsanyi, G.; Grant, S. K.; Pratt, W. P.; and Koenig, J. W. (eds.), Proceedings of the international conference on Mississippi Valley-type lead–zinc deposits: University of Missouri–Rolla Press, p. 234–242.

Coveney, R. M., Jr.; and Ragan, V. M., 1987, Pressures and temperatures from aqueous fluid inclusions in sphalerite from Midcontinent country rocks: Economic Geology, v. 82, p. 740–751.

Crawford, M. L., 1981, Phase equilibria in aqueous fluid inclusions, *in* Hollister, L. S.; and Crawford, M. L. (eds.), Fluid inclusions: applications to petrology: Mineralogical Association of Canada Short Course Handbook, v. 6, p. 75–100.

Dickson, J. A. D., 1965, A modified staining technique for carbonates in thin section: Nature, v. 205, p. 587.

Ebanks, W. J., Jr.; Brady, L. L.; Heckel, P. H.; O'Connor, H. G.; Sanderson, G. A.; West, R. R.; and Wilson, F. W., 1979, The Mississippian and Pennsylvanian (Carboniferous) Systems in the United States—Kansas: U.S. Geological Survey Professional Paper 1110-Q, 30 p.

Farr, M. R., 1989, Compositional zoning characteristics of late dolomite cement in the Cambrian Bonneterre Formation, Missouri: implications for parent fluid migration pathways: Carbonates and Evapo-

rites, v. 4, p. 177–194.
Galloway, W. E., 1984, Hydrogeologic regimes of sandstone diagenesis: American Association of Petroleum Geologists Memoir 37, p. 3–13.
Garven, G.; and Freeze, R. A., 1984, Theoretical analysis of the role of groundwater flow in the genesis of stratabound ore deposits. 1.—Mathematical and numerical model. 2.—Quantitative results: American Journal of Science, v. 284, p. 1085–1174.
Goldstein, R. H., 1986, Reequilibration of fluid inclusions in low-temperature calcium-carbonate cement: Geology, v. 14, p. 792–795.
_____1988, Cement stratigraphy of Pennsylvanian Holder Formation, Sacramento Mountains, New Mexico: American Association of Petroleum Geologists Bulletin, v. 72, p. 425–438.
_____1990, Petrographic and geochemical evidence for origin of paleospeleothems from pre-Pennsylvanian paleokarst, New Mexico: implications for the application of fluid inclusions to studies of diagenesis: Journal of Sedimentary Petrology, v. 60, p. 282–292.
Gregg, J. M., 1985, Regional epigenetic mineralization in the Bonneterre Dolomite (Cambrian), southeastern Missouri: Geology, v. 13, p. 503–506.
Gregg, J. M.; and Hagni, R. D., 1987, Irregular cathodoluminescent banding in late dolomite cements: evidence for complex faceting and metalliferous brines: Geological Society of America Bulletin, v. 98, p. 86–91.
Harris, J. W., 1984, Stratigraphy and depositional environments of the Krebs Formation—lower Cherokee Group (Middle Pennsylvanian) in southeastern Kansas: University of Kansas unpublished M.S. thesis, 139 p.
Hatch, J. R.; King, J. D.; and Daws, T. A., 1989, Geochemistry of Cherokee Group oils of southeastern Kansas and northeastern Oklahoma: Kansas Geological Survey Subsurface Geology Series 11, 20 p.
Heckel, P. H., 1977, Origin of phosphatic black shale facies in Pennsylvanian cyclothems of Mid-continent North America: American Association of Petroleum Geologists Bulletin, v. 61, p. 1045–1068.
_____1983, Diagenetic model for carbonate rocks in Midcontinent Pennsylvanian eustatic cyclothems: Journal of Sedimentary Petrology, v. 53, p. 733–759.
Jorgensen, D. G., 1989, Paleohydrology of the Anadarko basin, central United States, *in* Johnson, K. S. (ed.), Anadarko basin symposium, 1988: Oklahoma Geological Survey Circular 90, p. 176–193.
Leach, D. L., 1979, Temperature and salinity of the fluids responsible for minor occurrences of sphalerite in the Ozark Region of Missouri: Economic Geology, v. 74, p. 931–937.
Leach, D. L.; and Rowan, E. L., 1986, Genetic link between Ouachita foldbelt tectonism and the Mississippi Valley-type lead–zinc deposits of the Ozarks: Geology, v. 14, p. 931–935.
Leach, D. L.; Viets, J. G.; and Rowan, E. L., 1984, Appalachian–Ouachita orogeny and Mississippi Valley-type lead–zinc deposits [abstract]: Geological Society of America Abstracts with Programs, v. 16, p. 572.
McKibben, M. E., 1986, Ferroan carbonate cements in limestones and sandstones of southeastern Kansas: late diagenetic processes and conditions: University of Kansas unpublished M.S. thesis, 76 p.
Merriam, D. F., 1963, The geologic history of Kansas: Kansas Geological Survey Bulletin 162, 317 p.
Murphy, T. D., 1978, Strandplain and deltaic deposits and related coals of the Middle Cherokee Subgroup of southeastern Kansas and western Missouri: University of Texas–Austin unpublished M.S. thesis, 126 p.
Oliver, J., 1986, Fluids expelled from orogenic belts: their role in hydrocarbon migration and other geological phenomena: Geology, v. 14, p. 99–102.
Potter, R. W., II; Clynne, M. A.; and Brown, D. L., 1978, Freezing point depression of aqueous sodium chloride solutions: Economic Geology, v. 73, p. 284–285.
Prezbindowski, D. R.; and Larese, R. E., 1987, Experimental stretching of fluid inclusions in calcite—implications for diagenetic studies: Geology, v. 15, p. 333–336.
Roedder, E., 1967, Metastable superheated ice in liquid-water inclusions under high negative pressure: Science, v. 155, p. 1413–1417.
Sharp, J. M., Jr., 1978, Energy and momentum transport model of the Ouachita basin and its possible impact on the formation of economic mineral deposits: Economic Geology, v. 73, p. 1057–1068.
Shelton, K. L.; Reader, J. M.; Ross, L. M.; Viele, G. W.; and Seidemann, D. E., 1986, Ba-rich adularia from the Ouachita Mountains, Arkansas: implications for a post collisional hydrothermal system: American Mineralogist, v. 71, p. 916–923.
Woody, M. D., 1983a, Sedimentology, diagenesis, and petrophysics of selected Cherokee Group (Desmoinesian) sandstones in southeastern Kansas—Part 1: Shale Shaker, v. 33, p. 91–104.
_____1983b, Sedimentology, diagenesis, and petrophysics of selected Cherokee Group (Desmoinesian) sandstones in southeastern Kansas—Part 2: Shale Shaker, v. 33, p. 107–122.

Evolution of Formation Waters in Early Pennsylvanian Morrowan Sandstones in the Hugoton Embayment of the Anadarko Basin, Southern Midcontinent, U.S.A.

S. Chaudhuri and R. Robinson
Kansas State University

N. Clauer
Centre de Geochimie de la Surface, Strasbourg, France

L. M. Jones
Kansas State University

ABSTRACT.—Formation waters in the Early Pennsylvanian Morrowan rocks in the Hugoton embayment of southwestern Kansas, southeastern Colorado, and northwestern Oklahoma are of chloride-calcium type. Isotopic and chemical compositional changes appear to trend roughly along a northwest–southeast direction; the waters in the far northwest part of the basin have the lowest salinity, the highest ^{87}Sr content, and the lowest D and ^{18}O contents. The salinities of the waters range from ~75,000 mg/l to >243,000 mg/l. The δD values relative to SMOW range from about –7 to –62‰, whereas the $\delta^{18}O$ values are between –6.3 and +3.4‰. The $^{87}Sr/^{86}Sr$ of the waters ranges from 0.70906 to 0.71965. The compositional changes may be related to mixing of two waters, one of which is continental meteoric water. This meteoric water appears to have originated from an area of highly elevated landmass along the west margin of the Hugoton embayment. The recharge of the aquifers most likely occurred much earlier than Recent or Pleistocene time. The trends of isotopic and chemical changes of the formation waters correspond to the trends of isotopic changes of carbonate cements in the Morrowan sandstones. The chemical and isotopic compositions of formation waters in the Morrowan sandstones have a strong overprint of past hydrodynamic conditions in the basin. Evidence for cross-formation flow of water between the early Morrowan sandstones and the overlying Middle Pennsylvanian Cherokee or the underlying Mississippian aquifers is nearly absent in the Hugoton embayment. The isotopic data suggest that subnormal fluid pressures in the Morrowan sandstones could have developed due to dilation of pore volumes in the rocks and decrease in volume of the fluids from decreased temperature attendant with erosional removal of the overburden.

INTRODUCTION

The northern shelf provinces of the Anadarko basin in the southern Midcontinent of the U.S.A. have been explored for hydrocarbon production for more than half a century (Rascoe and Adler, 1983). Despite the long production activities in these areas, migration and accumulation history of the hydrocarbons and development of reservoir properties remain virtually unknown. The issues are complex, and the final solutions to these problems await integration of evidence which emerges from different lines of inquiry.

Geochemical investigations of oil-field waters can be useful in obtaining significant clues to hydrologic characteristics of a sedimentary basin. Although hydrocarbons can be transported as a separate phase, there is no doubt that at least part of the hydrocarbon migration entails solution in water. Hence studies of oil-field waters can provide potentially very useful information on the migration history of hydrocarbons. Knowledge of accumulations of hydrocarbons requires an understanding of the development of fluid potentials in the aquifers, and geochemical investigation of oil-field waters may shed important light on the development of fluid pressures in reservoir rocks with hydrocarbon accumulations. A critical assumption in the reconstruction of hydrocarbon migration and accumulation histories from investigations of oil-field waters is that the flow paths of hydrocarbons in the past were much the same as the flow paths of present-day formation waters. Information on paleohydrology of a basin is therefore important for full understanding of geochemical data on present-day formation waters in relation to associated hydrocarbon migration and accumulation.

This paper focuses on chemical and isotopic characteristics of formation waters in the Early Pennsylvanian Morrowan unit and of associated sandstone reservoirs in the Hugoton embayment of the Anadarko basin in eastern Colorado, southwestern Kansas, and northwestern Oklahoma. Figure 1 indicates the locations of wells used for this study. These wells were drilled into the Morrowan sandstones, which occur in lenticular bodies deposited in a wide range of environments, from continental alluvial through deltaic to marine (Busch, 1974; Swanson, 1979). The fluid pressures are subnormal in the Morrowan sandstones in the Hugoton embayment (Dickey and Cox, 1977). The geochemical data have been used to analyze hydraulic relations among different Morrowan aquifers, to depict paleohydrologic characteristics in the Hugoton embayment, and to assess the cause of development of subnormal fluid pressures in the Morrowan unit.

STRATIGRAPHIC AND STRUCTURAL FRAMEWORKS

During early and middle Phanerozoic time, northern and western Oklahoma, Texas–Oklahoma Panhandle, western and southern Kansas, and southeast Colorado constituted a broad shelf-like epicontinental basin, commonly referred to as the Oklahoma basin, in which thick extensive marine carbonate beds interbedded with thin essentially marine shales and sandstones were deposited. The southern Oklahoma aulacogen, which developed on the Precambrian craton in Early and Middle Cambrian time, was a W–NW trending graben in which >6,100 m of graywacke, chert, spillite, and rhyolite were deposited and later intruded by gabbro and granite (Johnson and others, 1989). With subsequent cooling and attendant increase in density of the lithosphere, it remained a negative tectonic feature in which sediments were deposited during much of the Paleozoic. The shelf sedimentation in much of the Oklahoma basin during early and middle Paleozoic time was interrupted by a series of orogenic movements beginning with development of the Cambridge arch and Central Kansas uplift (major transverse components of the NE-trending Transcontinental arch), the Nemaha ridge, and the Salina basin during Late Mississippian and Early Pennsylvanian time. Broad epeirogenic movements near the end of the Mississippian produced a widespread pre-Pennsylvanian unconformity. Toward the end of Early Pennsylvanian time, deformation of the southern Oklahoma aulacogen associated with the collision between the North

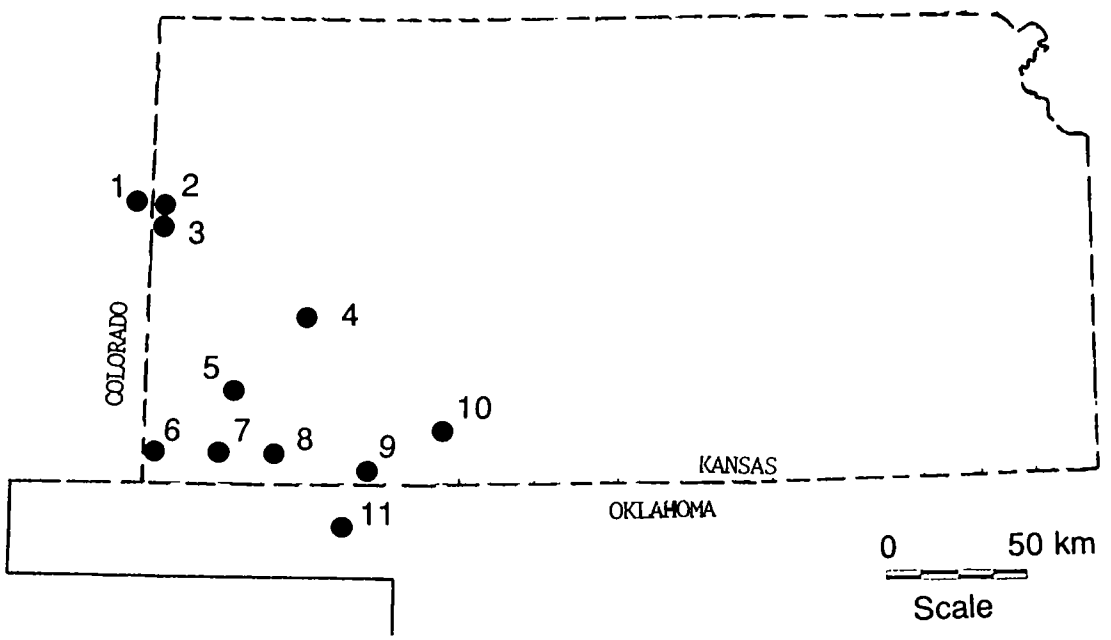

Figure 1. Locations of wells used in this study. 1—Arapahoe field, Cheyenne County, Colorado; 2—Arapahoekan field, Wallace County, Kansas; 3—Stockholm field, Greeley County, Kansas; 4—Stewart field, Finney County, Kansas; 5—Railroad Bend Spikes field, Grant County, Kansas; 6—Winter North field, Morton County, Kansas; 7—North Shuck field, Stevens County, Kansas; 8—Shuck Nix D1 field, Seward County, Kansas; 9—O'Brien Barly Fincham field, Meade County, Kansas; 10—Lexington field, Clark County, Kansas; 11—Mocane field, Beaver County, Oklahoma.

American and the South American plates created the Amarillo–Wichita uplift and the Anadarko and Ardmore basins. The collisional movement also produced some prominent positive and negative tectonic features around the Anadarko basin, such as the Apishapa uplift and Las Animas arch in southeastern Colorado, the Cimarron uplift across the Texas–Oklahoma Panhandle, the Ouachita Mountains and Arkoma basin in Oklahoma, and the Dalhart basin in Texas. A Late Pennsylvanian orogeny produced the Arbuckle Mountains and was responsible for some degree of rejuvenation of the older tectonic features (Adler and others, 1971). Major structural elements surrounding the Anadarko basin during the late Paleozoic are presented in Figure 2.

The Hugoton embayment, which is the northern shelf of the Anadarko basin, occupies much of southwestern Kansas, part of southeastern Colorado, and parts of the Texas–Oklahoma Panhandles and northwestern Oklahoma. It is separated from the Denver basin to the northwest by the Las Animas arch and from the Salina basin to the east by the Cambridge arch and Central Kansas uplift, and from the Dalhart basin to the southwest by the Cimarron arch. The late Paleozoic stratigraphic units in the Hugoton embayment area are indicated in Figure 3. The Early Pennsylvanian Morrowan unit unconformably overlies the Mississippian rocks and underlies the Atokan or the Middle Pennsylvanian Cherokee rocks. The Mississippian System consists essen-

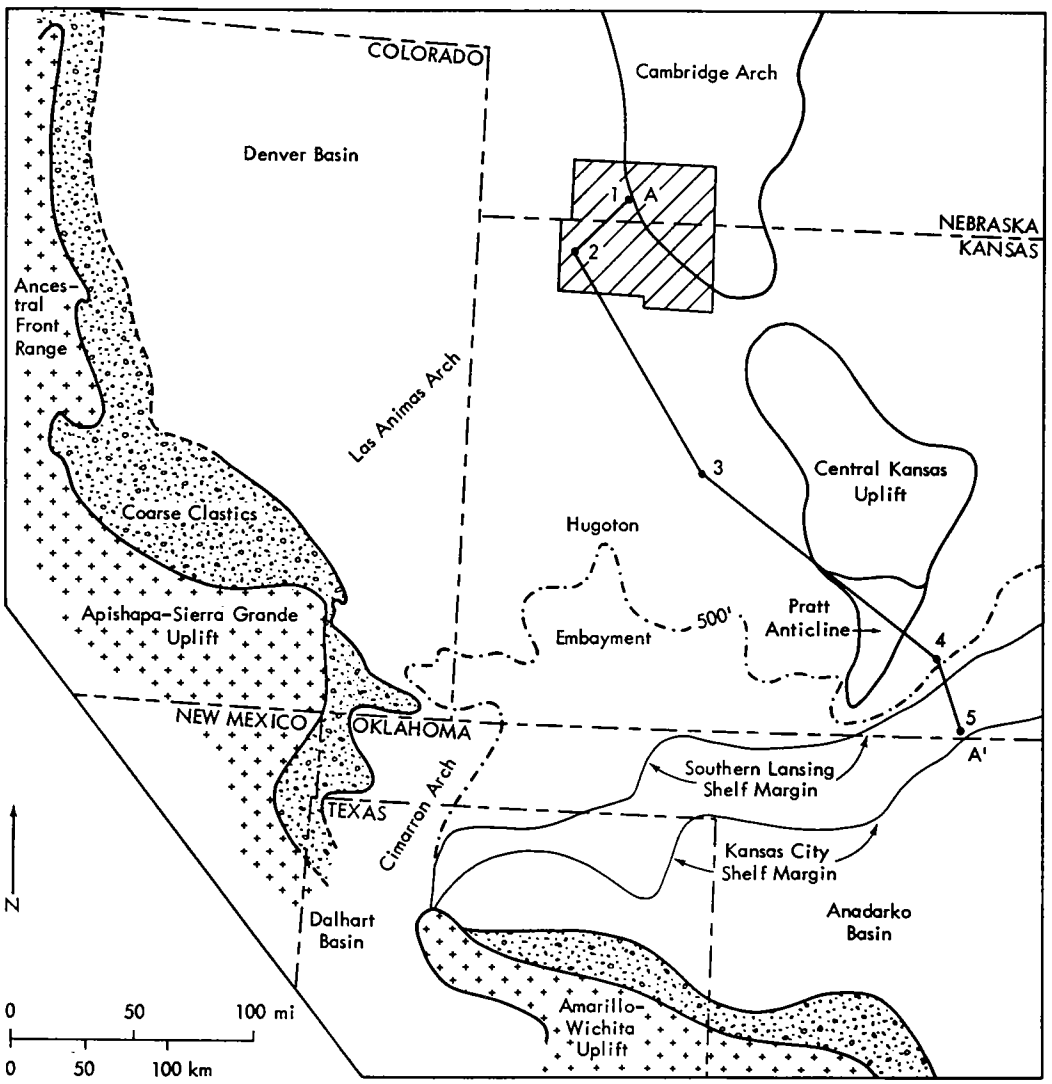

Figure 2. Structural elements surrounding the Anadarko basin and the Hugoton embayment during late Paleozoic time (after Watney, 1980).

tially of marine limestone with interbedded thin shales and sandstones. The top of the Mississippian System is marked by a pre-Pennsylvanian unconformity throughout the Hugoton embayment, but in the deeper parts of the Anadarko basin the sedimentation was continuous from Late Mississippian into Early Pennsylvanian time (Johnson and others, 1989). A major regression of the sea from the shelf area of the Anadarko basin produced a widespread erosional surface during Late Mississippian time. In Early Pennsylvanian Morrowan time, the sea transgressed northward over the erosional surface. The Morrowan transgression was interrupted by brief periods of minor regression during which clean, well-sorted sands accumulated in elongated bodies near shorelines in the Hugoton embayment and poorly sorted argillaceous sediments accumulated in the marine environment away from the shorelines. Farther offshore the argillaceous beds graded to marine muds and calcareous sands. In the southern part of the Hugoton embayment, marine depositional environments prevailed during Morrowan time; farther north in southwestern Kansas and southeastern Colorado alluvial and deltaic environments prevailed (McManus, 1959).

SYSTEM	SERIES	STAGE	GROUP
PENNSYLVANIAN	U. Pennsylvanian	Virgilian	Wabaunsee
			Shawnee
			Douglas
		Missourian	Lansing
			Kansas City
			Pleasanton
	M. Pennsylvanian	Desmoinesian	Marmaton
			Cherokee
		Atokan	
	L. Pennsylvanian	Morrowan	
MISSISSIPPIAN	U. Mississippian	Chesterian	
		Meramecian	
	L. Mississippian	Osagian	
		Kinderhookian	

Figure 3. Late Paleozoic stratigraphic column in the Hugoton embayment area.

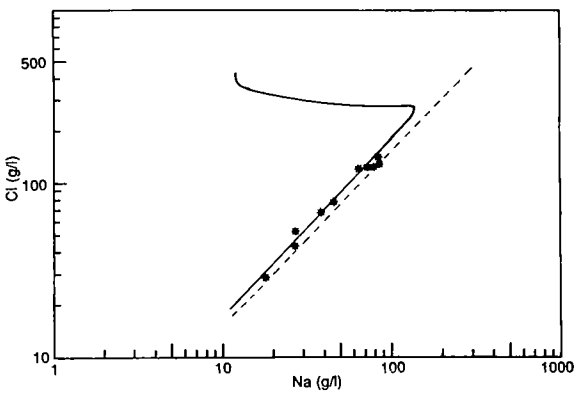

Figure 4. Na and Cl contents of formation waters in Morrowan sandstone relative to the contents of the same elements in evaporated seawaters (solid curve) and in solutions of halite (dashed line).

RESULTS

Chemical data of formation waters in Morrowan sandstones are presented in Table 1. The salinities of the waters range from ~52,000 mg/l to ~244,500 mg/l. Like many other formation waters, Na and Cl contents primarily determine the salinities of these waters. The molar Na/Cl of the waters in the Morrowan sandstones range from as low as 0.78 to slightly less than 1. On a graph of the Na versus Cl content, formation waters lie close to the compositional path for evaporated seawater (Fig. 4). Like nearly all formation waters, the oil-field waters in the Morrowan sandstones are enriched in Ca and Sr and depleted in Mg and K relative to evaporated seawater when the two types of water are compared at the same concentration of Cl. Figures 5 and 6 are illustrations of depletions and enrichments of some of the chemical constituents of Morrowan formation waters relative to evaporated seawaters. The chemical compositions of the formation waters can be related to combined effects of several different processes such as evaporation, mineral-water interactions, oxidation-reduction, and mixing of waters of different origin, but no attempt has been made in this study to provide a chemical evolutionary model which would explain all chemical characteristics of the waters.

Spatial variations in the chemical compositions of the waters are clearly evident. The Cl contents, reflecting the measure of total dissolved solids, appear to increase southeastward (Fig. 7). This trend in the salinity variation roughly corresponds to the trend of increasing thickness of the Morrowan unit as illustrated by Adler and others (1971). At the southeastern end of the study area, the salinity variation is minimal. This area of similar Cl contents occurs in the area of a potentiometric low in the potentiometric map constructed by Larson (1971) for waters in the Pennsylvanian rocks (Fig. 8).

The waters in the Morrowan sandstones in the Hugoton embayment are found to be of chloride-calcium type. Dickey and Soto (1974) reported a large collection of chemical data on waters in the Morrowan sandstones in the Texas–Oklahoma Panhandle region, southwestern Kansas near the Oklahoma/Kansas border, and northwestern Oklahoma immediately southeast of the Panhandle. They also observed that in much of the area, with the exception of the area to the southeast of the Panhandle, the waters are predominantly of

TABLE 1. — CHEMICAL ANALYSES OF FORMATION WATERS IN MORROWAN SANDSTONES IN THE HUGOTON EMBAYMENT
(Concentration given in mg/l)

Sample	Location	Cl	SO_4	Na	K	Mg	Ca	Sr
1	Cheyenne County, CO	29,220	2,277	18,500	170	230	1,475	19
2	Wallace County, KS	42,310	1,944	27,000	224	350	2,525	32
3	Greeley County, KS	50,620	1,175	26,500	215	420	3,300	37
4	Finney County, KS	69,700	868	39,060	460	1,650	6,750	220
5	Grant County, KS	85,080	—	43,000	105	—	9,540	1,000
6	Morton County, KS	88,940	700	45,350	180	1,150	13,100	815
7	Stevens County, KS	149,500	—	75,620	215	—	18,000	1,120
8a	Seward County, KS	140,000	149	82,500	140	2,200	15,250	1,410
8b	Seward County, KS	128,000	332	80,000	258	2,150	14,750	822
10a	Clark County, KS	125,310	—	65,800	630	2,520	8,550	710
10b	Clark County, KS	127,970	—	69,600	464	2,490	9,300	1,000
11	Beaver County, OK	132,000	169	70,880	475	2,025	13,050	1,000

chloride-calcium type with salinities ranging from about 100,000 to 200,000 mg/l. The Morrowan sandstone waters in the area to the southeast of the Panhandle are generally of bicarbonate-sodium type with average total dissolved solids of ~20,000 mg/l. The genetic relationship between these two types of water in the Morrowan unit has yet to be worked out.

Oxygen-hydrogen isotopic analyses of the waters in the Morrowan sandstones in southwestern Kansas (Table 2) indicate that the isotopic compositions are linearly related (Fig. 9). This linear relationship apparently represents a mixture in different proportions of a low-salinity continental meteoric water and a high-salinity, complexly evolved water. Although the isotopic composition of the highly evolved component could not be clearly identified, the isotopic composition of the meteoric water component appears to be limited to a δD value of about −102‰ and a $\delta^{18}O$ value of about −14‰, as determined by the intercept of the formation water line on the global meteoric water line (Fig. 9). The isotopic compositions of the formation waters vary approximately linearly with the salinity of the waters, the enrichment of D (Fig. 10) or ^{18}O contents occurring with increasing salinity.

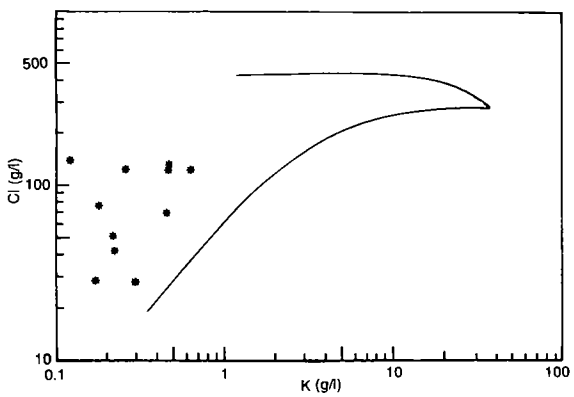

Figure 5. K and Cl contents of formation waters in Morrowan sandstones relative to the contents of the same elements in evaporated seawaters (solid curve).

Oxygen and carbon isotopic compositions were determined for ankeritic carbonate cements in samples of cores of Morrowan sandstones from two separate localities. One of the cores was taken from the Lexington oil field in Clark County, Kansas, just a few miles north of the Oklahoma/Kansas border (location 10, Fig. 1). The average salinity of formation waters in the Morrowan sandstones from this locality is >125,000 mg/l. The second core was from the vicinity of the Arapahoe oil field in Cheyenne County, Colorado (location 1, Fig. 1), where the formation waters are characterized by a relatively low salinity of ~52,000 mg/l. The oxygen and carbon isotopic compositions of carbonate cements of the sandstones at each locality are presented in Table 3. At each locality the isotopic values vary within narrow limits; however, the isotopic compositions of carbonate cements from the two localities are distinctly different. The cements in the Morrowan sandstones in Clark County, Kansas, have $\delta^{18}O$ values relative to SMOW between +25.1 and +28.4‰ and $\delta^{13}C$ val-

TABLE 2. — STRONTIUM, HYDROGEN, AND OXYGEN ISOTOPIC COMPOSITIONS OF FORMATION WATERS IN MORROWAN SANDSTONES IN THE HUGOTON EMBAYMENT
(Oxygen and hydrogen values expressed relative to SMOW)

Sample	Location	$^{87}Sr/^{86}Sr$ ($\pm 2\sigma$)	$\delta^{18}O$	δD
1	Cheyenne County, CO	0.718340 ±8	–6.3	–62
2	Wallace County, KS	0.719650 ±8	–4.4	–52
3	Greeley County, KS	0.719496 ±9	–4.3	–50
4	Finney County, KS	0.709941 ±9	–0.5	–34
5	Grant County, KS	0.710425 ±8	–1.8	–25
6	Morton County, KS	0.711950 ±9	–1.3	–29
7	Stevens County, KS	0.710599 ±8	—	—
8a	Seward County, KS	0.709680 ±9	+3.4	–7
8b	Seward County, KS	0.709631 ±9	—	—
9	Meade County, KS	0.709058 ±8	—	—
10a	Clark County, KS	0.710100 ±9	+3.2	–13
10b	Clark County, KS	0.709900 ±9	+3.2	–14
11	Beaver County, OK	0.709070 ±8	+3.2	–11

ues relative to PDB between –2.1 and +2.8. In Cheyenne County, Colorado, the carbonate cements have $\delta^{18}O$ values ranging from +20.6 to +23.8‰ and $\delta^{13}C$ values between –1.9 and –3.3‰. Figure 11 illustrates the contrast in the isotopic compositions of carbonate cements in Morrowan sandstones between these two localities, suggesting that composition of the fluids at the time of diagenetic deposition of the cements were as widely different between these two localities as the compositions of the present-day formation waters from the same two localities.

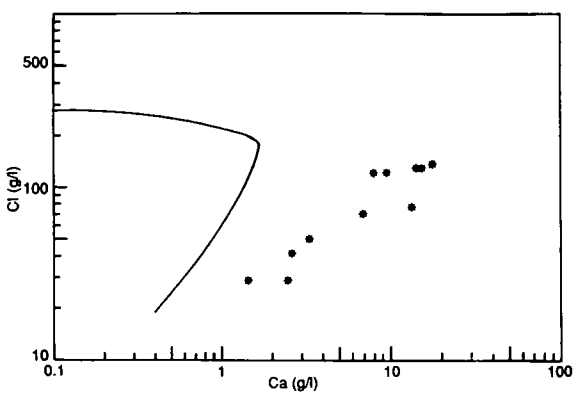

Figure 6. Ca and Cl contents of formation waters in Morrowan sandstones relative to the contents of the same elements in evaporated seawaters (solid curve).

The $^{87}Sr/^{86}Sr$ of the formation waters are between 0.70906 and 0.71965 (Table 2) with Sr contents ranging from 19 to 1,410 mg/l (Table 1). The radiogenic Sr content appears to increase northwestward (Fig. 12). Unlike the variations in oxygen-hydrogen isotopic compositions of the waters which can be ascribed to mixing of two waters of different evolutionary history, the variations in Sr isotopic compositions cannot be clearly attributed to mixing of two different waters because of the lack of a reasonably linear trend in the relationship between the $^{87}Sr/^{86}Sr$ and 1/Sr values (Fig. 13).

Strontium isotopic analyses of carbonate cements in the Morrowan sandstones from each of the two cores indicate that the $^{87}Sr/^{86}Sr$ are significantly varied. The isotopic values found are between 0.70843 and 0.70927 in Clark County, Kansas, and between 0.71184 and 0.71573 in Cheyenne County, Colorado (Table 3). These Sr isotopic values of the cements are distinctly different from the Sr isotopic values of associated present-day waters, suggesting the isotopic signatures of cements are from fluids of earlier times. Across the Morrowan sandstone beds, the cements are widely varied in their strontium isotopic compositions (Fig. 14). In the Lexington field, Kansas, the Sr isotopic values tend to be linearly related to the inverse of Sr concentrations (Fig. 15). The trend suggests that the fluids which accounted for the deposition of the carbonate cements in this locality may be defined by mixing different proportions of two chemically and isotopically different waters.

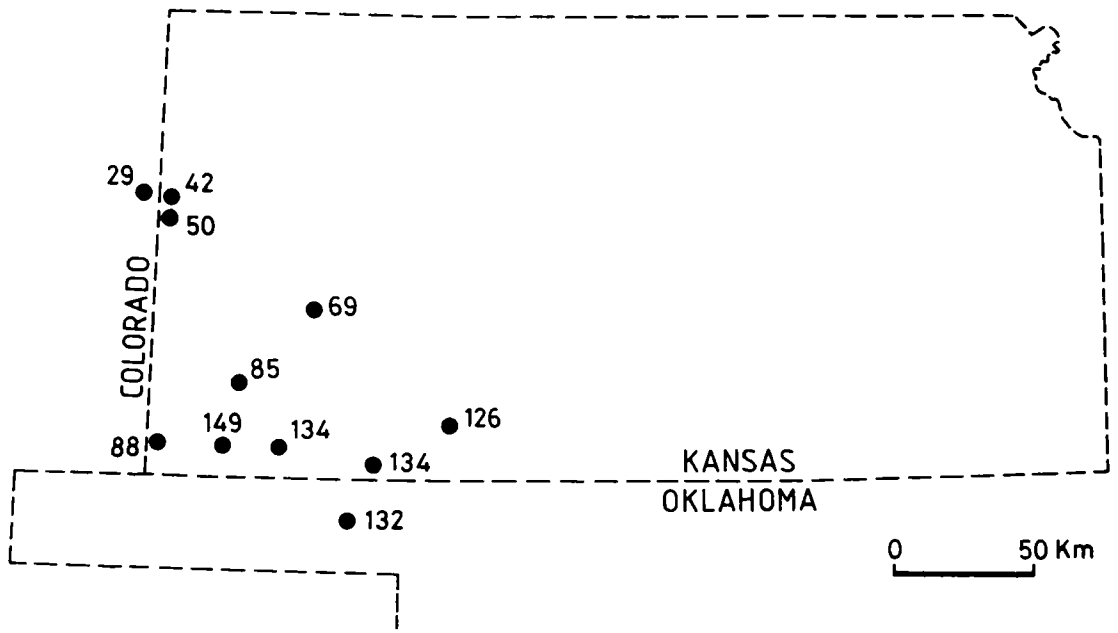

Figure 7. Spatial distribution of chloride contents (g/l) of formation waters in Morrowan sandstones.

DISCUSSION

The oil-field waters in the Morrowan sandstones in the Hugoton embayment appear to have the following chemical and isotopic trends: (1) the salinity tends to decrease northwestward, as evident from changes in Na and Cl contents of the waters; (2) both D and ^{18}O contents tend to increase southeastward; (3) D contents apparently increase with increasing Cl contents in a southeastward direction; and (4) ^{87}Sr contents tend to increase northwestward. The spatial variations in the chemical and isotopic compositions of the waters may be explained in terms of a model of mixing of two chemically and isotopically different waters. Any consideration of such a genetic model for the evolution of the formation waters should shed much light on the questions of the sources of waters and the nature of hydraulic communication not only among the Morrowan aquifers, but also between the Morrowan sandstones and the subjacent or the superjacent stratigraphic units.

The sources for formation waters are best identified by the variations in the D and the ^{18}O contents of the waters. The linear trend in these data for the waters in the Morrowan sandstones intersects the global meteoric line at δD value of $-102‰$ and $\delta^{18}O$ value of -14, which define the isotopic composition of the meteoric water component in the formation waters of the Morrowan sandstones (Fig. 9). The other component may be described as a chemically evolved seawater or diagenetically evolved water of unknown origin, with D and ^{18}O contents at least as high as those given by the sample with the highest D and ^{18}O contents. Two popular interpretations have been given as to the source of the meteoric water component in oil-field waters. One interpretation is that the meteoric water component in oil-field brines was derived locally in recent time because of its similarity in isotopic composition to the present-day local meteoric water. The other explanation is that the meteoric water component in oil-field brines either belongs to some cold climate period, possibly Pleistocene glacial time, or relates to recharge of the aquifers at high elevations, because the inferred isotopic values for the meteoric water component are decidedly more negative than the isotopic values of local recent meteoric water. In the case of the Morrowan aquifers, the D and ^{18}O contents of the meteoric water component are clearly much lower than the D and ^{18}O contents of recent meteoric waters in southwestern Kansas, which we found to have a δD value of about $-55‰$ and $\delta^{18}O$ value of about $-7.5‰$ (Fig. 9). Although a Pleistocene glacial water source appears reasonable based merely on the highly negative isotopic values, on geologic grounds we must also consider that the meteoric water component may have been derived from a recharge of the aquifers at high elevations in the eastern front of the Rocky Mountains in Colorado where outcrops and subcrops of steeply dipping Pennsylvanian strata are known to occur. However, the recent artesian condition does not necessarily translate into recharge of the Morrowan aquifers in recent time. Similar physiographic conditions also existed as far back in time as the Pennsylvanian (Fig. 2), suggesting

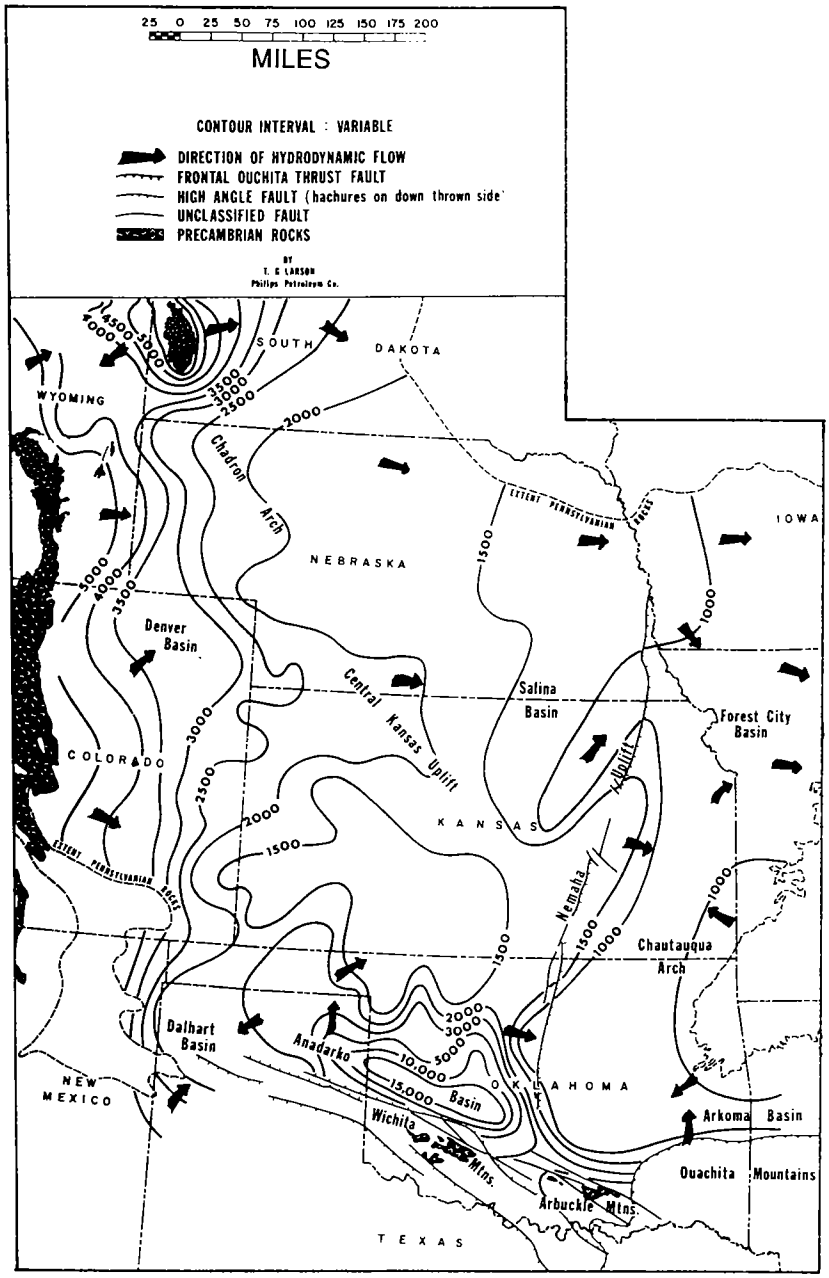

Figure 8. Potentiometric surface map of Pennsylvanian System in the Hugoton embayment and the Anadarko basin (after Larson, 1971).

that recharge of the Morrowan aquifer during times much earlier than the Holocene or Pleistocene cannot be ruled out.

The isotopic data presented in Table 3 indicate that the cements of sandstones from two widely separated localities, one in Colorado and the other in the southern part of southwestern Kansas, are markedly different from each other in their carbon, oxygen, and strontium isotopic compositions. The carbonate cements in the fluvial Morrowan sandstones to the north in Colorado are low in $\delta^{13}C$ (−3.3 to −1.9), low in $\delta^{18}O$ (+20.6 to +23.8), and high in $^{87}Sr/^{86}Sr$ (0.71184–0.71573) compared to the carbonate cements in the marine Morrowan sandstones to the south in Kansas, which have high $\delta^{13}C$ values (−2.1 to +2.8), high $\delta^{18}O$ values (+25.1 to +28.4), and low $^{87}Sr/^{86}Sr$ (0.70843–0.70927). This trend of heavy oxygen and low ^{87}Sr

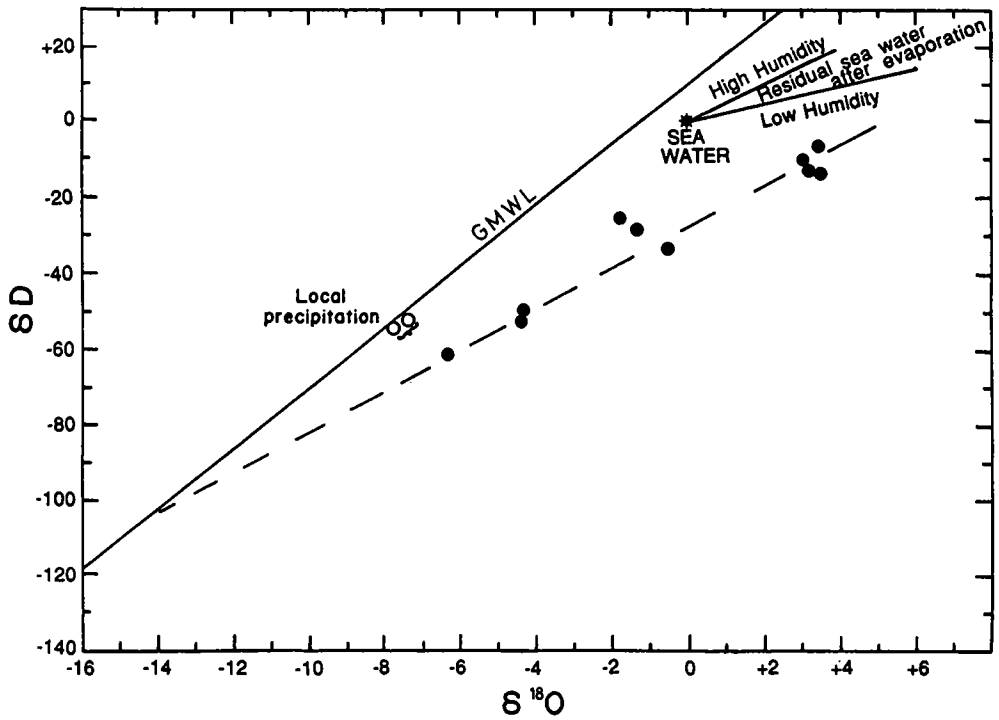

Figure 9. Oxygen and hydrogen isotopic compositions of formation waters in Morrowan sandstones (solid circles), sea water (asterisk), and present-day local precipitation (open circles). The solid line, GMWL, represents the global meteoric water line. The dashed line is the formation water line.

contents in the south and light oxygen and high ^{87}Sr contents in the north for the pore fluids during the episode of carbonate cementation is broadly similar to the trend of oxygen and Sr isotopic compositions of recent formation waters in the Morrowan aquifers. The apparent similarity in the isotopic trends of the recent formation waters and pore fluids during carbonate cementation, and the apparent physical discontinuity among the lenticular aquifers, strongly suggests that the evolutionary history of the meteoric water component of the formation waters in the Morrowan sandstones relates to past hydrodynamic conditions of the basin and not to the recent hydrologic cycle in the basinal area.

The Early Pennsylvanian Morrowan unit in the Hugoton embayment rests unconformably on carbonate rock dominated Mississippian sequence, the top of which represents a widespread erosional surface. This erosional surface is potentially an excellent avenue for hydraulic communication between Morrowan and Mississippian aquifers. But the isotopic data of the formation waters in the Morrowan sandstones, when compared with the isotopic data of waters in the underlying Mississippian strata in the same locality, strongly suggest lack of vertical communication between the Early Pennsylvanian Morrowan sandstones and the underlying Mississippian rocks. For example, in Cheyenne County, Colorado, the $^{87}Sr/^{86}Sr$ of the formation waters in the Morrowan sandstones is ~0.7183, whereas the $^{87}Sr/^{86}Sr$ of formation waters in the Mississippian rocks is ~0.7340 (Chaudhuri, 1978). Similar distinct differences in the Sr isotopic compositions between the two units also exist along the eastern margin of the Morrowan subcrops in southwestern Kansas. The waters in the Morrowan sandstones also appear to be somewhat enriched in both D and ^{18}O relative to the waters in the Mississippian rocks.

In a large part of the Hugoton embayment in southwestern Kansas, the Early Pennsylvanian Morrowan unit is unconformably overlain by rocks of the Middle Pennsylvanian Cherokee Group. Like the waters in Mississippian rocks, the waters in Middle Pennsylvanian Cherokee rocks are also high in $^{87}Sr/^{86}Sr$ relative to the waters in the Early Pennsylvanian Morrowan rocks. For example, Nicastro (1983) reported that the $^{87}Sr/^{86}Sr$ of waters in both the Mississippian carbonate rocks and the immediate overlying Middle Pennsylvanian Cherokee sandstones in the eastern part of the Hugoton embayment in southwestern Kansas are about 0.7230–0.7240, and we found that the

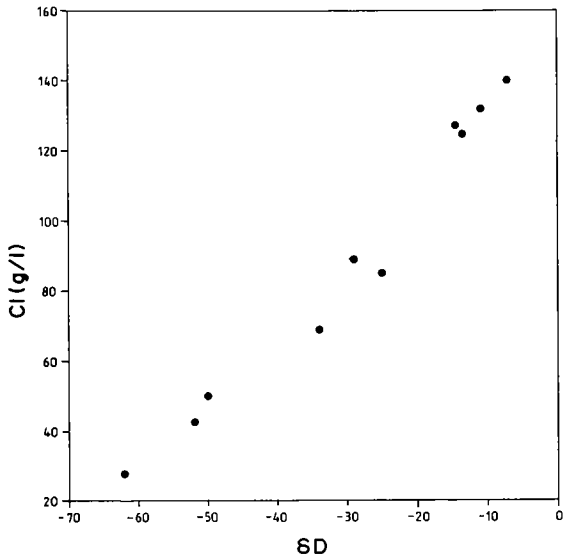

Figure 10. Variations of D with salinity of formation waters in Morrowan sandstones.

$^{87}Sr/^{86}Sr$ of formation waters in the Morrowan sandstones near the same area are about 0.7090–0.7100 (Table 2). In essence, hydraulic communication exists between the Mississippian and the superjacent Middle Pennsylvanian Cherokee rocks where the Morrowan rocks are absent, but not between the Morrowan sandstones and the underlying Mississippian or overlying Cherokee rocks, suggesting that considerable hydraulic isolation exists for the Morrowan sandstones in the Hugoton embayment in southwestern Kansas.

Hydraulic communication among the Morrowan aquifers also appears limited at the present time. Dickey and Cox (1977) pointed out, based on information that each reservoir has its own pressure decline curve, a lack of hydraulic continuity among the lenticular Morrowan aquifers. The strontium isotopic data for waters in the Morrowan sandstones also suggest a lack of hydraulic communication among the aquifers at the present time. The lack of linearity between the $^{87}Sr/^{86}Sr$ and the 1/Sr values, shown in Figure 13, may be used as evidence for the absence of hydraulic continuity among the aquifers.

Both the oxygen-hydrogen isotopic relationship and the trend of increasing D content with increasing salinity suggest a mixing of two isotopically and chemically different waters for the evolution of waters in the Morrowan sandstones. But this mixing trend is hardly evident from the relationship of $^{87}Sr/^{86}Sr$ and 1/Sr values (Fig. 13), especially for the waters from the southern part of the Hugoton embayment in southwestern Kansas and northwestern Oklahoma, which, as Larson (1971) presented, is apparently an area with a low potentiometric surface for the Pennsylvanian aquifers (Fig. 8). The failure of the Sr isotopic data to support the stable isotope evidence for mixing of two isotopically and chemically distinct waters has also been documented in several other studies on basinal waters (McNutt and others, 1987; Chaudhuri and others, 1987). This incompatibility between the two independent sets of evidence has not been clearly explained. An implication that is frequently made in the literature is that the nonlinearity in the Sr isotopic data could be related to reactions of the waters with isotopically and chemically varied minerals, especially carbonate minerals, of the reservoir rocks. But we believe that this implication may not be totally correct, at least not for waters in the lenticular Morrowan sandstones. Any reaction between formation waters and carbonate cements in the lenticular Morrowan reservoir sandstones appears minimal, as the anisotropy in the Sr isotopic compositions of the carbonate cements in a reservoir is still very much evident in the sandstone cores from two separate localities (Table 3). The comparison between the Sr isotopic data from the formation waters and the carbonate cements (Tables 2 and 3) strongly supports the interpretation that no Sr isotopic equilibration was achieved between the waters and their Morrowan reservoir rocks. Even selective dissolution of carbonate cements in a sample of sandstone shows small internal heterogeneity in the Sr isotopic compositions of the carbonate cements (Table 3). We contend that a lack of conclusive Sr isotopic evidence for mixing of two separate sources of water most likely relates to the process of development of subnormal fluid pressures in the Morrowan and other Paleozoic units in the Hugoton embayment of southwestern Kansas and northwestern Oklahoma.

Different mechanisms have been advocated to explain the development of subnormal fluid pressures in stratigraphic units: (1) increased water table with deposition of sediments on a stratigraphic unit containing a sealed high permeability formation (Bradley, 1975); (2) chemical osmosis across a semipermeable shale membrane (Berry, 1959; Hitchon, 1969; Bradley, 1975); (3) epeirogenic movements leading to reversal of tilting of an aquifer with pinch-out originally downdip and outcrop originally updip; after tilting, the recharge (outcrop) area becomes the discharge area resulting in loss of fluid from the aquifer (Bradley, 1975); (4) topographically driven fluid flow in tilted aquifers with hydraulic insulation within the basin separating the recharge zone from the more permeable discharge zone downdip (Fertl and others, 1976; Senger and Fogg, 1987; Belitz and Bredehoeft, 1988); (5) large scale erosion following uplift and tilting of basin with attendant decrease in volume of the fluid due to decreased temperature and dilation of pore volumes by greater amounts

TABLE 3. — ISOTOPIC DATA ON CARBONATE CEMENTS IN MORROWAN SANDSTONES

Depth (ft)	Sr (ppm)	$^{87}Sr/^{86}Sr$[a] (±2σ)	$\delta^{18}O$ per mil (SMOW)	$\delta^{13}C$ per mil (PDB)
		Arapahoe field, Cheyenne County, Colorado		
5,352[b]	—	0.715042 ±9	—	—
5,352[c]	—	0.715382 ±9	—	—
5,352[d]	208	0.715504 ±8	+20.9	-3.2
5,353	258	0.715727 ±9	—	
5,355	387	0.711845 ±8	+23.8	-2.0
5,357	703	0.713777 ±8	+22.7	-1.9
5,360	397	0.712391 ±9	+21.9	-2.9
5,362	177	0.714749 ±9	—	—
5,366	772	0.714666 ±8	—	—
5,368	95	0.714934 ±8	+20.6	-3.3
		Lexington field, Clark County, Kansas		
5,162 (I-32 McPhail)	—	0.709230 ±9	+26.1	-1.7
5,177 (I-32 McPhail)	—	0.709151 ±8	+26.7	-0.2
5,160 (2-20 Moore)	—	0.708712 ±9	+27.8	-0.1
5,191 (2-20 Moore)	—	0.708651 ±9	+28.4	-2.8
5,239 (5-19 Seacat)	—	0.708602 ±8	+27.6	+1.0
5,257 (5-19 Seacat)	—	0.708433 ±9	+26.9	+0.7
5,127 (2-29 Moore)	—	0.708737 ±9	+26.9	+0.9
5,141 (2-29 Moore)	—	0.708830 ±8	+27.7	+1.7
5,252 (1-18 Schieb)	—	0.709271 ±9	+25.1	-2.1

[a]All $^{87}Sr/^{86}Sr$ values have been corrected for fractionation by taking $^{86}Sr/^{88}Sr$ is equal to 0.1194. The $^{87}Sr/^{86}Sr$ value of NBS 987 strontium carbonate standard measured during this study was found to be 0.710228 ± 0.000008 (2σ).
[b]Leaching for 1 minute in 0.5 m HCl.
[c]Leaching for 5 minutes in 0.5 m HCl.
[d]Complete dissolution in 0.5 m HCl.

in shales than in sandstones which causes fluids to move from sandstones to shales (Dickey and Cox, 1977; Neuzil and Pollock, 1983).

The mechanism of osmotic pressure force, as advocated by Berry (1959), cannot be used to explain the apparent lack of evidence of mixing of waters in the light of the Sr isotopic data from waters in the Morrowan sandstones. Berry suggested that restriction of flow of ions but not of water through low permeability shale beds between fresh-water aquifer and saline-water aquifer will cause a decline in fluid pressure in the fresh-water aquifer due to the migration of the water molecules along the concentration gradient toward the saline-water aquifer. Larson (1971) noted a low potentiometric surface in the southern part of the Hugoton embayment in southwestern Kansas and northwestern Oklahoma (Fig. 8). Belitz and Bredehoeft (1988) argued that the low potentiometric surface is due to osmotic pressures. In much of southwestern Kansas, the sandstones in the Early Pennsylvanian Morrowan unit are separated from the overlying Middle Pennsylvanian Cherokee sandstones and the underlying Mississippian carbonate aquifers by sequences of shale and limestone beds. Our preliminary studies on chemical and isotopic compositions of formation waters in other stratigraphic units in southwestern Kansas suggest that the average salinity of waters in the Morrowan unit is much higher than that of waters in either the underlying or the overlying unit. As compared to waters of the Morrowan unit, those of the immediate overlying and underlying formations are depleted in both D and ^{18}O contents and enriched in ^{87}Sr (Nicastro, 1983). The osmosis effect on the isotopic compositions of Sr in waters is difficult to evaluate due to lack of any experimental data. No compelling reason exists at this time to suggest that osmosis would result in $^{87}Sr/^{86}Sr$ ratios to be generally inversely related to D or ^{18}O contents for the waters, which is a phenomenon that is common among formation waters.

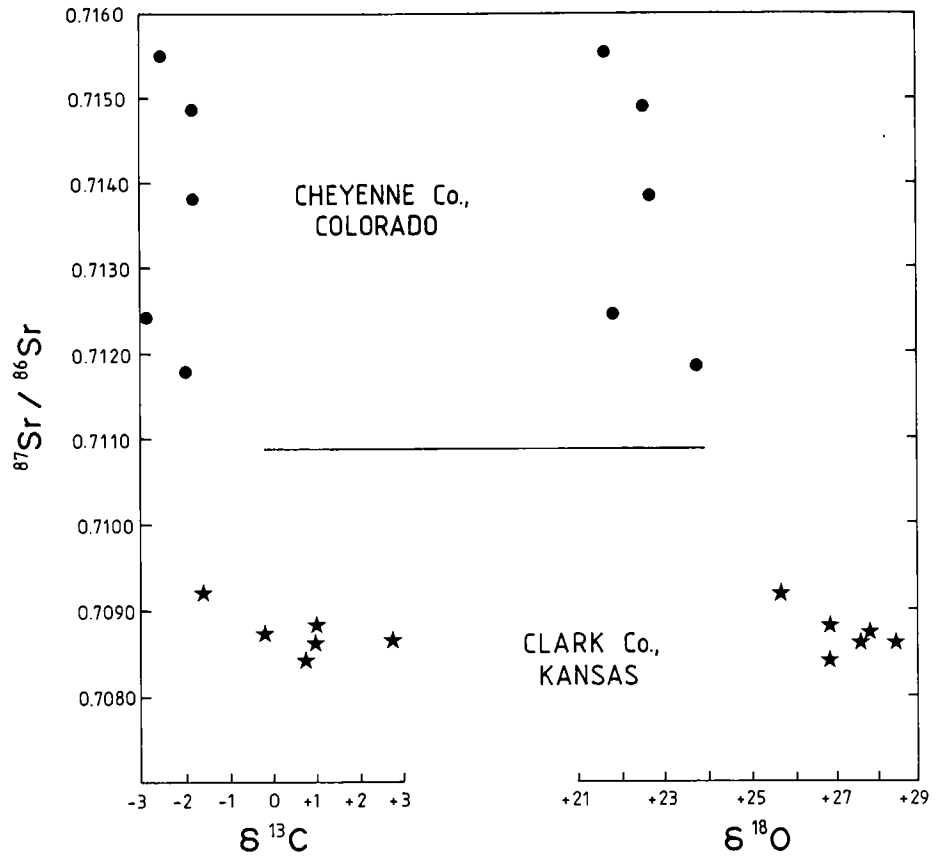

Figure 11. Carbon, oxygen, and strontium isotopic variations of carbonate cements in Morrowan sandstones in two separate oil fields.

The evidence of Sr isotopic data, stable isotopic data, and salinities of formation waters in the Morrowan sandstones also bears no relation to the effects of topography and relatively high rate of discharge through more permeable strata in the discharge zone which have been considered by some as a cause for the subnormal pressures in the Morrowan unit. The high rate of discharge through more permeable strata should have little influence on the Sr isotopic compositions of formation waters. Sr isotopic fingerprints can be attributed roughly to mixing of two different waters. Geologic evidence is lacking to give support to the use of the hypothesis by Bradley (1975) that the effect of epeirogeny attendant with transformation of a recharge area into a high permeability discharge area could be a cause for subnormal fluid pressures in the Morrowan sandstones.

The process of development of subnormal fluid pressures due to decrease in volume of the fluids in response to decreased temperature and increase in pore volumes in rocks following erosional removal of overburdens is the one which seems to explain clearly why the stable isotope data but not the Sr isotope data point to mixing of two sources of water for the origin of waters in the Morrowan unit. Dickey and Cox (1977) remarked that the removal of overburden would cause an elastic dilation of the pores in both sandstones and shales, the increase in pore volumes being more in shales than in sandstones, and a change in the volume of the water which is about half as much as the change in the pore volume. They suggested that relative changes in the pore volumes and waters will facilitate some water movement from sandstone beds to adjacent shale beds, which may explain the subnormal pressures in the sandstone beds. Neuzil and Pollock (1983) also provided laboratory evidence on the increase in pore volume due to erosional unloading of the overburden. Temperature decrease attendant with removal of overburden will decrease the volume of fluid and cause some additional decrease in pressures in the pore fluids (Dickey and Cox, 1977). We suggest that as the erosional removal of overburden opens communication between sandstones and adjacent shales, leaching of varied amounts of Sr from highly compacted shales (normally containing highly

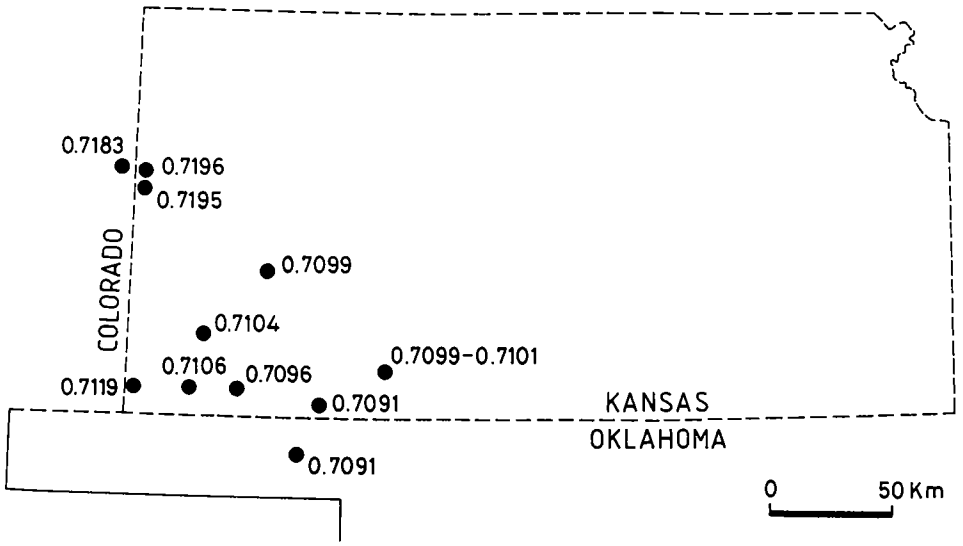

Figure 12. Spatial variations in strontium isotopic values of formation waters in Morrowan sandstones.

saline waters in the micropores) would tend to disrupt the linear trend in the relationship between the $^{87}Sr/^{86}Sr$ and 1/Sr values which might have existed for the waters in sandstones prior to the cross-stratal hydraulic communication with enclosing shale beds. The opening of hydraulic communication between sandstone beds and shale beds due to erosional unloading of overburden should not significantly affect the hydrogen and oxygen isotopic compositions of the formation waters in the sandstone because the waters in the two lithologic units were most likely genetically related and differed little in the isotopic compositions.

CONCLUSION

Formation waters in the Morrowan sandstones in the Hugoton embayment are generally of chloride-calcium type. Chemical and isotopic compositions of the waters appear to change roughly along a northwest–southeast direction and many of these trends may be related to mixing of two separate waters, one of which is continental meteoric water. The meteoric-water component was most likely derived from recharge of the aquifers at high altitudes along the western margin of the Hugoton embayment. Much of the recharge may not have occurred in the recent hydrologic cycle. The isotopic and chemical changes in many ways correspond to changes in the depositional environments of the sands and also to changes in the isotopic compositions of carbonate cements in the sandstones. The present formation waters in the Morrowan sandstones bear chemical and isotopic signatures which reflect chemical and isotopic signatures of past diagenetic waters in the Hugoton embayment. The isotopic data tend to support the conclusion that subnormal fluid pressures in the Pennsylvanian System in the Hugoton embayment developed due to decrease in volume of the fluids attendant with decrease in temperature and dilation of pore volumes in the rocks as a result of erosional removal of overburden following uplift and tilting of the basin.

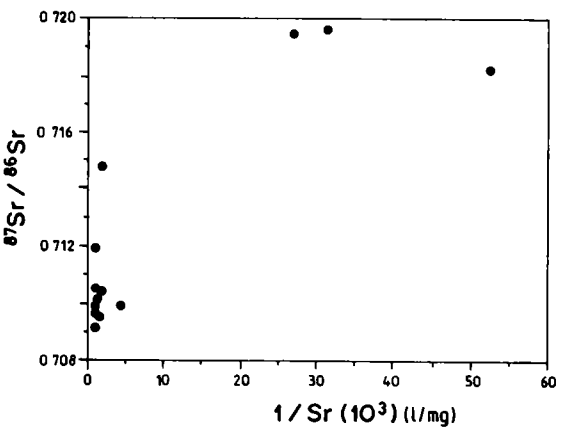

Figure 13. Relationship between strontium isotopic ratios and 1/Sr values of formation waters in Morrowan sandstones.

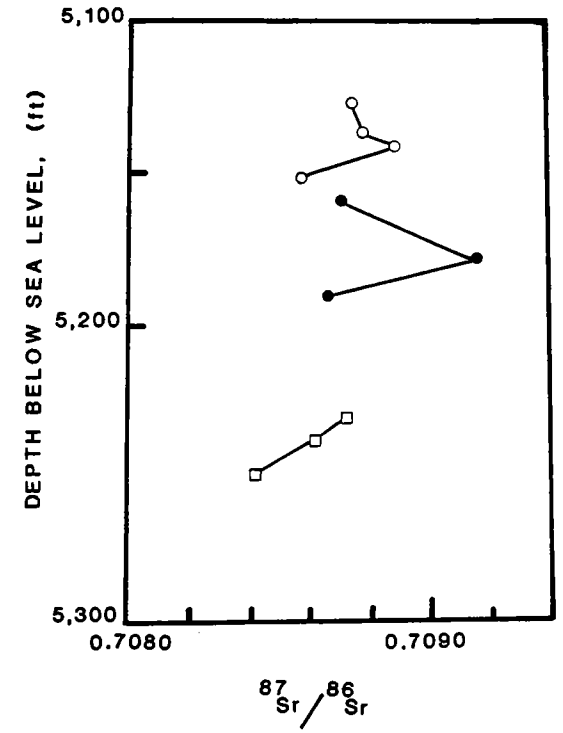

Figure 14. Changes in strontium ratios of carbonate cements in Morrowan sandstones with depth in the Lexington field, Kansas. (Three different symbols represent samples from three different wells in the field.)

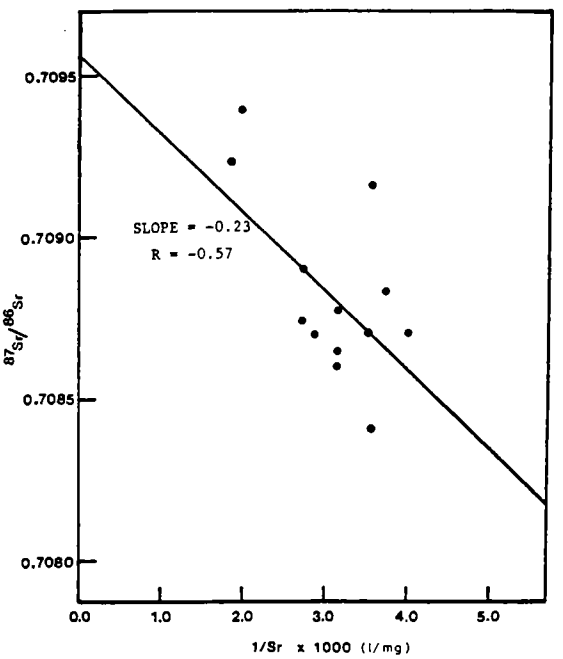

Figure 15. Strontium isotopic ratios versus 1/Sr values of carbonate cements of Morrowan sandstones in the Lexington field, Clark County, Kansas.

REFERENCES

Adler, F. J.; and others, 1971, Future petroleum provinces of the Mid-continent, region 7, *in* Cram, I. H. (ed.), Future petroleum provinces of the United States: their geology and potential: American Association of Petroleum Geologists Memoir 18, v. 2, p. 985–1120.

Belitz, K.; and Bredehoeft, J. D., 1988, Hydrodynamics of Denver basin: explanation of subnormal fluid pressures: American Association of Petroleum Geologists Bulletin, v. 72, p. 1334–1359.

Berry, F. A. F., 1959, Hydrodynamics and chemistry of the Jurassic and Cretaceous Systems in the San Juan basin, northwestern New Mexico and southwestern Colorado: Stanford University unpublished Ph.D. dissertation, 213 p.

Bradley, J. S., 1975, Abnormal formation pressure: American Association of Petroleum Geologists Bulletin, v. 59, p. 957–973.

Busch, D. A., 1974, Stratigraphic traps in sandstones—exploration techniques: American Association of Petroleum Geologists Memoir 21, 174 p.

Chaudhuri, S., 1978, Sr isotopic composition of several oil-field brines from Kansas and Colorado: Geochimica et Cosmochimica Acta, v. 42, p. 329–332.

Chaudhuri, S.; Broedel, V.; and Clauer, N., 1987, Strontium isotopic evolution of oil-field waters from carbonate reservoir rocks in Bindley field, central Kansas, U.S.A.: Geochimica et Cosmochimica Acta, v. 51, p. 45–53.

Dickey, P. A.; and Cox, W. C., 1977, Oil and gas in reservoirs with subnormal pressures: American Association of Petroleum Geologists Bulletin, v. 61, p. 2134–2142.

Dickey, P. A.; and Soto, C., 1974, Chemical composition of deep subsurface waters of the western Anadarko basin: Society of Petroleum Engineers of AIME, Paper No. SPE 5178, 17 p.

Fertl, W. H.; Chilingarian, G. V.; and Rieke, H. H., III, 1976, Abnormal formation pressures: implications to exploration, drilling, and production of oil and gas resources: Developments in Petroleum Science, v. 2, 382 p.

Hitchon, B., 1969, Fluid flow in western Canada sedimentary basin. I.—Effect of topography: Water Resources Research, v. 5, p. 186–195.

Johnson, K. S.; and others, 1989, Geology of the southern Midcontinent: Oklahoma Geological Survey Special Publication 89-2, 53 p.

Larson, T. G., 1971, Hydrodynamic interpretation of Mid-continent, *in* Cram, I. H. (ed.), Future petroleum provinces of the United States: their geology and potential: American Association of Petroleum Geologists Memoir 15, v. 2, p. 1043–1046.

McManus, D. A., 1959, Stratigraphy and depositional history of the Kearney Formation (Lower Pennsylvanian) in western Kansas: University of Kansas unpublished Ph.D. dissertation, 150 p.

McNutt, R. H.; Frape, S. K.; and Dollar, P., 1987, A strontium, oxygen and hydrogen isotopic composition of brines, Michigan and Appalachian basins, Ontario and Michigan: Applied Geochemistry, v. 2, p. 495–505.

Neuzil, C. E.; and Pollock, W. D. 1983, Erosional unloading and fluid pressures in hydraulically "tight" rocks: Journal of Hydrology, v. 91, p. 179–193.

Nicastro, L., 1983, Isotopic and chemical studies of oilfield waters associated with Upper Paleozoic rocks, Miner field, Ness County, Kansas: Kansas State University unpublished M.S. thesis, 89 p.

Rascoe, B., Jr.; and Adler, F. J., 1983, Permo–Carboniferous hydrocarbon accumulations, Mid-continent, U.S.A.: American Association of Petroleum Geologists Bulletin, v. 67, p. 979–1001.

Senger, R. K.; and Fogg, G. E., 1987, Regional underpressuring in deep brine aquifers, Palo Duro basin, Texas. 1.—Effects of hydrostratigraphy and topography: Water Resources Research, v. 23, p. 1481–1493.

Swanson, D. C., 1979, Deltaic deposits in the Pennsylvanian upper Morrowan formation of the Anadarko basin, *in* Pennsylvanian sandstones of the Mid-continent: Tulsa Geological Society Special Publication No. 1, p. 115–168.

Watney, W. L., 1980, Cyclic sedimentation of the Lansing–Kansas City Groups in northwestern Kansas and southwestern Nebraska: Kansas Geological Survey Bulletin 220, 72 p.

Arbuckle Oils—An Overview

Stephen W. Brown and Paul J. Swetland
Core Laboratories, Houston, Texas

Alan R. Daly
Chevron Overseas, San Ramon, California

ABSTRACT.—There are no known reports in the literature of a confirmed source-rock facies within the Arbuckle Group of Oklahoma. The lack of a documented source-rock facies and the fact that the great bulk of the Group is composed of carbonates have led many explorationists to infer that the Arbuckle Group has not generated significant amounts of hydrocarbons. However, carbonate source rocks have been documented in other basins, and relatively few geochemical analyses have been performed on Arbuckle samples. Therefore, the Arbuckle should be analyzed to determine its source-rock potential.

Recent oil and gas discoveries in the Arbuckle Group have given a practical significance to arguments for and against the existence of Arbuckle source rocks, and the outcome of the debate will undoubtedly influence future exploration strategies.

The source rocks from which particular oils originated can be identified by matching geochemical fingerprints of the oils and potential source rocks in a process known as oil-source correlation. This paper presents a fundamental discussion of oil-source correlation techniques and reviews the body of literature dealing with the analysis of oils in Arbuckle reservoirs. It specifically discusses (1) the stratigraphic units responsible for sourcing oils in Arbuckle reservoirs, (2) the hypothetical characteristics of an Arbuckle-sourced oil, and (3) the stratigraphic units responsible for sourcing oils throughout Oklahoma.

Vitrinite Reflectance and Deep Arbuckle Maturation at Wilburton Field, Latimer County, Oklahoma

Steven J. Hendrick
ARCO Oil and Gas Co., Bakersfield, California

ABSTRACT.—Various shale horizons have been sampled and analyzed for vitrinite reflectance (R_o) and source rock quality in wells from the area of Arbuckle production at Wilburton field. Total organic carbon (TOC) measurements suggest that Caney and Woodford Shales are the most likely sources for gas in the Arbuckle. These shales have been juxtaposed against the Arbuckle horst along its bounding faults.

Analyses of the Caney and Woodford Shales yielded R_o values as much as ~3.0%. Conventional wisdom indicates that dry gas is confined to rocks with <3.2% vitrinite reflectance. The Caney and Woodford Shales, which are positioned 1,000–1,500 ft above the Arbuckle at Wilburton field, approach this upper preservation limit. The Woodford Shale is the oldest shale unit from which reliable vitrinite measurements can be obtained. By vertically profiling these vitrinite data on log/linear graphs, one can extrapolate these data to deeper horizons. This allows for an approximation of the maturation level in the Arbuckle reservoir at Wilburton field. The results of this extrapolation show that the Arbuckle gas accumulation lies at vitrinite levels of 3.5% (top of Arbuckle) to 3.8% (dry gas/water contact). The large accumulation of methane in the Arbuckle at Wilburton field, therefore, occurs in rocks which would generally be considered over-mature for hydrocarbon preservation. Thus, it is reasonable to expect that preservation of large accumulations of methane can exist throughout the Arkoma basin in rocks approaching, and perhaps exceeding, vitrinite reflectance levels of 4.0%.

INTRODUCTION

Exploration in the Arkoma basin was forever changed in 1987 when ARCO Oil and Gas Co. discovered gas in Arbuckle Group dolomite deep beneath the existing shallower production at Wilburton field. The Yourman No. 2 discovery was the product of an exploratory tail added to an otherwise shallower development well. This discovery represents not only the first sustained economic production from the Arbuckle in the basin, but is one of the largest hydrocarbon discoveries (~500 BCFGIP) made in the conterminous United States in the past decade. Prior to the Yourman No. 2 well, the Arbuckle had been penetrated in >200 wells basinwide, and had generally been written off as a noneconomic unit. The most important indication of gas prior to the Yourman was the Amoco Reed "C" No. 2, drilled 30 mi to the northeast, in Le Flore County. This well initially tested for 5,451 MCF of gas per day, but watered out within a year after only 162 MMCF of production.

Wilburton field is located in the gas-prone Arkoma basin along the Pittsburg/Latimer county line in southeastern Oklahoma (Fig. 1). Wilburton field lies just north of the outcrop of the Choctaw thrust fault—the leading edge thrust fault of the Ouachita overthrust system. Rocks along the Choctaw fault represent shelf facies or "Arbuckle Facies" rocks which have been locally repeated by thrusting and imbrication. Gas production is from the basal Atokan Spiro sandstone (Fig. 2) which is encountered twice, and locally three times in two major thrust plates at Wilburton field. This production is in the footwall of the Choctaw fault.

Wilburton field was discovered in 1960 when the Ambassador Williams No. 1 was successfully completed as the first gas well in the Spiro sandstone. This completion was made in the shallower of two thrust plates. The deeper Spiro was found productive in 1985 at the ARCO Smith No. 2 and Samson Costilow No. 2 wells. In 1987, gas was discovered in the Morrowan Cromwell sandstone (Fig. 2) at Wilburton field. In that year the ARCO McAlester No. 2X discovered gas in the Cromwell of the shallow thrust plate, and the ARCO Yourman No. 2 added a deep plate Cromwell discovery to the Arbuckle discovery.

At the time of this writing, Arbuckle production has been established in 12 wells, with an additional three wells still drilling or testing (Fig. 3). These three wells will likely complete the Arbuckle development of this field. Each well is capable of producing from 15 to 40 MMCF of gas per day. One hundred BCF of gas were produced from the Arbuckle through March 1990.

The Arbuckle production at Wilburton field occupies a much smaller area than the Spiro produc-

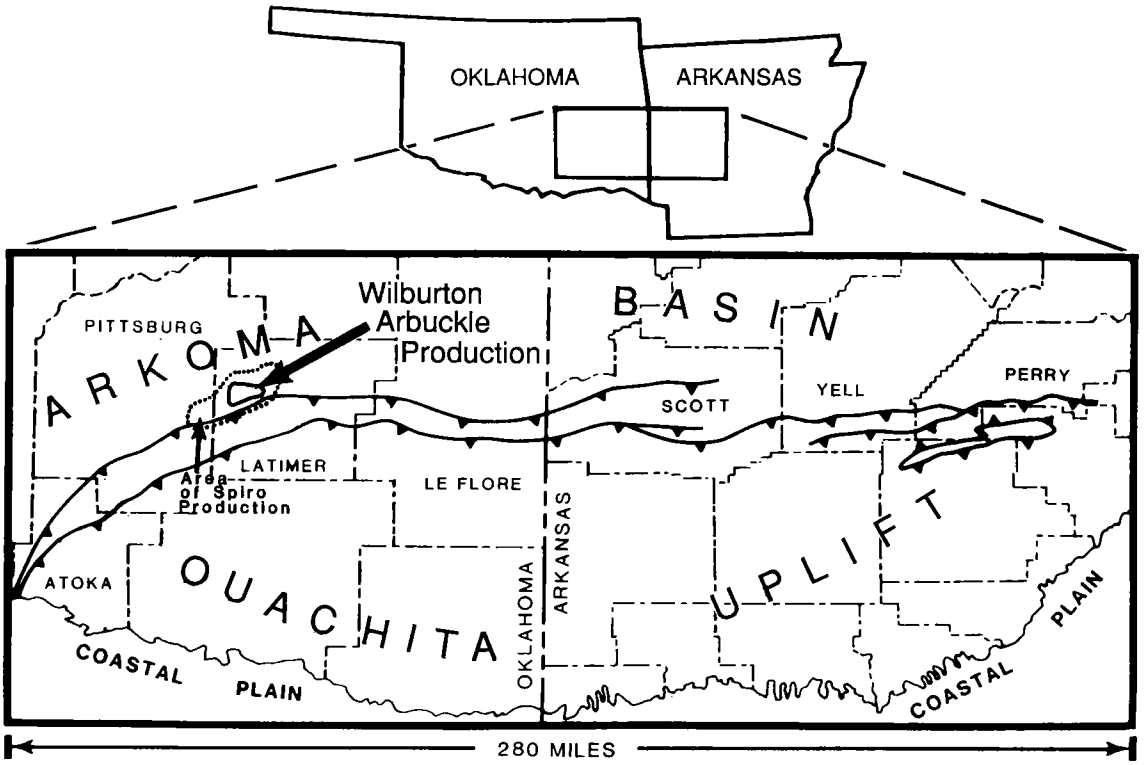

Figure 1. Map showing the location of Wilburton field (outlined by the area of Spiro production) and the location of Wilburton Arbuckle production.

tion (Fig. 1). The productive Arbuckle is currently confined to a single basement-involved horst block (Fig. 4). This horst block was likely formed in early Atokan time, during the initial formation of the Arkoma foreland basin. The formation of this basin postdates stable shelf deposition of the basal Atokan Spiro sandstone, and coincided with the rapid accumulation of >10,000 ft of Atoka shale and minor interbedded sandstone.

SOURCE ROCKS

Based on high total organic carbon (TOC) values (Table 1) and direct structural juxtaposition (Fig. 4), gas reservoired in the Arbuckle dolomite at Wilburton field was probably derived from the Devonian Woodford Shale and Mississippian Caney Shale (Fig. 2). Routine analyses for TOC were run for the entire stratigraphic section, from the Atoka shale at the surface to and including the Arbuckle Group. The highest TOC measurements were from the Woodford Shale; the second highest were from the Caney Shale. The Arbuckle at Wilburton is notably low in measurable organic material (<0.20% TOC). The TOC values at Wilburton are consistent with analyses from other ARCO wells in the Oklahoma portion of the Arkoma basin (Table 1). The Woodford Shale TOC values range from 2.06 to 6.52%, and the Caney Shale TOC values range from 2.02 to 4.04%. Because these analyses were derived from drill cuttings and represent 50-ft composites, it is likely that there has been some dilution from both cavings and the compositing process.

Because the highly organic Woodford Shale is known throughout Oklahoma as a prolific source rock, it was expected to yield source-quality TOC measurements prior to analyses. The high Caney Shale measurements, however, were not expected. Both the Woodford and Caney Shales contain oil-prone amorphous organic matter. This is consistent with the common presence of solid bitumen in samples throughout the lower Paleozoic section. The presence of solid bitumen, which is a residual by-product formed by thermal degradation of oil, suggests that the hydrocarbon initially generated was oil and that it was later cracked to gas, either during migration or while residing in the trap.

The Woodford Shale is 100–150 ft thick, and the Caney Shale is ~500 ft thick in the Wilburton area. This gives a combined 600–650 ft of highly organic source rocks, which are directly juxtaposed against the Arbuckle reservoir along bounding normal faults at Wilburton field (Fig. 4).

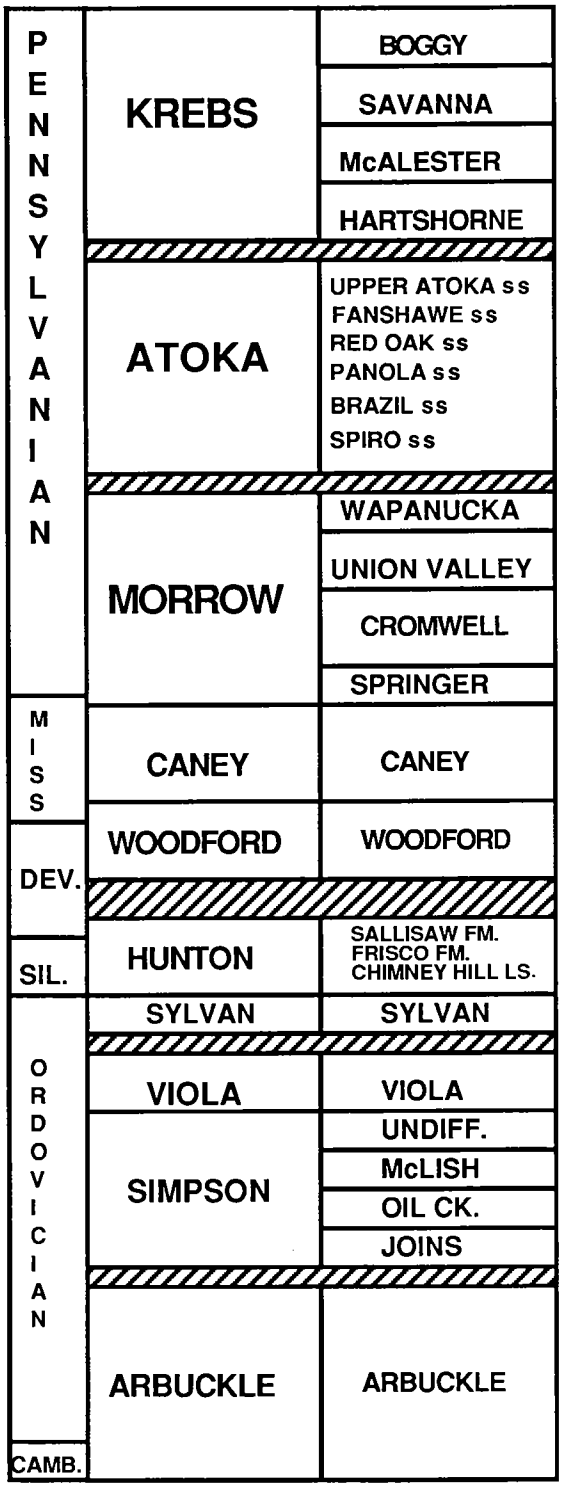

Figure 2. Generalized stratigraphic column and subsurface nomenclature of the Oklahoma Arkoma basin.

THERMAL MATURATION

In conjunction with the above TOC analyses, Devonian to Atokan age shales were measured for vitrinite reflectance, or % R_o (see Fig. 5) in order to determine the level of maturation in the strata at Wilburton field. The maturation level of the Arbuckle was of particular interest. Because vitrinite is confined to the post-Ordovician portion of the stratigraphic record (Katz and others, 1988), the Woodford is the lowest shale unit from which reliable R_o data can be obtained in the Wilburton area. Accurate estimates of maturation can be obtained for productive Atokan and Morrowan sandstones based on R_o measurements from the shales with which these sandstones are interbedded. The lack of vitrinite in pre-Silurian strata necessitates a different approach for determining maturation of the Arbuckle. A general lack of sufficient quantities of Arbuckle samples preclude widespread application of other, more direct, methods of maturation measurement, such as conodont alteration index (CAI), which requires a substantial amount of sample due to the paucity of conodonts in the Arbuckle.

The vitrinite extrapolation method is presented here as a tool that can easily be applied throughout the Arkoma basin due to the availability of shallow well control and the small sample-sizes required for vitrinite reflectance measurements. In this method, maturation profiles of a well, log/linear (semilog) graphs of depth vs. R_o are extrapolated to the depth of the Arbuckle. This approach is not without potential pitfalls, however. The pre-Woodford section is dominated by carbonates which may have conducted heat differently from the overlying shale-dominated strata. Problems can also arise from poor quality control during sampling and incorrect interpretation of kinks in the profiles which may be real or due to man-made causes, such as casing points in a well (Feazel and Aram, 1990). Vitrinite reflectance (% R_o) versus depth profiles for two wells in the area of Wilburton field Arbuckle production are presented in Figures 6 and 7. The results of the extrapolated Arbuckle maturation data presented here can serve as a yardstick for explorationists desiring to develop a "Wilburton Model" for Arbuckle gas exploration in the Arkoma basin.

Arbuckle Maturation

ARCO Oil and Gas Austin No. 3

Figure 6 is a profile of the Austin No. 3 well—a Spiro development well. This well is located in the same 640-acre unit as the Austin No. 2 well—an Arbuckle development well (Fig. 3). The Austin No. 3 well tested the lower of the two thrusted Spiro sandstones at Wilburton and was drilled to a total depth of 11,476 ft in Morrowan strata. A mud-

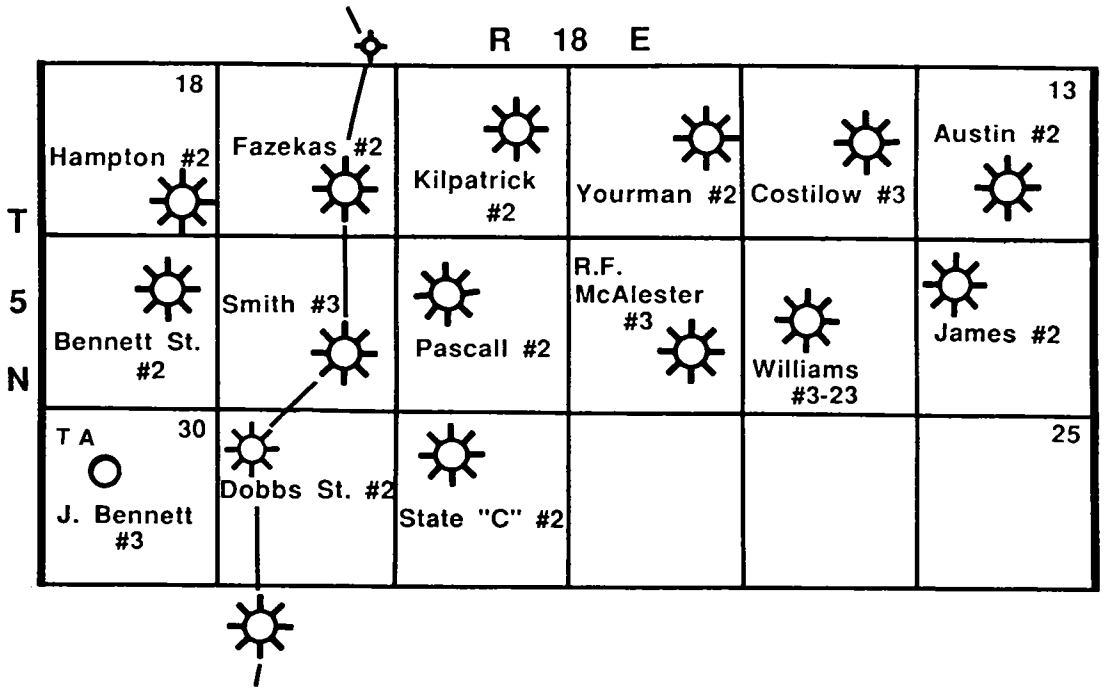

Figure 3. Location of Arbuckle wells (large symbols) in Wilburton field and location of cross section shown in Figure 4.

logger began sampling at the base of air drilling operations at ~7,500 ft depth. As can be seen on Figure 6, R_o values of 2.27–2.97% are distributed in a manner allowing easy visual straight-line fit. By extending this straight line to the estimated depth of the Arbuckle, the Arbuckle top is found to lie at an extrapolated R_o value of 3.5%, while the depth of water-free gas production within the Arbuckle extends to a depth of ~14,000 ft where the extrapolated R_o value is 3.7%. Both of these values are significantly above the conventionally accepted dry gas preservation limit of 3.2% (Fig. 5).

ARCO Oil and Gas Steve Fazekas No. 2

Figure 7 is a similar depth versus log R_o graph for the Steve Fazekas No. 2 well—an Arbuckle exploratory well drilled in 1988 to confirm the Yourman discovery. In this profile there is an offset of data which coincides with a thrust fault at a depth of ~9,600 ft. This fault is responsible for the repetition of the upper Morrow to lower Atoka in the Wilburton field area. The R_o data below the thrust fault ranges from 2.72% in the subthrust Atoka to 2.99% in the Caney. The three deepest values are anomalously low and are also questionable due to a small number of average reflectance measurements. These samples may also have significant contamination due to the caving of less-mature uphole zones. In general, however, the data distribution from 10,000 to 12,000 ft (Atoka through Caney) allows a straight-line fit and extrapolation to depth. According to this linear extrapolation, R_o is 3.5% at the top of the Arbuckle and 3.8% at the base of dry gas production. These data are in general agreement with data from the Austin well. Both profiles suggest that, based on extrapolated R_o data, the productive Arbuckle at Wilburton field may occur at vitrinite reflectance levels greater than those thought to represent the dry gas preservation limit (Fig. 8).

CONCLUSIONS

Based on the profiles of vitrinite reflectance (R_o) data on log/linear graphs from two wells in the area of Wilburton Arbuckle production, the Arbuckle reservoir lies within an extrapolated R_o range of 3.5 to 3.8% (Fig. 8). This is in line with ARCO conodont-derived data (CAI) from in-field cores. The CAI indices for the sparse conodont population of the Arbuckle are as great as 4+, which correlates with 3.0–4.0% R_o. It is suggested, therefore, that explorationists working in other portions of the Arkoma basin not confine themselves to exploring only within the realm of conventional gas preservation limits. Using the technique of extrapolating R_o data from shallower

TABLE 1. — TOTAL ORGANIC CARBON CONTENTS >2% FROM ARCO WELLS IN THE ARKOMA BASIN

Well name	Location	Total Organic Carbon (TOC%)		
		Atoka	Caney	Woodford
ARCO Browne No. 1	Sec. 28, T. 6 N., R. 17 E. Pittsburg County, OK	2.93 2.92*	3.95	4.62
ARCO Fazekas No. 2	Sec. 17, T. 5 N., R. 18 E. Latimer County, OK		3.07 2.47 2.62 2.91 3.07 2.17 2.02	6.31 4.90
ARCO Hart No. 1	Sec. 6, T. 4 N., R. 19 E. Latimer County, OK	2.42*	2.26	
ARCO Sharp No. 1	Sec. 2, T. 5 N., R. 17 E. Latimer County, OK	2.14*	4.04	5.47 6.52
ARCO Ingersoll No. 1-19	Sec. 19, T. 1 N., R. 13 E. Atoka County, OK	2.03 2.56*		
ARCO Runestone No. 1	Sec. 9, T. 5 N., R. 25 E. Le Flore County, OK		2.38 2.63 2.04 2.09 2.12 2.04	2.06 4.66 5.18 5.16 5.85

*Derived from the lowermost Atoka shale.

horizons to the Arbuckle, one should include any extrapolated value of as much as 4.0% in Wilburton exploration models.

REFERENCES

Dow, W. G., 1978, Petroleum source beds on continental slopes and rises: American Association of Petroleum Geologists Bulletin, v. 62, p. 1584–1606.

Feazel, C. T.; and Aram, R. B., 1990, Interpretation of discontinuous vitrinite reflectance profiles: discussion: American Association of Petroleum Geologists Bulletin, v. 74, p. 91–93.

Harris, A. G., 1983, Thermal maturation values (conodont color alteration indices) for Paleozoic and Triassic rocks, Chandler Lake, De Long Mountains, Howard Pass, Killik River, Misheguk Mountain, and Point Hope Quadrangles, northwest Alaska, and subsurface NPRA: U.S. Geological Survey Open-File Report 83-505, 15 p.

Katz, B. J.; Pheifer, R. N.; and Schunk, D. J., 1988, Interpretation of discontinuous vitrinite reflectance profiles: American Association of Petroleum Geologists Bulletin, v. 72, p. 926–931.

Perry, W. J., Jr.; Wardlaw, B. R.; Bostick, N. H.; and Maughan, E. K., 1983, Structure, burial history, and petroleum potential of frontal thrust belt and adjacent foreland, southwest Montana: American Association of Petroleum Geologists Bulletin, v. 67, p. 725–743.

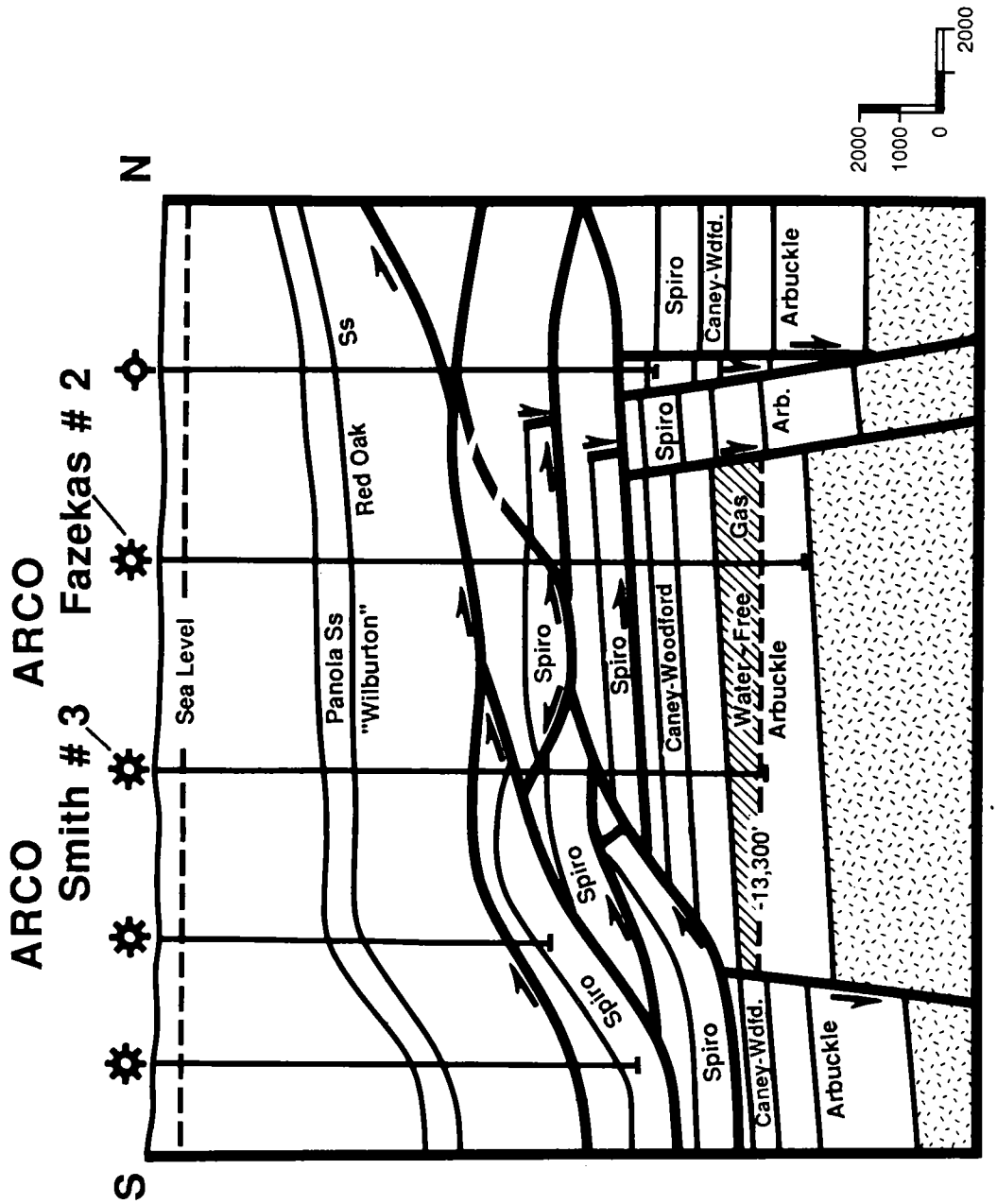

Figure 4. Cross section through the productive horst at Wilburton field.

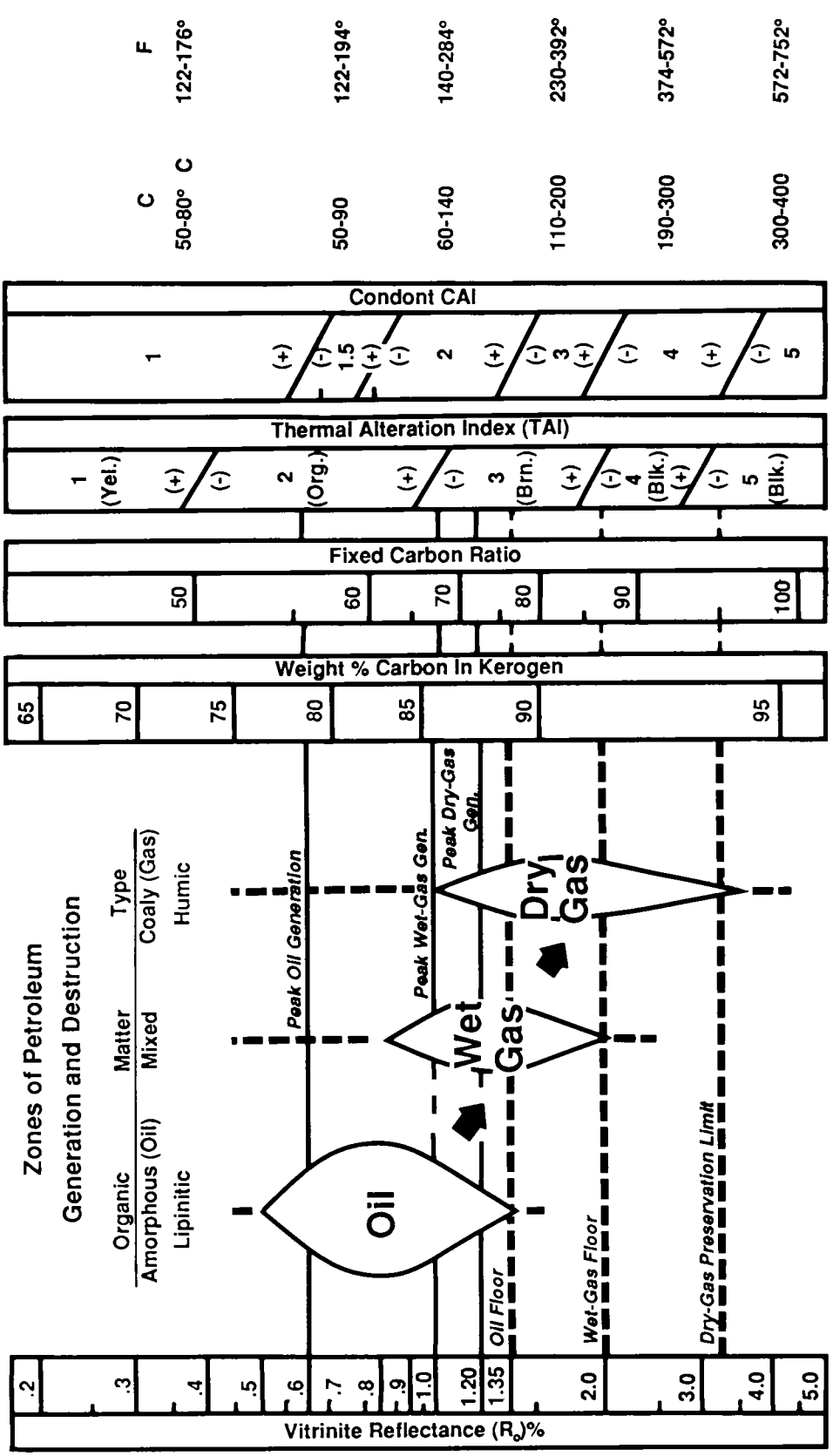

Figure 5. Correlation of maturation indices (modified from Dow, 1978, and Perry and others, 1983) with equivalent temperature ranges (from Harris, 1983).

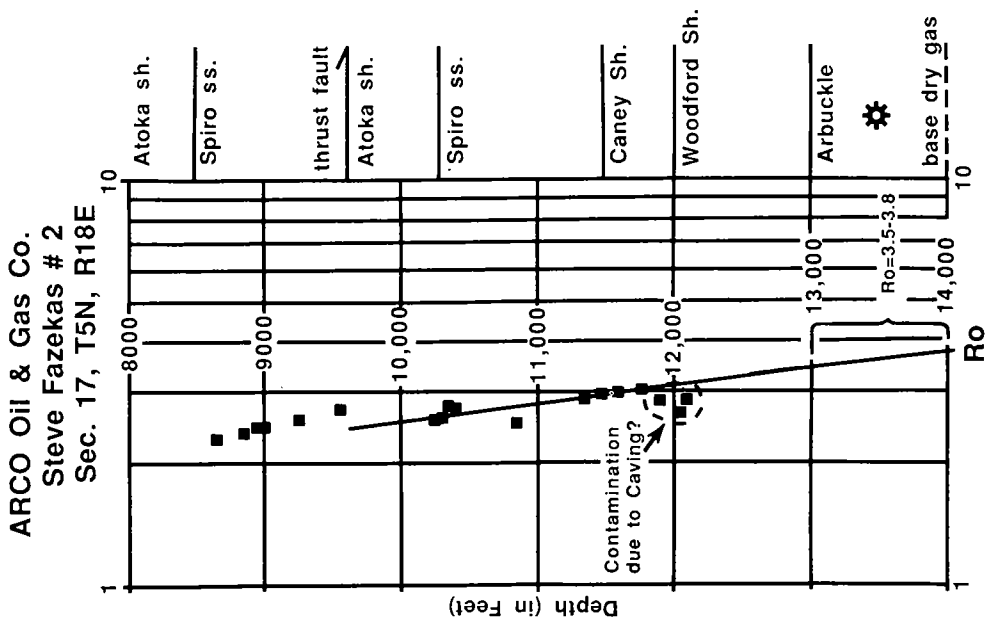

Figure 7. Depth versus vitrinite reflectance (R_o) from the Steve Fazekas No. 2 extrapolated to the base of the dry gas zone in the Arbuckle.

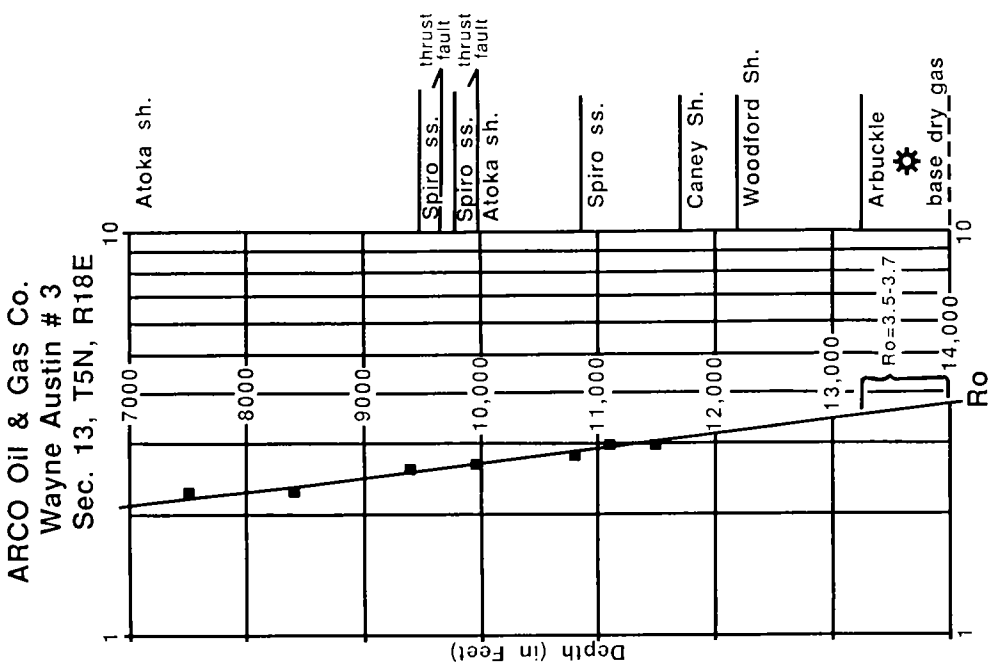

Figure 6. Depth versus vitrinite reflectance (R_o) from the Wayne Austin No. 3 extrapolated to the predicted depth of the base of the dry gas zone in the Arbuckle.

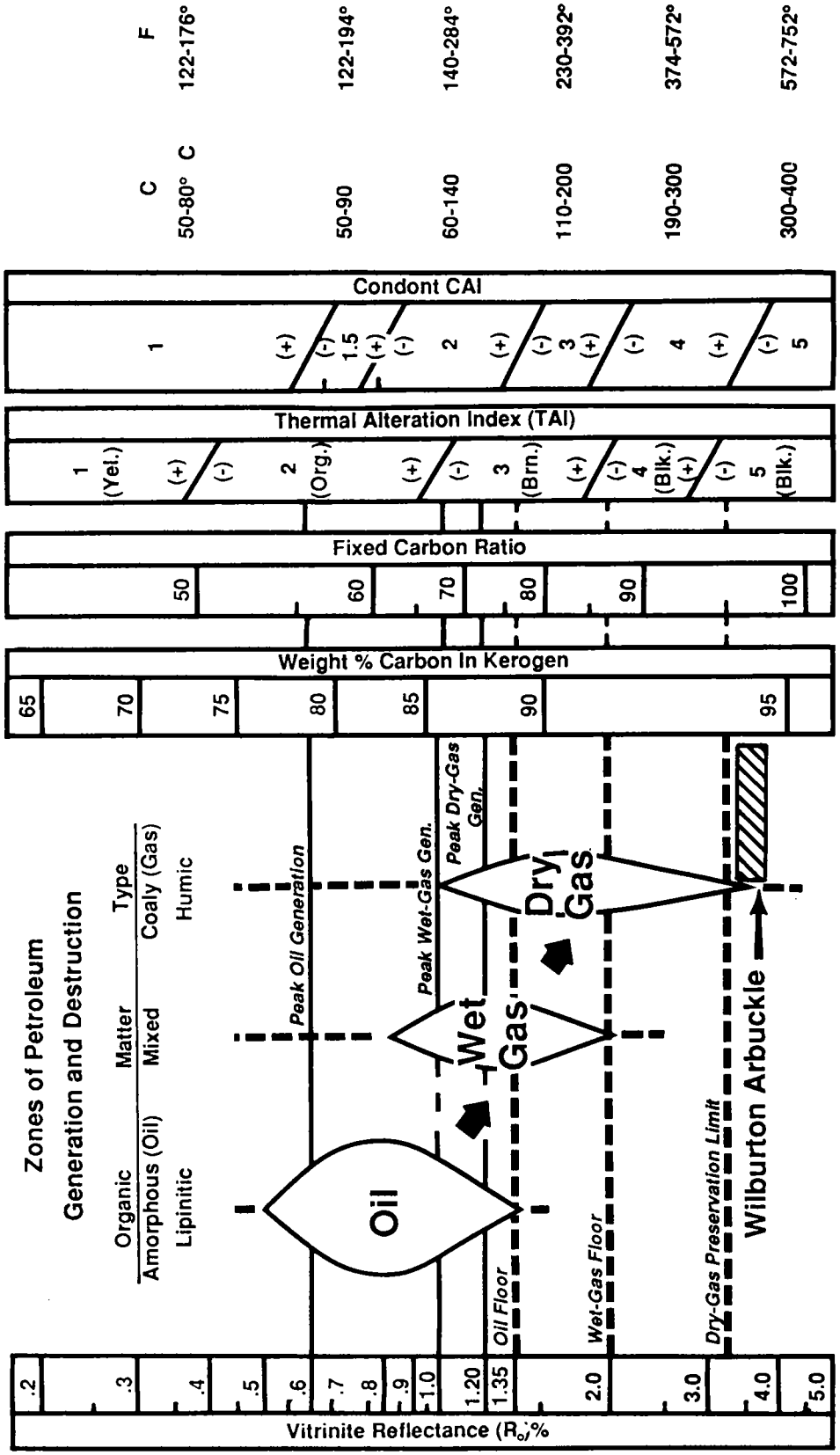

Figure 8. Correlation of maturation indices (modified from Dow, 1978, and Perry and others, 1983) with equivalent temperature ranges (from Harris, 1983) and the range of extrapolated R_o values for the Arbuckle at Wilburton field.

Characterization of Oil Types in the Ardmore and Marietta Basins, Southern Oklahoma Aulacogen

David A. Wavrek
University of Tulsa

ABSTRACT.—Gas chromatography analyses (GC–FID, GC–FPD, GC–MS) of 385 crude oils from the Ardmore and Marietta basins establishes the presence of seven oil families. These groups (types) are established by the distribution of n-alkanes, acyclic isoprenoids, alkylated cyclic hydrocarbons, alkylated sulfur compounds, steranes, hopanes, aryl-isoprenoids, and carbon isotopes. The type designations are reinforced by the stratigraphic distribution of oil types. In summary, oil Types A through E appear to correlate with source facies within Pennsylvanian (Atoka Formation?), Mississippian (Goddard, Caney, and Sycamore Formations), Devonian–Mississippian (Woodford Shale), upper Middle Ordovician (Viola Group), and Middle Ordovician (Simpson Group) rocks, respectively. The genetic interpretation of Type F oils is uncertain due to geochemical considerations, while Type G oils are complicated by their association with the Ouachita facies. The frequency distribution of these oil types indicates that Type C oils are dominant, but other oil types are locally abundant and provide new exploration targets.

INTRODUCTION

The southern Oklahoma aulacogen has been an area of significant hydrocarbon exploration for more than 75 years. Despite this fact, basic questions relating to the origins of southern Oklahoma oils remain unanswered. The number of oil families, their source beds, the nature of the migration paths, and the dominant alteration processes have not been adequately addressed. As an initial approach to answer these questions, I define the end-member oil types from gas chromatographic analyses of 385 oil samples collected throughout the study area.

Geologic Setting

The southern Oklahoma aulacogen has been defined by Hoffmann and others (1974), Pruatt (1975), Thompson (1976), and Wickham (1978a). This report covers the area bounded by the Arbuckle Mountains to the northeast, Ouachita facies to the southeast, Muenster uplift to the southwest, and the Wichita uplift/Anadarko basin to the northwest. Included in this area are the Ardmore basin, Marietta basin, and Criner Hills uplift (Fig. 1).

Samples

A total of 385 oil samples from 83 fields were obtained as part of a basin modeling research project. These samples provided complete stratigraphic control (Fig. 2), as well as a broad geographic base (Fig. 3). In some of the multipay fields, samples were obtained from each producing zone and in some cases, where faults offset equivalent producing horizons, samples were collected from both sides of the fault (Fig. 4).

Analytical Procedures

All oil samples were analyzed by whole-oil, capillary-column, gas chromatography using a Hewlett-Packard 5830 instrument equipped with a flame ionization detector (GC–FID). The capillary column was nonpolar with a bonded phase (Quadrex 007, 50 m × 0.25 mm ID with 0.5 μm film thickness). The oven was programmed from 35°C (10 min) to 300°C at 8°C/min with a final hold-time of 45 min. Other temperature zones include the split inlet (100:1) at 300°C and the detector at 350°C.

A total of 125 oil samples were analyzed for their sulfur-compound distribution by whole-oil gas chromatography using a Hewlett-Packard 5890A instrument equipped with a flame photometric detector (GC–FPD). A temperature programmed injector was used (50–300°C) in the split mode (100:1) along with the capillary column as described above. The oven was programmed from 35°C (2 min) to 225°C at 4°C/min and to 300°C at 8°C/min with a final hold-time of 25 min.

Fifty samples were analyzed by whole-oil gas chromatography–mass spectrometry (GC–MS) using an HP 5890A gas chromatograph interfaced to an HP 5970B mass selective detector. A conven-

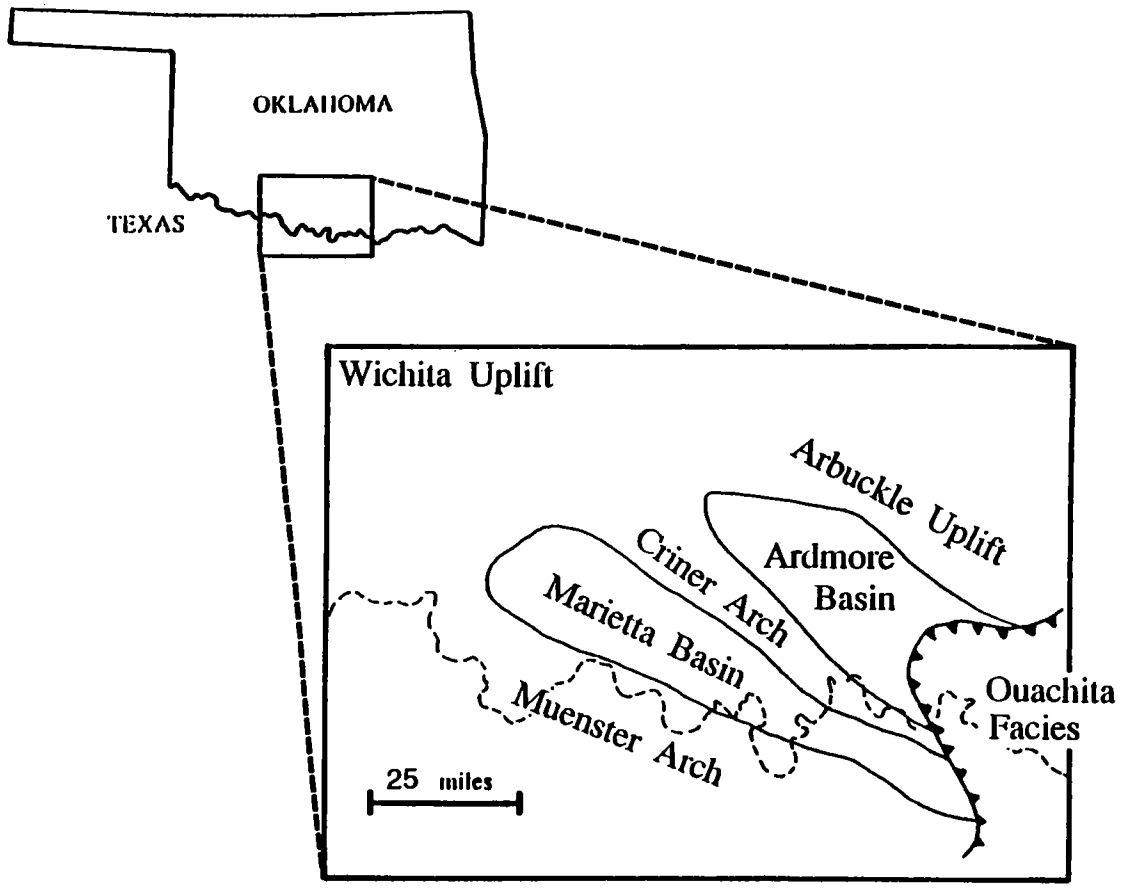

Figure 1. Major geologic provinces in the study area.

tional split injection (100:1) was used at 300°C. The capillary column used on this instrument was a J&W DB-5 (60 m × 0.25 mm ID with 0.25 μm film thickness). The oven was programmed from 35°C (2 min) to 325°C at 2°C/min with a 60 min hold-time. Data were collected in single-ion monitoring (SIM) mode for 20 ions with a 30 msec dwell time.

All chromatograms were quantified by peak height measurement and the data were transcribed to a spreadsheet for further analysis. Detailed data analysis is continuing, but the conclusions regarding the genetic oil types are reported at this time.

RESULTS

Gas chromatography of whole-oil samples revealed significant differences in the oil types reservoired in the study area. The parameters used to establish the oil groups (types) include the relative n-alkane distribution, acyclic isoprenoids, alkylated cyclic hydrocarbons, alkylated sulfur compounds, aryl-isoprenoids, hopanes, steranes, and carbon isotopes.

Type A Oils

Oils assigned to Type A are distinguished from the other oil types on the basis of their increased abundance of nC_{15+} alkanes, very little odd-carbon preference in the nC_{11}–nC_{20} range alkanes, and their more linear n-alkane profile (Figs. 5,6). They display moderate abundances of isoprenoids with typical Pr/Ph, Pr/nC_{17}, and Ph/nC_{18} values of 1.31, 0.52, and 0.47, respectively. A moderate amount of aryl-isoprenoids is observed along with minor alkylated cyclic compounds. The per mil carbon-isotope values obtained for two of these oils averaged –30.6, –30.8, and –30.3 for the whole oil, saturate, and aromatic fractions, respectively. Type A oils are generally located in Pennsylvanian reservoirs adjacent to areas where Pennsylvanian sediments are within the oil window (e.g., Leon North, Mountain Creek, and Isom Springs SW fields).

Type B Oils

Oils assigned to Type B have n-alkane profiles similar to the Type A oils (Figs. 5,6), but have increased abundances of acyclic isoprenoids. Typi-

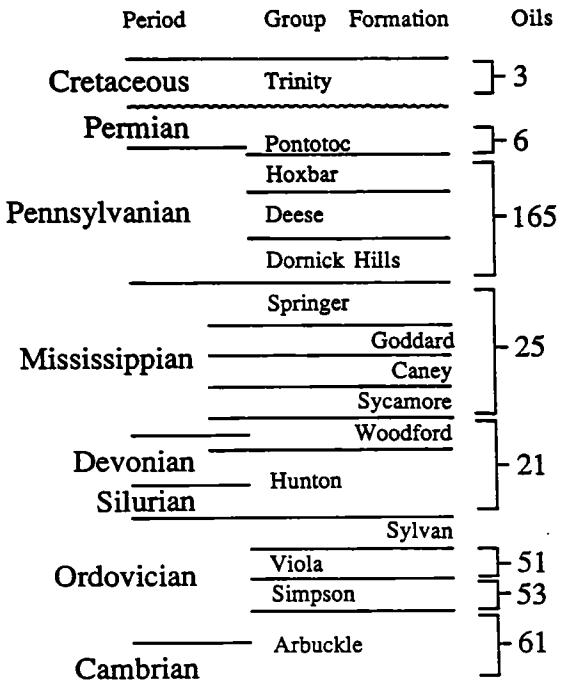

Figure 2. Stratigraphic distribution of 385 oil samples.

cal values for Pr/Ph, Pr/nC_{17}, and Ph/nC_{18} are 1.41, 0.85, and 0.70, respectively. Again, moderate amounts of aryl-isoprenoids are observed along with minor alkylated cyclic compounds. The per mil carbon-isotope values obtained for two of these oils averaged –30.8, –30.9, and –30.3 for the whole oil, saturate, and aromatic fractions, respectively. Type B oils commonly occur in Mississippian-age reservoirs, particularly within the Springer Group (e.g., Aylesworth SE, Sho-Vel-Tum, and Springer fields).

Type C Oils

Oils assigned to Type C have n-alkane profiles that decrease exponentially with increasing carbon number from a maximum in the mid-range n-alkanes (Figs. 5,6). These oils display a minor to trace odd-carbon preference in the nC_{11}–nC_{20} alkane range and contain relatively minor abundances of isoprenoids with typical Pr/Ph, Pr/nC_{17}, and Ph/nC_{18} values of 1.48, 0.32, and 0.27, respectively. The per mil carbon-isotope values obtained for two of these oils averaged –30.1, –30.4, and –29.9 for the whole oil, saturate, and aromatic fractions, respectively. Similar to Type A and B oils, Type C oils have a moderate amount of aryl-isoprenoids, minor alkylated cyclic compounds,

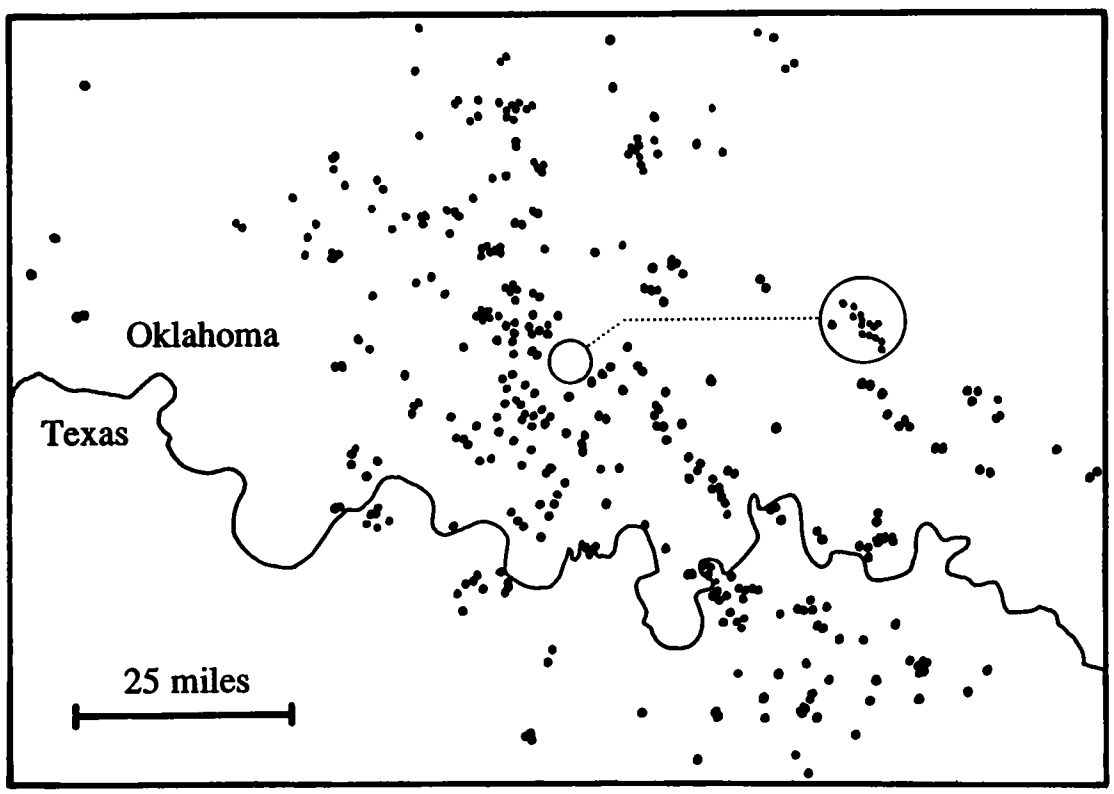

Figure 3. Geographic distribution of 385 oil samples.

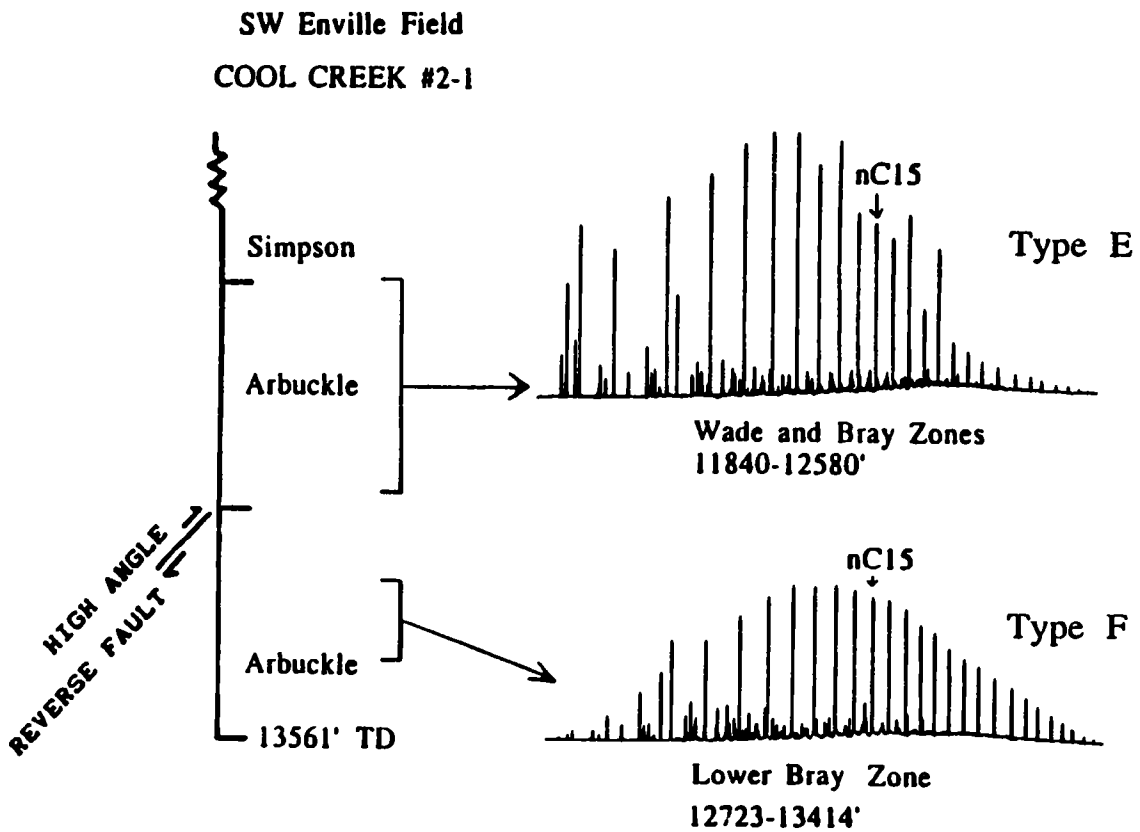

Figure 4. Illustration of the importance of systematic sample collection.

and trace concentrations of alkylated cyclic sulfur compounds. Type C oils are quite common in Hunton Group/Woodford Formation reservoirs (e.g., Aylesworth, Isom Springs, and Springer fields), but also occur in all the producing horizons.

Type D Oils

Oils assigned to Type D have some characteristics that may lead some investigators to interpret Type D as a mixed oil type (e.g., mixed Type C + Type E). However, because Type D oils contain some compounds that have not been observed in the other oil groups, a mixing origin is unlikely. Type D oils have an increased abundance of mid-range n-alkanes that contain a moderate odd-carbon preference in the nC_{11}–nC_{20} range (Figs. 5,6). They contain a moderate amount of aryl-isoprenoids and typical values for Pr/Ph, Pr/nC_{17}, and Ph/nC_{18} are 1.10, 0.31, and 0.51, respectively. The per mil carbon-isotope values for two of these oils averaged –31.1, –31.3, and –30.9 for the whole oil, saturate, and aromatic fractions, respectively. The hydrocarbons that make Type D oils unique include the anomalously high concentrations of alkylated cyclic compounds (e.g., n-alkylcyclohexanes and n-alkylbenzenes) with an odd-carbon preference (Fig. 7), and moderate concentrations of alkylated sulfur compounds (Fig. 8). The extended hopanes (C_{31}–C_{35} triterpanes) are relatively abundant (Fig. 9), but the C_{34}/C_{35} hopane ratio is generally less than one. The end-member Type D oils commonly occur in Ordovician-age Viola Group reservoirs, particularly within the Marietta basin (e.g., Joiner City, Reck East, and Atlee fields).

Type E Oils

Oils that are dominated by n-alkanes with a strong odd-carbon preference in the C_{11} to C_{20} range and contain relatively minor amounts of the nC_{20+} hydrocarbons are assigned to Type E (Figs. 5,6). These oils display minor to trace amounts of isoprenoids with typical Pr/Ph, Pr/nC_{17}, and Ph/nC_{18} ratios of 1.41, 0.15, and 0.18, respectively. While these oils contain only trace amounts of n-alkylated cyclic hydrocarbons, sulfur compounds, and aryl-isoprenoids, they contain relatively abundant hopanes (vs. steranes) and relatively high C_{29}/C_{30} hopane ratios. The carbon-isotope values obtained for two of these oils are anomalously light; average values from whole oil, satu-

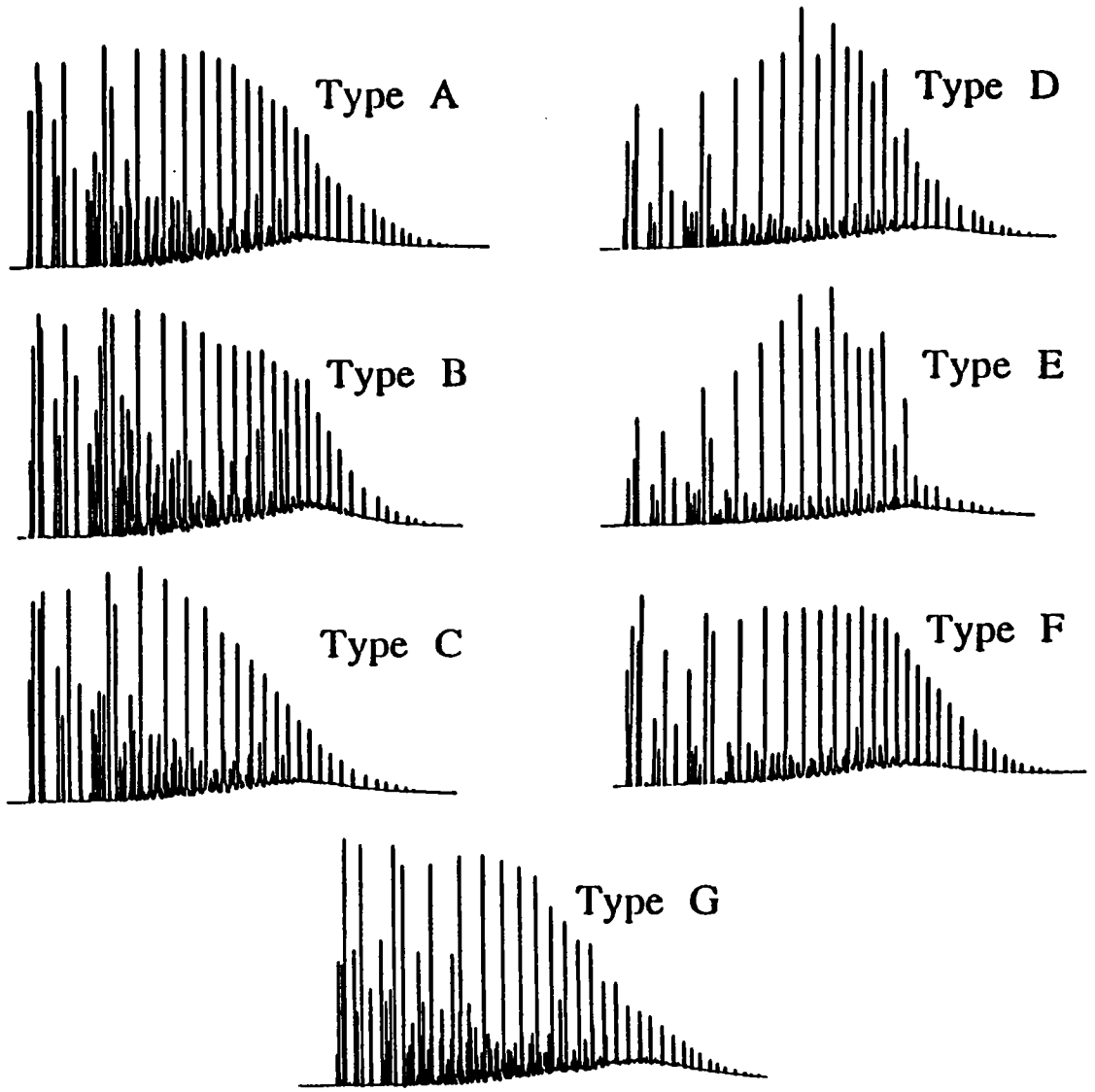

Figure 5. Gas chromatograms (GC–FID) of the end-member oil types.

rate, and aromatic fractions are –33.2‰, –33.5‰, and –32.9‰, respectively. As a group, Type E oils are generally restricted to Simpson and Arbuckle Group reservoirs (e.g., Robberson SE, Joiner City SE, and Ardmore SW fields).

Type F Oils

Oils assigned to Type F are unusual on both geochemical and stratigraphic grounds. These oils have smooth n-alkane profiles, minor isoprenoids (Figs. 5,6), and typical Pr/Ph, Pr/nC_{17}, and Ph/nC_{18} ratios of 1.64, 0.28, and 0.23, respectively. These oils contain relatively minor amounts of biomarker molecules (e.g., aryl-isoprenoids, hopanes, steranes) and have rather high maturity values (Fig. 10). The per mil carbon-isotope values obtained for two of these oils averaged –30.6, –30.7, and –30.3 for the whole oil, saturate, and aromatic fractions, respectively. These oils are restricted to Arbuckle Group reservoirs (e.g., drill stem test from McKenzie Hill and Cool Creek Formations at Cottonwood Creek field, Cool Creek Formation at Springer field, and the West Spring Creek Formation at Enville SW field).

Type G Oils

Oils assigned to Type G have some characteristics that may be interpreted as originating from mixing oil types, but because of their close proximity to the Ouachita facies (Fig. 1) these oils are assigned to one group for the purposes of this report until additional work can be completed.

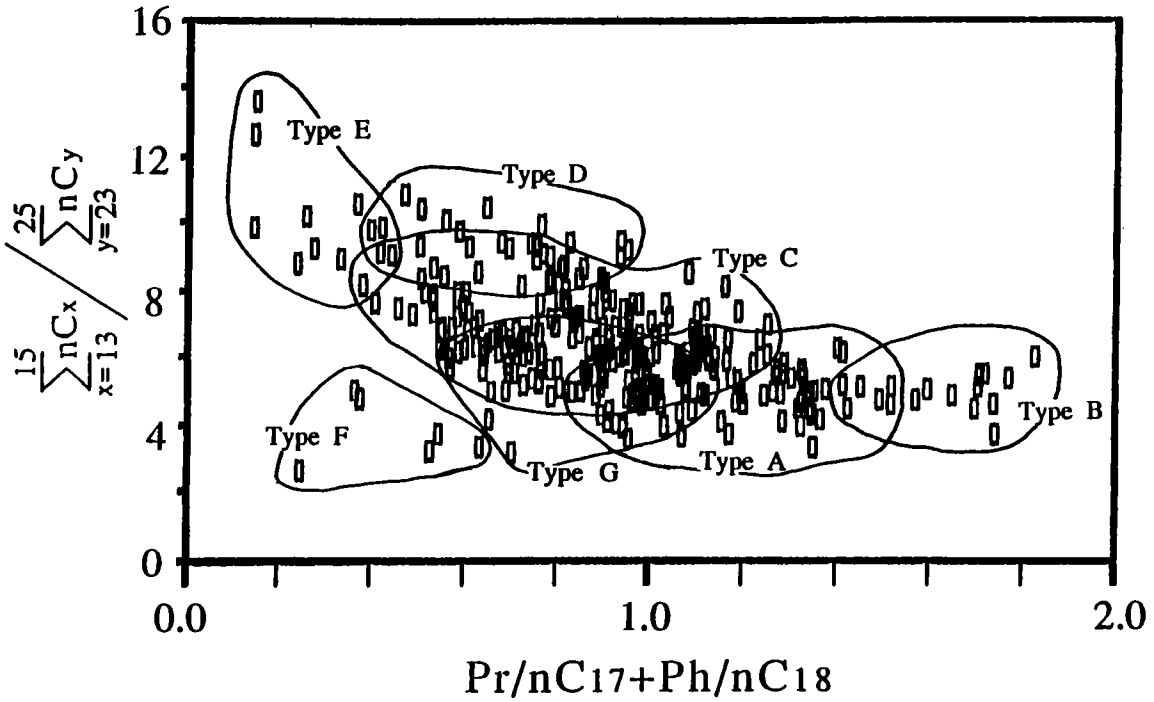

Figure 6. Plot showing typical end-member oil families using n-alkane and isoprenoid ratio values.

These oils are somewhat variable in composition, but are generally characterized by their relatively abundant C_{20+} n-alkanes and common odd-carbon preference (relatively minor) in the nC_{13}–nC_{20} range (Figs. 5,6). Typical values for Pr/Ph, Pr/nC_{17}, and Ph/nC_{18} can be considered to be 1.51, 0.39, and 0.37, respectively. The per mil carbon-isotope values obtained for two of these oils averaged –30.7, –30.5, and –30.5 for the whole oil, saturate, and aromatic fractions, respectively. These oils are commonly found in Simpson Group reservoirs in geographic proximity to the Ouachita facies (Fig. 1) (e.g., Cumberland and Sherman fields), but also occur in reservoirs in other stratigraphic units (e.g., Pennsylvanian reservoirs at Sherman and Case fields).

DISCUSSION

While the n-alkane and isoprenoid distributions are not universal source indicators, previous studies (e.g., Engel and others, 1988) have demonstrated their merit in Paleozoic geochemical programs. Burruss and Hatch (1989) reported that extracts from organic-rich Pennsylvanian sediments in the Anadarko basin are commonly enriched in higher molecular weight n-alkanes when compared to the older stratigraphic units. This relationship is likely to persist into the Ardmore and Marietta basins and remains consistent with a contribution of organic matter from higher plants (Albrecht and Ourisson, 1971; Tissot and Welte, 1984) in the source rocks for Type A oils. Furthermore, the general restriction of Type A oils to Pennsylvanian-age reservoirs adjacent to areas where Pennsylvanian-age sediments are within the oil window (Wavrek and Ferebee, 1991) supports the interpretation that the Type A oils were derived from Pennsylvanian-age source rocks. It is acknowledged, however, that possible complications involving active hydrocarbon generation (i.e., calculated maturity is increasing at a rate greater than a time function) and the possibility that some oils were derived from distant sources (i.e., Ouachita facies, Fort Worth basin, or Anadarko basin) are still under investigation.

The isoprenoid distributions in oils and source rocks are the result of complex interactions among precursor compounds, mechanisms of preservation, diagenesis, and catagenic alterations (Illich, 1983; Curry and Simpler, 1988). Despite their restricted utility, systematic trends have been observed in this study that help constrain a probable source for Type B oils. The enhanced isoprenoids and relatively abundant C_{20+} alkanes suggest that the depositional environment for these oils was relatively oxic and contained input from higher plant material (Tissot and Welte, 1984; Curry and Simpler, 1988). Based on the data available, lateral variations in organic content observed within Mississippian organic-rich rocks (e.g., Goddard, Caney, and Sycamore Formations) were appar-

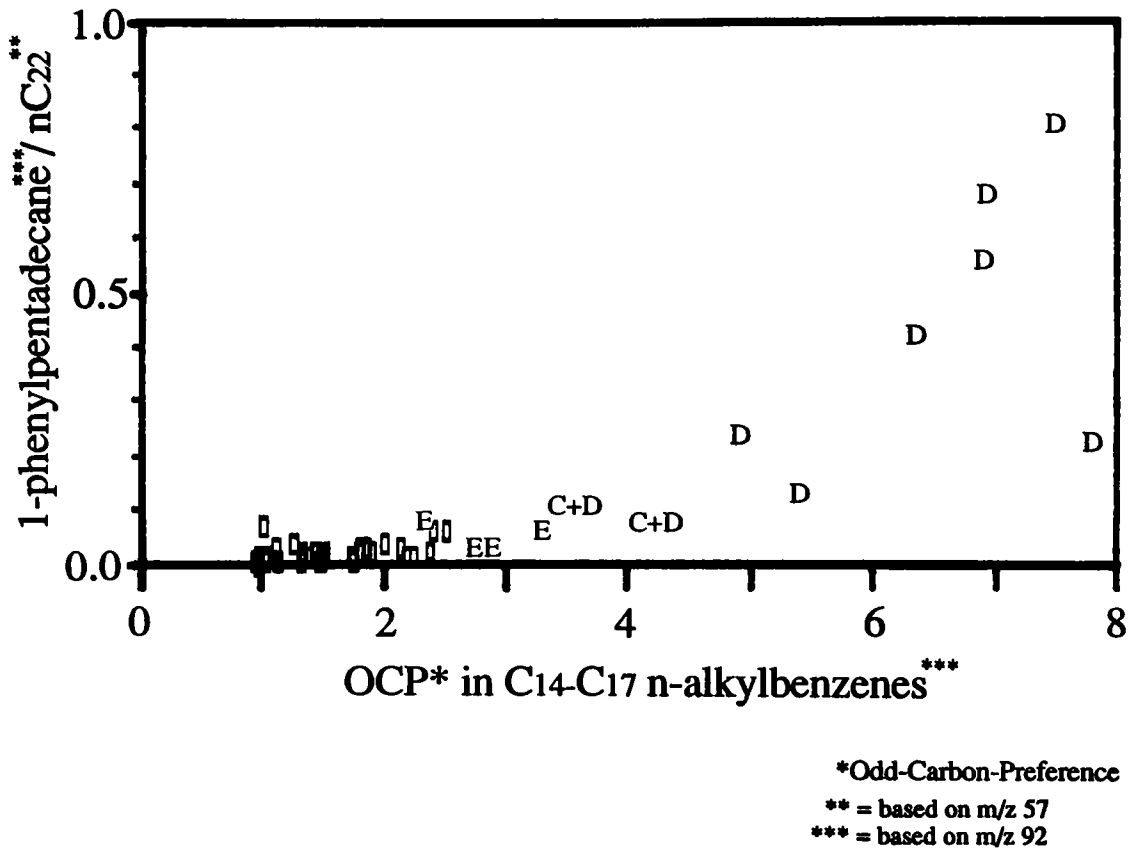

Figure 7. Illustration of the increased abundance and odd-carbon-preference of the n-alkylbenzenes in Type D oils. Data points without a letter designation (i.e., rectangles) are from oil Types A, B, C, F, and G. This figure also demonstrates the use of molecular parameters to unravel mixed oil types.

ently depositionally controlled; gas-prone kerogen facies accumulated on local highs, while oil-prone kerogen facies accumulated in depositional lows. In addition, the stratigraphic restriction of Type B oils to Mississippian-age reservoirs (i.e., particularly Springer Group) reinforces the correlation of Type B oils with Mississippian-age source rocks.

The Late Devonian–Early Mississippian Woodford Shale is a well-known petroleum source rock (Welte and others, 1975; Lewan and others, 1979; Winters and others, 1983; Comer and Hinch, 1987; Lewan, 1987; Burruss and Hatch, 1989; Wavrek, 1989,1990). It is generally agreed that the Woodford Shale is a laterally persistent, organic-rich rock interval with oil-prone kerogen of sufficient thermal maturity to source liquid hydrocarbons. Previous investigators have observed lateral variations on regional and local scales in organic content (Sullivan, 1985; Hester and others, 1990) and environmentally sensitive microfossils (Urban, 1960), but it is also acknowledged that some Pennsylvanian-age source rocks can yield a "Woodford-appearing" bitumen extract (R. C. Burruss, personal communication). Therefore, the effect of lateral variations in source rock facies will need to be addressed in future research. However, on the basis of the observed hydrocarbon distributions, I correlate Type C oils with the Woodford Shale.

Martin and others (1963) first reported the peculiar distribution of n-alkanes in crude oils from Ordovician-age reservoirs. Since that time, the strong odd-carbon preference in C_{11}–C_{20} n-alkanes, minor nC_{20+} alkanes, and the minor abundance of acyclic isoprenoids have become accepted as diagnostic of Ordovician-age source rocks on a global scale (Williams, 1974; Alexander and others, 1984; Fowler and Douglas, 1984; Jackson and others, 1984; Reed and others, 1986; Hoffmann and others, 1987; Longman and Palmer, 1987; Jacobson and others, 1988). Since both oil Types D and E share some of the "Ordovician character," additional clues must be used to distinguish the respective source intervals. Molecular indicators that support a correlation of Type D oils with carbonate source facies include the anomalously high concentrations of n-alkylcyclohexanes and n-alkylbenzenes with an odd-carbon preference (Fowler and Douglas, 1984; Connan and oth-

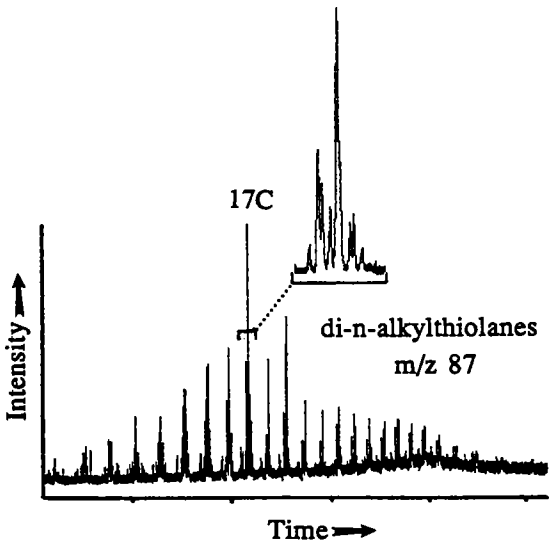

Figure 8. Ion trace of the di-n-alkylthiolanes that are prevalent in Type D oils. Compound identities are tentatively based on published data (e.g., Schmid and others, 1987; Sinninghe Damste and others, 1987; Strausz and others, 1990), although some of the minor peaks may originate from other alkylated molecules.

ers, 1986; Reed and others, 1986; Hoffmann and others, 1987; Williams and others, 1988), extended hopanes (McKirdy and others, 1983; Palacas and others, 1984; ten Haven and others, 1985,1988) and di-n-alkylthiolanes (Schmid and others, 1987; Sinninghe Damste and others, 1987,1989). Preliminary source-rock data, in conjunction with published reports (Galvin, 1983; Jones and Philp, 1990), support a correlation of Type D oils with the Viola Group. In particular, the Viola unit 1L (terminology of Glaser, 1965; Finney, 1988) contains significant source-rock potential in the basal chert layer (TOC average 1.31%, n = 30) and laminated marls (TOC average 2.4%, n = 7). While details of this source interval remain under investigation (Garcia, in preparation), the correlation is reinforced by the general stratigraphic restriction of Type D oils to Viola Group reservoirs.

While oil Types D and E share some chemical characteristics, Type E oils have distinct characteristics including a strong odd-carbon preference and the lack of the "carbonate-sourced" molecular indicators that are present in Type D oils. Support for a Type E oil/Simpson Group source-rock correlation is provided by extracts from Simpson Group sediments (TOC as much as 4.5%) within the study area, sedimentologic trends (Schramm, 1964; Wickham, 1978b), carbon isotope anomalies (Hatch and others, 1987), and the general stratigraphic restriction of Type E oils to Simpson and Arbuckle Group reservoirs.

The oils designated as Type F deserve discussion due to their low biomarker abundance (e.g., aryl-isoprenoids, hopanes, steranes), advanced maturity level, and stratigraphic restriction. The low biomarker abundance may be attributed to the advanced maturity level, low initial abundances, late generation from lean organic source facies, or selective destruction in the presence of sulfur species. While it is noted that Type F oils from the Cool Creek Formation and McKenzie Hill Formation drillstem tests (DST) at Cottonwood Creek are associated with reservoir anhydrite and hydrogen sulfide (David Read, personal communication), the oil samples have low total sulfur contents. Therefore, additional work will be required to unravel the status of Type F oils. Likewise, the genetic implications of Type G oils will require additional research due to their possible derivation from the Ouachita facies. Nevertheless, the compositional variability of Type G oils probably reflects multiple source intervals.

While the frequency distribution of oil types (Fig. 11) provides a useful summary of this research, several points need to be acknowledged. First, sample collection was biased toward the Lower Paleozoic (e.g., Arbuckle Group) and toward reservoirs likely to contain "non-Woodford"-sourced hydrocarbons. Second, oils suspected of being mixed oil types (10%) are included in the group with the closest end-members. This was done since extensive source-rock work will be required to accurately define the lateral variability in source-rock facies and to determine the effects of mixed kerogen types vs. mixed oil types. Third, oils that were mildly biodegraded (4%) were assigned a genetic oil type, but those oils that were severely biodegraded (6.5%) were excluded from the summary. Finally, it is believed that the frequency distribution of oil types (Fig. 11) would have an addi-

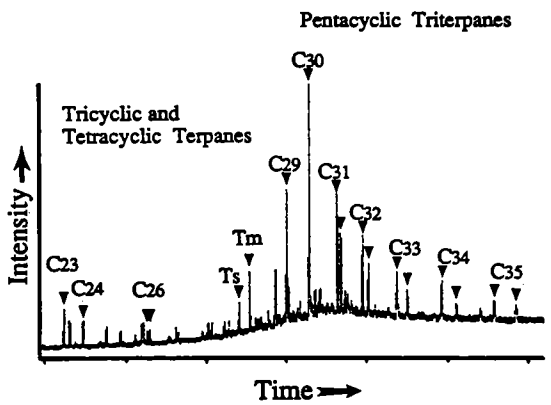

Figure 9. Ion trace of m/z 191 in a Type D oil.

tional skew toward Type C if the data were based on cumulative production.

CONCLUSIONS

The gas chromatographic analyses of 385 oils from the Ardmore and Marietta basins reveal the presence of seven oil types. Although the research is "in progress," tentative correlations have been established. Oil Types A through E appear to correlate with source facies within the Pennsylvanian (Atoka Formation?), Mississippian (Goddard, Caney, and Sycamore Formations), Devonian–Mississippian (Woodford Formation), upper Middle Ordovician (Viola Group), and Middle Ordovician (Simpson Group) rocks, respectively. Meanwhile, the "group" status of oil Types F and G along with the study of the lateral variations in source rock facies are still under investigation.

ACKNOWLEDGMENTS

The work described in this paper was supported by Amoco Research, ARCO, Chevron, Exxon, Mobil, Santa Fe Energy, and Unocal. I also wish to acknowledge Clive Ferebee (University of Tulsa) for his role in the exhaustive task of sample collection from the numerous operators (61), whose names will be published elsewhere.

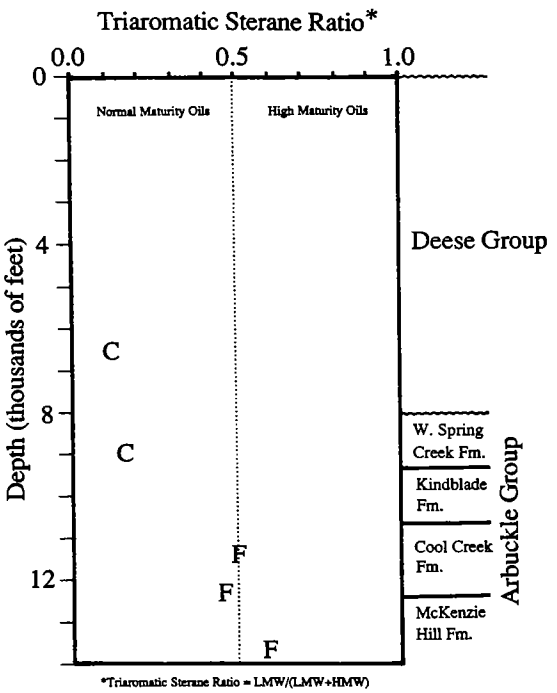

Figure 10. Maturity data plotted against reservoir depth at the Cottonwood Creek field. Letters refer to the oil type in each reservoir. LMW = low molecular weight; HMW = high molecular weight.

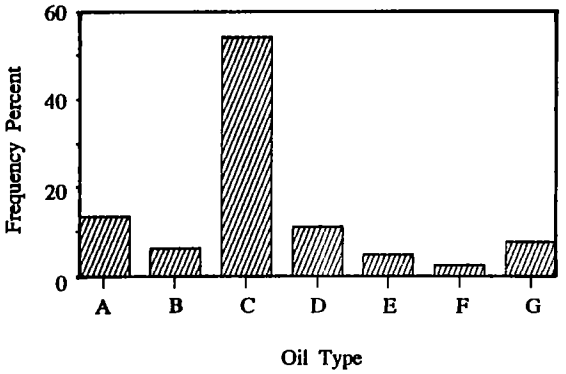

Figure 11. Frequency distribution of oil types reservoired in the Ardmore and Marietta basins.

REFERENCES

Albrecht, P.; and Ourisson, G., 1971, Biogenic substances in sediments and fossils: Angewandte Chemie International Edition, v. 10, p. 209–225.

Alexander, R.; Cumbers, M.; and Kagi, R. I., 1984, Geochemistry of some Canning basin crude oils, *in* Purcell, P. G. (ed.), The Canning basin, Western Australia: Proceedings of Geologic Society of Australia/Petroleum Exploration Society of Australia Symposium, p. 353–358.

Burruss, R. C.; and Hatch, J. R., 1989, Geochemistry of oils and hydrocarbon source rocks, greater Anadarko basin: evidence for multiple sources of oils and long-distance oil migration, *in* Johnson, K. S. (ed.), Anadarko basin symposium, 1988: Oklahoma Geological Survey Circular 90, p. 53–64.

Comer, J. B.; and Hinch, H. H., 1987, Recognizing and quantifying expulsion of oil from the Woodford Formation and age-equivalent rocks in Oklahoma and Arkansas: American Association of Petroleum Geologists Bulletin, v. 71, p. 844–858.

Connan, J.; Bouroullec, J.; Dessort, D.; and Albrecht, P., 1986, The microbial input in carbonate-anhydrite facies of a sabkha paleoenvironment from Guatemala: a molecular approach, *in* Leythaeuser, D.; and Rüllkotter, J. (eds.), Advances in organic geochemistry 1985: Pergamon, Oxford, p. 29–50.

Curry, D. J.; and Simpler, T. K., 1988, Isoprenoid constituents in kerogens as a function of depositional environment and catagenesis, *in* Mattavelli, L.; and Novelli, L. (eds.), Advances in organic geochemistry 1987: Pergamon, Oxford, p. 995–1001.

Engel, M. H.; Imbus, S. W.; and Zumberge, J. E., 1988, Organic geochemical correlation of Oklahoma crude oils using R- and Q-mode factor analysis: Organic Geochemistry, v. 12, p. 157–170.

Finney, S. C., 1988, Middle Ordovician strata of the Arbuckle and Ouachita Mountains, Oklahoma; contrasting lithofacies and biofacies deposited in

southern Oklahoma aulacogen and Ouachita geosyncline, *in* Hayword, O. T. (ed.), Geological Society of America, South-Central Section, Centennial field guide, p. 171–176.

Fowler, M. G.; and Douglas, A. G., 1984, Distribution and structure of hydrocarbons in four organic-rich Ordovician rocks: Organic Geochemistry, v. 6, p. 105–114.

Galvin, P. K., 1983, Deep-to-shallow carbonate ramp transition in Viola limestone (Ordovician), southwest Arbuckle Mountains, Oklahoma [abstract]: American Association of Petroleum Geologists Bulletin, v. 63, p. 466–467.

Garcia, M. A. [in preparation], Crude oil and source rock facies of the Viola Group in the Ardmore and Marietta basins, southern Oklahoma aulacogen: University of Tulsa M.S. thesis.

Glaser, G. C., 1965, Lithostratigraphy and carbonate petrology of the Viola Group (Ordovician), Arbuckle Mountains, south-central Oklahoma: University of Oklahoma unpublished Ph.D. dissertation, 197 p.

Hatch, J. R.; Jacobson, S. R.; Witzke, B. J.; Risatti, J. B.; Anders, D. E.; Watney, W. L.; Newell, D. K.; and Vuletich, A. K., 1987, Possible late Middle Ordovician organic carbon isotope excursion: evidence from Ordovician oils and hydrocarbon source rocks, Mid-continent and east-central United States: American Association of Petroleum Geologists Bulletin, v. 71, p. 1342–1354.

Hester, T. C.; Schmoker, J. W.; and Sahl, H. L., 1990, Effects of basin evolution on source-rock characteristics of the Woodford Shale, Anadarko basin, Oklahoma: U.S. Geological Survey Circular 1060, p. 34–36.

Hoffmann, P.; Dewey, J. F.; and Burke, K., 1974, Aulacogens and their genetic relation to geosynclines and a Proterozoic example from Great Slave Lake, Canada, *in* Dott, R. H., Jr.; and Shaver, R. H. (eds.), Modern and ancient geosynclinal sedimentation: Society of Economic Paleontologists and Mineralogists Special Publication 19, p. 38–55.

Hoffmann, C. F.; Foster, C. B.; Powell, T. G.; and Summons, R. E., 1987, Hydrocarbon biomarkers from Ordovician sediments and the fossil alga *Gloeocapsomorpha prisca* Zalessky 1917: Geochimica et Cosmochimica Acta, v. 51, p. 2681–2697.

Illich, H. A., 1983, Pristane, phytane, and lower molecular weight isoprenoid distributions in oils: American Association of Petroleum Geologists Bulletin, v. 67, p. 385–393.

Jackson, K. S.; McKirdy, D. M.; and Deckelman, J. A., 1984, Hydrocarbon generation in the Amadeus basin, central Australia: Australian Petroleum Exploration Association Journal, v. 24, p. 42–65.

Jacobson, S. R.; Hatch, J. R.; Teerman, S. C.; and Askin, R. A., 1988, Middle Ordovician organic matter assemblages and their effect on Ordovician-derived oils: American Association of Petroleum Geologists Bulletin, v. 72, p. 1090–1100.

Jones, P. J.; and Philp, R. P., 1990, Oils and source rocks from Pauls Valley, Anadarko basin, Oklahoma: Applied Geochemistry, v. 5, p. 429–448.

Lewan, M. D., 1987, Petrographic study of primary petroleum migration in the Woodford Shale and related rock units, *in* Doligez, B. (ed.), Migration of hydrocarbons in sedimentary basins: Editions Technip, Paris, p. 113–130.

Lewan, M. D.; Winters, J. C.; McDonald, J. H., 1979, Generation of oil-like pyrolyzates from organic-rich shales: Science, v. 203, p. 897–899.

Longman, M. W.; and Palmer, S. E., 1987, Organic geochemistry of Mid-continent Middle and Late Ordovician oils: American Association of Petroleum Geologists Bulletin, v. 71, p. 938–950.

Martin, R. L.; Winters, J. C.; and Williams, J. A., 1963, Distribution of n-paraffins in crude oils and their implication to origin of petroleum: Nature, v. 199, p. 110–113.

McKirdy, D. M.; Aldridge, A. K.; and Ypma, P. J. M., 1983, A geochemical comparison of some crude oils from pre-Ordovician carbonate rocks, *in* Bjorøy, M.; Albrecht, P.; Cornford, C.; de Groot, K.; Eglington, G.; Galimov, E.; Leythaeuser, D.; Pelet, R.; Rüllkotter, J.; and Speers, G. (eds.), Advances in organic geochemistry 1981: Wiley, Chichester, United Kingdom, p. 99–107.

Palacas, J. G.; Anders, D. E.; and King, J. D., 1984, South Florida basin—a prime example of carbonate source rocks of petroleum, *in* Palacas, J. G. (ed.), Petroleum geochemistry and source rock potential of carbonate rocks: American Association of Petroleum Geologists Studies in Geology No. 18, p. 71–96.

Pruatt, M. A., 1975, The southern Oklahoma aulacogen: a geophysical and geological investigation: University of Oklahoma unpublished M.S. thesis, 62 p.

Reed, J. D.; Illich, H. A.; Horsfield, B., 1986, Biochemical evolutionary significance of Ordovician oils and their sources, *in* Leythaeuser, D.; and Rüllkotter, J. (eds.), Advances in organic geochemistry 1985: Pergamon, Oxford, p. 347–358.

Schmid, J. C.; Connan, J.; and Albrecht, P., 1987, Occurrence and geochemical significance of long-chain dialkylthiacyclopentanes: Nature, v. 329, p. 54–56.

Schramm, M. W., Jr., 1964, Paleogeologic and quantitative lithofacies analysis, Simpson Group, Oklahoma: American Association of Petroleum Geologists Bulletin, v. 48, p. 1164–1195.

Sinninghe Damste, J. S.; de Leeuw, J. W.; Kock-van Dalen, A. C.; de Zeeuw, M. A.; de Lange, F.; Rijpstra, W. I. C.; and Schenck, P. A., 1987, The occurrence and identification of series of organic sulphur compounds in oils and extracts. I.—A study of Rozel Point oil (U.S.A.): Geochimica et Cosmochimica Acta, v. 51, p. 2369–2391.

Sinninghe Damste, J. S.; Rijpstra, W. I. C.; de Leeuw, J. W.; Schenck, P. A., 1989, The occurrence and identification of series of organic sulphur compounds in oils and sediment extracts: II.—Their presence in samples from hypersaline and non-hypersaline paleoenvironments and possible application as source, paleoenvironmental and maturity indicators: Geochimica et Cosmochimica Acta, v. 53, p. 1323–1341.

Strausz, O. P.; Lown, E. M.; and Payzant, J. D., 1990, Nature and geochemistry of sulfur-containing

compounds in Alberta petroleums, *in* Orr, W. L.; and White, C. M. (eds.), Geochemistry of sulfur in fossil fuels: American Chemical Society, Washington, D.C., p. 366–396.

Sullivan, K. L., 1985, Organic facies variation of the Woodford Shale in western Oklahoma: Shale Shaker, v. 35, p. 76–89.

ten Haven, H. L.; de Leeuw, J. W.; and Schenck, P. A., 1985, Organic geochemical studies of a Messinian evaporitic basin, northern Apennines (Italy). I.—Hydrocarbon biological markers for a hypersaline environment: Geochimica et Cosmochimica Acta, v. 49, p. 2181–2191.

ten Haven, H. L.; de Leeuw, J. W.; Sinninghe Damste, J. S.; Schenck, P. A.; Palmer, S. E.; and Zumberge, J. E., 1988, Application of biological markers in the recognition of paleo-hypersaline environments, *in* Fleet, A. J.; Kelts, K.; and Talbot, M. R. (eds.), Lacustrine petroleum source rocks: Geological Society of America Special Publication 40, p. 123–130.

Thompson, T. L., 1976, Plate tectonics in oil and gas exploration of continental margins: American Association of Petroleum Geologists Bulletin, v. 60, p. 1463–1501.

Tissot, B. P.; and Welte, D. H., 1984, Petroleum formation and occurrence [second revised edition]: Springer-Verlag, New York, 699 p.

Urban, J. B., 1960, Microfossils of the Woodford Shale (Devonian) of Oklahoma: University of Oklahoma unpublished M.S. thesis, 77 p.

Wavrek, D. A., 1989, Characterization of oil types along Hewitt trend, Carter County, Oklahoma [abstract]: American Association of Petroleum Geologists Bulletin, v. 73, p. 424.

_____1990, Southern Oklahoma aulacogen: an integrated basin model [abstract]: American Association of Petroleum Geologists Bulletin, v. 74, p. 788.

Wavrek, D. A.; and Ferebee, C. D., 1991, Ardmore and Marietta basins—an integrated basin model: University of Tulsa Research Consortium Report, 144 p.

Welte, D. H.; Hagemann, H. W.; Hollerbach, A.; Leythaeuser, D.; Stahl, W., 1975, Correlation between petroleum and source rock: Proceedings of the Ninth World Petroleum Congress, part 2, p. 179–191.

Wickham, J. S., 1978a, The southern Oklahoma aulacogen, *in* Structural style of the Arbuckle region: Geological Society of America, South-Central Section, Guidebook for field trip no. 3, p. 8–41.

_____1978b, Oil Creek Formation, *in* Structural style of the Arbuckle region: Geological Society of America, South-Central Section, Guidebook for field trip no. 3, p. 98–99.

Williams, J. A., 1974, Characterization of oil types in Williston basin: American Association of Petroleum Geologists Bulletin, v. 58, p. 1243–1252.

Williams, J. A.; Dolcater, D. A.; Torkelson, B. E.; and Winters, J. C., 1988, Anomalous concentrations of specific alkylaromatic and alkylcycloparaffin components in West Texas and Michigan crude oils, *in* Mattavelli, L.; and Novelli, L. (eds.), Advances in organic geochemistry 1987: Pergamon, Oxford, p. 47–59.

Winters, J. C.; Williams, J. A.; and Lewan, M. D., 1983, A laboratory study of petroleum generation by hydrous pyrolysis, *in* Bjorøy, M.; Albrecht, P.; Cornford, C.; de Groot, K.; Eglington, G.; Galimov, E.; Leythaeuser, D.; Pelet, R.; Rüllkotter, J.; and Speers, G. (eds.), Advances in organic geochemistry 1981: Wiley, Chichester, United Kingdom, p. 524–533.

Hydrocarbon-Induced Diagenetic Aureoles in Southwestern and Southern Oklahoma

Zuhair Al-Shaieb
Oklahoma State University

Janet Cairns
Amoco Production Co., Tulsa

R. A. Lilburn
Union Oil of California, Oklahoma City

ABSTRACT.—The Permian red beds that overlie some giant oil fields in southwestern and southern Oklahoma have undergone extensive mineralogical and chemical diagenesis. The diagenetic minerals occur within a distinctly zoned aureole that delineates the position of the oil field. The geometries of the aureoles strongly reflect the major structural elements that controlled emplacement of hydrocarbons in the underlying rocks. Calcite, ferroan calcite, manganese-rich calcite, dolomite, ankerite, pyrite, marcasite, and native sulfur are the major diagenetic minerals. The innermost zone of each aureole is characterized by abundant carbonate cementation and generally coincides with a major fault system. Pyrite and marcasite cements are commonly associated with carbonate-cemented zones; these minerals occur also in the bleached sandstones.

$\delta^{13}C_{PDB}$ values of carbonate cements indicate three major sources of carbon: (1) an organic source with $\delta^{13}C$ values of approximately –32‰, (2) a freshwater source with an average $\delta^{13}C$ value of -8.0 ± 3‰, and (3) a hybrid source (freshwater and organic). A mixing model was developed to calculate the proportion of organic carbon in carbonate cement.

$\delta^{34}S$ values of pyrite and marcasite average +6.1‰ and range from –9 to +16‰. The isotopic composition of sulfides is similar to that of oil in the underlying reservoir. Formation of diagenetic pyrite and marcasite is explained by reduction of iron oxides in red beds by hydrogen sulfide, and by other organic material associated with hydrocarbons.

The hydrocarbon-induced diagenetic aureoles (HIDA) concept can be used in exploration for oil and gas, specifically in structurally controlled reservoirs.

Geochemistry of Pennsylvanian Crude Oils and Source Rocks in the Greater Anadarko Basin, Oklahoma, Texas, Kansas, Colorado, and Nebraska: An Update

Robert C. Burruss and Joseph R. Hatch
U.S. Geological Survey, Denver

ABSTRACT.—Our previous work indicated that three basic factors affect the composition of petroleum throughout the basin: (1) three distinct types of crude oils, which occur in stratigraphically distinct reservoirs, were generated from three major source-rock sequences (Upper Ordovician Sylvan Shale, Upper Devonian–Lower Mississippian Woodford Shale, and Middle and Upper Pennsylvanian marine shales); (2) these oil types have intermixed; and (3) oils in all reservoirs are systematically depleted in benzene and toluene with increasing distance from the thermally mature to overmature basin depocenter, suggesting water-washing during migration over distances as great as 300 mi.

Recent exploration interest in Lower Pennsylvanian oil reservoirs along the western and northern margin of the basin led us to reevaluate evidence for Pennsylvanian source rocks, a Pennsylvanian oil type, and long-distance migration. Many samples of Lower, Middle, and Upper Pennsylvanian shales from the northern and western shelves of the basin are of low to moderate thermal maturity (T_{max} <450°C) and have total organic carbon values >1%. Rock-Eval pyrolysis of these shales reveals, however, that they differ greatly in quality as potential sources of oil. Shales from the Lower Pennsylvanian Morrow and Springer Formations in western Oklahoma have hydrogen indices (HIs) in the range of 20–80, whereas the thin, widespread, marine Middle and Upper Pennsylvanian shales in western Oklahoma and Kansas have HIs in the range of 200–350. These low and high ranges of HI are typical of source rocks containing, respectively, gas-prone (type III) terrestrial organic matter and oil prone (type II) marine organic matter. Both vitrinite reflectance and Rock-Eval T_{max} measurements indicate that the organic matter in Pennsylvanian rocks in western Kansas, southeastern Colorado, and parts of northern Oklahoma is thermally immature to marginally mature and did not generate the oil and gas that accumulated in these areas.

Crude oils in Pennsylvanian reservoirs share certain common characteristics (such as methylcyclohexane > n-heptane, relatively heavy carbon-isotopic composition, and abundant n-alkanes > n-C_{15}), but show relatively large ranges in composition compared to other oil types in the basin. Some of this variability is due to mixing with oils generated from the Woodford Shale and Ordovician shales, but a significant component appears to be due to variations in depositional environment and thermal maturity of source rocks throughout the Pennsylvanian section. For example, marginally mature, thin, Middle and Upper Pennsylvanian marine shales appear to be source rocks for oils that contain amounts of isoprenoids equal to or greater than adjacent n-alkanes, and that have pristane/phytane ratios in the range 1.0–1.3.

Pennsylvanian oils from western Kansas and southwestern Nebraska show systematic depletion of toluene with distance from the Anadarko basin depocenter, as do Pennsylvanian oils from the eastern flank of the Las Animas arch in southeastern Colorado. However, Pennsylvanian oils from the western flank of the Las Animas arch are not depleted in toluene. The whole-oil compositions from both sides of the arch are similar, but the contrast in the toluene content suggests the oils were affected by different hydrologic regimes. One possible explanation is that oils on the east side of the arch migrated from source rocks in the Anadarko basin, whereas those on the west side may have been derived from the Denver basin.

Oil in Permian Karst in the Slick Hills of Southwestern Oklahoma

R. Nowell Donovan and Arthur B. Busbey
Texas Christian University

R. Douglas Elmore and Michael H. Engel
University of Oklahoma

INTRODUCTION

The Slick Hills of southwestern Oklahoma are the exposed portion of the frontal Wichita fault zone, an area of considerable tectonic complexity lying between the Wichita Mountain uplift and the Anadarko basin (Fig. 1). Deformation occurred during Pennsylvanian and earliest Permian times; total stratigraphic displacement of Cambrian igneous basement rocks across the zone is as much as 45,000 ft. This often-cited and truly enormous displacement is the result of two distinct, yet juxtaposed, architectural elements. During the Pennsylvanian, an existing lower Paleozoic sedimentary basin was partly inverted. The Wichita Mountain uplift is the area of greatest inversion; up to 10,000 ft of lower Paleozoic sediments plus perhaps 5,000 ft of igneous basement rocks have been eroded from the uplift. To the north, across the frontal Wichita fault zone, the Anadarko basin developed as a complex syntectonic depocenter in which as much as 30,000 ft of Late Mississippian, Pennsylvanian, and Permian sediments were deposited. Thus the frontal Wichita fault zone is, quantitatively, the most significant line of inversion. Most of the displacement within the zone was accomplished by movements on large, oblique (left-lateral) reverse faults. These faults compartmentalized blocks of lower Paleozoic rocks that show various degrees of internal strain. Both drilling and seismic data suggest that a large part of the frontal Wichita fault zone, including the

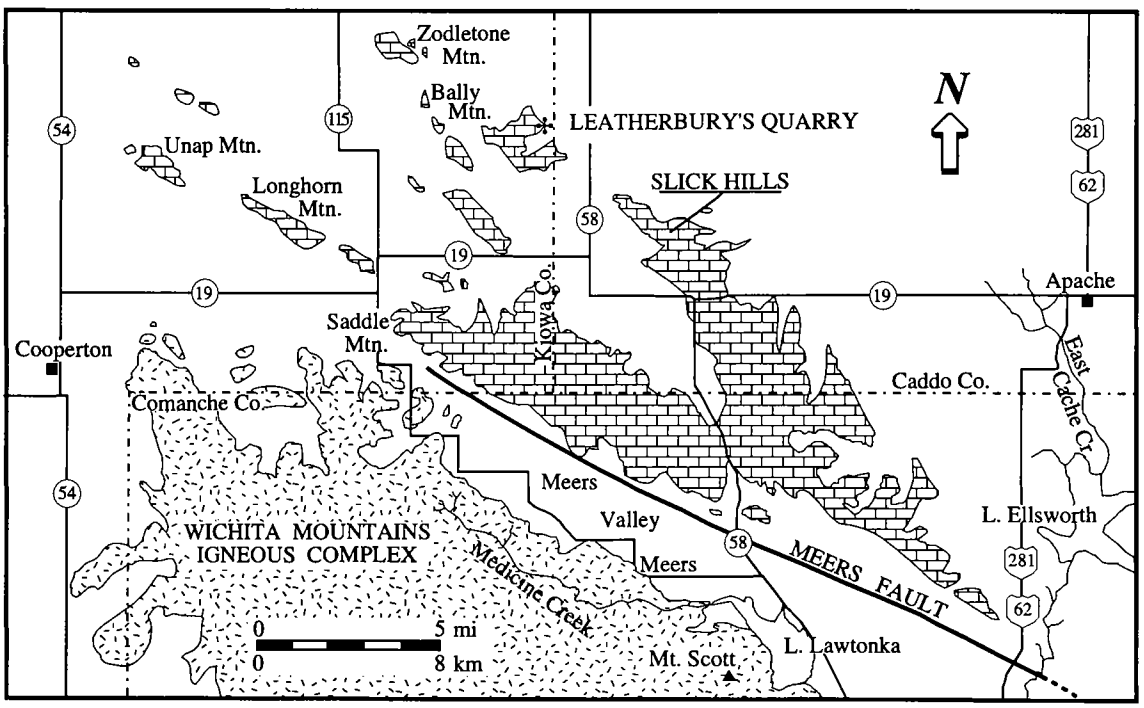

Figure 1. Map of the Slick Hills and adjacent parts of the Wichita Mountains showing the location of Leatherbury's Quarry.

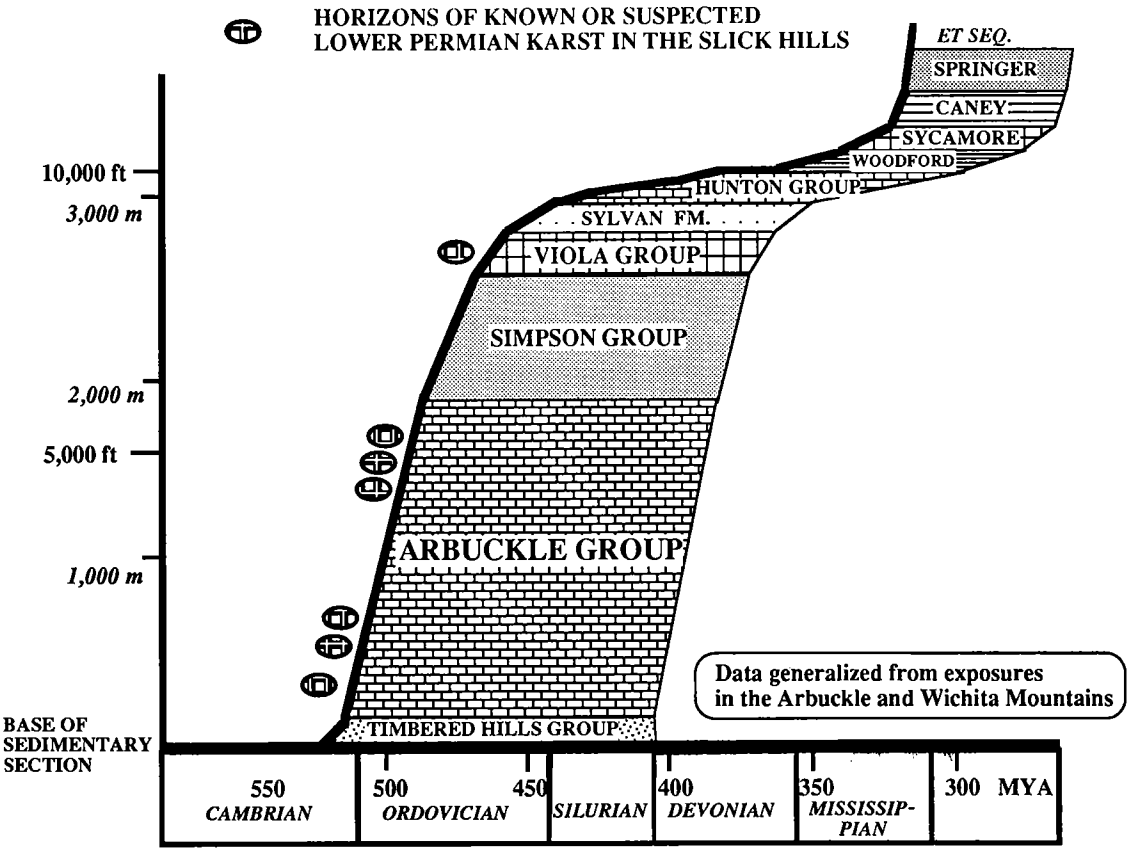

Figure 2. Stratigraphic section exposed in the Slick Hills and Arbuckle Mountains; stratigraphic intervals where known or suspected Permian karst is developed in the Slick Hills are shown.

northern part of the Slick Hills, overlies the Anadarko basin (Donovan, 1986; Donovan and others, 1989).

The Slick Hills are built of Cambrian and Ordovician sedimentary rocks (mostly carbonates) that unconformably overlie a Cambrian igneous basement (Fig. 2). The great bulk of the outcrop is formed by limestones (plus some dolomites) that are assigned to the Arbuckle Group.

The Wichita Mountains and the Slick Hills are an impressive example of exhumed topography. In essence, they were sculpted during the Early Permian and then buried beneath a blanket of later Permian alluvium, eolian sandstones, and evaporites (Donovan, 1986). In this paper we are concerned with analyzing the original Permian geomorphology of the Slick Hills, with particular emphasis on the development of karst. Small cave systems have previously been documented (Simpson, 1979; Donovan, 1982) and are securely dated as Permian on the basis of their vertebrate-fossil content. Of special interest in the present context is the fact that many of the speleothems that decorate the walls of the caves contain substantial traces of hydrocarbons (Donovan, 1987). Paleomagnetic data obtained from the speleothems have yielded Permian magnetic-pole positions (Elmore and others, 1987).

In this paper we describe a small development of karst exposed in Leatherbury's Quarry (SE¼ NE¼ sec. 25, T. 6 N., R. 14 W.) on the northeastern edge of the Bally Mountain range, which is the northwestern part of the Eastern Slick Hills (for location see fig. 1 in Donovan and Ragland, 1991; for preliminary description see Donovan and Busbey, 1991). First we describe physical aspects of the system, then the evidence for the age of the system, and finally the hydrocarbon imprint.

KARST IN THE SLICK HILLS

The surface of the Slick Hills displays a hierarchy of karst-solution features, including such small-scale features as pits, pans, trittkaren, rillenkarren, and solution runnels (classification from Ford and Williams, 1989). The dominant geomorphic element is provided by an interplay of fracture-controlled linear karren; splitkarren

(joint, stylolite, and vein-controlled solution fissures) and the larger kluftkarren and flachkarren (also known as grikes and clints, respectively) constitute the dominant elements of limestone pavement. Grikes (kluftkarren) are produced by solution along master joints; several that intersect the walls of the Bally cave open downward into cave systems. This relationship suggests that some of the surface karst imprint seen in the Slick Hills is of Permian vintage.

The well-known "tombstone topography," which characterizes outcrops in both the Slick Hills and Arbuckle Mountains, is a form of limestone pavement developed in steeply dipping beds. As a consequence of the steep dip, the limestone pavements are dominated by splitkarren that are due to solution along bedding planes and bedding-parallel stylolites.

THE CAVE SYSTEM IN LEATHERBURY'S QUARRY

The cave system was first exposed during quarrying operations about 30 years ago, but the quarry has been inactive for about 25 years (Doyle Leatherbury, personal communication, 1991). The quarry was cut in limestones of the upper part of the Ordovician Kindblade Formation (Arbuckle Group). This part of the section is characterized by relatively thick layers (as much as 5 ft) that dip consistently NE at angles of 15–20°. Two or three thin impermeable clay-rich layers are found in the section; they exert some control on modern seepage into the quarry. However, the development of Permian karst was controlled by tectonic fractures rather than bed boundaries. No signs indicate that water circulation was confined.

Fractures in the quarry show a complex bimodal arrangement (Fig. 3). The dominant NE-trending set, which is perpendicular to bedding, consists of vertical fractures. While many fractures in the secondary NW-dipping set are also vertical, some dip at high angles SW, which suggests that they may predate tectonic tilting of the section. Many fractures are filled by nonfibrous calcite and, more rarely, dolomite. In addition, numerous fractures are coated by thin veneers of solid bitumen.

The karst is principally developed as fissures (as much as 60 ft deep) that have developed from the solution of master joints in both joint sets, particularly the NE-trending set. In general, the fissures are very narrow; only two of them have opened to a width of more than 3 ft. As noted above, these fissures open at the surface into grikes (kluftkarren). The extent of the karst outside of the quarry cannot be readily ascertained, although deeply weathered grikes extend for several hundred yards up the hillside southwest of the quarry. Interestingly, the karst is developed on the crest of

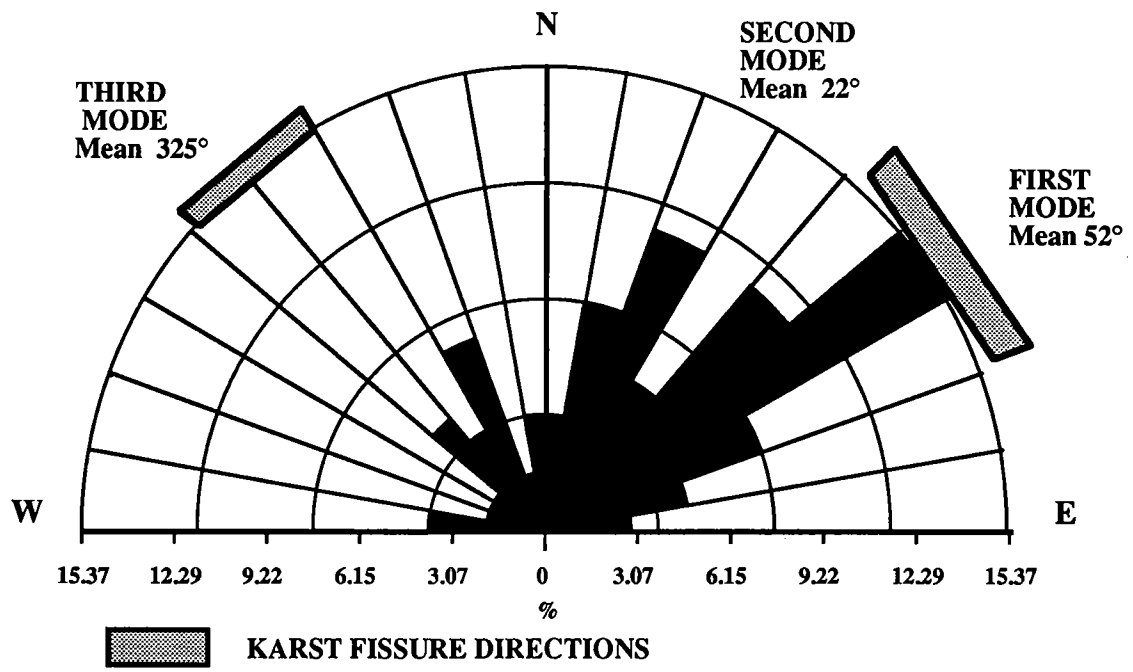

Figure 3. A joint and fissure analysis conducted in Leatherbury's Quarry shows that the two principal karst-fissure directions correspond with orthogonal joint sets in the quarry.

a convex hill spur and bears no relationship to any existing surface-drainage pattern. However, since the principal karst passages are aligned in the same general direction as the dip of the Arbuckle Group at this location, it could be argued that the underground drainage was inherited from a consequent drainage pattern at the surface.

OUTLINE OF THE PRINCIPAL FEATURES OF THE CAVE SYSTEM

Features of the cave system include the following characteristics.

1) A series of solution-widened linear fissures with some small chambers.

2) Calcite speleothems, many of which contain inclusions and coatings of hydrocarbons.

3) A variety of clastic deposits, including green illitic clay, limestone pebbles, bone fragments, rounded pebbles of speleothem (some with hydrocarbon inclusions), and large angular blocks of speleothem. Some of the clay is impregnated with hydrocarbons and is stained deep brown as a result.

Generally, lower levels in the caves are dominated by speleothems while upper levels contain more abundant and coarser clastic deposits. We emphasize, however, that the architectural relationships between the two levels are very complicated.

Solution Features in the Karst

The walls of the fissures display a large number of solution features, some of which are attributable to phreatic flow, others to vadose flow. Thus at lower levels in the quarry, as in the case of the "World's smallest oil field" (Donovan, 1987), the circular cross section of a conduit that is now filled by speleothem deposits suggests that it originated as a phreatic passage. On the other hand, other cave cross sections suggest that much vadose modification through entrenchment has taken place and that vadose features dominate the present form of the caves.

In detail, small-scale corrosional scalloping is developed on some fissure walls, while corrosion notches in some of the larger chambers suggest that at one time they were partially filled by pools of water. Corrosion notches cut some speleothems, suggesting that the caves have a complex history.

Speleothems

Calcite speleothems are the most obvious feature in the lower parts of the cave system. Among the varieties of speleothem that have been found are flowstone, cave popcorn, stalactites, and stalagmites. Given the small size of the chambers

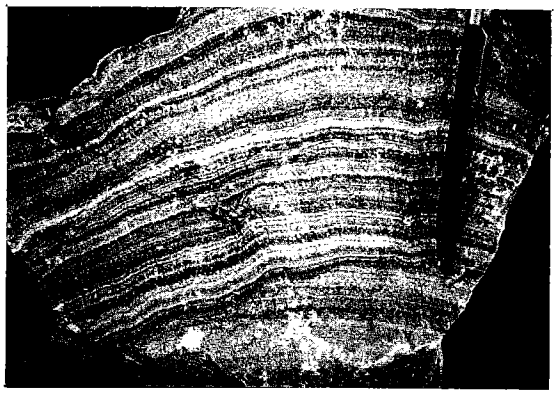

Figure 4. Loose block of flowstone; truncated laminae beneath the pencil tip indicate a discordant dissolution event.

(up to 3 ft across) and fissures, most of the deposits seen are types of flowstone. Flowstone coats are as much as 24 in. thick, and several varieties have been recognized. As outlined below, their detailed architecture reflects a complex history of deposition in both phreatic and vadose settings. Furthermore, it is clear that, on occasion, deposition was interrupted by corrosional events (Fig. 4).

Flowstone Type A

Type A flowstones are constructed of tiers of coalesced subparallel fibrous calcite crystals that display internal growth lines recording continuous syntaxial growth. Crystals of this type are generally characterized by width:length ratios of ~5, and individual crystals as much as 5 in. long have been noted. The orientation of the crystals is generally perpendicular to the substrate (mostly the walls of fissures, but also limestone pebbles within the cave). Individual tiers of crystals within a flowstone are separated by disconformable surfaces on which the succeeding generation of fibrous crystals grew from fresh nucleation sites (Fig. 5).

Growth lines in the flowstones are formed by detrital clay, hydrocarbons, or, less commonly, hematite. Where present in abundance, these substances may have temporarily inhibited calcite precipitation thus forming tier boundaries in the flowstone (Figs. 5,6). Two forms of growth line can be recognized. The first is generally concavo-convex, parallel to the surface of the flowstone deposit, and probably records precipitation under vadose conditions. The second is euhedral, "dog-tooth spar" form. Growth lines of this form presumably record precipitation under phreatic conditions. Both forms of growth line can be found in the same flowstone, suggesting that water levels within the cave system fluctuated considerably.

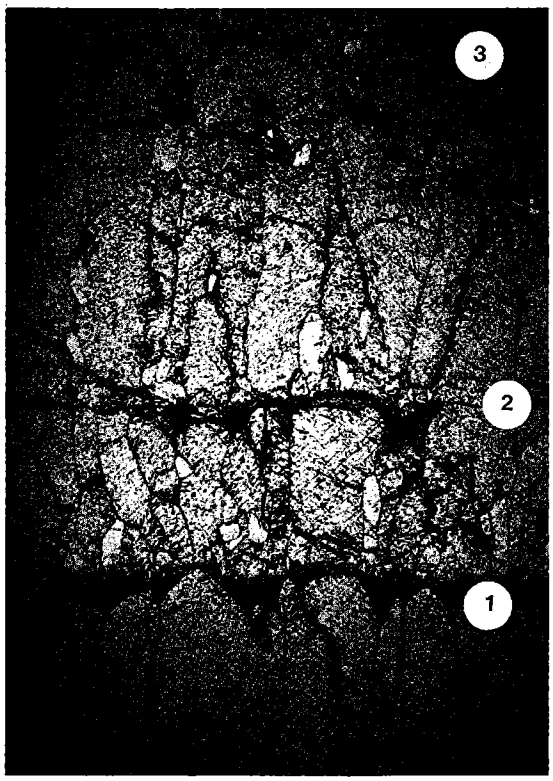

Figure 5. Photomicrograph, in plane-polarized light, of Flowstone Type A, showing three boundaries (1, 2, 3) separating tiers of subparallel coalescing fibrous crystals. Note curved (vadose) growth lines at 2 and dogtooth growth lines at 1, 3, and elsewhere. Field of view is 4 mm wide.

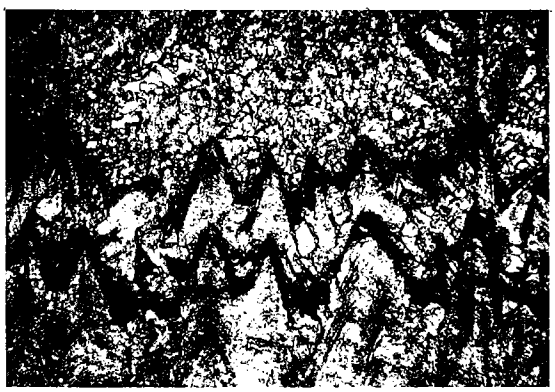

Figure 6. Photomicrograph, in plane-polarized light, of Flowstone Type A, showing hydrocarbon coats along dogtooth boundaries in phreatic flowstone. Apparently crystal growth was terminated on two occasions by an influx of hydrocarbons and clay. This deposit was precipitated in a small rimstone pool; the upper part of the view shows a mosaic of anhedral calcite mixed with detrital clay. Field of view is 3 mm wide.

Flowstone Type B

Type B flowstone consists of arrangements of coalescing subparallel fibrous crystals organized into a two-fold hierarchy. Large "crystals" as much as 12 in. long and 1 in. wide can be seen in thin section to be composed of nearly parallel bundles of numerous smaller crystals. Where growth lines are present, the smaller crystals are obvious. However, where they are absent, the larger "crystals" show slight differences in extinction across boundaries between the smaller crystals.

Growth lines invariably define crystal morphology, suggesting that Type B flowstone was deposited under phreatic conditions (Fig. 7). The final infill of the conduit described as the "World's smallest oil field" by Donovan (1987) consists of subvertical composite "crystals" of this type.

Flowstone Type C

Type C flowstone consists of tiers of subparallel acicular calcite crystals as much as 2.5 in. long.

Figure 7. Photomicrograph, in crossed-polarized light, of Flowstone Type B, showing how the larger fibrous "crystals" (e.g., 1, 2) are composite aggregates of smaller fibrous crystals. The latter are clearly demarcated by the dogtooth spar arrangement of hydrocarbon inclusions. Field of view is 4 mm across.

These crystals do not coalesce, so the texture is porous. In some cases the porosity is preserved. More commonly, it has been partially or completely filled by equant microspar (Fig. 8).

Typically the crystals do not have euhedral terminations, and growth lines are not generally found. The origin of this type of flowstone is unclear. It is conceivable that this texture records an inversion from an aragonite precursor.

Flowstone Type D

Rare opaque green flowstone, Type D, consists of crystals contaminated by abundant illite inclusions. Type D flowstone is always located at the junction of a speleothem and a younger clay infill. It appears to have been precipitated under phreatic conditions and, presumably, records the final contamination of the speleothem. Some of the crystal terminations observed are curved, probably because the increasing amount of clay detritus significantly distorted the crystal lattices.

Figure 8. Photomicrograph, in crossed-polarized light, of Flowstone Type C, showing acicular crystals that do not coalesce but are separated by a mosaic of equant microspar. The microspar appears to partly replace the acicular crystals. Field of view is 4 mm wide.

Stalactites

To date, no discrete stalactite has been found in place. However, some flowstone curtains appear to be nucleated around straw stalactites (Figs. 9,10). The concentric straws are filled by anhedral calcite that shows strained extinction, suggesting that growth within the straw was aggressively competitive. On the other hand, crystals nucleated on the exterior of the straw are unstrained.

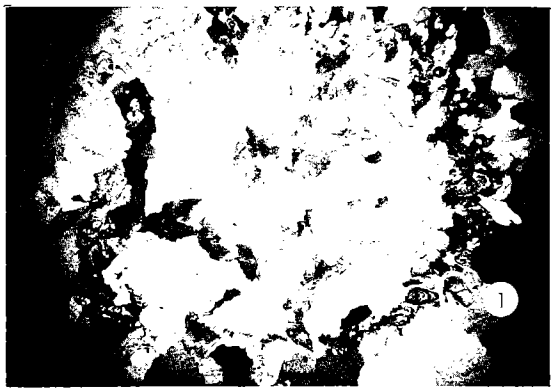

Figure 9. Photomicrograph, in crossed-polarized light, showing concentric outline of what is thought to be a stalactite enveloped by phreatic speleothem. Within the stalactite, the infilling anhedral calcite shows strained crystals, while crystals nucleated on the exterior of the stalactite show drusy growth patterns (Fig. 10 is a close-up of area "1"). Field of view is 12 mm across.

Figure 10. Photomicrograph, in crossed-polarized light, showing detail of the exterior surface of the stalactite shown in Figure 9. The exterior of the stalactite appears in the bottom right of the view (1). Presumably the stalactite was submerged and competitive drusy growth ensued. Notice the important role that hydrocarbon inclusions play in demarcating the growth of individual crystals. Field of view is 3 mm across.

Stalagmites

To date, a single discrete stalagmite has been found; this stalagmite was overlain by a thick deposit of clay (Fig. 11). Other stalagmites have been located, but their form is masked by an overgrowth of flowstone.

Cave Popcorn

Cave popcorn has been found on the walls of several fissures. The most impressive development consists of coalescing globules that resemble clusters of grapes (Fig. 12). In some instances, the vadose environment in which the popcorn grew eventually became phreatic, resulting in precipitation of an outer coating of dogtooth spar.

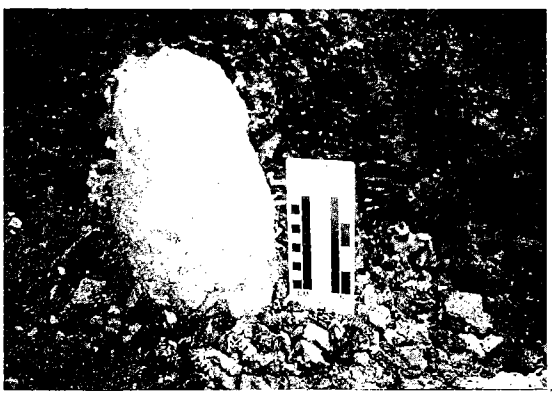

Figure 11. A stalagmite (13 in. tall) that grew from a base of limestone-pebble rubble excavated from a deposit of laminated illitic clay. Scale in centimeters and inches.

Figure 12. A cluster of cave popcorn 1.5 in. wide; notice prominent zone of hydrocarbon inclusions.

Euhedral Precipitates

The final precipitate that coats many of the speleothems at lower levels in the system is a partial coat of euhedral calcite (usually in the form of dogtooth spar, but in one area, of nailhead [rhombohedral] spar). Individual crystals as much as 0.5 in. long have been found. At the lowermost levels, these crystals are remarkably pure; at higher levels they are increasingly contaminated by clay.

Euhedral deposits of this type resemble, in a modest way, those found in "crystal caves" (Ford and Williams, 1989). They imply that, at a period late in the history of the cave, the water table rose substantially. At that time it is possible that both meteoric and basinal waters were entering the fissures. Small aggregates of euhedral pyrite in a few of the late speleothems suggest a slight hypogene imprint.

Other Forms of Calcite

In upper levels in the caves, deposits of marlstone are found in which micritic calcite is mixed with variable amounts of clay, bones, and pebbles. Textures, which include a ramifying network of calcite veins, resemble those of calcretes (fossil soils) found in contemporary Permian rocks (Donovan, 1986). If this calcite is of pedogenic origin, it offers support to the suggestion that the caves were preserved because of increasing aridity.

Detrital Deposits

Two types of detrital deposits have been recognized during the course of this study: those thought to have been washed into the cave system (allochthonous deposits) and those originating within the system (autochtonous deposits).

Autochtonous deposits are mostly fragments of speleothem derived from the cave walls. They include large angular pebbles (some of which have secondary speleothem coats) and smaller rounded pebbles (some with hydrocarbon inclusions). The latter are particularly noteworthy as they are present at the highest levels in the system and, hence, suggest that a considerable amount of erosion has taken place above the preserved land surface.

Most of the detritus washed into the caves appears to have come from the surface. It includes: (1) pebbles from the Arbuckle Group, including limestone, dolomite, and chert; (2) fragments of vertebrates (see below); and (3) green illitic clay.

In general, the coarser fragments (including bones) are found nearest to the surface in poorly sorted conglomerates. Clay has infiltrated down to a maximum depth of ~60 ft below the present land surface. The clay was probably not derived from the local limestones but may well be loess blown from the surrounding alluvial plains.

The stratigraphically youngest detritus in the caves consists of delicately laminated clay deposits as much as 6 ft thick (Figs. 11,13). Three deposits of this type have been found in the largest chambers in the system, one of which is only 6 ft from the present hill surface. In each deposit the clay is remarkably well sorted; it is uncontaminated by pebbles or bones (suggesting "difficult" communication with the surface) and yet, paradoxically, excavations have shown that it rests on such fragments. We suggest that the laminated clay infiltrated downward from a surface that was already covered by Permian sediments. Under such conditions, water could still percolate down from the surface, but could not transport coarse particles, only clay. The underlying coarse fragments were presumably washed into the system before its entombment.

One of these contains considerable soft-sediment deformation; this may record a seismic event or, more likely, local deformation caused by roof collapse (incasion) in the cave system (Fig. 13).

DATING OF THE CAVE DEPOSITS

The cave systems in Leatherbury's Quarry are securely dated by a rather extensive Permian reptile and vertebrate fauna. This fauna is currently under investigation; ~100,000 fragments of bone have been collected from several fissures in the quarry. The most distinctive and most common beast is the reptile *Captorhinus*. Our preliminary investigations show that at least four new species of vertebrates are present.

None of the fossils seem to represent animals that actually lived in the caves, but rather individuals that died and were washed into them. Some, for example the edaphosaurid pelycosaur *Edaphosaurus*, were quite large and could not have used the surface openings of the cave for protection. The smaller *Captorhinus aguti* was ~12 in. long and probably used the surface openings of the fissures as dens or hiding places. Plentiful *Captorhinus aguti* remains in the cave fill reflect varying degrees of water transport; some specimens are undamaged and others are well rounded and abraded. To date, no articulated specimens have been recovered. A preliminary faunal list from Leatherbury's Quarry is given in Table 1.

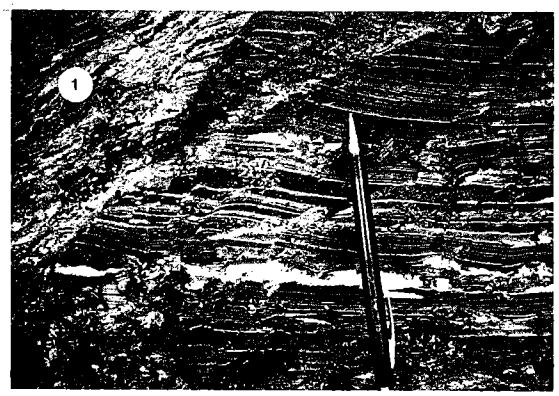

Figure 13. Laminated illitic clay that is the final infill of a chamber. Notice the small normal faults to the left of the pencil; these faults appear to have formed on the margin of a zone of complex shearing (1). The shearing may record a seismic event or a partial collapse (incasion) of the cave roof.

TABLE 1. — PRELIMINARY FAUNAL LIST, LEATHERBURY QUARRY

Osteichthyes

Indeterminate paleoniscoid teeth

Amphibia

Indeterminate labyrinthodont skull and jaw fragments

cf. *Euryodus primus*, microsaur

Reptilia

Indeterminate reptiles with laterally compressed, strongly recurved teeth, similar to Bolt's (1980) 'reptile X'

Captorhinus aguti

cf. *Captorhinikos* sp.

New caseid pelycosaur

cf. *Mycterosaurus* sp., a varanopseid pelycosaur

Thrausmosaurus sp., possibly a varanopseid pelycosaur

Delorhynchus priscus, possibly a varanopseid pelycosaur

Edaphosaurus sp., an edaphosaurid pelycosaur

The Leatherbury Quarry cave fauna may be given a tentative age assignment of Leonardian (Artinskian) age based on the work of Heaton (1979), who views all occurrences of *Captorhinus aguti* in Oklahoma as of Leonardian age. The presence of a possibly more-derived caseid pelycosaur in the fauna may indicate a slightly younger age or possible faunal mixing.

THE HYDROCARBON IMPRINT IN THE CAVES

In all types of speleothems, hydrocarbons occur in three forms: (1) as minute, three-micron inclusions within calcite crystals; (2) as larger inclusions along cleavage lines within the crystals; and (3) as biodegraded coatings on the surfaces of crystals.

Biodegraded hydrocarbons are also found impregnated in delicately laminated illitic clays. The lamination is a distinct alternation of dark-brown hydrocarbon-bearing layers with light-green hydrocarbon-free layers.

The Relationship Between Hydrocarbons and Magnetism

Paleomagnetic, rock-magnetic, petrographic, and geochemical studies of the hydrocarbon-saturated speleothems indicate there is a relationship between hydrocarbons and a chemical magnetization that resides in magnetite (Elmore and others, 1987; Elmore and Crawford, 1990). The dark bands in the speleothems contain calcite with hydrocarbon-filled primary fluid inclusions. Such calcites possess more than an order-of-magnitude-stronger natural remanent magnetization (NRM) than calcite in the lighter bands, which do not yield stable decay during demagnetization. Alternating field (AF) and thermal demagnetization of specimens of the dark bands reveal a Permian direction of magnetization (declination = 106°, inclination = 3°, k = 17, 95 = 5, n = 56). The results of rock magnetic experiments, and the fact that most maximum unblocking temperatures are below 580°C, suggest that the dominant component resides in magnetite. In some specimens, stable decay to 640°C suggests the presence of hematite. Magnetic extracts from the dark calcites contain spherical and other authigenic forms which, based on energy dispersive analysis, contain iron as the only detectable element. Powder X-ray diffraction patterns of extracts from the calcites indicate the presence of magnetite. The spherical forms are similar to authigenic magnetite reported in the literature.

The nature of the relationship between the hydrocarbons and authigenic magnetite is being evaluated via a detailed organic geochemical and petrographic investigation. Analysis by gas chromatography (GC) and gas chromatography–mass spectrometry (GC–MS) suggests that the most likely source of the oil was the Devonian Woodford Formation in the Anadarko basin. GC analyses of the C_{15} aliphatic fraction isolated from the speleothems indicate that the level of biodegradation is variable. Comparisons between magnetic intensity and various organic parameters suggest some interesting relationships. For example, samples with the highest magnetic intensity are apparently the least degraded. There may also be a direct relationship between the amount of extracted bitumen and magnetic intensity. There is no relationship, however, between intensity and percent asphaltenes (an alteration product of degradation), which does not support the suggestion that the presence of magnetite may be related to alteration of the hydrocarbons.

Stable carbon- and oxygen-isotope values for the light calcites ($\delta^{13}C_{PDB}$ –6.7‰; $\delta^{18}O_{PDB}$ –4.2‰) and dark calcites ($\delta^{13}C_{PDB}$ –6.2‰; $\delta^{18}O_{PDB}$ –4.7‰) are slightly depleted. The stable carbon-isotope value for the hydrocarbons in the speleothems is –30.7‰ (PDB). The isotopic values in the calcites could be slightly depleted due to the incorporation of some isotopically light carbon and oxygen from limited oxidation of hydrocarbons during precipitation of the speleothems. The fact that the calcites are not more depleted supports the interpretation that the hydrocarbons were not extensively degraded when trapped in the fluid inclusions. The values in the calcites are consistent with a shallow depth of formation from fresh water (Allan and Matthews, 1977). The similarity of the ^{13}C and ^{18}O values for the adjacent dark and light calcites also favors a common origin.

The magnetization in the speleothems was acquired in the Permian, resides predominantly in authigenic magnetite, and is interpreted to be chemical remanent magnetization (CRM). The fact that the cave deposits formed at relatively shallow depths, and that the Arbuckle Group speleothems were never deeply buried, probably eliminates the possibility of a thermoviscous origin for the magnetization. The stable isotope values for the speleothems are consistent with a shallow depth of formation (Allan and Matthews, 1977). The presence of authigenic magnetite spheres in magnetic extracts of the dark calcites supports a chemical origin for the magnetization.

The results from the light and dark speleothems suggest that there is a relationship between hydrocarbons and authigenic magnetite; the stronger magnetization invariably resides in the dark calcites, where the hydrocarbons are concentrated. This relationship between intensity of magnetization and abundance of hydrocarbons suggests that hydrocarbons caused precipitation of authigenic magnetite and acquisition of the associated CRM. The fact that the time of remanence acquisition (Permian) is consistent with the time of hydrocarbon migration and formation of the speleothems also provides evidence that hydrocarbons can cause acquisition of a stable secondary magnetization residing in magnetite.

WHAT WERE THE CONTROLS ON CAVE FORMATION?

As far as can be ascertained from the available exposures, outcrops of the Arbuckle Group in the Slick Hills are extensively perforated by small fossil cave systems of Early Permian age. Several of these cave systems in the Slick Hills have been exposed by quarrying and roadworks. Examples are exposed in the quarry at Richard's Spur, in the Cook Creek road cut (Donovan, 1982), and in

Leatherbury's Quarry described here (Donovan and others, 1986; Donovan, 1987). These three cave systems can be dated securely on the basis of their vertebrate fauna. Other examples have not yet yielded faunal evidence, although at least four display hydrocarbon-impregnated speleothems. Furthermore, a small Permian cave system is developed in an outcrop of Viola Limestone in the outlying Sugar Hills northwest of the main Slick Hills range. These caves are alike in their modest dimensions, linear geometry, decoration by calcite speleothems that are partially impregnated by hydrocarbons, and, in many cases, their vertebrate fauna.

We suggest that the important events in the development of such caves in Early Permian times were: (1) tectonism, mostly Pennsylvanian, that imparted a closely spaced fracture pattern to the lower Paleozoic limestones and left the Slick Hills emplaced structurally above the Anadarko basin, wherein the Woodford Formation (among others) had evolved to become a mature oil source rock; (2) the selective karstic opening of the ubiquitous Pennsylvanian joint systems to form long, narrow fissure systems dominated by vertical shafts; (3) an increasingly arid climate in the Late Pennsylvanian and Early Permian which led to a great reduction in the rate of weathering and the "fossilization" of a hilly, karsted land surface (Fig. 14); and (4) the gradual burial of this land surface, during

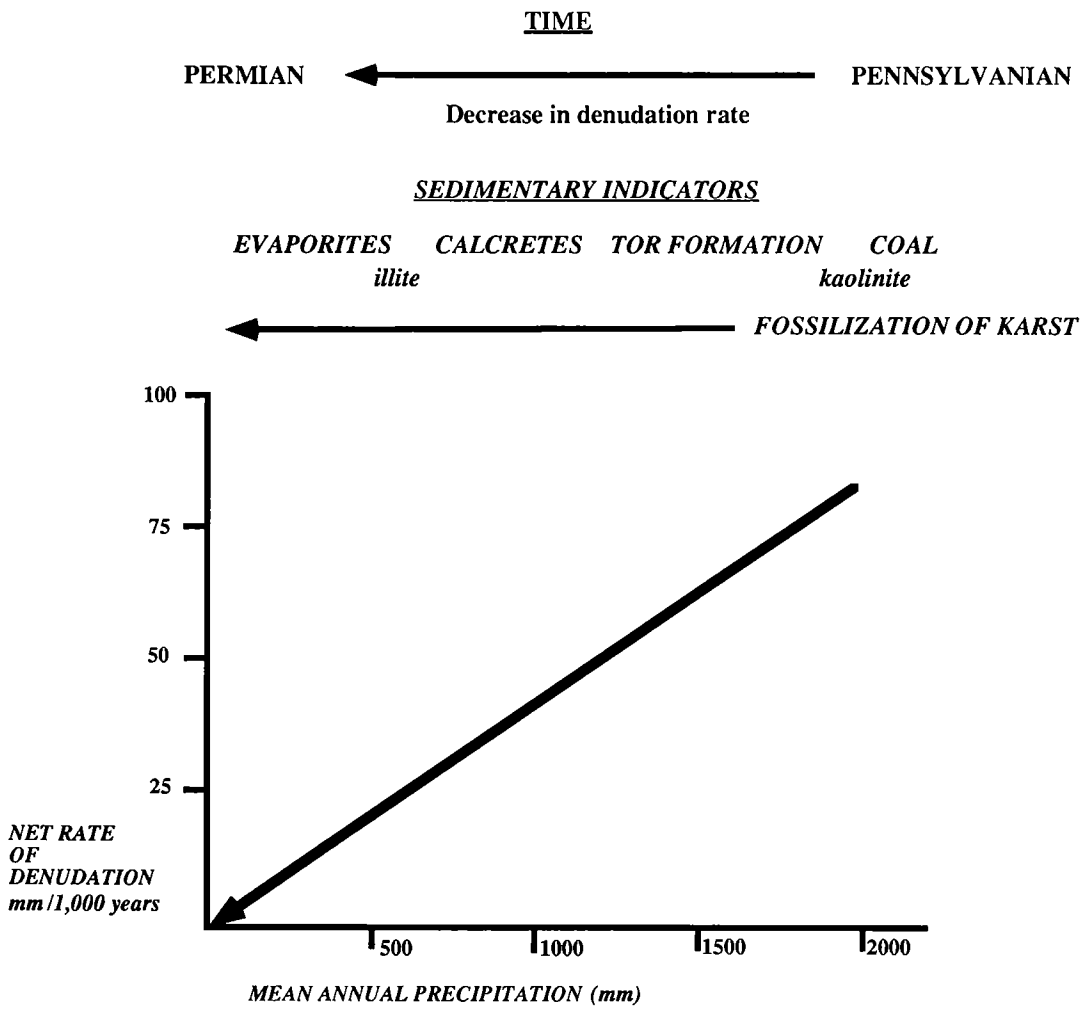

Figure 14. The upper part of the figure is a diagrammatic illustration of some of the sedimentary indicators of increasing aridity and gradual "fossilization" of the Wichita Mountains and Slick Hills during the Early Permian. The lower graph is the empirical relationship between rate of solution and mean annual rainfall in modern karst settings. While this relationship may not be precisely applicable to the evolution of karst surfaces in the Slick Hills during the Permian, it does indicate the likely driving mechanism behind the "fossilization" of karst processes at this time (data derived from Bridges, 1985).

Early Permian time, by fine-grained siliciclastic detritus deposited on alluvial plains.

HOW DID THE CAVE SYSTEM EVOLVE?

The geometry of the Leatherbury cave system is remarkably complex. Nevertheless, in several places the original water-corroded walls of the caverns exhibit horizontal rim lines which suggest that development of the cave system postdated tectonic tilting of the Arbuckle Group to the northwest at angles of ~20°.

The character of the deposits in the cave varies according to the level examined (Fig. 15). In general the following sequence of events seems to have occurred.

1) Opening of the fissures by meteoric dissolution; some phreatic imprint is preserved, but the morphology of the caves is primarily a vadose one.

2) Coating of the fissures by calcite speleothems, principally flowstone but also cave popcorn, stalactites, and stalagmites. The flowstones display complex textures indicative of discontinuous precipitation under both vadose and phreatic conditions.

3) Phreatic infill of the fissures in the lower part of the system. In some places phreatic speleothems closed the fissures; some of the last crystals deposited were remarkably pure calcite of the "iceland spar" variety. Initially, the suggestion that the water table within the caves was higher as speleothem deposition concluded does not seem to be compatible with the increasing aridity of the surface environment. The paradox can be resolved when it is realized that the land surface was still subsiding and being covered by Permian sediments, even though surface erosion had effectively ceased (Fig. 16). It is possible that some basinal water entered the caves at this late time.

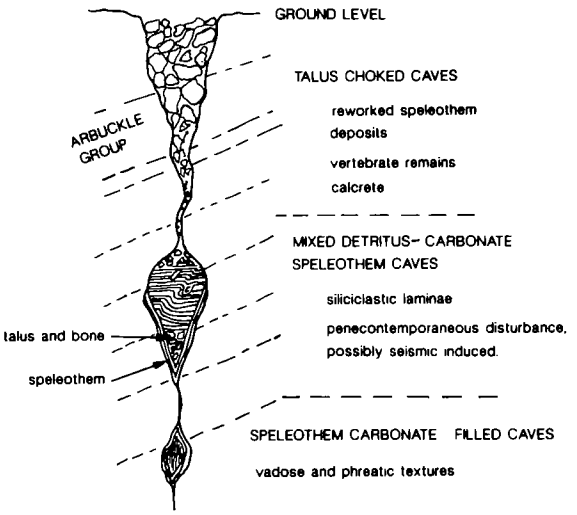

Figure 15. Schematic representation of the types of deposit found in the fissure fills in Leatherbury's Quarry. Within mid-level caves, spatial relationships clearly indicate that surface-derived talus, including reptile bones, probably arrived prior to infill by the laminated clays which are, for the most part, devoid of fossil remains. Note that the laminated clays that occur in mid-level caves may in fact be younger than the coarse talus found in the upper part of caves.

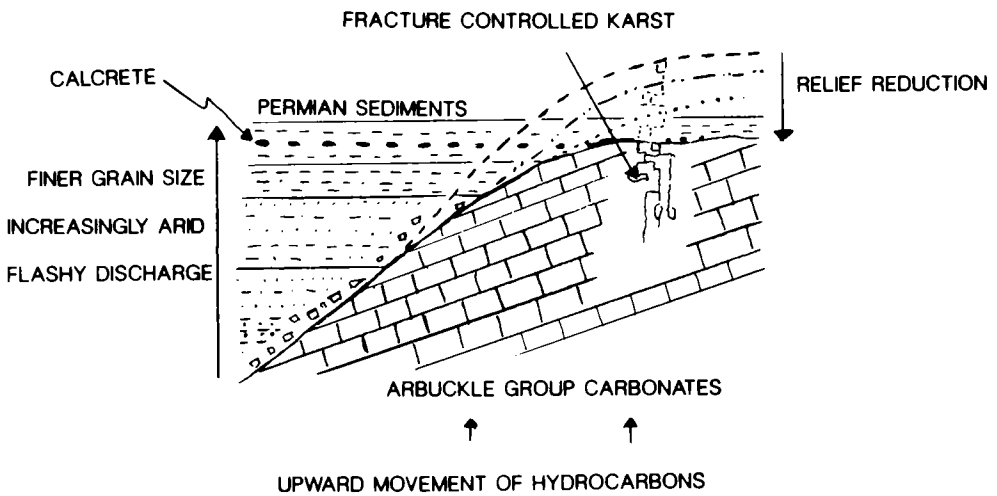

Figure 16. Schematic cross section illustrating how the cave system was gradually buried and preserved beneath Permian alluvium. As the climate became increasingly more arid, dissolution ceased and the karst was "fossilized." At the same time, tectonic uplift ceased, to be replaced by gentle regional subsidence. As a consequence of this subsidence, the Slick Hills were gradually buried beneath a veneer of alluvium (manifest in the cave systems as fine-grained siliciclastic detritus). This burial explains the apparent paradox whereby the final speleothems in the caves are phreatic, rather than vadose deposits.

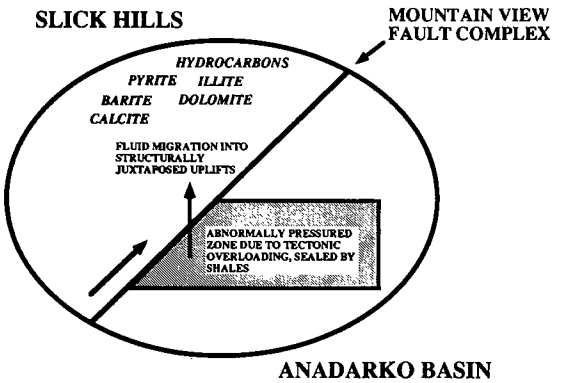

Figure 17. Schematic illustration showing the inferred route by which oil migrated from the Anadarko basin into caverns in the Slick Hills.

4) As the overlying surface of the Slick Hills was lowered by denudation, the tops of the fissures were partially filled by clastic detritus (including vertebrate-fossil remains) derived from the overlying land surface. As this detritus includes fragments of speleothems, it seems likely that the cave systems themselves were being "cannibalized" by surface erosion until the landscape was buried by Early Permian sediments. At any given level, the introduction of abundant clastics effectively terminated speleothem formation.

5) The final infill of the caves took place after the landscape was buried beneath a cover of Permian alluvium; it consists of finely laminated illitic clays that are devoid of both fossil reptiles and palynomorphs.

As noted previously, hydrocarbons may be found in all varieties of speleothems and in illitic clays. As the local rocks are neither organic rich nor mature, the hydrocarbons may have migrated upward from a structurally overpressured Woodford source in the Anadarko basin, through the faults of the frontal Wichita fault zone into tectonic fractures in the Arbuckle (Fig. 17). As noted previously, several bitumen-bearing veins cut the walls of the quarry. Escaping from these fractures, the hydrocarbons mingled with carbonate-saturated waters in the caves before being incorporated into the growing speleothems and clay deposits.

ACKNOWLEDGMENTS

Donovan, Elmore, and Engel are grateful for the support of the National Geographic Society (# 3926-88). Donovan further acknowledges the support of the Charles B. Moncrief Chair of Geology, while Busbey is grateful for the award of a grant from the Texas Christian University Research Fund.

REFERENCES

Allan, J. R.; and Matthews, R. K., 1977, Carbonate and oxygen isotopes as diagenetic and stratigraphic tools: surface and subsurface data, Barblades, West India: Geology, v. 5, p. 16–20.

Bolt, J. R., 1980, New tetrapods with bicuspid teeth from the Fort Sill locality (Lower Permian, Oklahoma): Neues Jahrbuch für Geologie und Paläontologie, v. 8, p. 449–459.

Bridges, S. D., 1985, Mapping, stratigraphy, and tectonic implications of Lower Permian strata, eastern Wichita Mountains, Oklahoma: Oklahoma State University unpublished M.S. thesis, 125 p.

Donovan, R. N., 1982, Stop 11—Highway 19 area, *in* Gilbert, M. C.; and Donovan, R. N. (eds.), Geology of the eastern Wichita Mountains, southwestern Oklahoma: Oklahoma Geological Survey Guidebook 21, p. 154–155.

_____1986, Geology of the Slick Hills, *in* Donovan, R. N. (ed.), The Slick Hills of southwestern Oklahoma—fragments of an aulacogen?: Oklahoma Geological Survey Guidebook 24, p. 1–12.

_____1987, The World's smallest oil field?: Oklahoma Geology Notes, v. 47, p. 238, 291.

Donovan, R. N.; and Busbey, A. B., 1991, Stop 13: Leatherbury's Quarry—the World's smallest oil field, *in* Johnson, K. S. (ed.), Arbuckle Group core workshop and field trip: Oklahoma Geological Survey Special Publication 91-3, p. 255–258.

Donovan, R. N.; and Ragland, D. A., 1991, Stop 10: The base of the Arbuckle Group at Bally Mountain, *in* Johnson, K. S. (ed.), Arbuckle Group core workshop and field trip: Oklahoma Geological Survey Special Publication 91-3, p. 244–246.

Donovan, R. N.; Ragland, D. A.; and Shaefer, D., 1986, Stop 4: Geology of the Cook Creek road cut, *in* Donovan, R. N. (ed.), The Slick Hills of southwestern Oklahoma—fragments of an aulacogen?: Oklahoma Geological Survey Guidebook 24, p. 100–105.

Donovan, R. N.; Marchini, W. R. D.; McConnell, D. A.; Beauchamp, W.; and Sanderson, D. J., 1989, Structural imprint on the Slick Hills, southern Oklahoma, *in* Johnson, K. S. (ed.), Anadarko basin symposium, 1988: Oklahoma Geological Survey Circular 90, p. 78–84.

Elmore, R. D.; and Crawford, L., 1990, Remanence in authigenic magnetite: testing the hydrocarbon-magnetite hypothesis: Journal of Geophysical Research, v. 95, p. 4539–4549.

Elmore, R. D.; Engel, M. H.; Crawford, L.; Nick, K.; Imbus, S.; and Sofer, F., 1987, Evidence for a relationship between hydrocarbon and authigenic magnetite: Nature, v. 324, p. 428–450.

Ford, D. C.; and Williams, P. W., 1989, Karst geomorphology and hydrology: Unwin Hyman, Ltd., London, 601 p.

Heaton, M. J., 1979, Cranial anatomy of primitive captorhinid reptiles from the Late Pennsylvanian and early Permian, Oklahoma and Texas: Oklahoma Geological Survey Bulletin 127, 84 p.

Simpson, L. C., 1979, Upper Gearyan and Lower Leonardian terrestrial vertebrate faunas of Oklahoma: Oklahoma Geology Notes, v. 39, p. 3–21.

Pressure Compartments and Seals in the Anadarko Basin

Zuhair Al-Shaieb, James Puckette, Patrick Ely, and Vanessa Tigert
Oklahoma State University

ABSTRACT.—Abnormally pressured zones have been recognized for more than two decades in the Anadarko basin. Pressure data demonstrate the presence of a "mega compartment complex" along with isolated and relatively smaller compartments in the basin. These compartments have produced large quantities of natural gas, particularly from the Pennsylvanian Red Fork and Morrow sandstone reservoirs. A study of these reservoirs indicates a significant increase in pressure gradients below 10,000 ft. This marked increase in gradient is characteristic of the transition from under- or normal-pressure zones to overpressured compartments in the basin. Preliminary data suggest the mega compartment complex is divided into a myriad of smaller units with their own distinct pressure gradients. On the other hand, local overpressured compartments are found outside the mega compartment complex. These compartments are isolated overpressured zones within normal or near-normal pressure regions.

The Anadarko basin regional overpressured compartment includes rocks from Pennsylvanian, Mississippian, and Devonian Systems. The top of this regional mega compartment complex is found approximately 10,000–11,000 ft below the surface. The base of this complex seems to coincide with the Devonian Woodford Shale. Local compartments are present in many stratigraphic intervals, but are most apparent in the Hunton and Simpson Groups.

Pressure data from the Gulf Oil Co. Weaver No. 1, McClain County, show the cored Simpson Group in the Weaver No. 1 to be part of a seal zone. The compositionally homogeneous Simpson sandstones in the Weaver No. 1 exhibit textural heterogeneity due essentially to diagenetic processes. These processes are cementation, intergranular pressure-solution, and mechanical brecciation. The textural heterogeneity is manifested as chemical and mechanical micro- and macrobanding. Pressure data from the Woods Switzer "C" No. 1, Roger Mills County, indicate that the Upper Red Fork reservoir in the Southwest Leedey field is an overpressured compartment. The Upper Red Fork is separated from the overlying Skinner reservoir by a lithologic seal with a diagenetic overprint.

INTRODUCTION

Abnormally pressured zones have been recognized for more than two decades in the Anadarko basin. In this paper, the evidence will be presented to demonstrate the presence of a "mega compartment complex" along with isolated and relatively smaller compartments within the Anadarko basin. These compartments have produced large quantities of natural gas, particularly from the Pennsylvanian Red Fork and Morrow sandstone reservoirs. A study of these reservoirs indicates a significant increase in pressure gradients below 10,000 ft. This marked increase in gradient is characteristic of the transition from zones of subnormal or normal pressure to overpressured compartments in the basin. Preliminary data suggest the mega compartment complex is divided into a myriad of smaller ones with their own distinct pressure gradients. On the other hand, local overpressured compartments are found outside the mega compartment complex. These compartments represent isolated overpressured zones within normal or near-normal pressure regions.

In the western Oklahoma portion of the Anadarko basin (Fig. 1), the regional overpressured compartment studied includes rocks from Pennsylvanian, Mississippian, and Devonian Systems. The top of this regional mega compartment complex is found approximately 10,000–11,000 ft below the surface. The base of this complex seems to coincide with the Devonian Woodford Shale (Figs. 2,3). Local compartments outside the mega compartment complex are present in many stratigraphic intervals, but are most apparent in the Hunton and Simpson Groups (Fig. 3).

The area of study (Fig.1) is the western Oklahoma portion of the Anadarko basin including Beckham, Custer, Dewey, Ellis, Roger Mills, and Washita Counties where abnormally pressured zones have been recognized (Breeze, 1970).

To systematically investigate pressure com-

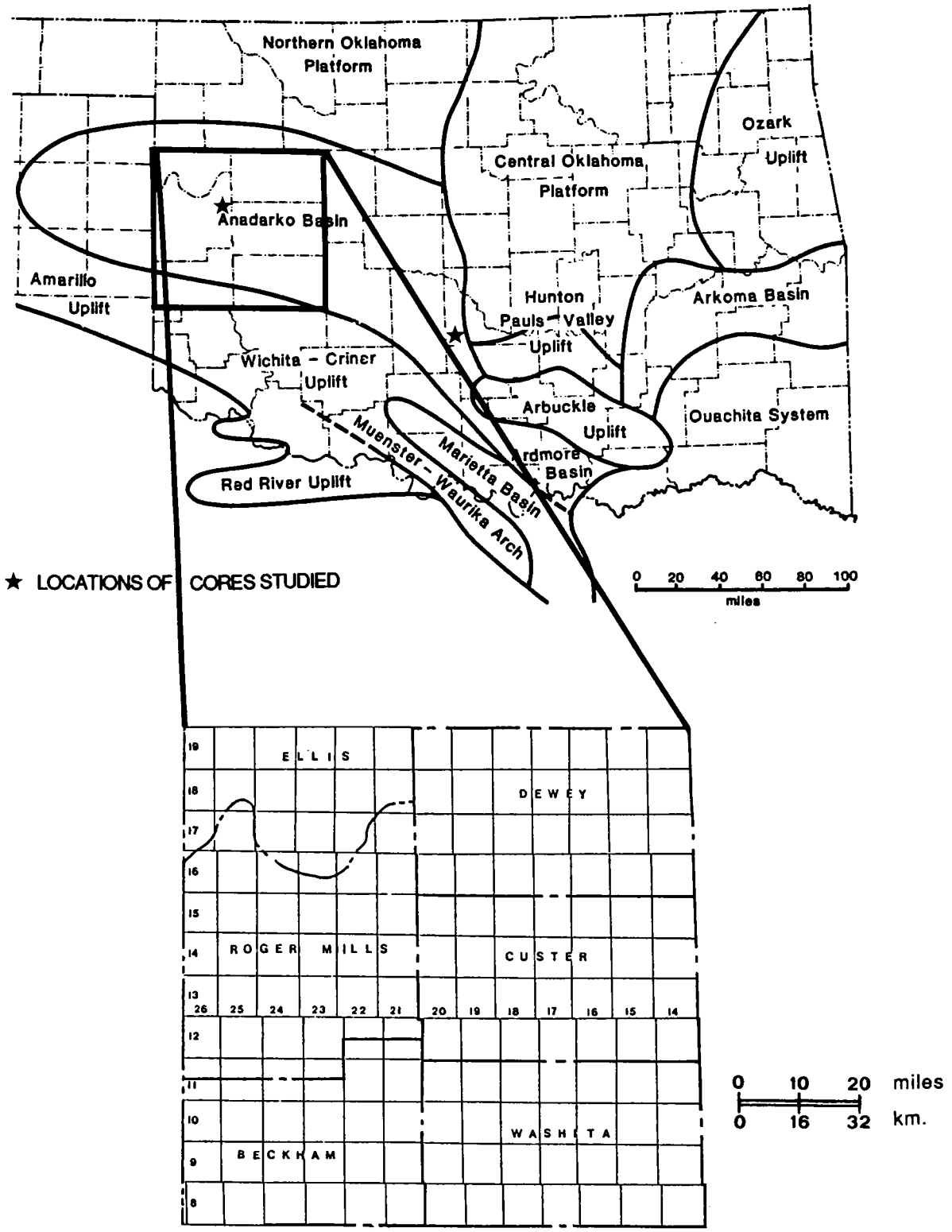

Figure 1. Area of study, locations of cores studied, and major geological provinces of Oklahoma (Al-Shaieb and Shelton, 1977; Arbenz, 1956).

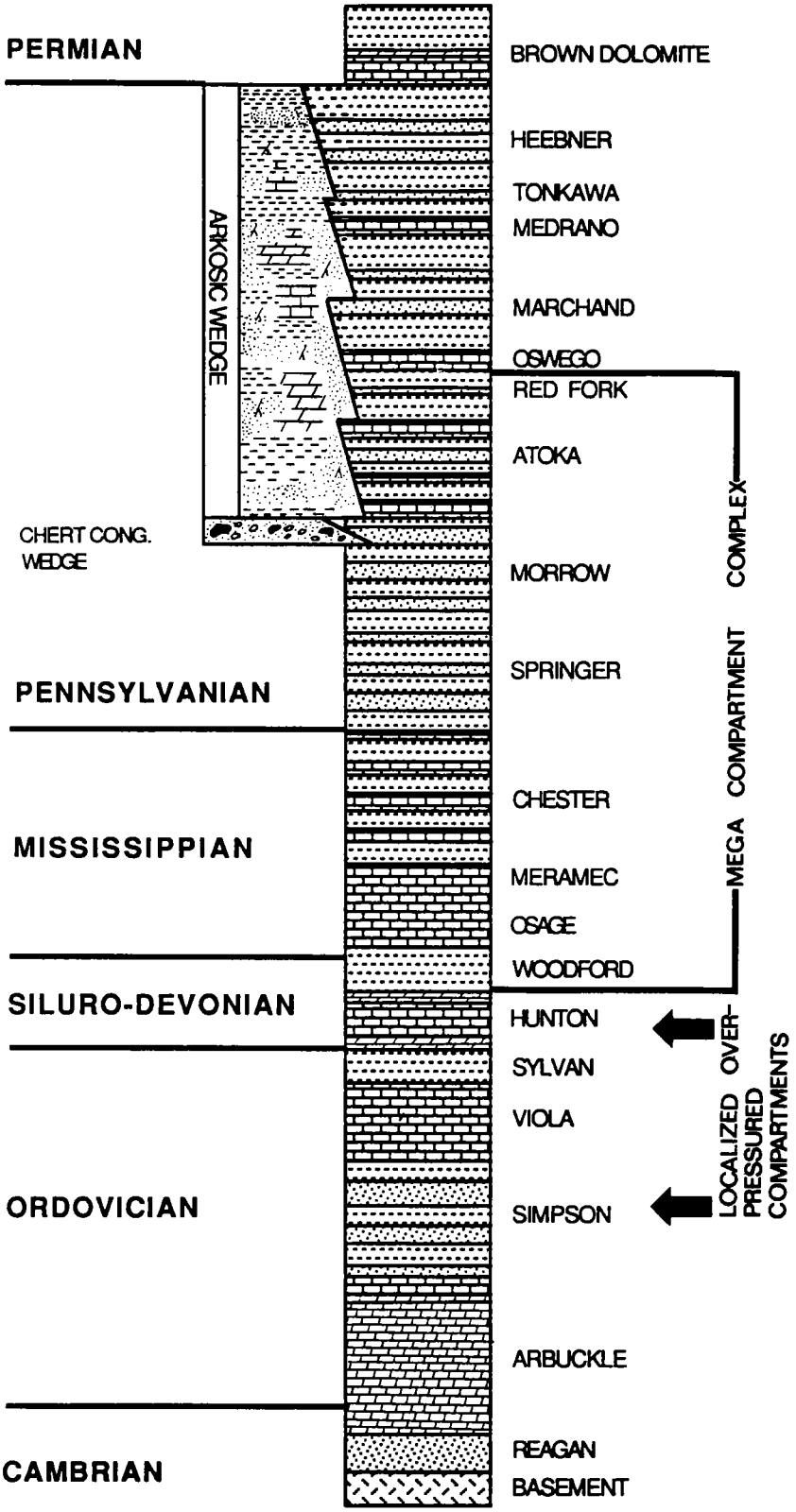

Figure 2. Generalized stratigraphic section of the overpressured rock units in the study area.

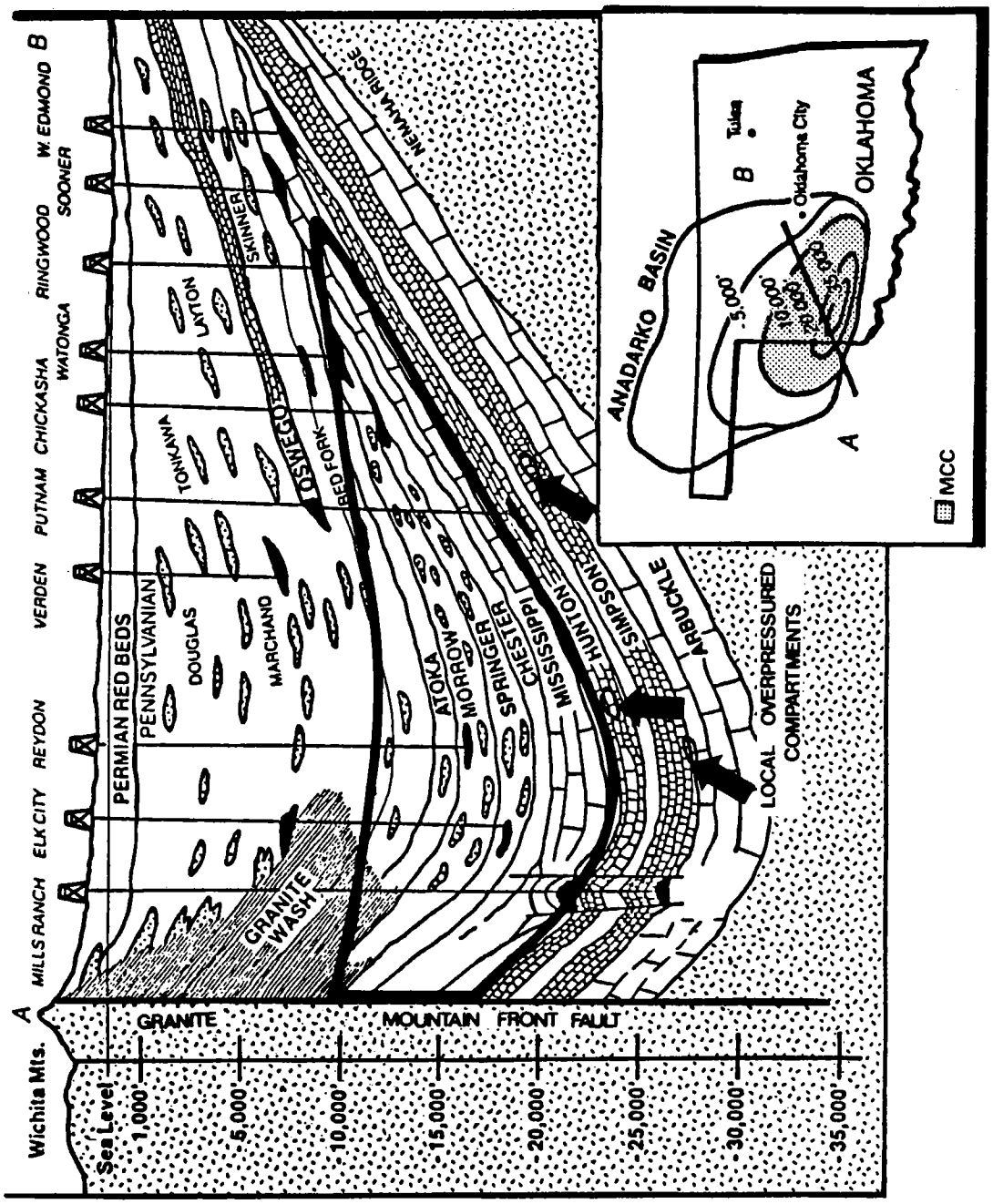

Figure 3. Schematic cross section of Anadarko basin showing regional mega compartment complex (outlined). Arrows identify local overpressured compartments (after Al-Shaieb and others, 1990).

partments and seals within the western Oklahoma portion of the Anadarko basin, the following set of research activities was undertaken. These were:

1) Verification of the presence of pressure compartments and seals using drilling and production data;

2) Identification of cores taken within seal intervals and overpressured zones;

3) Analysis of the petrology, mineralogy, and diagenetic overprints of these cored intervals;

4) Identification of compaction features, stylolites, pressure solution, and faults in cored seal intervals; and

5) Evaluation of the "low resistivity zones" and other wire-line log signatures of shale and other lithologies that might suggest undercompaction and overpressuring.

METHODOLOGY

Pressure Data

Pressure gradients are calculated by dividing static bottom-hole pressure (BHP), also known as reservoir pressure, by the depth of the reservoir from surface. Changes in surface elevation and the position and inclination of the ground-water table can affect pressure gradient reliability (Orr and others, 1985); however, because of the shallow water table and flat topography these effects in the study area are minimal.

One of the primary concerns of this study was to insure the high quality of reservoir (BHP) pressure data. Three types of pressure data were used: (1) shut-in pressure from drillstem tests (DSTs), (2) recorded bottom-hole pressure (BHP) from P/Z data listed in Dwight's Energy (1989) gas production books, and (3) reservoir pressure (BHP) calculated from static initial wellhead shut-in pressure.

Drillstem tests were the first data used in the study to calculate pressure gradients. Though DST pressures can be erroneously high, they are frequently low due to poor reservoir permeability. Some DST pressure values were omitted because the calculated gradient was anomalously low compared to nearby gradients in the same stratigraphic interval. On the other hand, DST pressures with abnormally high gradients were examined further to determine if these gradients reflected true formation fluid recoveries and pressures. The DST data obtained were insufficient to construct comprehensive maps and make valid interpretations of pressure gradients within the Desmoinesian, Atokan, Morrowan, and Springeran intervals. Therefore, bottom-hole pressures listed in Dwight's Energy gas production data books were also utilized. These pressures are basically static bottom-hole pressures which are calculated by Dwight's using "Z" or compressibility deviation factors. All BHP and Z-factor data used were recorded for the initial well test or within three

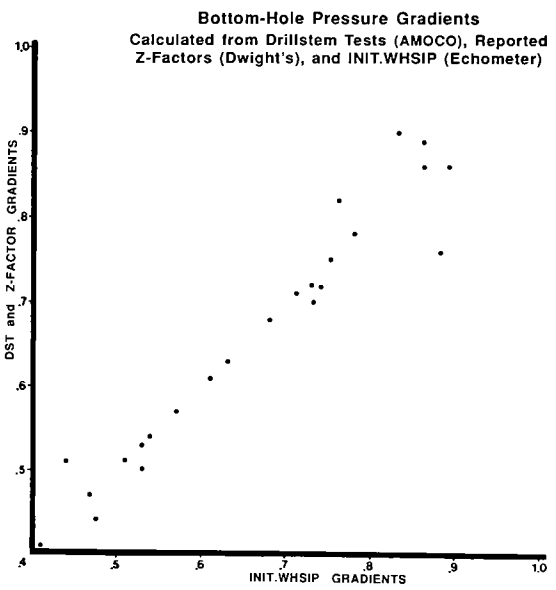

Figure 4. Relationship between pressure gradients calculated from various bottom-hole pressure sources.

months after the first production. In many instances the only pressure reported for a well was initial wellhead shut-in pressure (INIT. WHSIP). To determine initial reservoir pressure (BHP) from INIT. WHSIP, it was necessary to sum the recorded INIT. WHSIP and fluid column pressures in the production string. A commercially available program supplied by the Echometer Co. (1986) was used to convert INIT. WHSIP to BHP. This program provides mechanisms for calculating BHP from INIT. WHSIP using surface and fluid column pressures. In this study liquid column pressures were ignored because the wells generally have very high gas/liquid ratios, and there was no way of determining liquid column heights from available data. Since liquid column pressures were not used, the calculated reservoir pressures may be slightly lower than the actual pressures. The formula used by the program to determine gas column pressure calculated an average Z-factor based on surface and bottom-hole temperatures, gas gravity, and gas composition. The concentrations of nitrogen (<1%), hydrogen sulfide (negligible to absent), and carbon dioxide (less than 1–5%) are low in natural gas produced in the study area. Therefore, concentrations of these gases were not a factor in the calculation of average Z-factors for the Echometer BHP calculation. Where multiple sources of BHP were available, comparisons were made between the bottom-hole pressures calculated from INIT. WHSIP, DSTs, and reported BHP and Z-factors in Dwight's. A strong

positive correlation between data sources was evident (Fig. 4). Based on the comparison of data from various sources, it is believed the greatest potential for error is in the accuracy of reported data and not in calculation methods of BHP.

Cored Seal Intervals

Several cores were available for examination within the study area. In general, the cored intervals represent reservoirs within compartments; however, both seals and compartments are represented in a few cored intervals. One core that was studied was from the Woods Switzer "C" No. 1 in sec. 5, T. 15 N., R. 21 W., Roger Mills County (Fig. 1). The Woods Switzer "C" No. 1 core is from within the mega compartment complex and includes a probable seal and part of the underlying compartment. A second core studied was from the Gulf Weaver No. 1 in sec. 17, T. 5 N., R. 4 W., McClain County (Fig. 1). This core is from east of the study area and contains a diagenetically banded seal within the Simpson sandstone and carbonate sequence.

COMPARTMENT VERIFICATION AND IDENTIFICATION

Mega Compartment Complex

In the study area, pressure gradient maps of the Missourian/Virgilian (Fig. 5), Red Fork (Fig. 6), Morrowan (Fig. 7), and Hunton (Fig. 8) were constructed. These maps show significant increases in pressure gradients basinward for the Red Fork and Morrowan intervals. Red Fork gradients increase from 0.5 psi/ft to 0.75 psi/ft (Fig. 6). Morrow gradi-

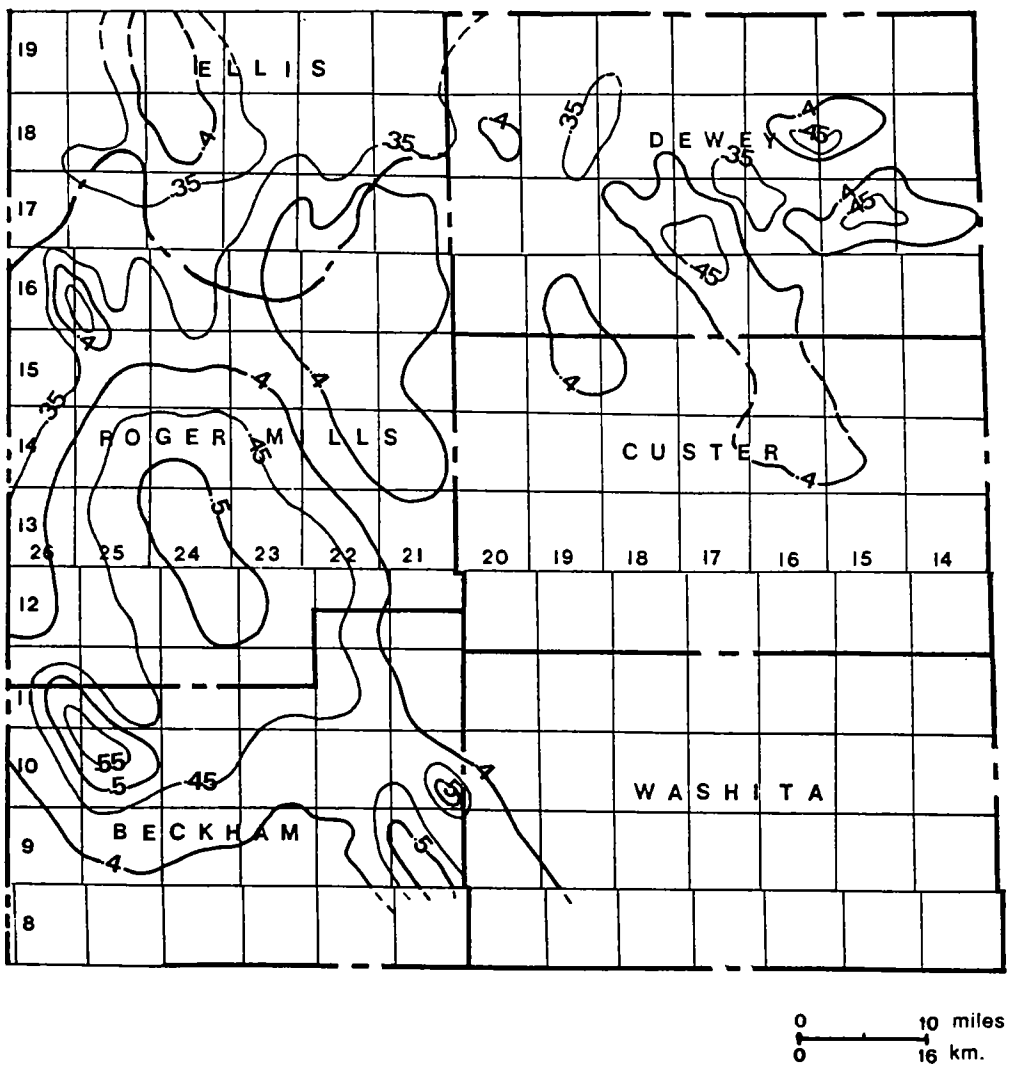

Figure 5. Pressure gradient (psi/ft) contour map of Missourian/Virgilian rocks.

ents increase from 0.5 psi/ft to >0.9 psi/ft (Fig. 7). Pressure gradient maps for the Missourian/Virgilian (Fig. 5) and Hunton (Fig. 8) intervals do not show a significant basinward increase. The maps indicate the presence of a regional overpressured mega compartment complex. The top seal is approximately 10,000–11,000 ft deep in the study area (Fig. 3). The bottom seal of this complex appears to coincide with the Woodford Shale. This mega compartment complex is basin wide, completely sealed, and overpressured.

Localized Compartments

Pressure data also indicate the presence of isolated abnormally high-pressured smaller compartments within the regional overpressured compartment. Localized, smaller overpressured compartments were also identified within regional normally pressured zones.

PRESSURE GRADIENT MAPS FOR WESTERN OKLAHOMA PORTION OF THE ANADARKO BASIN

Missourian/Virgilian

Figure 5 shows pressure gradient contours of the Missourian/Virgilian reservoirs. These reservoirs include both sandstone facies (Layton and Tonkawa) and arkosic facies (granite wash). Pressure gradients for the Missourian/Virgilian rocks indicate under- to normal-pressure conditions throughout most of the study area. Slight over-

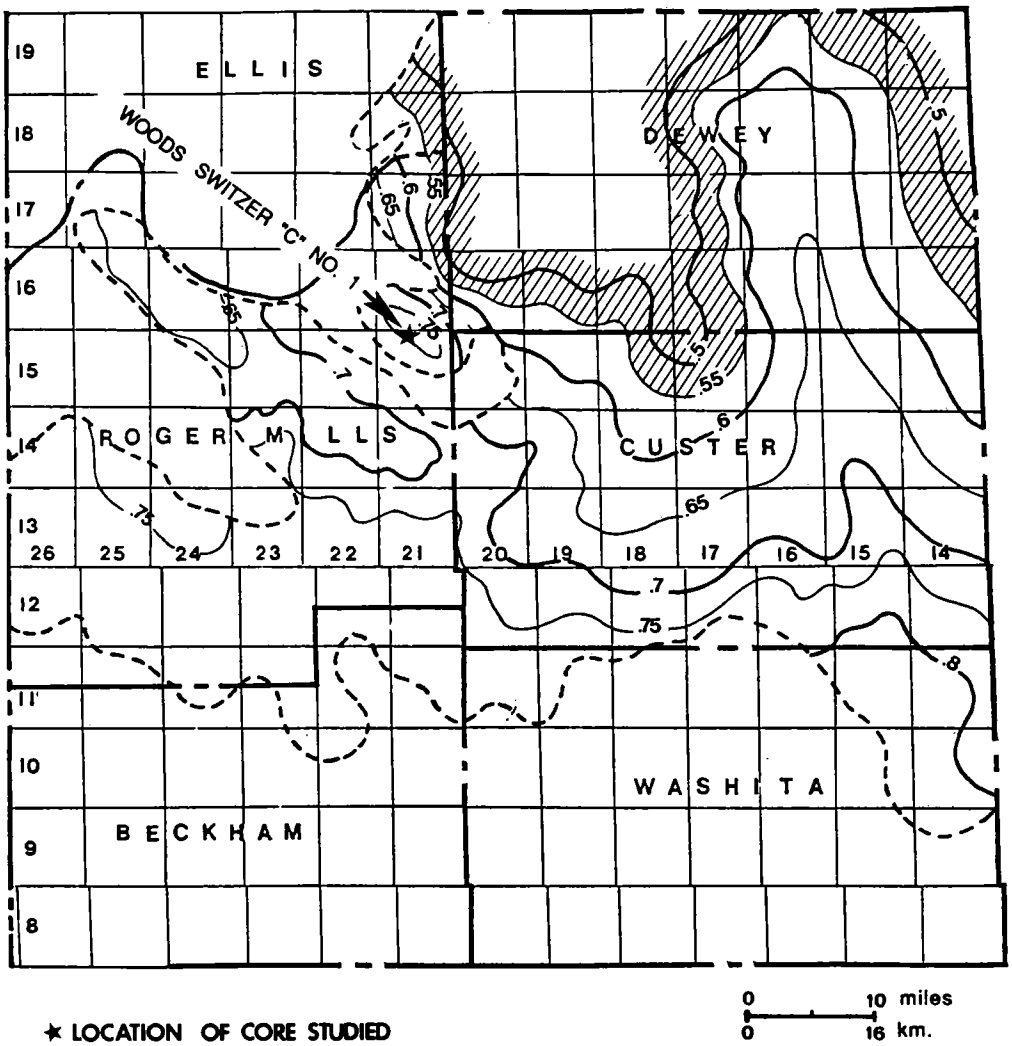

Figure 6. Pressure gradient (psi/ft) contour map of the Red Fork sandstone. Location of the Woods Switzer "C" No. 1 Red Fork core is identified. The limit of Red Fork sandstone deposition is shown by a dashed line. Transition zone from normal pressure regime to overpressuring is shaded.

pressuring observed in the southern part of the study area reflects deeper burial (>10,000 ft) of the Missourian granite wash. Due to the limited amount of Missourian/Virgilian production, nearly all pressure data used in this study are from drillstem tests.

Red Fork Sandstone

The Red Fork sandstone pressure gradient map (Fig. 6) shows a significant change from normal to elevated pressure gradients from shelf to basinal settings. The transition zone from normal to overpressured gradients is shaded; the limits of Red Fork sandstone deposition are shown by dashed lines (Fig. 6). The Red Fork pressure gradient map shows a uniform basinward increase in gradient over much of the study area. However, in T. 15 N., R. 21 W. and T. 16 N., R. 21 W. an anomalously high overpressured compartment is recognized. This compartment corresponds to an isolated Red Fork sandstone reservoir. The Woods Switzer "C" cored interval represents a Red Fork sandstone producer in this reservoir. Based on the setting, geometry, and sedimentary structures of the Switzer core, it is believed this sandstone reservoir was deposited in a shallow-marine delta-fringe setting. This anomalously high pressured reservoir represents deposition in a transitional setting between deltaic conditions to the north and east and the deeper-marine sandstones

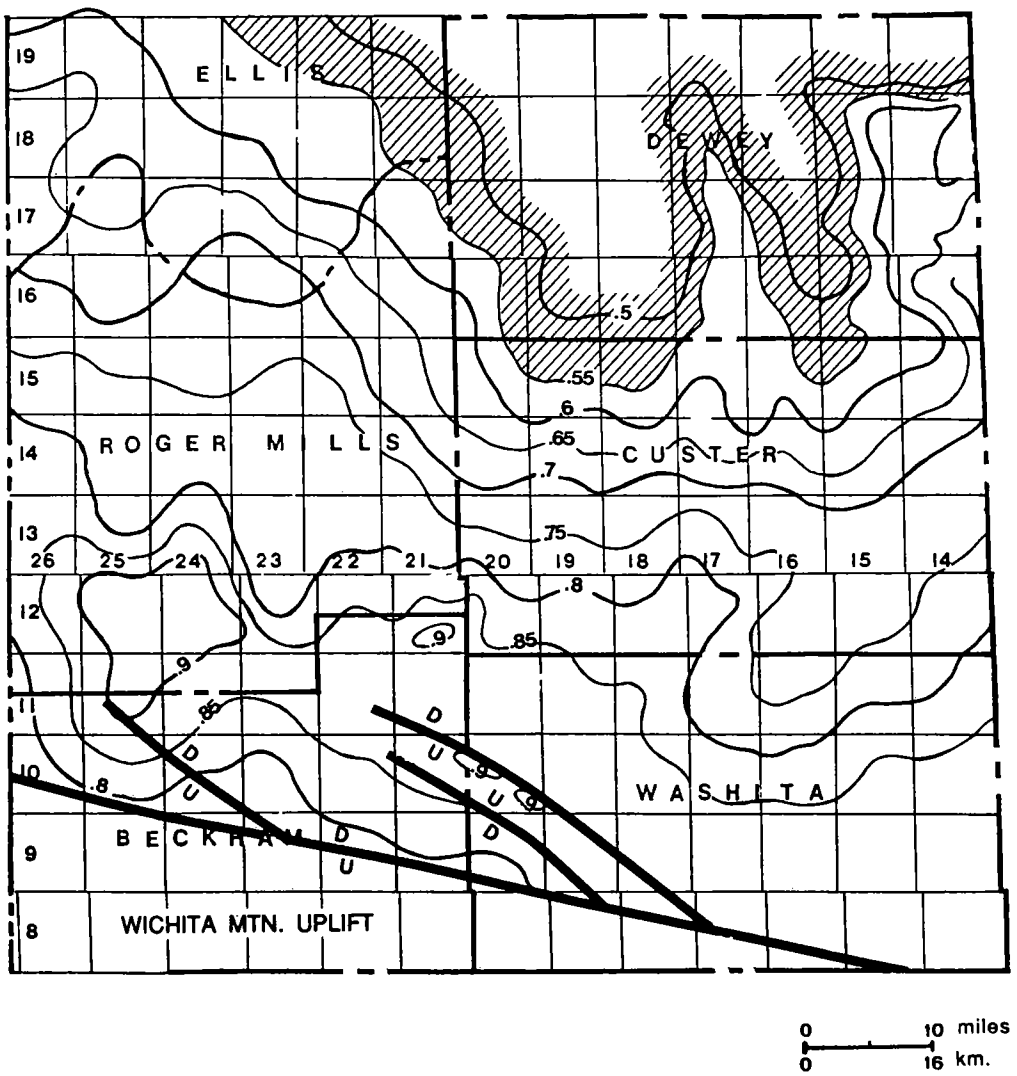

Figure 7. Pressure gradient (psi/ft) contour map of the Morrow sandstone. Transition zone from normal pressure regime to overpressuring is shaded.

basinward to the south. The isolation and shelf edge setting of this reservoir may have promoted seal development through extensive shale deposition around the sand body. Tectonic downwarping of the basin along the shelf edge and deep burial may have contributed to the reservoir's abnormal pressure.

Morrow Sandstone

Figure 7 shows the pressure gradients of the Morrowan reservoirs. The transition zone from normal to elevated pressure gradients is shaded on Figure 7. Deltaic and shallow-marine sandstone facies are dominant in the northern part of study area. Arkosic, chert conglomerate fan-delta facies are very prominent in the southern part of study area. Pressure gradients in chert conglomerate reservoirs are among the highest recognized in the basin and exceed 0.90 psi/ft. The southern boundaries of these reservoirs are the frontal fault zone of the Wichita Mountain uplift. This fault system also represents the southern lateral limit of the overpressured compartment. The Morrow reservoirs exhibit a fairly uniform increase in pressure gradients basinward with depth.

Hunton Group

The pressure gradient map for the Hunton Group (Fig. 8) provides the evidence of the lower boundary (bottom seal) of the regional overpressured mega compartment complex. Most reservoir pressures recorded for the Hunton Group re-

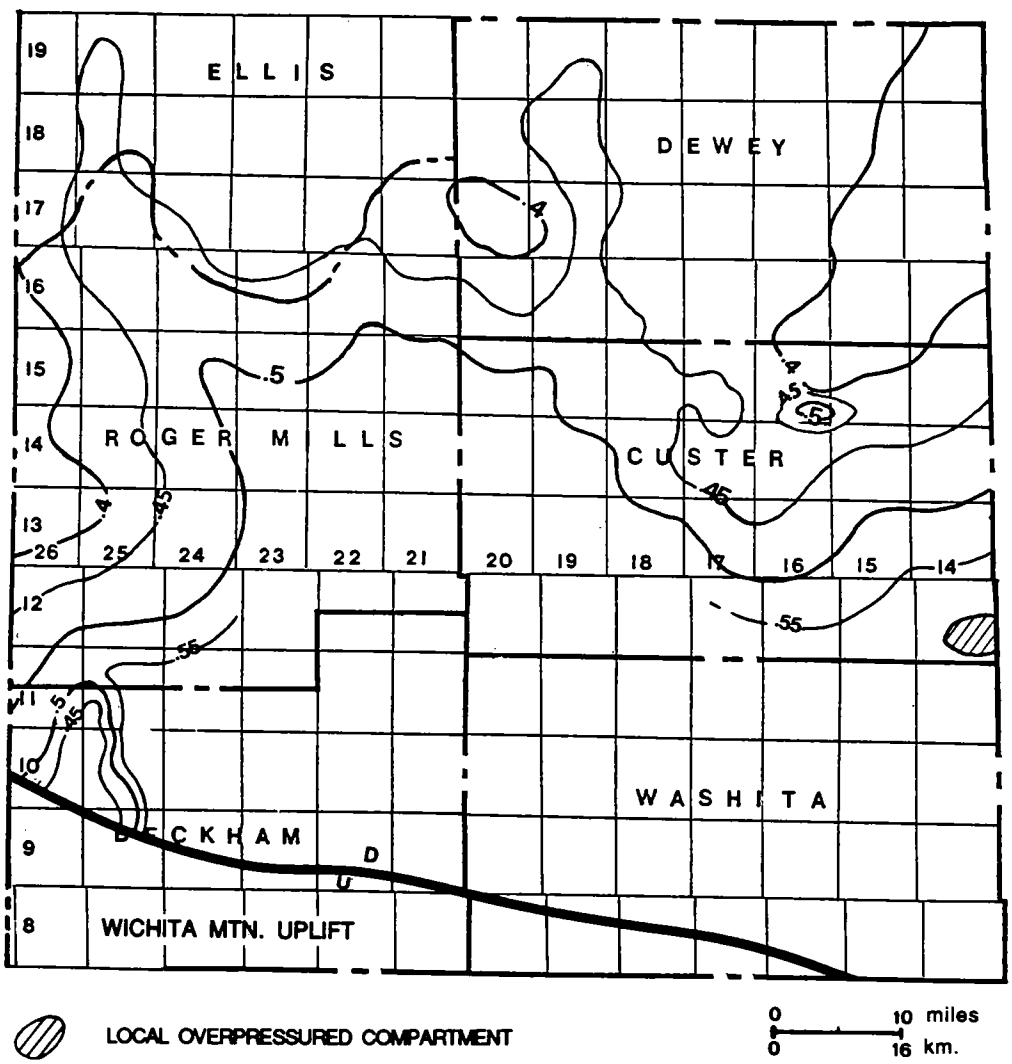

Figure 8. Pressure gradient (psi/ft) contour map of the Hunton Group showing a local overpressured compartment within normally pressured Hunton rocks.

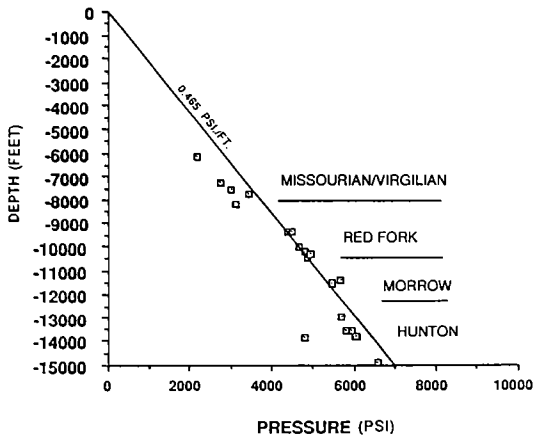

Figure 9. Pressure-depth profile from T. 17 N., R. 18 W. and T. 18 N., R. 18 W. on the shelf of the Anadarko basin. Note that all gradients plot along the projected 0.465 "normal" gradient slope.

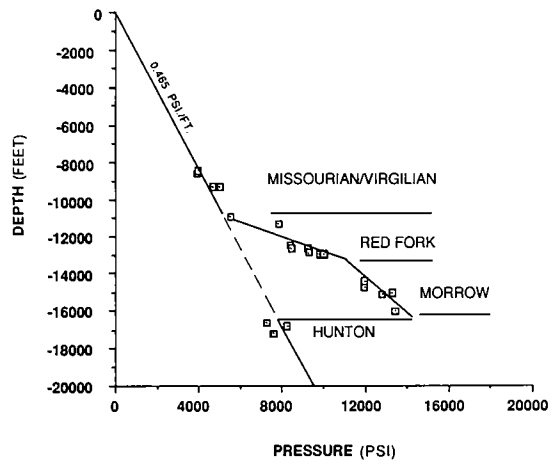

Figure 10. Pressure-depth profile from Roger Mills County, Oklahoma. Deviation of curve to right (higher pressure) identifies the mega compartment complex in the Red Fork and Morrow intervals. Hunton Group gradients cluster around the "normal" 0.465 psi/ft gradient.

flect near-normal gradients. An anomalous, highly pressured area observed in T. 12 N., R. 14 W. is interpreted as a local overpressured compartment enclosed in the near-normally pressured Hunton zone.

The near-normal Hunton pressure gradients indicate that the base of the regional overpressured compartment coincides with the Woodford Shale. In the study area, the stratigraphic intervals

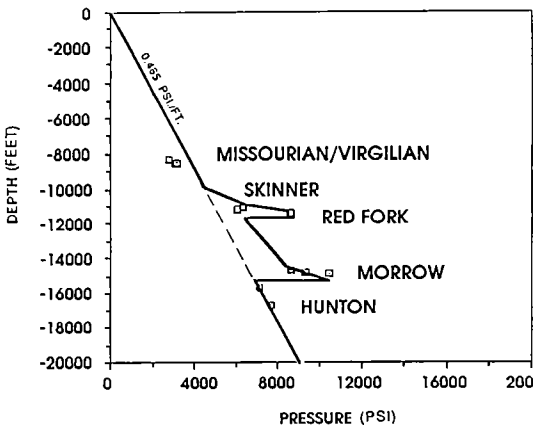

Figure 11. Pressure-depth profile in the vicinity of the Woods Switzer "C" No. 1 in the Southwest Leedey field. Deviations of curve to the right from the 0.465 psi/ft gradient curve indicate overpressured compartments. Change in slope of line connecting the Skinner and Red Fork data points indicates that a seal separates the two zones. The change in slope below the Red Fork indicates that a seal separates the Red Fork and Morrow zones.

below the Woodford Shale, including the Hunton, Simpson, and Arbuckle Groups, generally have near-normal pressure gradients. However, the intervals do contain local areas with abnormally pressured zones.

PRESSURE-DEPTH PROFILES

Within the shelf setting of the study area, a pressure-depth profile such as Figure 9 indicates the near-normal pressure gradients. Contrasting this gradient is a pressure-depth profile constructed in Roger Mills County in the deeper part of the basin. This profile (Fig. 10) indicates the development of overpressured conditions in the Red Fork and Morrowan intervals and near-normal pressure gradients in the Hunton Group. Based on the presence of high pressure gradients in overlying Springer and Mississippian reservoirs, the bottom seal of the regional compartment is inferred to be near the Woodford Shale stratigraphic position.

Evidence for compartments or units within the mega compartment complex is best seen in T. 15 N., R. 21 W. (Fig. 6). Red Fork gradients in this field (0.75 psi/ft) are situated between overlying Skinner gradients (0.56–0.67 psi/ft) and underlying Morrowan (0.6–0.7 psi/ft) gradients (Fig. 11). This Red Fork compartment appears to be confined to a stratigraphically isolated shallow-marine delta-fringe sandstone deposit situated along the shelf break of the Anadarko basin.

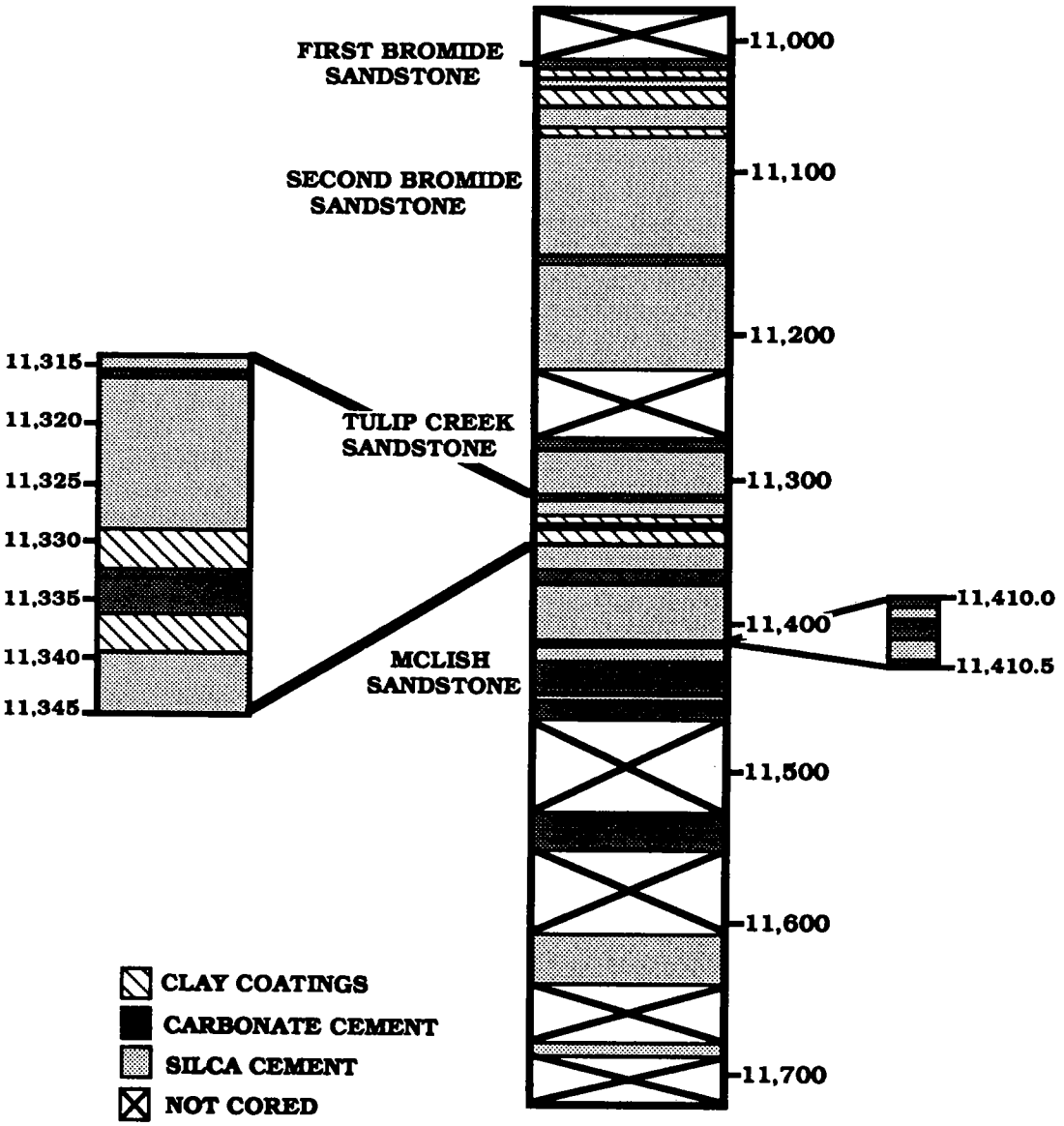

Figure 12. Large and small-scale diagenetic banding of seal interval in the Gulf Weaver core.

NATURE OF SEALS

The Gulf Weaver and Woods Switzer cores were selected because they contained thick cored intervals that included seals as defined by pressure data. Two different types of seals were identified in the Weaver and Switzer cores. The Weaver core contains large-scale (measured in feet) and small-scale (measured in tenths of feet) (Fig. 12) diagenetically banded zones within the Simpson sequences. In the Switzer core, the seal interval contains silicified carbonate mudstone and claystone zones overlying interlaminated silicified claystone and siltstone. This interval is a seal due primarily to lithology but also to significant silica and carbonate cementation.

Diagenetic and Lithologic Banding Patterns

Top and basal pressure seals generally exhibit a characteristic linear pressure change with increasing depth across the seal zone (Powley, 1987). Pressure data from the Gulf Oil Co., Weaver No. 1, McClain County indicate that the Simpson Group cored interval is part of a seal zone which can be

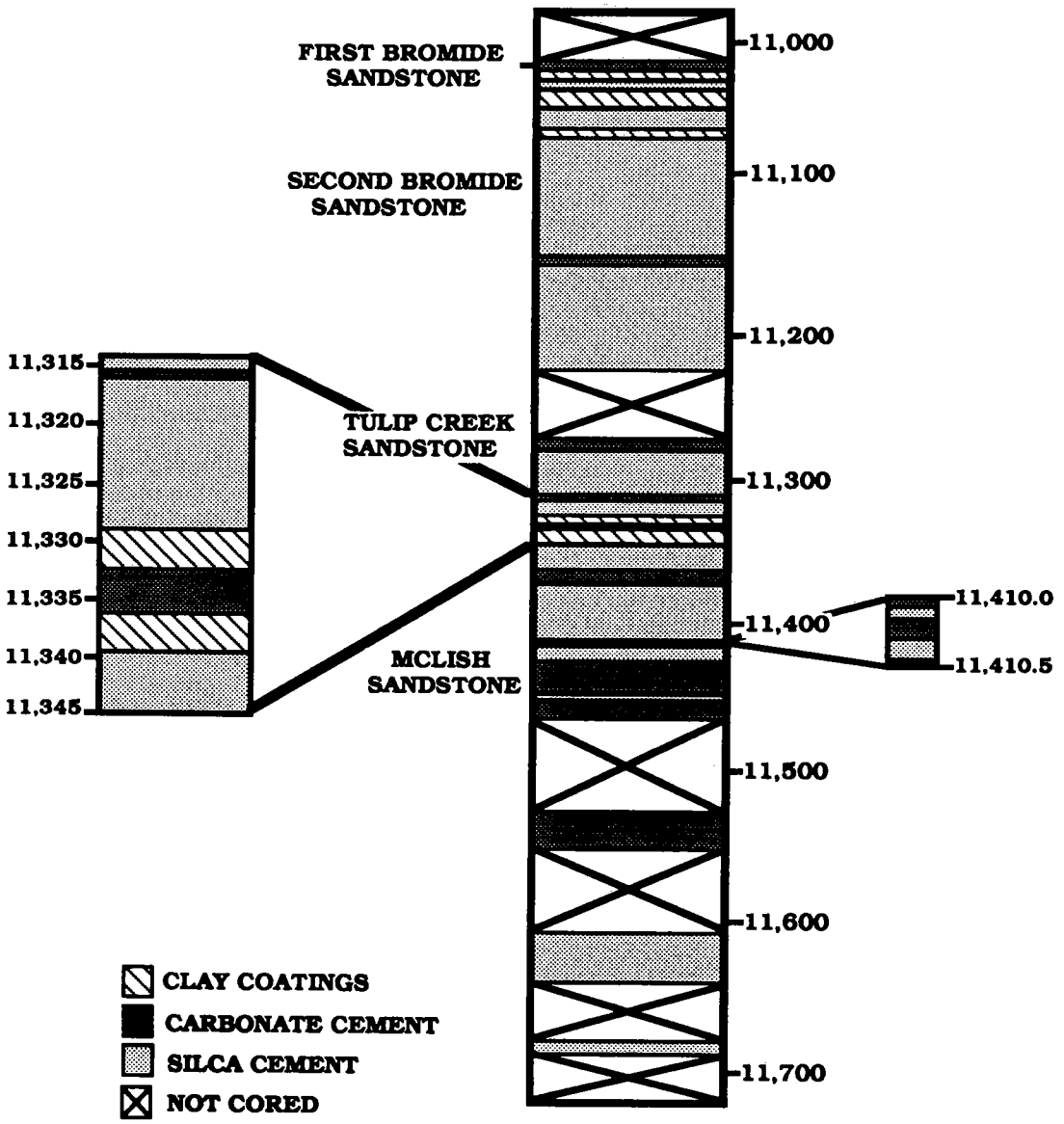

Figure 12. Large and small-scale diagenetic banding of seal interval in the Gulf Weaver core.

NATURE OF SEALS

The Gulf Weaver and Woods Switzer cores were selected because they contained thick cored intervals that included seals as defined by pressure data. Two different types of seals were identified in the Weaver and Switzer cores. The Weaver core contains large-scale (measured in feet) and small-scale (measured in tenths of feet) (Fig. 12) diagenetically banded zones within the Simpson sequences. In the Switzer core, the seal interval contains silicified carbonate mudstone and claystone zones overlying interlaminated silicified claystone and siltstone. This interval is a seal due primarily to lithology but also to significant silica and carbonate cementation.

Diagenetic and Lithologic Banding Patterns

Top and basal pressure seals generally exhibit a characteristic linear pressure change with increasing depth across the seal zone (Powley, 1987). Pressure data from the Gulf Oil Co., Weaver No. 1, McClain County indicate that the Simpson Group cored interval is part of a seal zone which can be

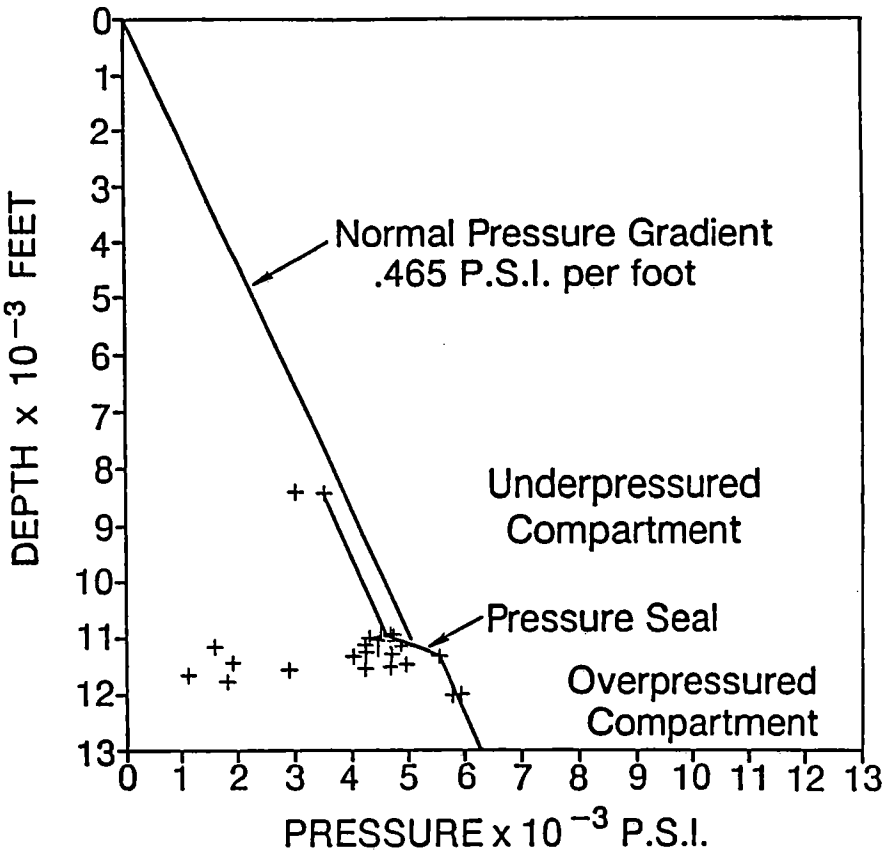

Figure 13. Pressure-depth profile in the vicinity of the Gulf Weaver No. 1 core in sec. 17, T. 5 N., R. 4 W., McClain County, Oklahoma.

correlated with the pressure-depth profile shown in Figure 13 (Tigert and Al-Shaieb, 1990).

The compositionally homogeneous Simpson Group sandstones exhibit textural heterogeneity due essentially to diagenetic processes. The diagenetic processes are cementation, intergranular pressure-solution, and mechanical brecciation. The textural heterogeneity in the Gulf Weaver No. 1 core is manifested as laminations and banding formed by chemical and mechanical diagenetic processes.

There are three distinct types of horizontal banding and lamination observed in the Simpson sandstone core: (1) poorly indurated sandstones alternate with well-indurated, silica-cemented sandstones (Fig. 14); (2) sharp contacts between silica-cemented and carbonate-cemented sandstone (Fig. 15), locally associated with stylolites; and (3) black to tan bands (oil-stained sandstone) alternate with light-colored bands (non-oil-stained sandstone) (Fig. 16).

Pressure solution and the formation of stylolites is related to rock compaction processes. Gouge and granulation textures (Fig. 17) are formed by deformational processes associated with faulting. These mechanical features, modified by chemical processes, may be part of the sealing mechanism associated with faults that serve as lateral seals. In the Gulf Weaver core, a single diagenetic band may not serve as a complete and laterally extensive seal, but the cumulative effect of multiple diagenetic banded zones may provide an effective seal. Both chemical and mechanical diagenetic banding patterns have been theoretically duplicated using a reaction-transport-mechanical model (Dewers and Ortoleva, 1990).

Immediately above the Red Fork sandstone reservoir in the Woods Switzer core is an interlaminated carbonate-claystone-siltstone sequence that is ~50 ft thick. This interlaminated sequence has a distinct diagenetic overprint and represents part of the seal. The pressure data supporting the presence of this seal are shown in Figure 18. The Skinner reservoir above the seal has a pressure gradient of 0.56–0.67 psi/ft while the Red Fork reservoir below the seal has a gradient of 0.75 psi/ft. The wire-line log signatures across this seal interval (Fig. 19) are similar to those observed for the transition to overpressured intervals reported by

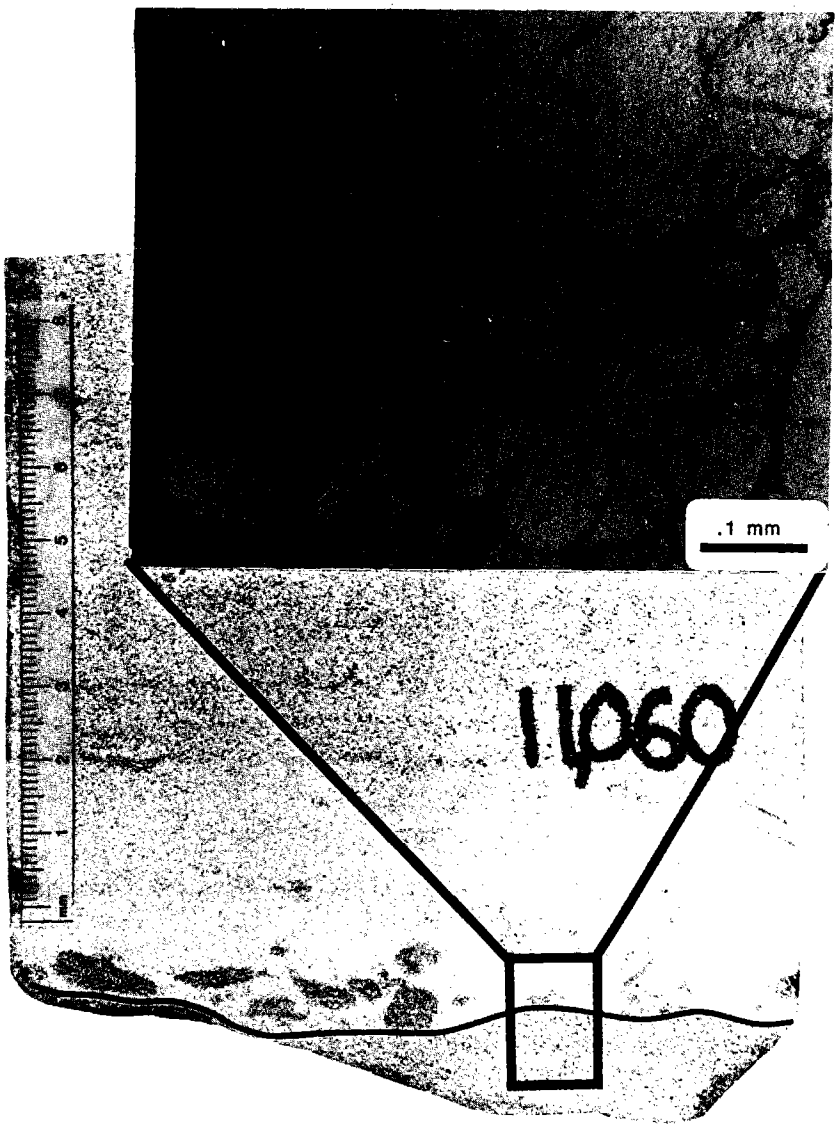

Figure 14. Well-indurated, silica-cemented sandstone alternating with clay-coated poorly indurated sandstone. Quartz overgrowth (QO) and primary intergranular porosity (PIP) is shown in photomicrograph.

Fertl and Timko (1970) (Fig. 20) and Breeze (1970). Normally, wire-line log signatures indicate shale resistivity and density increase with increasing depth. Features of the log signature across the transition zone include: (1) a decrease in shale resistivity with increasing depth, (2) a corresponding increase in conductivity, (3) an increase in acoustic traveltime (porosity) with depth, and (4) a corresponding decrease in bulk density and increase in neutron porosity. Once the overpressured interval is encountered the wire-line logs indicate that shale resistivity and density again increase with increasing depth.

CONCLUSIONS

The principal conclusions of this study are as follows:

1) Pressure measurements derived from drilling and production data can be utilized to locate and delineate sealed compartments.

2) A regional overpressured compartment called the mega compartment complex extends from ~10,000 ft to the base of the Woodford Shale.

3) Isolated abnormally higher-pressured compartments or units occur within the mega compartment complex.

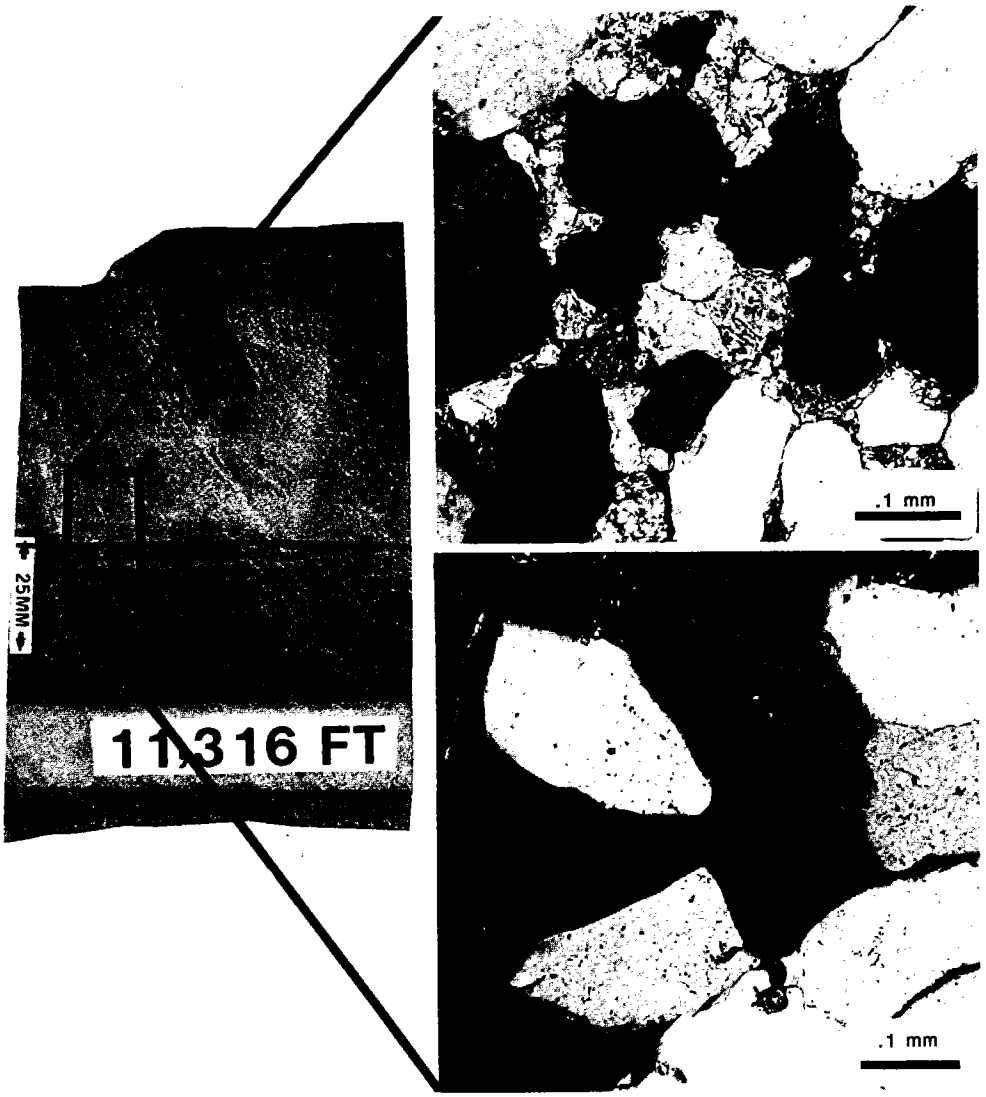

Figure 15. Silica-cemented sandstone (dark) in contact with carbonate-cemented sandstone (light).

4) Localized high pressured compartments within normally pressured zones were identified outside the mega compartment complex.

5) Seals can be both lithologically and diagenetically controlled.

6) Diagenetic seals in the Simpson sandstones are characterized by the abrupt change from alternating bands of non-cemented and silica-cemented sandstone to carbonate-cemented sandstone.

7) Mechanical deformation features, including stylolites, gouge, and granulation can produce seals within relatively homogeneous sandstones.

8) Seals are identifiable in cores and can be inferred from wire-line logs and subsurface mapping.

ACKNOWLEDGMENTS

We gratefully acknowledge the Gas Research Institute for generously funding this research through Contract No. 5089-26-1805. We thank David Powley and John Bradley of Amoco Production Co. who gave helpful suggestions concerning this study. Dwight's Energy Data Inc. provided gas well production histories that were essential to the completion of this study.

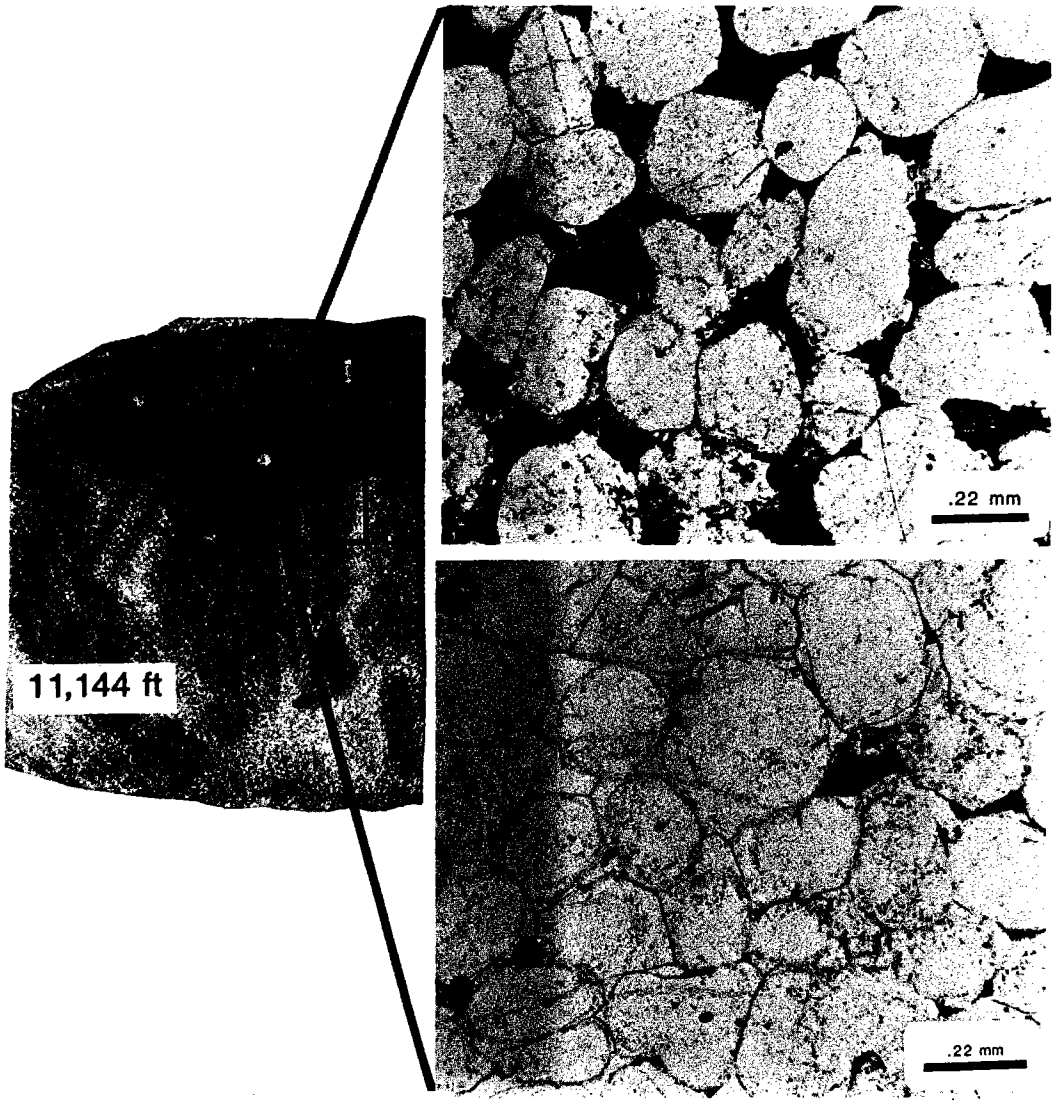

Figure 16. Oil-stained sandstone (dark) in contact with non-oil-stained sandstone.

REFERENCES

Al-Shaieb, Z.; Alberta, P. L.; and Gaskins, M., 1990, Depositional environment, petrology, diagenesis, and porosity of the Upper Morrow chert conglomerate in Oklahoma, in Transactions of the American Association of Petroleum Geologists Mid-Continent Section Meeting: Oklahoma City Geological Society, p. 1–53.

Al-Shaieb, Z.; and Shelton, J. W., 1977, Evaluation of uranium potential in selected Pennsylvanian and Permian units and igneous rocks in southwestern and southern Oklahoma: U.S. Department of Energy Open-File Report GJBX-35 (78), 248 p.

Arbenz, J. K., 1956, Tectonic map of Oklahoma: Oklahoma Geological Survey Map GM-3, scale 1:750,000.

Breeze, A. F., 1970, Abnormal-subnormal pressure relationship in the Morrow sands of northwestern Oklahoma: Shale Shaker Digest, no. 7, p. 45–66.

Dewers, T.; and Ortoleva, P., 1990, A coupled reaction/transport/mechanical model for intergranular pressure solution, stylolites, and differential compaction and cementation in clean sandstones: Geochimica et Cosmochimica Acta, v. 54, pt. 2, p. 1609–1625.

Dwight's Energy Data Inc., 1989, Natural gas well production histories: Richardson, Texas.

Echometer Co., 1986, Analyzing well performance: Wichita Falls, Texas.

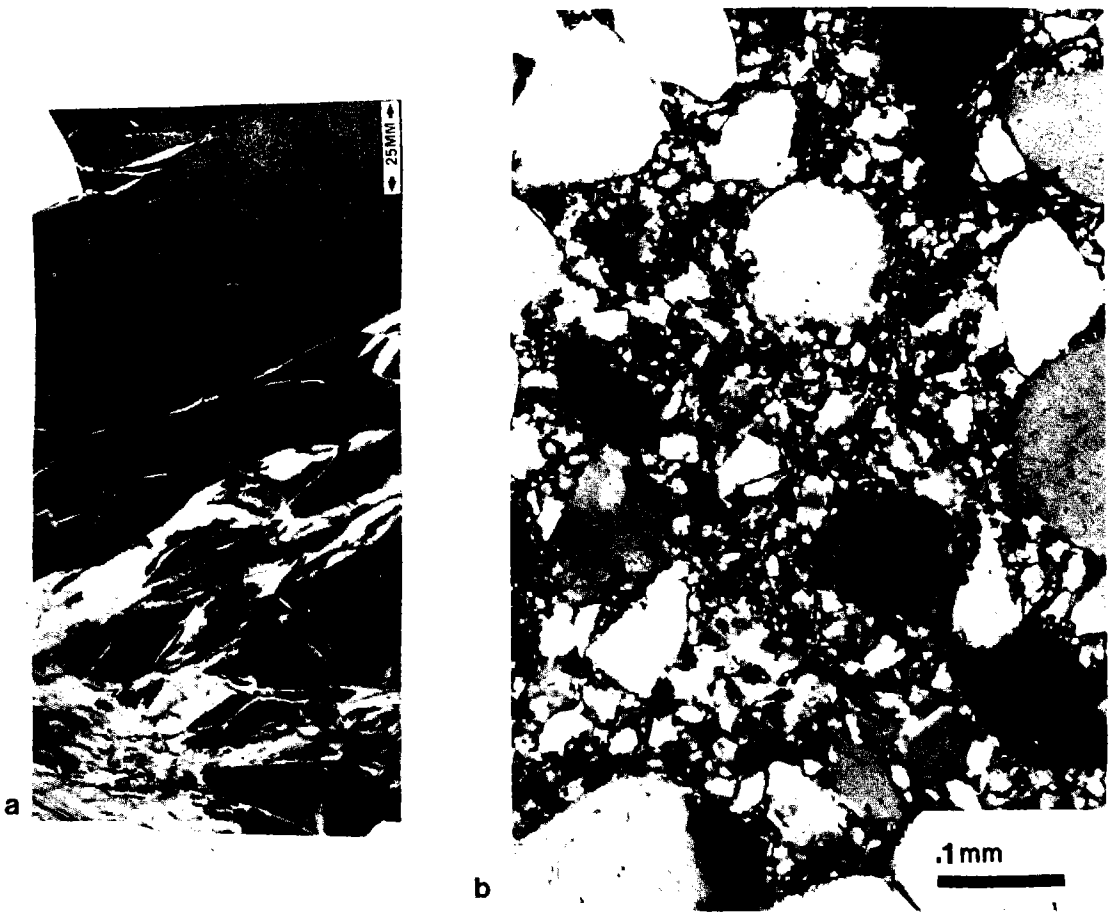

Figure 17. Gouge in sandstone. Depth 11,377 ft. *A*—Core photograph of light-colored gouge. *B*—Photomicrograph of shattered quartz grains in gouge zone (cross-polarized light).

Fertl, W. H.; and Timko, D. J., 1970, Occurrence and significance of abnormal pressure formations: Oil and Gas Journal, v. 68, p. 97–108.

Orr, E. D.; Kreitler, C. W.; and Senger, R. K., 1985, Investigation of underpressuring in the Deep-Basin Brine aquifer, Palo Duro basin, Texas: Texas Bureau of Economic Geology Circular 85-1, 44 p.

Powley, D. E., 1987, Subsurface fluid compartments: Gas Sands Workshop, Gas Research Institute, Chicago, 16 p.

Tigert, V. A.; and Al-Shaieb, Z., 1990, Pressure seals: their diagenetic banding patterns: Earth Science Reviews, v. 29, p. 227–240.

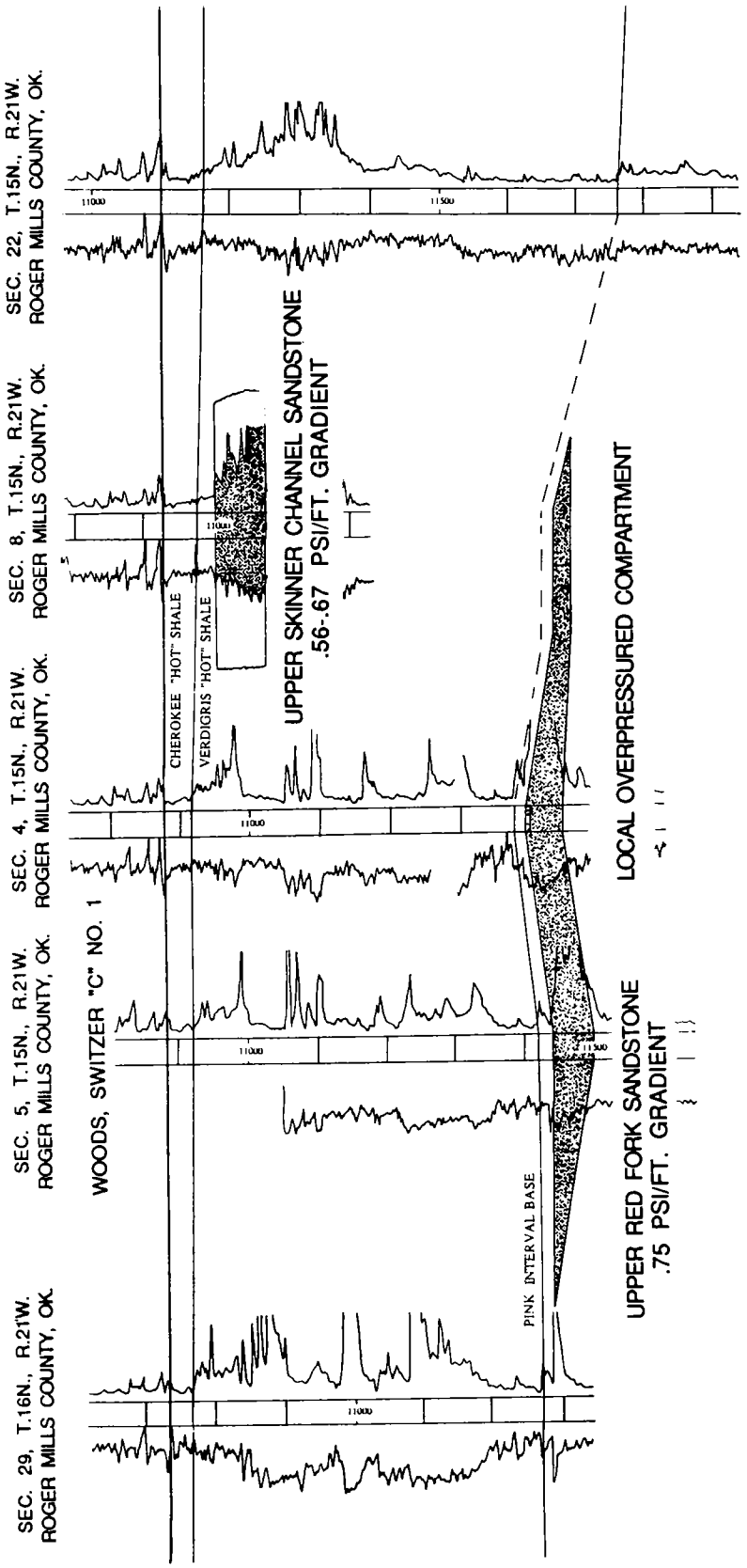

Figure 18. Stratigraphic cross section through Southwest Leedey field, Roger Mills County, Oklahoma. The Upper Red Fork sandstone reservoir in this field represents a completely sealed compartment or unit. The change in pressure gradient between the Upper Skinner reservoir (0.56–0.67 psi/ft) and Red Fork reservoir (0.75 psi/ft) indicates a seal exists between the zones.

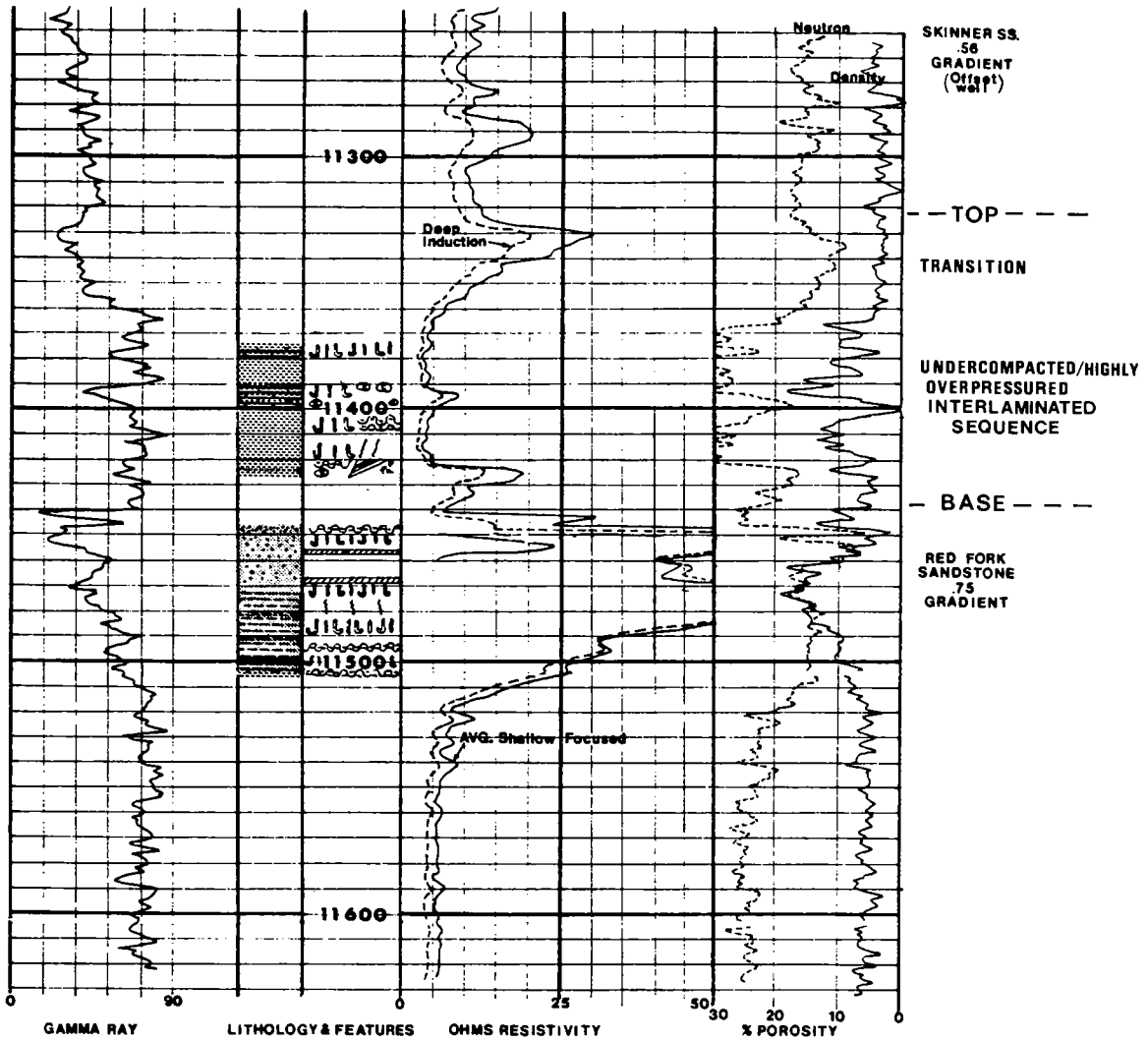

Figure 19. Wire-line log responses across the seal zone between the Skinner and Red Fork reservoirs in the Woods Switzer "C" No. 1.

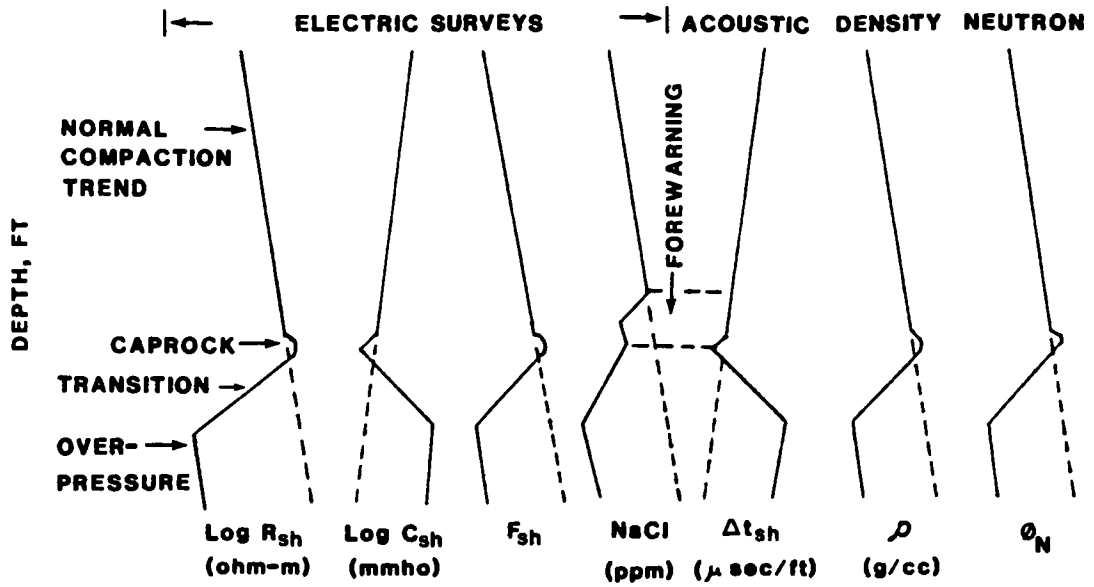

Figure 20. Wire-line log responses in normal and overpressured environments (Fertl and Timko, 1970).

Hydrocarbon Potential of Selected Permian Basin Shales as Classified Within the Organic Facies Concept

Charles R. Landis
ARCO Oil and Gas Co., Plano, Texas

Ali Trabelsi
AA Production, Inc., Lubbock, Texas

Gary Strathearn
University of California at Los Angeles

ABSTRACT.—Integrated organic petrography and geochemistry indicate that thermally immature Woodford, Atoka, Canyon, and Wolfcamp shales of the Permian and Val Verde basins were hydrocarbon source rocks of organic facies B (oil prone) and BC (oil/gas prone) at the onset of oil generation. Hydrocarbon potential of both organic facies evolved toward more gas-prone facies during catagenesis. Present hydrocarbon potential of these shales is mainly gas. The higher bench-mark H/C ratios of organic facies B (~1.30) correlate to blue-light primary liptinite content in immature shale (~0.50% R_o). Alginite in immature shale exhibits a strong greenish-yellow fluorescence (λ max = 520–560 nm). Overall, the ratio of blue-light to white-light liptinite content exceeds unity in immature and incipiently mature shale. With increasing maturity, this ratio falls below unity as primary liptinite fluorescence diminishes. Petrographic evidence of the dominant continuous hydrocarbon phase includes an unusual but conspicuous microfracture exsudatinite which exhibits a strong blue and blue-green fluorescence (λ max = 450–470 nm). Proton resonance spectra from bitumen document complex saturated fractions and electron-donating functionals associated with the aromatic fraction and in the saturated hydrocarbons. These data suggest that the potential role of generated molecules as sedimentary reductants in conduits and reservoir beds can be established in the source rock environment.

INTRODUCTION

The concept of petroleum generation commonly implies that hydrocarbons are derived at depth and driven toward highly permeable, receptive reservoir rocks. It is understood that these hydrocarbons are products of thermal decomposition of indigenous oil-prone organic material. To qualify as a liquid hydrocarbon source rock three criteria, enumerated by Cardott and Lambert (1985), must be met: (1) total organic carbon (TOC) content must exceed 0.5 wt%; (2) oil-prone parental organic matter (mainly type I and type II kerogen) must be present; and (3) thermal maturity must have reached at least that of the oil-window (Phillippi, 1965; Dow, 1977; Tissot and Welte, 1978; Brooks, 1981). Each criterion is critical for the generation of liquid hydrocarbons, as the absence of one nullifies the potential of the other two.

Catagenesis is characterized by relatively modest temperatures (50–150°C) and pressures (300–1,000 bars) and is commonly called the "oil window" (Tissot and Welte, 1978). Although in many ways broad and largely undifferentiated, this stage includes the onset of liquid hydrocarbon generation, peak hydrocarbon generation, and the thermal termination of liquid hydrocarbon preservation. Demarcations of these stages vary, but peak liquid hydrocarbon generation follows the onset of liquid hydrocarbon generation for type I and type II kerogen (Dow, 1977; Bostick, 1979; Dow and O'Connor, 1982; Saxby, 1982; Teichmüller, 1982). A summary of the chemistry of organic maturation is given by Waples (1982).

The term *source rock* is an encompassing term which has been further subdivided to express relative stages of generation or potential as a hydrocarbon-generating sedimentary succession (Waples, 1984). An effective source rock is "any sedimentary rock that has already generated and expelled hydrocarbons" (Waples, 1984, p. 93). His potential source rock is a sedimentary succession that meets the first two criteria listed above but fails the third; a possible source rock may be suspected of hydrocarbon generation but awaits evaluation (Waples, 1984). Currently, the evalua-

tion of all source rocks favors geochemical techniques that provide bulk chemical information from a sample.

The source-rock concept also implies that the generative products of indigenous oil-prone organic material must be expelled. This point is often not developed in the literature. The dominant mechanisms of primary migration, for example clay dewatering (Powers, 1967), the continuous hydrocarbon phase (Meissner, 1978; Momper, 1978; Jones, 1981), and hydrocarbon diffusion (Leythaeuser and others, 1980,1982,1983,1984) have only recently been incorporated into the evaluation of likely source rocks (Jones, 1987). Indeed, the mobilization of hydrocarbons from source rocks remains one of the most poorly understood of the processes related to the generation of oil.

The evaluation of source-rock potential and mechanisms of primary hydrocarbon migration are rarely integrated into one classification system. A step toward this end is the concept of organic facies (Jones, 1984,1987). Jones (1984, p. 163–164) defines organic facies as a "mappable rock unit, distinguishable from adjacent rock units by the character of its om [organic matter] without regard to the inorganic aspects of the sediment." This system predicts the hydrocarbon potential of thermally immature source rocks based upon "bench-mark" atomic hydrogen to carbon (H/C) ratios, Rock-Eval pyrolysis data, and organic petrology. By definition, organic facies classification applies only to thermally immature rocks (<0.50% R_o), but remaining hydrocarbon potential in mature source rocks may be evaluated within this concept as well.

To date, the classification of source rocks and the recognition of primary migration mechanisms are based largely upon geochemical data, although microscopy may eventually prove to be an excellent aid to these ends. Petrographic analysis is useful because (1) the sample is preserved during the analysis, (2) sample preparation cost is minimal, (3) varieties of bitumen may be identified, and (4) microscopic inspection reveals organic-mineral relationships not directly obtained from bulk chemistry. Petrographic techniques are utilized to characterize the thermal maturity and composition of a potential source rock. Preserved plant fragments and other organic material are microscopically observable and referred to as macerals. Spackman (1958) proposed that macerals as discrete substances possess diagnostic chemical and physical properties. Petrographically, macerals are diverse (see Stach and others, 1982). Among the three major maceral groups, the vitrinites and inertinites are either not, or perhaps marginally, prone to liquid hydrocarbon generation (Tissot and Welte, 1978).

The evidence to date has indicated that the liptinites are the most important maceral group with respect to the generation of liquid hydrocarbons. Alginite is a particularly important liptinite in many oil-prone shales. Typically, the chemistry of alginite is characterized by saturated hydrocarbons (Tissot and Welte, 1978). Their petrographic habit may be either colonial or unicellular (Hutton and others, 1980). *Tasmanites* is a unicellular marine alga preserved as the maceral alginite. In blue light, *Tasmanites* exhibits a strong fluorescence, particularly in immature and incipiently mature shale.

Liptinites may be distinguished from other macerals by the unusual property of conspicuous fluorescence. Liptinite spectral fluorescence has been studied in bituminous coals for many years (Teichmüller, 1974; Ottenjann and others, 1975; Ting and Lo, 1975; Spackman and others, 1976; Teichmüller and Wolf, 1977; Radke and others, 1980; Teichmüller and Durand, 1983). Visible fluorescence reveals secondary liptinite macerals thought to be related to oil generation (Teichmüller, 1974). Secondary liptinite macerals are formed from primary liptinite macerals during thermal maturation. Other varieties of secondary resinites identified in coals and shales fill fissures and cracks (Crelling, 1983; Mukhopadhyay and Gormly, 1984).

The correlation of the organic-facies concept and thermal maturation with the distinctive organic petrology of prolific hydrocarbon source beds remains as an important scientific study. Jones (1984,1987) used the diagenetic environment, bounded upwardly by vitrinite reflectance near 0.50% R_o, to provide benchmark H/C ratio data for the classification of organic facies. Still needed as additional corroborative data for organic facies classification are the quantitative fluorescence properties of the macerals most prone to the generation of liquid hydrocarbons. The effectiveness in documenting catagenesis in shales by blue-light inspection awaits comparison with the recent improvements documented for coal characterization (Spackman and others, 1976; Crelling, 1983).

Also, blue-light microscopy may reveal mechanisms of primary migration. Extremely oil-prone shales should reveal petrographic expressions of the development of the continuous hydrocarbon phase. If generation itself is the main factor controlling the events leading to the ultimate expulsion of oil, then liptinite spectral properties are a vital geologic probe into these processes. Also, if the continuous phase is the dominant migration mechanism in oil-prone source rocks, then petrographic documentation of its mode of formation is needed. Thus, the objectives of this study are twofold: (1) to characterize the organic facies of several Permian basin shales with integrated organic geochemistry and petrology, and (2) to identify

petrographic expressions of primary hydrocarbon migration.

GEOLOGIC SETTING

The Permian basin of western Texas and eastern New Mexico is a prolific petroleum province and is southernmost among several cratonic basins of the North American Midcontinent. The geologic history of the Permian basin records deposition of many likely hydrocarbon source beds. Today, petroleum and natural gas is produced in all of the comprising physiographic provinces (Fig. 1). Beginning in Ordovician time, the Tobosa basin was a broad, largely unstructured depression or continental margin sag of the late Paleozoic Permian basin (Galley, 1958; McGlassen, 1968). Reflective of this relative quiescence, its Silurian and Devonian rocks record significant carbonate and shale sequences. The late Paleozoic Alleghenian–Ouachita–Marathon Orogeny resulting from the continental collision of Gondwanaland and North America coupled with concommitant basement uplift of the ancestral Rocky Mountains probably initiated the suturing and subsequent uplift of the Central Basin Platform. As a result, two separate asymmetric depressions, the Delaware and Midland basins, were formed (Thomas, 1977; Kluth and Coney, 1981; Pindell, 1985; Armin, 1987). Subsequent shale, carbonate,

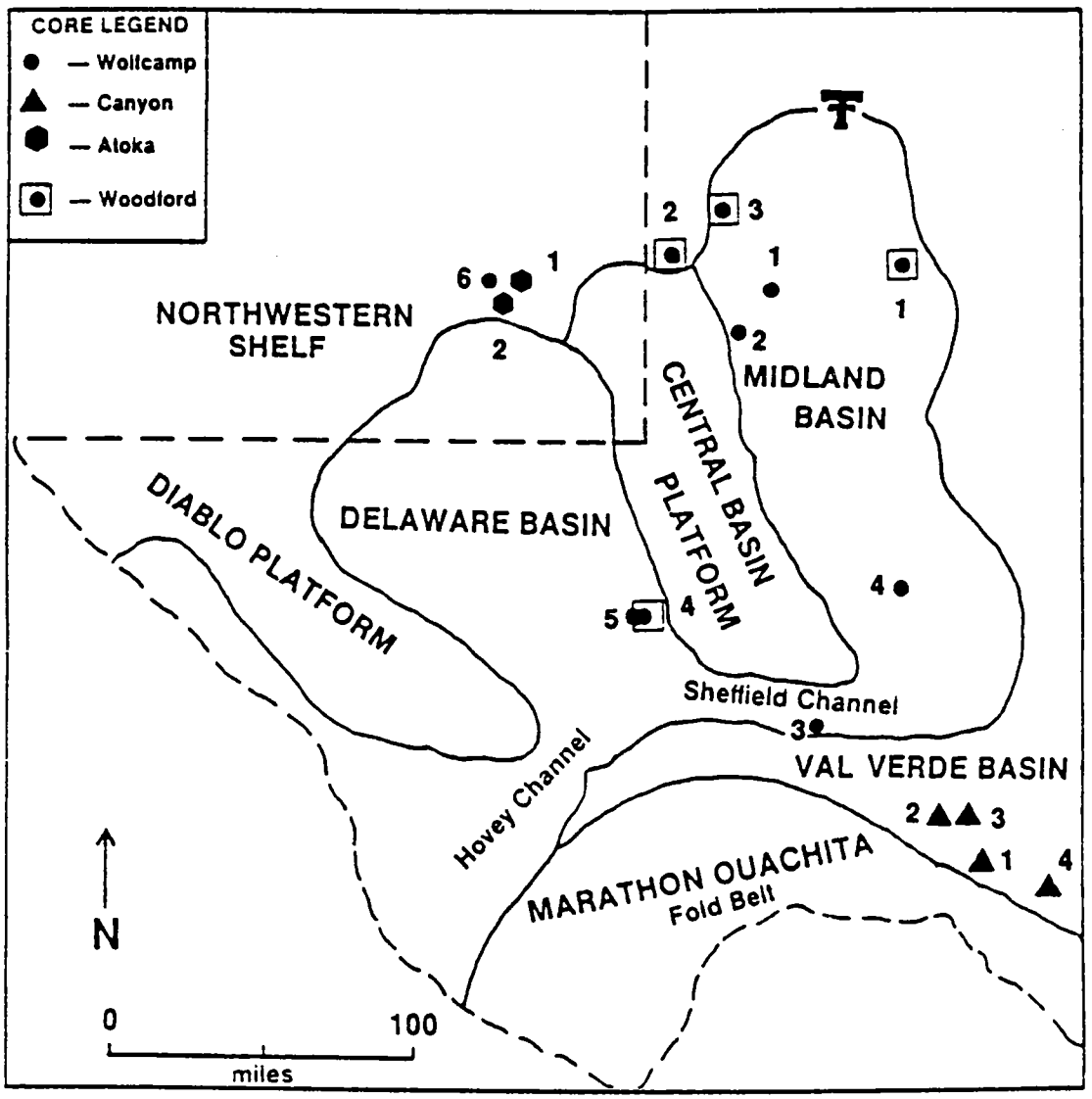

Figure 1. Physiography of Permian basin of western Texas and eastern New Mexico indicating its general tripartite nature.

and evaporite deposition continued to fill the Delaware and Midland basins and drape unconformably over the platform. Apart from late Paleozoic suturing, the two relatively stable basins experienced only mild tilting (Hills, 1984) and possible Mississippi Valley-type mineralization (Mazzullo, 1986).

The stratigraphy and sedimentology of the Permian basin has been well studied (Adams and others, 1951; Adams, 1965; Hills, 1970,1972,1984; Bloomer, 1977; Ward and others, 1986; Mazzullo and Reid, 1987; Reid and Mazzullo, 1988). Permian basin stratigraphy generally records thick lower Paleozoic carbonates that are overlain by middle Paleozoic clastics. However, unlike other cratonic analogs, thick Permian evaporite and carbonate reef complexes cap the stratigraphic column (Ward and others, 1986).

The Val Verde foreland basin represents part of the discontinuous arcuate foreland basin system produced by Alleghenian–Ouachita–Marathon orogenesis (Pindell, 1985). Much of the Val Verde early and middle Paleozoic stratigraphy records activity similar to other sequences in North America. After Late Precambrian–Early Cambrian rifting, carbonate and shale deposition along the passive margin of the craton mimics the sedimentology of the Permian basin. Up-section, thick late Paleozoic flysch and molasse sequences of the Val Verde basin indicate significant unroofing of the Ouachita–Marathon highlands (Graham and others, 1975). Thus, several thick basinal, slope, and shelf organic-rich shales occupy conspicuous stratigraphic positions throughout the generative Val Verde basin.

The following Paleozoic shale sequences in the Permian basin were studied: Upper Devonian Woodford Shale, Pennsylvanian (Atoka, Missourian [Canyon Equivalent]), and Permian (Wolfcampian) shale. In this study, no attempts have been made to conduct original investigations involving correlation of stratigraphic units. The stratigraphy of these rocks in the various physiographic provinces is well known (Fig. 2). Trabelsi (1990) provides a detailed study of depositional environments of the Woodford, Atoka, Canyon, and Wolfcampian shales in the subsurface of the Permian basin. Comer (1988) provides concise interpretations of the depositional environments of the Woodford Shale.

The Woodford Shale (Late Famennian) in the Midland basin displays two distinct lithofacies: (1) silty black shale and (2) shaly dolomitic facies (Trabelsi, 1990). The silty black shale is thinly laminated, organic rich, and contains maceral assemblages dominated by marine organic matter with notable concentrations of *Tasmanites*. This shale was deposited in relatively deep-water environments. Muds that formed this black shale possibly were deposited as dilute muddy suspensions or nepheloid layers (Trabelsi, 1990). The dark color, high organic content, fine laminations, and lack of bioturbation that characterize this facies suggest unusual conditions of anoxia or near-anoxia over the sea floor during the time of Woodford deposition (Trabelsi, 1990).

Other organic-rich shales include the Canyon, Atoka, and Wolfcamp shales. Atoka shale is dark grayish-black, silty, micaceous, thinly laminated, and is commonly intercalated with thin sandstones. This shale was deposited in a relatively calm, moderately deep, open shelf marine environment. A reducing environment is indicated by appreciable amounts of pyrite and mildly calcified fauna (Trabelsi, 1990).

Up section from the Atokan clastics are Canyon clastics of the Eastern Shelf, Midland, and Val Verde basins. Canyon sandstones display a suite of sedimentary structures, facies associations, and biogenic features indicative of deposition by turbidity currents. Lithologically, these turbidite deposits represent parts of submarine fan deposition comprising fine-grained sandstones, siltstones, and shale (Bloomer, 1977; Huang, 1989; Trabelsi, 1990).

The Lower Permian Wolfcamp section consists of carbonates, both limestone and dolomite, and siliciclastic rocks of basinal and slope origin (Hills, 1984; Ward and others, 1986; Mazzullo and Reid, 1987; Reid and Mazzullo, 1988). This stratigraphy is thought to represent the debouchment of ponded muds and other clastics from behind Late Pennsylvanian carbonate banks which developed along the margin of the basin (Hills, 1984). As a consequence, dolomitic and siliciclastic shales as well as carbonate debris flow breccias are interbedded with slope and basinal shale and limestones (Mazzullo and Reid, 1987; Reid and Mazzullo, 1988). The carbonates are known to be the hydrocarbon reservoir facies (Mazzullo and Reid, 1987).

ANALYTICAL PROCEDURE

Organic petrologic data were gathered with a modular Leitz MPV III microscope system capable of conventional white-light and fluorescence analyses. Criteria for the selection of suitable vitrinite were drawn from Bostick and Alpern (1977) and Bostick (1979). Vitrinite reflectance is now routinely applied to the evaluation of source rock maturity after its reliability was first demonstrated in coal (McCartney and Teichmüller, 1972). The difficulties associated with extending the use of vitrinite reflectance to pelitic rocks have been elucidated elsewhere (Bostick, 1979).

Maceral content was determined from point counts on whole-rock mounts in white light and blue light with glycerin and air objectives, respectively (Table 1). Five hundred counts from the pel-

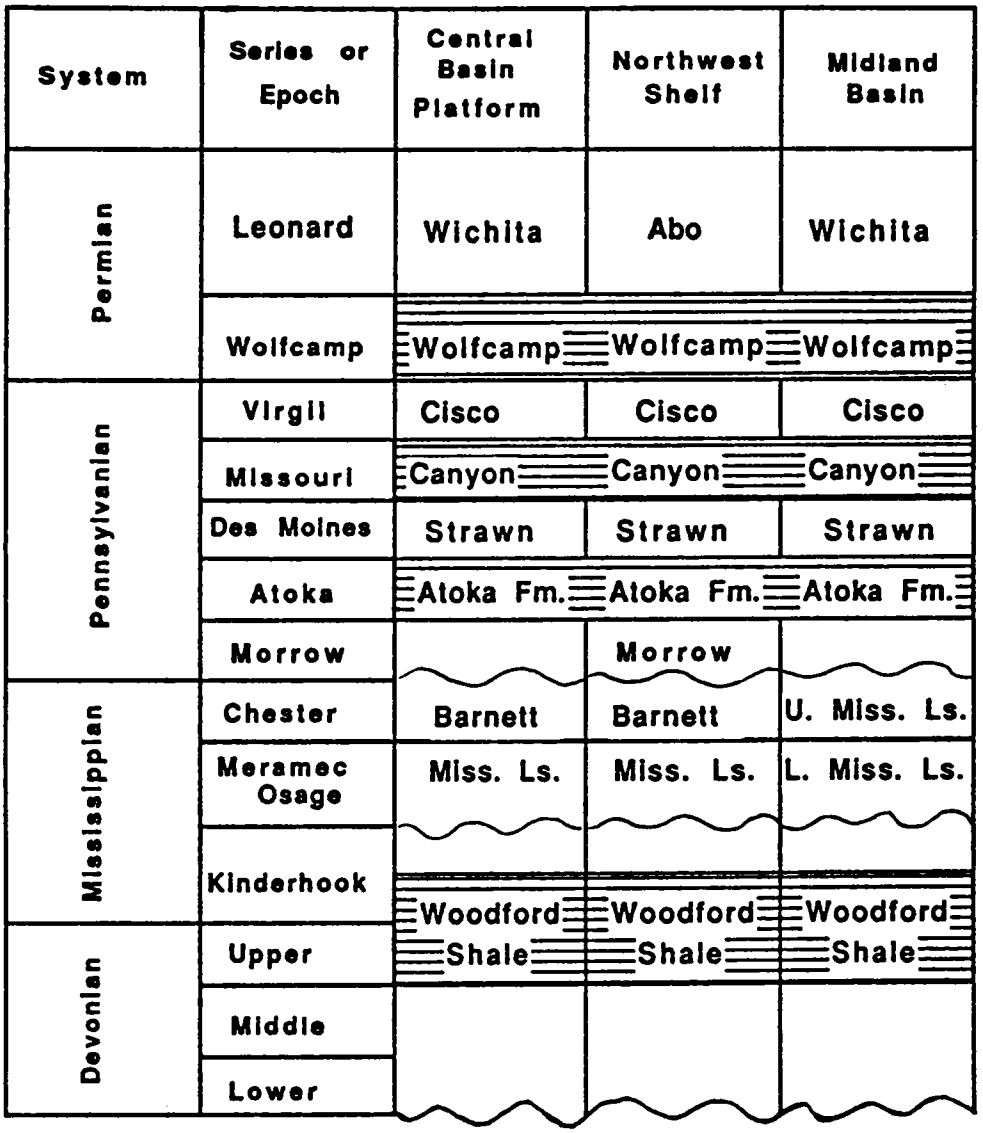

Figure 2. Stratigraphy of middle Paleozoic rocks of the Permian basin.

let surface were taken from fields of 20 points advanced in 150 μm steps perpendicular to bedding when stratification was apparent. Maceral classification drew from several systems used for coals and sedimentary rocks (Bostick, 1979; van Gijzel, 1982; Stach and others, 1982; Mukhopadhyay and others, 1987). Fluorescence analysis consisted of the above blue-light analysis and quantitative spectral analysis of primary and secondary liptinites.

Quantitative spectral analysis for the continuous excitation of liptinite fluorescence generally followed well-documented procedure (Crelling and others, 1989). The 365 nm line from a 100W Hg arc-lamp provided continuous wave (CW) excitation after passing through an input monochromator and microscope optics. Liptinite fluorescence passed through an exit monochromator to a cooled (-25°C) red-sensitive micro-channel plate photomultiplier (MCP). Cooling the MCP housing substantially reduced the ambient dark current, which becomes increasingly troublesome with increasing maturity.

Adherence to this procedure yielded an acceptable fluorescence spectrum that characterized the fluorescence color of the maceral. Two important parameters taken from each spectrum included the spectral maximum (peak or λ max) and the spectral quotient (Q). The former is the wavelength of maximum intensity. The latter is often

TABLE 1. — MACERAL CLASSIFICATION USED FOR PETROGRAPHIC CLASSIFICATION OF PERMIAN BASIN SHALE

I.	Vitrinite Group
	Indigenous vitrinite (1st cycle)
	Non-indigenous vitrinite (recycled)
II.	Liptinite Group
	Alginite
	Sporinite
	Resinite
	Liptodetrinite
	Exsudatinite (blue-light only)
	blue fracture fillings
	yellow to orange fillings
III.	Inertinite Group
	Fusinite
	Semifusinite
	Inertodetrinite
IV.	Amorphinite

called the red/green quotient as it compares intensities at 650 nm and 500 nm (650 $nm_{int.}$/500 $nm_{int.}$); both generally describe the shape of the acquired fluorescence spectrum.

Atomic hydrogen to carbon ratios (H/C) were obtained with an automated SIRA 12 mass spectrometer. Gas samples were prepared in the fashion described by Hayes and others (1983). Initial core samples were cleaned of surface contaminants by rinsing in dilute HCl/HF solutions (10%/10%) and then thoroughly with distilled water. Demineralization was accomplished with reagent grade HCl and HF solutions introduced to the sample in stepwise fashion. The residue was washed with distilled water until neutralized.

A fraction of the residual organic matter (10–20 mg) was combusted at 800°C for two hours in clean (500°C/2 hr) quartz tubes with cupric oxide and separated reduced-copper beads. Estimates of TOC contents were made as weight percentages from the residues of the above demineralization. These values are not equivalent to the total microscopic organic content (MOC) reported below. Elemental ratios were determined by gas pressure measurement in the mass spectrometer. Standardization was completed with known hydrocarbon molecules and precision among 22 of these compounds was 0.03.

Additional bulk chemical analysis included ^1H NMR spectroscopy of extractable organic matter in the shale completed with a Varian 200 mHz instrument. Organic material was obtained by Soxhlet extraction over 48 hours with benzene solvent. The sample cup was agitated at the midpoint of the extraction. Residual bitumen was cured with deuterochloroform ($CDCl_3$) standard and scanned from 1 to 12 ppm with signal averaging of least 10. Dominant organic functional groups were identified from their characteristic spectral region (Silverstein and others, 1981).

PRESENTATION OF DATA

As measured by mean random vitrinite reflectance (R_o), this suite of shale samples covers the entire oil window rather well (Table 2). TOC ranges from <1 to 35% by weight. In contrast, MOC totals <23% by volume. Alginite, primarily *Tasmanites*, exhibits a strong greenish-yellow fluorescence (λ max = 520–560 nm) in immature Woodford Shale (Figs. 3A,4,5). In white light, alginite macerals are transparent and often escape detection. In the other shales, similar unicellular Tasmanites alginite is evident. Alginite that exhibits discrete morphological forms has recently been classified as telalginite (Hutton, 1984; Sherwood and others, 1984; Cook, 1987). Typically, alginite spectra are broad and structureless (Fig. 4). Landis (1990) reports that the fluorescence of these macerals shifts to the red wavelengths with increasing thermal maturity.

Perhaps more conspicuous in mature shale (>0.80% R_o) are strongly radiative exsudatinites which fill microfractures along bedding (Fig. 3B). No obvious linear relationship between exsudatinite content and thermal maturity is apparent (Fig. 6) although peak abundances occur between 1.0 and 1.2% R_o. These macerals are typically 5–10 μm thick and may be as long as 200 μm, exhibit subtle flow structures, and include shale clasts.

The fluorescence spectra of these exsudatinites document a strong blue and blue-green fluorescence (Fig. 7). Unlike alginite, subtle spectral structure is apparent as a bulge in the yellow wavelengths (520–550 nm). Although the fluorescence properties of these secondary macerals differ greatly from those of the exsudatinite initially defined from coal (Teichmüller, 1974) and commonly reported in the literature (Teerman and others, 1987; Zhao and others, 1990), they are called exsudatinite in this study due to their origin as secondary exsudates derived from indigenous oil-prone organic material. In coal, exsudatinite exhibits a characteristically weak to moderate orange fluorescence (Teichmüller, 1974; Teerman and others, 1987; Zhao and others, 1990). As Zhao and others (1990) report, several varieties of exsudatinite macerals may be distinguished based upon their fluorescence spectra.

The petrography of these secondary macerals supports many of the observations reported previously in the literature. Secondary resinite, with spectral properties similar to exsudatinite, has been identified in coal (Crelling, 1983; Mukhopad-

hyay and Gormly, 1984). In Wolfcamp shale, local enrichments of resinites thought to be primary suggest that these macerals may be more precisely identified as "secondary resinites." In the other shales containing negligible primary resinite, these macerals must be classified more broadly as exsudatinite. Lewan (1987) observed parting separations in experimentally matured shale on the order of 100–150 μm, which were attributed to a lack of confining pressure in the apparatus. No such separations were observed from these Permian basin core samples.

Proton resonance spectra reveal important general traits about the bitumen (Figs. 8–10). The saturated region (0.9–2.0 ppm) is characterized by broad reflections indicative of complex environments for these protons. Thus, distinctions between chain and ring saturates is not possible. However, the tendency of the aromatic-associated protons to peak up-field from the reference benzene line (7.2 ppm) is meaningful. These data suggest that aromatic substituents with unpaired electrons on the atom directly attached to the aromatic ring dominate over other deactivating substituents. Similarly, peaks for protons associated with ether/alcohol functionals (3.2–3.6 ppm) are

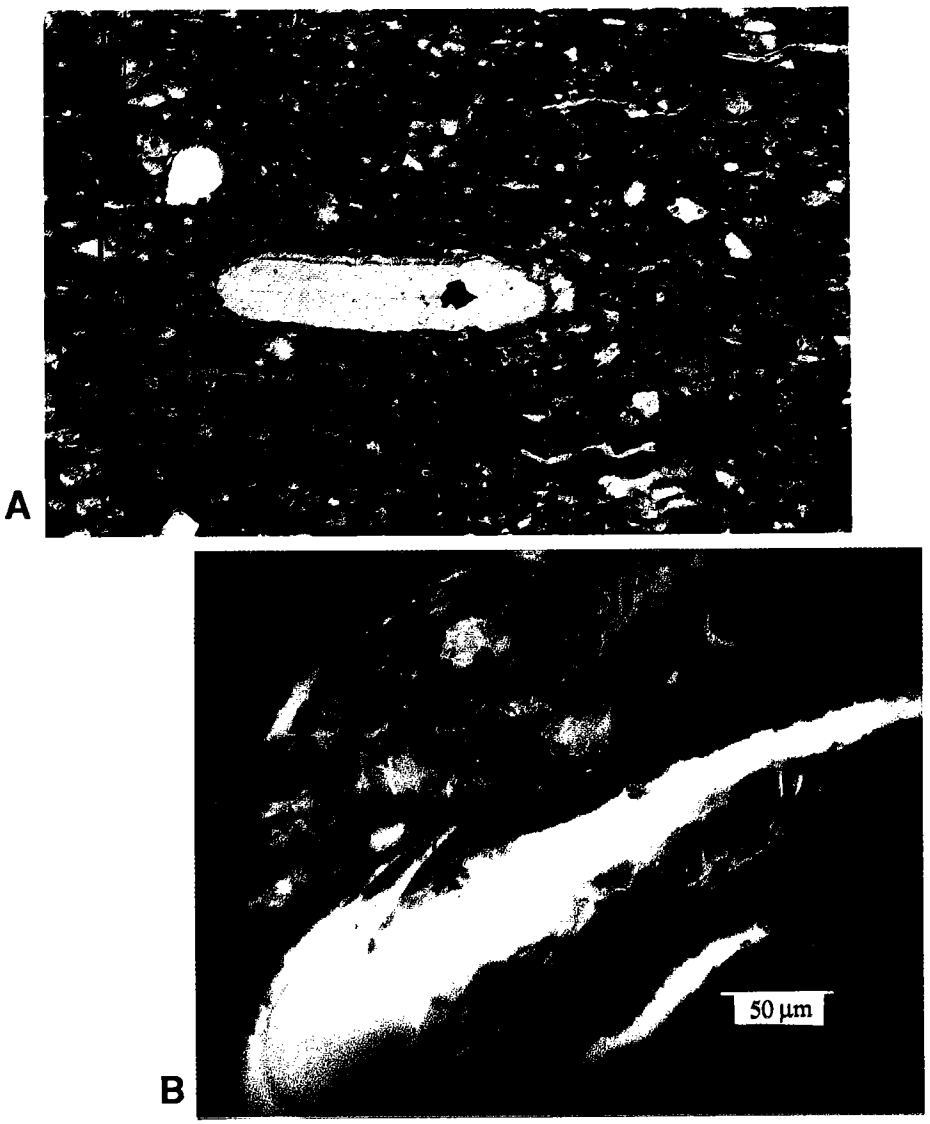

Figure 3. *A*—Photomicrograph in blue light of *Tasmanites* alginite in thermally immature shale exhibiting characteristically strong fluorescence. *B*—Photomicrograph in blue light (500×) of microfracture exsudatinite exhibiting characteristically strong blue emission.

TABLE 2. — BENCHMARK GEOCHEMICAL AND PETROLOGICAL DATA USED FOR ORGANIC FACIES CLASSIFICATION OF PERMIAN BASIN SHALES

Core	Sample	% R_O (s)[a]	H/C·	TOC (wt%)	MOC[b] (vol%)	BL/WL[c]
		Woodford Shale				
1	1	0.56(0.10)	0.81	1.0	13.4	1.3
1	2	0.50(0.06)	1.24	35.0	12.0	2.8
1	3	0.59(0.06)	1.27	32.9	15.0	8.8
1	4	0.57(0.10)	0.98	0.8	6.8	3.2
1	5	0.58(0.05)	0.75	3.8	11.6	1.2
2	1	0.68(0.07)	1.30	13.4	20.0	3.2
2	2	0.62(0.09)	1.27	8.4	9.0	—
2	3	0.59(0.05)	—	—	4.0	7.5
2	4	0.66(0.09)	1.28	3.6	13.0	3.5
3	1	0.93(0.14)	0.68	5.9	22.2	1.7
3	2	0.95(0.11)	0.67	6.2	13.4	1.0
4	1	1.02(0.14)	1.10	32.6	17.4	0.8
4	2	1.05(0.11)	1.08	15.1	16.6	0.8
		Atoka Formation				
1	1	1.29(0.07)	0.74	2.6	—	—
1	2	1.22(0.10)	0.47	16.7	8.0	0.9
1	3	1.23(0.09)	0.53	6.9	10.6	0.0
1	4	1.23(0.11)	0.63	7.3	—	—
2	1	1.01(0.11)	1.08	7.3	7.2	0.3
2	2	0.93(0.11)	0.93	9.5	11.0	0.0
2	3	0.92(0.08)	0.92	7.8	14.6	0.2
2	4	0.96(0.10)	—	15.9	18.2	0.3
2	5	0.99(0.07)	0.97	8.7	—	—
2	6	0.99(0.09)	0.51	3.2	—	—
2	7	0.94(0.11)	—	8.5	10.8	0.7
		Canyon shales				
1	1	1.36(0.11)	0.60	23.6	17.8	0.0
1	2	1.38(0.09)	0.57	26.2	17.6	0.0
1	3	1.39(0.09)	0.62	11.6	9.0	0.0
1	4	1.32(0.08)	0.45	24.6	14.0	0.0
1	5	1.32(0.08)	0.43	12.5	12.0	0.0
1	6	1.33(0.08)	0.44	8.2	12.2	0.1
1	7	1.40(0.08)	0.45	13.0	12.0	0.0
2	1	1.23(0.10)	0.94	12.2	9.4	0.0
2	2	1.27(0.05)	—	—	15.2	0.0
2	3	1.18(0.08)	1.01	12.4	8.8	tr.
2	4	1.19(0.07)	1.01	10.4	9.0	0.0
2	5	1.22(0.10)	1.05	9.5	11.2	0.0
2	6	1.17(0.07)	1.08	8.1	11.2	0.0
2	7	1.16(0.08)	1.10	14.0	12.4	0.0
2	8	1.12(0.09)	1.12	21.0	11.6	tr.
2	9	1.12(0.08)	1.12	12.2	10.8	tr.
2	10	1.11(0.09)	1.12	9.6	14.2	0.2
3	1	1.24(0.10)	0.70	6.9	6.6	0.6
3	2	1.18(0.11)	1.08	7.8	12.2	0.1
3	3	1.20(0.14)	1.18	9.0	7.4	0.1
3	4	1.27(0.14)	1.18	15.1	10.2	0.2
3	5	1.17(0.10)	1.19	11.3	11.6	0.1
3	6	1.21(0.09)	1.05	7.8	12.6	0.0
4	1	0.96(0.08)	1.07	5.3	11.2	0.6
4	2	1.01(0.11)	1.18	16.0	10.8	1.4
4	3	0.96(0.12)	1.17	12.9	7.8	1.3
4	4	0.93(0.10)	1.19	15.9	11.6	1.0

TABLE 2. — *Continued*

Core	Sample	% R_O (s)[a]	H/C	TOC (wt%)	MOC[b] (vol%)	BL/WL[c]
4	5	0.94(0.07)	1.21	8.0	10.2	0.5
4	6	1.06(0.07)	1.15	1.0	8.0	0.9
4	7	1.05(0.13)	1.06	6.4	8.0	0.5
4	8	1.01(0.07)	1.08	10.4	7.4	0.6
4	9	1.05(0.09)	1.11	10.0	9.4	0.9
4	10	1.04(0.12)	1.07	8.0	8.0	0.7
4	11	1.07(0.10)	1.07	2.5	11.2	0.4
4	12	1.07(0.17)	0.92	8.5	6.8	1.1
4	13	1.03(0.11)	0.78	4.2	11.2	0.4
4	14	1.12(0.07)	0.75	9.2	9.2	1.8
4	15	1.10(0.11)	0.75	4.2	12.4	0.6
4	16	1.09(0.06)	0.72	16.4	7.8	0.2
4	17	1.07(0.07)	0.76	27.3	6.8	0.8
4	18	1.13(0.08)	1.04	8.8	16.2	1.6
4	19	1.10(0.11)	1.09	8.8	10.6	1.2
4	20	1.16(0.11)	1.07	22.3	10.4	0.8
		Wolfcamp shales				
1	1	0.84(0.09)	0.85	26.8	16.6	0.6
1	2	0.89(0.09)	0.84	23.4	8.8	1.2
1	3	0.90(0.09)	0.87	20.7	10.4	1.5
1	4	0.85(0.11)	0.82	18.7	5.8	1.8
1	5	0.94(0.10)	0.88	26.3	7.0	1.1
2	1	0.90(0.08)	1.23	28.8	10.8	1.0
2	2	0.85(0.09)	1.20	20.8	8.8	0.7
2	3	0.88(0.13)	1.14	26.8	7.6	1.7
3	1	0.93(0.06)	1.06	29.1	10.8	1.3
4	1	0.91(0.07)	0.95	25.5	9.2	0.5
4	2	0.94(0.11)	0.93	24.9	8.6	0.5
4	3	0.92(0.09)	0.97	27.2	10.0	0.8
5	1	0.94(0.13)	0.71	18.4	5.0	0.2
5	2	0.90(0.06)	0.68	18.1	12.4	0.4
6	1	0.72(0.05)	0.81	18.8	10.2	0.2
6	2	0.72(0.07)	0.77	5.7	4.2	0.4
6	3	0.85(0.09)	0.87	3.1	2.8	1.3
6	4	0.85(0.06)	0.99	28.5	15.0	0.4
6	5	0.76(0.07)	1.04	19.6	12.6	0.1
6	6	0.75(0.10)	0.97	26.1	9.2	0.9
6	7	0.77(0.08)	0.93	17.5	10.0	0.5
6	8	0.87(0.09)	0.81	19.8	13.2	0.8
6	9	0.78(0.06)	1.04	14.8	8.6	0.6
6	10	0.84(0.13)	0.83	8.5	6.6	0.5
6	11	0.74(0.10)	0.89	4.4	6.6	0.6
6	12	0.89(0.10)	0.85	26.4	13.0	0.4
6	13	0.93(0.09)	0.82	25.3	8.0	0.3
6	14	0.73(0.11)	0.79	4.0	7.6	1.0
6	15	0.81(0.09)	0.84	9.8	7.6	0.2
6	16	0.72(0.11)	0.72	5.9	3.8	1.0
6	18	0.94(0.06)	0.81	23.2	11.6	0.7
6	19	0.88(0.11)	0.78	27.5	12.0	0.4
6	20	0.83(0.08)	0.78	9.7	7.2	1.0
6	21	0.86(0.09)	0.61	15.1	14.0	0.4
6	22	0.89(0.07)	0.73	4.8	11.4	0.5
6	23	0.82(0.08)	0.60	17.8	12.2	0.1

Note: Organic facies is established in thermally immature shale with atomic H/C ratios and mean random vitrinite reflectance data. These data may also be used within this framework to evaluate remaining hydrocarbon potential of mature shale.

[a] R_o (s) = Reflectance in oil immersion (standard deviation).

[b] MOC = Total microscopic organic material and is the sum of particulate organic material, i.e., liptinite, vitrinite, and inertinite.

[c] BL/WL = The ratio of blue-light to white-light liptinite content.

also evident. In general, these data suggest that functionality capable of electron donation at chemically reactive sites is present in the soluble fraction of the shale.

DISCUSSION

Evaluation of Source Rock Potential

The concept of source rock classification proposed by Jones (1984,1987) is extended to these Permian basin shales. Immature shale is classified within the concept of organic facies. Remaining hydrocarbon potential of mature shale is also evaluated with the bench-mark criteria of the organic facies system. Several of the primary and secondary criteria are met to satisfactorily classify these Paleozoic shales as excellent oil- and oil/gas-prone source rocks (Table 3). Petrographic and bulk geochemical data mutually suggest that: (1) these shales contain sufficient quantities of oil-prone organic material; (2) most of the basinal shales are thermally mature with respect to liquid hydrocarbon generation; and (3) these shales expulse generative products via well-known mechanisms of primary migration.

Organic facies of Woodford Shale range from oil-prone (facies B) to gas-prone (facies C). As Jones (1987) notes, source rock potential is bound to reflect the initial kerogen assemblage and the degree of organic matter preservation during deposition. This suggests that hydrocarbon potential of source rocks will vary considerably, on a basinal scale or even within a limited cored interval, depending upon depositional processes.

Based upon extrapolation of data from mature shale and those data from immature shale, the petrographic and geochemical data suggest that mature Woodford, Atoka, Canyon, and Wolfcamp shales were hydrocarbon source rocks of organic facies B and BC (Fig. 11). Remaining hydrocarbon potential is gas, or oil and gas. The important H/C ratio taken near 0.50% R_o distinguishes organic facies B from organic facies BC source rocks rather well during catagenesis. For Permian basin source rocks of organic facies B, the incipiently mature H/C value is ~1.30. More gas-prone shales extrapolate to ~1.05, suggesting an initial organic facies BC classification. There is again considerable variation in remaining hydrocarbon potential during thermal evolution of these shales. For example, mature Wolfcamp shale ranges from oil prone to gas prone.

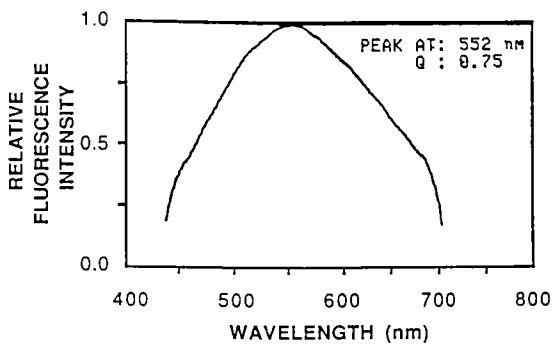

Figure 4. Average fluorescence spectrum of immature Woodford Shale alginite *Tasmanites* indicating greenish-yellow color.

TABLE 3. — LISTING OF INTERPRETED ORGANIC FACIES AND CORRESPONDING DOMINANT HYDROCARBON POTENTIAL OF PERMIAN BASIN SHALES AT THE ONSET OF CATAGENESIS

Source rock	Organic facies	Predominant HC potential
Wolfcamp	BC	oil/gas
Canyon	B	oil
Atoka	BC	oil/gas
Woodford	B	oil

Note: Organic facies for Wolfcamp, Canyon, and Atoka shales are interpreted from vitrinite reflectance vs. H/C trends shown in Figure 11. The remaining hydrocarbon potential for mature shale is gas or predominantly gas.

Both petrographic and geochemical analyses indicate that sufficient organic material is present in these shales for the generation of hydrocarbons. TOC by the residual demineralization technique indicates that as much as 35% by weight may be present with most shales falling between 5 and 20% by weight (Fig. 12). The microscopically detected particulate organic matter values (Fig. 13) are most often lower than corresponding TOC values. Visually detected organic matter reaches 22% by volume; most shales fall in the range of 5–18% by volume. However, the petrographic data indicate a bimodal distribution related to organic facies classification. Shales classified as oil prone, mainly Canyon shales, have a mean volumetric content of ~11% (Fig. 14). In contrast, organic material by volume averages ~8% in more gas-prone shale, mainly Wolfcamp shale (Fig. 15).

Petrographic properties further justify the above organic facies classification of these Permian basin source rocks. In immature Woodford Shale, large, discrete, greenish-yellow alginite, mainly *Tasmanites*, are evident. These liptinites exhibit strong fluorescence intensities. In the other mature shales, unicellular alginite is also present. Conspicuous liptodetrinite (i.e., fragmen-

tary primary liptinite) contributes to the primary liptinite assemblages in all shales. The similarity in fluorescence properties and morphology of large fragments link the liptodetrinite to the alginite and other, much less abundant, primary liptinites.

The amount of primary liptinite detected in blue light is related to the H/C ratio (Fig. 16). Clearly, higher H/C ratios are recorded for shales that are relatively enriched in fluorescent liptinites, as expected. Note that the blue-light volu-

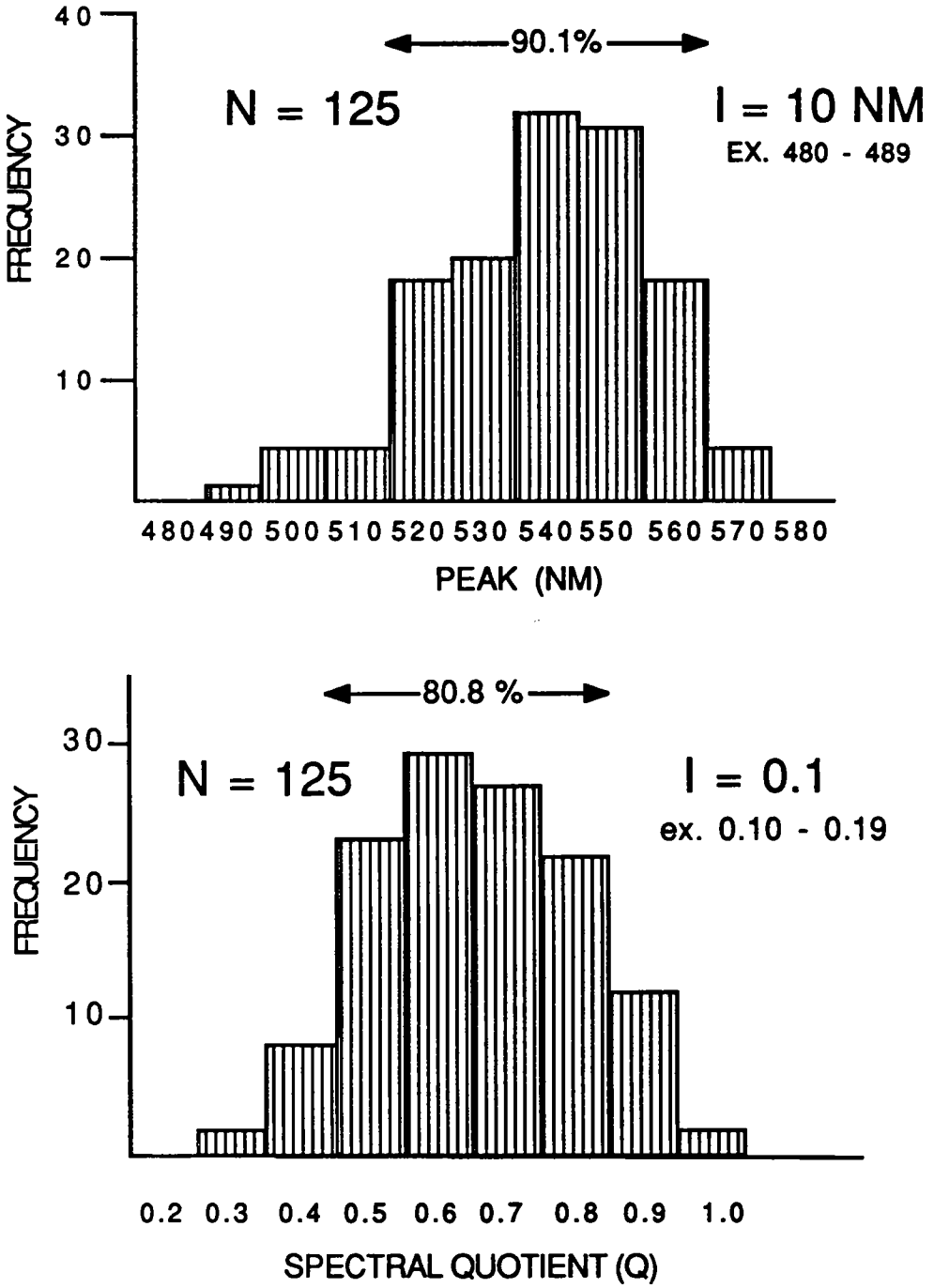

Figure 5. Histogram plots of peak wavelength and spectral quotient (Q) in immature (0.56% R_o) Woodford Shale.

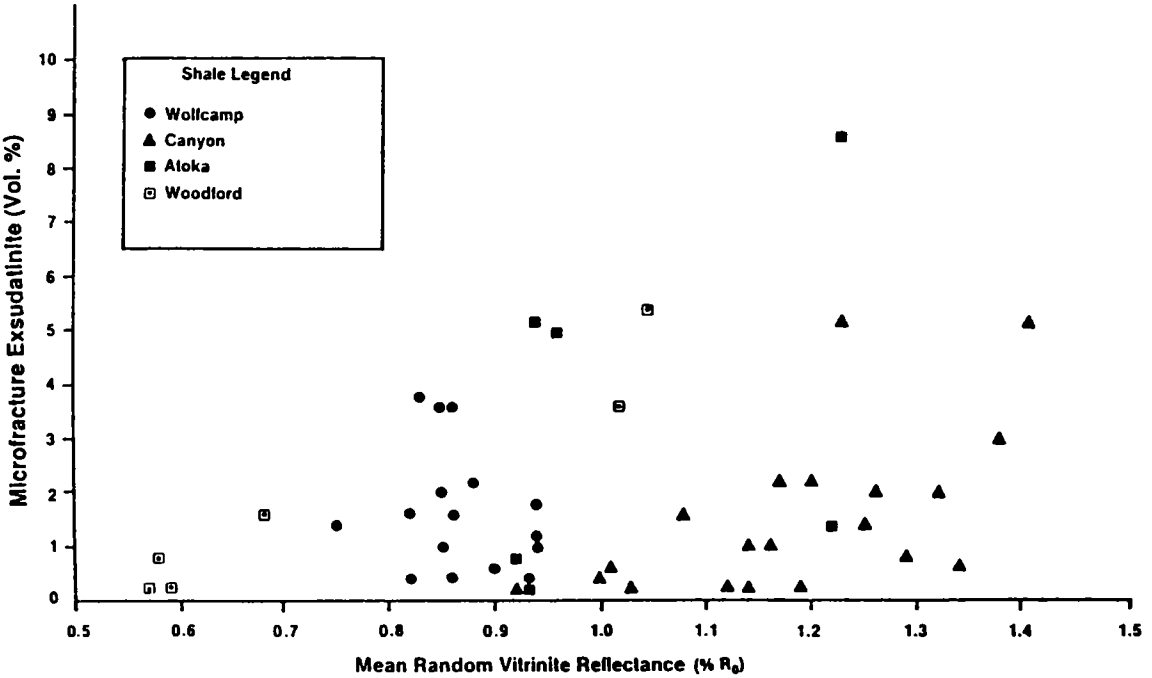

Figure 6. Plot of mean random vitrinite reflectance (% R_o) versus microfracture exsudatinite content (vol%) in Permian basin shales.

metric content of primary liptinites dominates the maceral distribution in organic facies B at the onset of catagenesis (i.e., H/C ratios near 1.30) (Fig. 16). On the other hand, the maceral distributions for shales with H/C ratios (0.95–1.15) characteristic of organic facies BC reveal the influence of terrestrially derived organic material in the form of measurable vitrinite and inertinite, and less liptinite. This is predicted for these organic facies (Jones, 1987), as it is well known that terrestrial organic assemblages drive the hydrocarbon potential toward natural gas and other light hydrocarbons (Tissot and Welte, 1978).

The results of this work suggest that the ratio of blue-light to white-light liptinite content is a helpful additional parameter for integrated source rock characterization (Fig. 17). Petrographic inspection must include blue-light point counts as it is very difficult to link H/C ratios to liptinite content based solely upon white-light maceral composition data. Ratios from immature and incipiently mature shales exceed unity. This ratio is near unity in mature shales (0.7–1.0% R_o). Above 1.00% R_o, this ratio falls below unity because as the fluorescence of the liptinites diminishes, their low-gray reflectance makes them visible in white light. Although it is well known that blue-light analyses improve petrographic coal characterization (Spackman and others, 1976; Crelling, 1983), the improved detection of liptinites at the critical reflectance of 0.5% R_o seems to be an important additional parameter by which to classify source rocks within the organic facies concept. However, these blue-light maceral data must be complemented in some way by white-light analyses in mature shale. Integrated petrography serves two main purposes: identification of liptinites in very mature shales and identification of the largely nonfluorescent terrestrial macerals.

Primary Hydrocarbon Migration

Bulk composition of potentially mobile hydrocarbons indigenous to these shales is revealed by ^1H NMR data from their companion bitumen. Although naphthenic-paraffinic oils characterize source rocks of organic facies B (Jones, 1987), exact determinations of the ratio between these two molecular groups is not possible from these data as the structure of the saturated fraction is lost in the broad peaks of the methyl region (0.9–2.0 ppm). These data do not refute past findings, however, as the saturated molecules are notable bitumen constituents.

More revealing is the potential role of these mobile molecules in oxidation-reduction reactions. Electron-donating functionality is identified as aromatic substituents, or as ether/alcohol nested in the saturated fraction. These data suggest that the role of organic matter as sedimentary reductants in carrier and reservoir beds may be established within the source-rock environment

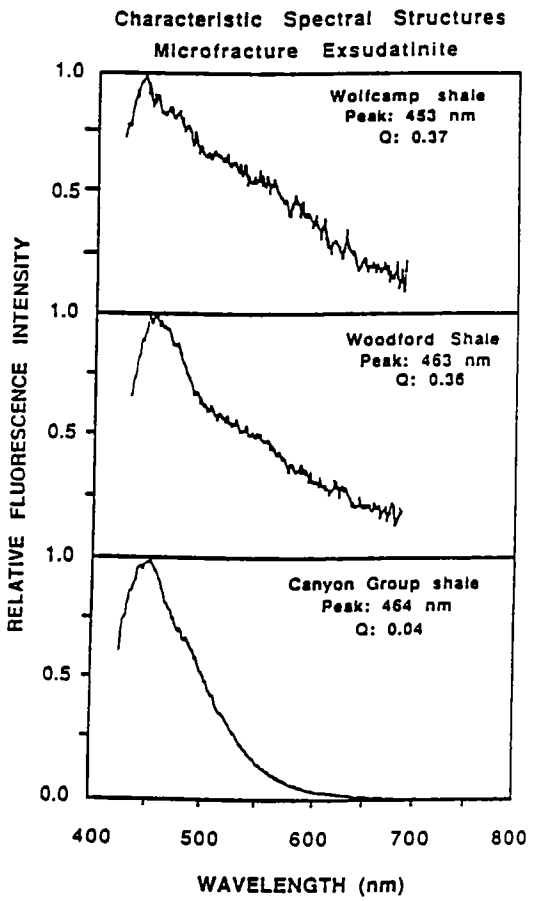

Figure 7. Fluorescence spectra of microfracture exsudatinite illustrating a range of spectral structure common for these macerals.

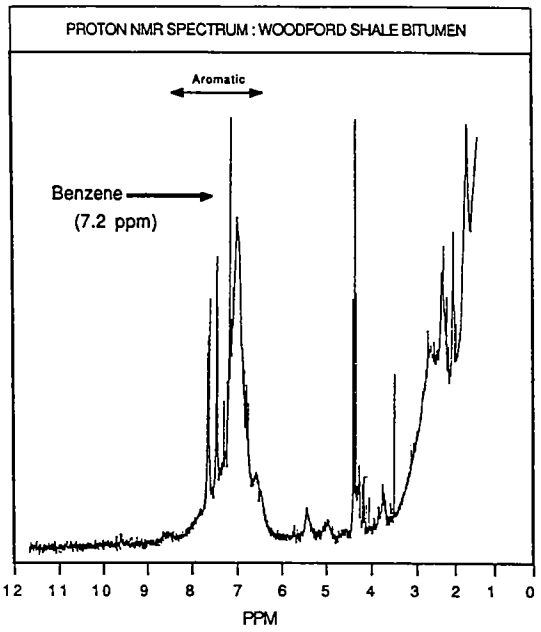

Figure 8. Proton resonance spectrum of Woodford black-shale facies bitumen. Line at 7.2 ppm is reference benzene.

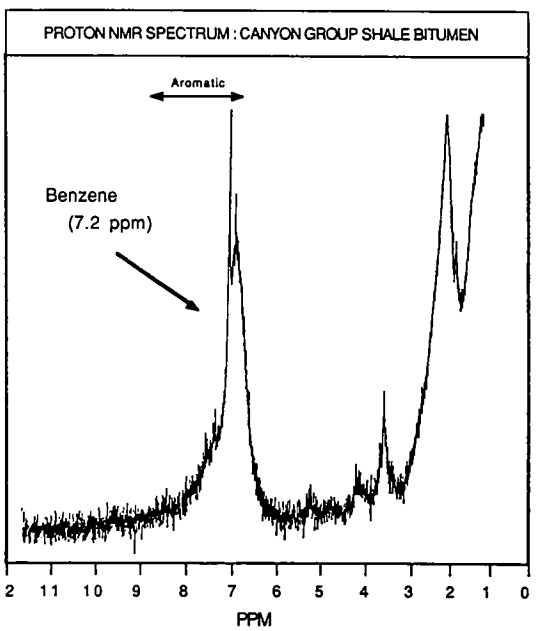

Figure 9. Proton resonance spectrum of Canyon black shale bitumen. Line at 7.2 ppm is reference benzene.

although most attention has focused upon activity outside the source-rock environment.

The diagenetic precipitation of ferroan dolomite and ankerite has been a well-studied geologic process, including in known oil reservoirs. Boles and Franks (1979) predicted that cations released during the conversion of smectite to illite could later precipitate as carbonate cement in reservoirs. Curtis (1978) points to decarboxylation reactions specifically within the sedimentary organic fraction as the source for the CO_2 needed for subsequent carbonate cementation. Others have documented the formation of late diagenetic ferroan carbonates (Katz, 1971; Al-Shaieb and Shelton, 1978; Boles, 1978). In the Permian Basin, Mazzullo (1986) reports zoned forms via cathodoluminescence in Mississippi Valley-type (MVT) dolomites which he ascribes to late stage diagenesis. It seems clear that if the correct cations (Mg^{2+}, Fe^{2+}, Ca^{2+}) become available outside of the source-rock en-

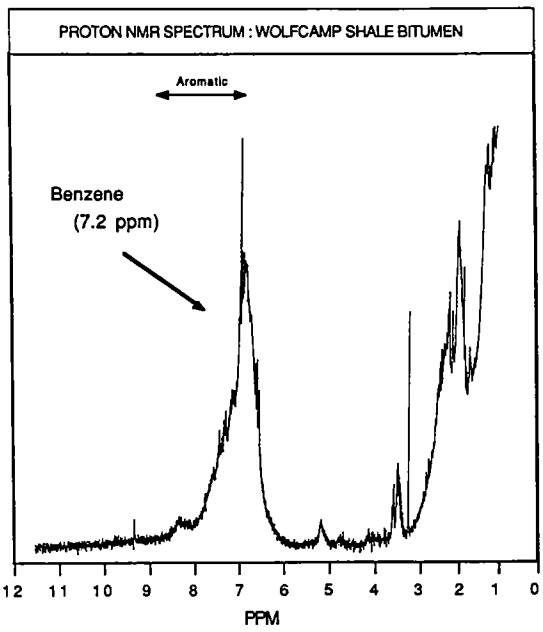

Figure 10 (left). Proton resonance spectrum of Wolfcamp black-shale facies bitumen. Line at 7.2 ppm is reference benzene.

vironment, the appropriate organic functional groups are at hand for carbonate cementation via some of the proposed mechanisms reported in the literature.

The results of this study suggest that an important mechanism of primary hydrocarbon migration may be identified petrographically in these shales. However, as Jones (1981) notes, several mechanisms of primary migration may be at work to various degrees in a source rock. Thus, the petrographic identification of one mechanism does not preclude the presence of other mechanisms less conspicuous in blue light. For example, a continuous hydrocarbon phase which occurs as an interconnected network in the mineral matrix would be subtly expressed at the microscope as a fluorescent mineral-bituminous groundmass.

The variety of bedding plane microfracture exsudatinite described above is interpreted to be

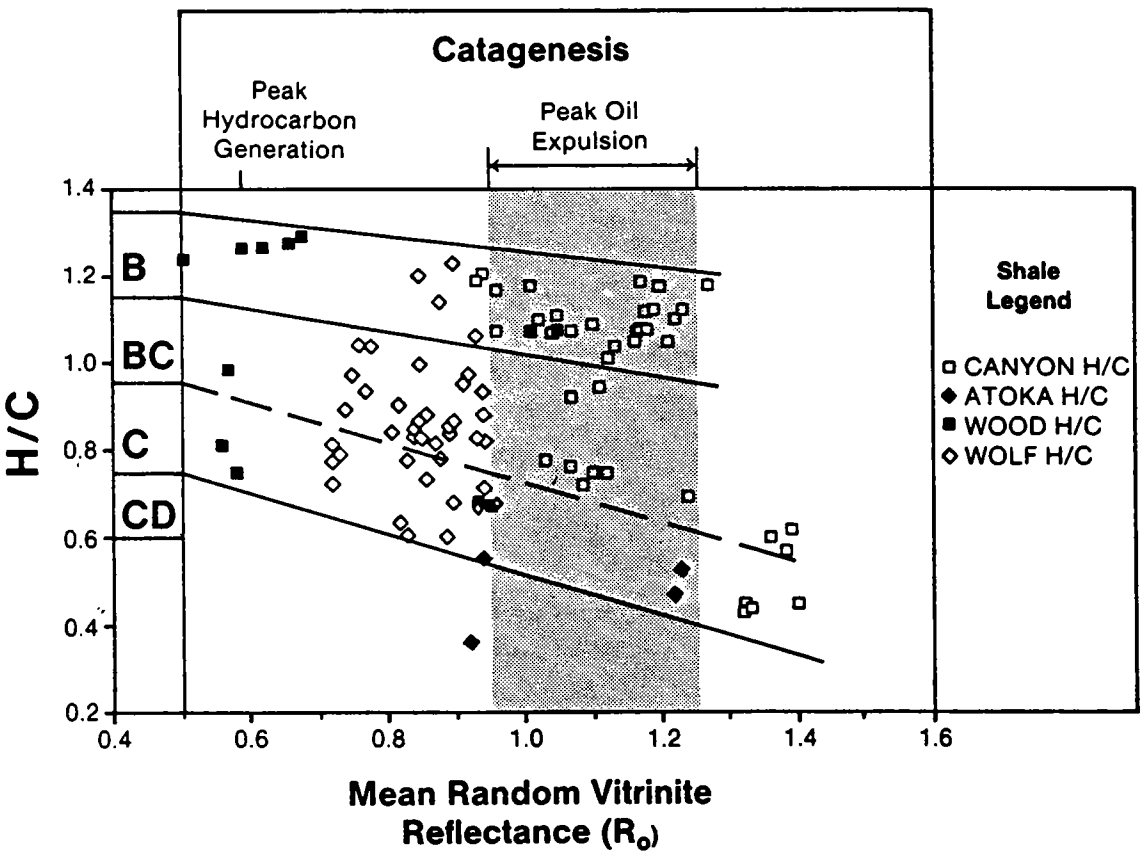

Figure 11. Plot of atomic H/C versus vitrinite reflectance for all shale. Although most shale is mature and past peak hydrocarbon potential, remaining hydrocarbon potential can be evaluated by translating laterally back to corresponding classification of source rock.

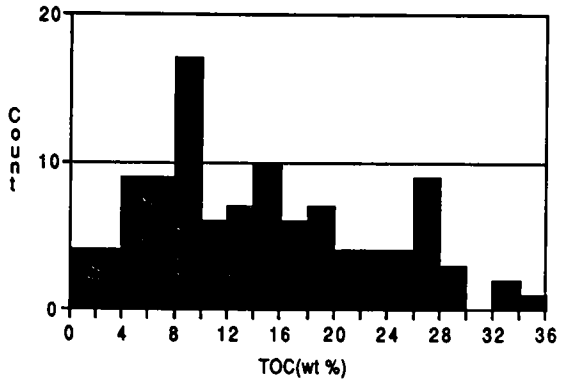

Figure 12. Composite histogram of total organic carbon content (TOC wt%) from Permian basin shales.

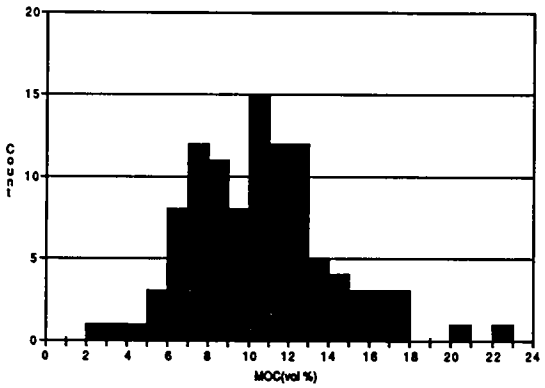

Figure 13. Composite histogram of particulate organic material petrographically counted (vol%) from whole rock mounts of shale.

an unusual manifestation of the continuous hydrocarbon phase. Central to the development of the continuous phase is the generation process itself. It is the volumetric increase in generated hydrocarbons that enhances the development of localized supernormal pressure (SNP) (Jones, 1981) if the hydrocarbons are detained in the source rock. Lewan (1987) notes that artificially matured source rocks may accommodate the net increase in hydrocarbons by generating submicron partings. Presumably, these fractures may be filled and reach petrographic proportions depending upon the amount of bitumen charge. This phenomenon is interpreted for the variety of exsudatinite in the Permian basin shales described above. Control of shale fabric upon the earliest stages of primary hydrocarbon migration is indicated by the preference of these secondary macerals to develop along bedding. The initial direction of movement via this mechanism is parallel to bedding until basin architecture dictates subsequent migration pathways.

CONCLUSIONS

The Paleozoic Woodford, Atoka, Canyon, and Wolfcamp shales of the Permian and Val Verde basins are source rocks of organic facies B and BC. They are oil and oil/gas prone after attaining thermal maturity. They become increasingly gas-prone during catagenesis. Similar organic facies determinations have been completed on Permian carbonates of the Delaware basin (Jones, 1987). Additional useful criteria offered by petrographic inspection are fluorescence spectral properties and integrated white-light and blue-light maceral analyses. Alginite exhibits strong greenish-yellow fluorescence in immature and incipiently mature

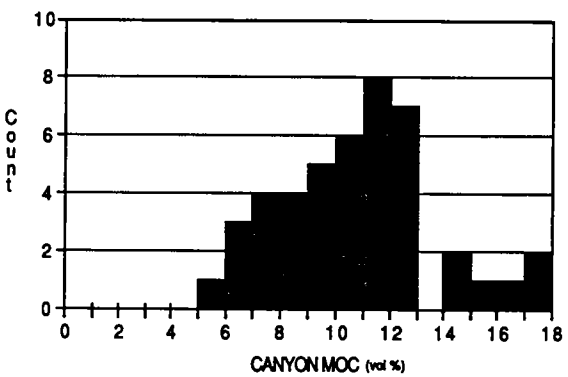

Figure 14. Histogram plot of particulate organic material counted (vol%) from whole rock mounts of Canyon shales.

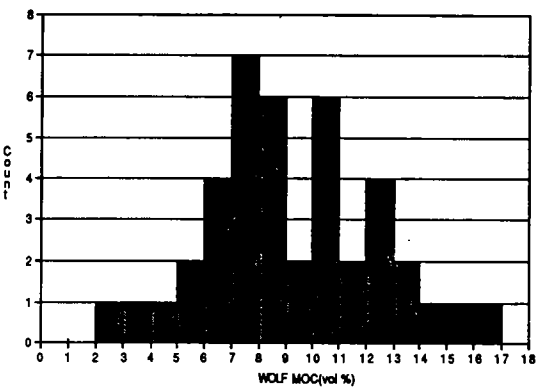

Figure 15. Histogram plot of particulate organic material counted (vol%) from whole rock mounts of Wolfcamp shale.

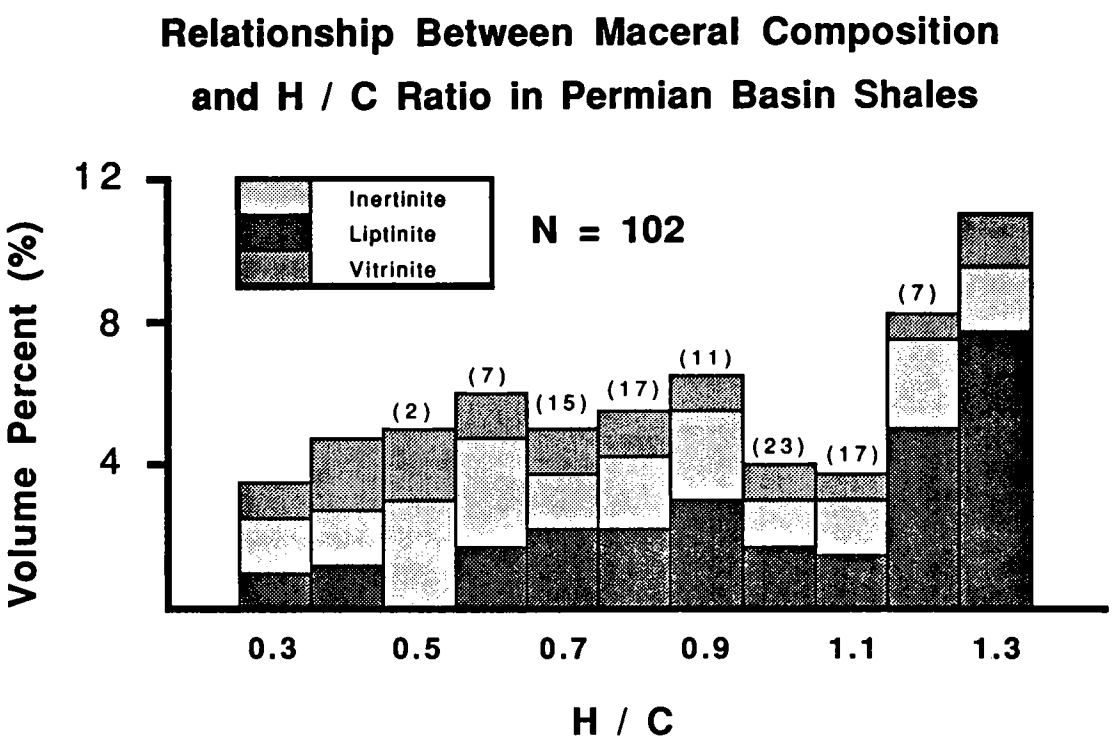

Figure 16. Plot of atomic H/C ratio versus the maceral composition at the group level. Vitrinite and inertinite are reported from white-light point counts; liptinite data are from blue-light maceral analyses. Note that higher H/C ratios are paired with a higher relative contribution of fluorescent liptinites.

shale. In immature and incipiently mature shale, ratios of blue-light to white-light liptinite content exceed one. In mature shale, this ratio approaches one and may fall below one after primary liptinite fluorescence is diminished. These data call for integrated maceral analyses.

Primary hydrocarbon migration from these shales is certainly complex. Several mechanisms may be responsible for the ultimate expulsion of oil from these shales. Among them, an unusual variety of continuous-phase hydrocarbon migration may be petrographically detected in blue light in these shales. Petrographic evidence of continuous-phase migration is revealed as a conspicuous variety of microfracture exsudatinite that exhibits a strong blue to blue-green fluorescence. This unusual manifestation does not preclude the development of a continuous phase disseminated in the mineral groundmass, perhaps more common in source rocks. Bitumen chemistry documents electron-donating functionals, mainly aromatic substituents with unpaired electrons attached directly to the ring structures and ether/alcohol functionals in the saturated fraction. This suggests that generated oil-precursors in the source rock and those migrating outside of the source rock are suitably structured for carbonate cementation during later stages of diagenesis.

ACKNOWLEDGMENTS

This research was supported by the Texas Advanced Technology Research Program. Additional support was provided by E. Leitz Inc. and Exxon (Midland) Co. We thank Stan C. Teerman of Chevron Oil Field Research Co. and Suzanne J. Russell of Shell Development Co. for the prompt and insightful review of this manuscript. We thank Dr. W. L. Borst for the use of the microscope system at Texas Tech University.

REFERENCES

Adams, J. E.; Frenzel, H. N.; Rhodes, M. L.; and Johnson, D. P., 1951, Starved Pennsylvanian Midland basin: American Association of Petroleum Geologists Bulletin, v. 35, p. 2600–2607.

Adams, J. E., 1965, Stratigraphic-tectonic development of Delaware basin: American Association of Petroleum Geologists Bulletin, v. 49, p. 2140–2148.

Al-Shaieb, Z.; and Shelton, J. W., 1978, Secondary ferroan dolomite rhombs in oil reservoirs, Chadra Sands, Gialo Field, Libya: American Association of Petroleum Geologists Bulletin, v. 62, p. 463–468.

Armin, R. A., 1987, Sedimentology and tectonic significance of Wolfcampian (Lower Permian) conglomerates in the Pedregosa basin: southeastern Arizona, southwestern New Mexico, and northern

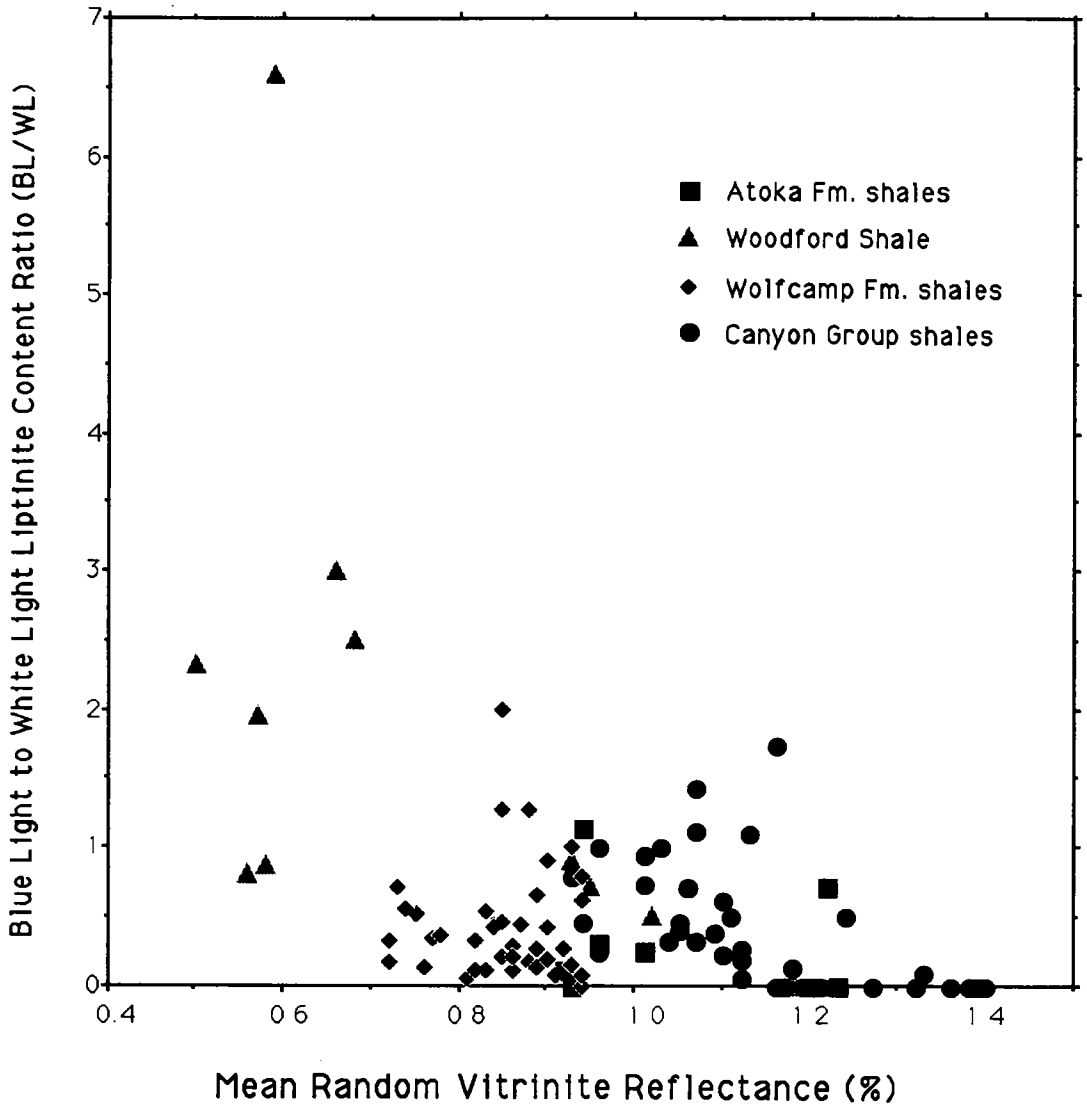

Figure 17. Plot showing the variation of the ratio of blue-light (BL) to white-light (WL) liptinite content (vol%) as a function of vitrinite reflectance.

Mexico: Geological Society of America Bulletin, v. 99, p. 42–65.

Bloomer, R. R., 1977, Depositional environments of a reservoir sandstone in west-central Texas: American Association of Petroleum Geologists Bulletin, v. 61, p. 344–359.

Boles, J. R., 1978, Active ankerite cementation in the sub-surface Eocene of southwest Texas: Contributions to Mineralogy and Petrology, v. 68, p. 13–22.

Boles, J. R.; and Franks, S. G., 1979, Clay diagenesis in Wilcox sandstones of southwest Texas: implications of smectite diagenesis on sandstone cementation: Journal of Sedimentary Petrology, v. 49, p. 55–70.

Bostick, N. H., 1979, Microscopic measurement of the level of catagenesis of solid organic matter in sedimentary rocks to aid exploration for petroleum and to determine former burial temperatures—a review: Society of Economic Paleontologists and Mineralogists Special Publication 26, p. 17–43.

Bostick, N. H.; and Alpern, B., 1977, Principles of sampling, preparation, and constituent selection of microphotometry in measurement of maturation of sedimentary organic matter: Journal of Microscopy, v. 109, pt. 1, p. 41–47.

Brooks, J., 1981, Organic maturation of sedimentary organic matter and petroleum exploration—a review, *in* Brooks, J. (ed.), Organic maturation studies and fossil fuel exploration: Academic Press, New York, p. 1–38.

Cardott, B. J.; and Lambert, M. W., 1985, Thermal maturation by vitrinite reflectance of Woodford Shale, Anadarko basin, Oklahoma: American Association of Petroleum Geologists Bulletin, v. 69, p.

1982–1998.
Comer, J. B., 1988, Lithology and depositional environment of the Woodford Formation (Upper Devonian) in the Permian basin: West Texas Geological Society, p. 17.
Cook, A. C., 1987, Organic petrological studies of oil shales: Society for Organic Petrology Abstracts and Program (fourth annual meeting), p. 15–25.
Crelling, J. C., 1983, Current uses of fluorescence microscopy in coal petrology: Journal of Microscopy, v. 132, pt. 3, p. 151–266.
Crelling, J. C.; Bensley, D. F.; Landis, C. R.; and Rimmer, S. M., 1989, Workshop on fluorescence microscopy (lecture notes): Society for Organic Petrology Workshop (sixth annual meeting), Carbondale, Illinois, 143 p.
Curtis, C. D., 1978, Possible links between sandstone diagenesis and depth-related geochemical reactions occurring in enclosing mudstones: Journal of the Geological Society of London, v. 135, p. 107–117.
Dow, W. G., 1977, Kerogen studies and geological interpretations: Journal of Geochemical Exploration, v. 7, p. 79–99.
Dow, W. G.; and O'Conner, D. I., 1982, Kerogen maturity and type by reflected light microscopy applied to petroleum exploration, *in* Staplin, F. L.; and others (eds.), How to assess maturation and paleotemperatures: Society of Economic Paleontologists and Mineralogists Short Course 7, p. 133–157.
Galley, J. E., 1958, Oil and geology in the Permian basin of West Texas and New Mexico, *in* Habitat of oil—a symposium: American Association of Petroleum Geologists Special Publication, p. 395–446.
Graham, S. A.; Dickinson, W. R.; and Ingersoll, R. V., 1975, Himalayan–Bengal Model for flysch dispersal in the Appalachian–Ouachita system: Geological Society of America Bulletin, v. 86, p. 273–286.
Hayes, J. M.; Kaplan, I. R.; and Wedeking, K. W., 1983, Precambrian organic geochemistry, preservation of the record, *in* Schopf, J. W. (ed.), Earth's earliest biosphere: Princeton University Press, p. 93–134.
Hills, J. M., 1970, Late Paleozoic structural directions in southern Permian basin, West Texas to southeastern New Mexico: American Association of Petroleum Geologists Bulletin, v. 54, p. 1809–1827.
_____1972, Late Paleozoic sedimentation in West Texas Permian basin: American Association of Petroleum Geologists Bulletin, v. 56, p. 2303–2322.
_____1984, Sedimentation, tectonism, and hydrocarbon generation in Delaware basin, West Texas and southeastern New Mexico: American Association of Petroleum Geologists Bulletin, v. 68, p. 250–267.
Huang, F.-Wen, 1989, Depositional environments, diagenesis and porosity relationships of the Canyon Sands, Edward and Sutton Counties, Texas: Texas Tech University unpublished Ph.D. dissertation, 244 p.
Hutton, A. C., 1984, Geology of oil shale deposits within the Narrows Graben, Queensland, Australia: discussion: American Association of Petroleum Geologists Bulletin, v. 68, p. 1055–1057.
Hutton, A. C.; Kantsler, A. J.; Cook, A. C.; and McKirdy, D. M., 1980, Organic matter in oil shales: Journal of Australian Petroleum Exploration Association, v. 20, pt. 1, p. 44–63.
Jones, R. W., 1981, Some mass balance and geological constraints on migration mechanisms: American Association of Petroleum Geologists Bulletin, v. 65, p. 103–122.
_____1984, Comparison of carbonate and shale source rocks, *in* Palacas, G. (ed.), Petroleum geochemistry and source rock potential of carbonate rocks: American Association of Petroleum Geologists Studies in Geology 18, p. 163–180.
_____1987, Organic facies, *in* Brooks, J.; and Welte, D. (eds.), Advances in petroleum geochemistry: Academic Press, New York, v. 2, p. 1–90.
Katz, A., 1971, Zoned dolomite crystals: Journal of Geology, v. 79, p. 38–51.
Kluth, C. F.; and Coney, P. J., 1981, Plate tectonics of the ancestral Rocky Mountains: Geology, v. 9, p. 10–15.
Landis, C. R., 1990, Organic maturation, primary migration, and clay mineralogy of selected Permian basin shales: Texas Tech University unpublished Ph.D. dissertation, 227 p.
Lewan, M. D., 1987, Petrographic study of primary petroleum migration in the Woodford Shale and related rock units, *in* Doligez, B. (ed.), Migration of hydrocarbons in sedimentary basins: Second IFP Exploration Research Conference, Carcans, France, June 15–19, p. 113–130.
Leythaeuser, D.; Schaeffer, R. G.; and Yukler, A., 1980, Diffusion of light hydrocarbons through near-surface rocks: Nature, v. 284, p. 522–525.
_____1982, Role of diffusion in primary migration of hydrocarbons: American Association of Petroleum Geologists Bulletin, v. 66, p. 408–429.
Leythaeuser, D.; Schaeffer, R. G.; and Pooch, H., 1983, Diffusion of light hydrocarbons in subsurface sedimentary rocks: American Association of Petroleum Geologists Bulletin, v. 67, p. 889–895.
Leythaeuser, D.; Mackenzie, A.; Schaeffer, R. G.; and Bjorøy, M., 1984, A novel approach for recognition and quantification of hydrocarbon migration effects in shale-sandstone sequences: American Association of Petroleum Geologists Bulletin, v. 68, p. 196–219.
Mazzullo, S. J., 1986, Mississippi Valley-type sulfides in Lower Permian dolomites, Delaware basin, Texas: implications for basin evolution: American Association of Petroleum Geologists Bulletin, v. 70, p. 943–952.
Mazzullo, S.J.; and Reid, A. M., 1987, Basinal Lower Permian facies, Permian basin. Part II.—Depositional setting and reservoir facies of Wolfcampian; Lower Leonardian basinal carbonates: West Texas Geological Society Bulletin, v. 26, no. 8, p. 5–10.
McCartney, J. T.; and Teichmüller, M., 1972, Classification of coals according to degree of coalification by reflectance of the vitrinite component: Fuel, v. 51, p. 64–68.
McGlassen, E. H., 1968, The Siluro–Devonian of West Texas and southeast New Mexico, *in* Delaware basin exploration: West Texas Geological Society Guidebook 68-55, p. 35–44.
Meissner, F. F., 1978, Petroleum geology of the Bakken

Formation Williston basin, North Dakota and Montana: Williston Basin Symposium, Montana Geological Society, p. 207–227.

Momper, J. A., 1978, Oil migration limitations suggested by geological and geochemical considerations: American Association of Petroleum Geologists Course Note Series 8, p. B1–B60.

Mukhopadhyay, P. K.; and Gormly, J. R., 1984, Hydrocarbon potential of two types of resinite: Organic Geochemistry, v. 6, p. 439–454.

Mukhopadhyay, P. K.; Hagemann, H. W.; and Gormly, J. R., 1987, Characterization of kerogens as seen under the aspect of maturation and hydrocarbon generation: Erdöel und Kohle, Erdgas, Petrochemie v. 38, pt. 1, p. 7–18.

Ottenjann, K.; Teichmüller, M.; and Wolf, M., 1975, Spectral fluorescence measurements of sporinites in reflected light and their applicability for coalification studies, *in* Alpern, B. (ed.), Pétrographie organique et potential pétrollier: Centre Nationale Recheiche Scientifique, Paris, p. 49–65.

Philippi, G. T., 1965, On the depth, time, and mechanism of petroleum generation: Geochimica et Cosmochimica Acta, v. 29, p. 1021–1049.

Pindell, J. L., 1985, Alleghenian reconstruction and subsequent evolution of the Gulf of Mexico, Bahamas, and Proto-Caribbean: Tectonics, v. 4, p. 1–39.

Powers, M. C., 1967, Fluid-release mechanisms in compacting marine mudrocks and their importance in oil exploration: American Association of Petroleum Geologists Bulletin, v. 51, p. 1240–1254.

Radke, M.; Schaffer, R. G.; Leythaeuser, D.; and Teichmüller, M., 1980, Composition of soluble organic matter in coals: relation to rank and liptinite fluorescence: Geochimica et Cosmochimica Acta, v. 11, p. 1787–1800.

Reid, A. M.; and Mazzullo, S. J., 1988, The Pennsylvanian–Permian boundary in shelf areas of the north platform of the Midland basin: West Texas Geological Society Bulletin, v. 27, no. 6, p. 5–8.

Saxby, J. D., 1982, A reassessment of the range of kerogen maturities in which hydrocarbons are generated: Journal of Petroleum Geology, v. 5, p. 117–127.

Sherwood, N. R.; Cook, A. C.; Gibling, M.; and Tantisukrit, C., 1984, Petrology of a suite of sedimentary rocks associated with some coal-bearing basins in NW Thailand: International Journal of Coal Geology, v. 4, p. 45–71.

Silverstein, R. M.; Bassler, G. C.; and Morrill, T. C., 1981, Spectrometric identification of organic compounds [fourth edition]: John Wiley and Sons, New York, 442 p.

Spackman, W., 1958, The maceral concept and the study of modern environments as a means of understanding the nature of coal: Transactions of the New York Academy of Science, series 2, v. 20, no. 5, p. 411–423.

Spackman, W.; Davis, A.; and Mitchell, G. D., 1976, The fluorescence of liptinite macerals: Brigham Young University Geology Studies, v. 22, pt. 3, p. 59–75.

Stach, E.; Mackowsky, M.; Taylor, G. H.; Chandra, D.; Teichmüller, M.; and Teichmüller, R., 1982, Stach's textbook of coal petrology: Gebrüder Borntraeger, Berlin, 535 p.

Teerman, S. C.; Crelling, J. C.; and Glass, G. B., 1987, Fluorescence spectral properties of resinite macerals from coals of the Hanna Formation, Wyoming, U.S.A.: International Journal of Coal Geology, v. 7, p. 315–334.

Teichmüller, M., 1974, Generation of petroleum-like substances in coal seams as seen as under the microscope, *in* Tissot, B.; and Bienner, F. (eds.), Advances in organic geochemistry 1973: Editions Technip, Paris, p. 379–407.

_____1982, Application of coal petrological methods in geology including oil and natural gas prospecting, *in* Stach, E. (ed.), Stach's textbook of coal petrology: Gebrüder Borntraeger, Berlin, p. 381–412.

Teichmüller, M.; and Durand, B., 1983, Fluorescence microscopical rank studies on liptinites and vitrinites in peats and coals, and comparisons with results of the Rock-Eval pyrolysis: International Journal of Coal Geology, v. 2, p. 197–230.

Teichmüller, M.; and Wolf, M., 1977, Application of fluorescence microscopy in coal and oil exploration: Journal of Microscopy, v. 109, pt. 1, p. 49–73.

Thomas, W. A., 1977, Evolution of Appalachian–Ouachita salients and recesses from reentrants and promontories in the continental margin: American Journal of Science, v. 277, p. 1233–1278.

Ting, F. T. C.; and Lo, H. B., 1975, Fluorescence characteristics of thermo-altered exinites (sporinites): Fuel, v. 54, p. 201–204.

Tissot, B. P.; and Welte, D. H., 1978, Petroleum formation and occurrence, a new approach to oil and gas exploration: Springer-Verlag, New York, 538 p.

Trabelsi, A., 1990, Sedimentology, petrography, and diagenesis of selected Paleozoic source rocks from the Permian basin: Texas Tech University unpublished Ph.D. dissertation.

van Gijzel, P., 1982, How to assess maturation and paleotemperatures: Society of Economic Paleontologists and Mineralogists Short Course No. 7, p. 195–207.

Waples, D. W., 1982, Organic geochemistry for exploration geologists: International Human Resources Development Corporation, Boston, 151 p.

_____1984, Modern approaches in source-rock evaluation, *in* Woodward, J.; Meissner, F. F.; and Clayton, J. L. (eds.), Hydrocarbon source rocks of the greater Rocky Mountain region: Rocky Mountain Association of Geologists, Denver, p. 35–49.

Ward, R. F.; Kendall, C. G. St. C.; and Harris, P. M., 1986, Upper Permian (Guadalupian) facies and their association with hydrocarbons—Permian basin, West Texas and New Mexico: American Association of Petroleum Geologists Bulletin, v. 70, p. 239–262.

Zhao, S.-Q.; Zhong, N.-N.; Xiong, B.; Simoneit, B. R. T.; and Wang, T.-G., 1990, Organic geochemistry and coal petrology of Tertiary brown coal in the Zhoujing mine, Baise basin, South China: Fuel, v. 69, p. 4–11.

PART II

PANEL DISCUSSION:
Can Carbonates Be Source Rocks for Commercial Petroleum Deposits?

Edited presentations made by four panelists, followed by an edited transcript of the discussion between the audience and panel. Panel members, in order of their presentation, are:

JOHN D. PIGOTT, University of Oklahoma

JAMES G. PALACAS, U.S. Geological Survey, Denver

JACK E. WILLIAMS, Amoco Production Co. (retired), Tulsa

LLOYD E. GATEWOOD, Independent Geologist, Oklahoma City

Can Carbonates Be Source Rocks for Commercial Petroleum Deposits? Considerations from a Rate Perspective

John D. Pigott
University of Oklahoma

INTRODUCTION: POSING THE PROBLEM

The question: "Can carbonates be source rocks for commercial petroleum deposits?" can be answered one of two principal ways: (1) with descriptive criteria of source quality, quantity, and maturity of ancient rocks; or (2) by considering physical-biochemical processes on different time scales. This paper takes the second approach by looking at the relative impact that diffusive and advective processes have upon microbially mediated reactions which tend to reduce the preservation potential of sedimentary organic matter.

PRESERVATION POTENTIAL IN BRIEF

The preservation potential of organic matter can be described in chemical terms as the inverse of its potential for oxidation; i.e., the greater the chances of its reaction with a potential electron acceptor, the lower its chances of preservation. However, such a simplified approach ignores the microbial mediation of such activities. A more proper way of viewing preservation potential, then, is that given a reactive organic matter as a substrate, restriction of the microorganisms from contact with electron acceptors (first oxygen, and then sulfate and nitrogen compounds) favors preservation of organic matter. The sequence of these microbial reactions has been delineated by Berner (1980).

As sediments are normally continually saturated with fluid during and following deposition, consideration of the aqueous chemistry and physical-transport processes are pertinent. It is the concentration of electron acceptors relative to the reactive organic matter, the sediment porosity and permeability, and the magnitude of advective and diffusive processes through time that are the principal factors governing the preservation potential of organic matter.

MATERIAL FACTORS

Oxygen

The material ratio of reactive organic matter to potential oxidizing agents determines to what extent the microbially mediated reactions can ultimately and stoichiometrically proceed, both during and following deposition. The oxygen content of the ambient waters initially directly affects the ability of aerobic microbes to oxidize the carbon and, potentially, destroy the organic matter. The oxygen amount in terms of biofacies has been classified in the following way (modified after Rhoads, 1974; and Byers and Larson, 1979): in those waters that are termed aerobic (1–8 ml/L of dissolved oxygen), massive bioturbation and aeration of the sediments generally provide an excess of oxidizing agent thereby decreasing the immediate preservation potential. In ambient waters of 0.1–1 ml/L of dissolved oxygen (dysaerobic waters), organic matter would be less likely attacked by aerobes and more likely to be immediately preserved unless attacked by facultative anaerobes. However, if the dissolved oxygen content were instead <0.1 ml/L (anaerobic), there would be insufficient oxygen to support benthic microaerobes and organic matter preservation would potentially be more likely.

Sulfate and Nitrogen Compounds

Although oxygen is classically treated as the chief oxidizing agent for the microbial oxidation of organic matter, anaerobic destruction of organics occurs in carbonates through microbial means. Indeed, conventional wisdom at present suggests that the genesis of most black shales occurred within euxinic basinal environments and that the oxidation of organic matter occurs only in the presence of aerobes under free oxygen. However, that anaerobes, both facultative and obligatory, also oxidize organics, and that TOC (total organic carbon) often correlates to productivity, suggests alternative considerations for the preservation and destruction of organic matter. For example, Pigott (1977) and Pigott and Land (1986) demonstrated from material-balance considerations that reef-sediment organic matter could be oxidized by sulfate reducers and nitrogen bacteria if advection sufficient for inorganic sulfate-nitrogen importation occurred. In terms of bacterial experiments, Kristensen and Blackburn (1987) found that the degradation rate of organic matter in natural shal-

low-water sediments, incubated under the absence of oxygen, was higher than the rate under oxygen. Therefore, for preservation, organic matter must also be isolated from electron acceptors other than oxygen.

Reactive Carbon

The amount of available organic matter provides the other parameter that is necessary to be considered. The amount which settles to the sea floor is a function of the primary organic production, its ratio with other sedimentary components, and the amount of time spent in the water column settling and exposed to grazers, i.e. water depth and burial rate. Calvert (1987) has shown the spatial distribution of modern organic productivity and TOC in the sediments below to be a function directly of the proximity to zones of coastal upwelling. In terms of the effects of water depth, Suess (1980) showed that for a given production rate, the settling flux of carbon is an inverse power function of the water depth, e.g., an increase in order of magnitude of one variable results in a decrease by an order of magnitude of another. Therefore, for coastal upwelling zones or areas proximal to shallow reefs where organic productivity is locally a maximum, the TOC would be potentially higher. Dilution is also a factor; yet, if sedimentary TOC is compared to the overall sedimentation rate, as Mueller and Suess (1979) have shown, a similar power relationship results. That is, the higher the sedimentation rate, the higher the resulting deposited TOC. Organic matter is preserved if the amount of reactive carbon is larger than the surrounding oxidant-supplied microbes' ability to destroy it. Preservation can be increased two ways. The first is to increase the amount of reactive carbon (accompanying or absorbed on the inorganic sediments). The other way, which we shall focus on, is to decrease the rate at which oxidizers can be transported in.

TRANSPORT EQUATION

The rate at which potential oxidants can be transported into the sediments to microbially react with the organic carbon can be described in terms of diffusive and advective processes. Diffusion, or Fd, in its simplest Fickian form can be written as:

$$Fd = -\phi D (dC/dZ) \qquad g\,cm^{-2}sec^{-1} \qquad (1)$$

where ϕ is sediment or rock porosity, D is the diffusion coefficient, and dC/dZ is the chemical gradient. Therefore, oxidants must diffuse into the sediments at some rate constant D to enable the microbially mediated destruction of the organic carbon.

We shall describe advection, Fu, or the rate at which dissolved oxygen is buried with the sediment organic particles as:

$$Fu = \phi U C \qquad g\,cm^{-2}sec^{-1} \qquad (2)$$

where U is the rate (cm/sec) and C is the concentration ($g\,cm^{-3}$).

Addition of these two quantities describes the transportation equation of flux, F, of materials into or out of the sediments:

$$F = Fd + Fu \qquad g\,cm^{-2}sec^{-1}. \qquad (3)$$

Let us consider this transport equation in its simplest case for oxygen. For sedimentary reactive organic carbon, then, the flux of oxygen can be characterized by a diffusion and an advection term. Physically, then, the oxygen content would be a function of that buried initially with the particles (the advective process) and the oxygen-concentration gradient between the sediment and the overlying water (the diffusive process).

But, such a simple treatment ignores the important question of geologic time and facies, and indeed of changes in the controlling parameters with burial. For example, the porosity term of equations (1) and (2) is neither facies- nor time-independent. Lerman (1979) has shown from considerations of tortuosity that D, the diffusion coefficient, varies as:

$$D = D_0(\phi)^2 \qquad cm^2sec^{-1} \qquad (4)$$

where D_0 is the diffusion coefficient in water (100% porosity). That is, as the porosity decreases (e.g., from a well-sorted, porous grainstone to a poorly sorted less porous mudstone) the diffusion coefficient decreases as the square of the porosity. Sediment porosity also changes with depth (and time), owing primarily to compaction of the sediments. This relationship, ϕ_z, can be described as a logarithmically declining function (Athy, 1930; Bond and Kominz, 1984):

$$\phi_z = \phi_0 \exp(-z/ck) \qquad wt\% \qquad (5)$$

where ϕ_0 is the initial porosity, z is depth, and c and k are lithologically dependent constants. Therefore, to determine the effects of chemical transport, one must determine the facies and time-depth dependency of porosity. Importantly, especially for carbonates, postdepositional diagenesis easily alters this simple relationship and facies- and mineralogy-dependent porosity relationships must be empirically determined.

DIRECT COMPARISON OF DIFFUSION WITH ADVECTION

Method

It is instructive to directly compare the diffusive and advective processes. We shall do this in two ways: first by determining the diffusion, LD, and

advection, LA, distances (after the manner of Lerman, 1979), and secondly by comparing rates. In terms of distance, one has:

$$LD = (Dt)^{1/2} \quad \text{cm} \quad (6)$$

and

$$LA = U\,t \quad \text{cm} \quad (7)$$

where t is time in sec.

Next, to compare the efficiencies by a dimensionless ratio of lengths, RL, we simply divide LA by LD to obtain:

$$RL = LA/LD = U(t/D)^{1/2}. \quad (8)$$

Importantly, as time increases, U becomes more important and diffusion less substantial a contributor to transport. Secondly, to determine the time at which the two processes equal each other, tE, one simply sets LA = LD and

$$tE = D/U^2 \quad \text{sec.} \quad (9)$$

In terms of a dimensionless rate comparison, RC, we have:

$$RC = \text{Log}\,[U/D^{1/2}]. \quad (10)$$

If RC = 0, the rate constants (not to be confused with rates) are equivalent. As the concentration gradients figure heavily into the rate magnitudes for diffusion, if RC < 0, then the diffusion-rate constant dominates, and if RC > 0, the advection-rate constant is more important. Table 1 documents some of the molecular and eddy-diffusion coefficients in modern environments, while Table 2 lists some of the ranges of characteristic advection velocities on the earth's surface.

TABLE 1. — DIFFUSION RATE CONSTANTS*

Media	Log_{10} diffusion coefficient (cm^2/sec)
Atmosphere (horizontal)	9 to 10
Oceans (horizontal)	6 to 10
Atmosphere (vertical)	4 to 6
Ocean, lakes (vertical)	–1 to 1
Gases in air	–1 to 0
Salts, gases in water	–7 to –4
Thermal diffusion (water)	–8 to –7

*Calculated from data compiled by Lerman (1979).

TABLE 2. — ADVECTION VELOCITIES*

Media	Log_{10} advective velocity (cm/sec)
Tropospheric winds	1 to 3
Surface water currents	0 to 2
Particles settling in air	–2 to 2
Particles settling in water	–3 to –1
Ground-water flow	–6 to 0
Evaporation; ocean upwelling	–6 to –5
Ocean floor spreading	–8 to –7
Sedimentation in lakes and oceans	–11 to –9

*Calculated from data compiled by Lerman (1979).

Application to Carbonate Biogeochemical Facies

We can summarize the preceding observations in a schematic reefal carbonate facies diagram as shown in Figure 1. The reefal textures are after the classification of Embry and Klovan (1971) and the carbonate textures are after Dunham (1962). Although these facies can vary in scale and in types of organisms through time, the general relationships hold. Importantly, these chemical and biofacies parameters vary both laterally and vertically with depth.

We shall now compare the ratio of advection distances to diffusion distances in the carbonate biogeochemical facies shown in Figure 1, utilizing the diffusion and advection information of Tables 1 and 2. Let us hold the diffusion rate constant at 1×10^{-5} cm^2/sec (at 70% porosity, SO_4^{-2} is 5.3×10^{-5}; and at 100% porosity, O_2 is 2.35×10^{-5} cm^2 sec).

Water Column

Within the water column, for a sedimentation rate of 10^{-2} cm/sec, tE is small, only 6 minutes, and RC is 0.5. Such tE and RC values imply that the advective supply of oxidants from the water column is substantially greater than that possible from mechanical diffusive processes (on the surface of the molecule). If organics are deposited within a lengthy (deep) water column with abundant oxygen, the time exposed to oxygen is long and the chances of their subsequent preservation are minimized. If, on the other hand, the ambient oxygen concentration were reduced (e.g., during a time of anoxia), the chances of preservation would by more favorable.

Basinal Deep

On a deep (>2 km) sea floor, with a slow sedimentation rate of 1 mm/1,000 yr, it would take billions of years for the advection distance to equal that of diffusion, as diffusion-rate constants in this scenario are much higher. RC is equal to –11, sug-

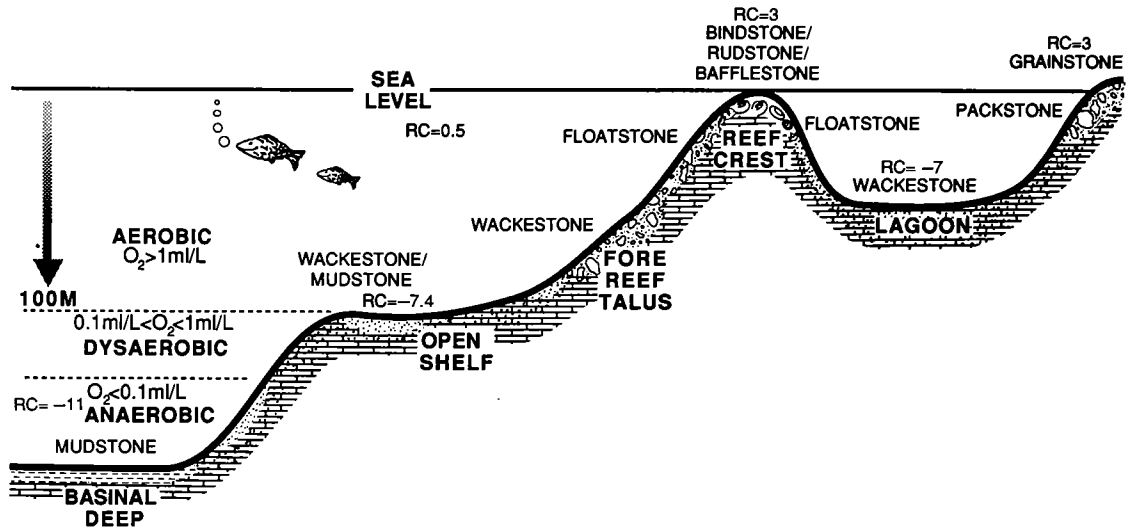

Figure 1. Schematic carbonate facies profile (variable horizontal and vertical scale) indicating oxygen biofacies and changes in the ratio of advective to diffusive rate constants: RC (see text for calculation). Carbonate texture names are after Dunham (1962) and reefal textures are after Embry and Klovan (1971). Note that oxygen biofacies can change their vertical and lateral distribution through geologic time and that the schematic facies tract is not species dependent.

gesting the enormously greater magnitude of diffusive processes in the importation of oxidants. Unless transported quickly through the overlying water column (e.g., by allodapic turbidity currents), the organics would suffer a similar fate of destruction as previously described.

Open Shelf

For an open-ocean carbonate platform, e.g., chalks (such as the Austin Chalk) where sedimentation rates have been estimated as high as 4 cm/1,000 yr, the tE would be 22 hrs and RC would be –7.4. Suess (1980) has shown that fine-grained sediments can absorb substantial organic matter. Therefore, by settling quickly, they are less likely to be oxidized, and TOCs as high as 17% have been reported.

Lagoon

Within an average lagoonal sediment with a sedimentation rate of 1 mm/yr, tE becomes 11.5 days and RC is –8. Therefore, it is not until almost 12 days that the ability of advection would become equivalent to that of diffusion. As it is highly unlikely that with such a sedimentation rate the sediments would continue to be aerobic, one must rely upon the diffusive supply of oxidants to destroy the organic matter. Thus there is a greater chance of preservation here than in the overlying water column.

SUMMARY

In terms of organic preservability, knowledge of the initial oxygen concentration is only half the story; the ability to transport in oxidants (e.g., O_2, SO_4, etc.) via advection or diffusion even under anerobic conditions in order to supply the microorganisms with sufficient electron acceptors is also important. Carbonates, owing to their mineral metastability in changing water chemistries, have a propensity for postdepositional change in their rock properties (porosity, permeability, etc.). Therefore, even a cursory model of a modern environment still has its limitations following deposition. However, in terms of the advective and diffusive processes considered, carbonates can potentially become source rocks if RC is generally <0. Predicting the initial preservation potential of carbonates then depends not only upon the determination of the initial concentration of available oxidants in the water column and the input amount of organic carbon, but also upon the assessment of the RC variation with biofacies and through time.

REFERENCES

Athy, L. F., 1930, Density, porosity, and compaction of sedimentary rocks: American Association of Petroleum Geologists Bulletin, v. 14, p. 1–24.

Berner, R. A., 1980, Early diagenesis: a theoretical approach: Princeton University Press, 241 p.

Bond, G. C.; and Kominz, M. A., 1984, Construction of tectonic subsidence curves for the early Proterozoic miogeocline, Southern Canadian Rocky Mountains: implications for subsidence mechanisms, age of breakup, and crustal thinning: Geological Society of America Bulletin, v. 95, p. 155–173.

Byers, C. W.; and Larson, D. W., 1979, Paleoenvironments of Mowry Shale (Lower Cretaceous), western and central Wyoming: American Association of Petroleum Geologists Bulletin, v. 63, p. 359–361.

Calvert, S. E., 1987, Oceanographic controls on the accumulation of organic matter in marine sediments, *in* Brooks, J.; and Fleet, A. (eds.), Marine petroleum source rocks: Blackwell Scientific, London, p. 137–151.

Dunham, R. J., 1962, Classification of carbonate rocks according to depositional texture, *in* Ham, W. E. (ed.), Classification of carbonate rocks: American Association of Petroleum Geologists Memoir 1, p. 108–121.

Embry, A. F.; and Klovan, J. E., 1971, A Late Devonian reef tract on northeastern Banks Island, N.W.T.: Bulletin of Canadian Petroleum Geology, v. 19, p. 730–781.

Kristensen, E.; and Blackburn, T. H., 1987, The fate of organic carbon and nitrogen in experimental marine sediment systems: influence of bioturbation and anoxia: Journal of Marine Research, v. 45, p. 231–257.

Lerman, A., 1979, Geochemical processes, water and sediment environments: John Wiley and Sons, New York, 481 p.

Mueller, P. J.; and Suess, E., 1979, Productivity, sedimentation rate, and sedimentary organic matter in the oceans. 1.—Organic carbon preservation: Deep-Sea Research, v. 26A, p. 1347–1362.

Pigott, J. D., 1977, Early diagenesis of sulfur and nitrogen species in Jamaican reef sediments (determined by in situ sampling): Third International Coral Reef Symposium, Miami, Florida, v. 2, p. 533–540.

Pigott, J. D.; and Land, L. S., 1986, Interstitial water chemistry of Jamaican reef sediment sulfate reduction and submarine cementation: Marine Chemistry, v. 19, p. 355–378.

Rhoads, D. C., 1974, Organism-sediment relationship on the muddy sea floor: Oceanographic Marine Biology Annual Review, v. 12, p. 263–300.

Suess, E., 1980, Particulate organic carbon flux in the oceans—surface productivity and oxygen utilization: Nature, v. 288, p. 260–263.

Can Carbonates Be Source Rocks for Commercial Petroleum Deposits?

James G. Palacas
U.S. Geological Survey, Denver

ABSTRACT.—Carbonate rocks, such as lime mudstones and dolomudstones, are shown to be source beds of commercial amounts of petroleum by presenting examples of well-documented carbonate source rocks. These examples are based on both geochemical and geologic data and were selected to illustrate their worldwide occurrence and their distribution throughout the geologic column. Geochemical and/or geologic highlights are given for the following source rocks: Miocene Alcanar Formation, Tarragona basin, Spain; Paleocene and Eocene Green River Formation, Uinta and Piceance basins, Utah and Colorado, U.S.; Upper Cretaceous Niobrara Formation, eastern Denver basin, U.S.; Upper Cretaceous Austin Chalk, south-central Texas, U.S.; Upper Cretaceous La Luna Formation, Maracaibo basin, Venezuela; Lower Cretaceous Sunniland Limestone, South Florida basin, U.S.; Jurassic Callovian–Oxfordian rocks, Saudi Arabia; Jurassic Smackover Formation, Gulf Coast, U.S.; Triassic Burano Formation and Emma Limestone, Italy; Permian Bone Spring Limestone, Delaware basin, New Mexico, U.S.; Devonian Duvernay Formation, Western Canada basin, Alberta, Canada; Silurian Salina A-1 carbonate facies of the Salina Group, Michigan basin, U.S. and Canada; Lower Cambrian Observatory Hill Beds, East Officer basin, South Australia; and upper Proterozoic Huqf Group, Oman.

In addition, a few important depositional and geochemical characteristics of carbonate source rocks are summarized. Key compositional features of carbonate- versus shale-derived oils are also given in tabular form. This kind of information should assist the explorationist in correlating an oil to its source and, hence, in defining migration pathways.

INTRODUCTION

Prior to about the mid 1960s to early 1970s, the prevalent view of many, if not the majority, of petroleum geologists was that carbonate rocks were not quantitatively important source beds of petroleum. One of the principal papers given at the Second World Petroleum Congress in 1937, in Paris, France, entitled "Petroleum Cannot be Generated in Limestones" (Von Hettinga Tromp, 1938), summed up the consensus of thinking at that time.

We have come a long way since then. Nearly 50 years later, another paper on the same subject (carbonate source rocks) was given at the Eleventh World Petroleum Congress in 1983, in London, England. This paper, based on abundant geologic and geochemical evidence, including source rock–crude oil correlations, demonstrated that certain carbonate rocks are good to excellent petroleum source rocks. I had the privilege of delivering that paper, entitled "Carbonate Rocks as Sources of Petroleum: Geological and Chemical Characteristics and Oil-Source Correlations" (Palacas, 1984a).

To avoid possible misunderstandings, it is appropriate to define the term "carbonate rock." The simplest and probably most widely accepted definition is that a carbonate rock is a sedimentary rock that contains ≥50% carbonate minerals, predominantly calcite and dolomite. A "pure" carbonate rock generally contains >90% carbonate minerals. Carbonate rocks commonly include marls or marlstones that contain 35–65% clay and 35–65% carbonate (Oehler, 1984). Most carbonate source rocks are fine grained and, as such, are referred to as micrites or lime mudstones and dolomudstones.

EXAMPLES OF CARBONATE SOURCE ROCKS

Well-documented examples of carbonate source rocks and their location, age, range, and average total organic carbon (TOC) content are presented in Table 1, and selected key points are highlighted below. At least two observations should be made: carbonate source rocks occur throughout the world, and they are present throughout most of the geologic column.

Cenozoic Examples

In the Cenozoic Era, one well-documented carbonate source rock is the Miocene Alcanar Formation, Tarragona basin, Spain (Table 1) (Demaison and Bourgeois, 1984). The Alcanar carbonates, consisting of pelagic marlstones and limestones

TABLE 1. — WORLDWIDE EXAMPLES OF CARBONATE SOURCE ROCKS

Source unit	Location	Geologic position	TOC wt% Range	TOC wt% Avg.
Alcanar Formation	Tarragona basin, Spain	Miocene	3.2–4.7	4.0
Green River Formation: (open lacustrine facies)	Uinta and Piceance basins, Utah and Colorado	Eocene & Paleocene	~1.0–22.3[a] ~1.0–4.2[b]	8.7[a] 1.6[b]
Niobrara Formation	Eastern Denver basin, Colorado	U. Cretaceous	0.4–5.8	3.2
Austin Chalk (>9,000′ deep)	Gulf Coast, Texas	U. Cretaceous	0.8–7.4	3.0
La Luna Formation	Maracaibo basin, Venezuela	U. Cretaceous	1.5–9.6	3.8
Sunniland Limestone	South Florida basin, Florida	L. Cretaceous	0.4–12.3	1.8
Carbonates of Oxfordian–Callovian age	Northeastern Saudi Arabia	U. & M. Jurassic	—	≥4.0
Smackover Formation	Eastern Gulf Coast, U.S.	U. Jurassic	0.1–4.0	0.5[c]
Burano Formation; Emma Limestone	Central-southern Italy; Adriatic Sea	U. Triassic	0.1–1.5; 0.3–17.0	— —
Bone Spring Limestone	Delaware basin, New Mexico	L. Permian	0.3–2.2	1.3[c]
Duvernay Formation	Western Canada basin, Alberta	U. Devonian	1.6–17.0	5–10
Salina A-1 carbonates	Michigan basin, U.S.	Silurian	0.1–0.6	0.3[c]
Observatory Hill Beds	East Officer basin, South Australia	L. Cambrian	0.2–1.3	0.5
Huqf Group	South Oman	Precambrian	~2.2–6.2	~4.0

NOTE: References for source rock units and TOC data are cited in text; — = not available; U. = Upper, L. = Lower.
[a]Immature to marginally mature marlstones, generally <8,000 ft deep.
[b]Mature source rocks, generally 8,000–14,000 ft in depth.
[c]This average TOC value may be biased on the low side; see text.

(containing type II organic matter), illustrate a somewhat uncommon geologic phenomenon that seems worthy of mention. Rather than charging laterally equivalent or overlying, younger reservoir rocks, as is commonly observed, the oils generated from these Miocene rocks have migrated downward into underlying older (Jurassic and Cretaceous) reservoir rocks, resulting in at least nine oil fields in the Tarragona basin (Demaison and Bourgeois, 1984; Albaiges and others, 1986).

The classic lacustrine oil-shale sequence of the Eocene and Paleocene Green River Formation, Uinta and Piceance basins, Utah and Colorado, U.S., is another economically important Cenozoic body of rock that contains carbonate and calcareous claystone petroleum source rocks (Hunt and others, 1954; Robinson and Cook, 1971; Tissot and others, 1978; Anders and Gerrild, 1984; Anders and others, 1992). Through long-time usage, the highly kerogenous (type I) rocks of the Green River Formation have been referred to as "shales." Yet, in reality, in the well-known upper part of the Eocene "oil shale" section, which includes the very organic rich "Mahogany zone," the rocks are more accurately described as dolomitic mudstones or marlstones. The kerogen-rich marlstones are associated with the lithologic assemblage referred to as the open-lacustrine (i.e., offshore or deeper water) facies as opposed to the marginal-lacustrine and fluvial facies (Ryder and others, 1976). These marlstones, which were deposited in a saline to hypersaline environment, contain abundant carbonate minerals, chiefly dolomite and calcite, with quartz and feldspar comprising the major noncarbonate minerals; the marlstones contain surprisingly little or no illite or other clay minerals, especially in the chemical depocenter of the basin (Dyni, 1976). The upper or Eocene "oil shale" section also contains a varied assemblage of evaporitic minerals, notably nahcolite ($NaHCO_3$), dawsonite $NaAL(OH)_2CO_3$, and halite (NaCl) and subordinate amounts of shortite ($Na_2CO_3 \cdot 2CaCO_3$) and trona

($Na_2CO_3 \cdot NaHCO_3 \cdot 2H_2O$). The latter two minerals occur in significant abundances in the Green River "oil shales" of Wyoming (Eugster and Hardie, 1978). The lower part of the Eocene "oil-shale section" was deposited under less saline to fresh water conditions and contains principally calcareous claystones that are characterized by abundant illite and subordinate amounts of carbonate and saline minerals.

The hydrocarbon resources attributed to the marlstones and calcareous claystones ("oil shales") of the Green River Formation of Eocene and Paleocene age are quite varied and extraordinary. The shallower (generally <8,000 ft deep), lower maturity (immature to marginally mature), Eocene kerogen-rich rocks are first and foremost noted for their potential to yield as much as 2.4 trillion bbl of shale oil upon closed retort (destructive distillation). Such volumes apply to the combined Green River oil shale in Utah, northwestern Colorado, and southwestern Wyoming (Culbertson and Pitman, 1973). Second, these same immature–marginally mature rocks, principally in the Uinta basin, have generated and expelled lower maturity hydrocarbons such as (1) conventional oils (Tissot and others, 1978; Anders and Gerrild, 1984; Anders and others, 1992); (2) "heavy oils" in excess of 10 billion bbl that are now present as biodegraded tar-sand deposits (Ritzma, 1973; Kuuskraa and others, 1987; Palacas and others, 1989; Anders and others, 1992); and (3) variable but significant amounts of solid bitumens, such as gilsonite (volumetrically most important), wurtzilite, ozocerite, albertite, and ingramite (Hunt and others, 1954; Curiale, 1986; Palacas and others, 1989; Anders and others, 1992). Interestingly, the gilsonite deposits alone have been estimated to amount to ~300 million bbl of oil in-place (Cashion, 1967). With reference to the tar-sand deposits investigated in the Uinta basin (e.g., Sunnyside, P.R. Spring, Asphalt Ridge, Whiterocks, and Raven Ridge), biomarker compounds indicate that only the Raven Ridge "oils" exhibit a higher level of thermal maturation, ranging from marginally mature to mature. The other tar-sand oils have been tentatively assigned a marginally mature ranking at best. The above thermal maturity assessments have been made on the assumption that specific biomarker distributions, such as the ratio of monoaromatic to triaromatic steroids, have undergone little or no biodegradation and are not source dependent.

The more deeply buried (>8,000 ft), more thermally mature and less organic-rich (average TOC = 1.6%) Green River rocks of dominantly earliest Eocene and Paleocene age (Table 1) (Fouch, 1975, 1981), on the other hand, have generated predominantly mature to very mature oils and natural gases (Tissot and others, 1978; Anders and Gerrild, 1984; Anders and others, 1992).

Mesozoic Examples

Numerous carbonate source rocks of Mesozoic age have been well documented. One example is the Upper Cretaceous Niobrara Formation of the eastern Denver basin which consists principally of organic-rich chalks that contain type II kerogen (Table 1) (Rice, 1984). Although the Niobrara chalks are a source of undetermined amounts of oil in the more deeply buried, more thermally mature western part of the Denver basin, they are noteworthy in that they are the source of large quantities of bacterial gas in the thermally immature, shallow shelf area of the eastern Denver basin (Rice, 1984). The National Petroleum Council (1980) estimated recoverable gas reserves of ~1 trillion cubic feet (TCF). Rice (1984) presented convincing evidence that these bacterial gases are indigenous to the Niobrara chalks, thus, in essence, acknowledging that Niobrara chalks play a dual role as both source rocks and reservoir rocks. It would be remiss not to point out that comparable thermally immature Niobrara chalks in the Williston basin of North and South Dakota are estimated to have also generated massive amounts of bacterial gas (on the order of 60 TCF of in-place reserves) (Shurr and Rice, 1987).

Another Upper Cretaceous carbonate source rock in the United States that functions both as a source and reservoir rock is the Austin Chalk of south-central Texas (Table 1) (Grabowski, 1984). The Austin Chalk consists of interbedded thick, light-colored, organic-lean (<1.5% TOC) beds and thin, dark-colored, organic-rich beds characterized by type I and II kerogens and TOC contents generally >4%. These chalks are thermally mature and have generated significant amounts of commercial oil and thermogenic gas (as opposed to bacterial gas). Also, because the Austin Chalk possesses both ideal source and reservoir characteristics, it stands out as a prime target for horizontal drilling. This innovative drilling technology has dramatically increased the recoverable petroleum reserves in the Austin Chalk.

Another well-documented carbonate source rock of Late Cretaceous age is the La Luna Formation, Maracaibo basin, Venezuela (Table 1) (Talukdar and others, 1986) and Magdalena Valley, Colombia (Zumberge, 1984). The La Luna Formation, consisting of organic-rich argillaceous limestones and calcareous shales, is the source for giant oil accumulations (Carmalt and St. John, 1986).

One example of Early Cretaceous age is the Sunniland Limestone, South Florida basin (Table 1). Generally laminated, mainly type II kerogen-rich limestone beds in the lower Sunniland, especially the downdip basinal facies, have been shown to be the probable source for oils accumulated in the updip, upper Sunniland carbonate

reef-like reservoir rocks (Palacas, 1978,1984a,b; Palacas and others, 1984).

Probably the most prolific carbonate source rock for generating and expelling massive amounts of conventionally recoverable oil (i.e., excluding unconventionally recovered oil such as oil in tar sand deposits) is the Jurassic (Callovian–Oxfordian) sequence of carbonate rocks in northeastern Saudi Arabia (Ayres and others, 1982; Jones, 1985). These algal-rich (type II kerogen), thinly laminated, thermally mature, pelloidal limestones, deposited in euxinic intrashelf basins on a stable carbonate-evaporite platform, expelled as much as 400 billion bbl of oil (Jones, 1985). Most, if not all, of this expelled oil migrated vertically upward into the overlying reservoirs, charging principally the Upper Jurassic Arab Formation carbonate grainstone reservoirs that are as much as 1,000 ft above the source rock. Farther upward migration was prevented by the widespread impervious evaporite beds of the 500-ft-thick Upper Jurassic Hith Anhydrite.

Another notable Upper Jurassic carbonate source rock is the Smackover Formation in the northern rim of the Gulf Coast, U.S., extending from the Florida Panhandle through Texas (Oehler, 1984; Sassen and Moore, 1988; Claypool and Mancini, 1989; Sassen, 1990). The algal-rich, laminated lime mudstones are confined chiefly to the lower part of the Smackover. Although averaging only ~0.5% TOC (Table 1), they are the source of "giant-size" volumes of oil and gas in carbonate grainstone reservoirs of the upper part of the Smackover as well as in other overlying reservoirs. The presently low TOC value is attributed in large part to the advanced stage of thermal maturity; the TOC values, consequently, must have been much higher in the geologic past, prior to thermal transformation of the organic matter. Furthermore, the average TOC value is also undoubtedly biased toward the low side primarily because the basinal laminite facies are rarely drilled or cored. Despite the high levels of thermal maturation, the basinal laminites still exhibit up to several percent TOC values. Originally these values most likely ranged from 4 to 6% or more (G. T. Grabowski, Exxon Production Research Co., unpublished data; G. E. Claypool, Mobil Research and Development Corp., and R. Sassen, BP Production Co., personal communication).

As in Saudi Arabia, the oil expelled from the lower Smackover moved predominantly upward into the overlying Upper Jurassic and Cretaceous reservoirs. In Florida and Alabama, some oil also migrated downward into the underlying sandstone reservoirs in the Upper Jurassic Norphlet Formation.

Triassic carbonate source rocks are well represented in Italy (Pieri and Mattavelli, 1986; Riva and others, 1986; Novelli and others, 1987; Brosse and others, 1988; Mattavelli and Novelli, 1990). In fact, the Middle and Upper Triassic rocks, containing type II kerogens, are the source of 95% of the discovered oil reserves in Italy (5.3 billion bbl of in-place oil) (Mattavelli and Novelli, 1990). The areal distribution of the main oil families can be delineated into three geographic regions: (1) Po basin, northern Italy, (2) central and southern peninsular Italy, including the adjoining Adriatic Sea, and (3) Sicily. Examples of geochemically identified carbonate source rocks for the central geographic region are shown in Table 1. The Upper Triassic, sulfur-rich facies of the onshore Burano Formation (TOC generally 0.1–0.6%, but as much as 1.5%) and equivalent facies of the offshore Emma Limestone (TOC commonly 0.3–5.0%; 17.0% maximum) are the main source rocks for the Adriatic oils and, presumably, for adjacent onshore oils (Paulucci and others, 1988; Mattavelli and Novelli, 1990). Of significant interest is the fact that 70% of all the oils in Italy, including for most of the Adriatic Sea and Sicilian oils, are nonbiodegraded, sulfur-rich, low maturity ("immature") heavy oils with API gravities commonly ranging from 5 to 20°.

Paleozoic Examples

Carbonate source rocks of Paleozoic age are also not uncommon. A Permian example, although not well documented in the published literature, is the Bone Spring Limestone in the northwest shelf of the Delaware basin in southeastern New Mexico. Most of the data and interpretations were derived from Williams (1977) (a written version of a talk given at the American Association of Petroleum Geologists Southwest Section meeting, Abilene, Texas), J. A. Williams (unpublished data), and Palacas (unpublished data). The Bone Spring consists of as much as 3,500 ft of rocks of Leonardian age that are the slope and basin facies equivalents of the shelf facies of the northern Delaware basin. The Bone Spring is composed of three carbonate units commonly referred to as the First, Second, and Third Bone Spring carbonates, separated by three clastic units, the First, Second, and Third Bone Spring sands composed of silty, quartzose sandstone intercalated with laminated lime mudstone or dolomudstone (Gawloski, 1988).

TOC contents of the Bone Spring carbonate rocks were assessed from composited drill cuttings (sample intervals commonly 100–300 ft thick; up to 430 ft thick) from three wells in New Mexico: (1) Pan Am No. 7, Big Eddy, sec. 19, T. 20 S., R. 31 E., Eddy County—1,737 ft analyzed out of a 3,100-ft section; (2) Pan Am No. 1, Little Eddy, sec. 5, T. 20 S., R. 33 E., Lea County—2,090 ft analyzed out of a 2,760-ft section; and (3) Bass et al. No. 1, North Custer Mountain, sec. 28, T. 23 S., R. 35 E., Lea County—2,870 ft analyzed out of a 2,870-ft sec-

tion. The weighted TOC values are as follows: (1) average 0.9%, range 0.3–1.5%; (2) average 1.4%, range 0.4–2.1%; and (3) average 1.4%, range 0.5–2.2%, respectively, with an overall weighted average TOC of ~1.3%. It would not be surprising to find upon analysis of smaller sample intervals that numerous thin zones, much richer in oil-prone organic matter (perhaps 2.5–5.0% TOC), are also present.

The oils generated by the Bone Spring carbonate rocks have accumulated in Bone Spring carbonate and/or sandstone reservoirs and in other overlying Permian reservoirs. It is very possible that a large proportion of the oil in San Andres reservoirs on the west side of the Central Basin Platform and on the northwest shelf of the Delaware basin was derived from Bone Spring sources (Williams, 1977; J.A. Williams, personal communication).

An excellent example of a Devonian carbonate source rock is the exceedingly organic-rich Duvernay Formation in the Western Canada basin, east-central Alberta (Stoakes and Creaney, 1985; Creaney and Allan, 1990). This Upper Devonian carbonate unit, composed of dark-gray to black, bituminous (type II kerogen), laminated lime mudstones, with insoluble residues generally much less than 10%, was deposited under marine, deep-water, low-energy, euxinic basinal conditions between Leduc Formation reef complexes. TOC contents of the lime mudstone are generally between 5 and 10% and as high as 17% (Table 1); hydrogen indices are in the 500–600 mg HC/g TOC range (Creaney and Allan, 1990). The thermally mature Duvernay carbonate rocks are the source of oils produced from the adjoining Leduc reef buildups and from other nearby reservoirs that contain as much as 14 billion bbl of in-place oil (Creaney and Allan, 1990).

Silurian carbonate source rocks have been well documented in the Michigan basin, U.S. and Canada (Powell and others, 1984; Gardner and Bray, 1984; McMurray, 1985; Rullkötter and others, 1986). In a study of the U.S. portion of the Michigan basin, Gardner and Bray (1984) concluded that the carbonaceous, laminated interreef Salina A-1 carbonate facies of the Salina Group, characterized by strong petroliferous odors and apparently indigenous oil and gas shows, are the principal source of hydrocarbons that charged the adjacent Niagaran pinnacle reefs. An upper algal or "Brown Niagaran" dolomite facies was also proposed as a subordinate source of petroleum. Both carbonate facies were believed to have been deposited in a mesosaline environment. The TOC values for the A-1 carbonates, averaging 0.3%, are unusually low compared to other carbonate-evaporite source rock facies illustrated in Table 1. One possible explanation is that the hydrogen-rich, laminated, thermally mature A-1 carbonates might have experienced maximum efficiency in the generation and expulsion of hydrocarbons, leaving only a minor remnant of the original organic matter content. Another possibility is that the richer source rock units, probably occurring in thin beds, were not examined. Support for this latter possibility is provided by the analysis of other borehole core samples in which TOC contents as high as 1.4% were detected (J. A. Williams, personal communication). Furthermore, on the Ontario side of the Michigan basin, McMurray (1985) reported TOC contents as high as 3.3% in equivalent Salina A-1 carbonates.

Lower Cambrian carbonate source rocks have been identified in the East Officer basin, South Australia (McKirdy and others, 1984). In the northeastern part of the basin, source rocks of the Observatory Hill Beds, containing as much as 1.3% TOC (Table 1), consist of algal, laminated, pyritic, dolomitic and argillaceous mudstones, including alkaline evaporite minerals, notably trona and shortite. Geologic criteria and detailed crude oil–source rock correlations have demonstrated that, under marginally mature conditions, these evaporite-bearing carbonate rocks have generated black, low sulfur (0.3%), naphthenic, heavy oils (~14° API) that are rich in acyclic isoprenoids. The Observatory Hill Beds, characterized by type II kerogens, are believed to have formed in a nonmarine, highly alkaline, reducing, playa-lacustrine environment. The oils generated by these 550–570(?) Ma lacustrine carbonates are unique in that they are similar to some of the oils and bitumens generated by the much younger (~50? Ma) lacustrine, evaporite-bearing dolomitic mudstones of the Eocene Green River Formation, Utah and Wyoming (McKirdy and others, 1984).

Precambrian Example

Hydrocarbon-generating carbonate rocks have also been reported in the Precambrian. Perhaps one of the most exciting examples recently cited in the literature is the occurrence of upper Proterozoic Huqf Group carbonate-evaporite source rocks in southern Oman (Grantham and others, 1987; Brett Mattes, reported in Fritz, 1989). These carbonate-evaporite rocks have been clearly shown to be the source of ~12 billion bbl of oil and undetermined amounts of gas that accumulated mainly in overlying Paleozoic reservoirs but that also accumulated in Precambrian reservoirs (Bret Mattes, reported in Fritz, 1989). The Precambrian oils generally have low API gravity and are sulfur rich. They are characterized by pristane/phytane ratios <1, a striking series of monomethylalkanes and presumed dimethylalkanes (Klomp, 1986), a strong predominance of C_{29} steranes, an absence or very low content of diasteranes (Grantham, 1986), and highly negative whole-oil $\delta^{13}C$ values

(around –36‰—values considered to be among the most negative crude oil values reported) (Grantham and others, 1987). The Huqf Group source rocks "contain type-II organic matter, most probably originating from bacteria and cyanobacteria" (Grantham and others, 1990, p. 321). Based on data of four source rock samples (Grantham and others, 1987, table 1), TOC contents of the Huqf Group source rocks reach as high as 6.2% (Table 1).

CHARACTERISTICS OF CARBONATE SOURCE ROCKS AND OILS

In this section, a few important features of carbonate source rocks, in particular carbonate-evaporite source facies, are summarized. Emphasis is placed on key compositional characteristics of carbonate-derived oils in contrast to shale-derived oils that might assist the explorationist in correlating oils to their source rocks and, in turn, in determining migration pathways. For more details on carbonate source rocks, the reader is referred to the other papers dealing with carbonate rocks in this volume, the references listed at the end of this paper, and the collection of carbonate source-rock papers in Palacas (1984b).

Carbonate-evaporite facies, which account for most of the source rocks shown in Table 1 (e.g., Green River open lacustrine facies, Sunniland Limestone, Oxfordian–Callovian rocks of Saudi Arabia, Smackover Formation, Duvernay Formation, Salina A-1 carbonates, Observatory Hill Beds, and Huqf Group), accumulated in hypersaline depositional environments such as lagoons, restricted marine basins, sabkhas, and lacustrine basins. These environments are characterized by low influx of terrigenous debris, high organic productivity in the upper water column, usually anoxic conditions in the lower water column, and always highly reducing conditions beneath the sediment-water interface. In such highly reducing environments, carbonate evaporite source facies, characterized by oil-prone type II or type I kerogens, commonly contain 1–5% TOC and range as high as 10–30% (Spiro and others, 1983; Palacas, 1984a; Powell, 1984; Stoakes and Creaney, 1985). Significantly, these same facies, in their thermally immature state (R_o = 0.3–0.6%), are characterized by extremely high yields (10–25%) of lipid-like extractable organic matter relative to total organic carbon. Moreover, even higher yields (30–80%) have been observed in some carbonate-evaporite facies (Palacas, 1984a; Palmer and Zumberge, 1981; Powell, 1984; Tannenbaum and Aizenshtat, 1985).

One explanation for generation of abundant lipid-like extractable organic matter at low levels of thermal maturity is that, during early diagenesis, in the highly reducing environment where abundant H_2S is generated and iron contents are low, sulfur becomes incorporated into the kerogen structure (designated as type II-S kerogen) (Orr, 1986). Cleavage of relatively weak sulfur-carbon bonds results in generation of resin- and asphaltene-rich petroleum at low levels of thermal stress. J. A. Williams (this volume) elaborates more fully on the important role of sulfur in early generation of hydrocarbons. Another explanation is that the extreme reducing conditions in the depositonal environment cause retardation of the condensation or polymerization of kerogen precursor molecules, resulting in abnormally high ratios of lipid-like soluble organic matter (predominantly resins and asphaltenes) to insolubles (kerogen) (Powell, 1984). Should this latter hypothesis be true, then the resins and asphaltenes, in addition to kerogen, may also serve as major precursors of hydrocarbons generated later under higher thermal stress (Powell and others, 1975; Palacas, 1984a).

Table 2 (modified after Palacas, 1988) summarizes many of the compositional features of carbonate-derived oils. (For comparison, corresponding compositional features are also given for shale-derived oils.) Although it is recognized that, under certain depositional conditions, a similar organic facies can develop regardless of the inorganic aspects of the sediment (Jones, 1984,1987; Williams, this volume), enough data have accumulated to show that in the majority of petroliferous sedimentary basins, carbonate-derived and shale-derived immature to moderately mature oils can be distinguished from one another. Accordingly, Table 2 lists compositional characteristics for the low- to medium-maturity oils. In very mature oils, many of the key correlation parameters, such as biomarker compounds, are altered or even destroyed. Basic to the data in Table 2 are the assumptions that oils have undergone little or no alteration due to biodegradation, migration, and in-reservoir maturation. Obviously, caution should be exercised in using this table because, on a worldwide basis, there are oils that contain combinations of the two categories of geochemical characteristics listed. Also, some oils may be mixtures of oils derived from two or more sources, sometimes of different lithologies. Also, secondary processes may selectively alter the parameters. Therefore, no single parameter can be used to pinpoint the origin of an oil. Rather, interpretation of multiple bulk and molecular parameters and an understanding of the geology are needed to determine oil-source bed relationships with some degree of confidence.

CONCLUSIONS

Fourteen examples of worldwide carbonate source rocks (Table 1), based on solid geologic and geochemical data, including source rock–

TABLE 2. — CHARACTERISTICS OF LOW- TO MEDIUM-MATURITY OILS DERIVED FROM CARBONATE VERSUS SHALE SOURCE ROCKS

Parameter	Carbonate rocks	Shales	References[a]
API gravity	Low–medium	Medium–high	6,10,16
Total sulfur	High (>1%)[b]	Low (<1%)	1,6,10,12,16
HC/(resins+asphaltenes)	Low–medium	Medium–high	1,4,9,10,11,12
Naphthenes/paraffins	High–medium	Medium–low	6,13,16
Sat HC/Arom HC	Low–medium	Medium–high	6,11,12,16
CPI, C_{22}–C_{32} n-alkanes	≤1	≥1	1,6,10,11,12,17
Pristane/phytane	≤1	≥1	1,3,6,10,12,13
Phytane/n-C_{18}	High (0.3–1.5+)	Low (≤0.3–0.4)	1,10,11,12
Steranes+triterpanes/ n-alkanes	High–medium	Low–medium	1,11,12
Steranes[c]	High aquatic to mixed aquatic/terrestrial ($C_{27} \geq C_{29}$)	High terrestrial to mixed aquatic/terrestrial ($C_{27} \leq C_{29}$)	5,6
Diasteranes	Low–medium	Medium–high	6,8,14,15
Hopane/C_{27}–C_{29} steranes	>20	<20	2
C_{35}/C_{34} extended hopanes	≥1	≤1	8
Diterpanes: C_{24} tetracyclic/C_{26} tricyclic	High–medium	Medium–low	2,10,11
V pattern in four isomeric methyldibenzothiophenes	Common	Absent or rare	6
Thiophenic sulfur	High in benzo-thiophenes	Low in benzo-thiophenes	6

NOTE: HC = hydrocarbons; Sat = saturated; Arom = aromatic; CPI = carbon preference index.
[a]References: (1) Connan, 1981; (2) Connan and others, 1986; (3) Didyk and others, 1978; (4) Grabowski, 1984; (5) Huang and Meinschein, 1979; (6) Hughes, 1984; (7) Hunt and McNicol, 1984; (8) McKirdy and others, 1983; (9) Murris and DeGroot, 1979; (10) Palacas, 1984a; (11) Palacas and others, 1984; (12) Powell, 1984; (13) Renard and others 1977; (14) Rubenstein and others, 1975; (15) Rullkötter and others, 1985; (16) Tissot and Welte, 1984; (17) Welte and Waples, 1973.
[b]Oils derived from lacustrine carbonate rocks are commonly low in sulfur.
[c]Sterane distributions may also be affected by geologic time (Grantham and Wakefield, 1988).

crude oil correlations, provide ample proof that carbonate rocks are viable source rocks of commercial amounts of petroleum. The fact that ~40% of the world's giant oil fields are in carbonate reservoirs, most of which are believed to be charged with oil from carbonate source beds, also attests to the importance of these non-shale source rocks. It should also be emphasized that most carbonate rocks, like most siliceous rocks, contain non-hydrocarbon-generative organic facies (Jones, 1984) (i.e., those containing low TOC) which are not sources of economic amounts of petroleum. In order for a carbonate rock (or any other sedimentary rock) to be an effective source of conventional oil, it must meet certain criteria: it must have or contain (1) an adequate amount of organic matter, (2) the right type of organic matter (e.g., hydrogen-rich material), (3) a sufficient level of thermal maturity, and (4) the ability to expel hydrocarbons.

From the well-documented examples of carbonate source rocks (Table 1), it is readily seen that most carbonate source rocks contain an adequate amount of organic matter—an average of

1–5% TOC. Low values of TOC (<1%) observed for some of the source rocks can, in some cases, be explained by the effects of over-maturation or by limited sampling wherein the organically richer facies were not encountered or perhaps overlooked in drill cuttings. It is also evident that the predominant type of organic matter of these source rocks is the oil-prone type II kerogen. In some cases, type I or a combination of type I and II kerogens are present. Clearly, these carbonate source rocks, by virtue of their hydrogen-rich organic facies, have unequivocally been shown to be good to excellent source rocks of petroleum.

ACKNOWLEDGMENTS

Thoughtful and constructive reviews were provided by Jerry Clayton, Dudley Rice, Jack Williams, and Steve Creaney. The section on marlstones of the Green River Formation was certainly improved by the helpful comments and inputs of Bill Cashion, Tom Fouch, Ron Johnson, Jack Dyni, and Janet Pitman.

REFERENCES

Albaiges, J.; Algaba, J.; Clavell, E.; and Grimalt, J., 1986, Petroleum geochemistry of the Tarragona basin (Spanish Mediterranean offshore), *in* Leythaeuser, D.; and Rullkötter, J. (eds.), Advances in organic geochemistry 1985: Organic Geochemistry, v. 10, p. 441–450.

Anders, D. E.; and Gerrild, P. M., 1984, Hydrocarbon generation in lacustrine rocks of Tertiary age, Uinta basin, Utah—organic carbon, pyrolysis yield and light hydrocarbons, *in* Woodward, J.; Meissner, F. F.; and Clayton, J. L. (eds.), Hydrocarbon source rocks of the greater Rocky Mountain region: Rocky Mountain Association of Geologists, Denver, p. 513–529.

Anders, D. L.; Palacas, J. G.; and Johnson, R. C., 1992, Thermal maturity of rocks and hydrocarbon deposits, Uinta basin, Utah, *in* Fouch, T. D.; Nuccio, V. F.; and Chidsey, T. C. (eds.), Hydrocarbon and mineral resources of the Uinta Basin: Utah Geological Association Guidebook 20, p. 53–76.

Ayres, M. G.; Bilal, M.; Jones, R. W.; Slentz, L. W.; Tartir, M.; and Wilson, A. O., 1982, Hydrocarbon habitat in main producing areas, Saudi Arabia: American Association of Petroleum Geologists Bulletin, v. 66, p. 1–9.

Brosse, E.; Loreau, J. P.; Juc, A. Y.; Frixa, A.; Martellini, L.; and Riva, A., 1988, The organic matter of interlayered carbonates and clay sediments—Trias/Lias, Sicily, *in* Mattavelli, L.; and Novelli, L. (eds.), Advances in organic geochemistry 1987: Organic Geochemistry, v. 13, p. 433–443.

Carmalt, S. W.; and St. John, B., 1986, Giant oil and gas fields, *in* Halbouty, M. T. (ed.), Future petroleum provinces of the world: American Association of Petroleum Geologists Memoir 40, p. 11–53.

Cashion, W. B., 1967, Geology and fuel resources of the Green River Formation, southeastern Uinta basin, Utah and Colorado: U.S. Geological Survey Professional Paper 548, 48 p.

Claypool, G. E.; and Mancini, E. A., 1989, Geochemical relationships of petroleum in Mesozoic reservoirs to carbonate source rocks of Smackover Formation, southwestern Alabama: American Association of Petroleum Geologists Bulletin, v. 73, p. 904–924.

Connan, J., 1981, Biological markers in crude oils, *in* Mason, J. F. (ed.), Petroleum geology in China: PennWell, Tulsa, p. 48–70, 257–258.

Connan, J.; Bouroullec, J.; Dessort, D.; and Albrecht, P., 1986, The microbial input in carbonate-anhydrite facies of a sabkha palaeoenvironment from Guatemala: a molecular approach, *in* Leythaeuser, D.; and Rullkötter, J. (eds.), Advances in organic geochemistry 1985: Organic Geochemistry, v. 10, p. 29–50.

Creaney, S.; and Allan, J., 1990, Hydrocarbon generation and migration in the Western Canada sedimentary basin, *in* Brooks, J. (ed.), Classic petroleum provinces: The Geological Society, London, Special Publication No. 50, p. 189–202.

Culbertson, W. C.; and Pitman, J. K., 1973, Oil shale, *in* Brobst, D. A.; and Pratt, W. P. (eds.), United States mineral resources: U.S. Geological Survey Professional Paper 820, p. 497–503.

Curiale, J. A., 1986, Origin of solid bitumens, with emphasis on biological marker results, *in* Leythaeuser, D.; and Rullkötter, J. (eds.), Advances in organic geochemistry 1985: Organic Geochemistry, v. 10, p. 559–580.

Demaison, G.; and Bourgeois, F. T., 1984, Environment of deposition of middle Miocene (Alcanar) carbonate source beds, Casablanca field, Tarragona basin, offshore Spain, *in* Palacas, J. G. (ed.), Petroleum geochemistry and source rock potential of carbonate rocks: American Association of Petroleum Geologists Studies in Geology, no. 18, p. 151–161.

Didyk, B. M.; Simoneit, B. R. T.; Brassell, S. C.; and Eglington, G., 1978, Organic geochemical indicators of paleoenvironmental conditions of sedimentation: Nature, v. 272, p. 216–222.

Dyni, J. R., 1976, Trioctahedral smectite in the Green River Formation, Duchesne County, Utah: U.S. Geological Survey Professional Paper 967, 14 p.

Eugster, H. P.; and Hardie, L. A., 1978, Saline lakes, *in* Lerman, A. (ed.), Lakes—chemistry, geology, and physics: Springer-Verlag, New York, p. 237–293.

Fouch, T. D., 1975, Lithofacies and related hydrocarbon accumulations in Tertiary strata of the western and central Uinta basin, Utah, *in* Bolyard, D. W. (ed.), Rocky Mountain Association of Petroleum Geologists Symposium on Deep Drilling Frontiers of the Central Rocky Mountains, p. 163–174.

_____1981, Distribution of rock types, lithologic groups, and interpreted depositional environments for some lower Tertiary and Upper Cretaceous rocks from outcrops at Willow Creek–Indian Canyon through the subsurface of Duchesne and Altamont oil field: U.S. Geological Survey Oil and Gas Investigations Map Chart OC-81, 2 sheets.

Fritz, M., 1989, An old source surfaces in Oman: American Association of Petroleum Geologists Explorer,

v. 10, no. 9, p. 1, 14–15.
Gardner, W. C.; and Bray, E. E., 1984, Oils and source rocks of Niagaran reefs (Silurian) in the Michigan basin, *in* Palacas, J. G. (ed.), Geochemistry and source rock potential of carbonate rocks: American Association of Petroleum Geologists Studies in Geology, no. 18, p. 33–44.
Gawloski, T. F., 1988, Nature, distribution, and petroleum potential of Bone Spring detrital sediments, northern Delaware basin, *in* A symposium of oil and gas fields of southeastern New Mexico: Roswell Geological Society, p. 44–72.
Grabowski, G. J., Jr., 1984, Generation and migration of hydrocarbons in Upper Cretaceous Austin Chalk, south-central Texas, *in* Palacas, J. G. (ed.), Petroleum geochemistry and source rock potential of carbonate rocks: American Association of Petroleum Geologists Studies in Geology, no. 18, p. 97–115.
Grantham, P. J., 1986, The occurrence of unusual C_{27} and C_{29} sterane predominances in two types of Oman crude oil: Organic Geochemistry, v. 9, p. 1–10.
Grantham, P. J.; and Wakefield, L. L., 1988, Variations in the sterane carbon number variations of marine source rock derived crude oils through geologic time: Organic Geochemistry, v. 12, p. 61–73.
Grantham, P. J.; Lijmback, G. W. M.; and Posthuma, J., 1990, Geochemistry of crude oils in Oman, *in* Brooks, J. (ed.), Classic petroleum provinces: The Geological Society, London, Special Publication No. 50, p. 317–328.
Grantham, P. J.; Lijmbach, G. W. M.; Posthuma, J.; Hughes Clark, M. W.; and Willink, R. J., 1987, Origin of crude oils in Oman: Journal of Petroleum Geology, v. 11, no. 1, p. 61–80.
Huang, W. Y.; and Meinschein, W. G., 1979, Sterols as ecological indicators: Geochimica et Cosmochimica Acta, v. 43, p. 739–745.
Hughes, W. B., 1984, Use of thiophenic organosulfur compounds in characterizing crude oils derived from carbonate versus siliciclastic sources, *in* Palacas, J. G. (ed.), Petroleum geochemistry and source rock potential of carbonate rocks: American Association of Petroleum Geologists Studies in Geology, no. 18, p. 181–196.
Hunt, J. M.; and McNichol, A. P., 1984, The Cretaceous Austin Chalk of South Texas, *in* Palacas, J. G. (ed.), Petroleum geochemistry and source rock potential of carbonate rocks: American Association of Petroleum Geologists Studies in Geology, no. 18, p. 117–125.
Hunt, J. M.; Stewart, F.; and Dickey, P. A., 1954, Origin of hydrocarbons of Uinta basin, Utah: American Association of Petroleum Geologists Bulletin, v. 38, p. 1671–1698.
Jones, R. W., 1984, Comparison of carbonate and shale source rocks, *in* Palacas, J. G. (ed.), Petroleum geochemistry and source rock potential of carbonate rocks: American Associaton of Petroleum Geologists Studies in Geology, no. 18, p. 163–180.
_____1985, Hydrocarbon habitat in main producing areas, Saudi Arabia: reply: American Association of Petroleum Geologists Bulletin, v. 69, p. 2031–2033.
_____1987, Organic facies, *in* Brooks, J.; and Welte, D. (eds)., Advances in petroleum geochemistry, vol. 2: Academia Press, New York, p. 1–90.
Klomp, U. C., 1986, The chemical structure of a pronounced series of iso-alkanes in South Oman crudes, *in* Leythaeuser, D.; and Rullkötter, J. (eds.), Advances in organic geochemistry 1985: Organic Geochemistry, v. 10, p. 807–814.
Kuuskraa, V. A.; Hammershaimb, E. C.; and Paque, M., 1987, Major tar sand and heavy-oil deposits of the United States, *in* Meyer, R. F. (ed.), Exploration for heavy crude oil and natural bitumen: American Association of Petroleum Geologists Studies in Geology, no. 25, p. 123–134.
Mattavelli, L.; and Novelli, L., 1990, Geochemistry and habitat of the oils in Italy: American Association of Petroleum Geologists Bulletin, v. 74, p. 1623–1639.
McKirdy, D. M.; Aldridge, A. K.; and Ypma, P. J. M., 1983, A geochemical comparison of some crude oils from pre-Ordovician carbonate rocks, *in* Bjorøy, M.; and others (eds.), Advances in organic geochemistry 1981: John Wiley and Sons, Chichester, p. 99–107.
McKirdy, D. M.; Kantsler, A. J.; Emmett, J. K.; and Aldridge, A. K., 1984, Hydrocarbon genesis and organic facies in Cambrian carbonates of the Eastern Officer basin, South Australia, *in* Palacas, J. G. (ed.), Petroleum geochemistry and source rock potential of carbonate rocks: American Association of Petroleum Geologists Studies in Geology, no. 18, p. 13–31.
McMurray, M. G., 1985, Geology and organic geochemistry of Salina A-1 carbonate oil source-rock lithofacies (Upper Silurian), southwestern Ontario, Canada: University of Waterloo, Ontario, M.S. thesis.
Murris, R. J.; and de Groot, K., 1979, Oil habitat of carbonate provinces: Congresso Panamericano de Ingenieri a Petroleo, Mexico, Proceedings, sec. 1, paper 5.
National Petroleum Council, 1980, Denver basin tight gas reserves, Part II, p. 15-1–15-39.
Novelli, L.; Chiaramonte, M. A.; Mattavelli, L.; Pizzi, G.; Sartori, L.; and Scotti, D., 1987, Oil habitat in northwestern Po basin, *in* Doligez, B. (ed.), Migration of hydrocarbons in sedimentary basins: Editions Technip, Paris, p. 27–57.
Oehler, J. H., 1984, Carbonate source rocks in the Jurassic Smackover trend of Mississippi, Alabama, and Florida, *in* Palacas, J. G. (ed.), Petroleum geochemistry and source rock potential of carbonate rocks: American Association of Petroleum Geologists Studies in Geology, no. 18, p. 63–69.
Orr, W. J., 1986, Kerogen/asphaltene/sulfur relationships in sulfur-rich Monterey oils, *in* Leythaeuser, D.; and Rullkötter, J. (eds.), Advances in organic geochemistry 1985: Organic Geochemistry, v. 10, p. 499–516.
Palacas, J. G., 1978, Preliminary assessment of organic carbon content and petroleum source rock potential of Cretaceous and lower Tertiary carbonates, South Florida basin: Gulf Coast Association of Geological Societies Transactions, v. 28, p. 357–381.
_____1984a, Carbonate rocks as sources of petro-

leum: geological and chemical characteristics and oil-source correlations: 11th World Petroleum Congress Proceedings, 1983, London, v. 2, p. 31–43.

_____(ed.), 1984b, Petroleum geology and source rock potential of carbonate rocks: American Association of Petroleum Geologists Studies in Geology, no. 18, 208 p.

_____1988, Characteristics of carbonate source rocks of petroleum, *in* Magoon, L. B. (ed.), Petroleum systems of the United States: U.S. Geological Survey Bulletin 1870, p. 20–25.

Palacas, J. G.; Anders, D. E.; and King, J. D., 1984, South Florida basin—prime example of carbonate source rocks of petroleum, *in* Palacas, J. G. (ed.), Petroleum geochemistry and source rock potential of carbonate rocks: American Association of Petroleum Geologists Studies in Geology, no. 18, p. 71–96.

Palacas, J. G.; Anders, D. E.; King, J. D.; and Lubeck, C. M., 1989, Use of biological markers in determining thermal maturity of biodegraded heavy oils and solid bitumens, *in* Meyer, R. F.; and Wiggins, E. J. (eds.), The fourth UNITAR/UNDP international conference on heavy crude and tar sands: Alberta Oil Sands Technology and Research Authority, Edmonton, Alberta, Canada, p. 575–592.

Palmer, S. E.; and Zumberge, J. E., 1981, Organic geochemistry of Upper Miocene evaporite deposits in the Sicilian basin, Sicily, *in* Brooks, J. (ed.), Organic maturation studies and fossil fuel exploration: Academic Press, London, p. 393–426.

Paulucci, G.; Novelli, L.; Bongiorni, D.; and Cesaroni, R., 1980, Deep offshore exploration in the southern Adriatic Sea: Offshore Technology Conference 5730 Proceedings, p. 413–421.

Pierri, M.; and Mattavelli, L., 1986, Geologic framework of Italian petroleum resources: American Association of Petroleum Geologists Bulletin, v. 70, p. 103–130.

Powell, T. G., 1984, Some aspects of the hydrocarbon geochemistry of a Middle Devonian barrier-reef complex, Western Canada, *in* Palacas, J. G. (ed.), Petroleum geochemistry and source rock potential of carbonate rocks: American Association of Petroleum Geologists Studies in Geology, no. 18, p. 45–61.

Powell, T. G.; Cook, P. J.; and McKirdy, D. M., 1975, Organic geochemistry of phosphorites: relevance to petroleum genesis: American Association of Petroleum Geologists Bulletin, v. 59, p. 618–632.

Powell, T. G.; Macqueen, R. W.; Barker, J. F.; and Bree, D. G., 1984, Geochemical character and origin of Ontario oils: Bulletin of Canadian Petroleum Geology, v. 32, p. 289–312.

Renard, B.; Du Rouchet, J.; and Connan, J., 1977, Les roches-méres carbonatés, *in* Essai de caractérisation sédimentologique des dépots carbonatés. 2.—Eléments d'interprétation: Boussens et Pau, Elf Aquitaine, p. 139–149.

Rice, D. D., 1984, Occurrence of indigenous biogenic gas in organic-rich, immature chalks of late Cretaceous age, Eastern Denver basin, *in* Palacas, J. G. (ed.), Petroleum geochemistry and source rock potential of carbonate rocks: American Association of Petroleum Geologists Studies in Geology, no. 18, p. 135–150.

Ritzma, H. R., 1973, Location map, oil-impregnated rock deposits of Utah: Utah Geological and Mineralogical Survey, map 33.

Riva, A.; Salvatori, T.; Cavaliere, R.; Ricchiuto, T.; and Novelli, L., 1986, Origin of oil in Po basin, northern Italy, *in* Leythaeuser, D.; and Rullkötter, J. (eds.), Advances in organic geochemistry 1985: Organic Geochemistry, v. 10, p. 391–400.

Robinson, W. E.; and Cook, G. L., 1971, Compositional variations of the organic material of Green River oil shale–Colorado No. 1 core: U.S. Bureau of Mines Report of Investigations 7492, 32 p.

Rubenstein, I.; Sieskind, O.; and Albrecht, P., 1975, Rearranged sterenes in shale: occurrence and simulated formation: Journal Chemical Society Perkin Transactions, v. 1, p. 1833–1836.

Rullkötter, J.; Myers, P. A.; Schaefer, R. G.; and Dunham, K. W., 1986, Oil generation in the Michigan basin: a biological marker and carbon isotope approach, *in* Leythaeuser, D.; and Rullkötter, J. (eds.), Advances in organic geochemistry 1985: Organic Geochemistry, v. 10, p. 359–375.

Rullkötter, J.; Spiro, B.; and Nissenbaum, A., 1985, Biological marker characteristics of oils and asphalts from carbonate source rocks in a rapidly subsiding graben, Dead Sea, Israel: Geochimica et Cosmochimica Acta, v. 49, p. 1357–1370.

Ryder, R. T.; Fouch, T. D.; and Elison, J. H., 1976, Early Tertiary sedimentation in the western Uinta basin, Utah: Geological Society of America Bulletin, v. 87, p. 496–512.

Sassen, R., 1990, Geochemistry of carbonate source rocks and crude oils in Jurassic salt basins of the Gulf Coast, *in* Schumacher, D.; and Perkins, B. F. (eds.), Gulf Coast oils and gases: Gulf Coast Section, Society of Economic Paleontologists and Mineralogists Foundation, Ninth Annual Research Conference Proceedings, p. 11–22.

Sassen, R.; and Moore, C. H., 1988, Framework of hydrocarbon generation and destruction in eastern Smackover trend: American Association of Petroleum Geologists Bulletin, v. 72, p. 649–663.

Shurr, G. W.; and Rice, D. D., 1987, Geologic setting and potential for natural gas in the Niobrara Formation (Upper Cretaceous) of the Williston Basin, *in* Peterson, J. A. (ed.), Williston basin—exploration model for a cratonic petroleum province: Rocky Mountain Association of Geologists, Denver, p. 245–257.

Spiro, B.; Welte, D. H.; Rulkötter, J.; and Schaefer, R. G., 1983, Asphalts, oils, and bituminous rocks from the Dead Sea area—a geochemical correlation study: American Association of Petroleum Geologists Bulletin, v. 67, p. 1163–1175.

Stoakes, F. A.; and Creaney, S., 1985, Sedimentology of a carbonate source rock: the Duvernay Formation of Alberta, Canada, *in* Longman, M. W.; Shanley, K. W.; Lindsay, R. F.; and Eby, D. E. (eds.), Rocky Mountain carbonate reservoirs: a core workshop: Society of Economic Paleontologists and Mineralogists Core Workshop No. 7, p. 343–375.

Talukdar, S.; Gallango, O.; and Chin-A-Lien, M., 1986,

Generation and migration of hydrocarbons in the Maracaibo basin, Venezuela: an integrated basin study, *in* Leythaeuser, D.; and Rullkötter, J. (eds.), Advances in organic geochemistry 1985: Organic Geochemistry, v. 10, p. 261–279.

Tannenbaum, G.; and Aizenshtat, Z., 1985, Formation of immature asphalt from organic-rich carbonate rocks. I.—Geochemical correlation: Organic Geochemistry, v. 8, p. 181–192.

Tissot, B.; Deroo, G.; and Hood, A., 1978, Geochemical study of the Uinta basin: formation of petroleum from the Green River Formation: Geochimica et Cosmochimica Acta, v. 42, p. 1469–1485.

Tissot, B.; and Welte, D. H., 1984, Petroleum formation and occurrence: Springer-Verlag, Berlin, 538 p.

Von Hettinga Tromp, I. H., 1938, Petroleum cannot be generated in limestones: Second World Petroleum Congress Proceedings, 1937, Paris, p. 371–381.

Welte, D. H.; and Waples, D., 1973, Über die Bevorzugung geradzahliger n-alkane in sedimentgesteinen: Naturwissenschaften, v. 60, p. 516–517.

Williams, J. A., 1977, Characterization of oil types in the Permian basin: Paper presented at the American Association of Petroleum Geologists Southwest Section meeting, Abilene, Texas.

Zumberge, J. E., 1984, Source rocks of the La Luna Formation (Upper Cretaceous) in the Middle Magdalena Valley, Colombia, *in* Palacas, J. G. (ed.), Petroleum geochemistry and source rock potential of carbonate rocks: American Association of Petroleum Geologists Studies in Geology, no. 18, p. 127–133.

Can Carbonates Be Source Rocks for Commercial Petroleum Deposits?

Jack A. Williams
Amoco Production Co. (retired), Tulsa

There no longer seems to be any question as to whether carbonate rocks can be sources for commercial oil accumulations. Palacas (1988) published a long list of papers containing documented correlations between produced oils and carbonate source rocks. Included in the list are examples from several major oil provinces. I believe it is now the overwhelming consensus among petroleum geochemists that carbonates have generated a significant portion of known worldwide petroleum reserves, and there remains very little argument over this point.

There still exists, however, some difference of opinion regarding identification of carbonate sources and evaluation of their oil-generating capability. I will discuss some of those areas where misinterpretation is possible and caution should be used.

A major concern is an apparent tendency among many geochemists to be overly optimistic about the oil-generating potential of carbonates. Carbonate source rocks have been shown to generate, on the average, more oil per unit of organic carbon than do clastic sources. The explanations given for this observation are valid. Among organic-rich rocks, a higher percentage of the carbonates, particularly carbonate muds, are deposited in anoxic environments which are conducive to higher oil-generating capability. Also, in carbonates there normally is less terrestrial organic matter that would tend to adversely affect the amount of oil generated per unit organic carbon. However, clastic source rocks deposited under the same optimum conditions have comparable oil-generating potential. Consequently, there is no clear difference between carbonates as a group and shales as a group with regard to generation efficiency. It can only be said that, among organic-rich rocks, proportionately more carbonates than shales have been deposited under near-optimum conditions for oil generation. This overlap of generating potential for carbonates and clastics necessitates the following consideration: a potential source rock should be evaluated strictly on the basis of quality and quantity of its organic matter, without regard to its lithology. Jones (1984) has discussed this point in some detail. He arrived at the same conclusion: the organic matter requirement for significant oil generation should be the same for carbonates as it is for clastics.

A comparison of two well-known limestone intervals—the La Luna of Venezuela and Colombia, and the Arbuckle of Oklahoma—serves to emphasize the need to have organic richness for significant oil generation. Based on several published reports, the La Luna averages somewhere around 5% organic carbon (Zumberge, 1984). It clearly has been the source for a considerable quantity of oil in Venezuela. The Arbuckle, on the other hand, appears to average well below 1% overall. Data from Amoco Production Co. analyses showed an average of only ~0.1% organic carbon for 77 samples representing several zones in the Arbuckle, but figures published by Trask and Patnode (1942) showed a somewhat higher average value, <1% but with occasional values >1%. Little, if any, of the vast production in southern Oklahoma has been reliably related to an Arbuckle source (Wavrek, 1992; Brown and others, 1992). Most of the oil in this area has been related to the Woodford Shale and Pennsylvanian shales, with minor contributions from Ordovician sources. In all probability, at least a small portion of presently known reserves, or some remaining to be discovered, will some day be related to an Arbuckle source, and localized organic-rich zones will almost certainly be found somewhere in the thick Arbuckle section. Nevertheless, the statistics cannot be ignored when evaluating the merits of the relatively organic-poor Arbuckle compared to those of the organic-rich La Luna. Such a comparison serves to emphasize the need for organic richness if a source is to be effective, whether or not it is dominantly carbonate.

With regard to establishing a minimum organic requirement for an effective source, it would appear that the frequently quoted value of 0.4 wt% organic carbon (OC) (Hunt, 1979) is far from sufficient. Colin Barker (personal communication) has commented that there must be sufficient oil generated to fill pore spaces and saturate the kerogen before any oil can be expelled from the rock. Only 0.4% OC (~0.6% total organic matter) would not provide enough oil to do this, regardless of its generation efficiency. A minimum of 1.0% OC used by some geochemists (Hunt, 1979) is more

realistic, and even that concentration of organic matter may provide no better than marginal expulsion efficiency.

It also is possible for misinterpretation to occur when attempting to identify carbonate source rocks from composition of the oil derived from it. It has become popular in recent years to assume that compositional features such as even carbon number paraffin predominance, low pristane/phytane, and high sulfur content are almost unfailingly diagnostic of carbonate source rocks. However, all of these attributes are either directly or indirectly a function of depositional environment rather than lithology; that is they are all related to an anoxic environment. The fact that a higher proportion of carbonate source rocks was deposited in this kind of environment does lend some statistical credence to attributing the aforementioned compositional features to carbonate sources, but there are many important exceptions. Most notably, the Monterey siliceous facies in California (Curiale and Odermatt, 1989) and the Phosphoria phosphatic shales of Montana–Idaho–Utah (Lewan and others, 1986) are sources of considerable quantities of oil having the compositional features typically assigned to carbonate-sourced oils. On the other hand, oils derived from the Austin Chalk of eastern Texas (Grabowski, 1984) and the Green River marlstone do not possess the carbonate "fingerprint." The point to be made is simply that source-rock lithology, whether carbonate or clastic, cannot reliably be concluded simply on the basis of oil composition, and caution is in order when attempting this kind of determination.

Selected biomarker ratios, measured by gas chromatography–mass spectroscopy (GC–MS) are also frequently invoked as indicators of carbonate sources. For example, two indicators used for this purpose are (1) the proportion of higher (extended) hopanes, C_{34} and C_{35}, relative to total hopanes present, and (2) the ratio of diasteranes (rearranged steranes) to regular steranes. A high proportion of extended hopanes is another compositional feature attributed to anoxic conditions in the source. Anoxic conditions permit chemical reduction rather than oxidative cleavage of the acyclic portions of hopane precursors, resulting in higher carbon number molecules. The chemical reduction is not lithology dependent, but once again there will be a statistical preference for carbonate sources over clastic sources, and again there are major exceptions, most notably the examples previously mentioned. Similar arguments might pertain to other biomarker ratios listed by Palacas (1988) that have been proposed as characteristic of carbonate sources.

A low proportion of diasteranes, often cited as an indicator of carbonate sources, has not been suggested to be related to anoxicity, but instead has been attributed to a lack of clay catalysis in carbonate rocks. This indicator might also be misleading. First, there has not been any evidence presented showing that a high diasterane content is not simply an indicator of thermal maturity rather than clay catalysis, with the regular steranes having a relatively higher thermal destruction rate than diasteranes. Any statistical association of low diasterane content to carbonate sources may be a result of earlier oil generation and expulsion from highly anoxic sources due to high-sulfur kerogen. It is well known that carbon-sulfur bonds cleave more readily than carbon-carbon bonds when subjected to thermal exposure. In cases of earlier generation, thermal destruction of steranes may not have proceeded far enough to significantly affect their relative concentrations. A statistical relationship between high sulfur content and carbonate sources would be expected because the carbonates are less likely to contain the iron necessary to remove sulfur from the system by precipitation of iron sulfides; however, there are again the same major exceptions. Thus it might be concluded that diasterane concentration is at least an indirect function of anoxicity. Laboratory experimentation in this area is badly needed.

SUMMARY

1. It has been clearly established that carbonate rocks can be major sources for oil.

2. Organic richness is a prerequisite for effective carbonate sources, just as it is for clastics. The same minimum organic carbon requirement should be used regardless of lithology, and any rock containing <1.0% organic carbon is probably not capable of generating enough oil for expulsion to occur.

3. Oil component ratios usually deemed to be characteristic of carbonate sources actually are indicative of anoxic depositional environments and independent of lithology. A statistical preference of these ratios for carbonate sources is observed because a higher proportion of effective carbonate sources than clastic sources were deposited in anoxic environments. The number of major exceptions tends to preclude the use of any such indicators as definitive for carbonate sources, and caution should be observed when attempting to define source lithology based on oil composition.

REFERENCES

Brown, S. W.; Swetland, P. J.; and Daly, A. R., 1992, Arbuckle oils—an overview, *in* Johnson, K. S.; and Cardott, B. J. (eds.), Source rocks in the southern Midcontinent, 1990 symposium: Oklahoma Geological Survey Circular 93, p. 176

Curiale, J. A.; and Odermatt, J. R., 1989, Short term

biomarker variability in the Monterey Formation, Santa Maria basin: Organic Geochemistry, v. 14, p. 1–13.

Grabowski, G., 1984, Generation and migration of hydrocarbons in Upper Cretaceous Austin Chalk, south-central Texas, *in* Palacas, J. G. (ed.), Petroleum geochemistry and source rock potential of carbonate rocks: American Association of Petroleum Geologists Studies in Geology, no. 18, p. 97–115.

Hunt, J. M., 1979, Petroleum geochemistry and geology: W. H. Freeman and Co., San Francisco, 617 p.

Jones, R. W., 1984, Comparison of carbonate and shale source rocks, *in* Palacas, J. G. (ed.), Petroleum geochemistry and source rock potential of carbonate rocks: American Association of Petroleum Geologists Studies in Geology, no. 18, p. 163–180.

Lewan, M. D.; Bjorøy, M.; and Dolcater, D. L., 1986, Effects of thermal maturation on steroid hydrocarbons as determined by hydrous pyrolysis of Phosphoria retort shale: Geochimica et Cosmochimica Acta, v. 50, p. 1977–1987.

Palacas, J. G., 1988, Characteristics of carbonate source rocks of petroleum, *in* Magoon, L. B. (ed.), Petroleum systems of the United States: U.S. Geological Survey Bulletin 1870, p. 20–25.

Trask, P. D.; and Patnode, H. W., 1942, Source beds of petroleum: American Association of Petroleum Geologists, Tulsa, 566 p.

Wavrek, D. A., 1992, Characterization of oil types in the Ardmore and Marietta basins, southern Oklahoma aulacogen, *in* Johnson, K. S.; and Cardott, B. J. (eds.), Source rocks in the southern Midcontinent, 1990 symposium: Oklahoma Geological Survey Circular 93, p. 185–195.

Zumberge, J. E., 1984, Source rocks of the La Luna Formation (Upper Cretaceous) in the middle Magdelena Valley, Columbia, *in* Palacas, J. G. (ed.), Petroleum geochemistry and source rock potential of carbonate rocks: American Association of Petroleum Geologists Studies in Geology, no. 18, p. 127–133.

Can Carbonates Be Source Rocks for Commercial Petroleum Deposits?

Lloyd E. Gatewood
Independent Geologist, Oklahoma City

INTRODUCTION

As one of four moderators on the posed question, I have chosen the Arbuckle Group carbonates as my subject for discussion. In regard to commercial Arbuckle oil and gas production, I believe that there are examples of oil and gas being self-sourced in the Arbuckle Group. The question of the source of oil and gas in the Arbuckle Group is not entirely an academic one. The finding of 300 oil and gas fields in Oklahoma, under many different structural and stratigraphic conditions, has established a good many facts which lead me to the conclusion that hydrocarbons are indigenous to the Arbuckle. These facts include the following:

1) Shows of asphalt, gilsonite, oil, and gas have been reported from almost every formation of the Arbuckle Group and in many areas.

2) Oil and gas is produced in large quantities 600–1,000 ft or more below the top of the Arbuckle Group.

3) Some important Arbuckle fields have produced oil and gas from heterogeneous multizones and formations at great depths.

4) Oil is produced beneath salt-water zones in some of the fields shown and numbered in Figure 1: (10) Pettit Dome, (11) Dilworth, (2) Oklahoma City, (4) S.W. Mayfield, (5) S.E. Hoover, (6) Springer, (7) Healdton, and (8) Cottonwood Creek.

5) Parts of the Arbuckle are notably rich in organic remains, especially algae.

6) Formation waters of the Arbuckle Group differ in composition from those of overlying formations.

7) Oil and gas originating with a hydrogen sulfide byproduct is common in some very good fields.

8) Evaporites, such as anhydrite, serve as caps or seals for underlying dolomites that produce oil and gas.

9) Finally, much more Arbuckle oil and gas has been produced from zones far below the top of the Arbuckle than has ever been produced from the upper part of Arbuckle.

The accompanying information and discussion of the history of the environment of deposition of Arbuckle and Ellenburger Group rocks show clearly the factors necessary for commercial oil and gas production. These necessary ingredients are dolomite reservoirs, porosity, heterogeneity for migration, and timely trapping mechanisms. These have in the past been the most important ingredients for finding commercial quantities of Arbuckle and Ellenburger oil and gas.

ARBUCKLE PRODUCTION IN OKLAHOMA

To date, Oklahoma has 300 Arbuckle oil and gas fields or areas that produce from the Arbuckle Group, since the first Arbuckle discovery in 1912.

The most important of these fields, in terms of heterogeneous, multizone porosity and cumulative Arbuckle production, are (Fig. 1): (1) Cushing (0–300 ft*); (2) Oklahoma City (200–700 ft*); (3) S.E. Apache (West Spring Creek gas, 42 ft* and 292 ft*); (4) Mayfield (West Spring Creek, 1,200 ft*); (5) S.E. Hoover (West Spring Creek–Kindblade, 1,300–1,400 ft*; Butterly, 4,687 ft*); (6) Springer (West Spring Creek gas, 812 ft*; Cool Creek, 3,782 ft*); (7) Healdton (West Spring Creek, 200–350 ft*; Brown zone, 1,000 ft*; Cool Creek, 3,600 ft*); (8) Cottonwood Creek (West Spring Creek–Brown zone, average, 1,000 ft*; Cool Creek, >2,000 ft*; McKenzie Hill, >3,000 ft*); and (9) Wilburton (West Spring Creek gas, 466 ft*; Cool Creek gas, 1,435 ft*).

ELLENBURGER PRODUCTION IN TEXAS

The Texas Panhandle has had 10 fields producing from the Ellenburger, which includes the Mills Ranch field (Fig. 1, no. 12) with the deepest gas production in the world (23,418–26,518 ft). This gas production was 3,100 ft below the top of the Ellenburger. Other Ellenburger producers shown in Figure 1 are (13) Gageby Creek, (14) Locke, and (15) Laketon fields.

North Texas has 14 Ellenburger fields (Fig. 1) with (16) Conley, (17) KMA, (18) S.E. Dillard, and (19) Walnut Bend probably the most important.

*Asterisk indicates depth of Arbuckle production below top of Arbuckle Group.

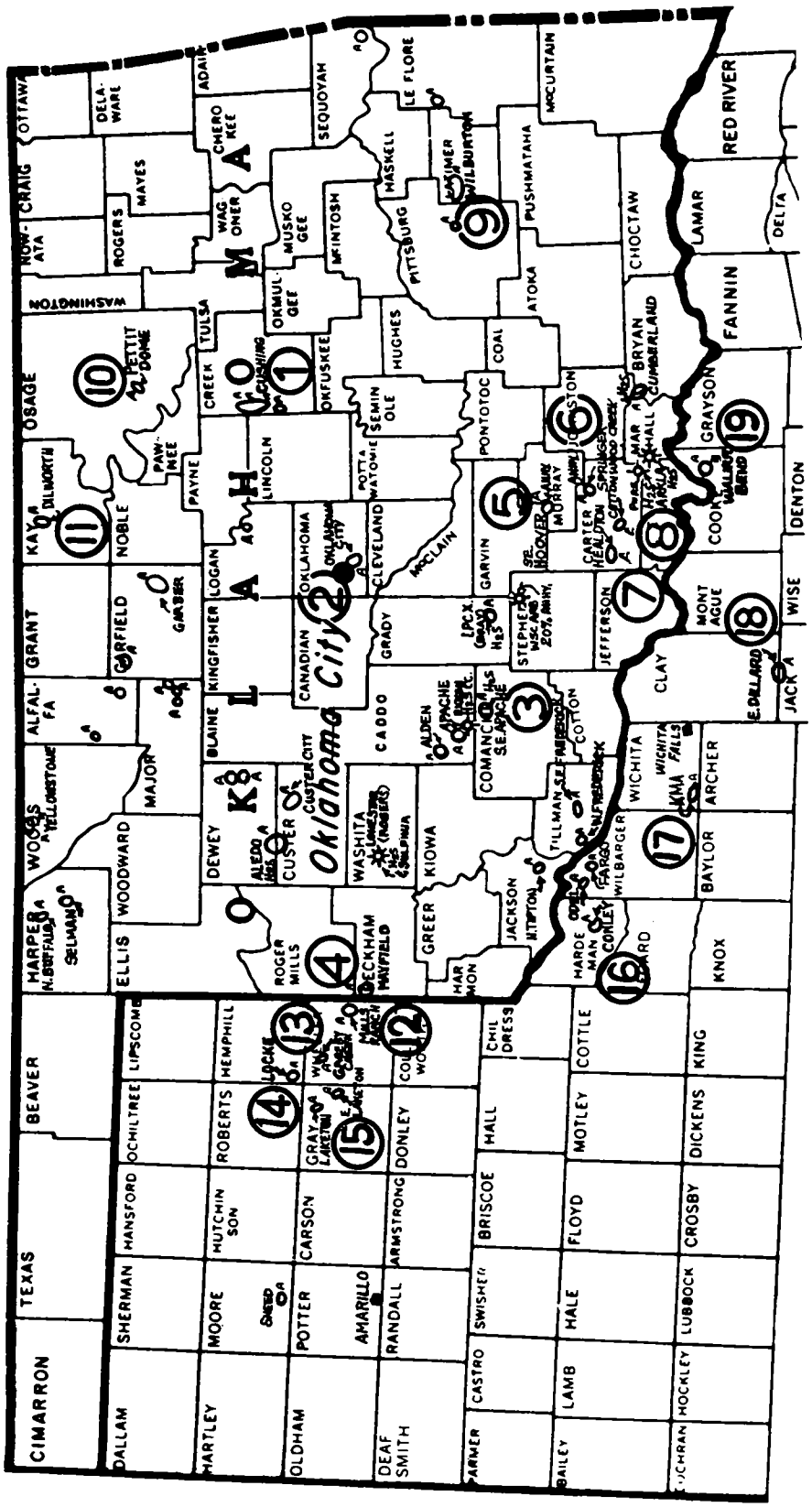

Figure 1. Arbuckle production in heterogeneous multizone fields and fields that produce from beneath salt-water zones. Fields are numbered and referred to in text.

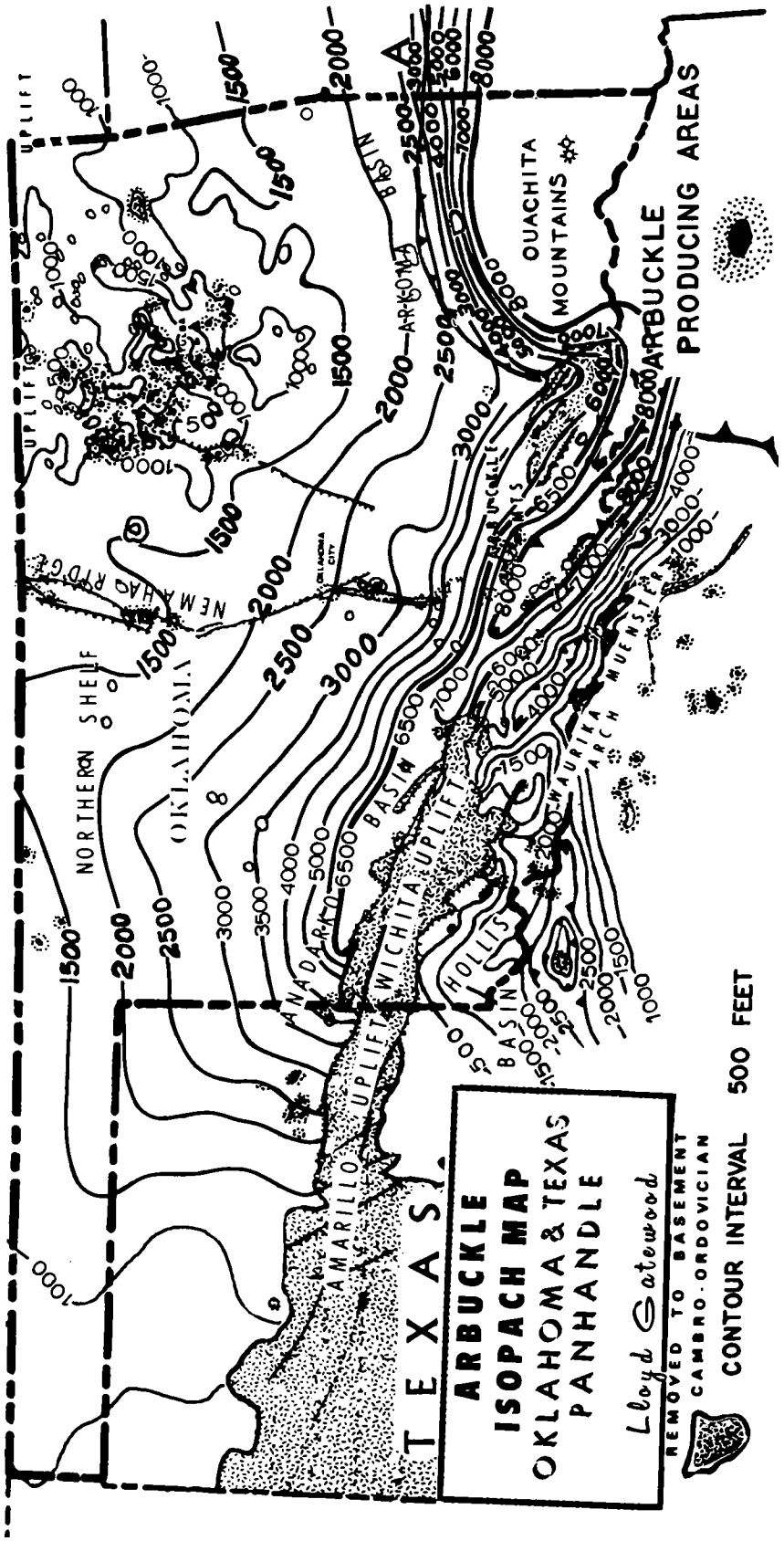

Figure 2. Thickness of Arbuckle Group in Oklahoma and Texas Panhandle. Maximum thickness is >8,000 ft in depocenter.

COMMON CHARACTERISTICS OF FIELDS PRODUCING FROM THE ARBUCKLE AND ELLENBURGER GROUPS

These Arbuckle/Ellenburger producing fields all have at least four common physical and lithologic characteristics:

1) The Arbuckle/Ellenburger producing zone is dolomite;

2) The producing zone almost invariably has some sort of induced (secondary) porosity;

3) The Arbuckle/Ellenburger production is related to a structure of early growth or origin; and

4) The fields have both lateral and vertical heterogeneity which signifies that the Arbuckle/Ellenburger rocks have lithologic, physical, and porosity characteristics which vary within the formations, depending in part on the environment of deposition.

ROLE OF BASEMENT ROCKS IN LATE CAMBRIAN AND EARLY ORDOVICIAN SEDIMENTATION

The basement rocks have had a profound influence on the stratigraphic and structural evolution of southern Oklahoma. During Precambrian time, an extensive continental mass was injected by granites, forming a relatively rigid cratonic block. The eastern part of this block, the eastern Arbuckle province, has been a stable element from the time of its formation to the present. It received a relatively thin cover of Paleozoic sedimentary rocks, which have been deformed by gentle folding and block faulting; the Tishomingo–Belton–Hunton uplift constitutes the eastern Arbuckle province. A somewhat similar block is represented in the subsurface by the Muenster–Waurika arch along the Red River in southern Oklahoma and northern Texas, where thinner intervals of Cambrian–Ordovician Arbuckle carbonates were deposited.

A great, foundered intracratonic sag developed in the Precambrian granitic basement in southern Oklahoma, forming the southern Oklahoma geosyncline, which was destined to receive as much as 45,000 ft of Paleozoic rocks. Before the early stage of the Oklahoma geosyncline ended with widespread extrusion of the Middle Cambrian Carlton Rhyolite, major faults along opposite margins of the basin were rejuvenated. The basin itself dropped at least a mile as a graben.

This transverse zone of weakness was the site of Early and Middle Cambrian volcanics, lava flows, and metasediments. The weakened trough foundered and was depressed under this burden, receiving 8,000 ft of Reagan Sandstone, Honey Creek Limestone, and the Arbuckle Group carbonate rocks (Fig. 2).

With downwarping, the basement surface was irregular and the water was deeper toward the southeastern end. The underlying igneous rocks provided locally prominent platforms, shelves, and shorelines in the Cambrian and Ordovician seas. Thus, there were different depositional environments, generally with shallow-water dolomites deposited along the margins, and limestones near the center of the basin (Figs. 3,4). Local changes in sedimentation occurred, including progradation, with regression and transgression of the sea. The result was to produce many vertical and lateral heterogeneities in lithology and porosity; thus, a number of stratigraphic traps were formed (Fig. 3).

The Cambrian–Ordovician depocenter was approximately the area embraced by the present-day 3,500-ft isopach line (Figs. 2,4). In the depocenter, these carbonate sediments are of shallow-marine origin; they consist mainly of interbedded, thin carbonate mudstones, intraclast calcarenites, oolitic calcarenites, stromatolites, and laminated dolomites or dolomitic limestones. The strata are, in part, richly fossiliferous and contain trilobites, brachiopods, mollusks, pelmatozoans, sponges, algae, and, well toward the top, graptolites.

DEEP-WATER MARINE CIRCULATION IN THE BASIN

Circulation of water within the basin was characterized by upwelling along the sides of the basin of cold water from the deepest part of the basin. The upwelling was at its maximum while an incipient Wichita–Criner geanticline was rising across the center of the basin (Fig. 4), and while the rest of the basin was being depressed.

As the incipient geanticlinal structure rose, it moved northward within the trough, so that incipient anticlinal folds were formed within the trough. With some of these folds, the push did little more than create minor changes of slope. Larger folds eventually became thrusted anticlines, directed toward the northeast. If a structure remained minor, it tended to become the site for deposition and/or formation of reefs, shoals, and carbonate banks. These features also formed along the "hinge line" around the perimeter of the depocenter, and thus contributed to the development of a vertical interface between limestone and dolomite along the "hinge line" (Figs. 3–5).

SEALS FOR TRAPS

Without a reasonably effective seal or other migration barrier, it is impossible for commercial quantities of crude oil or gas to accumulate. Probably the most effective seals are beds of evaporites, typically anhydrite or halite (salt), or the more common beds of shale with high clay contents. If a reservoir rock changes facies updip into one of

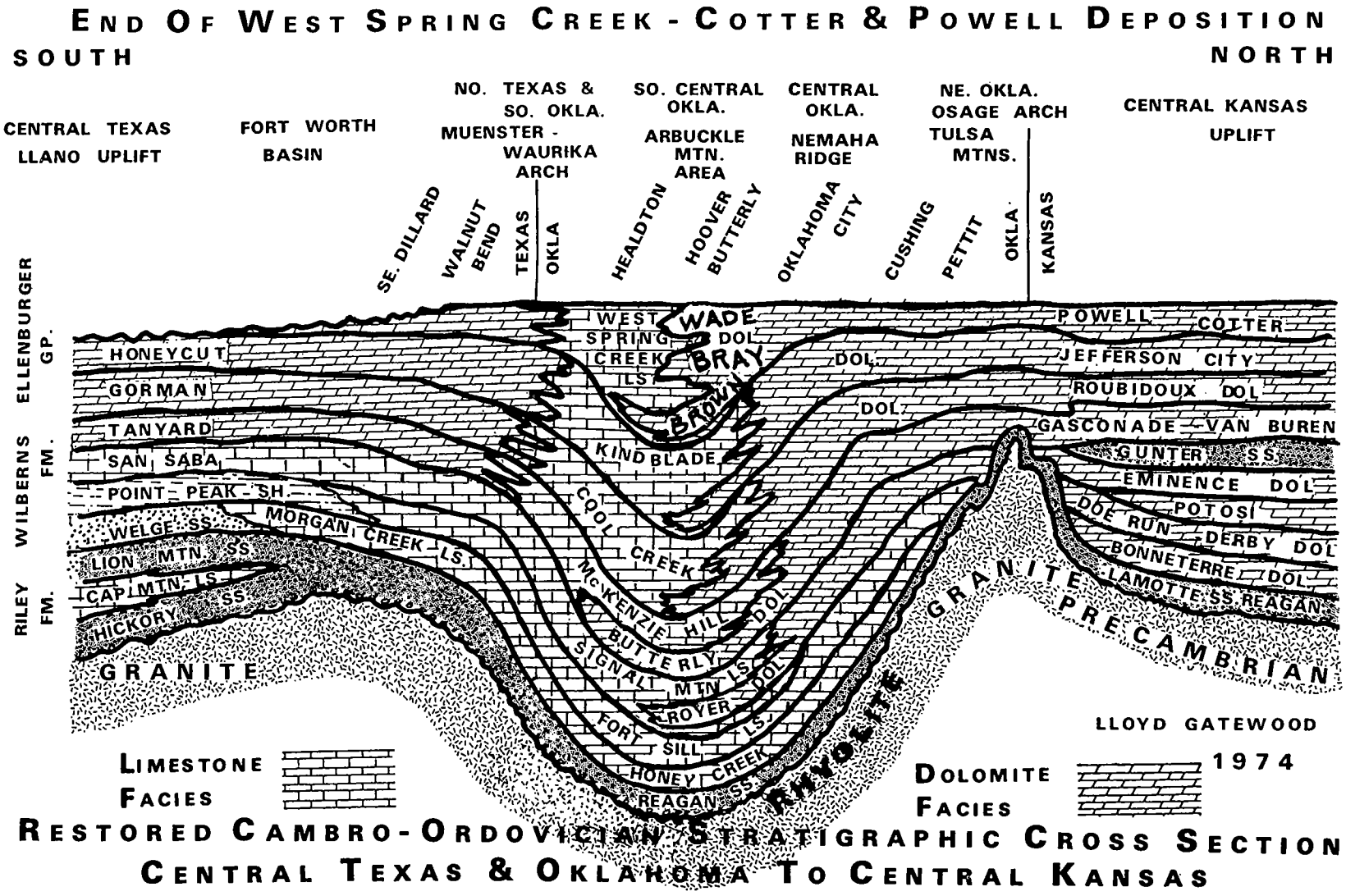

Figure 3. North–south cross section showing dominant lithology and facies changes of Late Cambrian–Early Ordovician strata from central Texas to central Kansas.

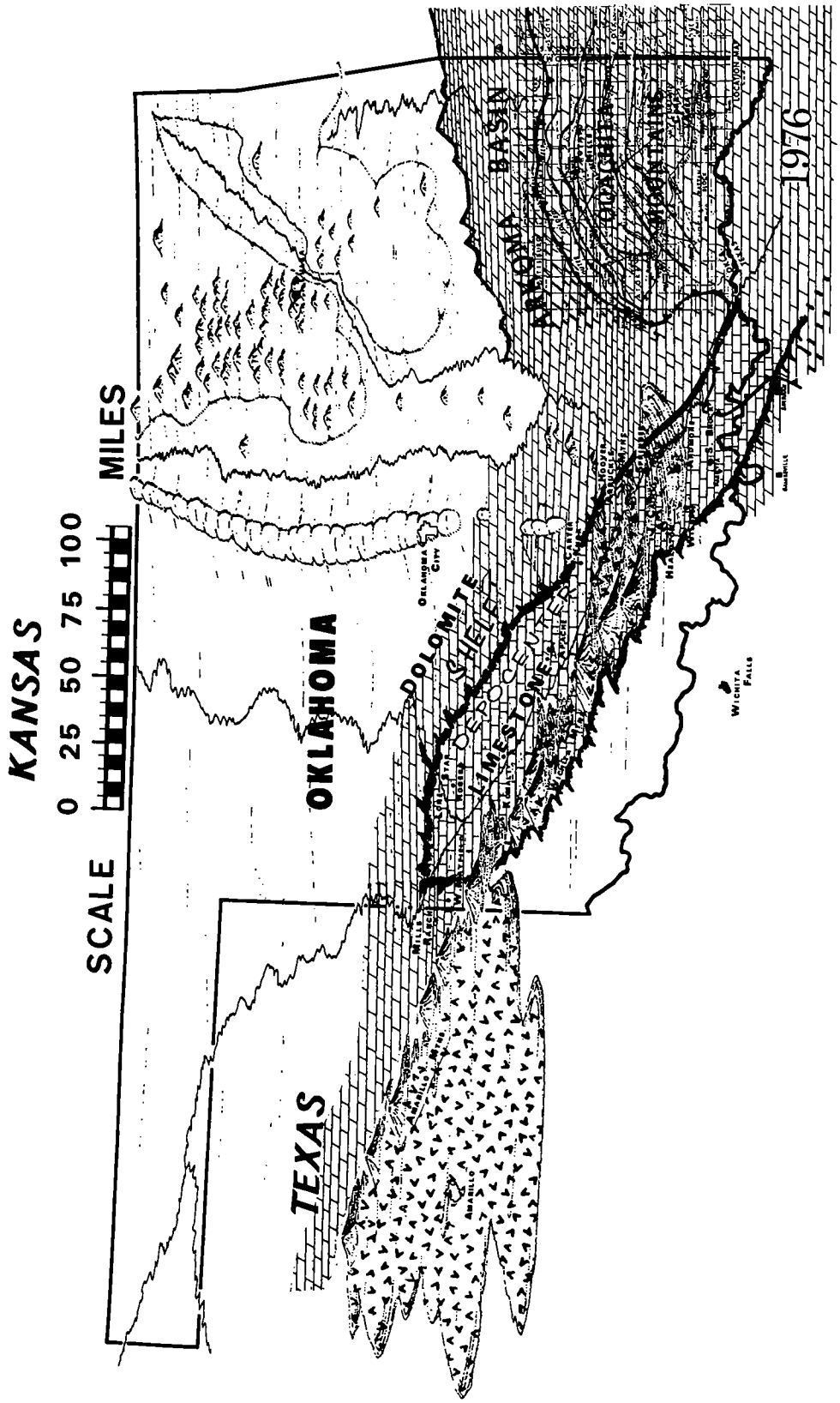

Figure 4. Paleogeography of the Arbuckle Group showing carbonate depocenter in the southern Oklahoma geosyncline and distribution of limestone and dolomite facies in the depocenter and on the platforms.

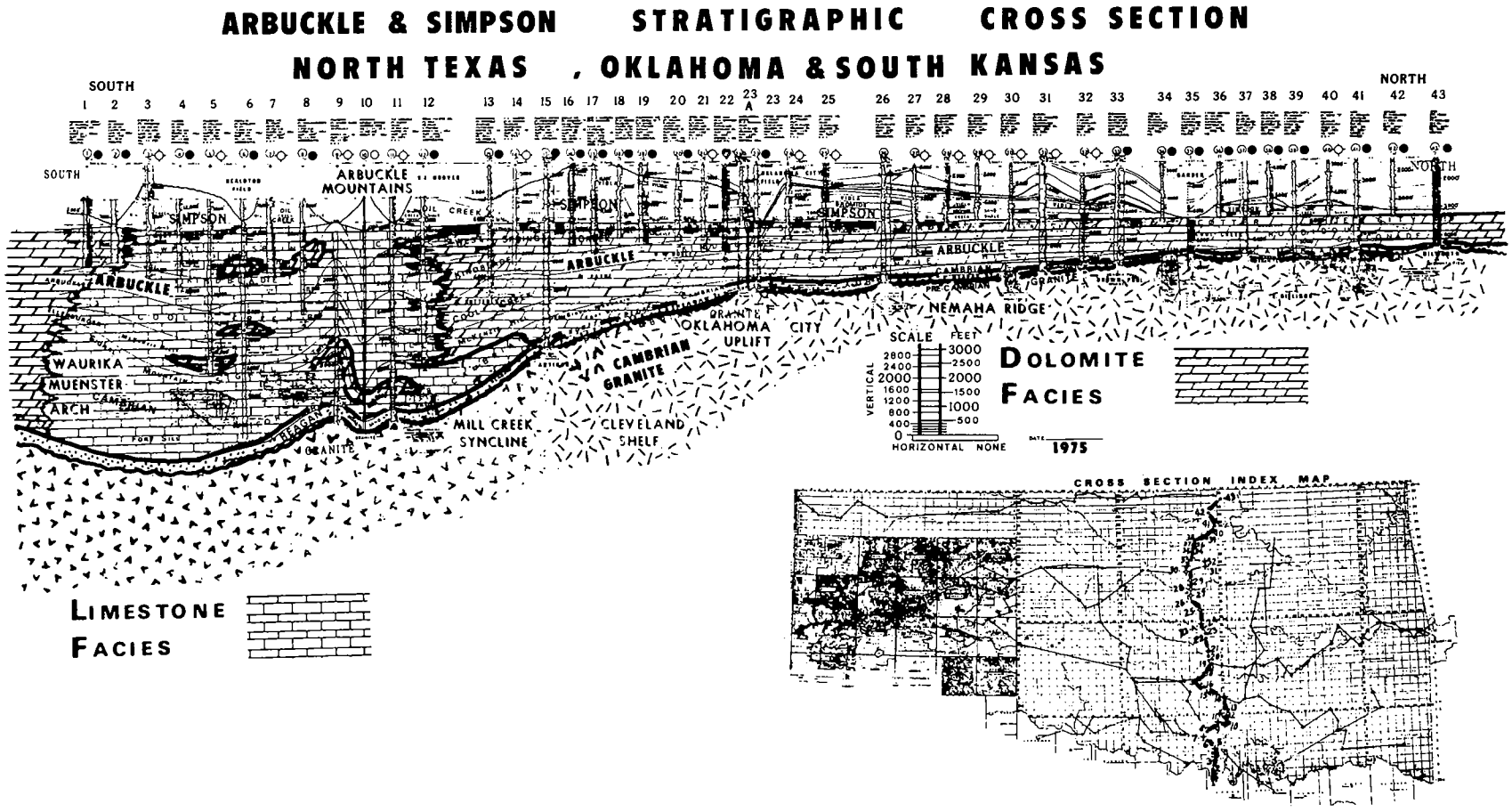

Figure 5. North–south stratigraphic cross section (215 mi long) showing major carbonate facies in the Arbuckle Group.

these rock types, and also is overlain by one of them, the seal conditions should be ideal for a stratigraphic or structural trap.

The chart of evaporite maxima shows that evaporites were at a maximum during Cambrian–Ordovician time (Fig. 6). For this reason, evaporite seals could very well have been formed during the many regression cycles of Arbuckle seas. Since, there are few shales in the Arbuckle Group, shale seals are highly unlikely.

SOURCE OF HYDROGEN SULFIDE

Petroleum generation, with hydrogen sulfide (H_2S)as a byproduct, can occur where organic matter and plankton are deposited in a partly silled or barred basin with restricted circulation. Hypersaline water entering a-sea that contains a rich fauna can cause sudden death. The animal and plant remains then sink to the bottom of the sea, are covered with sediment, and form petroleum later through their decomposition. Hydrogen sulfide is generated from these plant and animal remains by the putrefaction process.

BASIN CONDITIONS POOR IN OXYGEN AND RICH IN HYDROGEN SULFIDE

What makes the bottom waters of the basin poor in oxygen and rich in H_2S? It was generally assumed to be a consequence of stagnation. Euxinic waters or sediments form in restricted-circulation, barred-basin environments, such as those in the Black Sea, Caspian Sea, and Sea of Aral. Hydrologists and biologists state that the primary cause of euxinic conditions is hypertrophy, or excessive production of plankton. In highly hypertrophic waters, this production is so great that the benthonic life is almost totally suppressed.

Mrs. M. B. Sanders, a Dutch biochemist, showed that hypertrophy is produced only in waters in which intense upwelling brings nutrients from the depths to the surface in a planetary circulation system. The waters do not need to be deep, nor even fully marine. Hypertrophy is also characteristic of inland seas with no communication with the ocean, such as the Caspian Sea. It is best developed in shallow, semi-separated parts of the sea. The conditions required to produce hypertrophy are: (1) evaporation must be high; (2) the supply of fresh river water must be high and continuous; (3) the drainage area of the rivers must be fertile, to supply organic nutrients; and (4) the supply of fine sediments should also be high, to provide mineral nutrients (such as lime muds of the Arbuckle).

The characteristic organic features of hypertrophic waters are these:

1) Very thick water bloom, particularly of dinoflagellates. This causes the phenomenon known as "red water," and gives the Red Sea its name. It is an annual (commonly springtime) occurrence in many bodies of water (as for example, off the coast of southwest Africa). L. G. Weeks has discussed this in papers and lectures on the sources of oil.

2) Great mortality among fish and benthonic vertebrates, particularly during periods of water bloom. It is these two groups of organisms that are richest in both phosphorus and nitrogen, and the supply of these two elements is the chief limiting factor in plankton growth.

3) Formation of sapropel, an organic sediment preserving chlorophyll. Sapropelic organic matter cannot be preserved, except under completely anaerobic conditions, and without the formation of sapropelic organic matter, no oil can be generated, in the opinion of North (1985). Chlorophyll in this sediment contains porphyrins which form oil when they are broken down.

THE BLACK SEA AND HYDROGEN SULFIDE CONCENTRATIONS

The deeper waters of the Black Sea, beginning at a depth of 600 ft, contain hydrogen sulfide. At a depth of 1,200 ft, the water holds so much H_2S that life cannot exist in these waters down to a depth of 6,000 ft. Many scientists have attributed high amounts of hydrogen sulfide in the depths of the Black Sea to accumulation of the same types of animal and plant substances that are the primary source of petroleum.

Surface currents, where the surface waters to depths of 450–550 ft contain oxygen, flow from regions of low salinity to regions of higher salinity in response to hydrostatic head. This is accompanied, at depth, by currents that flow in the opposite direction, from regions of high salinity to low salinity, because of density distribution.

HYDROGEN-SULFIDE-RICH SOUTHERN OKLAHOMA CARBONATE GEOSYNCLINE

The hydrogen-sulfide-rich portion of the southern Oklahoma geosyncline extends from the Texas Panhandle southeastward through the Arbuckle, Marietta, and Sherman basins, merging with the deeper Ouachita-facies rocks in Bryan and Marshall Counties (Figs. 7,8). Most all the known occurrences of hydrogen sulfide gas, black smelly oil, and even molten sulphur are within the area enclosed by the 3,500-ft isopach contour of the Arbuckle Group (Fig. 2). Some examples are shown on Figure 8 and listed in the Appendix.

SOURCE BEDS OF PETROLEUM

Curiosity as to the source of petroleum has prompted geologists and others to examine not only the composition of the oils, but also of the rocks from which the oils come.

Fifty years ago, Parker Trask and Whitman Patnode (1942) completed a 10-year investigation and study of source beds for petroleum. Approximately 32,000 well samples were examined from seven petroliferous provinces and 15 states with oil and gas production. They made a basic assumption that, in general, oil is more likely to accumulate nearer than farther from its place of origin, and oil was assumed to move both parallel and transverse to the bedding. In stratigraphic migration, once oil starts to migrate, it will continue until something stops its migration or movement. It was finally assumed, arbitrarily, in the investigation of Trask and Patnode (1942) that beds 200 ft above or below known oil horizons are relatively near, and those >500 ft above or below oil horizons are remote.

PROPERTIES FOR SOURCE-ROCK INVESTIGATIONS

Twelve properties are commonly reported in source-rock investigations: texture, organic content, carbon content, reduction number, nitrogen

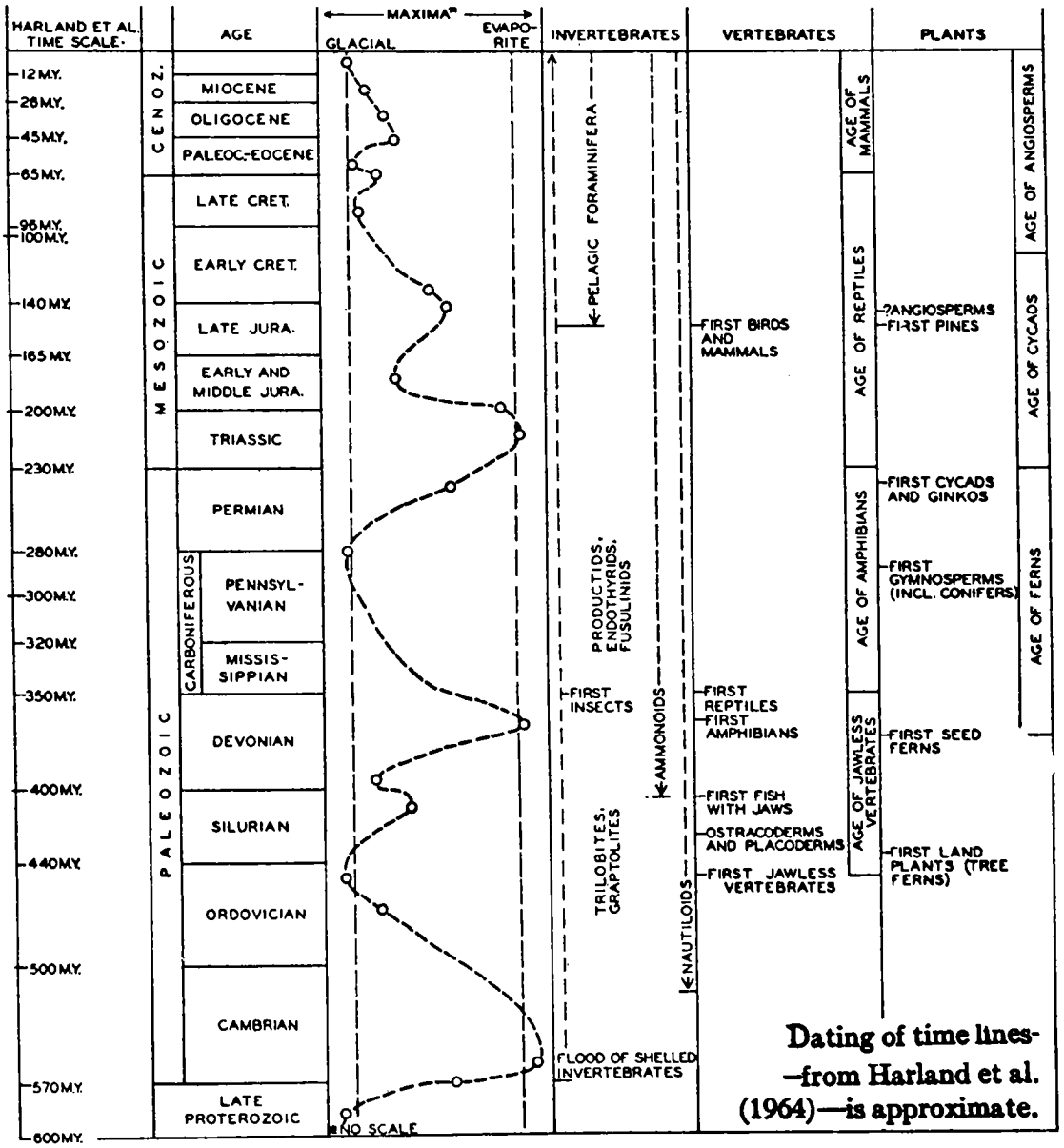

Figure 6. Chart showing evaporite maxima through time. Note that proliferation, or "explosions," of numerous life forms apparently are related to evaporite maxima, and not to episodes of mountain building.

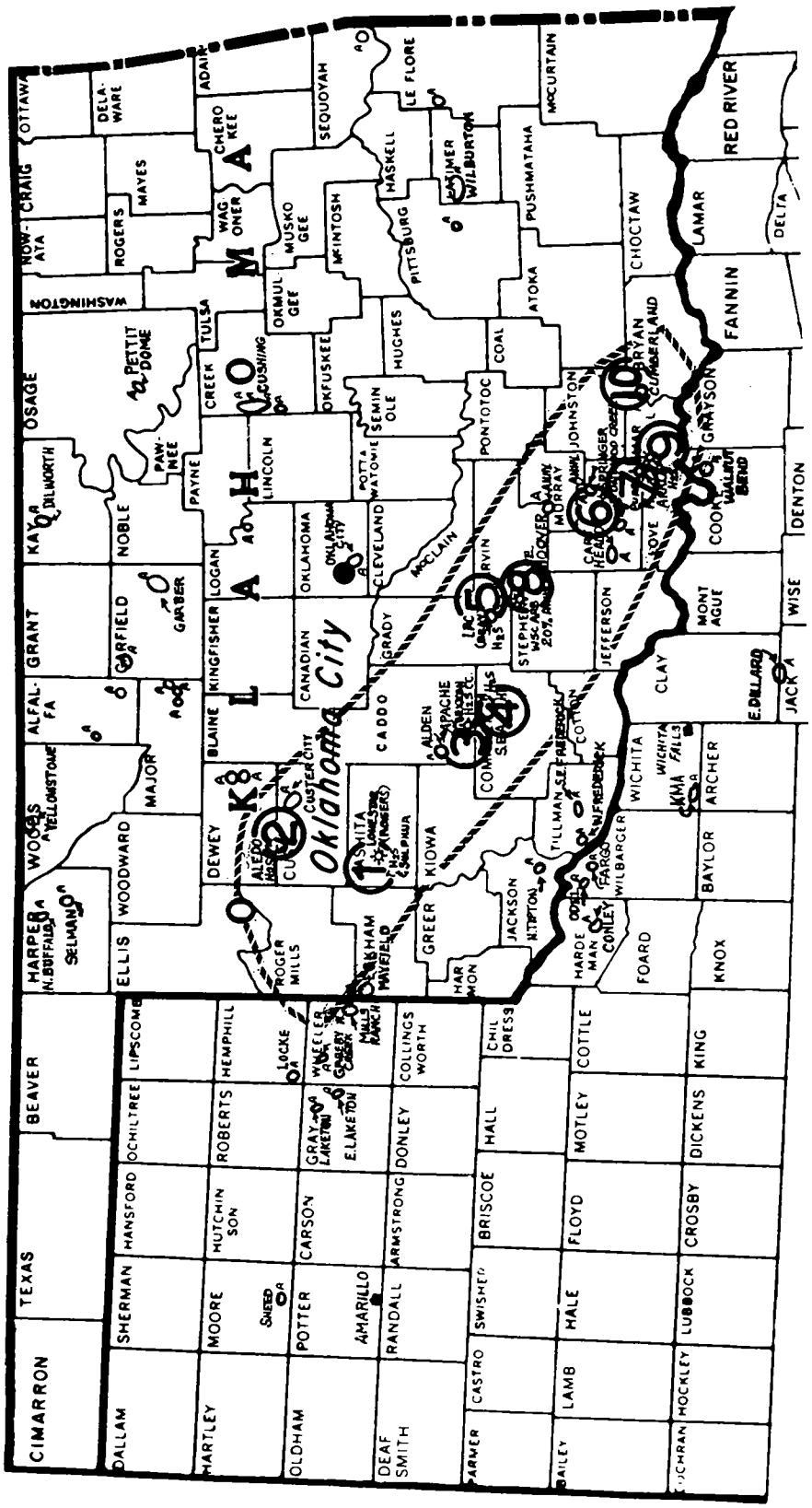

Figure 7. Location of 10 gas wells in the Arbuckle Group (in the depocenter) that contained hydrogen sulfide. Numbers refer to wells listed in the Appendix.

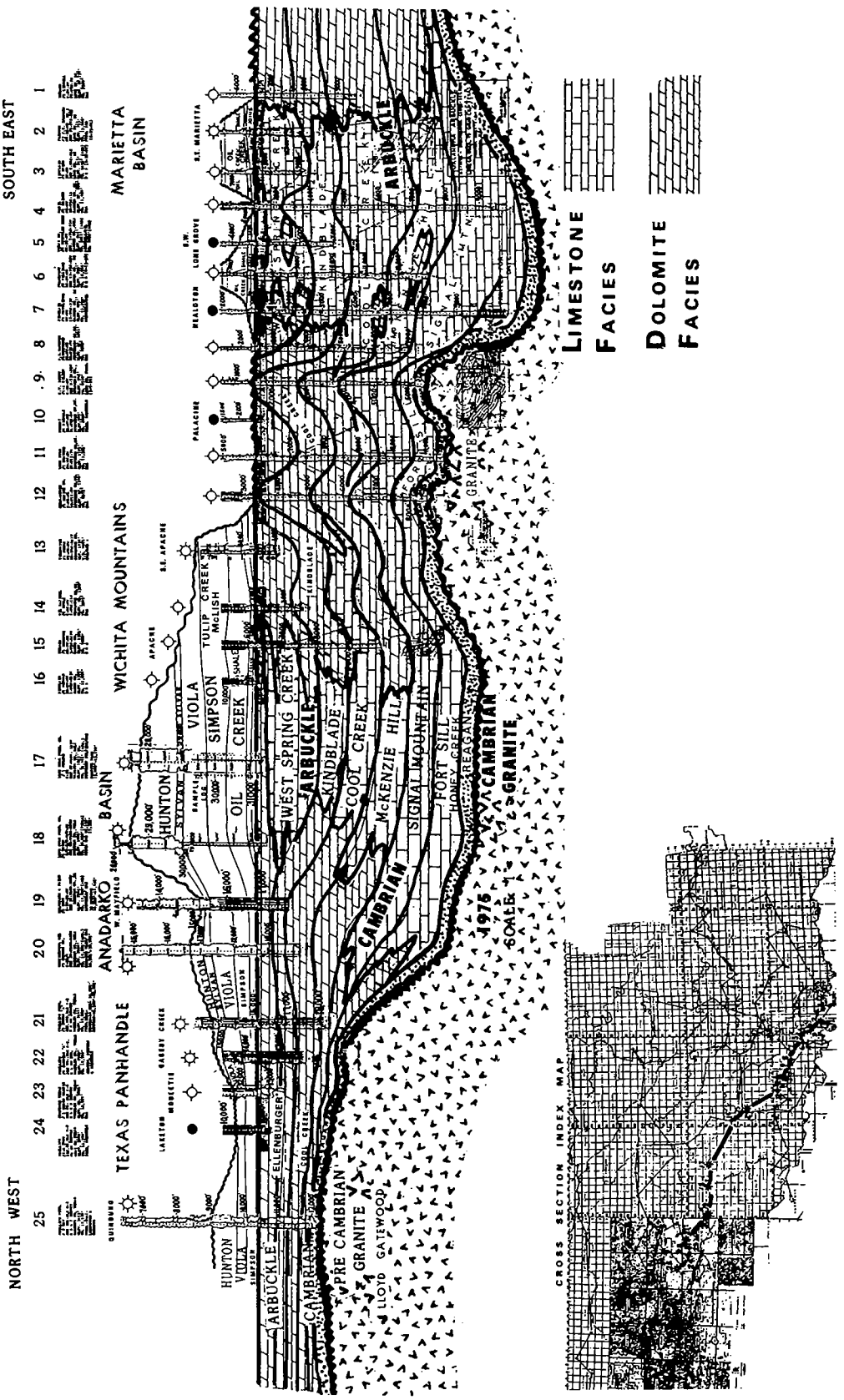

Figure 8. Northwest–southeast stratigraphic cross section (246 mi long) showing major carbonate facies of the Arbuckle Group along the depocenter (rich in hydrogen sulfide).

content, color, assay number, relative volatility, nitrogen-reduction ratio, oxidation factor, carbon-nitrogen ratio, and calcium carbonate content. The following is a brief discussion of some of these properties.

Petroleum is not derived entirely from the carbon of the organic matter; part of it consists of other elements. Consequently, in attempting to study the relations of organic constituents with respect to their ability to generate oil, it is more satisfactory to think in terms of the total quantity of organic matter than in terms of the major component (carbon) of the organic matter. However, in evaluating source beds, it is preferable to discuss their organic content in terms of their carbon content, because carbon is the element that is actually measured.

When the carbon content forms the basis for estimates of the organic content of source beds, the factor of 1.6 has been used. Two other properties, the reduction number and nitrogen content, are also used as guides to the organic content. When the reduction number is used, the organic content is assumed to be 1.4 times the reduction number; and when the nitrogen content is employed, the organic content is taken as 24 times the nitrogen content.

Because of the consistent relationship between the low nitrogen-reduction ratios and the occurrence of oil, one might assume that the oil comes mainly from the beds having low ratios; and the inference follows that most individual beds having low nitrogen-reduction ratios may be source beds.

The nitrogen-reduction ratio also seems to be related to metamorphism of the beds. In southeastern Oklahoma and in the Appalachian area, this ratio increases in the direction of the greater degree of metamorphism of the sediments, as indicated by the high carbon ratio of the coals. The high carbon ratio of the Appalachian region and in some of the Ouachita Mountain sediments may account for the generally large size of the nitrogen-reduction ratios.

The average quantity of carbon in ancient sediments is about 0.8–1.1%. Inasmuch as the organic content is estimated to be 1.6 times the amount of carbon present, the average organic content of ancient sediments is between 1.3 and 1.7%, for an average of 1.5%.

The color of sediments is also a rough index of the organic content. Light-colored sediments contain little organic matter, whereas dark sediments contain relatively more. Also, light-colored sediments have high reflectivity and dark sediments have low reflectivity.

Two properties of sediments that have been regarded as criteria for recognizing source beds, namely, the organic content and color, were not found to be related to the occurrence of oil, and the conclusion is reached that they are not valid criteria for recognizing source beds.

SOURCE ROCKS AND POROSITY RELATED TO OIL AND GAS GENERATION

It is very clear, I think, that when looking at source rocks and optimum types of porosity (i.e., intergranular, fracture, vugs, and karst), the carbonate source-rock environment, on average, with its potentially thick pay zones, will generate more oil per unit of organic carbon than will the shales. There may be some negative side effects if the oil or gas produced is associated with H_2S or CO_2.

CONCLUSION: THE ARBUCKLE GROUP IS A SOURCE ROCK

The thick Arbuckle marine-carbonate sequence is a rich oil and gas source rock, and its inherent heterogeneity also makes it a good reservoir rock. The presence of much organic and carbonaceous materials interbedded with the limestones and dolomites make the Arbuckle a favorable rock unit for generation of oil and gas.

I think, in the case of the Arbuckle Group, there are well-documented cases of oil and gas being sourced by carbonate rocks, and it is all dependent upon the depositional environment. You have to look at the rocks which do produce Arbuckle oil and gas, and compare the related lithology, composition, minerals, and organic constituents of the carbonates. However, no matter how high the source potential may appear to be, if there is no porosity and no timely development of a trapping mechanism (whether structural or stratigraphic), there will be no commercial accumulation of Arbuckle oil or gas.

REFERENCES

Harland, W. B.; Smith, A. G.; and Wilcock, B. (eds.), 1964, The Phanerozoic time scale—a symposium: Journal of the Geological Society of London Quarterly, v. 120, suppl., 458 p.

North, F. K., 1985, Petroleum geology: Allen and Unwin, Boston, 607 p.

Trask, P. D.; and Patnode, H. W., 1942, Source beds of petroleum: American Association of Petroleum Geologists, Tulsa, 566 p.

APPENDIX

List of Representative Wells with Arbuckle H_2S Gas

1) Lone Star No. 1 Rogers, wildcat, Washita County, Oklahoma. CSE¼ sec. 27, T. 10 N., R. 19 W. TD 31,441 ft (West Spring Creek, Arbuckle). High H_2S and liquid sulphur at TD. Gas well (plugged back) in the S.W. Burns Flat field. Drilled in 1974.

2) Gadsco No. 1-32 Michael, Aledo field, Dewey County, Oklahoma. N½N½SW¼ sec. 32, T. 16 N., R. 18 W. TD 17,700 ft (West Spring Creek, Arbuckle). High H_2S gas to TD. Arbuckle plugged off. Drilled in 1985.

3) Exxon No. 1 Apache gas Unit, wildcat, Caddo County, Oklahoma. NE¼NE¼SW¼ sec. 19, T. 5 N., R. 11 W. TD 24,715 ft (Cool Creek, Arbuckle). High H_2S gas at TD. Abandoned well. Drilled in 1979.

4) Tidewater No. 1 Meyers, SE Apache gas field, Caddo County, Oklahoma. NE¼NE¼ SW¼ sec. 10, T. 4 N., R. 11 W. TD 4,071 ft (West Spring Creek, Arbuckle). H_2S with gas production. Drilled in 1951.

5) LPCX No. 1 Bray, Knox field, Grady County, Oklahoma. CSW¼NE¼ sec. 35, T. 4 N., R. 6 W. TD 19,915 ft (Kindblade, Arbuckle). High H_2S at TD. Drilled in 1981.

6) Sarkeys No. 1 Pruitt, Caddo field, Carter County, Oklahoma. E½NE¼NW¼ sec. 26, T. 3 S., R. 1 E. TD 11,475 ft (Cool Creek, Arbuckle). High H_2S gas at TD. Corroded pipe, abandoned well. Drilled in 1971.

7) Pure No. 1 Resources Board, wildcat, Carter County, Oklahoma. SW¼NE¼SW¼ sec. 30, T. 5 S., R. 3 E. TD 21,539 ft (Joins, Simpson). High BHP (19,715 PSI) and high H_2S gas at TD. Abandoned well. Drilled in 1964.

8) British American No. 1 Krieger, Carter-Knox field, Stephens County, Oklahoma. NE¼ NW¼SW¼SW¼ sec. 3, T. 2 N., R. 5 W. TD 17,484 ft. Top Arbuckle (West Spring Creek) at 16,827 ft. Cored 650 ft of Arbuckle; described as 50% limestone, 30% dolomite, and 20% anhydrite. Some H_2S gas reported on test. Well completed in Bromide sand as gas well. Drilled in 1957.

9) Arkla No. 1-11 Cobb-Tipperary, wildcat, Marshall County, Oklahoma. CSE¼SE¼ sec. 11, T. 6 S., R. 3 E. TD 24,050 ft (Kindblade, Arbuckle). H_2S gas in West Spring Creek and Kindblade. Gas well (plugged back). Drilled in 1979.

10) Union Oil No. 106 Little, Cumberland field, Bryan County, Oklahoma. E½SW¼SW¼

Discussion Between Audience and Panel on the Subject: Can Carbonates Be Source Rocks for Commercial Petroleum Deposits?

Kenneth S. Johnson, *Moderator*
Oklahoma Geological Survey

Wallace G. Dow (DGSI, The Woodlands, TX):

There is one thing that hasn't been mentioned here about carbonates and other sources as well. The Arbuckle Group, wherever we see it, is pretty high in rank. It has gone through the oil-generation phase. In so doing, it has lost a lot of the organic matter that was originally there, converted it to oil and gas, which then migrated out. So if we look at a relatively high-rank Arbuckle rock today, which has perhaps 0.5% TOC, at the time of oil generation it could have had twice as much TOC. Good oil source rocks containing kerogens with high initial hydrogen contents, such as those described by Williams, will lose about half of their original organic carbon. Average shale source rocks with a lot of terrestrial organic matter, on the other hand, may lose only 25% of their initial TOC content. So if we see an Arbuckle rock with a vitrinite reflectance of ~3.0, it could have had twice that TOC content initially. That could change your whole way of looking at things. Also, as Jack mentioned, if we look at well cuttings, we may mix many lithologies and see only the average organic-carbon content. We have seen many places, such as in the Smackover, where the organic matter is concentrated in thin, sometimes argillaceous zones in the carbonates. Although the average TOC content is very low, the TOC content of that portion which expelled oil could be very high.

Jim Palacas (USGS, Denver):

I believe Wally Dow posed the following two questions: (1) What affect does thermal maturity have in assessing TOC contents in carbonate rocks of the Arbuckle Group? and (2) Could thin, organic-rich, oil-generating units be overlooked in drill cuttings due to dilution of preponderant organic-lean rocks?

In answer to the first, I agree with Wally's thesis that because the Arbuckle, for the most part, has undergone high thermal stress, it now displays only minimum TOC values. Consequently, the higher TOC contents in the geologic past, coupled with the oil-prone (type II-I) nature of the organic matter, have more than likely enabled at least portions of the Arbuckle to generate commercial amounts of petroleum. A somewhat analogous example is the Smackover Formation in Alabama and Mississippi. The Smackover carbonates, which are also very mature to overmature in the deeper portions of the basin, also show generally low TOC contents—an average of ~0.5%. Yet, these carbonate rocks are known to be the source of giant-size accumulations of oil and gas.

In answer to the second question, I also agree with Wally Dow that TOC contents of certain portions of the Arbuckle could be underestimated in drill cuttings by virtue of thick organic-lean rocks masking thin organic-rich units. These carbonate units commonly occur as oil-prone, algal-dominated laminae and bands and kerogen-rich stylolites, and although quite thin, nevertheless, when composited they could indeed have generated and expelled significant volumes of oil and gas. In addition, cuttings caved from shallower horizons could also contribute to the masking of the thin organic-rich units.

Let me also suggest another factor that might affect the general perception that the Arbuckle is pervasively low in TOC content and hence poor in source-rock potential. It may simply be a matter of not locating and analyzing the "right" organic-rich sections of rock. In support of this possibility, the monumental studies of Trask and Patnode (1942) indicated some promising TOC data (Fig. 1). In compiling Arbuckle data on ~178 non-oil-stained subsurface samples from 18 wells in the Anadarko basin, ~46% of the samples showed TOC contents ranging from 0.4 to 1.4%. According to many previous source-rock studies, carbonate rocks with such values can be considered as adequate source beds of petroleum.

The graph (Fig. 1) was put together yesterday [February 6, 1990] on the spur of the moment, during a break in th Source Rock Workshop. Neil Peterson (Worldwide Geosciences, Inc.) alerted me to the data and helped in the construction of the graph. It seems that in light of these promising data, the geologic community needs to reevaluate the source potential of Arbuckle Group rocks.

Louis W. Elrod (Texaco, Houston):

Jack Williams talked quite a bit about early generation of oil in carbonates. Most of the work

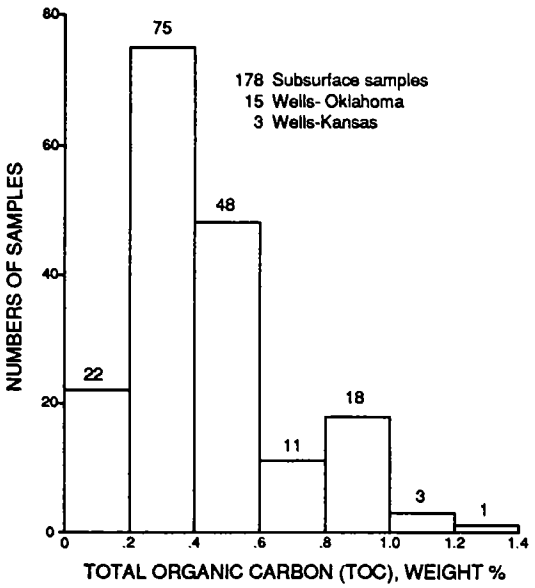

Figure 1. Bar graph showing total organic carbon in the Arbuckle Group of the Anadarko basin (data from Trask and Patnode, 1942).

that I have looked at has been in California, in the Santa Maria, Ventura, and San Joaquin basins, and some other areas. In every area, where I have either studied or looked at studies, there seems to be ample source rock that is buried deeply enough (in zone 3 or higher) to have generated oil at a normal maturity. I wonder, if I were to look for the definitive demonstration of early oil generation, where would I go?

Jack Williams (Amoco [retired], Tulsa):

Actually, the Monterey has been a classic example of early generation of oil, or it has been since it was recognized several years ago that most of the Santa Maria basin oils resulted from early generation. There are a lot of other early-generation oils around the world. Offhand, I can think of the oil in Sicily, which is very clearly early generation. We have had a lot of examples of it. But you are saying that you haven't found oil in the Santa Maria basin that seemed to be generated early. Is that correct?

Louis Elrod:

We looked at studies in the Ventura, Santa Maria, and San Joaquin basins, and we found Monterey that was certainly in zone 3 or higher. The Monterey had migration pathways that led to all of the accumulated oil that we were aware of, and we didn't see any real reason to invoke early generation of oil in any of those areas.

Jack Williams:

What was the sulfur content in those cases?

Louis Elrod:

I think the sulfur content was what you would normally associate with these oils, but I don't recall specifically.

Jack Williams:

Wilson Orr published, or at least he mentioned, several years ago that there is sort of a breakover point at about 5 or 6% sulfur. I don't remember the figure at which you effectively get into very early generation; I didn't know whether the value was below 3 or 4%, in which case there probably would not be a situation of early generation.

John A. Taylor (Independent, Oklahoma City):

I would like to make a comment on something that most people aren't aware of. In the late 1950s and in the earliest 1960s, Mobil Oil Corp. conducted an interesting research program on the Ellenberger and Arbuckle Groups. They collected samples from outcrops and from cores. They concentrated on sampling the more argillaceous parts of the Ellenberger and Arbuckle, and they performed spectrographic analysis on the samples. Certain characteristics of many samples were correlated and tied to oil samples collected from the Simpson and Arbuckle. Mobil has been trying to find a copy of that report, as a result of my call to them. It is important to note that the conclusion of that work was that there was organic material in the Arbuckle that was oil-type (using the words of that era) oriented. And there was some reasonable correlation, but not with great certainty, of the Arbuckle oil to some of the organic shales they found in the Arbuckle. I thought that might be of interest. There was definitely a conclusion that the Arbuckle argillaceous limestones had material that was petroliferous in nature. That was 30 years ago, and I remember only the highlights of the report. I was the person who had requested the study while I was exploration manager for Mobil.

Gunther J. Weisbrich (Hunt Oil Co., Dallas):

A question on Cottonwood Creek. One of the earlier talks today had indicated, I believe, that the oil was typed to the Woodford Shale as a source rock. I would like an explanation on how the Woodford oil migrates down through 500–600 ft of very dense limestone to the Brown zone? As I understand it, there is no juxtaposition of Woodford against the Arbuckle. So how does the oil get down there?

Lloyd Gatewood (Independent, Oklahoma City):

Well, I have the same quandary (I am just answering for myself). I have the same quandary of trying to get that much gas, or what is converted into gas, down through a few of those faults in such a heterogeneous carbonate as is present at

Wilburton or as is present at Mills Ranch, where the Arbuckle is ~25,000 ft deep, or at Mayfield where it is about 16,000–17,000 ft deep. I don't intend to imply that depth has that much to do with this. It is the thickness that tells us where the depocenters are, the total thickness. But I have the same problem trying to get what we normal people, who are explorationists, try to sell as a prospect—a prospect that has a fault as a trap, maybe a vertical fault, and some sort of a barrier at the top, such as an unconformity, a shale, or anhydrite. We try to sell the prospect, believing that oil or gas can migrate downward through all these heterogeneous carbonates. It is a mystery to me, and I don't know either.

Maybe the gentleman from CNG can help us.

David L. Read (CNG Producing Co., Denver):

If you examine and process properly the group-shoot seismic data available in the area, namely PGI 25 and Petty line G, you will find that there is a large thrust fault beneath the Cottonwood Creek structure. We believe that we can seismically trace units as young as Mississippian into the footwall beneath the Cottonwood Creek thrust block.

Lloyd Gatewood:

What was the juxtaposition there?

David Read:

Probably at least 4,000–5,000 ft of overthrust movement has taken place on what we call the Cottonwood Creek thrust. We believe that if you drill deep enough on the Cottonwood Creek structure, you would cut that thrust and encounter units as young as Mississippian. Of course, this means the Woodford is in the subthrust position and in an excellent position to source the overlying anticline.

Kenneth S. Johnson (moderator, OGS):

Let me ask the panel, what should we do in the future to help address the carbonate source-rock problem, specifically for the Arbuckle? Do we need to work specifically on the cores and analyze them for their TOC, look at the thermal maturities, and other studies like that? Do you have any comments as to what we should do in the future?

John Pigott (University of Oklahoma):

Let me make one comment that was raised by the Texaco gentleman, and also by the last talk. I think our knowledge about the lateral geometry of the TOC in the Arbuckle, its association with facies differences, and our knowledge about migration pathways is, by far, incomplete at this time. I really think we need to focus in the future tremendously upon the heterogeneities of carbonate source-rock content, and upon migration pathways.

Jim Palacas:

I agree with John Pigott that our present knowledge of TOC distribution in the Arbuckle Group is incomplete. This is highlighted by the recent revelation that nearly 50 years ago, Trask and Patnode (1942) showed that non-oil-stained carbonate rocks of the Arbuckle Group contained TOC as high as 1.4%. In fact, higher values ranging from 2 to 5% were also shown, but other analyses indicated that the rocks were oil stained. But even the presence of oil staining is critically important. Efforts should be made to determine if the oil stain is indigenous, migrated, or related to nearby oil accumulations. Because of the above information, I recommend that researchers evaluate the data to determine stratigraphic positions of the richer units, possible geographic trends, and possible migration routes of expelled hydrocarbons.

Lloyd Gatewood:

Let me make a plea, implore you to not defer drilling until you can identify a bona fide source. Please, do your homework well, like CNG did, as far as the paleogeology, and the structure, and drill it for the porosity; as a result, their drill bit fell into a 25-ft cave. You can't find anything unless you do your homework. And do your homework in such a way that when you do drill it, you've got a good idea that you are going to have structure, porosity, and a good paleogeologic pattern to show that you are not drilling into a structure formed too late to trap the oil. I would just add that, along the way, you utilize all of these things that you have heard today. ARCO and CNG and other companies are working to try to find out the answers of source, but please don't defer drilling just because we don't know where the source is. At the least, have a little faith that either on the shelf or in the basin there are additional reserves to be had in something as unpredictable as the Arbuckle.

David Read:

You were asking for suggestions on future work. At CNG, we are not completely sure what controls the presence of the Brown zone dolomitization. We know that the shelf lithology is primarily dolomite, but the key to finding production in the aulacogen is to find good coarse-crystalline dolomite in what is primarily a massive section of dense limestone. Addressing the topic of dolomitization mechanisms and distribution in the Ardmore basin area would be very valuable and possibly should be considered for a future symposium.

Kenneth Johnson:

Let me ask one final question. Steve Brown raised a very interesting question earlier, before the panel discussion. He conducted a vote on whether people in the audience believe the Ar-

buckle was a source for some of its own hydrocarbons, and the vote seemed to be split evenly. Let's see if there is any change of opinion as a result of this discussion. All those who think the Arbuckle may, in fact, be a significant source of hydrocarbons, please raise your hands [about half the audience raised their hands]. All those who think that it is not a significant source of hydrocarbons, please raise your hands [again, about half the audience raised their hands].

Well, there appears to have been no change in the collective opinion of those in the audience. Perhaps an equal number of people have changed their earlier opinions. The issue of whether the Arbuckle rocks can be a significant source of hydrocarbons still appears to be open to debate.

I want to thank the panelists for their excellent contributions, and with that we will close the panel discussion.

REFERENCE

Trask, P. D.; and Patnode, H. W., 1942, Source beds of petroleum: American Association of Petroleum Geologists, Tulsa, 566 p.

PART III

ABSTRACTS AND SHORT REPORTS RELATED TO POSTER PRESENTATIONS

Paleomagnetic Dating of Basinal Fluid Migration, Base-Metal Mineralization, and Hydrocarbon Maturation in the Arbuckle Mountains, Oklahoma

D. S. Bagley, D. London, D. Fruit, K. D. Cates, and R. D. Elmore
University of Oklahoma

ABSTRACT.—Paleomagnetic and rock magnetic results from the Ordovician Viola limestone in south-central Oklahoma indicate the presence of two chemical remanent magnetizations (CRMs). One is a CRM that is pervasive in the unfractured, non-mineralized Viola and resides in magnetite. An incremental fold test shows that this CRM was acquired during Pennsylvanian folding. Previous work has shown that the Viola was nonporous at the time of folding which probably excludes the possibility of remagnetization by externally derived fluids. A thermoviscous origin of this remagnetization can probably also be ruled out due to low maximum-burial temperatures. Because of this, an in situ chemical process of remagnetization, such as the maturation of hydrocarbons, is invoked to explain the pervasive synfolding magnetization.

A Permian CRM residing in hematite occurs in alteration halos around mineralized fractures. Geochemical studies indicate that the fluids that caused the mineralization and alteration were primarily basinal in origin, although multiple types of fluids were involved. The migration of basinal fluids through the fractures caused the remagnetization residing in hematite.

INTRODUCTION

The purpose of this paper is to describe paleomagnetic, petrographic, and geochemical results from the Viola limestone in the northern Arbuckle Mountains. The results have implications for understanding the timing and origin of base-metal precipitation in the northern Arbuckle Mountains (i.e., the Davis zinc field; Fay, 1981). In addition, the paleomagnetic results may have implications for determining the time of hydrocarbon maturation in the Viola.

GEOLOGIC SETTING

The study area is located within the Sooner rock and sand (SRS) quarry, secs. 11 and 14, T. 1 S., R. 1 E., Murray County, Oklahoma (Fig. 1). The quarry is in the Late Ordovician Viola limestone and is located ~3 km northeast of the Davis zinc field (Fay, 1981).

The Viola limestone is a widespread carbonate sequence as much as 300 m thick in the Arbuckle Mountains. At the base of the Viola are laminites that grade upward to coarse grainstones at the top of the unit. The Viola shallows upward and records deposition on a deep to shallow carbonate ramp (Ham, 1973; Galvin, 1983). The exposed limestone in the study area is interpreted to be lower to middle Viola. The limestones sampled are predominantly gray in color and consist primarily of fossiliferous mudstones, wackestones and some packstones that contain chert nodules. Primary porosities in these lithologies, particularly the mudstones and wackestones, are low. The limestones are tight, and other workers have suggested that any original porosity was occluded by an early phase of meteoric cementation (e.g., Grammer, 1985). The Viola does produce oil in some areas, but the porosity is a result of fracturing caused by deformation (Allen, 1983).

The Viola, which is found within the southern Oklahoma aulacogen (e.g., Wickham, 1978), was

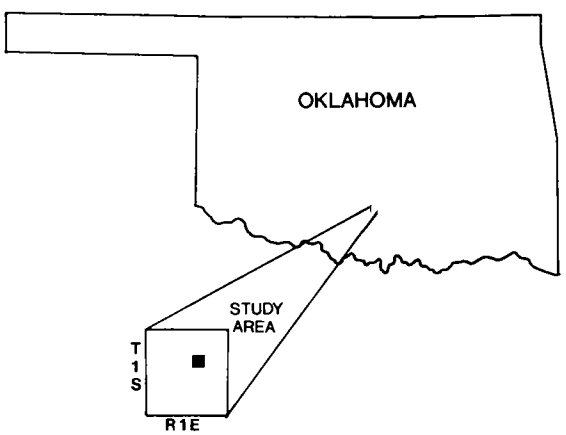

Figure 1. Map of Oklahoma showing study area located in Murray County, south-central Oklahoma.

deposited during the subsidence stage that followed the rifting stage of the aulacogen. The aulacogen was reactivated during the Late Paleozoic, and during the deformation stage, the rocks in the aulacogen were intensely folded and faulted.

Within the SRS quarry is an anticline/syncline couplet (Fig. 2). The axes of the folds trend NNW–SSE and both plunge gently (5–6°) to the south. The limbs of the folds can be traced continuously in the quarry. Located on the eastern portion of the study area (east limb of easternmost anticline) (Fig. 3) is a fractured zone. The fractures in this zone have two general orientations. One set strikes approximately N. 25° W. and dips 50° to the southwest. This fracture set is apparently axial planar to the trend of the folds seen in the quarry. The second set of fractures strikes between N. 55° E. and N. 60° E., approximately normal to the axis of the folds and therefore likely to be extension fractures (Wiltse, 1978). In one area the rocks are highly fractured and brecciated. This zone, which contains an abundance of small-scale slickensides, is interpreted to be the surface expression of a fault which trends NNW–SSE and dips to the west.

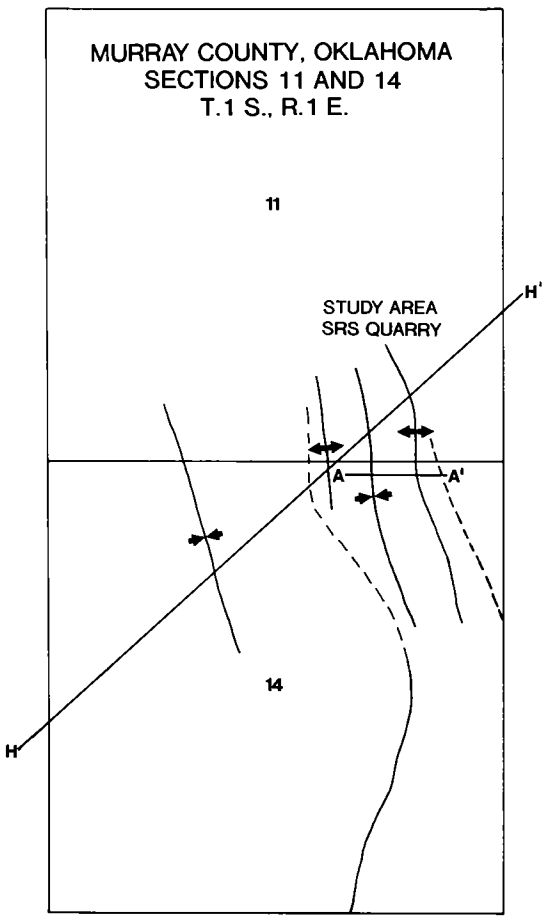

Figure 2. Figure showing structural features in the vicinity of the Sooner rock and sand quarry (after Wiltse, 1978). Dashed lines and solid lines connect to show the outline of the Viola outcrop in the study area.

Some of the fractures are mineralized with calcite. The calcite mineralization provides evidence of fluid migration through the fault zone. Also associated with the calcites in the fractures are Mississippi Valley-type base-metal oxides and sulfides including sphalerite, pyrite, marcasite, and goethite. In addition to the calcite mineralization, the fractures in this zone often exhibit a pipe-like appearance (Fig. 4), and some of the fractures are conduits for tar seeps. This zone will be referred to as the "mineralized zone" (Fig. 3).

The Viola in direct contact with the mineralized fractures and in the brecciated zone is commonly altered from the normal gray Viola to a yellow to reddish color. The calcite in the fractures also extends into the rock along what are apparently small fractures. In addition, a red to yellow, fine-grained carbonate-clay material can occur at the contact between the host limestone and the calcite in the fractures. This material also partially to completely fills some vugs and small fractures in the limestones. This material is clearly secondary and is probably related to the mineralizing event.

The western limb of the anticline and the adjacent syncline exhibit significantly less fracturing, and calcite mineralization and tar seeps are absent (Fig. 5). This zone will be referred to as the "non-mineralized zone" (Fig. 3).

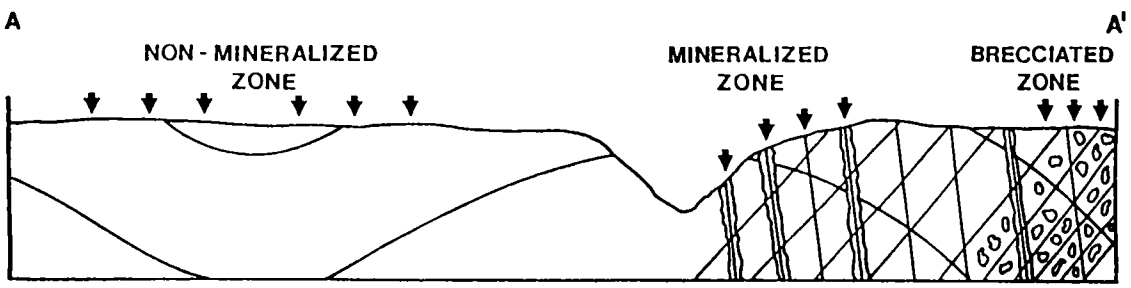

Figure 3. Sketched cross section A–A' of the study area showing the zones sampled and the sample-site locations (arrows).

Within and around the limestone quarry are a number of oil wells that comprise the Southwest Davis oil field. Oil production in the field comes primarily from the Oil Creek sandstones at depths of 1,000–1,600 m. Previous work has shown that the hydrocarbons in the field were trapped as a result of a thrust-fault system and its associated en echelon faults (Wiltse, 1978). Evidence for thrust faulting is shown by demonstrating that the Oil Creek is repeated a number of times in different wells within the field.

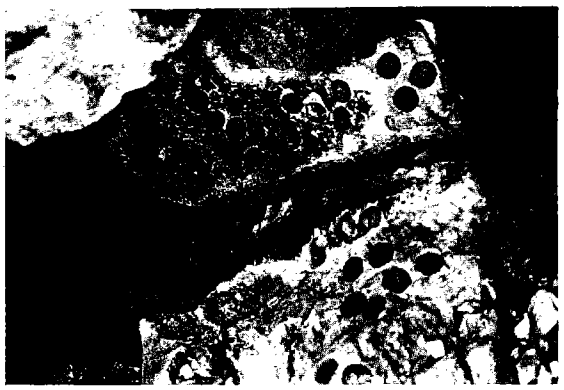

Figure 4. Field photograph from the mineralized zone. Note the hollow, pipe-like fracture that is lined with calcite.

MINERALOGY OF CALCITE-FILLED VEINS

The mineralogy of the calcite vein-filling is surprisingly complex, but can be subdivided into two stages of growth: early, basal scalenohedra that project into the fractures and cavities, and later, crystallographically complex rhombic overgrowths on the scalenohedra. The calcite veins can also be subdivided into two groups: those that are covered with natural asphalt and those that lack associated asphalt. Thus, there are four parageneses of calcite, which have distinctive characteristics or associated minerals.

Fluorescence.—In shortwave UV light, scalenohedra in asphalt-absent veins show white fluorescence and strong phosphorescence at their bases, changing to orange fluorescence at the tips of crystals. Rarely, scalenohedra associated with asphalt exhibit the same white fluorescence and phosphorescence at their bases, but most such scalenohedra do not fluoresce. Rhombic calcite in asphalt-absent veins fluoresces red, especially within inner growth zones of included minerals. Rhombic calcite from asphalt-bearing veins does not fluoresce.

Morphology.—Rhombic calcite overgrowths occur with two different morphologies. Rhombs from asphalt-absent veins are flat-faced, simple rhombohedra, sometimes twinned on {0001} with smooth, slightly etched surfaces. Rhombs in asphalt-bearing veins are rounded rhombohedra

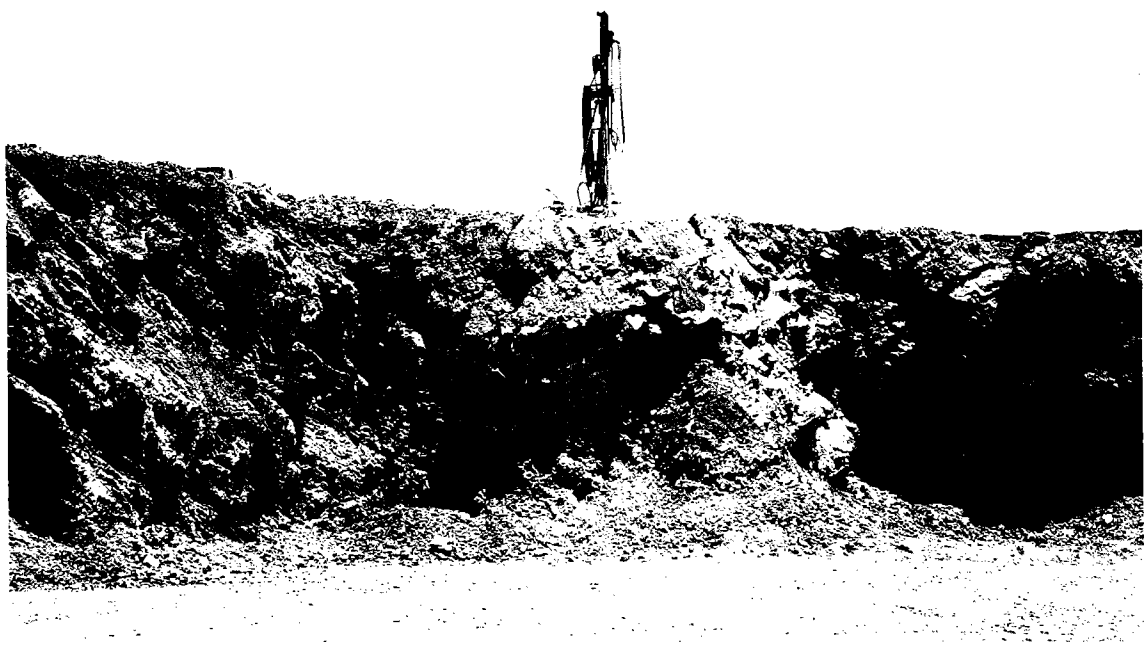

Figure 5. Field photograph of folded Viola limestone in the non-mineralized zone.

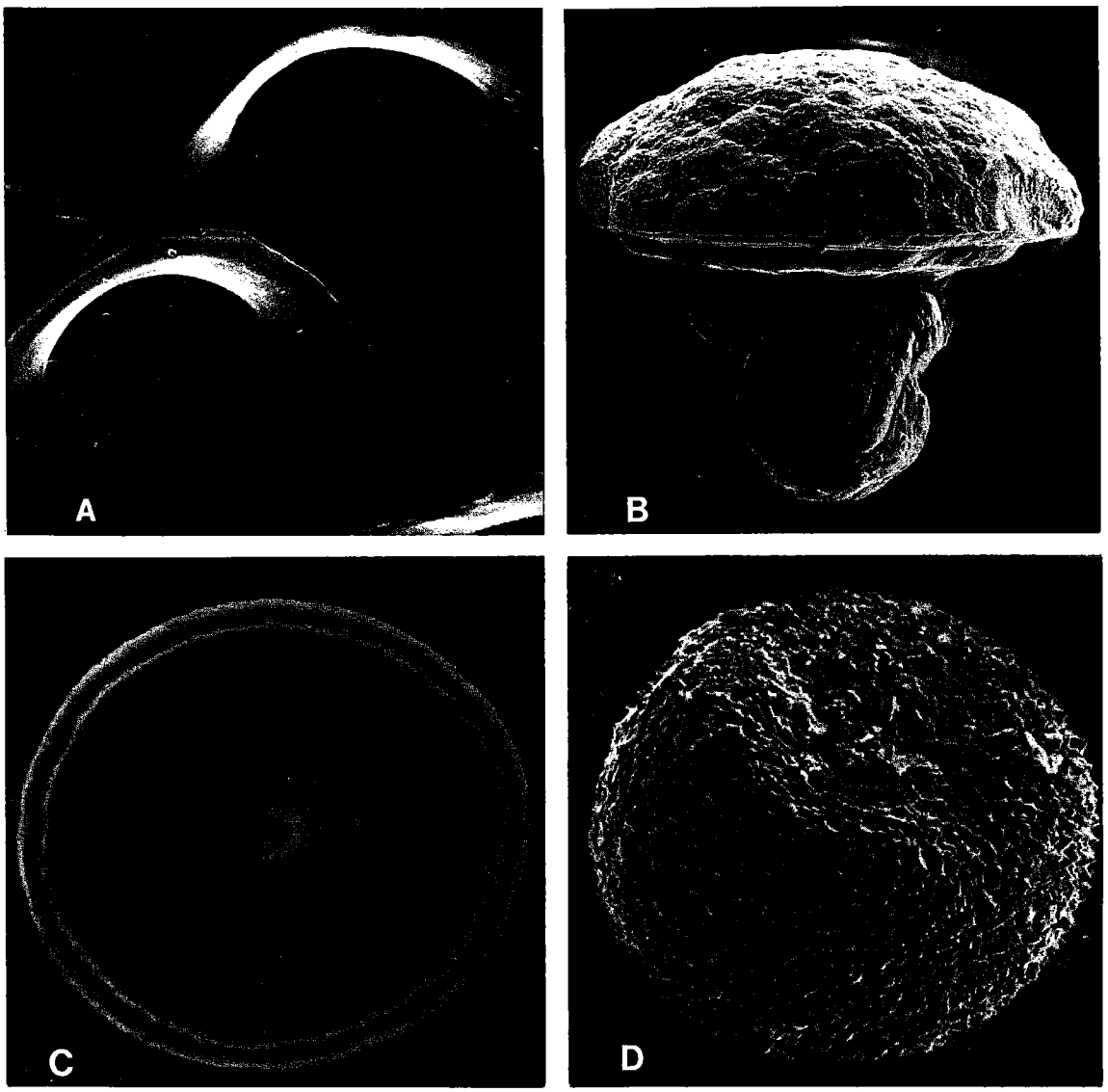

Figure 6. Electron photomicrographs of calcite and some commonly associated oxide and sulfide phases. *A*—Surface topography of rhombic calcite, showing the flat-topped circular growth platforms that are found only on rhombic calcite overgrowths associated with asphalt seeps (magnification 100×). Commonly associated base-metal phases not shown in this figure are pyrite (modified octahedra that coat the altered limestone matrix) and sphalerite (complex octahedral and tetrahedral composite crystals that are found mostly on the exterior tips of scalenohedra where these project through rhombic overgrowths). *B*—Cross section of primary, mushroom-shaped goethite or hematite crystal aggregate, dissolved out of an inclusion-rich layer within rhombic calcite from an asphalt-absent vein. The stems of the mushrooms point to the interior of the calcite rhombs, the caps lie toward the exterior of calcite crystals. Such Fe-oxide inclusions were deposited on the growth surfaces of these rhombic calcites and subsequently overgrown by calcite to form inclusions within rhombs (magnification 70×). *C*—View from the base of an Fe-oxide mushroom, showing the radial composite structure (mushroom gills) of very fine-grained Fe-oxide needles that constitute the cap of such aggregates (magnification 700×). *D*—A composite radial sphere of pyrite crystals from an asphalt-bearing vein, removed from the tip of a calcite scalenohedron where it projected through the rhombic overgrowth (magnification 275×).

with very shiny surfaces marked by macroscopic, flat-faced, circular growth steps (Fig. 6A).

Associated Minerals.—The scalenohedral calcite from both associations lacks solid inclusions. In asphalt-absent veins, marcasite + sphalerite are deposited along the contact between basal scalenohedra and rhombic overgrowths. The rhombic calcite in asphalt-absent veins also contains multiple growth zones of goethite + marcasite or pyrite (Fig. 6B,C). In asphalt-bearing veins, an assemblage of Fe-rich sphalerite + pyrite occurs as fine-grained druses covering the open undersurfaces of the vein calcite, and as crystal clusters where the tips of calcite scalenohedra project through the rhombic overgrowths (Fig. 6D).

Fluid Inclusions.—Primary fluid inclusion populations in calcite scalenohedra are indistinguishable between the veins with and without asphalt; both are marked by aqueous Na–Ca-brines entrapped at approximately 80–90°C. In rhombic calcite of asphalt-absent veins, primary spherical fluid inclusions associated with goethite + Fe-sulfides mostly contain Na-brines entrapped at approximately 50–60°C. In this association, there is inclusion evidence for mixing between the earlier Na–Ca-brine and the later Na-brine. No fluid inclusions have been found in rhombic calcite from asphalt-bearing veins. All calcites contain secondary fluid inclusions (non-saline, low temperature) that apparently represent entrapment of near-surface meteoric water.

The inferred chemistry and depositional sequence based on fluid inclusions and petrographic/microprobe studies are summarized below.

1) Calcite scalenohedra were deposited from a normal basin aqueous fluid (Na–Ca-brine) at temperatures of approximately 80–90°C.

2) Rhombic calcite overgrowths in asphalt-absent veins were deposited from a different brine (Na-dominated) at temperatures of 50–60°C. There is fluid inclusion evidence for mixing of the earlier, Na–Ca-brine and later Na-brine during the deposition of these rhombic calcite overgrowths. Fluid mixing with cooling, dilution, and perhaps a change in Eh (increase) or pH (decrease) may have caused precipitation of the goethite + marcasite or pyrite assemblage.

3) Fluid and solid inclusions are absent in rhombic calcite from asphalt-bearing veins. In this setting, however, the abundance of Fe-rich sphalerite + pyrite records a lower Eh and higher pH than existed in asphalt-absent veins. Petroleum would maintain the high sulfide activity and low Eh necessary to promote deposition of this reduced assemblage. The circular growth phenomena on the surfaces of rhombic calcites are interpreted as the result of selective surface wetting by an immiscible mixture of aqueous and hydrocarbon fluids during deposition of the rhombic calcites and associated sphalerite + pyrite in veins that currently contain asphalt. These inferences raise the question of the timing of the asphalt seeps relative to that of the deposition of the vein calcite. The current interpretation is that the asphalt is not modern, but rather a residue of hydrocarbons that filled at least some veins during the stage of rhombic calcite deposition.

4) Low temperatures of formation and the general absence of Cu-sulfides and galena suggest that the SRS quarry lies near an outer (cooler, shallower?) edge of the Davis zinc field. At this level of burial, apparently four distinct fluids, Na–Ca-brine, Na-brine, meteoric water, and petroleum, were introduced through fractures and mixed to various degrees. This resulted in variable Eh, pH, sulfide activity, salinity, and temperature, which promoted oxide and sulfide mineral precipitation and gross oxide/sulfide zoning patterns.

PALEOMAGNETISM

Mineralized Zone

Thermal demagnetization of specimens taken from within the calcite-filled fractures indicates the presence of two magnetic minerals. One phase shows significant decay by 100°C, while the other decays to 680°C (Fig. 7). Because goethite has a Curie temperature of 100°C and hematite has a Curie temperature of 680°C, these two minerals are the likely magnetic phases present in the calcites. Random directions were recorded for samples from the goethite and hematite in coarse vein-filling calcites.

Rock magnetic experiments conducted on the limestones in direct contact with the fractures indicate the predominance of a high coercivity mineral (Fig. 8A) with maximum unblocking temperatures of 680°C (Fig. 8B). In these specimens, the magnetization resides predominantly in hematite.

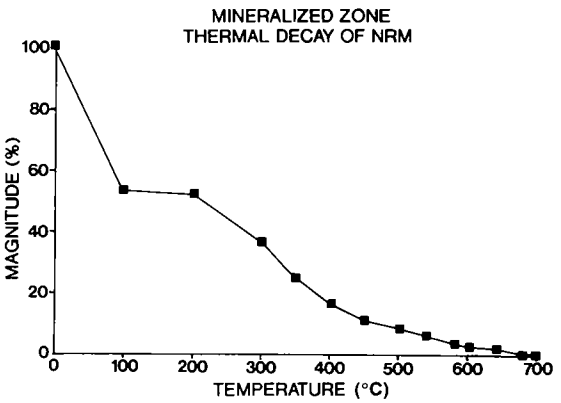

Figure 7. Representative thermal demagnetization curve for a specimen from the calcite in the veins. NRM refers to natural remanent magnetization.

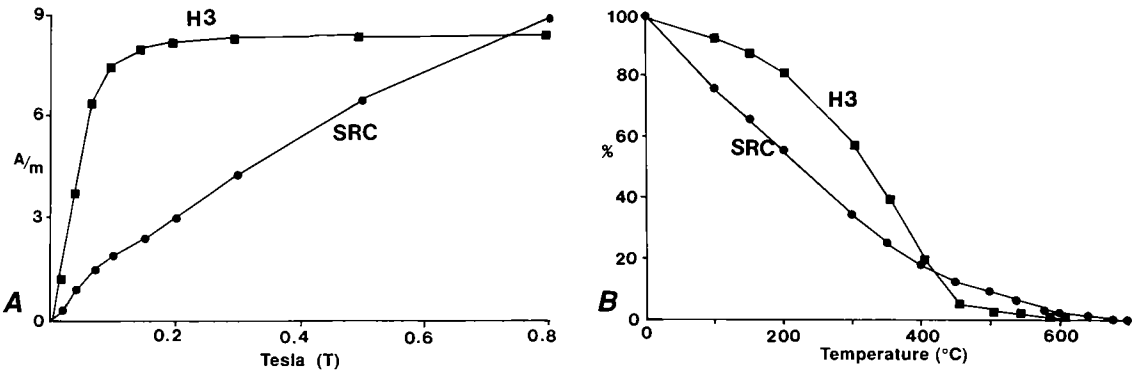

Figure 8. *A*—Representative isothermal remanent magnetization (IRM) acquisition curves for limestone specimens in the mineralized (SRC) and non-mineralized (H3) zones. Curve SRC does not achieve saturation by 0.63 T. Note small cusp in curve at 0.1 T, which suggests the presence of a minor amount of a low coercivity phase. The rise in the curve above 0.2 T indicates the presence of a high coercivity phase. Curve H3 reaches saturation by 0.2 T, indicating the presence of a low coercivity mineral. *B*—Representative thermal decay of IRM curves for specimens in the mineralized and non-mineralized zones. Decay above 580°C in SRC suggests the presence of hematite. Note maximum unblocking temperatures of 580°C for curve H3, which suggests the magnetic phase is magnetite.

With increased distance from the fractures, the amount of alternating field (AF) decay increases significantly, suggesting the emergence of a low coercivity phase. The low coercivity mineral is probably magnetite, while the high coercivity mineral that decays to 680°C is hematite. All lines of evidence indicate that as distance from the fractures increases, the relative ratio of the high coercivity hematite to the low coercivity magnetite decreases. It is apparent, then, that there is an alteration halo surrounding fractures with a magnetization residing in hematite (Fig. 9). It is believed that the fluids moving through the fractures and causing the mineralization were also responsible for the remagnetization and change in magnetic mineralogy.

The mean direction for the limestones in direct contact with the fractures was south–southeasterly and shallow (Fig. 10). The pole position for specimens in direct contact with the fractures is 109° E. longitude, 51° N. latitude, which corresponds to a Late Permian pole (Fig. 11) on the North American Apparent Polar Wander Path of Irving and Irving (1982). A similar pole position was also found for the rocks in the highly fractured and brecciated zone (Fig. 11).

Non-Mineralized Zone

The results of rock magnetic experiments indicate that the samples from the non-mineralized zone are dominated by a single, low coercivity magnetic phase (Fig. 8A) that decays completely by 580°C (Fig. 8B). Magnetite is a low coercivity mineral with a Curie temperature of 580°C and carries the magnetization in the non-mineralized zone. The directions for this component are southeasterly and shallow, and the directions from the limbs of the fold cross when the rocks are corrected for the tilt (Fig. 12). The results of an incremental fold test indicate that the magnetization was acquired during Pennsylvanian folding (Fig. 13). A statistically significant grouping of site means occurs at 70% unfolding (Fig. 13). The resultant pole position (126.5° E. longitude and 34.8° N. latitude) plots near the Early Carboniferous segment of Irving and Irving's (1982) Apparent Polar Wander Path (Fig. 11).

The origin of the magnetization in the non-mineralized zone is somewhat problematic. Thermoviscous processes can be ruled out as the Viola experienced only relatively low burial temperatures (e.g., Metcalf, 1985). Thus a chemical origin of remagnetization is invoked. It is also likely that the process by which the magnetization was acquired was an in situ process, as the limestone is extremely tight and any original porosity was probably eliminated by an early phase of meteoric cementation (Grammer, 1985).

In a previous study of the Viola on the Arbuckle Anticline (south of the SRS study area) Peck and Elmore (1984) reported that the unit contains a magnetization, interpreted to be a chemical remanent magnetization (CRM), residing in magnetite. The directions from each flank crossed during unfolding, although the corrected directions from the south flank (141/3) are close to the uncorrected directions from the north flank (146/3). The directions from the south flank of the Arbuckle Anticline are important because they are similar to the direction at the SRS locality. The SRS locality is in the area between the Washita Valley and Reagan

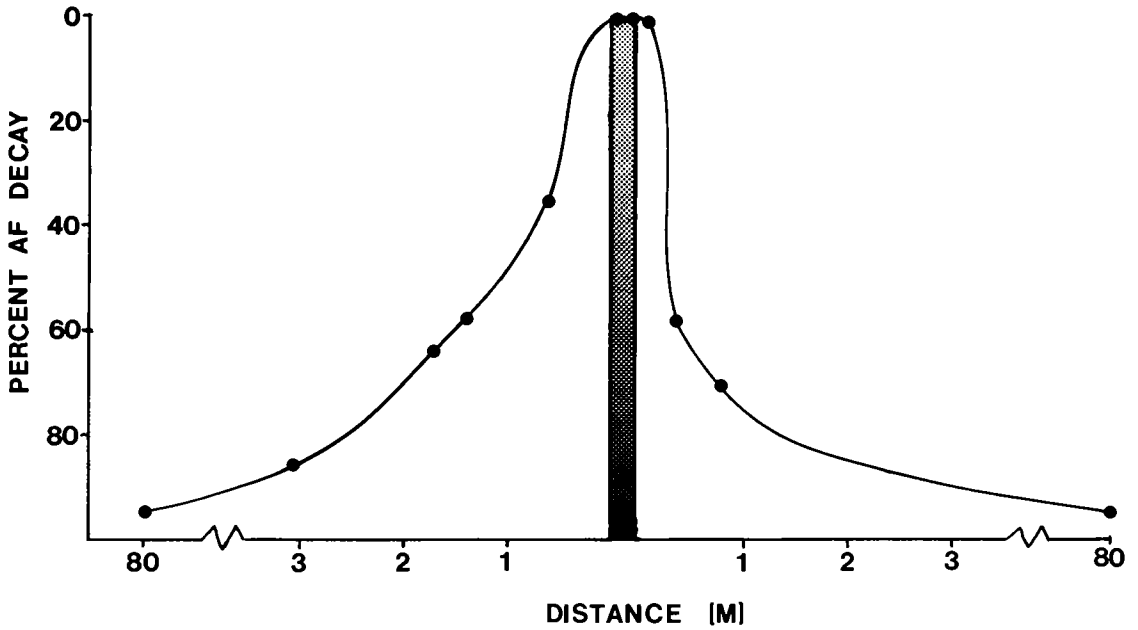

Figure 9. Summary diagram showing percent of AF decay of NRM as a function of distance from the calcite-filled fractures. Note that the low AF decay (highest coercivity) specimens are located within or very close to the fracture, but as distance increases high AF decay reflects the emergence of a low coercivity phase.

faults. This is a structurally complex area deformed by wrench faulting (Wickham, 1978) and perhaps gravity sliding (Phillips, 1983). These processes could have rotated structural blocks around a vertical axis. However, the similarity in the directions between the SRS locality, where there is the possibility of rotation, and the south flank of the Arbuckle Anticline, where rotation is unlikely, suggests that the SRS locality has not been rotated. The north flank of the Arbuckle Anticline is in the area that could have been rotated; the strike of the beds (N. 60° W.) is significantly different from the strike of the SRS locality (N. 25° W.). The directions from the north flank could be rotated or, alternatively, they could indicate asymmetrical folding.

DISCUSSION

The Viola Formation in the Arbuckle Mountains contains a pervasive Pennsylvanian synfolding CRM in magnetite and a local Permian CRM in hematite that is related to migration of basinal fluids. Based on comparisons with blocking temperature/relaxation time curves (e.g., Middleton and Schmidt, 1982), the magnetizations cannot be thermoviscous in origin due to the low burial temperatures.

The pervasive CRM in magnetite is similar to other synfolding magnetizations, some interpreted to be CRMs, reported from other carbonate units (e.g., McCabe and others, 1983). Lateral migration of orogenic fluids has been suggested as the agent of remagnetization for some of these units, although this interpretation probably does not apply to the Viola. In the areas studied, except for the fractured zones, the Viola does not contain

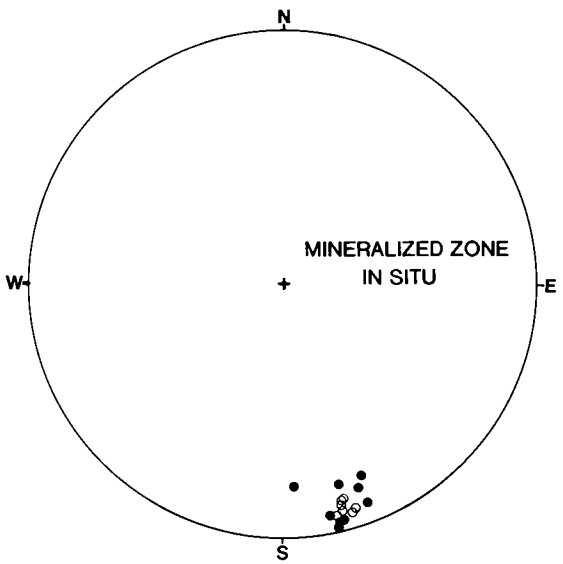

Figure 10. Schmidt equal-area projection for specimens in the mineralized zone in direct contact with a calcite-filled fracture. Direction (in situ) is south–southeast and shallow. Solid symbols represent projections in the lower hemisphere; open symbols represent projections in the upper hemisphere.

significant porosity and probably did not prior to folding (Grammer, 1985). Because the unit was probably tight at the time of folding, fluids could not have pervasively entered the rock. An in situ chemical mechanism, therefore, is needed to explain the remagnetization.

Several diagenetic processes that occurred in the Viola could possibly be related to magnetite authigenesis. For example, the Viola contains organic matter in the study area and one possible in situ mechanism could be related to diagenesis of this organic matter. Total organic carbon (TOC) values range between 0.04 and 0.54% for the Viola in the study area and, based on preliminary Rock-Eval pyrolysis, S_1/S_1+S_2 ratios range from 0.06 to 0.21 and T_{max} ranges from 434 to 442°C. These results suggest that some of the rocks are immature but others have just entered the oil window (Tissot and Welte, 1984). The results are also consistent with the interpretation that the hydrocarbons

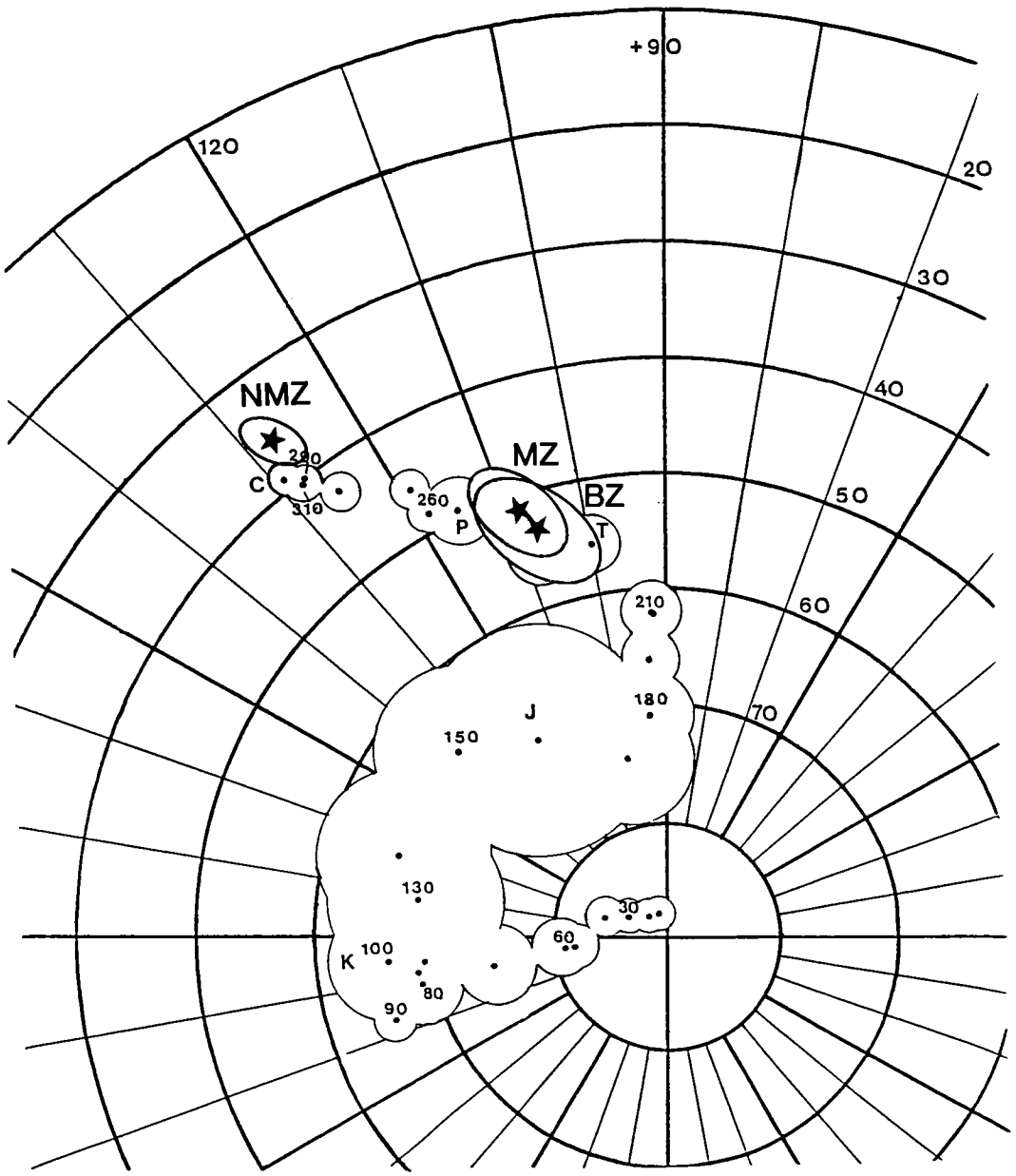

Figure 11. North American Apparent Polar Wander Path (Irving and Irving, 1982), with paleo-poles (★) calculated from the mean magnetic directions of the non-mineralized zone (NMZ), the mineralized zone (MZ), and the brecciated zone (BZ). The poles are plotted with their ellipses of confidence.

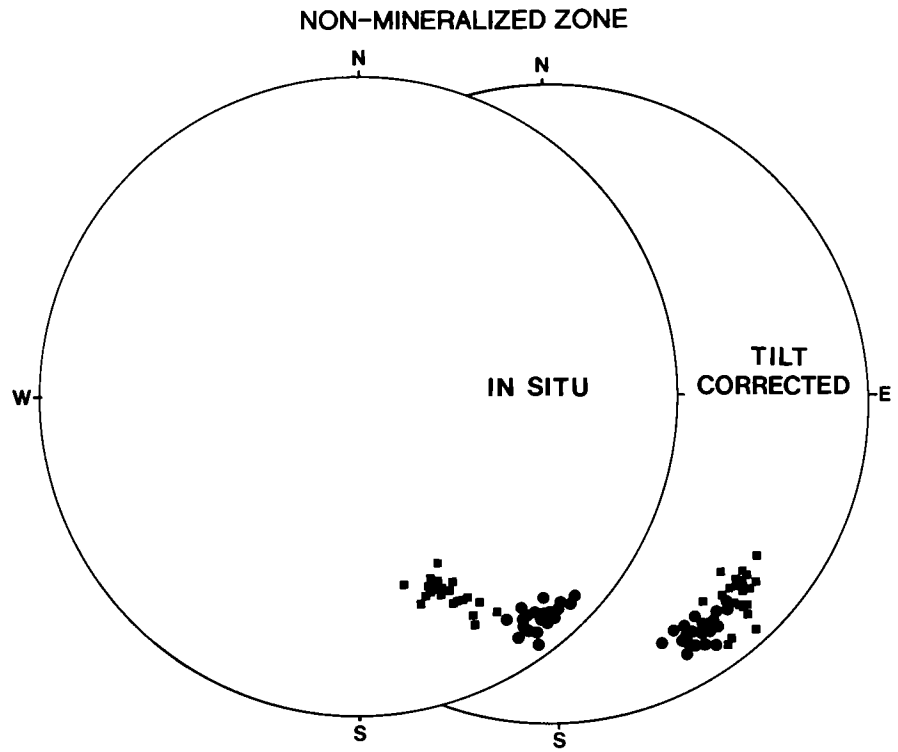

Figure 12. Schmidt equal-area projection of specimens from six sites in the non-mineralized zone, before and after tilt correction. Square symbols represent specimens from E-dipping limb; circles are from W-dipping limb (all specimens plot on lower hemisphere). Note that the directions cross during complete tilt correction, indicating a synfolding magnetization.

were generated in situ. The chemical conditions created by the maturation of the hydrocarbons may have caused precipitation of authigenic magnetite and acquisition of the synfolding CRM. This interpretation is reasonable in that both maturation of hydrocarbons and folding probably occurred during maximum burial and heating. Another possible mechanism that may be related to magnetite authigenesis is the transformation of smectite to illite which releases iron (Boles and Franks, 1979). The Viola contains some illite, and relatively thick volcanic ash deposits are found in the lateral equivalent of the Viola to the southeast (Sediqi, 1985).

Both maturation of hydrocarbons and the smectite–illite reaction can be caused by burial temperatures (~100°C) that are not high enough to cause a thermoviscous remagnetization. These, or other, in situ chemical processes mediated by relatively low burial temperatures could explain the pervasive CRM in the Viola as well as other pervasive magnetizations in carbonates. These hypotheses for in situ chemical remagnetization, however, are untested.

The Permian CRM residing in hematite is primarily related to basinal fluids that migrated along the fracture and fault zones. We suggest that mix-

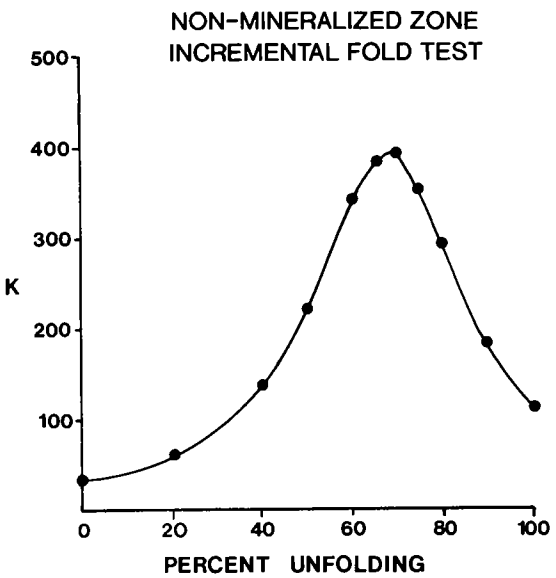

Figure 13. An incremental fold test was performed on the site means from six sample sites from the non-mineralized zone, and it was determined that the best grouping (K) of specimens came at 70% unfolding, indicative of a synfolding magnetization.

ing of different fluids (basinal, meteoric) and interactions between these fluids and the organic-rich Viola caused precipitation of the iron oxides and remagnetization around the fractures.

ACKNOWLEDGMENTS

The authors thank Karen Cochran and Mike Engel for input on the organic geochemistry of the Viola. Support was provided by grants from the National Science Foundation (EAR 8917181) and the Oklahoma Mining and Minerals Resources Research Institute to Elmore and London.

REFERENCES

Allen, G. D., 1983, Origin and genesis of fracture porosity in Viola limestone (Ordovician) [abstract]: American Association of Petroleum Geologists Bulletin, v. 67, p. 411.

Boles, J. R.; and Franks, S. G., 1979, Clay diagenesis in Wilcox sandstones of southwest Texas: implications of smectite diagenesis on sandstone cementation: Journal of Sedimentary Petrology, v. 49, p. 55–70.

Fay, R. O., 1981, Geologic map of southwest Davis zinc field, Arbuckle Mountains, Oklahoma: Oklahoma Geological Survey Map GM-20, 1 sheet, scale 1:7,920, 16-page text.

Galvin, P. K., 1983, Deep-to-shallow carbonate ramp transition in Viola limestone (Ordovician), southwest Arbuckle Mountains, Oklahoma [abstract]: American Association of Petroleum Geologists Bulletin, v. 67, p. 466.

Grammer, G. M., 1985, Diagenetic destruction of primary reservoir porosity in Viola limestone, south-central Oklahoma [abstract]: American Assocation of Petroleum Geologists Bulletin, v. 69, p. 258.

Ham, W. E., 1973, Regional geology of the Arbuckle Mountains, Oklahoma: Oklahoma Geological Survey Special Publication 73-3, 61 p.

Irving, E.; and Irving, G. A., 1982, Apparent polar wander paths Carboniferous through Cenozoic and the assembly of Gondwana: Geophysical Surveys, v. 5, p. 141–188.

McCabe, C.; Van der Voo, R.; Peacor, D. R.; Scotese, C. R.; and Freeman, R., 1983, Diagenetic magnetite carries ancient yet secondary remanence in some Paleozoic sedimentary carbonates: Geology, v. 11, p. 221–223.

Metcalf, W. J., 1985, Investigation of paleotemperatures in the vicinity of the Washita Valley fault, southern Oklahoma: University of Oklahoma unpublished M.S. thesis, 94 p.

Middleton, M. F.; and Schmidt, P. W., 1982, Paleothermometry of the Sydney basin: Journal of Geophysical Research, v. 87, no. B7, p. 5351–5359.

Peck, C. J.; and Elmore, R. D., 1984, Paleomagnetism of the Ordovician Viola limestone, south-central Oklahoma [abstract]: EOS, v. 65, p. 197–198.

Phillips, E. H., 1983, Gravity slide thrusting and folded faults in western Arbuckle Mountains and vicinity, southern Oklahoma: American Association of Petroleum Geologists Bulletin, v. 67, p. 1363–1390.

Sediqi, A. S., 1985, A sedimentologic and geochemical study of the Bigfork chert in the Ouachita Mountains and the Viola limestone in the Arbuckle Mountains: University of Oklahoma unpublished Ph.D. dissertation, 155 p.

Tissot, B. P.; and Welte, D. H., 1984, Petroleum formation and occurrence [second edition]: Springer-Verlag, New York, 699 p.

Wickham, J. S., 1978, The southern Oklahoma aulacogen, *in* Wickham, J. S.; and Denison, R. E. (eds.), Structural style of the Arbuckle region: Geological Society of America Guidebook for South-Central Section Annual Meeting, Field Trip 3, p. 9–41.

Wiltse, E. W., 1978, Surface and subsurface study of the southwest Davis oil field, sections 11 and 14, T. 1 S., R. 1 E., Murray County, Oklahoma: University of Oklahoma unpublished M.S. thesis, 72 p.

Burial History and Thermal Maturation of Pennsylvanian Rocks, Cherokee Basin, Southeastern Kansas

C. E. Barker
U.S. Geological Survey, Denver

R. H. Goldstein
University of Kansas

J. R. Hatch
U.S. Geological Survey, Denver

A. W. Walton and K. M. Wojcik
University of Kansas

ABSTRACT.—Vitrinite reflectance (R_m), Rock-Eval pyrolysis and organic carbon data, measured in core samples from >60 wells in southeastern Kansas, indicate that hydrocarbon generation has occurred, at least locally, in the organic-matter-rich Pennsylvanian rocks. R_m averages 0.7% (number of samples, n = 104) which is within the oil window, and R_m in six wells exceeds 1.5%. Rock-Eval T_{max} data (n = 156) generally parallel and confirm the R_m profiles. Hydrogen and oxygen indices (n = 93) from Rock-Eval pyrolysis indicate that the organic matter has highly variable hydrogen and oxygen contents. Some stratigraphic intervals have S_2 to S_3 ratios averaging 6.5, indicating they contain oil-prone organic matter which produces an appreciable S_1 peak—an indication of hydrocarbon generation (average S_1 = 0.8 mg HC/g rock; n = 94). Organic carbon content in mudstone and sandstone (n = 149) averages 1.2 and ranges up to 12.4 wt%, indicating sufficient levels for hydrocarbon expulsion are locally present.

Heating at the reconstructed peak burial depth alone does not account for the observed organic matter thermal maturation. Interpretation of the R_m data using an empirical geothermometer suggests temperature reached regional levels of 110°C, and in the warm spots exceeded 150°C. The geothermal gradient suggested by these data is very low, indicating a local development of an upward flow system in the Cherokee basin.

INTRODUCTION

The Cherokee basin is bounded by the Nemaha fault system and Sedgwick basin to the west, Bourbon arch and Forest City basin to the north, and the Ozark uplift to the east, and extends into the Arkoma basin and Ouachita Mountains to the south. This region contains significant hydrocarbon and Mississippi Valley-type Pb–Zn deposits. A locally complex thermal history in the Cherokee basin is suggested in this study by regional vitrinite-reflectance values of ~0.7% with values reaching 0.9–1.5% in some clusters of wells (warm spots).

This paper is an overview of our ongoing investigation of thermal history in the Cherokee basin. As such, the scope of this paper will not allow detailed presentation of methods or analytical results. The data are listed in the Appendix and summarized in Table 1. The data were derived from >220 samples of mudrock, coal, sandstone, and limestone. The general methodology used is found in Peters (1986; Rock-Eval method) and Robert (1988; Lopatin, vitrinite-reflectance and coal analysis).

PEAK BURIAL DEPTH AND BURIAL HISTORY RECONSTRUCTION

Pennsylvanian to Permian

Pennsylvanian deposition in the Cherokee basin began ~314 Ma (absolute ages from Hills and others, 1983) with the deposition of Atokan age sediments over the regional Mississippian unconformity. Sediment deposition in this area, except for the western portion along the Nemaha Ridge, continued without major interruption until near

TABLE 1. — STATISTICAL SUMMARY OF ORGANIC GEOCHEMISTRY ANALYTICAL RESULTS, CHEROKEE BASIN, SOUTHEAST KANSAS

Analysis Parameter Lithology	Sample size	Range	Mean	Standard deviation	Units
Organic carbon					
Coal[a]	73	14.1–79.3	54.8	18.7	weight-percent
Other rocks[b]	149	0.05–12.4	1.2	1.5	weight-percent
Vitrinite reflectance					
All samples	104	0.4–1.54	0.7	0.2	% mean random in oil (R_m)
Rock-Eval					
T_{max}[a,b]	156	410–592	436	38	°C
S_1					
Coal[a]	73	0.59–35.1	7.2	7.6	mg hydrocarbon/g rock
Other rocks[b]	94	0.01–5.48	0.8	1.4	mg hydrocarbon/g rock
Hydrogen Index					
Coal[a]	73	70–418	256	73	mg hydrocarbon/g C_{org}
Other rocks[b]	93	2–523	128	105	mg hydrocarbon/g C_{org}
Oxygen Index					
Coal[a]	73	2–42	13	8	mg CO_2/g C_{org}
Other rocks[b]	92	2–550	72	88	mg CO_2/g C_{org}
S_2/S_3					
Coal[a]	73	3.57–98.27	28	18	mg hydrocarbon/mg CO_2
Other rocks[b]	89	0.14–72.76	6.5	12	mg hydrocarbon/mg CO_2

[a]Coal = Coal or coaly mudrocks that were arbitrarily grouped as those samples with >14 wt% C_{org}.

[b]Other rocks (mudrocks and sandstones) = samples with 0.5–14 wt% C_{org}. Results from samples with <0.5 wt% C_{org} or samples in which bitumen was visually detected are not included.

the end of the Permian. Stratigraphic reconstructions indicate as much as 250 ft of Ochoan rocks were deposited, but these rocks must have been soon removed and seem negligible in estimating burial depth. Merriam (1963, figs. 77,94) showed in his geologic and pre-Mesozoic paleogeologic maps that erosion of most of the Permian section was completed before the Triassic. For this reconstruction, Merriam's concept is slightly modified in accord with the reconstructions of McKee and others (1959,1967) and Stewart (1975), which allows for a more gradual erosion of the Permian section extending through the Triassic and Jurassic.

Post-Paleozoic

Paleogeographic reconstruction shows eastern Kansas was a positive element during the Triassic (McKee and others, 1959) and apparently persisted as such until the Cretaceous when as much as 100 ft of sediments were deposited in the Cherokee basin. Cretaceous and Cenozoic deposits are of minor thickness (as much as 300 ft; Merriam, 1963), and because their deposition followed significant exhumation of the Cherokee Group, they are negligible in calculating peak burial depth and paleotemperature. Also Cretaceous lamproite intrusions in the Cherokee basin (Merriam, 1963) could not have significantly contributed to heating of the study area because the intrusions are too small, occur too far north, and were intruded after ore deposition (Table 2).

The paleothickness of Permian overburden present at peak burial was estimated by projecting the preserved Permian section in the Sedgwick basin over the Cherokee basin (Fig. 1). This indicates ~3,600 ft of pre-Ochoan Permian section has been removed by erosion. Adding the eroded thickness to present burial depth suggests a peak burial of ~6,000 ft for the basal Cherokee Group at Union Gas Leffingwell 16 in west-central Cherokee basin (Fig. 2).

TABLE 2. — AGES OF SELECTED GEOLOGIC EVENTS, CHEROKEE BASIN REGION

Event (significance)	Age	Reference
OLDEST		
Anadarko basin/Wichita uplift (potential for lateral fluid flow into Cherokee basin from the south)	315–330 Ma	Johnson (1989)
Pennsylvanian deposition commences in Cherokee basin	314 Ma*	Merriam (1963)
Ouachita uplift (initial stage) (potential for lateral fluid flow into Cherokee basin from the south)	~310 Ma	Johnson (1988)
Ore deposition (a time of oil migration)	310–250 Ma	Leach and Rowan (1986)
Permian evaporite deposition (potential brine source)	275–250 Ma	Merriam (1963)
Peak burial in Cherokee basin	255–250 Ma	this paper
Ozark uplift and deep erosion in Cherokee basin (potential for flow from east and local meteoric recharge)	~250 Ma	Merriam (1963)
YOUNGEST		

*Geologic age converted to absolute age using Hills and others (1983).

EVIDENCE FOR HYDROCARBON GENERATION

Composition and Concentration of Organic Matter

Organic petrography observations on samples from Pennsylvanian mudrocks indicate terrestrial material (type III) is the common identifiable phytodetritus and that amorphous debris is also present. Hydrogen index (HI) versus oxygen index (OI) data (Table 1; data in Appendix) are consistent with petrographic observations and the pyrolysis data of Hatch and others (1989) that show mixtures of types II (oil-prone) and III (gas-prone) organic matter in marine mudrock and type III organic matter in the mudrocks associated with coal. The S_2 to S_3 ratio is a second indicator of organic matter type in that it is a measure of gas and oil generative capability. S_2/S_3 averages 6.5 (Table 1), indicating that the organic matter is generally oil prone (Peters, 1986). Organic carbon content (C_{org}) in the mudrocks averages 1.2 wt% and ranges up to 12.4 wt%, amounts locally sufficient for hydrocarbon expulsion.

Thermal Maturity

A composite profile of mean random vitrinite-reflectance (R_m) measurements versus reconstructed peak burial depths (Fig. 3) indicates a very low gradient based on samples taken from wells throughout the Cherokee basin. The regional thermal maturity level is about 0.5–0.8% R_m. In portions of some wells, however, R_m is ~1.5% (Appendix). The R_m data suggest that on a regional basis the rocks are marginally mature to mature with respect to oil generation (Dow, 1977).

The mean vitrinite reflectance of 0.7% R_m (Table 1) is equivalent to an average T_{max} of 436°C (equation in Appendix) or mature with respect to oil generation. In samples from individual wells that have appreciable C_{org} (generally >0.5 wt%)

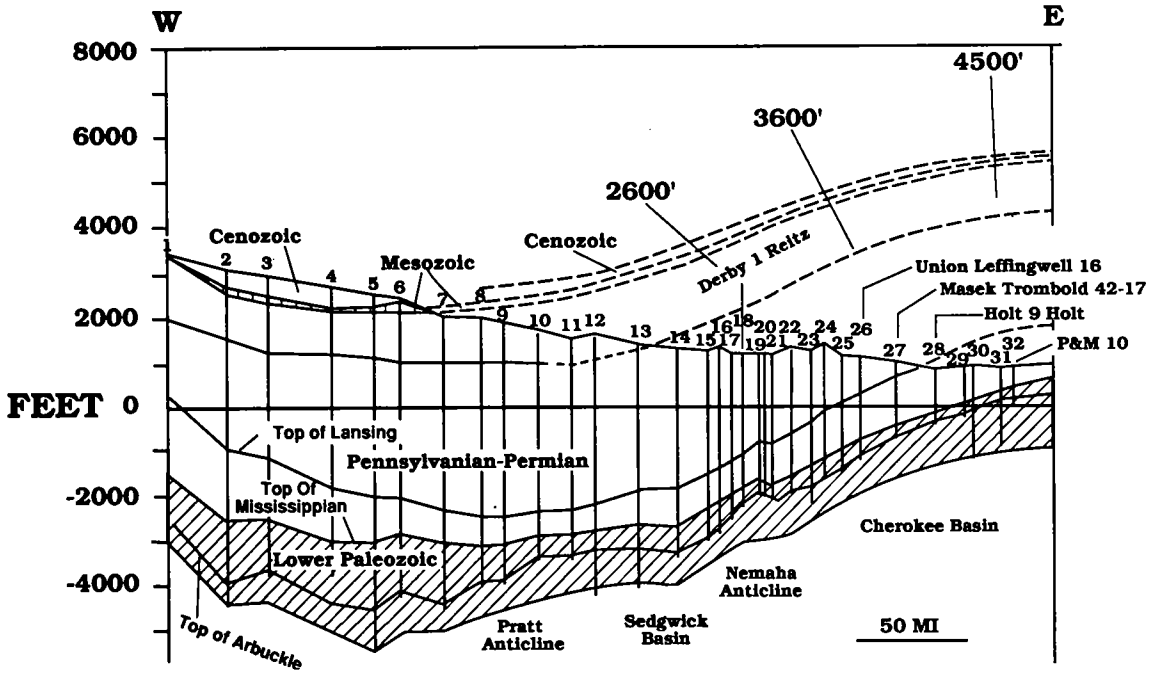

Figure 1. Stratigraphic projection of the Permian overburden over the now eroded Cherokee basin. Based on a W–E cross section across southern Kansas by Merriam (1963; the numbers on Fig. 1 refer to his well numbers used). The erosion depths (2,600, 3,600, and 4,500 ft) across southeastern Kansas are based on the preserved thickness of Pennsylvanian and Early Permian rocks. The thickness of Ochoan (Late Permian), Mesozoic, and Cenozoic rocks is considered insignificant to the magnitude of the burial depth and was not included in reconstructing peak burial depth. Selected wells used in this study are labeled on the cross section.

Rock-Eval T_{max} mimics the changes in R_m, which confirms that the variation in the R_m values with depth is a valid signal of thermal maturity. This is an important confirmation because laboratory and operator biases in both parameters (Dembicki, 1984) can lead to spurious measurements.

If hydrocarbon migration into the rocks is negligible, a significant Rock-Eval S_1 peak indicates the organic matter has generated volatile hydrocarbon. Because most of the sampled rocks are impermeable, hydrocarbon migration into the samples is probably not pervasive. Therefore, the detection of a significant S_1 peak in Pennsylvanian samples (mudrock and sandstone samples average 0.8 mg HC/g rock; coal samples average 7.2 mg HC/g rock) that have no visible oil stain indicates that oil generation occurred in the Cherokee basin.

Peak Paleotemperature

Interpretation of the R_m data using an empirical geothermometer (Barker and Goldstein, 1990) suggests the regional temperature reached 110°C and locally exceeded 150°C. These paleotemperatures are consistent with temperatures derived from fluid inclusion homogenization temperatures reported by Coveney and others (1987) and Wojcik and others (this volume). A series of Lopatin analyses using a 25°C Permian surface temperature and increasing geothermal gradient in 5°C/km steps suggests oil generation at peak burial in the Cherokee basin would require a geothermal gradient of >40°C/km (Fig. 2). The modern regional geothermal gradient is ~35°C/km, although it reaches 55°C/km across the thin basal interval of the Cherokee mudrocks (Kinney, 1976; Stavnes and Steeples, 1982). The modern mean annual surface temperature is 13°C. These present-day measurements are a reasonable starting point to estimate paleogeothermal gradients, because this area is part of the central stable region of North America, and it is unlikely that heat flow from the basement was substantially higher at any time since the Pennsylvanian. Paleosurface temperature of about 20–25°C coincided with peak burial in the Late Permian and early Mesozoic, because the area was in an equatorial position at that time (Habicht, 1979). The modern thermal regime would predict temperatures of <90°C in the most deeply buried mudrocks (1.8 km), significantly lower than the peak paleotemperature indicated for the Pennsylvanian rocks. Thus, the paleo-

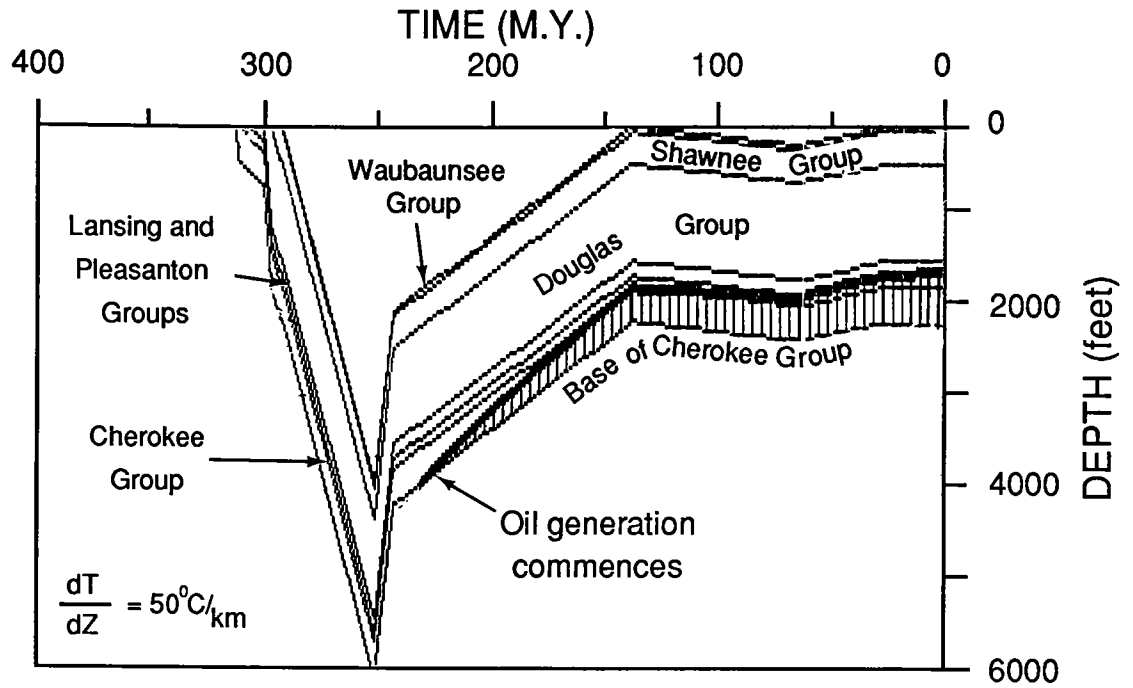

Figure 2. Burial history, Cherokee basin, southeast Kansas, based on formation tops from Union Gas Leffingwell 16 and 50°C/km geothermal gradient. Permian surface temperatures are estimated at 25°C decreasing to 14°C at present. No oil generation occurred at any time in models with geothermal gradients <40°C/km.

temperatures indicated by the geothermometers are not accounted for by simple burial heating in the modern thermal regime. Moreover, the regional geothermal gradient indicated by vitrinite reflectance is low (<20°C/km; calculated using data in Fig. 3 and the geothermometer of Barker and Goldstein, 1990), unlike the modern 35°C/km regional gradient.

Discussion

The discrepancy between modern and ancient thermal conditions is explained by invoking local zones of upward flow from pre-Pennsylvanian aquifers into fractured portions of the generally impermeable Pennsylvanian rocks. Evidence for upward flow is the R_m-depth profiles in individual wells (Fig. 3) and samples from small geographic areas that have a significantly higher R_m than the regional level (average 0.7% R_m) indicating warm spots (Fig. 4) in the Pennsylvanian rocks. R_m-depth profiles before erosion are considered to connect with a near-surface value of 0.2% R_m (Dow, 1977) suggesting that a shallower, high R_m-depth gradient existed above the very low R_m-depth gradient seen in the composite data (Fig. 3). The form of the R_m-profile with the very low gradient segment and conjectured shallow high-gradient segment above is like that resulting from thermal convection (Barker and Elders, 1981) or upward flow (Law and others, 1989). However, the extreme anisotropy of permeability in the Pennsylvanian rocks would seem to preclude convection.

The data presented here and from Wojcik and others (this volume) suggest regional temperatures of 110°C with warm spots of >150°C in the Pennsylvanian rocks. The 110°C paleotemperatures are consistent with predictions based on a lateral brine flow model and the distance of the Cherokee basin (~300 km) from the Ouachita Mountains/Arkoma basin front (see summary by Leach and Rowan, 1986). However, the presence of warm spots, locally higher temperatures (to 150°C), and a low regional geothermal gradient suggest upward, not horizontal, flow. This evidence, along with the evidence for intrabasin hydrocarbon generation, is inconsistent with predictions of, or the postulated need for, lateral brine flow. Lateral flow of hydrocarbons from deeply buried source rocks to the south is unnecessary to account for hydrocarbons in the Cherokee basin (Hatch and others, 1989; and this paper).

SPECULATION ON HEAT AND FLUID SOURCES

The burial history of the Cherokee basin suggests a mechanism for this complex fluid history. Initially, the Pennsylvanian and Wolfcampian rocks would remain at relatively low temperature (until upward flow ensued) because of high thermal conductivity of postulated overlying Late Permian evaporites. The underlying Wolfcampian–Pennsylvanian rocks have been influenced by low temperature brine (Wojcik and others, this volume) possibly infiltrating into the section from Permian evaporites. Orogeny to the south emplaced warm deep-basin-derived brines (Sharp, 1978; Oliver, 1986) into the permeable Mississippian and older rocks, below the confining beds of the mudrock-rich lower Cherokee Group (Jorgensen, 1989). The timing of geologic events (Table 2) suggests that connate and early diagenetic fluids would have been displaced during Permian time by the upward flow of brines followed by the dispersal of the brines into permeable beds in the Pennsylvanian strata.

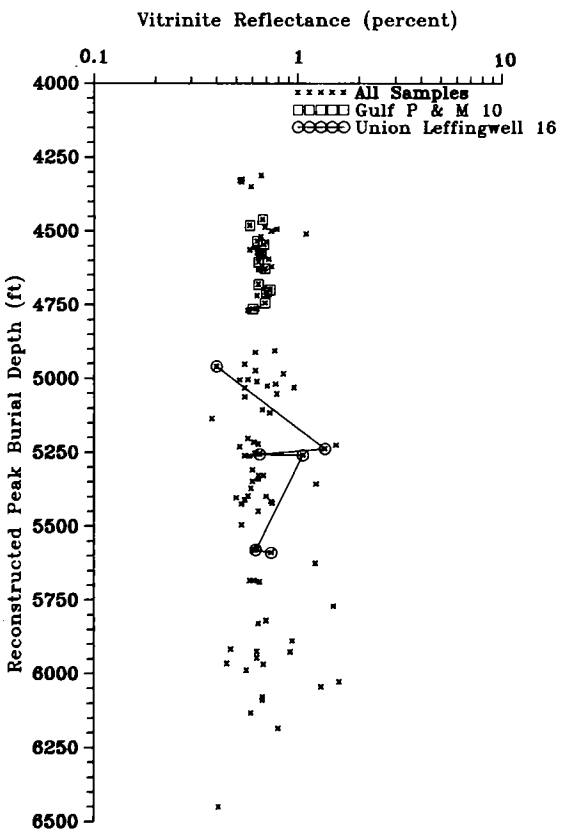

Figure 3. Composite profile of vitrinite reflectance (mean random R_m in percent) versus reconstructed peak burial depth, Cherokee basin wells, southeast Kansas. Peak burial depth estimated by projecting position of well onto the Figure 1 cross section and measuring the thickness of the overburden at that point. The open squares indicate a single well to show that some individual wells also show a lack of gradient like that observed in the composite figure. The open circles indicate one of the warm spot wells with locally high R_m.

Subsequently, uplift related to formation of the Ozark Dome in the late Paleozoic to early Mesozoic made the area of the Cherokee basin a positive element. Erosion of the Permian and Pennsylvanian rocks ensued and the flow system was disrupted. Another fluid derived from a topographically driven recharge system may have been introduced from the Ozark uplift. Evidence for meteoric influenced recharge is suggested by the presence of a low-salinity water now present in the Cambrian, Ordovician, and Mississippian rocks which are overlain by Pennsylvanian rocks containing significantly higher salinity fluids (Dingman and Angino, 1969). At present there is no fluid inclusion record of this low-salinity water intruding into the Pennsylvanian section.

CONCLUSIONS

The organic geochemistry and thermal history of the Cherokee basin indicates that some source rocks have enough thermally mature organic matter for hydrocarbon generation and for expulsion to have occurred. The heating required for oil generation is speculated to be related to warm water discharge from the adjacent basins to the south. We suggest that the warm spots are formed by warm upward flow along fractures and/or faults discharging into locally permeable rock packages within the Pennsylvanian strata of the Cherokee basin.

REFERENCES

Barker, C. E.; and Elders, W. A., 1981, Vitrinite reflectance geothermometry and apparent heating duration in the Cerro Prieto geothermal field: Geothermics, v. 10, p. 207–223.

Barker, C. E.; and Goldstein, R. H., 1990, A fluid inclusion technique for determining peak temperature and its application to establish a refined calibration for the vitrinite reflectance geothermometer: Geology, v. 18, p. 1003–1006.

Coveney, R. M., Jr.; Goebel, E. D.; and Ragan, V. M., 1987, Pressures and temperatures from aqueous fluid inclusions in sphalerite: Economic Geology, v. 82, p. 740–751.

Dembicki, H., Jr., 1984, An interlaboratory comparison of source rock data: Geochimica et Cosmochimica Acta, v. 48, p. 2641–2649.

Dingman, R. J.; and Angino, E. E., 1969, Chemical composition of selected Kansas brines as an aid to interpreting change of water chemistry with depth: Chemical Geology, v. 4, p. 325–339.

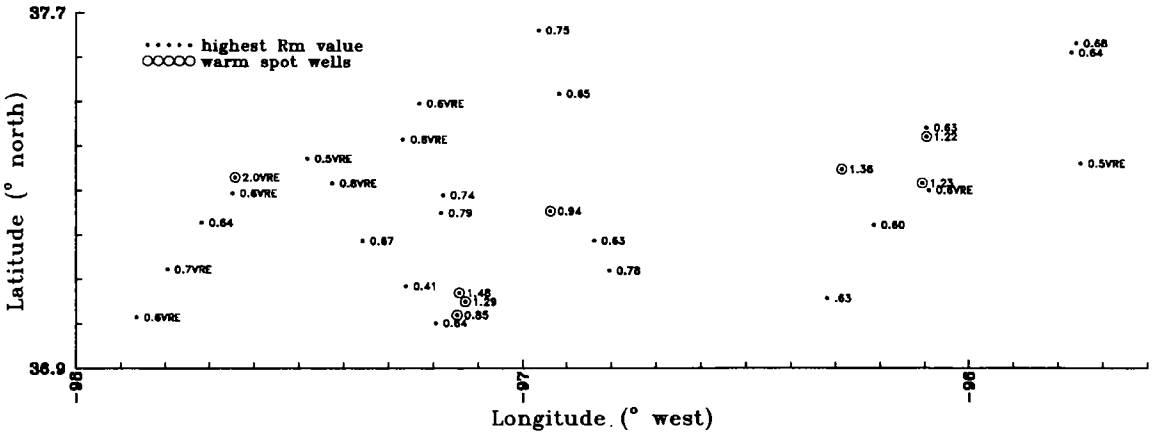

Figure 4. Preliminary map of warm spots in the Cherokee basin, southeast Kansas. Warm spots indicated by clusters of wells with (R_m) or vitrinite reflectance equivalent (VRE) higher than the regional mean random vitrinite reflectance. Point labels indicate the highest R_m or VRE value measured in the well. Circled points indicate wells with R_m >0.85%. Clusters of circled points constitute the warm spots discussed in the text.

Dow, W. G., 1977, Kerogen studies and geological interpretations: Journal of Geochemical Exploration, v. 7, p. 79–99.

Habicht, J. K. A., 1979, Paleoclimate, paleomagnetism, and continental drift: American Association of Petroleum Geologists, Studies in Geology 9, 31 p.

Hatch, J. R.; King, J. D.; and Daws, T. A., 1989, Geochemistry of Cherokee Group oils of southeastern Kansas and northeastern Oklahoma: Kansas Geological Survey Subsurface Geology Series 11, 20 p.

Hills, J. M.; and others, 1983, Southwest/southwest Midcontinent region; Correlation of Stratigraphic Units in North America (COSUNA) project: American Association of Petroleum Geologists, Tulsa.

Johnson, K. S., 1988, General geologic framework of the field-trip area [Arkoma–Ouachita area]: Oklahoma Geological Survey Guidebook 25, p. 1–5.

_____1989, Geologic evolution of the Anadarko basin, *in* Johnson, K. S. (ed.), Anadarko basin symposium, 1988: Oklahoma Geological Survey Circular 90, p. 3–12.

Jorgenson, D. G., 1989, Paleohydrology of the Anadarko basin, central United States, *in* Johnson, K. S. (ed.), Anadarko basin symposium, 1988: Oklahoma Geological Survey Circular 90, p. 176–193.

Kinney, D. M. (ed.), 1976, Geothermal gradient map of North America: American Association of Petroleum Geologists and U.S. Geological Survey, 2 sheets, scale 1:5,000,000.

Law, B. E.; Nuccio, V. F.; and Barker, C. E., 1989, Kinky vitrinite reflectance profiles: evidence of paleopore pressure in low permeability, gas-bearing sequences in Rocky Mountain foreland basins: American Association of Petroleum Geologists Bulletin, v. 73, p. 999–1010.

Leach, D. L.; and Rowan, E. L., 1986, Genetic link between Ouachita foldbelt tectonism and the Mississippi Valley-type lead–zinc deposits of the Ozarks: Geology, v. 14, p. 931–935.

McKee, E. D.; and others, 1959, Paleotectonic maps of the Triassic System: U.S. Geological Survey Map I-300, plate 6, 33 p.

McKee, E. D.; and others, 1967, Paleotectonic maps of the Permian System: U.S. Geological Survey Map I-450, 164 p.

Merriam, D. F., 1963, The geologic history of Kansas: State Geological Survey of Kansas Bulletin 162, 317 p.

Oliver, J., 1986, Fluids expelled tectonically from orogenic belts: their role in hydrocarbon migration and other geologic phenomena: Geology, v. 14, p. 99–102.

Peters, K. E., 1986, Guidelines for evaluating petroleum source rock using programmed pyrolysis: American Association of Petroleum Geologists Bulletin, v. 70, p. 318–329.

Robert, P., 1988, Organic metamorphism and geothermal history: D. Reidel Publishing Co., Boston, 311 p.

Sharp, J. M., Jr., 1978, Energy and momentum transport model of the Ouachita basin and its possible impact on the formation of economic mineral deposits: Economic Geology, v. 73, p. 1057–1068.

Stavnes, S. A.; and Steeples, D. W., 1982, Relationships between geology and geothermal gradients in Kansas, *in* Ruscetta, C. A. (ed.), Proceedings, Geothermal direct heat program roundup technical conference: Earth Science Laboratory, University of Utah Research Institute, Publication ESL-98, v. 1, p. 88–104.

Stewart, G. F., 1975, Kansas, *chapter H of* Paleotectonic investigations of the Pennsylvanian system in the United States: U.S. Geological Survey Professional Paper 853, p. 127–156.

APPENDIX: Organic Geochemistry Data, Cherokee Basin, Southeast Kansas

Rock-Eval pyrolysis and measurement of total organic carbon (C_{org}) are used to qualitatively evaluate organic matter geochemistry and thermal maturity. However, they must be used with qualification and(or) exclusion of results from low-organic content (less than about 0.5 wt % C_{org}) rocks and used with caution if organic contamination is present (Peters, 1986). The source rocks are characterized by C_{org} and pyrolysis assay to indicate the potential for generation and expulsion of hydrocarbons. Source rock richness is assessed by measuring C_{org}, which reflects the total quantity of organic matter present. Pyrolysis is used to determine: 1. the amount of volatile hydrocarbons present in the rock (S_1 parameter), an indication that petroleum generating reactions have occurred; 2. the potential for further generation of hydrocarbon (S_2 parameter); and 3. thermal maturity of the rock which is estimated from the temperature of the inflection point in the S_2 pulse (T_{max}). The S_3 pulse is a semi-quantitative measure of the amount of oxygen in the organic matter, and the S_2 pulse is one of the hydrogen content. By normalizing S_2 and S_3 to C_{org}, a qualitative van Krevelen diagram can be constructed, with the hydrogen index ($HI=[S_2/C_{org}] \times 100$), a measure of the H/C ratio in the organic matter and the oxygen index ($OI=[S_3/C_{org}] \times 100$), a measure of the O/C ratio of the organic matter. Further, the oil or gas generation potential of the rock is shown by the S_2/S_3 (HI/OI) ratio. In rocks that are just within the thermally mature stage window an S_2/S_3 below 3 indicates gas-prone organic matter, an S_2/S_3 above 5 indicates an oil-prone organic matter (Peters, 1986). Lithology should also be considered in the interpretation. For example, coals often generate very high S_2/S_3 ratios (>>5) indicating an overly oil-prone character (Peters, 1986).

Well name, Location	Present depth (ft)	Peak[1] depth (ft)	Lithology[2]	R_m[3] (%)	C_{org} (wt %)	T_{max} (°C)	HI mg HC/ g C_{org}	OI mg CO_2/ g C_{org}	S_1 mg HC/ g rock	S_2/S_3 mg HC/ mgCO_2
Union Gas Co.	1359	4959	stylocumulate (+bitumen)	0.4?	0.53	412	432	52	1.84	8.17
Leffingwell 16,										
sec.[4] 14, T.31S., R.10E.	1638	5238	dk gray mdst	1.36	0.45	N/R[5]	55	148	0.17	0.37
	1656.5	5256.5	black mdst	0.65	0.76	N/R	121	65	0.46	1.84
	1659	5259	dark gray mdst	N/A[6]	0.73	N/R	254	65	1.28	3.87
	1660	5260	med gray mdst	1.06	0.54	N/R	120	90	0.90	1.32
	1979	5579	stylocumulate	0.62	1.07	N/R	241	50	2.34	4.77
	1989	5589	stylocumulate	0.74	0.52	426	128	71	0.24	1.81
Colt 18 A.O. Keown,	832	5032	coal	0.55	72.03	430	338	27	22.05	12.53
sec. 22, T.23S., R.18E.	1003	5203	coal	0.57	74.49	440	257	21	33.09	11.73
	1031.5	5231.5	coal	0.52	69.91	428	260	19	3.03	13.63
	1063	5263	coal	0.58	47.80	432	240	N/R	4.25	N/R
	1109	5309	coal	0.60	67.10	432	277	5	1.76	52.80
	1198	5398	coal	0.57	63.00	432	300	6	2.07	45.56
Pittsburg Midway	19	4219	lt gray mdst	N/A	0.34	N/R	26	55	0.07	0.47
CH-13 Equildson,	21	4221	med gray mdst	N/A	0.33	N/R	30	45	0.06	0.66
sec. 19, T.34S.,R.18E.	29	4229	med gray mdst	0.5VRE	0.64	420	23	46	0.06	0.50
	63	4263	lt gray mdst	N/A	0.44	432	54	36	0.08	1.50
Brazos W-1 Pierpoint,	1016	5316	med gray mdst	0.7VRE	3.56	443	127	120	0.72	1.06
sec. 9, T.28S., R.15E.	1026	5326	coal	0.7VRE	41.24	435	307	31	35.10	9.61
	1029	5329	coal	0.64	63.77	433	271	23	16.22	11.47
	1049	5349	coal	0.60	31.30	443	198	42	8.44	4.66
	1059	5359	coal	0.68	56.05	446	285	22	18.30	12.93
	1067	5367	med gray mdst	0.8VRE	1.54	447	100	212	0.50	0.47
Brazos O-11 Pierpoint,	333.5	4533.5	med gray mdst	0.6VRE	0.75	429	85	62	0.11	1.36
sec. 9, T.28S., R.15E.	360	4560	carb mdst	0.5VRE	0.55	421	58	52	0.07	1.10
	376	4576	dk gray mdst	0.6VRE	1.39	430	124	27	0.29	4.55
	385	4585	stylocumulate	0.6VRE	4.01	434	256	17	1.45	14.47
Kansas Geological Survey	85	4485	med gray mdst	N/A	0.31	385	58	41	0.07	1.38
JJ	93.5	4493.5	coal	0.79	20.56	437	132	12	0.59	10.85
sec. 26, T.27S.,R.25E.	93.5	4493.5	dk gray mdst	0.6VRE	2.29	434	90	86	0.18	1.04
	100	4500	coal	0.74	36.25	435	237	7	2.65	30.69
	220	4620	carb mdst	0.6VRE	2.16	434	112	45	0.43	2.45
	231	4631	coaly fossil	0.68	56.77	439	234	17	1.01	13.51
	236.5	4636.5	dk gray mdst	0.7VRE	1.79	436	84	8	0.31	10.06

Well name, Location	Present depth (ft)	Peak[1] depth (ft)	Lithology[2]	R_m[3] (%)	C_{org} (wt %)	T_{max} (°C)	HI mg HC/ g C_{org}	OI mg CO_2/ g C_{org}	S_1 mg HC/ g rock	S_2/S_3 mg HC/ mgCO_2
Shell Scroggins 3A,	2403	5003	stylocumulate	0.57	0.88	435	26	71	0.10	0.36
sec. 14, T.32S., R.2E.	2405	5005	dk gray mdst	0.52	0.54	427	48	116	0.08	0.41
	2430	5030	med gray mdst	0.96	0.28	N/R	57	217	0.06	0.26
	2825	5425	dk gray mdst	0.53	0.67	426	55	22	0.16	2.46
Shell Rothwell 6,	2342	4942	med gray mdst	0.55	0.57	430	61	115	0.08	0.53
sec. 14, T.32S., R.2E.	2804	5404	med gray mdst	0.5?	1.01	432	103	86	0.13	1.2
	2810	5410	med gray mdst	0.55	0.49	389	59	42	0.20	1.38
	2816	5416	med gray mdst	0.74	2.49	564	2	9	0.01	0.21
Sinclair-Prairie	2212	4912	med gray mdst	0.62	0.73	428	31	109	0.09	0.28
1 Schurtz,	2699	5399	coaly debris	0.70	0.15	603	326	113	0.09	2.88
sec. 29, T.34S., R.3E.	2876	5576	coaly debris	0.63	0.86	437	61	62	0.13	0.98
	3329	6029	med gray mdst	1.6	0.16	529	162	106	0.04	1.52
	3345	6045	med gray mdst	1.3	0.07	503	271	714	0.05	0.38
Sinclair-Prairie 1 Weir,	2749	5449	coaly debris	0.64	0.46	432	108	28	0.17	3.84
sec. 30, T.34S., R.3E.	3071	5771	lt gray sdst	1.5	0.13	N/R	84	123	0.04	0.68
	3120	5820	coaly mdst	0.7	5.90	444	118	13	0.93	8.93
	3433	6133	med gray mdst	0.59	1.80	445	83	13	0.30	6.00
Conoco 17-1 Rahn Unit,	2110	5010	coaly debris	0.63	15.81	443	211	25	4.88	8.30
sec. 5, T.34S., R.6E.	2119	5019	coaly fossil	0.78	35.14	445	177	15	6.79	11.58
	2125	5025	coaly debris	0.71	17.93	440	208	13	6.77	15.29
Sinclair 1 Collinson,	2273	4973	coaly debris	0.62	1.43	434	110	19	0.39	5.64
sec. 31 T.34S., R.3E.	2284	4984	dk gray mdst	0.85	4.53	N/R	11	19	0.15	0.57
	3485	6185	coaly fossil	0.80	1.52	448	75	14	0.20	5.26
Stelbar 4 Floyd,	1973	5573	dk gray mdst	barren	0.22	N/R	54	131	0.02	0.41
sec. 31, T.32S., R.11E.	1981	5581	breccia matrix	0.60	0.28	409	396	96	0.45	4.11
Sinclair 25 Kukuk,	2989	5889	coaly debris	0.94	18.26	450	176	22	4.9	7.68
sec. 24, T.32S., R.4E.	3027	5927	coaly fossil	0.92	14.07	451	155	35	2.87	4.32
Shell 1 Buffington,	2452	5052	med gray mdst	0.79	1.05	439	94	61	0.24	1.52
sec. 14, T.32S., R.2E.	2462	5062	coal	0.55	75.94	426	342	17	3.6	19.92
	2895	5495	carb mdst	0.53	1.46	439	69	59	0.24	1.17
Terra Resources	3682	5682	lt gray mdst	N/A	0.06	N/R	350	233	0.09	1.50
Peasel 1,	3697	5697	lt gray mdst	N/A	0.46	N/R	234	115	1.50	2.03
sec. 33, T.31S., R.1W.	4087	6087	dk gray mdst	0.7VRE	3.31	444	339	35	1.72	9.60
	4104	6104	dk gray mdst	0.7VRE	3.30	443	361	22	1.36	15.90
Petrodynamics	2053	4053	med gray mdst	0.5VRE	0.63	421	30	211	0.02	0.14
Castleman 1,	2056	4056	med gray mdst	0.6VRE	0.62	425	56	256	0.05	0.22
sec. 4, T.31S., R.1W.	2074	4074	coaly debris	0.7VRE	1.00	437	45	99	0.13	0.45
Derby 1 Ritz	2535.5	5225.8	med gray mdst	0.38?	0.65	N/R	52	10	0.10	4.85
sec. 25, T.31S. R.3E.	2625.8	5225.8	med gray mdst	1.54?	0.32	N/R	56	12	0.05	4.50
	2654	5254	carb mdst	0.62	3.12	440	117	N/A	0.52	N/A
	2661	5261	dk gray mdst	0.55	4.23	432	43	N/A	0.28	N/A
Wheeler 1 Richardson,	3017	5917	lt gray lmst	0.47?	0.08	N/R	52	10	0.10	4.85
sec. 12, T.33S., R.5E.	3025	5925	stylocumulate	0.63?	0.18	N/R	94	188	0.07	0.50
Anadarko Rusk A	3780	6080	stylocumulate	0.67	0.16	586	631	31	0.53	20.20
sec. 18, T.33S., R.1E.	3789	6089	stylocumulate	0.67	0.12	592	766	33	0.22	23.00
IPI Hadlock 2,	1457	5357	lt gray mdst	1.23?	0.12	458	308	25	0.05	12.33
sec. 28, T.31S.,R.12E.	1472	5372	med gray mdst	0.59	1.28	443	131	18	0.24	7.00
McBride 1 Kinland,	3550	6450	lt gray mdst	0.41?	0.05	N/R	320	120	0.04	2.66
sec. 24, T.34S., R.1E.										
Masek Day 24-17,	1784	5684	stylocumulate	0.58	0.07	586	485	14	0.12	34.00
sec. 17, T.30S., R.12E.										
Masek Day 31-21,	864	4764	coaly debris	0.63	1.23	442	156	3*	0.59	48.25
sec. 21, T.30S., R.12E.	868	4768	coaly debris	0.57	0.18	N/R	155	22	0.12	7.00
Kiska Forbeck 2,	2740	5340	coaly fossil	0.64	1.66	443	163	2	0.55	68.00
sec. 15, T.35S., R.2E.										
Phillips 1 Lena,	3068	5968	lt gray sdst	0.68	0.30	N/R	420	50	1.23	8.40
sec. 17, T.32S., R.5E.	3047	5947	lt gray sdst	0.63	0.18	N/R	361	150	0.43	2.40
Wheeler Rockwell 2	3065	5965	med gray sdst	0.45?	3.82	443	253	13	6.84	18.96
sec. 12, T.33S., R.5E.			(+ bitumen)							

Well name, Location	Present depth (ft)	Peak[1] depth (ft)	Lithology[2]	R_m[3] (%)	C_{org} (wt %)	T_{max} (°C)	HI mg HC/ g C_{org}	OI mg CO_2/ g C_{org}	S_1 mg HC/ g rock	S_2/S_3 mg HC/ mgCO_2
Wheeler Rockwell 3	3088	5988	stylocumulate	0.56?	0.07	N/R	171	928	0.06	0.18
sec. 12, T.33S., R.5E.										
Masek 13-16 Sherwin,	1130	5330	med gray mdst	N/A	0.26	N/R	130	223	0.24	0.58
sec. 16, T.31S., R.15E	1138.5	5338.5	med gray mdst	0.8VRE	0.45	449	124	46	0.35	2.66
Texas Bing 2,	2791	5891	med gray mdst	N/A	0.09	N/R	266	388	0.13	0.68
sec. 2, T.28S., R.7E.	2827	5927	stylocumulate	N/A	0.50	N/R	84	64	0.14	1.31
Holt Holt 9,	866	5066	med gray mdst	N/A						
sec. 25, T.31S., R.16E.	873	5073	med gray mdst	N/A	0.36	N/R	419	58	0.91	7.19
Masek 43-17 Sherwin,	1152	5352	med gray sdst	0.5VRE	1.20	424	221	140	1.44	1.58
sec. 17, T.31S., R.15E.										
Masek 3-22-25 Watson,	982	4882	carb mdst	0.7VRE	10.22	440	205	10	5.18	19.40
sec. 25, T.34S., R.13E.										
Masek 2-21-29 Barnett	810	4710	coaly debris	0.6VRE	1.28	434	161	17	0.75	9.00
sec. 29 T.34S., R.13E.	819	4719	coaly fossil	0.63	16.24	439	94	22	1.02	4.09
Neal 6 Tartar	989	5189	dk gray sdst	0.6VRE	4.73	434	295	19	6.79	15.20
sec. 16, T.28S., R.15E.	1016	5216	coal	0.61	53.54	437	310	22	20.16	13.92
	1022	5222	coal	0.64	22.66	433	331	25	13.13	13.26
DiCo Hazel Estes 7	857	5057	med gray mdst	N/A	0.41	N/R	100	19	0.32	5.12
sec. 30, T.29S., R.17E.	887	5087	coaly fossils	0.7VRE	10.83	441	278	28	5.48	9.81
	905	5105	coaly fossils	0.67	59.50	435	405	11	10.17	36.57
	916	5116	coaly fossils	0.73	10.44	442	203	33	3.81	6.08
Masek 33-10 Jones	706	4906	coal	0.77	20.50	444	154	16	4.90	9.30
sec. 10, T.31S., R.15E.										
Masek 42-17 Trombold,	680	4580	lt gray sdst	N/A	0.21	N/R	409	52	0.41	7.81
sec. 17, T.31S., R.13E.	683	4583	medgray mdst	N/A	0.43	435	155	37	0.42	4.18
Atlas Minerals	3991	5791	stylocumulate	0.4VRE	0.73	410	156	72	0.47	2.15
Phillips 1	4030	5830	stylocumulate	0.64?	1.50	432	234	200	1.28	1.16
sec. 35, T.32S., R.4W.										
IPI Dyer 7,	1178	5078	mdst	N/A	0.44	446	81	79	0.14	1.02
sec. 33, T.31S., R.12E.	1190	5090	med gray sdst	0.7VRE	0.55	436	116	34	0.20	3.36
	1310	5210	coaly sdst.	0.7VRE	17.98	435	292	10	5.85	29.01
Trico Jameson	411.5	4311.5	med gray mdst	0.66?	0.78	N/R	55	46	0.20	1.19
1A, 2A, 3A,	425	4325	coal	0.53	45.77	427	251	21	27.75	11.51
sec. 14 T.32S., R.12E.	429	4329	med gray mdst	0.52	1.09	432	81	21	0.24	3.86
	434	4334	coal	0.53	39.30	431	70	14	17.50	4.81
	441	4341	dk gray mdst	N/A	1.29	N/R	320	40	1.20	7.94
	450	4350	coal	0.59	47.57	435	96	27	10.57	3.57
Sinclair 20 Skaer	2089	4989	stylocumulate	0.5VRE	0.65	421	243	86	1.05	2.82
sec. 35, T.27S., R.4E.	2507	5407	med gray mdst	N/A	0.29	N/R	65	175	0.05	0.37
	2522	5422	coal	0.75	68.53	458	81	15	6.00	5.10
	2571	5471	med gray mdst	N/A	0.19	420	200	136	0.07	1.46
	2623	5523	lt gray sdst	N/A	0.12	N/R	250	433	0.06	0.57
Mack Misak 1,	4725	6525	dk gray mdst	0.8VRE	3.36	448	231	11	1.21	19.94
sec. 6, T.34S., R.4W.										
Commonwealth Farber 1A,	3529	5129	med gray mdst	0.7VRE	1.48	439	419	12	0.52	34.50
sec. 29, T.29S., R.2E.	3538	5138	dk gray mdst	0.7VRE	12.37	438	523	7	4.52	72.76
Beardmore Haines 1,	3774		lt gray mdst	N/A	0.43	431	60	93	0.16	0.65
sec. 12, T.31S., R.2W.										
Masek Day 42-16	1725	5625	coal or bitumen	0.8VRE	6.52	448	203	52	7.06	3.90
sec. 16, T.30S., R.12E.	1725.5	5625.5	stylocumulate (+ bitumen)	1.2?	42.13	453	201	23	24.80	8.71
Shell 1 Williams,	4866	6666	dk gray mdst	N/A	0.44	439	131	72	0.19	1.81
sec. 9, T.35S., R.5W.	4756	6556	dk gray mdst	0.7VRE	0.65	439	129	63	0.25	2.04
Petrodynamics Graham 1,	2110	3910	med gray mdst	0.6VRE	0.62	429	27	224	0.02	0.12
sec. 21, T.31S., R.3W.	2126	3926	med gray mdst	5.4VRE	0.63	567	103	22	0.07	4.64
	2142	3942	med gray mdst (+ sulfides)	5.4VRE	0.60	567	96	21	0.08	4.46

Well name, Location	Present depth (ft)	Peak[1] depth (ft)	Lithology[2]	R_m[3] (%)	C_{org} (wt %)	T_{max} (°C)	HI mg HC/ g C_{org}	OI mg CO_2/ g C_{org}	S_1 mg HC/ g rock	S_2/S_3 mg HC/ mgCO_2
D.E.I. Goyer 1,	3505	5805	dk gray mdst	0.7VRE	2.35	437	405	15	1.16	25.78
sec. 25, T.30S., R.1E.	3518	5818	dk gray mdst	0.7VRE	2.19	440	394	17	1.10	22.15
Atlas 1 Zook,	3938	5738	med gray mdst	N/A	0.08	442	237	137	0.02	1.72
sec. 35, T.32S., R.4W.	3948	5748	stylocumulate	N/A	2.24	N/R	33	179	0.32	0.18
	3957	5757	med gray mdst	N/A	0.05	553	400	200	0.01	2.00
	3963	5763	stylocumulate		0.18	431	88	144	N/R	0.61
	3963	5763	coaly debris	0.7VRE	2.43	439	130	28	0.69	4.59
	3971	5771	lt gray sdst	N/A	0.13	N/R	13	200	0.03	0.06
Kansas Geological Survey	35	1835	med gray mdst	N/A	0.37	N/A	10	51	0.01	0.21
Cu1,	61.5	1861.5	med gray mdst	N/A	0.32	N/R	6	115	0.01	0.05
sec. 33, T.28S., R.3W.										
Kansas Geological Survey	40	1840	med gray sdst	N/A	0.17	N/R	29	117	0.08	0.25
Cu2,	80	1880	med gray mdst	N/A	0.45	N/R	28	80	0.03	0.36
sec. 35, T.28S., R.4W.	118.5	1918.5	med gray mdst	0.5VRE	2.45	422	20	109	0.03	0.18
Kansas Geological Survey	60	1860	med gray mdst	0.5VRE	0.80	422	26	23	0.02	1.10
Cu3,	68.3	1868.3	med gray mdst	0.4VRE	0.63	414	39	266	0.02	0.14
sec. 11, T.28S., R.4W.										
Kansas Geological Survey	24	1824	lt gray mdst	N/A	0.33	414	202	94	0.41	2.46
Cu5,										
sec. 20, T.31S., R.2W.										
Kansas Geological Survey	86	4486	coal	0.69	49.13	437	164	9	10.72	16.47
Z,	155	4555	coaly debris	0.62	36.70	436	335	11	5.27	29.48
sec. 26, T.27S., R.25E.	164	4564	coal	0.58	68.22	431	328	9	1.78	33.07
Brazos Pierpoint O-5,	1010	5310	med gray mdst	0.7VRE	2.18	441	120	129	0.75	0.92
sec. 9, T.8S., R.15E.	1038	5338	med gray mdst	0.7VRE	1.61	437	185	133	0.87	1.39
	1052.5	5352.5	med gray mdst	0.6VRE	1.19	426	277	80	1.38	3.43
Range Pottoiff 3	2784.3	5684.3	coal	0.61	74.06	428	333	15	17.70	21.92
sec. 20, T.29S., R.5E.	2788.6	5688.6	coal	0.65	72.74	434	337	14	18.78	22.91
H. Corr Core Test 1,	200	2300	med gray mdst	N/A	0.43	604	362	262	0.04	1.38
sec. 21, T.29S., R.2W.	330	2430	med gray mdst	N/A	0.50	N/R	82	354	1.33	0.23
	460	2560	med gray mdst	0.5VRE	1.41	419	70	132	0.55	0.52
Gulf Minerals,	45.5	4445.5	coal	0.7VRE	8.30	438	56	7	0.55	7.37
P and M 10	60	4460	coal	0.67	69.36	434	276	5	2.70	54.14
sec. 22, T.31S., R.22E.	80	4480	coal	0.58	52.06	438	289	7	3.46	39.26
	134	4534	coal	0.63	51.46	436	418	7	2.40	55.81
	145.5	4545.5	coal	0.68	66.51	434	221	6	1.70	33.55
	175.5	4575.5	coal	0.66	57.67	435	263	5	1.42	47.35
	205	4605	coal	0.64	76.49	437	289	8	2.98	36.11
	227.5	4627.5	coal	0.69	67.25	438	287	8	6.04	32.03
	281	4681	coal	0.64	29.57	437	237	11	0.98	19.94
	300	4700	coal	0.73	58.44	438	235	6	1.14	33.66
	307	4707	coal	0.70	70.66	437	288	7	2.50	38.85
	344	4744	coal	0.69	55.34	437	302	7	3.88	41.13
	364	4764	coal	0.60	52.97	437	252	7	5.78	31.76
	378	4778	med gray mdst	N/A	0.50	N/R	N/R	334	0.01	N/R
	380	4780	stylocumulate	0.5VRE	0.69	415	31	81	0.18	0.39
	385	4785	stylocumulate	0.6VRE	2.07	426	128	37	1.03	3.45
	400	4800	lt gray sdst	N/A	0.08	N/R	75	250	0.03	0.30
	430	4830	stylocumulate	N/A	0.76	N/R	28	28	0.05	1.00
	480	4880	stylocumulate	0.7VRE	3.58	437				
	503	4903	stylocumulate	0.7VRE	5.09	436	138	14	0.34	9.26
	506.5	4906.5	stylocumulate	0.7VRE	1.08	440	131	57	0.19	2.29
	520	4920	stylocumulate	0.6VRE	2.82	434	36	49	0.17	0.74
	546	4946	stylocumulate	N/A	0.30	429	20	73	0.02	0.27
	587	4987	stylocumulate	0.6VRE	0.72	434	77	45	0.10	1.69
	643	4943	med gray mdst	N/A	0.08	N/R	62	250	0.04	0.25
	718	5018	med gray mdst	N/A	0.51	N/R	7	47	0.01	0.16
	797	5097	med gray mdst	N/A	0.46	N/R	50	50	0.05	1.00

Well name, Location	Present depth (ft)	Peak[1] depth (ft)	Lithology[2]	R_m[3] (%)	C_{org} (wt %)	T_{max} (°C)	HI mg HC/ g C_{org}	OI mg CO_2/ g C_{org}	S_1 mg HC/ g rock	S_2/S_3 mg HC/ mgCO_2
Gulf Minerals,	808	5108	med gray lmst	N/A	0.02	N/R	250	550	0.05	0.45
P and M 10	848	5148	stylocumulate	0.5VRE	0.50	418	80	44	0.14	1.81
(continued)	875	5175	med gray mdst	N/A	0.38	413	78	50	0.08	1.57
	904.5	5204.5	med gray mdst	N/A	0.36	398	86	58	0.09	1.47
	980	5280	med gray mdst	N/A	0.14	N/A	50	114	0.05	0.43
Gulf Minerals,	100	4500	Bevier coal	0.7VRE	71.05	435	257	11	7.17	21.55
P and M 20	120	4520	Croweberg coal	0.8VRE	68.63	445	174	15	2.38	11.46
sec. 8, T.31S., R.22E.	128	4528	Fleming coal	0.7VRE	72.89	436	280	10	6.55	26.93
	153	4553	Mineral coal	0.7VRE	69.33	435	284	6	2.43	44.89
	178	4578	Scammon coal	0.7VRE	66.70	436	297	7	3.04	41.47
	231	4631	Tebo coal	0.64	35.82	441	198	8	1.02	22.27
	240.5	4640.5	carb mdst	0.8VRE	1.82	446	43	30	0.24	1.41
	272	4672	Abj coal	0.7VRE	55.45	435	297	7	5.95	40.86
	300	4700	Cbj coal	0.7VRE	69.14	436	321	7	8.31	40.79
	318	4718	Dbj coal	0.7VRE	79.32	438	221	9	10.32	22.67
	353	4753	Rowe coal	0.7VRE	67.70	438	238	8	2.45	28.15
	402	4802	Aw coal	0.7VRE	60.78	440	223	10	1.70	22.26
	410.5	4810.5	Bw coal	0.7VRE	52.93	440	267	8	4.78	32.58
	428.5	4828.5	Cw coal	0.7VRE	76.27	443	211	13	5.60	16.16
	439.5	4839.5	Dw coal	0.7VRE	69.46	435	316	9	5.83	31.70
	469	4869	Riverton coal	0.7VRE	72.41	442	295	8	6.51	34.12
	484	4884	black mdst	0.7VRE	2.88	438	83	10	0.55	8.31
	591	4991	med gray mdst (top Miss.)	0.6VRE	1.08	434	77	18	0.20	4.20
Job Service Center 7	27	4427	Weir coal	0.7VRE	62.96	443	296	8	2.59	36.03
sec. 30, T.30S., R.25E.	60	4460	Abj coal	0.8VRE	73.60	448	207	5	2.00	35.49
	70.5	4470.5	Bbj coal	0.6VRE	69.70	434	315	6	1.48	51.66
	104	4504	Dbj coal	0.7VRE	76.39	438	267	5	2.89	45.68
	109.5	4509.5	Drywood coal (R_s = 0.35)	1.1? 0.8VRE	24.04	444	39	10	0.36	3.71
	118	451	Rowe Coal	0.66	59.68	436	299	8	3.43	35.75
	137.5	537.5	Neutral Coal	0.70	65.88	438	287	2	4.83	98.27
	173.5	573.5	Aw coal	0.63	49.97	436	282	7	8.00	38.86
	178	4578	Bw coal	0.67	58.86	438	286	7	3.68	37.67
	195	4595	Cw coal	0.72	68.85	439	308	9	4.09	33.44
	222	4622	Dw coal	0.74	62.53	440	292	6	5.26	46.48
	232	4632	coal	0.64	66.73	441	299	3	7.36	76.04
	238	4638	carb mdst	0.7VRE	2.57	439	77	10	0.52	7.37
	239	4639	carb mdst (top Miss.)	0.6VRE	2.74	432	40	16	0.55	2.50
	240	4640	lt gray mdst	N/A	0.03	N/R	366	333	0.07	1.10

1. Peak depth = maximum burial depth estimated from burial reconstruction (fig.1).
2. Lithology abbreviations: mdst = mudstone; sdst = sandstone; lmst = limestone; carb = carbonaceous; med = medium; lt = light; Miss. = Mississippian; HC = hydrocarbon.
3. R_m = mean random vitrinite reflectance; R_s = mean random sporinite reflectance; VRE = Vitrinite reflectance equivalent estimated from a regression analysis of measured Rock-Eval T_{max} and R_m pairs in the Cherokee basin (R_m = 0.00055 exp 0.016T_{max}) or where indicated by using R_s data; barren = a sample in which no usable vitrinite was recovered; A question mark indicates a difficult reflectance analysis usually due to sparse or multiple populations of vitrinite present or undetected bitumen in the sample.
4. Sec. = section
5. N/R = not reported.
6. N/A = not available.

Hydrodynamics of Deep-Basin Flow: Constraints on Timing of Midcontinent MVT Deposits and a Mechanism for Heating Pennsylvanian Coal

Lorraine H. Filipek
U.S. Geological Survey, Denver

Paleotopographic reconstructions suggest that major changes in regional ground-water flow systems occurred in the southern Midcontinent from Late Mississippian through Pennsylvanian time. Some of these flow systems are believed to be responsible for the formation of the world-class Mississippi Valley-type lead–zinc deposits (MVTs) of the region. The temporal evolution of these systems may have caused the decreasing south-to-north regional thermal gradient that is reflected in Pennsylvanian coals and fluid-inclusion filling temperatures of the MVTs and associated pre-Permian rocks. This presentation synthesizes the literature on MVTs, deep-basin flow, and the Quinlan and Beaumont (1984) model of flexural interaction between basins in order to constrain further the timing of the regional shifts in ground-water flow and the thermal events that produced the MVTs and heated the coals.

Several researchers have presented evidence that MVTs were formed by hot ground water that flowed out of deep basins. The driving force for fluid migration is believed to be either basin compaction (Sharp, 1978) or normal hydrologic gradients ("gravity flow"—e.g., Garven and Freeze, 1984). One group of MVTs, those of southeast and central Missouri, northern Arkansas, and the Tri-State district, is believed by some geologists (e.g., Leach and others, 1984) to have formed mainly by deep flow from the Arkoma basin during Pennsylvanian–Permian time. Several geochemical studies (Viets and others, 1989; Goldhaber and others, 1989) suggest that the southeast Missouri ores formed from fluids of two or more compositions. Based on paleodrainage patterns described by Howard (1979) and Greb (1989), the first stages of the southeast Missouri deposits could have formed by flow out of the Illinois basin or Reelfoot Rift during Late Mississippian/Early Pennsylvanian time. Alternately, they could have formed from compaction fluids that migrated northward from the rapidly subsiding Arkoma and Black Warrior foredeeps during early Middle Pennsylvanian time. In either case, the later stages of these deposits and most of the other MVTs in the region could have formed in Middle to Late Pennsylvanian time. During this period, appropriate hydrologic conditions were present for significant northward, gravity-driven flow out of the Arkoma or Black Warrior basins. Also during this period, the regional thermal gradient was probably the reverse of that preserved in the geologic record. Erosion of the Ouachita Mountains and uplift of the Ozark Dome in Late Pennsylvanian/Early Permian time probably caused a gradual shift in the deep ground-water flow system from a regional northward flow to a more localized and generally westward flow, thereby cutting off the supply of hot fluids to the MVTs, while simultaneously heating the rocks and coal nearer the ground-water source. By Early Permian time, through-to-basement faulting in the Arkoma basin "short-circuited" the horizontal water flow by moving hot water up the faults and heating the coals in the basin to anthracite rank. As these examples show, hydrologic models are useful for testing geologic hypotheses and for focusing research objectives.

REFERENCES

Garven, G.; and Freeze, R. A., 1984, Theoretical analysis of the role of groundwater flow in the genesis of stratabound ore deposits. 1.—Mathematical and numerical model: American Journal of Science, v. 284, p. 1085–1124.

Goldhaber, M. B.; Church, S. E.; and Doe, B. R., 1989, Pb isotopic constraints on fluid flow paths for Mid-Continent Mississippi Valley type (MVT) Pb–Zn ores [abstract]: Geological Society of America Abstracts with Programs, v. 21, no. 6, p. A4.

Greb, S. F., 1989, Structural controls on the formation of the sub-Absaroka unconformity in the U.S. Eastern Interior basin: Geology, v. 17, p. 889–892.

Howard, R. H., 1979, The Mississippian–Pennsylvanian unconformity in the Illinois basin; old and new thinking, *in* Palmer, J. E.; and others (eds.), Depositional and structural history of the Pennsylvanian System of the Illinois basin: Illinois State Geological Survey Guidebook 15, part 2, p. 34–42.

Leach, D. L.; Viets, J. G.; and Rowan, L., 1984, Appalachian–Ouachita orogeny and Mississippi Valley-type lead–zinc deposits [abstract]: Geological Society of America Abstracts with Programs, v. 16, p. 572.

Quinlan, G. M.; and Beaumont, C., 1984, Appalachian thrusting, lithospheric flexure, and the Paleozoic stratigraphy of the Eastern Interior of North America: Canadian Journal of Earth Sciences, v. 21, p. 973–996.

Sharp, J. M., Jr., 1978, Energy and momentum transport model of the Ouachita basin and its possible impact on formation of economic mineral deposits: Economic Geology, v. 73, p. 1057–1068.

Viets, J. G.; Leach, D. L.; and Mosier, E. L., 1989, Two distinct ore fluids in the Viburnum trend; genetic implications, *in* Hagni, R. D.; and others (eds.), Mississippi Valley-type mineralization of the Viburnum trend, Missouri: Society of Economic Geologists Guidebook, p. 155–165.

Geochemical and Fluid Inclusion Evidence for Regional Alteration of Upper Cambrian Carbonates by Basinal Fluids in Southern Missouri

Jay M. Gregg, Kevin L. Shelton, and Rita M. Bauer
University of Missouri

ABSTRACT.—The southeast Missouri Mississippi Valley-type Pb–Zn–Cu district formed during influx of massive volumes of saline fluids from nearby sedimentary basins. The timing of fluid migration likely coincided with Ouachita tectonism (Late Pennsylvanian to Early Permian). These fluids, which were chemically similar to petroleum-reservoir waters, altered rocks over an area >25,000 km² in southern Missouri.

Distinct minor- and trace-element trends were observed in the basal Bonneterre dolomite. The data are interpreted to indicate south-to-north flow of fluid originating in the Arkoma basin and northeast-to-southwest flow from the Illinois basin. Microthermometric measurements of fluid inclusions in the Bonneterre Dolomite indicate that at least two distinct fluids were present during epigenetic dolomitization and sulfide mineralization. No discernible temperature gradient was observed over the study area, as had been postulated by previous studies.

INTRODUCTION

The world class southeast Missouri Mississippi Valley-type (MVT) lead–zinc–copper district, including the Viburnum trend subdistrict, formed during the influx of massive volumes of saline fluids from nearby sedimentary basins (Fig. 1) (Gerdemann and Myers, 1972; Gregg and Shelton, 1989a). These fluids altered rocks over an area >25,000 km² in southern Missouri. This paper presents a synopsis of the ongoing research at the University of Missouri on regional basinal fluid flow associated with epigenetic dolomitization and Mississippi Valley-type (MVT) mineralization (Gregg and Shelton, 1989b; Bauer, 1989). Trace-element and fluid-inclusion analyses provide powerful tools in documenting the sources and pathways of basinal fluids as well as timing relative to petroleum migration, epigenetic dolomitization, and ore mineralization. These studies show that epigenetic dolomitization and sulfide mineralization in southern Missouri were the results of a complex, hydrologic system involving multiple basin sources, as opposed to a single Arkoma basin source as suggested by previous studies (e.g., Leach and Rowan, 1986).

MVT mineralization is common in cratonic carbonate sequences throughout the world (Anderson and Macqueen, 1982; Sverjensky, 1986). These deposits are characterized by galena, sphalerite, and other metal sulfides associated with epigenetic dolomite and calcite cements. MVT mineralization and petroleum are closely associated in the geological record (e.g., Fowler, 1933; Marikos and others, 1986; Mazzullo, 1986). Both result from coeval processes that occur in sedimentary basins. The basinal fluids which precipitated MVT sulfide minerals are thought to be chemically similar to

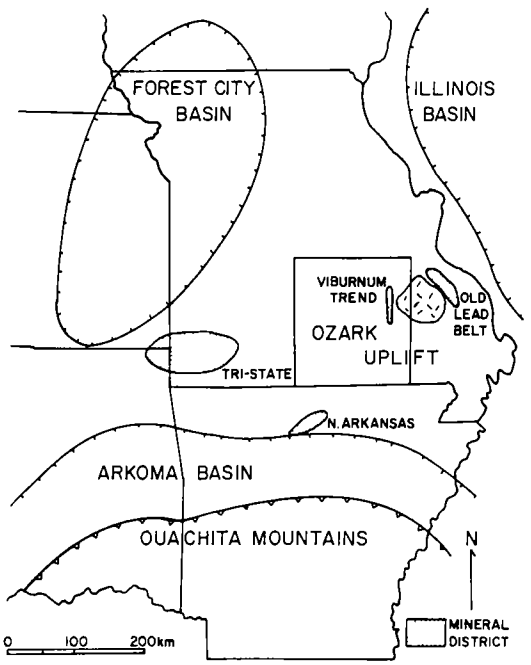

Figure 1. Location of the study area in southern Missouri, the igneous St. Francois Mountains (hachured), major sedimentary basins, and MVT mineral districts.

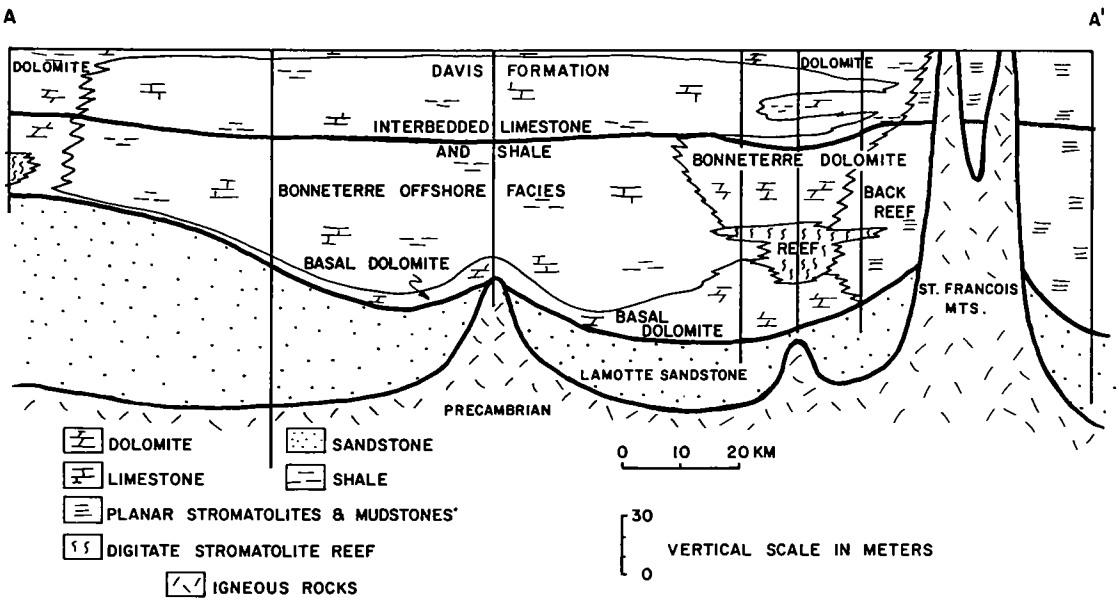

Figure 2. Stratigraphic section showing the relationship of Bonneterre facies to the underlying Lamotte Sandstone and Precambrian basement. Note the basal Bonneterre dolomite overlying the Lamotte–Bonneterre contact. Vertical lines show the locations of cores used in the cross section. The location is shown on Figure 3.

many petroleum-reservoir waters (Sverjensky, 1984). Therefore, geochemical reconstruction of basin fluid-flow patterns and pathways will also prove invaluable in understanding the migration of petroleum in the Midcontinent.

GEOLOGIC SETTING

The Bonneterre Dolomite forms the lower part of an Upper Cambrian platform-carbonate sequence in southeastern Missouri and is the primary host of the MVT ore bodies of the region (for detailed discussions see Skinner, 1977). The Bonneterre was deposited as a series of facies belts: intracratonic basin (offshore), algal stromatolite bioherm-grainstone (reef), and peritidal mudstones and cryptalgalaminates (back reef) facies in a shallow sea surrounding islands formed by the Precambrian igneous St. Francois Mountains (Fig. 2). The reef and back reef facies are pervasively dolomitized. Initial dolomitization of these facies likely occurred soon after deposition by Cambrian seawater. Further dolomitization and neomorphism of preexisting dolomite occurred in the subsurface during the period of sulfide mineralization (Gregg and Gerdemann, 1989; Gregg and Shelton, 1990). The offshore facies consists of interbedded marine limestones and shales (Gregg, 1988). The Bonneterre is underlain by the Lamotte Sandstone, the regional aquifer through which basinal fluids were transmitted (Gerdemann and Myers, 1972). A regional basal Bonneterre dolomite, averaging 6 m thick (Fig. 2), was formed during circulation of basinal fluid in the underlying Lamotte Sandstone (Gregg, 1985,1988; Gregg and Shelton, 1989b).

TRACE-ELEMENT STUDIES

A fluid will leave its chemical signature on a dolomite which precipitates from it. Distribution theory predicts that fractionation of a trace or minor element between an aqueous fluid and a growing crystalline phase is controlled by its distribution coefficient (K_d, defined as the ratio of concentration in the solid to concentration in the fluid). When a K_d is >1, the species will fractionate preferentially into the crystalline phase; when K_d is <1, the species will fractionate preferentially into the aqueous phase (McIntire, 1963). Several divalent ions commonly substitute into dolomite and their K_d values are: Fe>1, Mn>1, and Sr<1 (Veizer, 1983). Fe and Mn substitution in dolomite should increase and Sr should decrease in the down-flow direction of the dolomitizing solution (Machel, 1989).

Samples of epigenetic replacement dolomite were collected from 35 drill cores in the basal Bonneterre dolomite (Figs. 2,3). Powders of individual crystals were collected with a microdrill and analyzed for Fe, Mn, and Sr using ICP analysis. West of the Viburnum trend, in the basal dolomite underlying offshore facies of the Bonneterre (Fig. 3; Gregg and Shelton, 1989b), distinct regional

trends in concentrations of these elements were observed. Concentrations range from 3.47 wt%, 0.38 wt%, and 27 ppm in the south to 0.82 wt%, 0.12 wt%, and 55 ppm in the north for Fe, Mn, and Sr, respectively (Figs. 3,4).

In and near the Viburnum trend MVT subdistrict, in the basal dolomite underlying the reef facies of the Bonneterre, the trends in concentrations of these elements are reversed; from 0.50 wt%, 0.10 wt%, and 105 ppm in the south to 3.15 wt%, 0.55 wt%, and 32 ppm in the north, respectively (Figs. 3,4). Fe and Mn contents, determined using electron microprobe, of gangue dolomite cement in the Viburnum trend show a similar south-to-north enrichment, ranging from 1.41 mole % $FeCO_3$ and 0.11 mole % $MnCO_3$ in the south to 2.34 mole % and 0.23 mole % in the north, respectively (Gregg and Shelton, 1989b). (For a full discussion of the petrology of dolomite cements, see Voss and others, 1989; Farr, 1989.)

The chemical trends are interpreted to indicate a regional south-to-north flow of basinal fluid from the Arkoma basin through the Lamotte Sandstone. This regional flow likely resulted from a gravity-driven system originating in the Ouachita Mountains (Garven and Freeze, 1984; Bethke and others, 1988; Garven and Sverjensky, 1989). Potassium-argon analysis of dickite associated with galena in the Lamotte Sandstone (Rothbard, 1982) and fluid-inclusion and K–Ar studies of Ba-rich adularia and quartz veins in the Ouachita Mountains (Shelton and others, 1986) are consistent with a Late Pennsylvanian to Permian age for the basinal fluid migration event in southeastern Missouri.

A second fluid-flow system with a probable Illinois basin source (Gregg and Shelton, 1989b) is indicated by the chemical trends observed in the replacement basal Bonneterre dolomite and ore associated dolomite cements in and near the Viburnum trend subdistrict (Fig. 3). A gravity-driven system originating in the Appalachian region during Late Pennsylvanian time, and flowing through the Illinois basin (Garven and Sverjensky, 1989) may have produced these chemical trends.

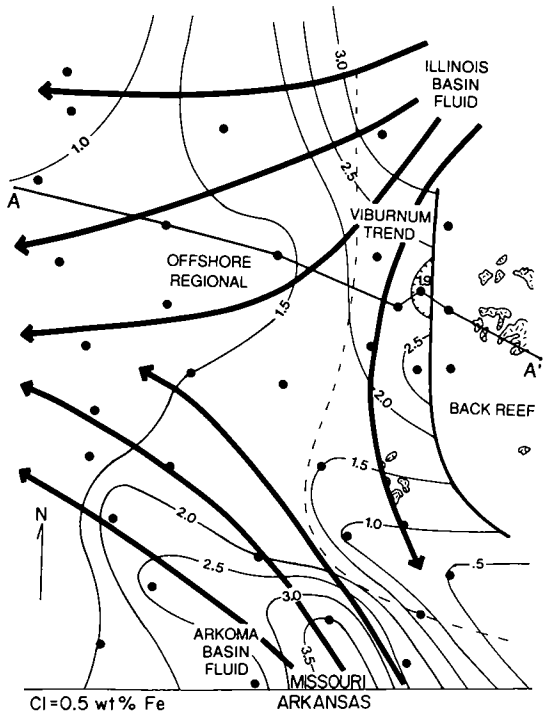

Figure 3. Contour map showing distribution of iron in the basal Bonneterre dolomite. The Viburnum trend area is separated from the back-reef area by a medium-weight line on the east and from the rest of the study area, to the west, by a dashed line. Wide lines with arrows illustrate hypothesized fluid-flow paths of two basinal fluids, one from the south (Arkoma basin) and one from the northeast (Illinois basin). Bullets show locations of cores used in this study. Section A-A' is shown in Figure 2.

FLUID-INCLUSION STUDIES

Microthermometric measurements of >350 two-phase fluid inclusions in replacement dolomite and dolomite cement (Fig. 5) indicate at least two, and possibly three, distinct fluids were present during epigenetic dolomitization and sulfide mineralization (Bauer, 1989). The two-fluid model is characterized by a warmer, less saline fluid (120–187°C, <8 wt% equivalent NaCl), and a cooler, more saline fluid (60–80°C, >30 wt% equivalent NaCl). A three-fluid interpretation would involve two fluids of similar salinity but different temperatures (fluid 1: 60–120°C; fluid 2: 120–180°C), and a third fluid (fluid 3) with variable temperature and salinity (Fig. 6). A pattern of fluid-inclusion temperatures and salinities, similar to that observed in southeast Missouri, exists in east Tennessee MVT zinc district sphalerites. These data have been interpreted to indicate fluid mixing during mineralization (Zimmerman and Kesler, 1981; Taylor and others, 1983). Intermediate fluid compositions and temperatures in the Bonneterre indicate that the end-member fluids likely mixed as they flowed through the region (Bauer, 1989; Bauer and others, 1989).

Previous studies have suggested a cooling gradient of ~0.09°C for basinal fluid flowing northward out of the Arkoma basin (Leach and Rowan, 1986; Bethke and others, 1988). This interpretation was based on fluid inclusions in sphalerite samples that were widely scattered both stratigraphically and aerially. No temperature gradient is discernible from the distribution of homogenization

temperatures of >500 two-phase fluid inclusions in both replacement dolomite and dolomite cement in the study area (Fig. 7). These data are incompatible with a steady-state model of fluid flow from a single-basin source. Instead, they are believed to indicate the presence of two or more basinal fluid interactions coeval with epigenetic dolomitization and MVT sulfide mineralization. This interpretation is further supported by trace and minor element distributions discussed above (Gregg and Shelton, 1989b; Bauer, 1989; Bauer and others, 1989; Shelton and others, 1992).

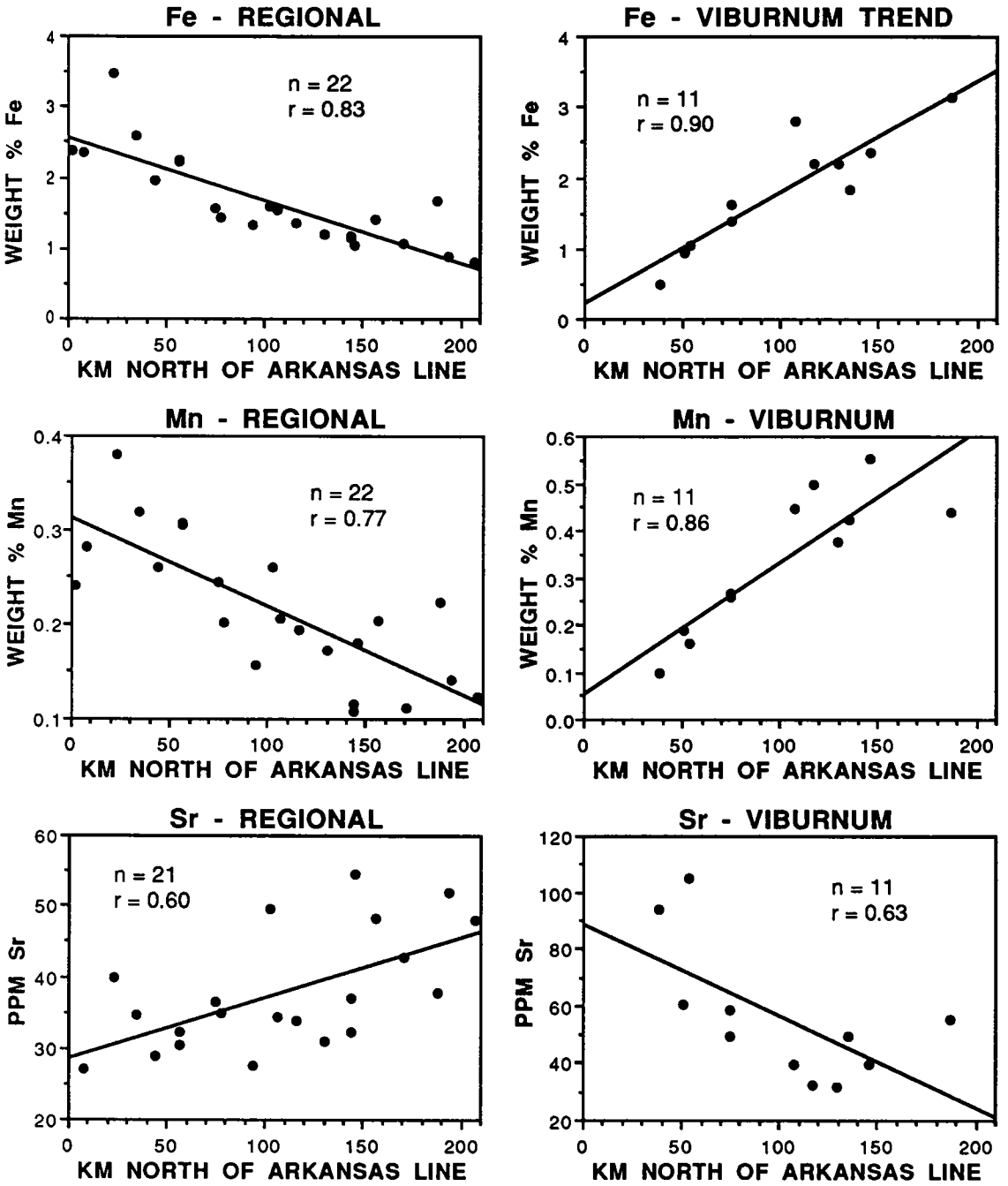

Figure 4. Concentrations of Fe, Mn, and Sr in the basal Bonneterre dolomite relative to distance north of the Missouri–Arkansas state line (36°15′ N lat.). Note the northward decreasing Fe and Mn regional trends and northward increasing Sr regional trends which are opposite to those in the Viburnum trend area.

SUMMARY

Strong trends in Fe, Mn, and Sr concentrations were observed at the Lamotte Sandstone–Bonneterre Dolomite contact and in later gangue dolomite cements associated with MVT sulfide mineralization. These trends are interpreted as resulting from fractionation of trace and minor elements in a fluid-dolomite system during regional epigenetic dolomitization and MVT mineralization. Fluid-flow patterns inferred by the chemical trends indicate a southern (Arkoma) basinal-fluid source as well as a northeastern (Illinois) basinal-fluid source during MVT mineralization and epigenetic dolomitization in southeastern Missouri.

Fluid inclusion temperature-salinity relationships reflect at least two, and possibly three, end-member fluids were present during dolomitization and mineralization. The absence of an areal

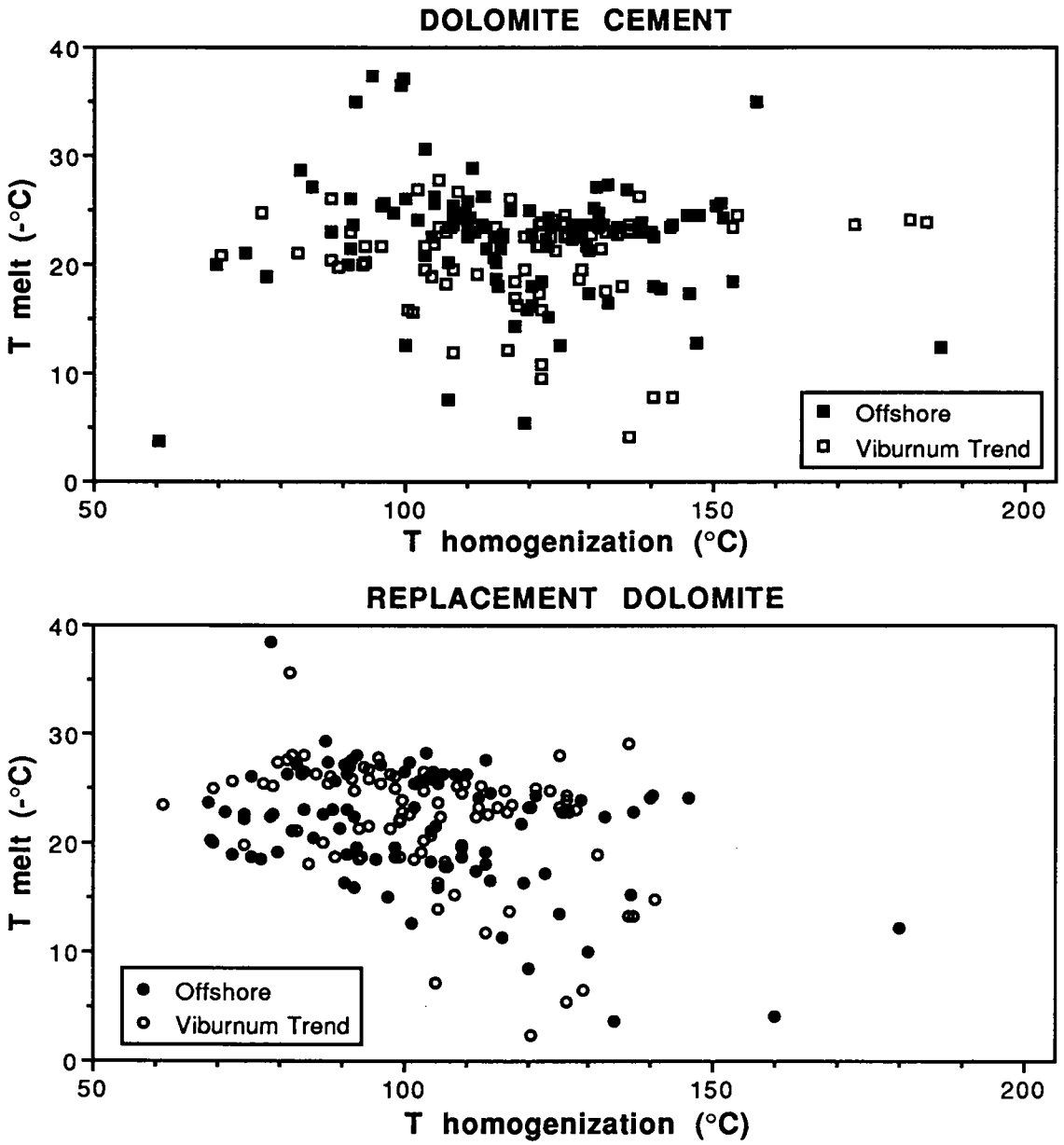

Figure 5. Distributions of last ice-melt and homogenization temperatures for data pairs from replacement dolomite and dolomite cement from the basal Bonneterre dolomite and Viburnum trend ore bodies.

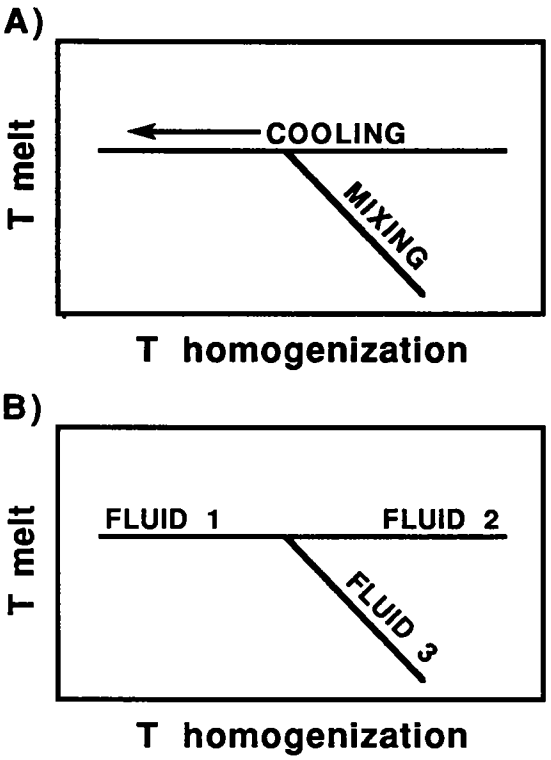

Figure 6. Possible interpretations of the distribution of fluid inclusion data (Fig. 5). *A*—Cooling of one fluid as a second fluid enters and mixes with the first. *B*—Three distinct fluid components: two with similar salinities but different temperatures, and a third with variable temperature and salinity.

temperature gradient in the fluid inclusion data indicates that it is unlikely that a single basinal source provided fluids for MVT sulfide mineralization and associated dolomitization in the study area. Instead, different fluids were derived from at least two basins, the Arkoma basin to the south and the Illinois basin to the northeast.

ACKNOWLEDGMENTS

Acknowledgement is made to the donors of the Petroleum Research Fund, administered by the American Chemical Society (PRF-19809-AC2 to K. L. Shelton), to the Weldon Spring Endowment Fund of the University of Missouri (to J. M. Gregg and K. L. Shelton), and to Texaco E&P Technology Division for partial support of this research. St. Joe Minerals Corp. provided access to core and aided in sample preparation for fluid inclusion studies. We thank R. L. Voss and R. D. Hagni for providing us with samples from most of the ore bodies of the Viburnum trend. We thank P. I. Nabelek and J. R. Palmer for their helpful reviews of this paper.

REFERENCES

Anderson, G. M.; and Macqueen, R. W., 1982, Ore deposit models. 6.—Mississippi Valley-type lead-zinc deposits: Geoscience Canada, v. 9, p. 108–117.

Bauer, R. M., 1989, Fluid inclusion study of the regionally extensive, epigenetic dolomite of the Bonneterre Formation, southeast Missouri: University of Missouri, Columbia, unpublished M.S. thesis, 102 p.

Bauer, R. M.; Shelton, K. L.; and Gregg, J. M., 1989, Fluid inclusion studies of regionally extensive epigenetic dolomites, Bonneterre Dolomite, S. E. Missouri: evidence of multiple fluids during Pb–Zn mineralization [abstract]: Geological Society of America Abstracts with Programs, v. 21, no. 6, p. A3.

Bethke, C. M.; Harrison, W. J.; Upson, C.; and Altaner, S. P., 1988, Supercomputer analysis of sedimentary basins: Science, v. 239, p. 261–267.

Farr, M. R., 1989, Compositional zoning characteristics of late dolomite cement in the Cambrian Bonneterre Formation, Missouri: implications for parent fluid migration pathways: Carbonates and Evaporites, v. 4, p. 177–194.

Fowler, G. M., 1933, Oil and oil structures in Oklahoma–Kansas zinc–lead mining field: American Association of Petroleum Geologists Bulletin, v. 17, p. 1436–1445.

Garven, G.; and Freeze, A. R., 1984, Theoretical analysis of the role of groundwater flow in the genesis of stratabound ore deposits. 1.—Mathematical and numerical model. 2.—Quantitative results: American Journal of Science, v. 248, p. 1085–1174.

Garven, G.; and Sverjensky, D. A., 1989, Hydrogeology of regional flow systems associated with the formation of Mississippi Valley-type ore deposits in the Midcontinent [abstract]: Geological Society of America Abstracts with Programs, v. 21, no. 6, p. A9.

Gerdemann, P. E.; and Myers, H. E., 1972, Relationship of carbonate facies patterns to ore distribution and to ore genesis in the southeast Missouri lead district: Economic Geology, v. 67, p. 426–433.

Gregg, J. M., 1985, Regional epigenetic dolomitization in the Bonneterre Dolomite (Cambrian), southeastern Missouri: Geology, v. 13, p. 503–506.

_____1988, Origins of dolomite in the offshore facies of the Bonneterre Formation (Cambrian), Missouri, *in* Shukla, V.; and Baker, P. A. (eds.), Sedimentology and geochemistry of dolostones: Society of Economic Paleontologists and Mineralogists Special Publication 43, p. 67–83.

Gregg, J. M.; and Gerdemann, P. E., 1989, Sedimentary facies, diagenesis, and ore distribution in the Bonneterre Formation (Cambrian), southeast Missouri, *in* Gregg, J. M.; Palmer, J. R.; and Kurtz, V. E. (eds.), Field guide to the Upper Cambrian of southeastern Missouri: stratigraphy, sedimentology, and economic geology: University of Missouri–Rolla, p. 43–55.

Gregg, J. M.; and Shelton, K. L., 1989a, Geochemical and petrographic evidence for fluid sources and pathways during dolomitization and lead–zinc mineralization in southeast Missouri: a review: Carbonates and Evaporites, v. 4, p. 153–175.

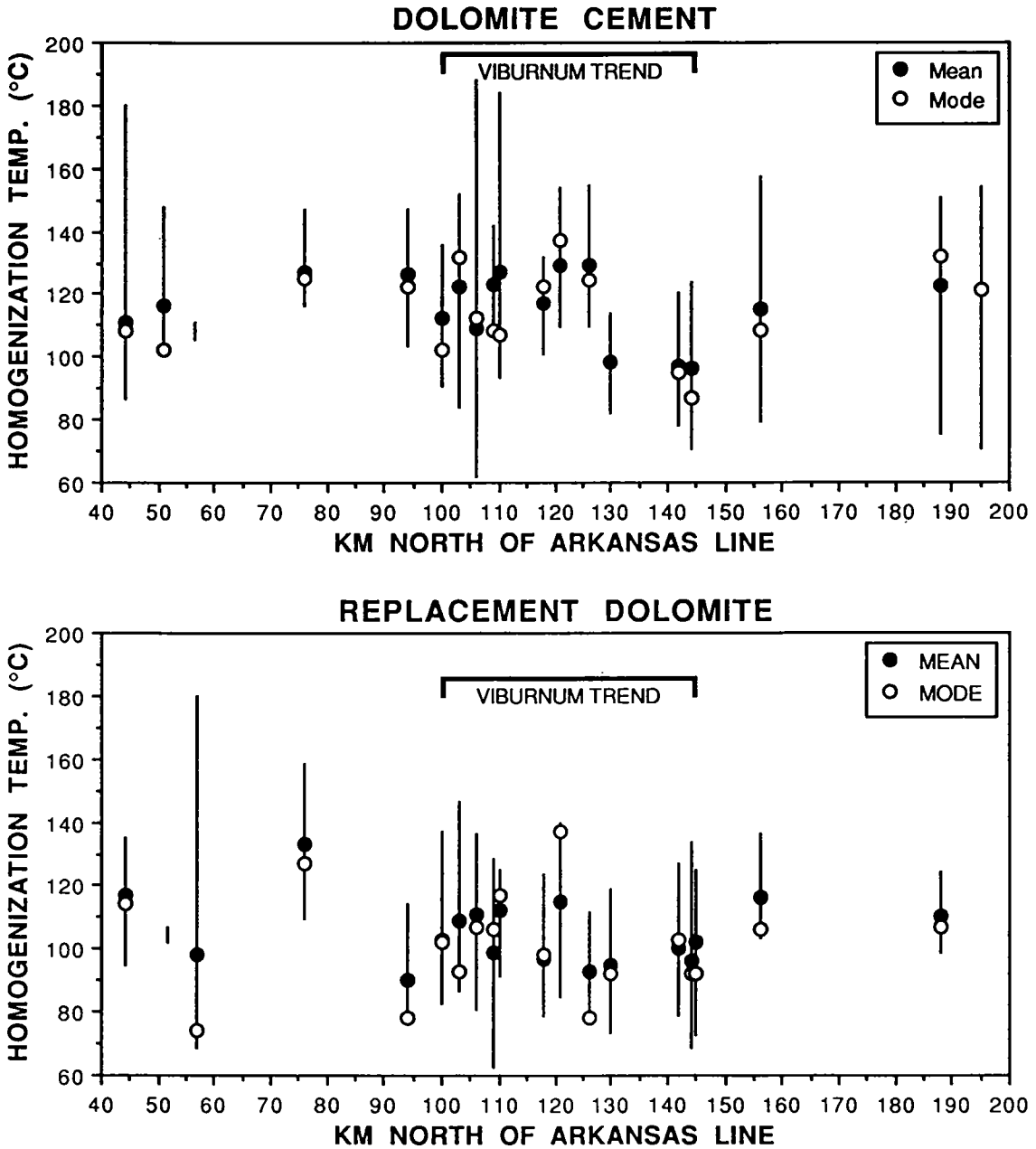

Figure 7. Ranges, means, and modes of fluid inclusion homogenization temperatures of dolomite cements. Note the lack of discernible thermal gradients.

_____1989b, Minor and trace element distributions in the Bonneterre Dolomite (Cambrian), southeast Missouri: evidence for possible multiple basin fluid sources and pathways during lead–zinc mineralization: Geological Society of America Bulletin, v. 101, p. 221–230.

_____1990, Dolomitization and dolomite neomorphism in the back reef facies of the Bonneterre and Davis Formations (Cambrian), southeastern Missouri: Journal of Sedimentary Petrology, v. 60, p. 549–562.

Leach, D. L.; and Rowan, E. L., 1986, Genetic link between Ouachita foldbelt tectonism and Mississippi Valley-type deposits of the Ozarks: Geology, v. 14, p. 931–934.

Machel, H.-G., 1989, Fluid flow direction during dolomitization as deduced from trace element trends, *in* Shukla, V.; and Baker, P. A. (eds.), Sedimentology and geochemistry of dolostones: Society of Economic Paleontologists and Mineralogists Special

Publication 43, p. 115–125.
Marikos, M. A.; Laudon, R. C.; and Leventhal, J. S., 1986, Solid insoluble bitumen in the Magmont West orebody, southeast Missouri: Economic Geology, v. 81, p. 1983–1988.
Mazzullo, S. J., 1986, Mississippi Valley-type sulfides in Lower Permian dolomites, Delaware basin, Texas: implications for basin evolution: American Association of Petroleum Geologists Bulletin, v. 70, p. 943–952.
McIntire, W. L., 1963, Trace element partition coefficients—a review of theory and applications to geology: Geochimica et Cosmochimica Acta, v. 27, p. 1209–1264.
Rothbard, D. R., 1982, Diagenesis of the Lamotte Sandstone in the southeast Missouri lead district: University of Missouri, Columbia, unpublished Ph.D. dissertation, 232 p.
Shelton, K. L.; Reader, J. M.; Ross, L. M.; Viele, G. W.; and Seidemann, D. E., 1986, Ba-rich adularia from the Ouachita Mountains, Arkansas: implications for a post-collisional hydrothermal system: American Mineralogist, v. 71, p. 916–923.
Shelton, K. L.; Bauer, R. M.; and Gregg, J. M., 1992, Fluid inclusion studies of regionally extensive epigenetic dolomites, Bonneterre dolomite (Cambrian), southeast Missouri: evidence of multiple fluids during dolomitization and lead–zinc mineralization: Geological Society of America Bulletin, v. 104.
Skinner, B. J. (ed.), 1977, An issue devoted to the Viburnum trend, southeast Missouri: Economic Geology, v. 72, p. 337–525.
Sverjensky, D. A., 1984, Oil field brines as ore-forming solutions: Economic Geology, v. 79, p. 23–37.
_____1986, Genesis of Mississippi Valley-type lead–zinc deposits: Annual Reviews of Earth and Planetary Science, v. 14, p. 177–199.
Taylor, M.; Kesler, S. E.; Cloke, P. L.; and Kelly, W. C., 1983, Fluid inclusion evidence for fluid mixing, Mascot–Jefferson City zinc district, Tennessee: Economic Geology, v. 78, p. 1425–1439.
Veizer, J., 1983, Trace elements and isotopes in sedimentary carbonates: Reviews in Mineralogy, v. 11, p. 265–300.
Voss, R. L.; Hagni, R. D.; and Gregg, J. M., 1989, Sequential deposition of zoned dolomite and its relationship to sulfide mineral paragenetic sequence in the Viburnum trend, southeast Missouri: Carbonates and Evaporites, v. 4, p. 195–209.
Zimmerman, R. K.; and Kesler, S. E., 1981, Fluid inclusion evidence for solution mixing, Sweetwater (Mississippi Valley-type) district, Tennessee: Economic Geology, v. 76, p. 134–142.

Structural Controls on Sediment Distribution and Thermal Maturation of the Woodford Shale, Anadarko Basin, Oklahoma

Timothy C. Hester, James W. Schmoker, and Howard L. Sahl
U.S. Geological Survey, Denver

ABSTRACT.—The Upper Devonian–Lower Mississippian Woodford Shale is informally divided here, on the basis of wire-line log character, into lower, middle, and upper members. Higher kerogen content of the middle member is the primary physical basis for this subdivision.

Depositional patterns of the Woodford Shale in the Oklahoma part of the Anadarko basin reveal a positive paleotopographic feature, parallel to and ~75 mi north of the Amarillo–Wichita uplift. This feature divided the Woodford into northeast and southwest depocenters and was a hinge line separating areas of regional basement flexure during Woodford deposition. From the hinge line, each member thickens to the southwest, reflecting subsidence along the central trough of the southern Oklahoma aulacogen. To the northeast, nearly uniform thickness of the lower and middle members records deposition on a stable shelf, whereas increasing thickness of the upper member reflects downwarping toward the Sedgwick basin of south-central Kansas.

The Woodford Shale was deposited between two major stages of structural development that together shaped the present-day Anadarko basin: the first stage, subsidence of the southern Oklahoma aulacogen, and the second-stage, foreland-style subsidence. Varying burial depths of the Woodford during the second stage of Anadarko basin development resulted in an unusually broad range of thermal maturities of the Woodford Shale. As a result, Woodford Shale on the shallow northeast shelf, with thickness dominated by the upper member, remains thermally immature to marginally mature with respect to oil generation. In contrast, Woodford Shale in the deep basin to the southwest, with thickness dominated by the lower and middle members, is thermally mature to post-mature with respect to oil generation. Thus, most hydrocarbons sourced by the Woodford Shale have been generated by the lower and middle members.

INTRODUCTION

The Woodford Shale is one of several organic-rich, "black" shales of Late Devonian and Early Mississippian age present in basins of the North American craton. Where thermally mature, these shales are economically important as hydrocarbon source rocks. The Woodford Shale is widely regarded as a major source of oil and gas in the Anadarko basin. This report describes the effects of Anadarko basin evolution on regional depositional trends and thermal maturation of the Woodford Shale in the Oklahoma portion of the Anadarko basin.

GEOLOGIC SETTING

The Woodford Shale is a highly radioactive, carbonaceous and siliceous, dark-gray to black shale. In terms of wire-line character, the Woodford can be generally described as two similar shales separated by a less dense, more radioactive, and often more resistive middle member. To better document variations and regional trends within the Woodford, the formation is considered here in terms of three, informal, log-derived members (Hester and others, 1988): the lower, middle, and upper members of the Woodford Shale (Fig. 1). Higher kerogen content of the middle member is the primary physical basis for this subdivision. Total organic carbon (TOC), calculated from log-derived formation density (Hester and others, 1990), averages 3.2, 5.5, and 2.7 wt%, respectively, for the lower, middle, and upper members of the Woodford Shale in the study area (Fig. 1).

The Woodford overlies a major regional unconformity developed in the Late Devonian (Amsden, 1975) and is conformably overlain by shales and limestones of Mississippian age. Total thickness ranges from near zero to ~125 ft on the northern shelf, and increases to >700 ft in limited parts of the deep Anadarko basin (Amsden, 1975). Maximum thickness in the area of this study is ~300 ft (Fig. 2).

The Anadarko basin is a two-stage Paleozoic

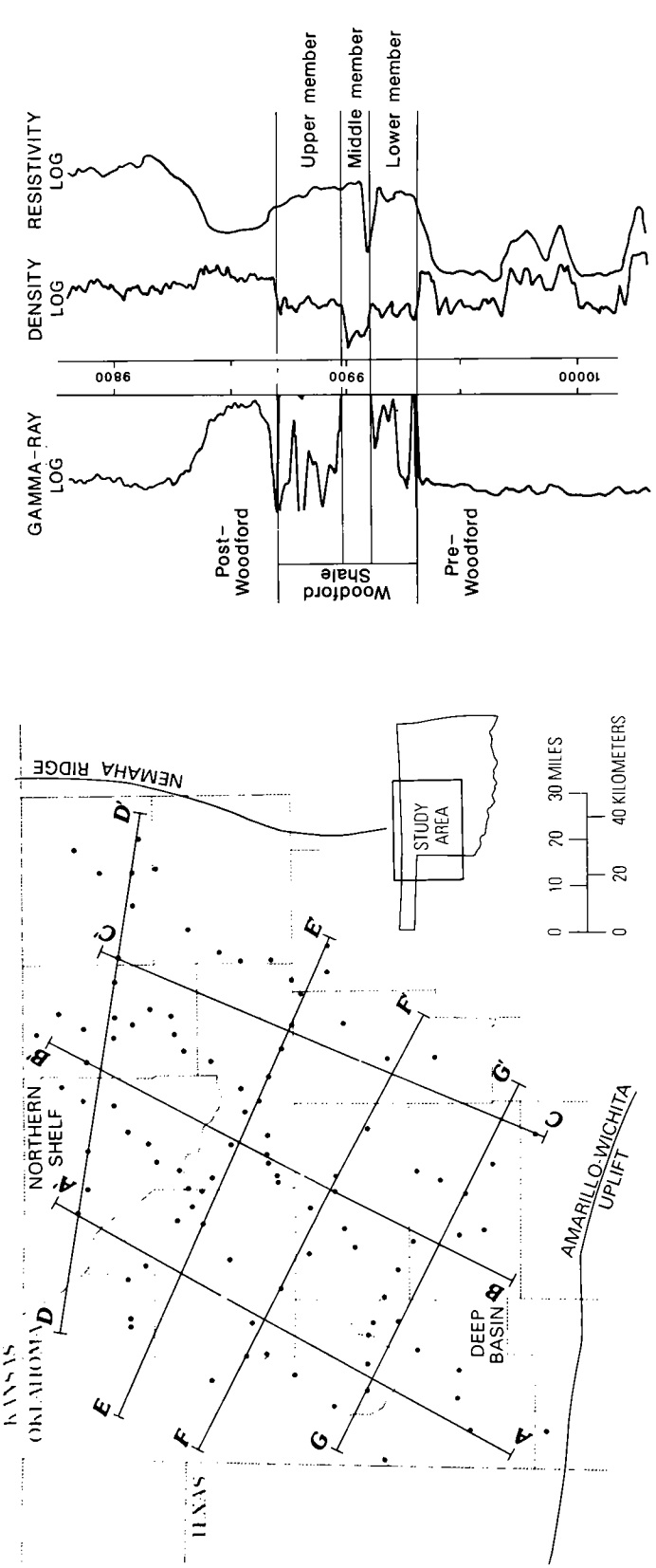

Figure 1. Study area, lines of cross sections, and locations of wells used in this study, and characteristic log signatures of lower, middle, and upper informal members of Woodford Shale.

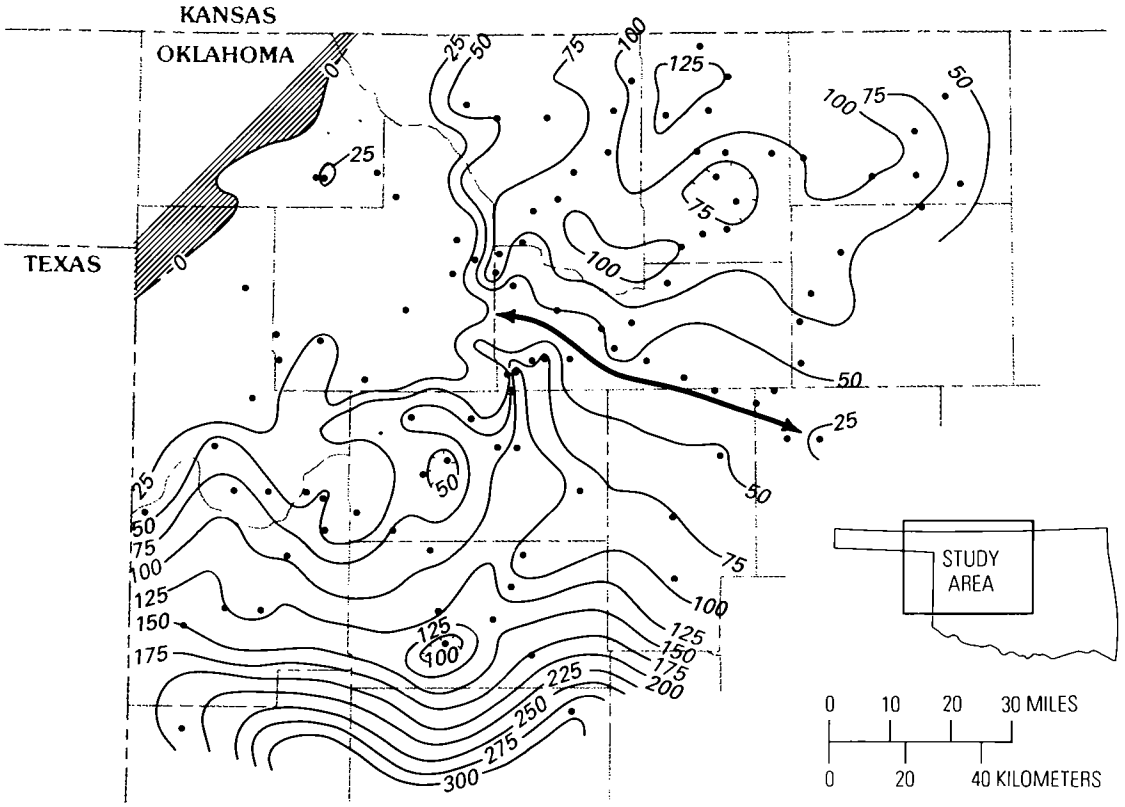

Figure 2. Thickness (ft) of Woodford Shale. Heavy line with arrows marks axis of positive topographic feature that separates Woodford into northeast and southwest depocenters. Area where Woodford Shale is absent is hachured. Contour interval = 25 ft.

basin. The Woodford postdates the predominately carbonate sediments of the first-stage, early Paleozoic southern Oklahoma aulacogen (Feinstein, 1981), and predates formation of the present-day basin, which developed primarily as a Carboniferous and Permian, second-stage, foreland-style basin.

SEDIMENT DISTRIBUTION

The heavy line with arrows shown on the Woodford Shale isopach map (Fig. 2) marks the axis of a positive paleotopographic feature, parallel to and ~75 mi north of the Amarillo–Wichita uplift, that divided the Woodford Shale into southwest and northeast depocenters. This positive feature influenced deposition throughout Woodford time and was a hinge line separating areas of regional basement flexure and subsidence.

Depositional relationships between the three members of the Woodford Shale, depicted in the smoothed regional cross sections of Figure 3, show the effects of Anadarko basin structural evolution. From the hinge line, each member of the Woodford thickens to the southwest, in response to renewed subsidence along the central trough of the southern Oklahoma aulacogen and/or the slow compaction through time of the thick pre-Woodford sedimentary section (Schmoker and Gautier, 1989). To the northeast, the nearly uniform thickness of the lower and middle members records deposition on a stable shelf, whereas increasing thickness of the upper member records downwarping toward the Sedgwick basin of south-central Kansas.

The middle member of the Woodford Shale onlaps the lower member in the central, northwestern, and extreme northeastern parts of the study area (Fig. 3), suggesting a general marine transgression during middle Woodford time. The upper member, however, offlaps the middle member in the west-central part of the study area and appears to onlap the middle member in the northeastern part of the study area, reflecting differential movement of the basement on each side of the northwest-trending positive feature of Figure 2.

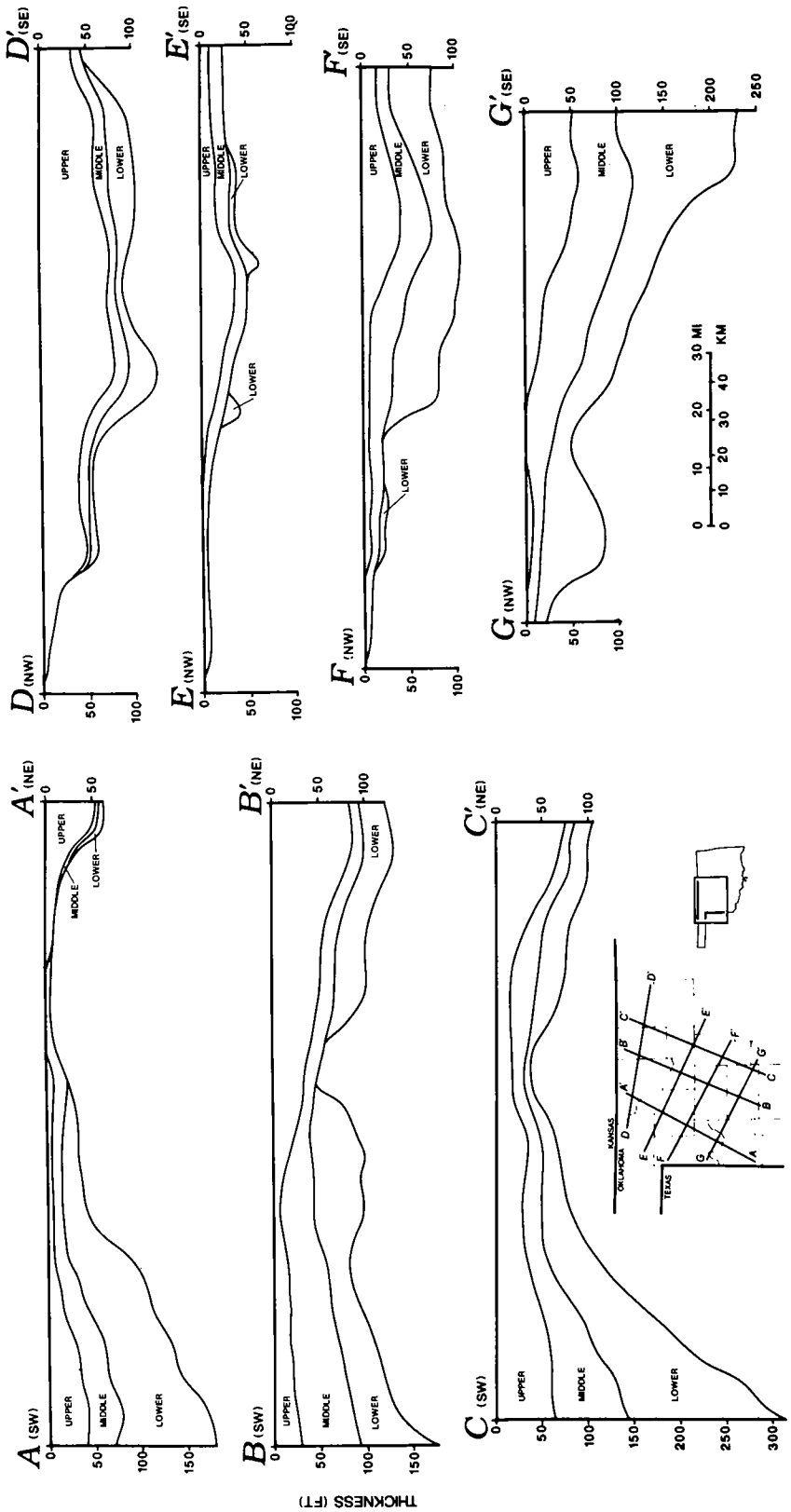

Figure 3. Smoothed regional cross sections showing lower, middle, and upper informal members of Woodford Shale. Datum is top of upper member.

Seas were deepening to the north of the hinge line and shallowing to the south of the hinge line during upper Woodford deposition.

As a result of these depositional trends, the thickness of the Woodford Shale is dominated by the upper member in the northeast region of the study area, and by the middle and lower members in the southwest region of the study area. When coupled with patterns of thermal maturation, these depositional patterns significantly influence the source-rock properties of the Woodford shale.

THERMAL MATURITY PATTERNS

The Woodford Shale was deposited during the time interval between two major stages of structural development that together shaped the present-day Anadarko basin: the first stage, subsidence of the southern Oklahoma aulacogen, and the second-stage, foreland-style subsidence. Differential burial of the Woodford Shale during the second stage of Anadarko basin development subjected the formation to an unusually broad range of thermal regimes (Cardott and Lambert, 1985). Vitrinite reflectance (R_o) ranges from slightly less than 0.5% on the northern shelf to well over 2.0% in the deep basin (Fig. 4). Large areas of the formation have reached thermal-maturity levels required for hydrocarbon generation (Schmoker, 1986).

The Woodford Shale on the shallow northeast shelf, with thickness dominated by the upper member, is generally immature to marginally mature with respect to oil generation. In contrast, the Woodford Shale in the deep basin to the southwest, with thickness dominated by the lower and middle members, is generally mature to postmature with respect to oil generation. About three-fourths of the thermally mature organic carbon in the Woodford Shale of the study area resides in the lower and middle members (Hester and others, 1990). Thus, most hydrocarbons sourced by the Woodford Shale have been generated by the lower and middle members.

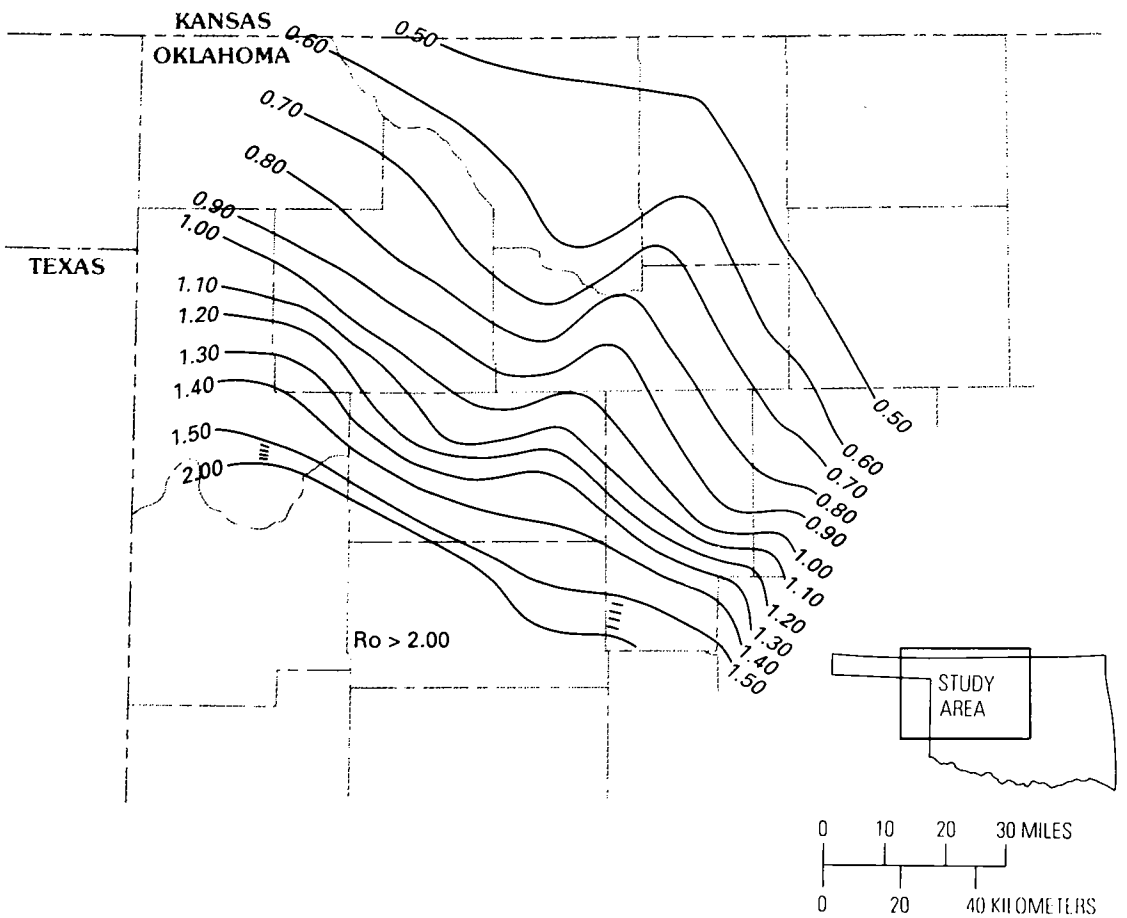

Figure 4. Vitrinite reflectance (R_o) of Woodford Shale, contoured from data of Cardott and Lambert (1985) and Cardott (personal communication, 1987). Contour interval = 0.1%.

SUMMARY AND CONCLUSIONS

A positive paleotopographic feature parallel to and ~75 mi north of the Amarillo–Wichita uplift divided the Woodford Shale into northeast and southwest depocenters. This positive feature was a hinge line separating areas of regional basement flexure during Woodford time. Lower and middle members of the Woodford Shale thicken to the southwest into the central trough of the southern Oklahoma aulacogen. The upper member thickens to the northeast toward the Sedgwick basin of south-central Kansas.

In the southwest region of the study area, present-day thermal maturity of the Woodford is generally greater than that corresponding to peak oil generation, whereas in the northeast region of the study area the Woodford is generally immature to marginally mature with respect to oil generation. Based on the combination of thermal-maturity and depositional trends described here, it can be concluded that most hydrocarbons sourced by the Woodford Shale of the study area have been generated from the middle and lower members.

The Woodford Shale consists of three depositional units (Fig. 1), each with significantly different physical properties and with laterally varying stratigraphic relationships to one another (Fig. 3). Geochemical, source-rock, and other physical-property studies of the Woodford should take into account the stratigraphic variations within the formation. In particular, studies related to horizontal drilling, which has spurred new interest in hydrocarbon production from black shales, should recognize that the Woodford is not a single homogeneous unit, but incorporates a rather complex set of regional stratigraphic and thermal-maturity patterns.

REFERENCES

Amsden, T. W., 1975, Hunton Group (Late Ordovician, Silurian, and Early Devonian) in the Anadarko basin of Oklahoma: Oklahoma Geological Survey Bulletin 121, 214 p.

Cardott, B. J.; and Lambert, M. W., 1985, Thermal maturation by vitrinite reflectance of Woodford Shale, Anadarko basin, Oklahoma: American Association of Petroleum Geologists Bulletin, v. 69, p. 1982–1998.

Feinstein, S., 1981, Subsidence and thermal history of southern Oklahoma aulacogen: implications for petroleum exploration: American Association of Petroleum Geologists Bulletin, v. 65, p. 2521–2533.

Hester, T. C.; Sahl, H. L.; and Schmoker, J. W., 1988, Cross sections based on gamma-ray, density, and resistivity logs showing stratigraphic units of the Woodford Shale, Anadarko basin, Oklahoma: U.S. Geological Survey Miscellaneous Field Studies Map 2054, 2 plates.

Hester, T. C.; Schmoker, J. W.; and Sahl, H. L., 1990, Log-derived, regional source-rock characteristics of the Woodford Shale, Anadarko basin, Oklahoma: U.S. Geological Survey Bulletin 1866-D, 38 p.

Schmoker, J. W., 1986, Oil generation in the Anadarko basin, Oklahoma and Texas: modeling using Lopatin's method: Oklahoma Geological Survey Special Publication 86-3, 40 p.

Schmoker, J. W.; and Gautier, D. L., 1989, Compaction of basin sediments: modeling based on time-temperature history: Journal of Geophysical Research, v. 94, p. 7379–7386.

Thermal Maturation of the Eastern Anadarko Basin, Oklahoma

Mark J. Pawlewicz
U.S. Geological Survey, Denver

Vitrinite reflectance (R_m) measurements on samples from wells along a line extending for 200 km from the northern shelf area of the Anadarko basin near the Kansas state line south to the deep part of the basin (Fig.1) show that the level of thermal maturity was set after maximum burial. Burial history reconstruction curves show the tectonic evolution of this area: minimal subsidence occurred in the northern part of the basin in the early Paleozoic, and moderate to rapid subsidence occurred throughout most of the remaining part of the basin from the Middle Ordovician to Permian. Temperatures determined from reflectance values are higher than those generally accepted for the onset of hydrocarbon generation and are also higher than temperatures obtained from similar studies in the basin. Regression analysis yields a reflectance gradient of 0.33% R_m/km

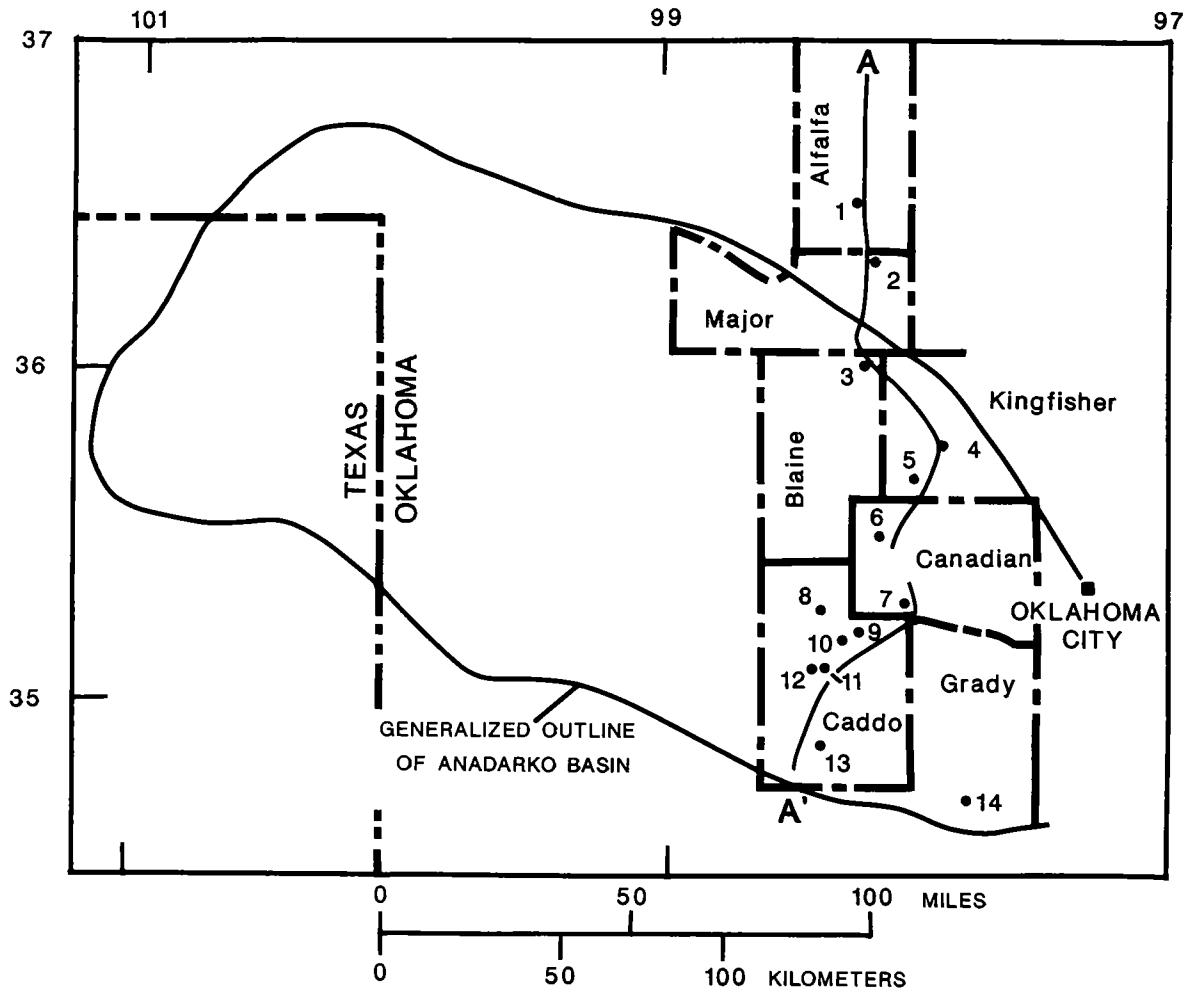

Figure 1. Location of Anadarko basin and lines of well profile. Modified from Adkison (1960).

along the profile. Isoreflectance lines, 0.6 and 1.3% R_m, show the depth and thickness of the window of oil generation (Fig. 2). The isoreflectance lines can be used to estimate the level of thermal maturity above or below them.

Vitrinite reflectance was measured on samples from a series of wells from the eastern part of the basin to determine the paleogeothermal history. The samples for this study are core and cuttings samples that range in age from Permian to Silurian and span a depth interval from 1,160 to 5,240 m. The aim of the study was to make generalizations about the use of paleogeothermal models to predict thermal maturation in any part of the basin. The vitrinite-reflectance data, interpreted using the relation of Barker and Pawlewicz (1986), suggest paleotemperatures were higher than temperatures derived from bottom-hole temperature data.

The oil window is generally considered to fall within the range of 50–65°C to 130–145°C, corresponding to vitrinite-reflectance values between 0.6 and 1.3%. In the well along the profile that has the largest depth range and best individual correlation, the highest reflectance values are significantly higher than the oil window, greater than 1.3% R_m. The deeper part of the well probably was subjected to higher temperatures that have since decreased.

The present-day geothermal gradient for the region of the well profile is 24°C/km (~1.3°F/100 ft) (Harrison and Luza, 1986), similar to the gradient of 1.2°F/100 ft used by Pusey (1973). Twenty-nine bottom-hole temperatures, from 18

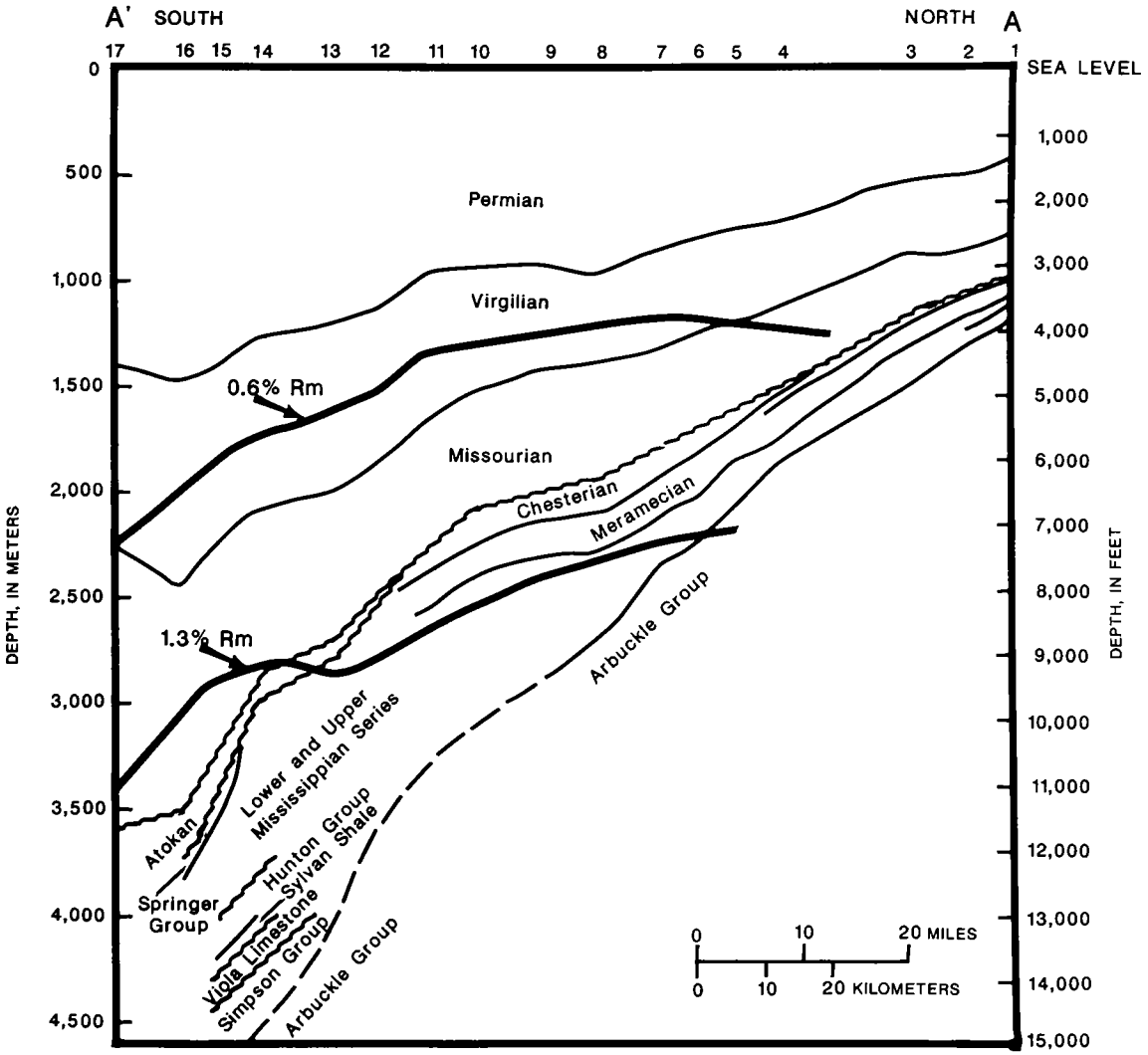

Figure 2. Cross section along well profile showing isoreflectance lines at 0.6 and 1.3% R_m. Wavy lines indicate unconformities. Dashed lines indicate uncertain formation boundaries.

wells parallel to the well profile, are in partial agreement with this gradient if the temperature correction scheme of Harrison and others (1982) is applied.

Barker and Pawlewicz (1986) showed that time has much less effect on the rank of organic matter than indicated by Lopatin (1971). Isoreflectance lines in the cross section, drawn from points connecting depths calculated for several wells, cross formation boundaries at an angle (Fig. 2). This is taken as evidence for maturation being a function of increased temperatures resulting from burial or renewed heating after subsidence of the basin stopped.

REFERENCES

Adkison, W. L., 1960, Subsurface cross section of Paleozoic rocks from Barber County, Kansas, to Caddo County, Oklahoma: U.S. Geological Survey Oil and Gas Investigations Chart OC-61, 2 sheets.

Barker, C. E.; and Pawlewicz, M. J., 1986, The correlation of vitrinite reflectance with maximum temperature in humic organic matter, *in* Buntebarth, G.; and Stagena, L. (eds.), Paleogeothermics; lecture notes in earth sciences, vol. 5: Springer-Verlag, Berlin, p. 79–93.

Harrison, W. E.; and Luza, K. V., 1986, Temperature-gradient information for several boreholes drilled in Oklahoma: Oklahoma Geological Survey Special Publication 86-2, 42 p.

Harrison, W. E.; Luza, K. V.; Prater, M. L.; and Cheung, P. K., 1982, Geothermal resource assessment in Oklahoma, *in* Ruscetta, C. A. (ed.), Geothermal direct heat program roundup technical conference proceedings: University of Utah Earth Science Laboratory, v. 1, p. 187–204.

Lopatin, N. V., 1971, Temperature and geologic times as factors in coalification: Akademiya Nauk SSSR Izvestiya Seriya Geologicheskaya, no. 3, p. 95–106.

Pusey, W. C., 1973, The ESR-kerogen method; a new technique of estimating maturity of sedimentary rocks: Petroleum Times, January 12, p. 21–23.

Laminated Black Shale–Bedded Chert Cyclicity in the Woodford Formation, Southern Oklahoma

Charles T. Roberts
ARCO Exploration and Production Technology, Plano, Texas

Richard M. Mitterer
University of Texas at Dallas

ABSTRACT.—In southern Oklahoma, the Woodford Formation consists of cyclic deposits of laminated black shales and bedded cherts. Organic carbon ranges from 3 to 9% in cherts and from 10 to 25% in black shales. Pyrolysis-gas chromatography, Rock-Eval and carbon isotopic analyses signify that the Woodford contains marine, oil-prone (type II) kerogen. Except for the difference in organic carbon content, the kerogens of the bedded chert–black shale couplets are analytically similar. The high organic carbon concentrations and the presence of laminated black shales throughout the entire thickness of the formation in southern Oklahoma indicate that deposition in this region occurred continuously under anoxic conditions. The cyclicity exhibited by the couplets represents pulses of high siliceous productivity superimposed on continuous deposition of black shales and may have been caused by external orbital forcing (Milankovitch cycles).

INTRODUCTION

The Woodford Formation, a Late Devonian–Early Mississippian (Frasnian–Tournaisian) siliceous black shale, is an important hydrocarbon source rock in the southern Midcontinent region of the United States. The formation is, in part, stratigraphically equivalent to several other organic carbon-rich shales, including the Antrim, Bakken, Chattanooga, New Albany, and Ohio, that together indicate the presence of widespread anoxic conditions over the North American craton during this time.

The organic geochemistry of the Woodford has been studied extensively, and much of the oil produced in central and southern Oklahoma has been correlated with bitumen from the formation (Cardott and Lambert, 1985; Comer and Hinch, 1987). Shales and cherts in the formation contain oil-prone (type II) kerogen with a range of thermal maturities from marginally mature in outcrop areas to metamorphic in the deeply buried portion of the Anadarko basin (Cardott and Lambert, 1985; Houseknecht and Matthews, 1985).

The Woodford Formation occurs in the subsurface over an extensive part of the southern Midcontinent and outcrops in the Arbuckle–Ouachita region of southern Oklahoma and western Arkansas. Lithologically, the formation consists predominantly of black shales in the west, becoming more siliceous eastward (Cardott and Lambert, 1985). In the Arbuckle uplift, cherts and black shales are rhythmically interbedded throughout the formation.

The Woodford is ~91 m thick where it is partially exposed in a road cut (I-35) on the south flank of the Arbuckle uplift, Carter County, Oklahoma. The basal 2–3 m of the formation, immediately above the unconformity marking the top of the Hunton Group, consist of thinly bedded alternating shales and cherts. The middle 67 m are dissected by creek drainage and is extensively covered by vegetation. The almost continuously exposed upper 22 m of Woodford, comprised of alternating beds of organic carbon-rich shales and cherts, constitute the focus of this study.

GEOCHEMISTRY

In the study area, Woodford shales are black to blackish-brown laminated beds ranging from 0.1 to 29 cm thick (average = 3.2 cm). Cherts are black to blackish-brown, blocky, dense, resistant beds ranging from 0.5 to 32 cm thick (average = 3.5 cm). Thicknesses of both lithologies increase within the top 5 m of the formation. The upper part of the Woodford section contains two zones rich in phosphorite nodules. One zone, 2.3 m from the top of the formation, is 4 m thick, and the second, 10.5 m from the top, is 2 m thick. The majority of the phosphorite nodules are found in chert beds.

A significant amount of poorly preserved radiolarian tests and megaspores are associated with cherts, most notably in phosphate nodules pres-

ent in the cherts. Microfossils are not observed in the shales. The abundance of siliceous microfossils associated with the cherts indicates that these beds are primary in origin and were not formed as a result of diagenetic processes.

Laminated black shales are highly enriched in organic carbon (C_{org}) with concentrations ranging from 10 to 25% (mean = 13.7%). C_{org} in cherts ranges from about 3 to 9% with a mean of 5.4%. Total sulfur in the shales varies from 0.4 to 4.9% (mean = 1.6%). Total sulfur in the cherts ranges from 0 to 1.0% with a mean of 0.5%. Variations in C_{org} and sulfur correlate entirely with lithology, with shales having more and cherts having less of both elements (Fig. 1). Comer and Hinch (1987) suggested that cherts of the Woodford are deficient in C_{org} relative to the laminated shales because cherts: (1) had higher initial concentrations of biogenic silica (i.e., C_{org} was diluted), (2) were cemented with silica soon after deposition, and (3) underwent little compaction.

A plot of C_{org} and sulfur from Woodford chert and shale samples displays a positive correlation with an approximate zero intercept (Fig. 2). Although both C_{org} and S concentrations in black shales are higher than in cherts, the S/C values for both lithologies fall on the same general trend. The average S/C ratio for all Woodford samples is 0.11. For shales, S/C is 0.12, while for cherts this ratio is 0.09. Thus, S/C is virtually identical in both shales and cherts. For comparison, the average S/C value for normal marine Holocene sediments is 0.36, and for normal marine (i.e., bioturbated) Phanerozoic shales the average S/C is 0.40 (Berner, 1982; Berner and Raiswell, 1983). The results for the Woodford also differ from S/C values obtained from coeval Devonian shales of the Appalachian basin; the latter have a positive S-axis intercept for the S/C trend and have S/C ratios greater than 0.40 (Leventhal, 1987).

The low S/C values for the Woodford samples indicate either that pyrite formation in the depositional environment was limited or that S/C values have been altered subsequent to deposition and do not represent original concentrations. Post-depositional changes, such as a decrease of or-

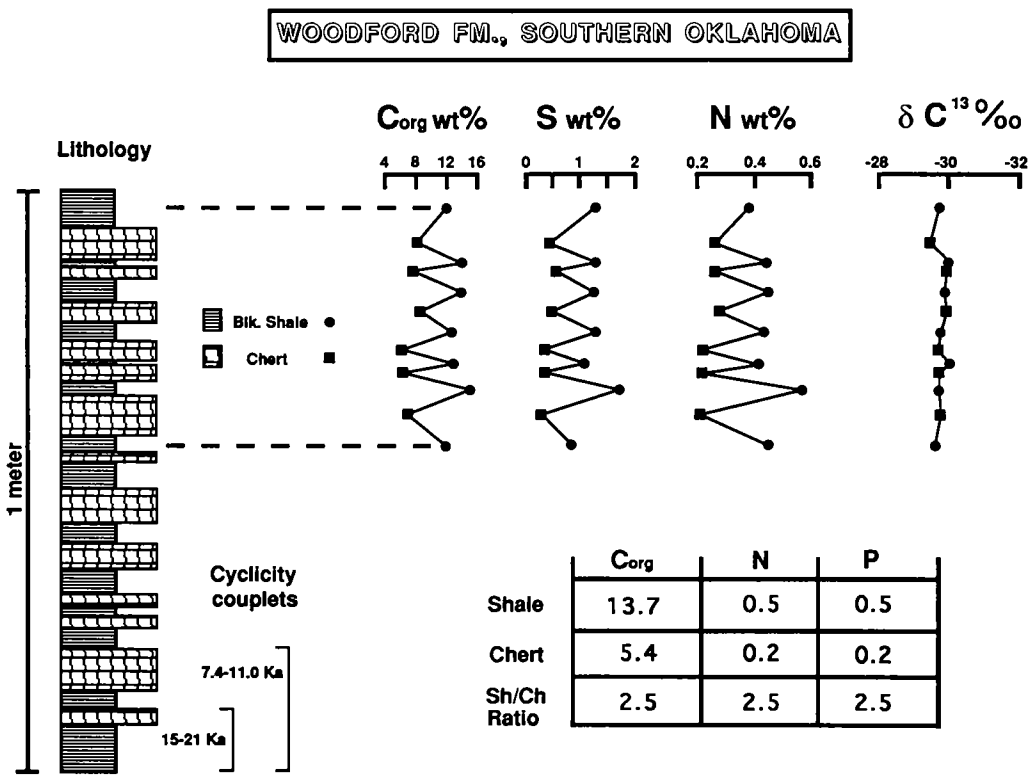

	Corg	N	P
Shale	13.7	0.5	0.5
Chert	5.4	0.2	0.2
Sh/Ch Ratio	2.5	2.5	2.5

Figure 1. A schematic diagram of a 1-m section of the Woodford Formation at its outcrop on the southern flank of the Arbuckle uplift, Interstate 35, Carter County, Oklahoma, illustrating the rhythmic deposition of laminated black shale and chert. Variations in organic carbon (wt%), total sulfur (wt%), total nitrogen (wt%) and carbon isotopic composition (‰) of kerogen are plotted for a portion of this section. Average concentrations (of organic carbon, nitrogen, and phosphorous) for shales and cherts and the ratios between shale and chert concentrations are indicated in the box at bottom.

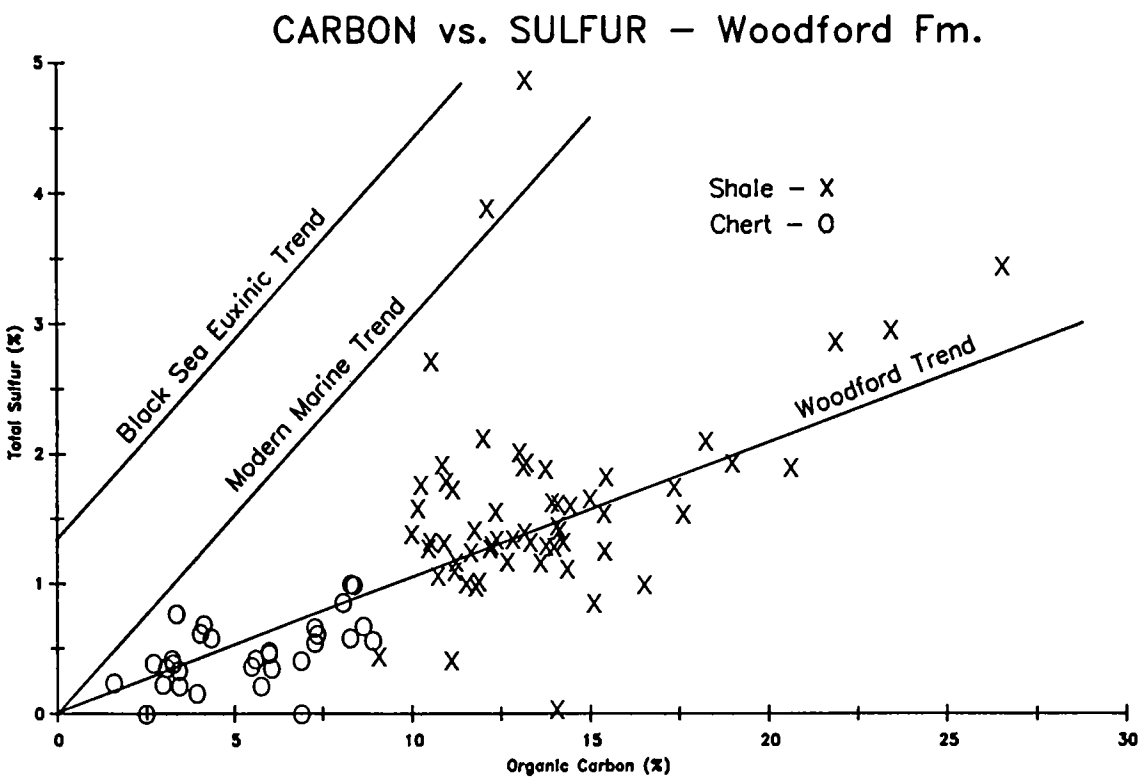

Figure 2. Organic carbon vs. total sulfur for chert and shale samples of the Woodford Formation compared to trends obtained for normal marine (Berner and Raiswell, 1983) and Black Sea (Leventhal, 1983) sediment samples.

ganic carbon due to hydrocarbon generation or weathering of pyrite and oxidation of sulfur to more soluble sulfate salts, cannot account for the S/C trend as they would either lead to an increase in the S/C values or cause the data to be more randomly scattered.

Pyrite formation is generally limited by deficiencies in organic carbon, sulfate, or reactive iron (Berner, 1982). High concentrations in both shales and cherts show that organic carbon was not a limiting factor in Woodford sediments. With deposition of Woodford sediments occurring in a marine basin, sulfate also was not limiting. Consequently, the most likely factor limiting pyrite formation in the Woodford was low concentrations of reactive iron transported to the basin. This inference is supported by the low iron content of Woodford samples (shale—1.5 wt% Fe; chert—0.4 wt% Fe) compared to coeval Chattanooga Shale (6.9 wt% Fe) (Brownlow, 1979) and to Cretaceous Mowry and Pierre Shales of the Western Interior Seaway (about 2–4 wt% Fe) (Dean and Arthur, 1989). Furthermore, the data for the Woodford samples fall on the constant S/Fe line for pyrite (S/Fe = 1.15), representing an iron-limited system, in the Fe–S–C_{org} ternary diagram (Fig. 3). Thus, there is essentially no reactive iron remaining after pyrite formation, and the degree of pyritization is virtually 100%. Iron was probably delivered to the sediments as a metal-organic matter complex, accounting for the linear trend in S/C values (Raiswell and Berner, 1985).

Rock-Eval pyrolysis data for 30 shale and chert samples, plotted as hydrogen index (HI) and oxygen index (OI), fall along a vertical trend in the intermediate hydrogen index range (Fig. 4). This trend represents the maturation pathways for types I and II kerogen (Tissot and others, 1974). Shales and cherts show considerable overlap in the type II region. Mean values for the production index and T_{max} for both shale and chert samples are 0.028° and 431°C, respectively. Conclusions drawn from the Rock-Eval data are that the Woodford cherts and shales from the outcrop region examined in this study contain marine oil-prone (type II) kerogen, that they exhibit a submature to slightly mature level of thermal maturation, and that, in general, they show a high degree of genetic source-rock potential.

Carbon-isotope analyses of several samples from the middle of the study interval further characterize the nature of organic matter in the cherts

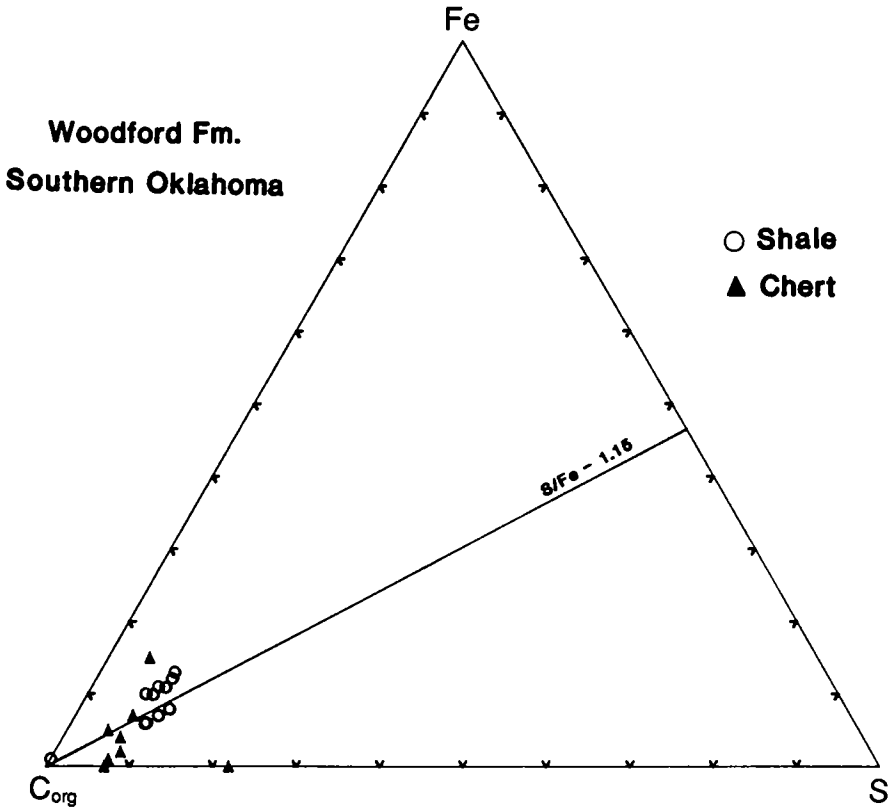

Figure 3. Fe–S–C_{org} ternary diagram for samples of the Woodford Formation. The line represents the constant value for the ratio (by weight) of sulfur-to-iron in pyrite (S/Fe = 1.15). Samples falling on this line are inferred to have been deposited in an iron-limited system.

and shales. The mean $\delta^{13}C$ value of Woodford kerogen for both cherts and shales is –29.8‰ (Fig. 1). Isotopic values range from –29.5 to –30.0‰, with no difference in $\delta^{13}C$ values for the kerogens of the two lithologies. The mean isotopic value falls within the general range of marine kerogens of Devonian age (Maynard, 1981).

Despite the differences in C_{org} content, Rock-Eval and carbon isotopic data indicate that shales and cherts contain essentially the same kind of kerogen. Lower organic carbon content of the cherts is inferred to be due to sedimentary dilution of organic matter during periods of high siliceous productivity rather than to differences in type of organic matter.

DEPOSITIONAL MODEL

The Woodford Formation accumulated in a shallow to deep, euxinic epicontinental sea on the southern margin of the North American craton. Deeper portions of the sea existed within the southern Oklahoma aulacogen, which includes the study site. The euxinic environment was favorable for accumulation and preservation of large amounts of organic carbon, as evidenced by the high concentrations in both cherts and shales. Although both lithologies are rich in organic carbon, shales are far more enriched than cherts.

Lower concentrations of C_{org} in cherts are inferred to be due to dilution by syngenetically deposited biogenic silica. Cherts were deposited during relatively short periods of high siliceous productivity as organic carbon-rich siliceous oozes. In contrast, shale deposition occurred over longer intervals of time with lower levels of siliceous productivity and less dilution of organic carbon by siliceous sediments. Figure 5 is a model illustrating the two alternating phases of sedimentation.

Relative rates of deposition of chert and shale can be estimated from elemental abundance data. Carbon, nitrogen, and phosphorus are derived almost exclusively from organic matter; consequently, the relative proportion of these constituents in shales and cherts is a measure of the dilution factor by biogenic silica sedimentation. The shale-to-chert ratio for each of these elements, based on their average concentrations, is 2.5 (Fig. 1). That is, due to dilution by biogenic silica, cherts contain 0.4 times the concentration of C_{org}, N, and

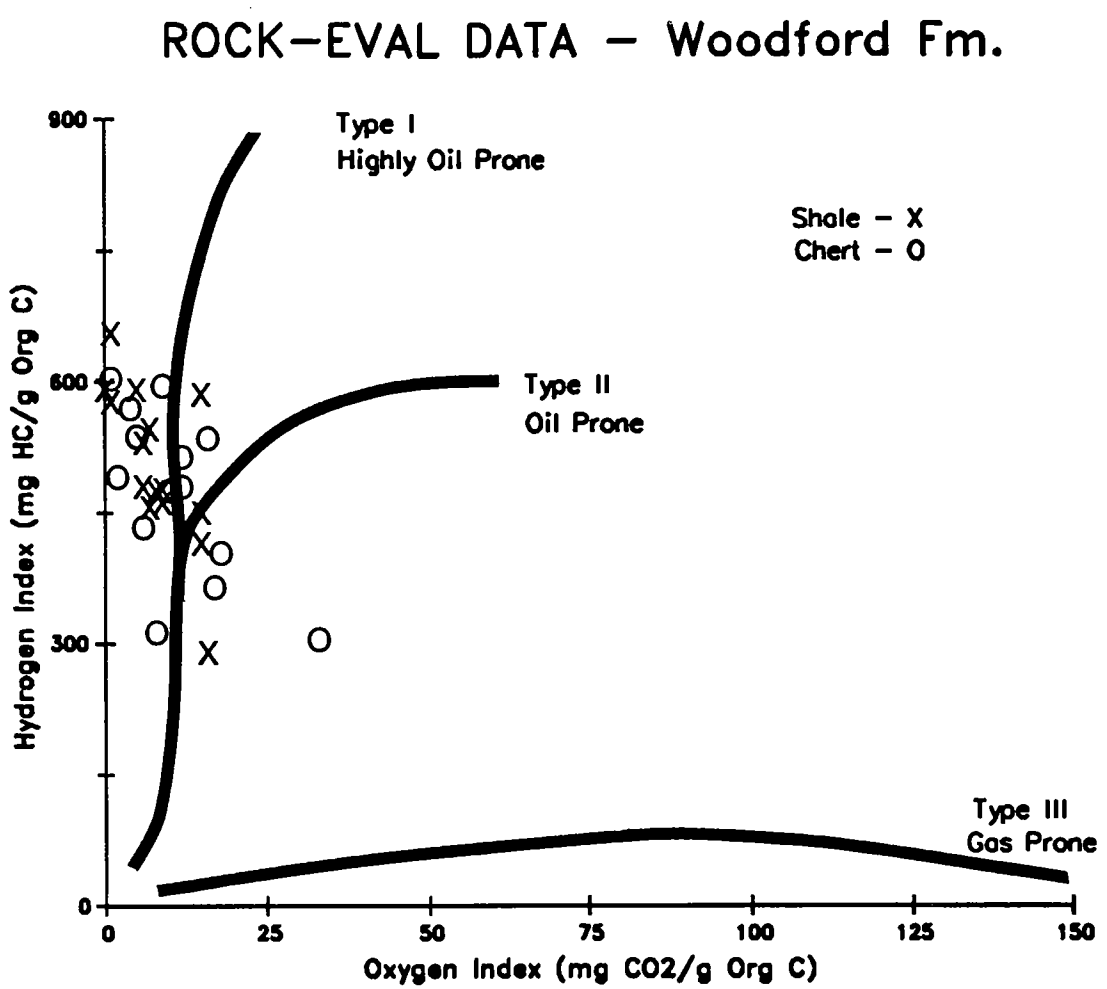

Figure 4. Rock-Eval hydrogen index (HI) vs. oxygen index (OI) for 30 whole rock chert and shale samples of the Woodford Formation.

P that is present in shales. Accordingly, cherts accumulated at least 2.5 times faster than shales. The dilution factor, however, may have been even greater than 2.5 if carbon accumulation rates were higher during chert deposition due to greater productivity at this time.

The time represented by a single chert-shale couplet can only be estimated because of the uncertainty in age range of the Woodford. Deposition of the Woodford lasted from Frasnian (Late Devonian) into Tournaisian (earliest Mississippian) time (Hass and Huddle, 1965; Ham, 1973). There is uncertainty as to how much of the Frasnian and Tournaisian is represented by this section because of the virtual absence of fossils except for poorly preserved radiolarians and conodonts. The Devonian–Mississippian boundary occurs between 4 and 5 m from the top of the formation (Hass and Huddle, 1965), so only a portion of the Tournaisian may be represented. Thus, the time span for Woodford deposition can be estimated minimally and maximally between 10 and 15 Ma.

Based on the average couplet thickness of 6.7 cm and an overall formation thickness of 91 m, individual couplets are estimated to have accumulated in 7.4–11.0 Ka (Fig. 1). Lower frequency periodicities of about 15–21 Ka and 90–125 Ka, representing megacycles of two and 10 couplets, are obtained from time series analysis of bedding thicknesses assuming depositional time spans of 10 and 15 Ma. Within the limits of age uncertainty of Woodford deposition, the shale–chert rhythmic periodicities in the Woodford fall within the frequency bands of Milankovitch orbital cycles.

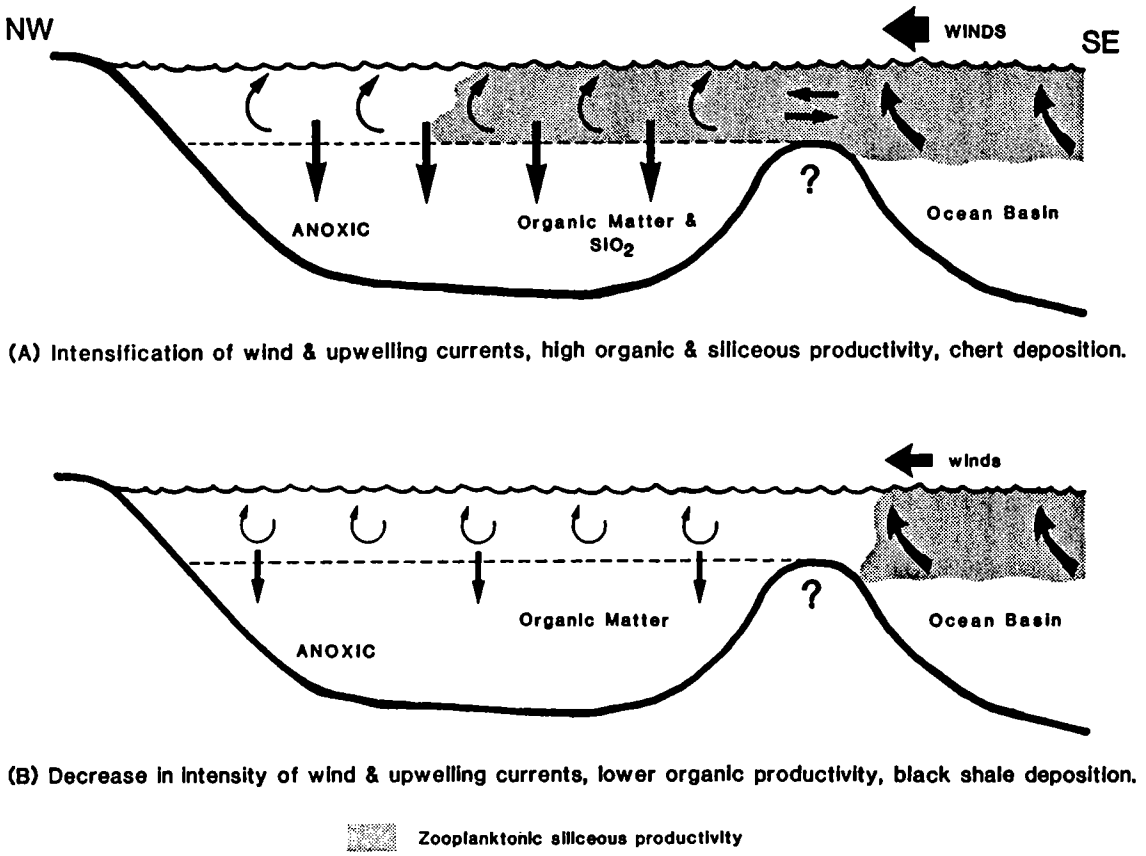

Figure 5. Depositional model for the Woodford Formation in the southern Oklahoma aulacogen.

SUMMARY

The Woodford Formation accumulated in a shallow to deep, euxinic epicontinental sea proximal to the southern margin of the North American craton. The euxinic environment was favorable for accumulation and preservation of large amounts of organic matter, as evidenced by the very high organic carbon values in chert and shale lithologies. Although differences exist between the organic carbon concentrations in shales and cherts, the kerogens of the chert and shale are analytically the same (oil-prone type II). The lower organic carbon concentrations in cherts are considered to be due to dilution by syngenetically deposited biogenic silica. Cherts were most likely deposited during relatively short periods of siliceous productivity as organic-carbon-rich siliceous oozes. In contrast, shale deposition probably occurred over a longer period of time during lower levels of siliceous productivity and less dilution of organic matter. Ultimate control over the depositional cycles of the Woodford Formation was probably by astronomical (Milankovitch) forcing.

REFERENCES

Berner, R. A., 1982, Burial of organic carbon and pyrite sulfur in the modern ocean: its geochemical and environmental significance: American Journal of Science, v. 282, p. 451–473.

Berner, R. A.; and Raiswell, R., 1983, Burial of organic carbon and pyrite sulfur in sediments over Phanerozoic time: a new theory: Geochimica et Cosmochimica Acta, v. 47, p. 855–862.

Brownlow, A. H., 1979, Geochemistry: Prentice-Hall, Englewood Cliffs, New Jersey, 498 p.

Cardott, B. J.; and Lambert, M. W., 1985, Thermal maturation by vitrinite reflectance of Woodford

Shale, Anadarko basin, Oklahoma: American Association of Petroleum Geologists Bulletin, v. 69, p. 1982–1998.

Comer, J. B.; and Hinch, H. H., 1987, Recognizing and quantifying expulsion of oil from the Woodford Formation and age-equivalent rocks in Oklahoma and Arkansas: American Association of Petroleum Geologists Bulletin, v. 71, p. 844–858.

Dean, W. E.; and Arthur, M. A., 1989, Iron-sulfur-carbon relationships in organic carbon-rich sequences I: Cretaceous Western Interior Seaway: American Journal of Science, v. 289, p. 708–743.

Ham, W. E., 1973, Regional geology of the Arbuckle Mountains, Oklahoma: Oklahoma Geological Survey Special Publication 73-3, 61 p.

Hass, W. H.; and Huddle, J. W., 1965, Late Devonian and Early Mississippian age of the Woodford Shale in Oklahoma, as determined by conodonts: U.S. Geological Survey Professional Paper 525-D, p. 125–132.

Houseknecht, D. W.; and Matthews, S. M., 1985, Thermal maturity of Carboniferous strata: American Association of Petroleum Geologists Bulletin, v, 69, p. 335–345.

Leventhal, J. S., 1983, An interpretation of carbon and sulfur relationships in Black Sea sediments as indicators of environments of deposition: Geochimica et Cosmochimica Acta, v. 47, p. 133–137.

_____1987, Carbon and sulfur relationships in Devonian shales from the Appalachian basin as an indicator of environment of deposition: American Journal of Science, v. 287, p. 33–49.

Maynard, J. B., 1981, Carbon isotopes as indicators of dispersal patterns in Devonian–Mississippian shales of the Appalachian basin: Geology, v. 9, p. 262–265.

Raiswell, R.; and Berner, R. A., 1985, Pyrite formation in euxinic and semi-euxinic sediments: American Journal of Science, v. 285, p. 710–724.

Tissot, B.; Durand, B.; Espitalié, J.; and Combaz, A., 1974, Influence of nature and diagenesis of organic matter in petroleum formation: American Association of Petroleum Geologists Bulletin, v. 58, p. 499–506.

A Reevaluation of the Geochemical Characteristics of Solid Bitumens from the Ouachita Mountains, Oklahoma

Tim E. Ruble and R. Paul Philp
University of Oklahoma

ABSTRACT.—The extracts of six solid bitumen samples (grahamites and impsonite) from the frontal and central Ouachita Mountains of southeastern Oklahoma have been examined. Previous studies have proposed that these solid bitumens originate from near-surface, low-temperature alteration of genetically related crude oils (Curiale, 1981,1986; Curiale and others, 1983). The purpose of this study was to utilize recent advances in analytical procedures to undertake a more detailed geochemical study of the bitumens and to reevaluate the conclusions from the previous investigations on the basis of the new data.

Hydrocarbon distributions of the extracts examined in the present study support the view that these solid bitumens are products of limited biodegradation, water washing, and devolatilization. However, biomarker distributions previously interpreted as indicators of biodegradation are now thought to reflect the influence of thermal maturity. Specifically, sterane and terpane distributions suggest that impsonite has undergone significant thermal alteration, while grahamite samples appear to be relatively unaffected. This observation is consistent with that of Jacob (1989) for the thermal origin of impsonite.

INTRODUCTION

Solid bitumen deposits occur in southeastern Oklahoma, primarily in the frontal and central Ouachita Mountains region (Fig. 1) and were first described geologically by Taff (1899,1909). A general summary of the bitumen deposits is given by Ham (1956) and Fay (1982). Petrographic and bulk chemical characterization of these bitumens has been investigated (Eldridge, 1901; Abraham, 1945; Jacob and Wehner, 1981; Cardott, 1991). Detailed geochemical investigations have also been presented (Curiale, 1981,1983,1986,1988; Curiale and Harrison, 1981; Curiale and others, 1983; Jacob and Wehner, 1981).

The general conclusion from previous geochemical studies has been that the solid bitumens in the Ouachita Mountains region originate from near-surface, low-temperature alteration of genetically related crude oils (Curiale, 1983). Specific processes proposed for this alteration include limited biodegradation, water washing, and devolatilization (Curiale, 1983). The two principal varieties of solid bitumen which occur in the Ouachita Mountains region are grahamite, found in the central and western sections, and impsonite, which has been found at a single site located in the eastern section (Fig. 1). These two solid bitumens are thought to be genetically related to each other with their differences resulting from the thermal alteration of grahamite to impsonite (Curiale, 1983; Jacob, 1989). The purpose of this study was to utilize recent advances in analytical procedures to undertake a more detailed geochemical analysis of the bitumens and reevaluate the conclusions from the previous investigations regarding the differences between the solid bitumens, grahamite and impsonite.

EXPERIMENTAL

Samples

Paleozoic solid bitumen samples were collected by J. A. Curiale and B. J. Cardott from fields and deposits in the Ouachita Mountains region in southeastern Oklahoma. Oil and solid bitumen pyrolysis data used for comparative purposes in this investigation came from Curiale (1981,1983). Detailed sample site locations and stratigraphic information have been presented elsewhere (Curiale, 1983; Cardott, 1991) and are summarized in Table 1 and noted in Figure 1.

Extraction and Fractionation

Crushed native bitumen samples were soxhlet extracted for 48 hours using a 1:1 mixture of methylene chloride and methanol. Asphaltenes were removed from the total bitumen extracts by precipitation with n-pentane. The deasphaltened bitumen extract was then separated into saturate, aromatic, and polar (NSO) fractions by thin layer chromatography using 100% hexane as solvent. Ultraviolet light and rhodamine indicator were used to distinguish the various fractions. Curiale's procedure differed slightly in that soxhlet extrac-

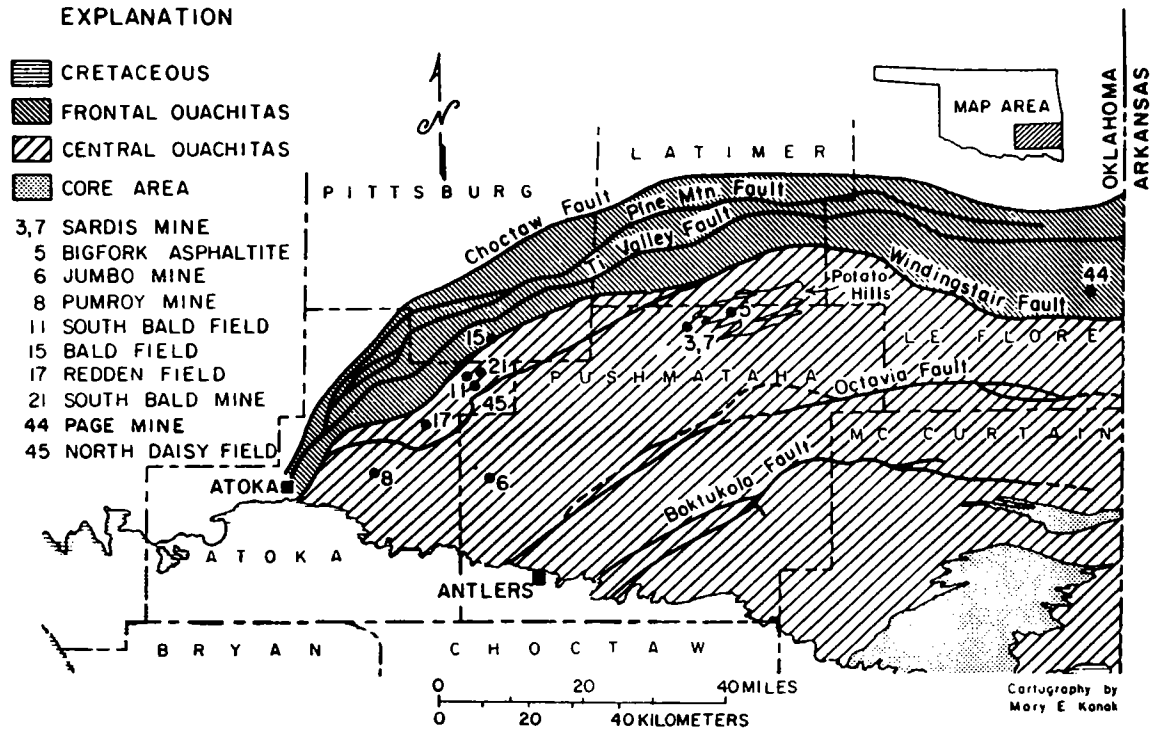

Figure 1. Map of Oklahoma Ouachita Mountains region, showing sample locations (Curiale and others, 1983).

tion was done for 24 hours using only methylene chloride as solvent. Asphaltenes were removed from the extract with n-heptane and column chromatography was used to separate the three fractions. In Curiale's study, fractionation was done only on the oils and not the solid bitumen pyrolyzates (Curiale, 1981).

Gas Chromatography–Mass Spectrometry (GC–MS)

GC–MS analyses were conducted using a Finnigan MAT TSQ 70, a triple stage quadrupole mass spectrometer coupled to a Varian 3400 gas chromatograph inlet system. Chromatographic separations were undertaken using a 25-m × 0.25-mm aluminum-coated fused silica capillary column coated with a 0.1 μm film of the HT-5 phase. The column was temperature programmed from 40 to 120°C at 10°C/min and then from 120 to 300°C at 1.8°C/min and held isothermally at 300°C for 18 min. The injector temperature was 280°C, transfer-line temperature 300°C, and ion-source temperature 200°C. The ion source was operated in the electron impact (EI) mode at an electron energy of 70 eV. Collision activated decomposition (CAD) spectra were obtained with argon as the collision gas at 0.28 mTorr and the collision energy was generally –10 eV. The mass spectrometer was also operated in the single stage mode using selected ion monitoring techniques for biomarker determinations.

Curiale's GC–MS analyses were completed using a Finnigan MAT 4000 instrument linked to an INCOS 2400 (Nova 3) data system. A Hewlett-Packard 5840A gas chromatograph inlet system was used with a 30-m × 0.25-mm fused silica capillary column coated with DB-5 phase. The column was temperature programmed from 40°C (isothermal for 1 min) to 150°C at 12°C/min and then from 150 to 310°C at 8°C/min (held until the homohopanes eluted). Injection temperature was 250°C, transfer-line temperature 250°C, and ion-source temperature 250°C. Ionization voltage was 70 eV and scans were taken from 35 to 450 amu every 2 sec (Curiale, 1981).

Low Temperature Pyrolysis

In Curiale's pyrolysis procedure, solid bitumen samples were placed in a prewashed quarter-inch stainless-steel tube in an atmosphere of dry nitrogen gas, and the tube was heated in a muffle furnace at 300°C for 23–24 hours. After removal and cooling to room temperature, the tube was opened and flushed with methylene chloride and the solution was filtered. The filtrate was then dried under a flow of nitrogen. Asphaltenes were removed with excess n-pentane and the filtrate was treated with a molecular sieve to remove any

TABLE 1.—LOCATIONS AND RESERVOIR INFORMATION FOR SAMPLES USED IN THIS AND PREVIOUS STUDIES
(Curiale and others, 1983; Cardott, 1991)

Sample Number and Type	Field or Deposit	County	Location	Reservoir	Comments
3 Grahamite	East Sardis	Pushmataha	9-T2N-R18E	Stanley Group (Mississippian)	----
5 Grahamite	Bigfork Veins	Pushmataha	1-T2N-R19E	Bigfork Formation (Ordovician)	Samples from veins and fractures in Bigfork chert
6 Grahamite	Jumbo	Pushmataha	28-T1S-R15E	Stanley Group (Mississippian)	----
8 Grahamite	Pumroy	Atoka	25-T1S-R13E	Stanley Group (Mississippian)	----
11 Oil	South Bald	Atoka	5-T1N-R15E	Jackfork Group (Pennsylvanian)	Producing interval: 188-236 feet
15 Oil	Bald	Pittsburg	28-T2N-R15E	Stanley Group (Mississippian)	Producing depth: 350 feet
17 Oil	Redden	Atoka	9-T1S-R14E	Stanley Group (Mississippian)	Producing depth: 148 feet
21 Grahamite	South Bald	Atoka	4-T1S-R15E	Stanley Group (Mississippian)	----
44 Impsonite	Page	Le Flore	24-T3N-R26E	Jackfork Group (Pennsylvanian)	----
45 Oil	North Daisy	Atoka	8-T1N-R15E	Stanley Group (Mississippian)	Loman No. 1 well

n-alkanes. This pyrolyzate fraction, devoid of n-alkanes, was then analyzed by GC and GC–MS without further column chromatography separation (Curiale, 1981).

RESULTS

Thermal maturity effects were evaluated from the pentacyclic terpane distributions as determined from the m/z 191 fragmentograms of the solid bitumen extracts, solid bitumen pyrolyzates, and the associated oils (Fig. 2). The ratio of 18α-22,29,30-trisnorhopane (T_s) to 17α-22,29,30-trisnorhopane (T_m) has been shown to increase with increasing maturity for oils with the same source (Seifert and Moldowan, 1978). Comparison of the T_s/T_m ratio for the two solid bitumen extracts analyzed in this investigation shows that the impsonite extract has a higher value (0.90) relative to that of the grahamite extracts (0.53). The T_s/T_m ratio was also determined for the pyrolyzates and oils examined in previous investigations (Curiale, 1981,1983). A peak previously identified as a tricyclic terpane (and possibly co-eluting with a monoaromatic compound in the pyrolyzates) is now thought to be 18α-22,29,30-trisnorhopane (T_s). The peak originally assigned by Curiale (1981) as 18α-22,29,30-trisnorhopane (T_s) is now thought to be 17α-22,29,30-trisnorhopane (T_m). These reassignments are based upon comparisons of the bitumen extracts examined in the current investigation and the presence of an unusual compound, tentatively identified as 25,28,30-trisnorhopane by Curiale (1988), observed in the m/z 191 and m/z 177 fragmentograms to elute between T_s and T_m

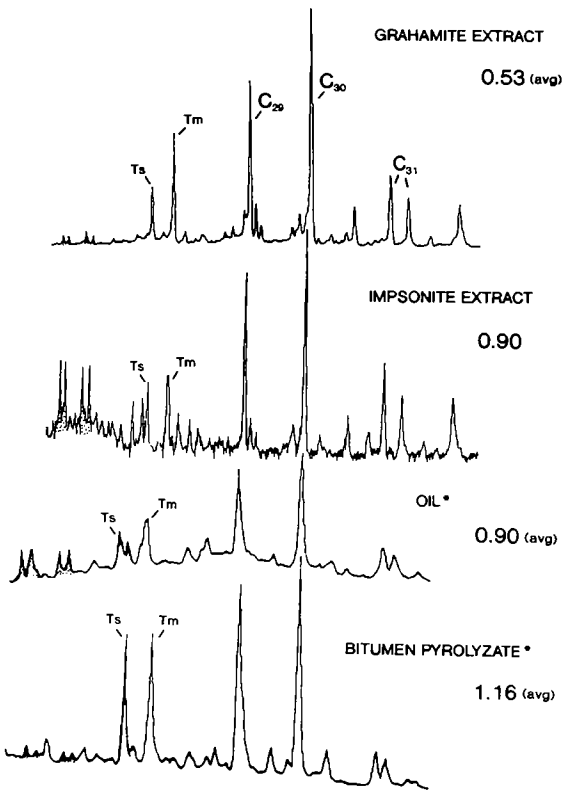

Figure 2. m/z 191 mass fragmentograms with the C_{27}–C_{31} regular hopanes labeled and tricyclic terpanes shaded. Number in the upper right corner is the average T_s/T_m ratio of the various samples. Asterisk (*) indicates data from Curiale (1981).

(Fig. 3). Based upon these new peak identifications both the oils and pyrolyzates have relatively high T_s/T_m ratios (0.90 and 1.16, respectively) in comparison to the grahamite extract ratios (0.53).

The effects of thermal maturity upon regular sterane distributions in oils has been well documented (Philp, 1985, and references therein). However, biodegradation can also affect steranes, and this could affect maturity determinations based upon regular sterane distributions. A more useful maturity parameter for characterizing these solid bitumen extracts was the ratio of C_{21} and C_{22} steranes (pregnane and homopregnane, respectively) to the regular C_{27}–C_{29} steranes. The pregnane/sterane ratio has been previously found to increase with increasing maturity (Wingert and Pomerantz, 1986). Examination of the m/z 218 fragmentograms (Fig. 4) shows that the impsonite extract has a higher pregnane/sterane ratio (0.40) than the grahamite extracts (0.32).

In extensively biodegraded oils, regular steranes are removed, leaving the more resistant diasteranes (Seifert and Moldowan, 1979). In a previous investigation of these solid bitumens, Curiale and others (1983) found that the diasterane to

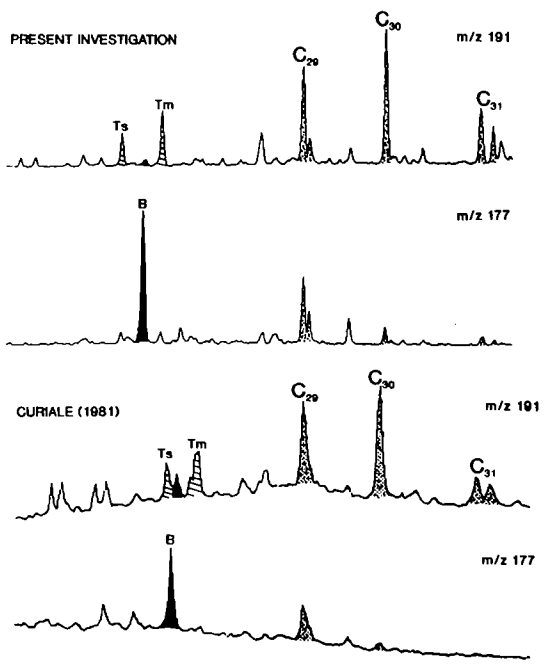

Figure 3. m/z 191 and m/z 177 fragmentograms of samples examined in the present investigation and from Curiale (1981). Note reassignment of the T_s and T_m peaks in the m/z 191 fragmentogram. Curiale (1981) had previously identified these peaks as a tricyclic terpane and T_s, respectively. The peak labeled B has been previously identified as 25,28, 30-trisnorhopane (Curiale, 1988).

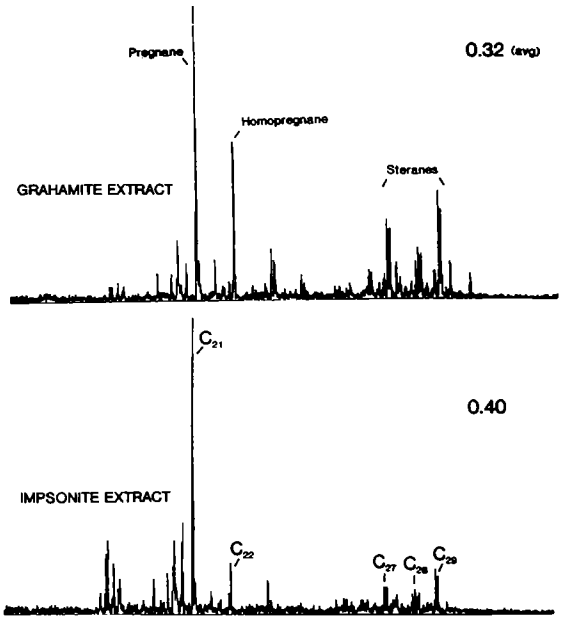

Figure 4. m/z 218 mass fragmentograms with pregnane, homopregnane and the regular C_{27}–C_{29} steranes labeled. Number in the upper right corner is the average pregnane/sterane ratio. This ratio is a measurement of the pregnane and homopregnane peak areas versus the peak areas of all sterane isomers from C_{27} to C_{29}.

regular sterane ratio was higher in the solid bitumen pyrolyzates than in the oils from the same geographic location. In the present study, the diasterane/sterane ratio was determined for the solid bitumen extracts and compared to that of the pyrolyzates and oils (Fig. 5). High relative abundances of diasteranes were observed only in the impsonite extract and not in the grahamite extracts. Thus, the oils and grahamite extracts have relatively low diasterane/sterane ratios (0.33 and 0.22, respectively), while all the pyrolyzates and the impsonite extract have higher ratios (0.57 and 0.49, respectively) and relatively higher abundances of diasteranes.

DISCUSSION

Based on petrographic characterization of solid bitumens, Jacob (1989) has suggested that impsonite is a thermal alteration product. In a petrographic study of the impsonite from the Ouachita Mountains region, Cardott (1991) concurred with this conclusion stating, "The presence of grahamite deposits in the area and the level of thermal maturity of the region suggest indirectly that the Page impsonite originated as a thermally altered grahamite formed from an asphaltene-rich as-

phalt." Curiale (1983) proposed that thermal alteration of grahamite to impsonite could explain the relatively low H/C and high fixed-carbon values of the impsonite, although no biomarker evidence was presented to support this premise. In the present investigation biomarker maturity parameters strongly suggest that impsonite is indeed a thermal alteration product of grahamite.

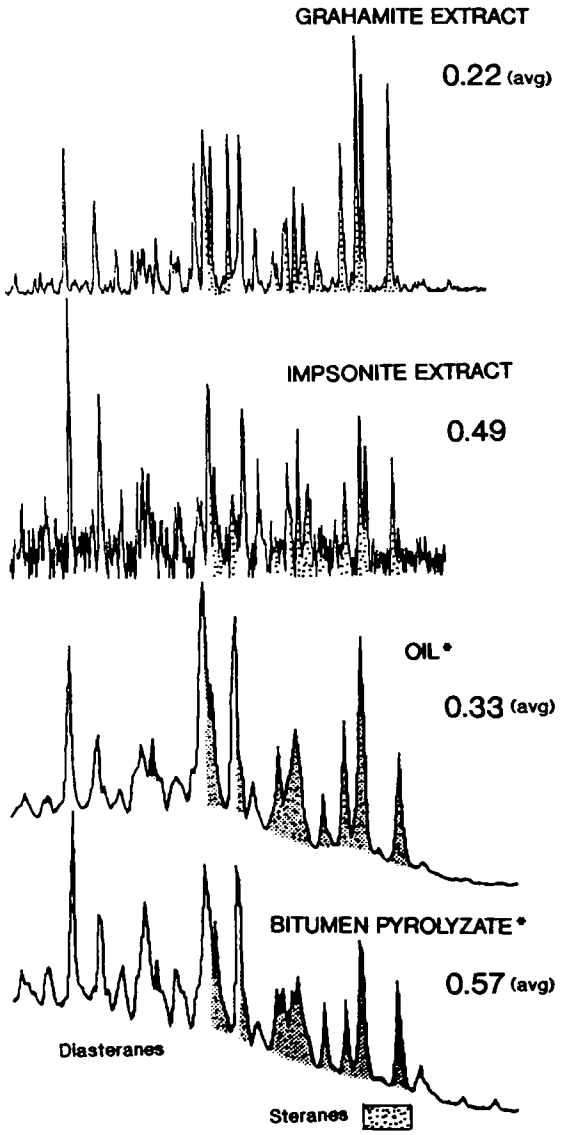

Figure 5. m/z 217 mass fragmentograms with the regular steranes shaded and the diasterane region labeled. Number in the upper right corner is the average diasterane/sterane ratio. This ratio is a measurement of the 13β,17α-diacholestane(20S+20R) peak areas versus the 24-Ethylcholestane peak areas. Asterisk (*) indicates data from Curiale (1981).

Pregnane/sterane ratios clearly indicate that the impsonite extract is more thermally mature than the grahamite extracts. Further biomarker evidence is provided by the T_s/T_m ratios, which show that the grahamite extracts are significantly less mature than the impsonite extract or the associated oils. The T_s/T_m ratio also shows that the pyrolyzates (grahamites and impsonite) are more mature than the oils or either of the extracts. A probable explanation of this observation is that the pyrolysis has "artificially matured" these samples. It is also possible that, since the pyrolyzates were analyzed without fractionation, a coelution of an aromatic compound (Curiale, 1981) could be affecting the T_s/T_m ratio.

Curiale and others (1983) previously concluded that the increase in diasterane/sterane ratio in the bitumen pyrolyzates versus the oils was indicative of a bitumen origin due to biodegradation of the oils. In the present study, the ratio of diasteranes to regular steranes was found to be higher only in the impsonite extract and not in the grahamite extracts. The geochemical implications of this finding are that the increased relative abundances of diasteranes in these solid bitumens cannot be due to biodegradation effects as was previously proposed. Since only the impsonite extract and the bitumen pyrolyzates show this trend, a possible explanation for the observed ratios is that the relative increase in diasteranes is a consequence of increased thermal maturity.

CONCLUSIONS

Hydrocarbon distributions of the extracts examined in this study support the view that these solid bitumens are products of limited biodegradation, water washing, and devolatilization. However, biomarker distributions previously interpreted as indicators of biodegradation are now thought to reflect the influence of thermal maturity. Specifically, sterane and terpane distributions suggest that impsonite has undergone significant thermal alteration while grahamite samples appear to be relatively unaffected. High relative abundances of diasteranes, which have often been attributed to biodegradation effects, appear to be related to maturity differences in these samples. Terpane peak identifications from previous investigations have been reevaluated to assess maturity differences and they now suggest that pyrolysis experiments may have "artificially matured" the solid bitumens.

REFERENCES

Abraham, H., 1945, Asphalts and allied substances [fifth edition]: Van Nostrand, New York, 2142 p.

Cardott, B. J., 1991, Organic petrology of epi-impsonite at Page, Oklahoma, U.S.A.: Organic Geochemistry, v. 17, p. 185–191.

Curiale, J. A., 1981, Source rock geochemistry and liquid and solid petroleum occurrences of the Ouachita Mountains, Oklahoma: University of Oklahoma unpublished Ph.D. dissertation, 286 p.

_____1983, Petroleum occurrences and source-rock potential of the Ouachita Mountains, southeastern Oklahoma: Oklahoma Geological Survey Bulletin 135, 65 p.

_____1986, Origin of solid bitumens, with emphasis on biological marker results, *in* Leythaeuser, D.; and Rullkötter, J. (eds.), Advances in organic geochemistry 1985: Pergamon Press, New York, p. 559–580.

_____1988, Biological markers in grahamites and pyrobitumens, *in* Yen, T. F.; and Moldowan, J. M. (eds.), Geochemical biomarkers: Harwood Academic Publishers, New York, p. 1–24.

Curiale, J. A.; and Harrison, W. E., 1981, Correlation of oil and asphaltite in Ouachita Mountain region of Oklahoma: American Association of Petroleum Geologists Bulletin, v. 65, p. 2426–2432.

Curiale, J. A.; Harrison, W. E.; and Smith, G., 1983, Sterane distribution of solid bitumen pyrolyzates; changes with biodegradation of crude oil in the Ouachita Mountains, Oklahoma: Geochimica et Cosmochimica Acta, v. 47, p. 517–523.

Eldridge, G. H., 1901, The asphalt and bituminous rock deposits of the United States, *in* 22nd annual report of the Geological Survey, 1900–1901: Government Printing Office, Washington D.C., v. 22, pt. 1, p. 209–452.

Fay, R. O., 1982, Asphaltite deposits in Pushmataha County, *in* Geology of Pushmataha County, Oklahoma: Eastern New Mexico University Studies in Natural Sciences, Special Publication 2, p. 46–58.

Ham, W. E., 1956, Asphaltite in the Ouachita Mountains of southeastern Oklahoma: Oklahoma Geological Survey Mineral Report 30, 12 p.

Jacob, H., 1989, Classification, structure, genesis and practical importance of natural solid oil bitumens ("migrabitumen"): International Journal of Coal Geology, v. 11, p. 65–79.

Jacob, H.; and Wehner, H., 1981, Microscope-photometric analysis of dispersed solid bitumina in sediments [in German]: DGMK Project 232, 257 p.

Philp, R. P., 1985, Biological markers in fossil fuel production: Mass Spectrometry Reviews, v. 4, p. 1–54.

Seifert, W. K.; and Moldowan, J. M., 1978, Applications of steranes, terpanes and monoaromatics to the maturation, migration and source of crude oils: Geochimica et Cosmochimica Acta, v. 42, p. 77–95.

_____1979, The effect of biodegradation on steranes and terpanes in crude oils: Geochimica et Cosmochimica Acta, v. 43, p. 111–126.

Taff, J. A., 1899, An albertite-like asphalt in the Choctaw Nation, Indian Territory: American Journal of Science, 4th series, v. 8, p. 219–224.

_____1909, Grahamite deposits of southeastern Oklahoma, *in* Hayes, C. W.; and Lindgren, W. (eds.), Contributions to economic geology 1908: U.S. Geological Survey Bulletin 380, p. 286–297.

Wingert, W. S.; and Pomerantz, M., 1986, Structure and significance of some twenty-one and twenty-two carbon petroleum steranes: Geochimica et Cosmochimica Acta, v. 50, p. 2763–2769.

Rock Heterogeneity and Geostatistical Methods Applied to Petroleum Migration in Source Rocks

Ahmad J. Sultan and John P. Heller
New Mexico Institute of Mining and Technology

This extended abstract is concerned with the mathematical descriptions of the variability of source-rock permeability.

Several types of rock heterogeneity may be found at different scales of length. They are all considered to be the result of environmental variability associated with one or more of three closely related processes in source-rock development. These processes are characterized as: sedimentary (including composition), diagenesis (the gradual chemical and physical changes that occurred after deposition), and tectonic (modification caused by large-scale changes, since deposition, of the geological environment).

The defining influences on rock properties are the compositions of sediment and inorganic or organic saturating fluids, and the processes involved in transport and deposition. Thus, the primary causes of rock heterogeneity are the spatial differences and temporal changes in sediment composition and sedimentary processes.

After deposition and subsequent burial of the source rock, many different chemical and physical changes occur. Nonuniform diagenetic processes are also responsible for significant spatial variability in permeability and other rock properties. Nonuniform postdepositional influences include spatial variations in temperature, chemical content, and flow velocity of the saturating fluid, as well as spatial variation in mechanical stresses on the formation.

Closely related to diagenetic changes, and sometimes difficult and/or pointless to separate from them, are postdepositional changes of the source rock that resulted from tectonic forces and events, such as deformation, uplift, and the intrusion of volcanic dikes.

A threefold classification of source-rock heterogeneity is given by Alpay (1972); similar ideas were published by Bear (1972) and Haldorsen and Lake (1984). These authors distinguished heterogeneity at several different scales: microscopic (the scale of only a few pores), macroscopic (the size of conventional core samples), megascopic (the size of large grid blocks in field models), and gigascopic (total formation or regional scale). Illustrations modeled after Haldorsen and Lake (1984) and Bear (1972) are shown in Figure 1. A semiquantitative description of heterogeneity types which may affect various source-rock parameters has been given by Weber (1986).

The question arises as to how spatial variability of source rocks could be modeled. We concentrate on permeability, which we consider to be the most important parameter in the fluid migration process. Moreover, this variability occurs at many scales. The somewhat unpredictable (or random) nature of rock properties, including spatial distribution, can be modeled by employing geostatistical techniques from modern probability theory and statistical methods. Describing these variations stochastically instead of deterministically deals mathematically with the variability of petrogeological parameters and with the uncertainty arising from incomplete information about their spatial distribution. Each parameter is treated as a random variable with its spatial fluctuations being the realization of a stochastic process. However, treating each parameter as a random variable is not the mathematical equivalent of saying that the parameters vary without cause or that there is no relationship between their values at different locations. We are driven to the stochastic approach by the lack of specific information about the values of permeability or other values. At the same time, we can anticipate that a purely statistical description will be useful in deriving overall properties of the formation. These techniques have already been used with some success in characterizing the variability of mineral deposits. A good reference to these techniques is given by Journel and Huijbregts (1978).

The geostatistical techniques are used to establish spatial correlation among the required reservoir rock properties. With the help of these techniques, unconditioned and conditioned simulations can be carried out to generate possible representations of a source-rock property field which has the statistically correct random behavior (as expressed in the mean and variogram). Several methods have been developed to generate or synthesize unconditioned fields: the Source Point Method developed by Heller (1972); the Fast Fourier Transform Method introduced by Gutjahr (1989); and the Turning Bands Method originated by Matheron (1973) and further developed by

Montoglou and Wilson (1982). A field generated by one of these methods is called an unconditioned simulation.

Although an unconditioned simulation has the same statistical character as the known observed data, the values it specifies for the field variable (at the locations of the original data points) probably do not coincide with the actual data at particular points. In a conditioned simulation this defect is remedied, at the cost of some additional calculation, by using a technique called "kriging" and generating a new unconditioned field. Kriging is the local estimation technique which provides the best linear unbiased estimator (often abbreviated BLUE) of the unknown value. The estimates provided by kriging are optimal in a mean-square sense and minimize the estimation error.

In this study, we have characterized the permeability distribution of a petroleum reservoir using the stochastic approach. Spatially correlated con-

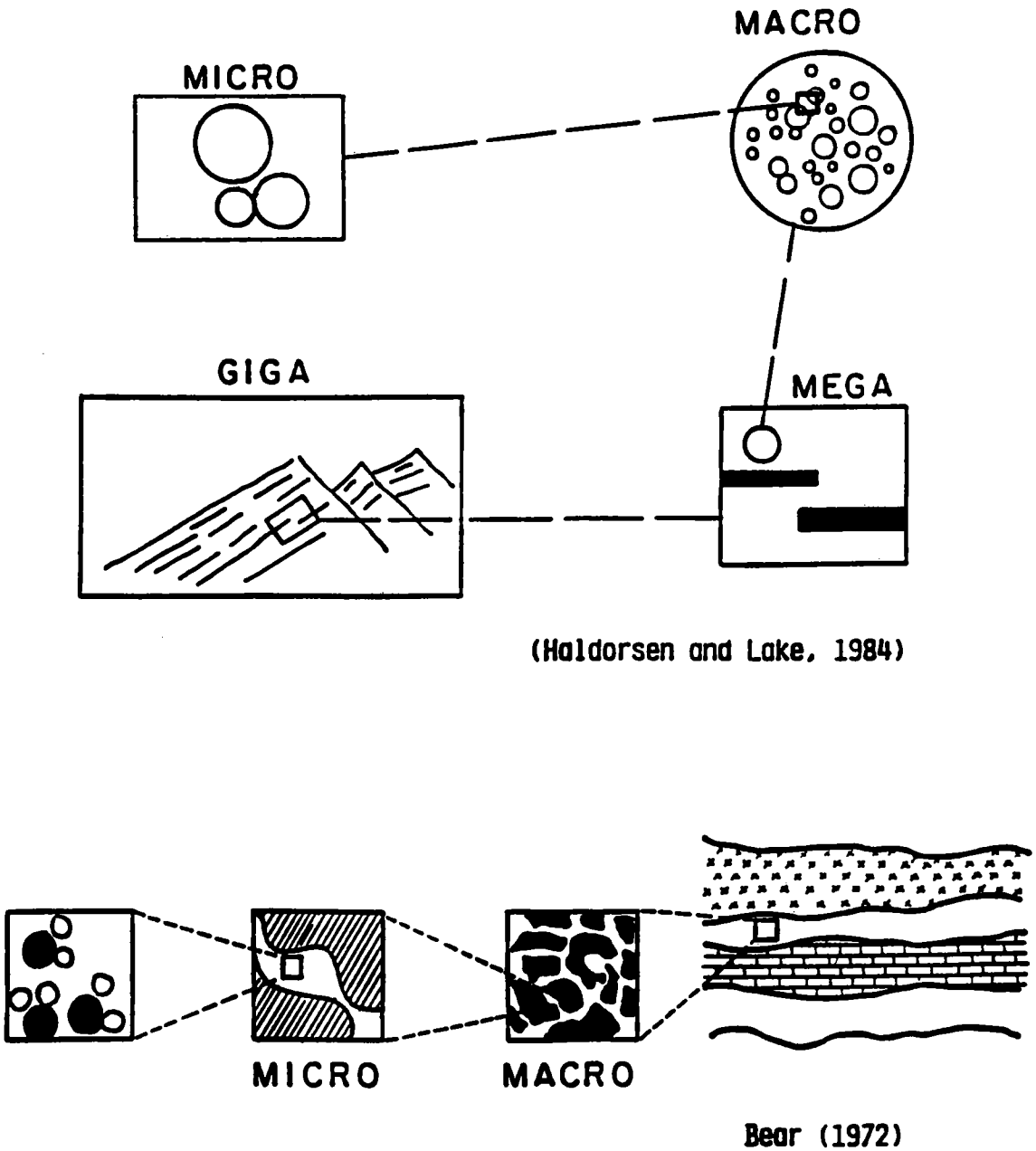

Figure 1. Schematic representations of scales of rock heterogeneity.

ditioned permeability fields were generated which could be used to further investigate the movement of petroleum fluid in a source rock.

REFERENCES

Alpay, O. A., 1972, A practical approach to defining reservoir heterogeneity: Journal of Petroleum Technology, v. 20, no. 7, 841–848.

Bear, J., 1972, Dynamics of fluids in porous media: Elsevier, New York, 764 p.

Gutjahr, A. L., 1989, Spatial variability: geostatistical methods: New Mexico Tech Project Report, LANL Contract 4-R58-2690R.

Haldorsen, H. H.; and Lake, L. W., 1984, A new approach to shale management in field-scale models: Society of Petroleum Engineers Journal, v. 24, no. 4, p. 447–457.

Heller, J. P., 1972, Observations of mixing and diffusion in porous media, *in* Fundamentals of transport phenomena in porous media: Proceedings, Second Symposium, International Association for Hydraulic Research/International Society of Soil Science, Guelph, Ontario, p. 1–26.

Journel, A. G.; and Huijbregts, C. J., 1978, Mining geostatistics: Academic Press, London, 600 p.

Matheron, G., 1973, The intrinsic random functions and their applications: Advanced Applied Probability, v. 5, p. 439–468.

Montoglou, A.; and Wilson, J. L., 1982, The turning bands methods for simulation of random fields using line generation by a spectral methd: Water Resources Research, v. 18, no. 5, p. 1379–1394.

Weber, K. J., 1986, How heterogeneity affects oil recovery, *in* Lake, L. W.; and Carroll, H. B., Jr. (eds.), Reservoir characterization: Academic Press, Orlando, p. 487–544.

Investigation of the Pyrolysis Process from Pyrolyzing the Woodford Shale and the Excello Shale

Longjiang Wang and Colin Barker
University of Tulsa

ABSTRACT.—We have used samples of the Woodford Shale, Oklahoma, and Excello Shale, Kansas, to study the process of source-rock pyrolysis. Bitumens in a source rock can be classified as free bitumens in pores, adsorbed bitumens on kerogen, or adsorbed bitumens on the mineral matrix. During pyrolysis, the free bitumens in pores evolve at the lowest temperature to form the first peak (Peak 1) on a pyrogram. The mechanism of bitumen release obeys a second order kinetic law. The bitumens adsorbed on kerogen and the mineral matrix then evolve, forming the intermediate peak(s). The mechanism involved here is a desorption process. With further increasing temperature, kerogen in the source rock starts to thermally break down, forming the second peak (Peak 2) on the pyrogram. The mechanism involved here is thermal cracking, and the evolution of Peak 2 obeys a first order kinetic law.

Pyrolysis experiments with model systems in which nC_{20} alkane, dibenzothiophene, and phenanthrene have been adsorbed onto Excello Shale samples have clarified the nature of the rock-bitumen interactions. Surfaces appear to be coated with a monolayer first; then multilayers develop. It is the multilayers which are released with second order kinetics. This is very important to source-rock behavior because the temperature for the evolution of the bitumens (i.e., expulsion) decreases with increasing bitumen content. This is in contrast to first order kinetic behavior in which peak position does not shift with amount.

Organic Matter Content of Outcrop Samples from the Ouachita Mountains, Oklahoma

Jane L. Weber
Oklahoma Geological Survey

The potential of a sedimentary rock to generate hydrocarbons is determined by three criteria: the abundance and type of organic matter present in the rock and its level of thermal maturity. The first two criteria must always be met, with 0.5% generally considered as the minimum quantity of organic carbon necessary to generate and expel oil and/or gas from clastic rocks. For outcrop samples, maturity level is a less important criterion, since at greater burial depths the same source interval could be mature enough to produce hydrocarbons.

As part of its comprehensive regional review of the Ouachitas, the Oklahoma Geological Survey (OGS) collected 50 samples of possible source rocks from exposed strata in the Ouachita Mountains of Oklahoma. Ranging in age from Early Ordovician to Early Pennsylvanian (Fig. 1), the sample set includes 37 rocks from the frontal belt (between the Choctaw and Windingstair faults); 12 from the central belt (south of the Windingstair fault); and one from the Broken Bow uplift in the southern Ouachitas (Fig. 2).

Geochemical data relating only to the quantity

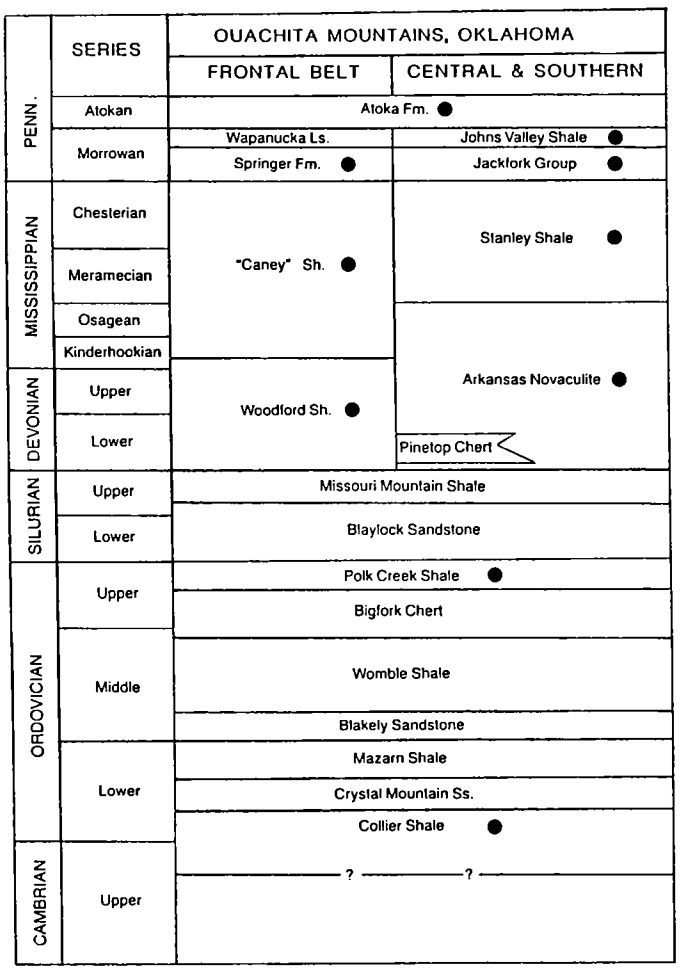

Figure 1. Stratigraphic chart for the Ouachita Mountains, Oklahoma. Dots (•) indicate units sampled. Modified from Johnson (1988) and Suneson (1988).

TABLE 1. — SAMPLE LOCATION AND GEOCHEMICAL DATA

Sample	Location	Total Organic Carbon (%)	Extractable Org. Matter (ppm)
	Atoka Formation		
1*	Sec. 32, T3N, R15E	0.95	167
2*	Sec. 21, T2N, R15E	0.66	87
3	Sec. 35, T4N, R16E	0.22	10
4	Sec. 23, T4N, R18E	0.41	20
5	Sec. 28, T4N, R19E	0.51	14
6	Sec. 32, T5N, R20E	0.32	10
7*	Sec. 29, T5N, R19E	0.89	160
8	Sec. 23, T5N, R21E	0.62	16
9	Sec. 5, T4N, R22E	0.59	10
10	Sec. 21, T5N, R22E	0.78	10
11*	Sec. 21, T5N, R23E	1.2	63
12	Sec. 30, T5N, R24E	0.49	10
13*	Sec. 2, T4N, R17E	1.0	116
14	Sec. 34, T5N, R18E	0.42	42
15*	Sec. 5, T4N, R18E	0.50	134
16*	Sec. 24, T4N, R17E	1.5	168
17*	Sec. 28, T4N, R18E	1.2	146
18	Sec. 21, T4N, R18E	0.74	30
19*	Sec. 4, T4N, R23E	1.8	1212
	Range:	0.22–1.8	10–1212
	Average:	0.78	128
	Johns Valley Shale		
20	Sec. 9, T1S, R16E	0.34	65
21	Sec. 3, T3N, R19E	0.30	10
22	Sec. 26, T4N, R20E	0.77	38
23	Sec. 24, T4N, R22E	0.45	15
24*	Sec. 2, T3N, R17E	3.0	356
25*	Sec. 12, T3N, R18E	2.4	573
	Range:	0.30–3.0	10–573
	Average:	1.21	176
	Springer Formation		
26	Sec. 1, T1N, R12E	0.52	50
27	Sec. 5, T4N, R18E	0.30	75
	Range:	0.30–0.52	50–75
	Average:	0.41	62
	Jackfork Group		
28*	Sec. 19, T1N, R15E	2.0	310
29	Sec. 34, T4N, R23E	0.82	22
30	Sec. 25, T2N, R21E	0.29	10
31	Sec. 31, T4N, R23E	0.49	52
	Range:	0.29–2.0	10–310
	Average:	0.90	98

TABLE 1. — *Continued*

Sample	Location		Total Organic Carbon (%)	Extractable Org. Matter (ppm)
		Caney Shale		
32*	Sec. 4, T1S, R16E		5.4	1570
33*	Sec. 11, T4N, R21E		4.6	6294
34*	Sec. 6, T4N, R21E		4.4	2816
		Range:	4.4–5.4	1570–6294
		Average:	4.8	3560
		Stanley Shale		
35	Sec. 9, T1S, R14E		0.39	120
36*	Sec. 26, T2N, R25E		0.94	170
37	Sec. 16, T3N, R20E		0.32	46
38	Sec. 2, T3N, R21E		0.19	32
39	Sec. 1, T2N, R21E		0.24	49
40	Sec. 2, T2N, R21E		0.17	12
41	Sec. 7, T2N, R23E		0.23	41
42	Sec. 33, T3N, R23E		0.22	44
		Range:	0.17–0.94	12–170
		Average:	0.34	64
		Woodford Shale		
43*	Sec. 5, T2N, R15E		3.3	1153
44*	Sec. 11, T4N, R21E		3.6	2436
45*	Sec. 15, T4N, R20E		2.0	514
46*	Sec. 6, T4N, R21E		8.5	3342
47*	Sec. 4, T2N, R15E		5.3	2248
		Range:	2.0–8.5	514–3342
		Average:	4.5	1939
		Arkansas Novaculite		
48*	Sec. 13, T2S, R11E		12.5	3300
		Polk Creek Shale		
49*	Sec. 14, T2S, R11E		6.1	980
		Collier Shale		
50	Sec. 17, T5S, R24E		0.29	50

*Merits further evaluation as a potential source rock.

of organic matter found in these samples is presented here. Investigations concerning the quality and maturity level of contained organic matter are currently underway at the OGS and will be reported later. Organic matter content was determined for each sample by measuring total organic carbon (TOC) with a Leco WR-12 Carbon Determinator and extractable organic matter (EOM) by soxhlet-extracting crushed rock for 24 hours with methylene chloride (Table 1).

The hydrocarbon-generating potential of each sample is estimated with a log-log plot of EOM vs. TOC (Fig. 3). This plot functions primarily as a screen, indicating samples that have essentially no capacity for producing (or having produced) significant hydrocarbons. It also indicates whether a potential source rock is more likely to produce oil or gas.

Roughly one-half the samples in this study, including the lone Collier and two Springer samples, lack sufficient organic matter (TOC ≥0.5% and EOM ≥60 ppm) to qualify them as potential source rocks. Four samples, including one Woodford, two Caney, and one Atoka collected from T. 4 N., R. 21–23 E. in the Ouachita frontal belt, fall in the "fair oil-source" area on the plots in Figure 3. Nineteen other samples, including representatives from all sampled formations except the Collier and Springer and taken from locations throughout the Ouachitas, contain sufficient organic carbon and extractable organic compounds to warrant further examination as potential source rocks for gas.

ACKNOWLEDGMENTS

The author appreciates the advice and support of Dr. Jock A. Campbell (OGS) and Dr. Neil H. Suneson (OGS) and the typing assistance of Diana Gilstrap (OGS).

REFERENCES

Johnson, K. S., 1988, General geologic framework of the field-trip area, *in* Johnson, K. S. (ed.), Shelf-to-basin geology and resources of Pennsylvanian strata in the Arkoma basin and frontal Ouachita Mountains of Oklahoma: Oklahoma Geological Survey Guidebook 25, p. 1–5.

Suneson, N. H., 1988, The geology of the Ti Valley fault in the Oklahoma Ouachita Mountains, *in* Johnson, K. S. (ed.), Shelf-to-basin geology and resources of Pennsylvanian strata in the Arkoma basin and frontal Ouachita Mountains of Oklahoma: Oklahoma Geological Survey Guidebook 25, p. 33–47.

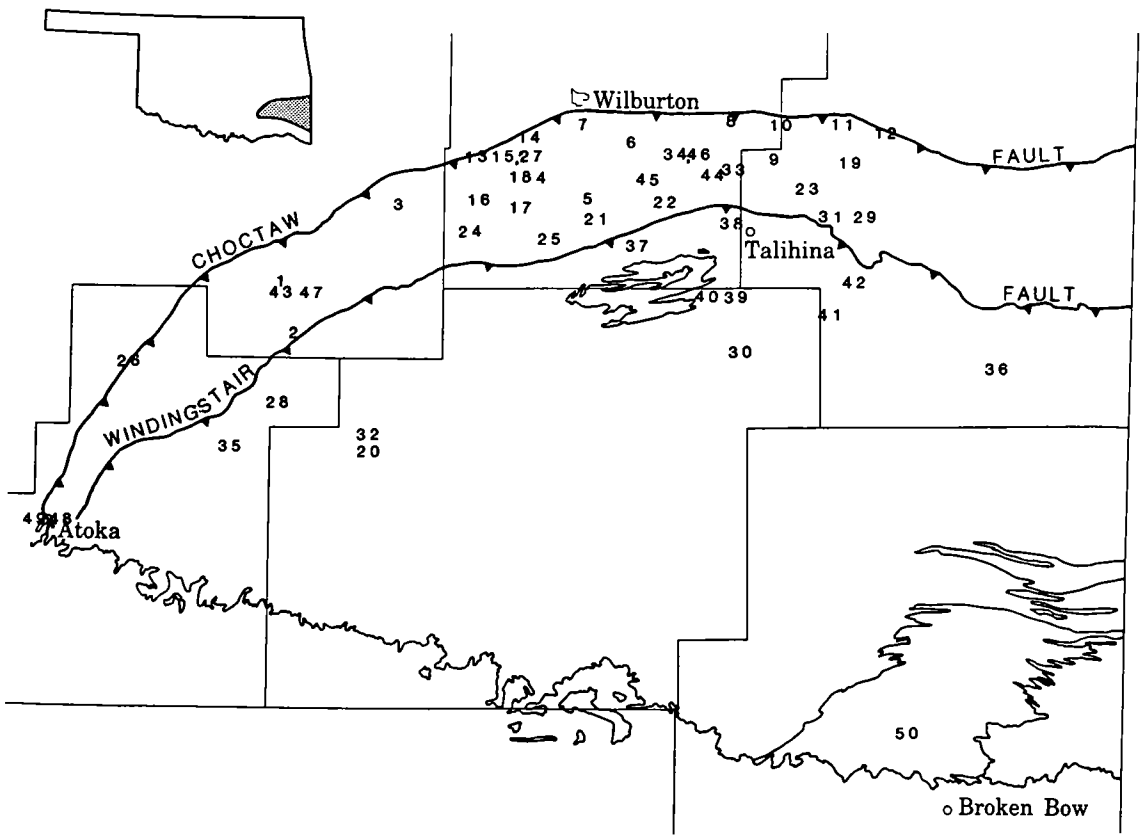

Figure 2. Locations of outcrops sampled in the frontal belt, central belt, and southern portion of the Ouachita Mountains, Oklahoma.

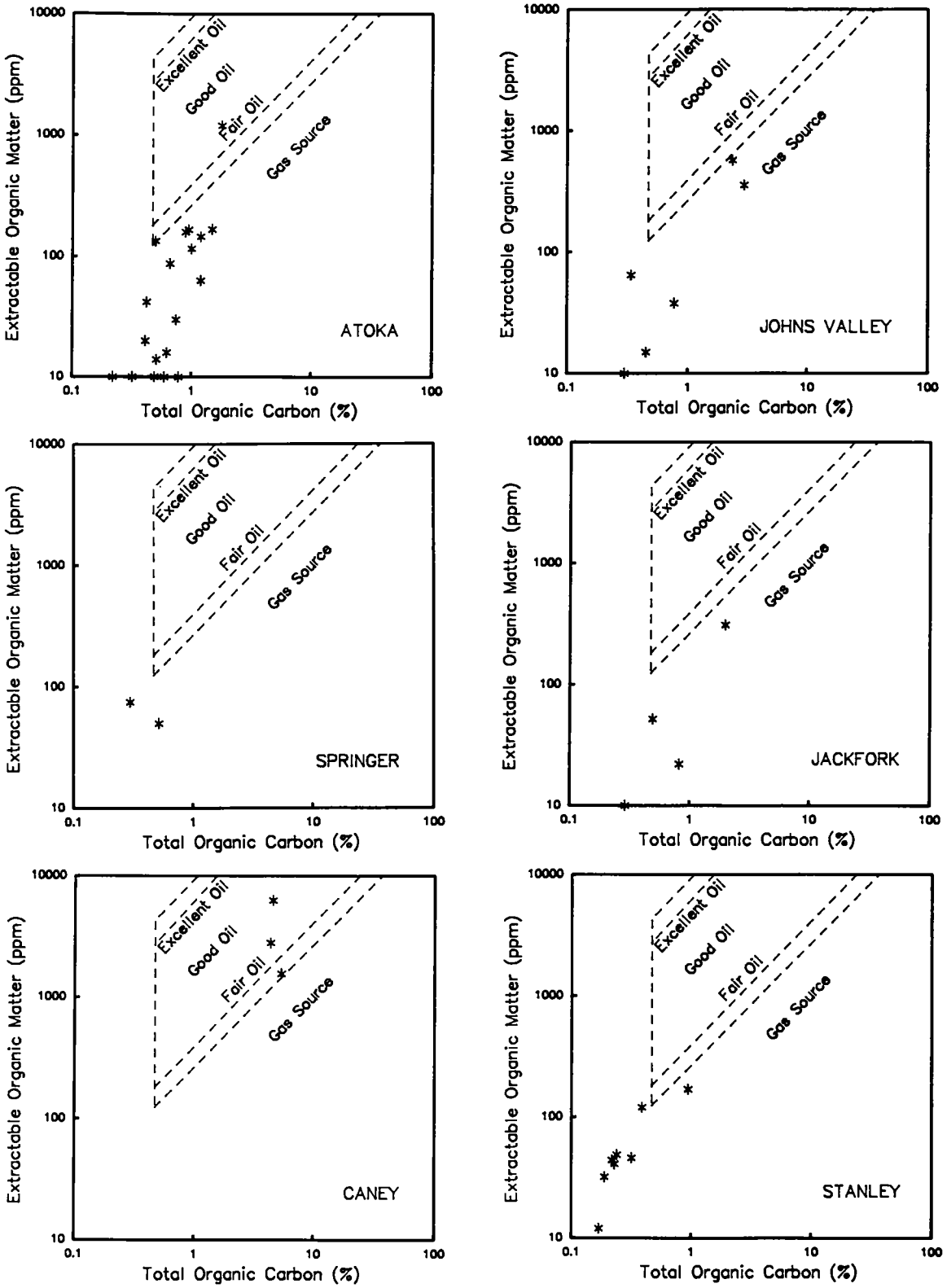

Figure 3. Log-log plots of EOM vs. TOC showing source-rock potential of outcrop samples from the Ouachita Mountains, Oklahoma.

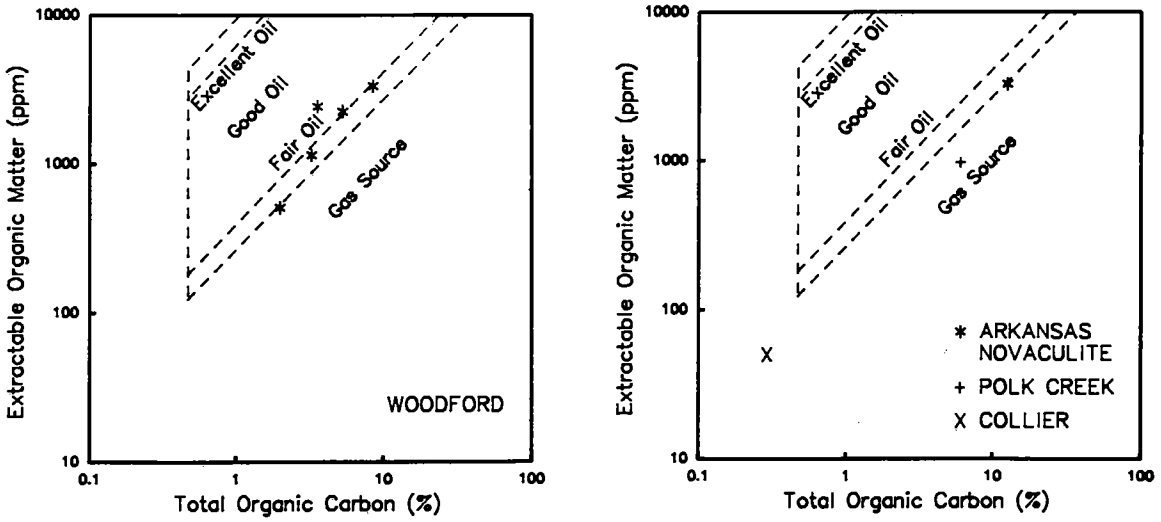

Figure 3. *(Continued)*